Synthesis and Reactivity of Lewis Base Stabilized Pnictogenylboranes

DISSERTATION

ZUR ERLANGUNG DES
DOKTORGRADES DER NATURWISSENSCHAFTEN
(DR. RER. NAT.)
DER FAKULTÄT FÜR CHEMIE UND PHARMAZIE
DER UNIVERSITÄT REGENSBURG

vorgelegt von
Christian Marquardt
aus Roding
im Jahr 2015

Diese Arbeit wurde angeleitet von Prof. Dr. Manfred Scheer.

Promotionsgesuch eingereicht am: 28. Oktober 2015
Tag der mündlichen Prüfung: 04. Dezember 2015

Vorsitzender: Prof. Dr. Arnd Vogler
Prüfungsausschuss: Prof. Dr. Manfred Scheer
Prof. Dr. Nikolaus Korber
Prof. Dr. Frank-Michael Matysik

Universität Regensburg

Eidesstattliche Erklärung

Ich erkläre hiermit an Eides statt, dass ich die vorliegende Arbeit ohne unzulässige Hilfe Dritter und ohne Benutzung anderer als der angegebenen Hilfsmittel angefertigt habe; die aus anderen Quellen direkt oder indirekt übernommenen Daten und Konzepte sind unter Angabe des Literaturzitats gekennzeichnet.

_____

Christian Marquardt

This thesis was elaborated within the period from January 2012 till October 2015 in the Institute of Inorganic Chemistry at the University of Regensburg, under the supervision of Prof. Dr. Manfred Scheer.

Parts of this work have already been published or submitted:
(* = Co-First Authorship: These authors contributed equally to this work.)

C. Marquardt, A. Adolf, A. Stauber, M. Bodensteiner, A. V. Virovets, A. Y. Timoshkin, M. Scheer, *Chem. Eur. J.* **2013**, *19*, 11887–11891.

C. Thoms, C. Marquardt, M. Bodensteiner, M. Scheer, *Angew. Chem. Int. Ed.* **2013**, *52*, 5150–5154.

C. Marquardt, C. Thoms, A. Stauber, G. Balazs, M. Bodensteiner, M. Scheer, *Angew. Chem. Int. Ed.* **2014**, *53*, 3727–3730.

C. Marquardt, O. Hegen, M. Hautmann, G. Balázs, M. Bodensteiner, A. V. Virovets, A. Y. Timoshkin, M. Scheer, *Angew. Chem. Int. Ed.* **2015**, *54*, 13122–13125.

C. Marquardt,* T. Jurca,* K.-C. Schwan, A. Stauber, A. V. Virovets, G. R. Whittell, I. Manners, M. Scheer, *Angew. Chem. Int. Ed.* **2015**, *54*, 13782–13786.

“An expert is a person who has found out by his own painful experience all the mistakes that one can make in a very narrow field.”

Niels Henrik David Bohr

To my family

Preface

During the period of this thesis (January 2012 – October 2015) some results have already been published (*vide supra*). These are also summarized in the present work, reprinted with permission of the respective scientific publisher. The corresponding license numbers are given at the end of the particular chapters.

At the beginning of each chapter a list of authors, who contributed to the respective part, is given. In addition, each chapter contains the section ‘author contributions’, which accurately describes the extent of involvement. If results from collaborations are in part also discussed in other theses, it is stated there.

To ensure a uniform design of this work, all chapters are subdivided into ‘Introduction’, ‘Results and Discussion’, ‘Conclusion’, ‘References’, ‘Supporting Information’ and ‘Author Contributions’. Furthermore, all chapters have the same text settings and the compound numeration begins anew. Due to different requirements of the journals and different article types, the presentation of figures for single crystal X-ray structures or the ‘Supporting Information’ may differ. In addition, a general introduction is given at the beginning and a comprehensive conclusion of all chapters is presented at the end of this thesis.

Table of Contents

1. Introduction

One of the first reports on a group 13/15 compound – the ammonia-borane adduct $H_3N{\cdot}BF_3$ by *Gay-Lussac* – dates back over 2 centuries.[1] Several decades later in 1890, the first phosphine-borane adduct $H_3P{\cdot}BCl_3$ was reported by *Besson*.[2] The high importance of those kind of borane adducts on materials sciences is reflected by numerous publications and review articles, which have been published on this topic over the last decade.[3] Since those initial studies, a great variety of Lewis acid/base (≙ LA/LB) adducts (Figure 1, type I, E' = group 13 element, E = group 15 element) has been synthesized and characterized. Besides the simple 1:1 LA/LB adducts, also hypercoordinated adducts (Figure 1, type II) which contain five-coordinated group 13 element centers, were thoroughly studied. Apart from the LA/LB adducts, organometallic group 13/15 compounds show a broad variety of different monomeric, heterocyclic and cage-like structural motifs of the type $[R_2E'ER'_2]_x$ (Figure 1, types III - IV) and $[RE'ER']_x$ (x ≥ 2) (Figure 1, types VI - VIII) (R, R' = H, F, Cl, Br, I, alkyl, aryl) containing regular *σ*-bonds consisting of 2-electron-2-center-bonds between the group 13 and the group 15 elements.[4]

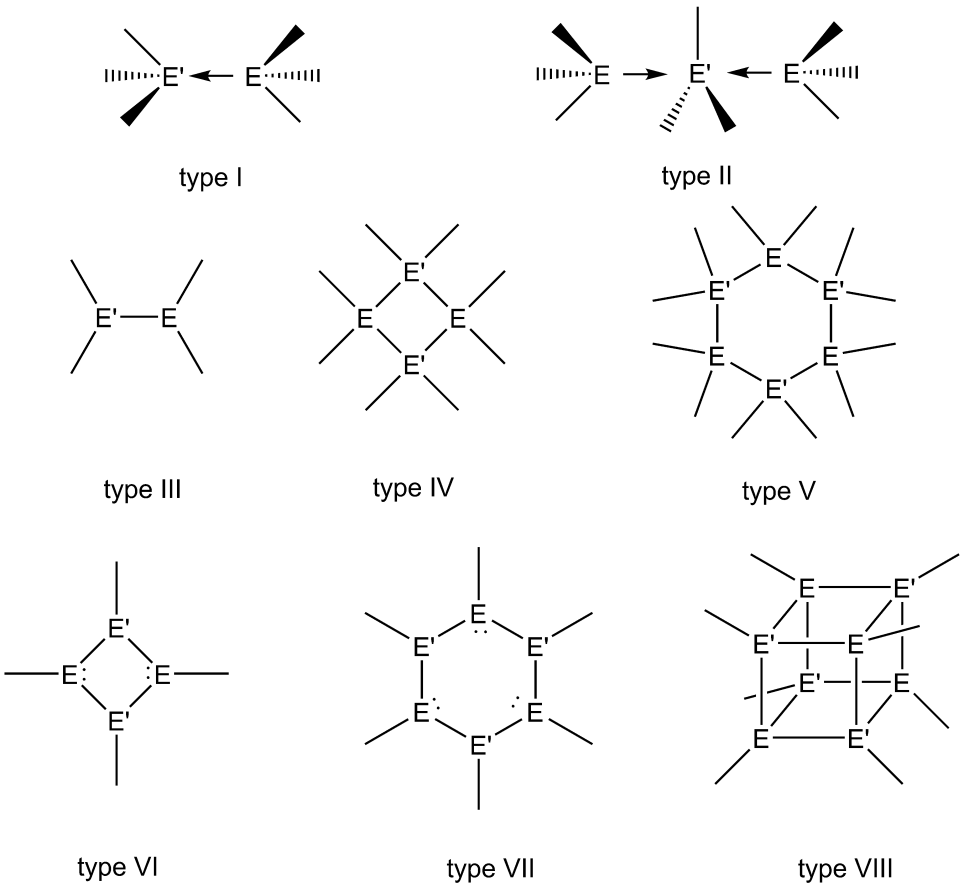

Figure 1. Different structural motifs for group 13/15 compounds.

Besides the pure academic interest of group 13/15 compounds they can be used for different applications. Binary group 13/15 materials for instance possess semiconducting properties and are often implemented in opto- and micro-electronic devices.[5] These so called III-V materials are deposited as thin films on substrates via the MOCVD (**m**etal**o**rganic **c**hemical **v**apor **d**eposition) process. This process was introduced by *Manasevit* in 1968,[6] describing the deposition of GaAs by thermolysis of $GaEt_3$ and AsH_3. GaAs has several applications in the industry, due to its desirable semiconducting properties.

In contrast small molecular units like $H_3N{\cdot}BH_3$ are in the focus of current research. The high hydrogen content (up to 19.6 wt-%) makes them to ideal candidates for hydrogen storage purposes.[7] To accentuate the significance of this class of compounds, the most important aspects of group 13/15 compounds will be discussed in the following separate chapters.

1.1 Isoelectronic relationship between organic CC-groups/units and group 13/15-compounds

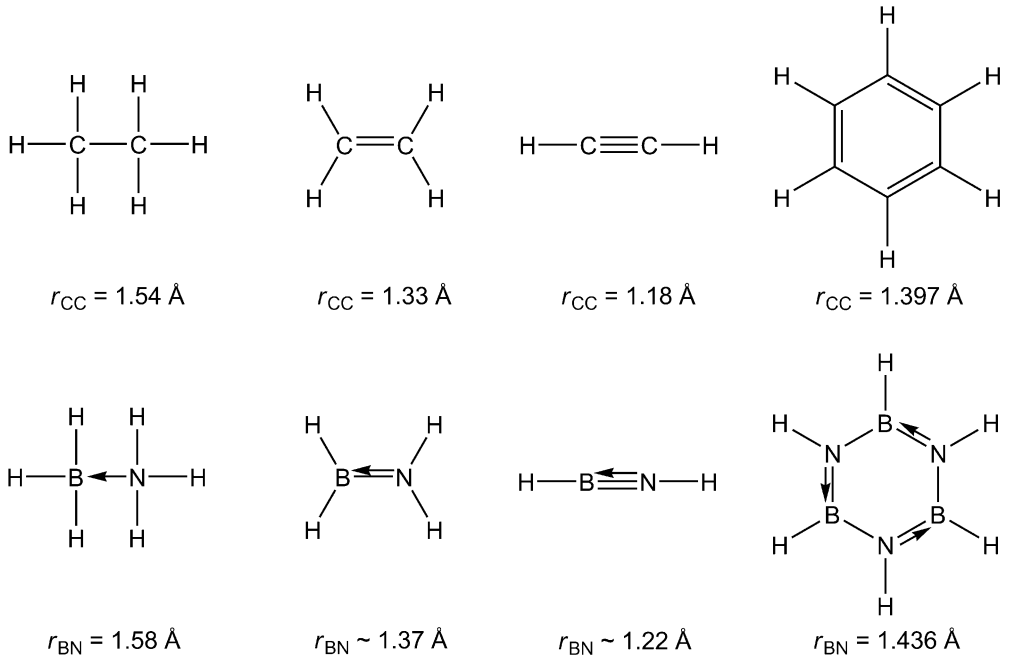

Figure 2. Structural and electronic relationship between containing compounds BN- and CC-units.

The combination of an atom of group 13 and group 15 of the periodic table is isoelectronic compared to a C-C bond, as both possess 8 valence-electrons. This will be described in the following for the example of boron-nitrogen (BN) compounds.[8] The structure of BN compounds is essentially identical to the corresponding C-C compounds. In all examples the same arrangements of the hydrogen substituents and a slightly

elongated B-N bond length (compared to the corresponding C-C compound) can be observed (Δr ~ 0.04 Å). Due to the differences in electronegativity (EN_B = 2.0, EN_N = 3.0, ΔEN_{NB} = 1.0) BN compounds exhibit polarized bonds. Calculations have shown, that only about $0.2e^-$ are transferred to the boron atom, which means, that most of the electron density is localized on the nitrogen atom.[9] Although the BN compounds are isolobal to C-C compounds, the polarization of the B-N-bond leads to different properties and an altered chemical behavior. While ethane is a gas at ambient conditions, the ionicity in $H_3N{\cdot}BH_3$ is responsible, that the latter is a solid. Borazine ($B_3N_3H_6$), the inorganic benzene – reported in 1926 by *Pohland* and *Stock*[10] –, which was a milestone for inorganic chemistry, has similar features like benzene, as it is a clear colorless liquid, exhibiting a typical aromatic odor. However the aromaticity is lower and borazine is more prone towards hydrolysis and easily undergoes addition reactions with e.g. hydrochloride. Upon coordination to transition metals the initial planar geometry of borazine is rearranged to a chair-like conformation exhibiting η^3-coordination of the nitrogen atoms towards the metal center, in contrast to benzene, which forms η^6-complexes. In the solid state some BN compounds exhibit similar physical properties. *α*-boron nitride for instance exhibits a comparable layered structure as graphene and can be used as a high temperature lubricant or as a coating for high-temperature applications, whereas in contrast *β*-boron nitride possesses a diamond type lattice and is classified as one of the hardest materials and is applied for the fabrication of abrasives.

An interesting difference is, that in the case of $[R_2E'–ER'_2]$ (R = H or small organic substituent) the group 15 element possesses an accessible lone pair in combination with a vacant p-orbital at the group 13 element. While the organic analog ethylene is stable under ambient conditions, these group 13/15 compounds (Figure 3, **I**) are very fragile towards head-to-tail-polymerization or oligomerization. This can be prevented if sterically demanding substituents are present (for example $Ph_2P–BMes_2$, Figure 3, **II**)[11] or by donor-acceptor- (LA/LB-) or only LB-stabilization, which will be discussed in more detail in a later chapter.

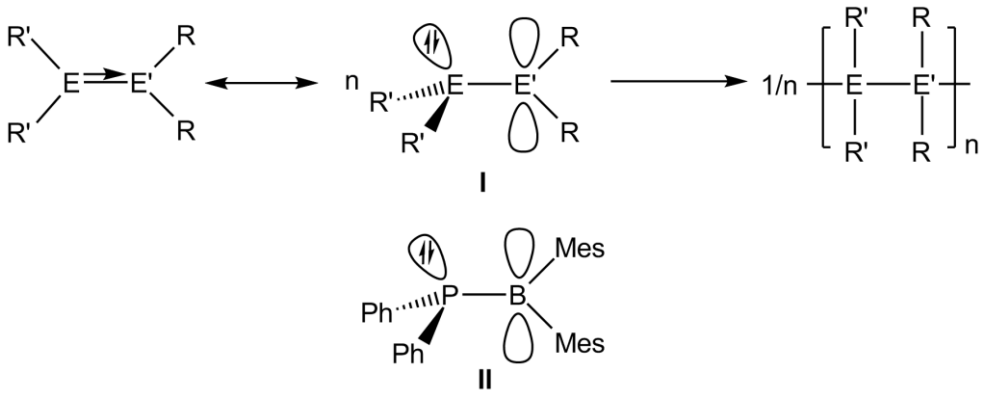

Figure 3. Polymerization and stabilization of monomers of the type $[R_2E'ER'_2]$.

1.2 Amine- and phosphine-borane adducts - valuable starting materials for oligomers and inorganic polymers

As mentioned before, one of the first amine-borane adducts was discovered over 2 centuries ago. However, it was not until 1937 that $Me_3N{\cdot}BH_3$ was reported by *Burg* and *Schlesinger* as the first amine-borane containing exclusively hydride substituents on the boron atom.[12] Recently, compounds of this type, and particular $H_3N{\cdot}BH_3$ experienced growing interest, as they are seen as possible hydrogen storage materials because of their high hydrogen content.[3] Especially dehydrocoupling reactions of amine- and phosphine-borane adducts, either induced thermally or with metal catalysts have been intensively studied. The first dehydrocoupling reaction of amine-boranes was mentioned in 1989.[13] However, the first detailed study of a catalytic reaction was published in 1999 by *Manners* and coworkers. The dimerization of the group 13/15 adduct $Ph_2HP{\cdot}BH_3$ was achieved with the transition metal catalysts $[Rh(1,5\text{-cod})_2][OTf]$ and $\{Rh(1,5\text{-cod})(\mu\text{-Cl})\}_2$ (1,5-cod = cycloocta-1,5-diene) (Figure 4).[14]

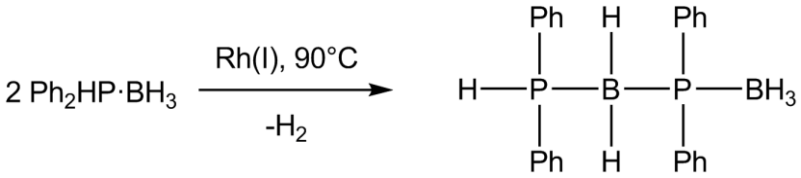

Figure 4. Rh(I) mediated dehydrocoupling of $Ph_2HP{\cdot}BH_3$.

The first detailed report on a truly catalytic dehydrocoupling of amine-boranes focused on Rh(I) and Rh(III) based catalysts.[15] Subsequently, the reaction was further explored and $[Rh(1,5\text{-cod})(\mu\text{-Cl})]_2$ proved to be the most effective catalysts.[16] Secondary amine-borane adducts tend to form cyclic dimers $[R'R''NBH_2]_2$ upon dehydrocoupling (Figure 5, **I**). In the case of bulky substituents on nitrogen, the corresponding aminoborane monomer can also be obtained (figure 5, **II**). Primary amine-borane adducts initially form cyclotriborazanes, which readily loose H_2 upon heating and are transformed into borazines (Figure 5, **III**).

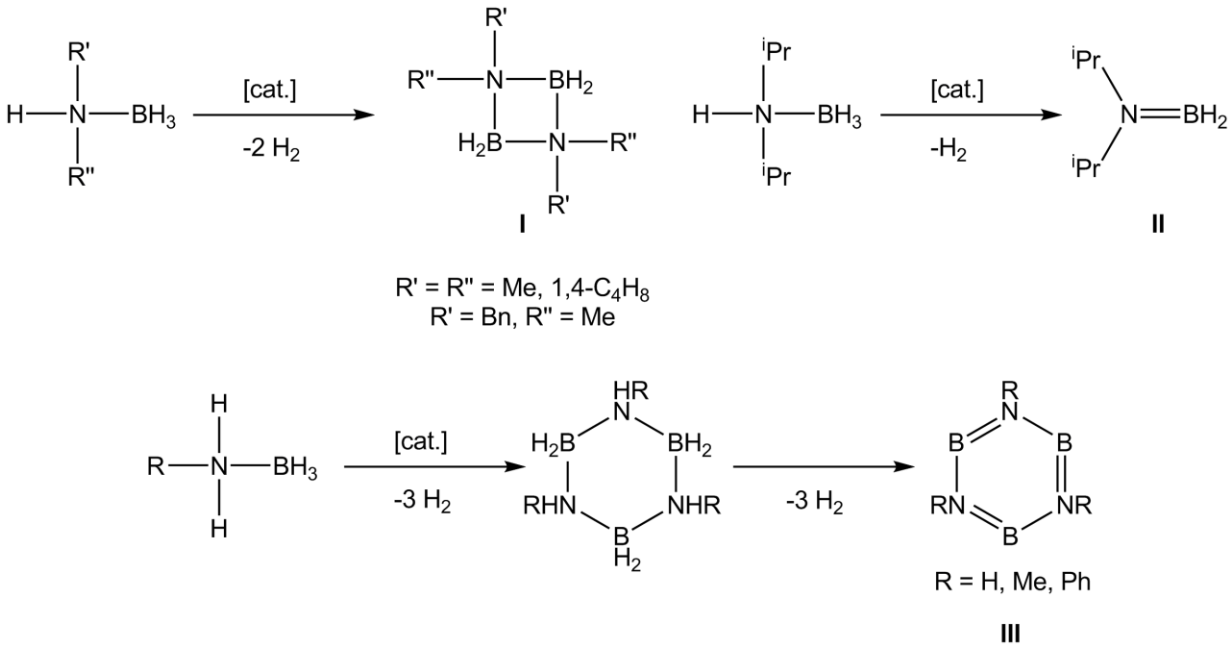

Figure 5. Dehydrocoupling of primary and secondary amine-boranes.

Since then, significant efforts have been taken to search for alternative catalysts. Another very effective catalytic system is based on Cp_2Ti, generated in situ from Cp_2TiCl_2 with 2 equivalents of $^{n}BuLi$.[17] The secondary amine-borane adducts $Me_2NH{\cdot}BH_3$ and $^{i}Pr_2NH{\cdot}BH_3$ were successfully dehydrogenated by Cp_2Ti already at room temperature to form quantitatively the same products as the Rh(I) catalyst. However, this system was completely inactive towards ammonia-borane and it showed only negligible reaction rates towards primary amine-boranes. In 2007 several titanium and zirconium sandwich complexes were investigated towards their catalytic activity in dehydrocoupling reactions of amine-boranes.[18] Among these the best results enabled the dehydrocoupling of $Me_2HN{\cdot}BH_3$ at 23 °C within minutes. Besides small oligomeric cyclic poly(aminoborane)s (PABs), linear polymers can be obtained as well. The parent poly(aminoborane) $[H_2N–BH_2]_n$ is probably the most investigated polymer in this class of materials. It has been claimed to be a thermal decomposition product of $H_3N{\cdot}BH_3$. Pyrolysis at temperatures between 150 and 180 °C produces $NH_2{=}BH_2$ as an intermediate, which rapidly polymerizes to give $[H_2N–BH_2]_n$. Due to the insolubility in all organic solvents, the postulated polymeric product could not be confirmed in those studies. In 2006, it was shown, that $H_3N{\cdot}BH_3$ could be very efficiently dehydrocoupled using *Brookhart's* $[IrH_2(POCOP)]$ catalyst (POCOP = $[\mu_3$-1,3-$(OP^{t}Bu_2)_2C_6H_3]$).[19] The resulting insoluble product was postulated to be a cyclic pentamer $[H_2N–BH_2]_5$. However, reinvestigation of the same reaction in more concentrated solutions by the *Manners* group, suggests the formation of a polymeric material.[20] Furthermore it was found that similar reactions of *N*-monoalkylamine-borane adducts in concentrated solutions yield

soluble linear PABs, while lower concentrations lead to the formation of oligomers.[20,21] Very recently the metal-free H_2-transfer between amine-borane and aminoboranes was also described.[22] *Denis* and *Gaumont* reported on the LA-catalyzed dehydrocoupling of $H_3P{\cdot}BH_3$ giving the parent polymer of the poly(phosphinoboranes) (PPB) $[H_2P–BH_2]_n$. Since $H_3P{\cdot}BH_3$ is thermally not stable, it had to be generated *in situ* by bubbling PH_3 and B_2H_6 through a solution of $B(C_6F_5)_3$. Elevated temperatures lead to polymerization of the monomer $H_3P{\cdot}BH_3$ under loss of dihydrogen. NMR analysis of the product suggests a polymeric structure, but the material was not characterized by high resolution mass spectrometry or IR, due to its high sensitivity. The reaction of $B(C_6F_5)_3$ with the $PhPH_2{\cdot}BH_3$ monomer leads to the formation of poly(phenylphosphinoborane) $[PhHP–BH_2]_n$. NMR analysis is consistent with $[PhHP–BH_2]_n$ concomitant with poorly resolved peaks which had been observed for the thermal polymerization of $PhPH_2{\cdot}BH_3$.[23] The first soluble, high molecular weight PPB was reported 4 years before in 1999.[14] When $PhPH_2{\cdot}BH_3$ was reacted with a Rh(I) catalyst in the absence of a solvent $[PhHP\text{-}BH_2]_n$ was cleanly formed. The average molecular weight of 31.000 Da was confirmed by static light scattering. When no catalyst is used the obtained molecular weight was considerably lower,[14] the reaction is less clean[24] and the resulting polymer is only poorly soluble in THF.[25] The PPBs are reasonably stable toward air and moisture in the solid state. Since those initial reports on high molecular weight PPBs a wide range of substituted PPBs has been synthesized.[26] Very recently, it was shown, that an earth abundant Fe-catalyst can also be used for the synthesis of PPBs with control of the molecular weight of the resulting polymers.[27] A variety of transition metal catalysts (Ru,[28] Pt,[29] Ir,[30] Ni,[31] Cu-Co-particels[32] and transition-metal-nanoparticels[33]) were studied and the mechanisms of the dehydrocoupling reactions (mainly for amine-boranes) were elucidated. Recent studies of the coordination chemistry of phosphine-borane ligands at d-block metal centers allowed the elucidation of the fundamental P-B bond formation processes leading to dehydrogenative oligomerization and polymerization.[34] Those studies revealed a two-fold role for P-H bonds: the activation of the P-H bond by metal centers to form metal-phosphidoborane intermediates, and the promotion of dehydrogenative coupling of P-H (protic H) with B-H (hydridic H) to release dihydrogen under formation of a P-B bond.[27a,34] However, as P-H bonds are nearly non-polar (electronegativity: P = 2.19, H = 2.20),[35] catalytic dehydrocoupling routes rely on electron withdrawing effects from aryl groups on phosphorus to promote the reaction, resulting in a relatively limited substrate scope. The only examples of poly(alkylphosphinoboranes) (alkyl = electron donating group), which have been prepared by the dehydrocoupling of $^{i}BuPH_2{\cdot}BH_3$[25] and $FcCH_2PH_2{\cdot}BH_3$[36] in the presence of Rh(I) catalysts are of modest molar mass. Although Rh(I) catalyzed reactions

generally lead to appreciable chain branching and crosslinking the poly(alkylphosphinoboranes) obtained from this reactions revealed a very high polydispersity index (PDI) value (e.g. > 5).[25] PABs are discussed as preceramic materials which could be processed into a desired shape and then pyrolyzed to give hexagonal boron nitride (α-boron nitride). A potential application for PPBs is as well their use as precursors for boron phosphide monoliths and fibers. Boron phosphide has significant interest due to its semiconducting properties.[37] Polymer films based on [(*p*-$CF_3C_6H_4$)PH-BH_2]$_n$ were successfully tested for a potential application in electron beam lithography.[38]

1.3 Frustrated Lewis Pairs (FLPs) – activation of small molecules

It is well-known, that electron-deficient Lewis acids and electron-rich Lewis bases form strong adducts. *Lewis* described this behavior already in 1923, which is very typical for compounds consisting of electron-pair-donors and electron-pair-acceptors.[39] Very characteristic for LAs are energetically low-lying lowest unoccupied molecular orbitals (LUMOs) which consequently can interact with the vacant electron-pairs of LBs which are typically located in the energetically high-lying highest occupied molecular orbital (HOMO). In 1942 *Brown* and co-workers investigated the behavior of different simple boranes towards lutidine (2,6-dimethylpyridine) as a base. While lutidine readily reacted with BF_3 to yield a LA/LB adduct, no reaction was observed for BMe_3.[40] This observation was attributed to the steric repulsion of the methyl groups, but no further investigations were made. Few years later, the special nature of Lewis pairs with sterically demanding substituents, which do not form classical LA/LB adducts was also observed by *Wittig* and *Tochtermann*, leading to the introduction of the German term “antagonistisches Paar”.[41] If an interaction between the group 13 and the group 15 element is inhibited by sterically demanding substituents, nowadays such compounds are entitled as “frustrated Lewis pairs” (FLPs). This term was primarily influenced by *Stephan,* who subsequently explored the chemistry of those FLPs and initially reported on the FLP-System $(Me_3C_6H_2)_2PC_6F_4B(C_6F_5)_2$ (Figure 6). This famous example, which exhibits a LA site and a LB site in one molecule, is able to cleanly cleave dihydrogen under ambient conditions giving a zwitterionic phosphonium/hydridoborate.[42] This reaction is reversible and by heating up of this system H_2 can be liberated.

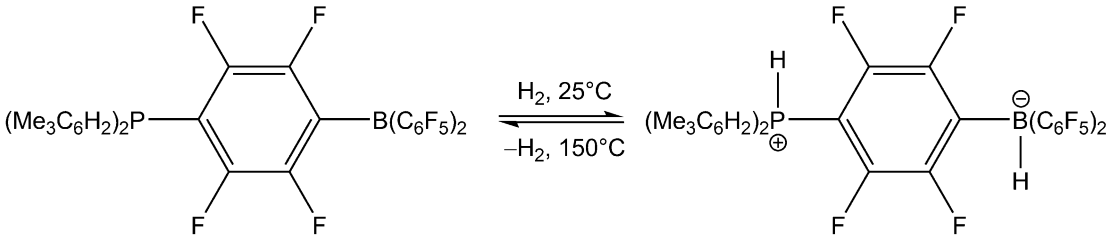

Figure 6. Reversible H_2-activation by FLP-System.

Subsequently, it was shown, that intermolecular systems of bulky phosphines and perfluorinated boranes can also be used as FLPs (Figure 7, **I**).[43] *Erker* reported on an ethylene-bridged FLP, which was also capable to cleave dihydrogen at room temperature (Figure 7, **II**).[44]

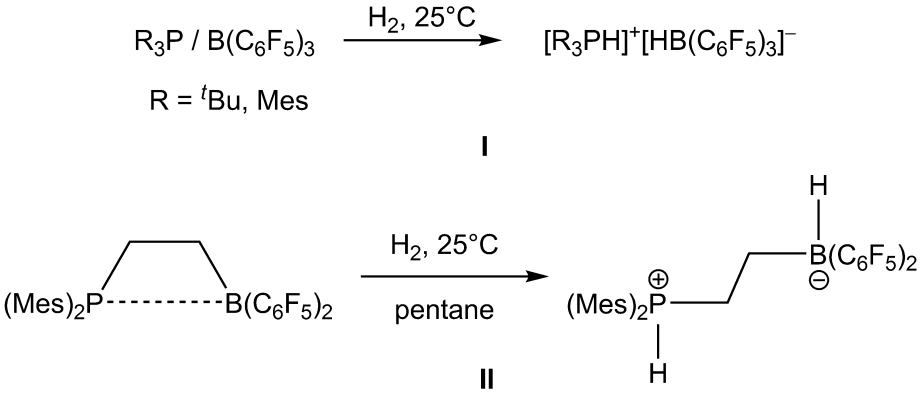

Figure 7. Inter- and intramolecular FLP-Systems.

Since those first examples for a metal-free H_2-activation the chemistry involving FLPs showed remarkable developments. Two recent reviews show the high capability of those FLP systems.[45] Recent reports include hydrogenation of a big variety of different substrates, capture of CO_2, SO_2, N_2O, reduction of CO and the promotion of polymerization reactions. *Lammertsma* reported on preorganized FLPs which are capable of the activation of small molecules without perfluorinated substituents.[46] Besides P/B based FLPs, P/Al based system are also well known and are investigated with major contribution by *Uhl* and coworkers.[47] *Stephan et al.* reported very recently on a N/B based system for the hydrogenation of CO_2.[48]

1.4 Synthesis of monomeric and oligomeric compounds of the type [$R_2E'ER'_2$]

The following chapters focus on the synthesis of the pnictogenyltrielanes. This term describes compounds of the general formula $[R_2E'ER'_2]_x$. Different methods for the bond formation between a group 13 and a group 15 element are known.[49] A feasible and

probably the most used method is the salt metathesis reaction, as illustrated in figure 8 for phosphinoboranes. Most commonly a salt metathesis starting from haloboranes R_2BX (X = halogen) and metal phosphides R'_2PM (M = alkaline metal) is used (Figure 8, route **I**).[50] Recently *Gudat* and coworkers reported on the utilization of a B-centered nucleophile in the reaction of a lithio-borane and a chlorophosphine (Figure 8, route **II**).[51] Another possibility is the elimination of Me_3SiCl (Figure 8, **III**).[52] This route was also extended to the synthesis of diborylphosphines ($R'P(BR)_2$) and the first triborylphosphine ($P(BR)_3$).[53] Pd-catalysed cross-coupling (Pd-catalysed P–B coupling reaction)[54] and reductive coupling under 1,2-aryl migration have also been described,[55] although these are not widely used.

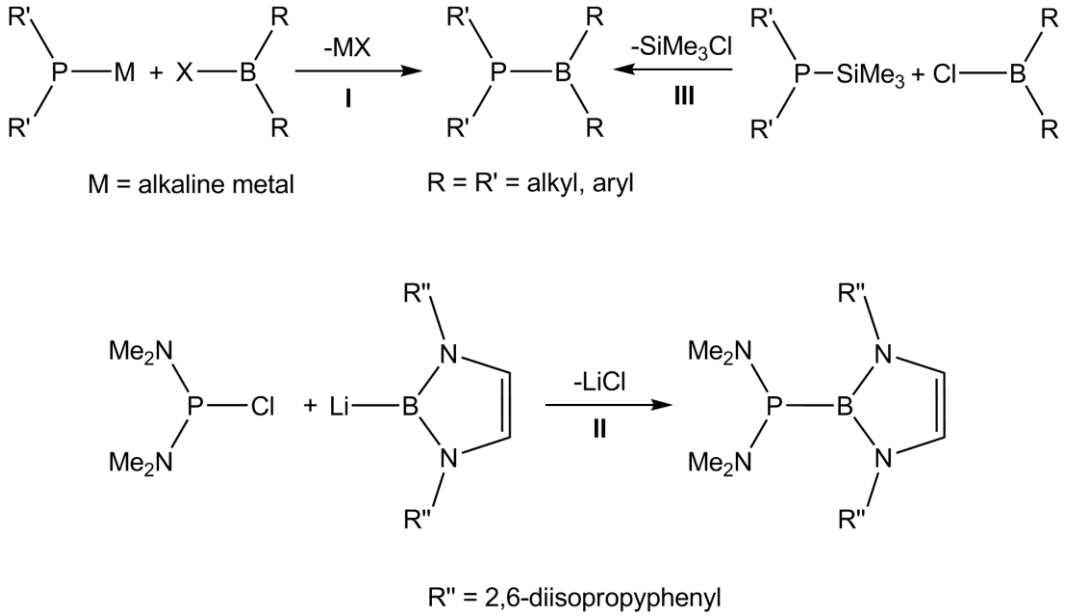

Figure 8. Salt metathesis and Me_3SiCl-elimination reaction for the synthesis of phosphinoboranes.

The heavier group 13 elements readily form E'–E bonds under elimination of H_2 (Figure 9, **I**),[56] $HSiMe_3$ (Figure 9, **II**) [57] or alkanes (Figure 9, **III**).[58]

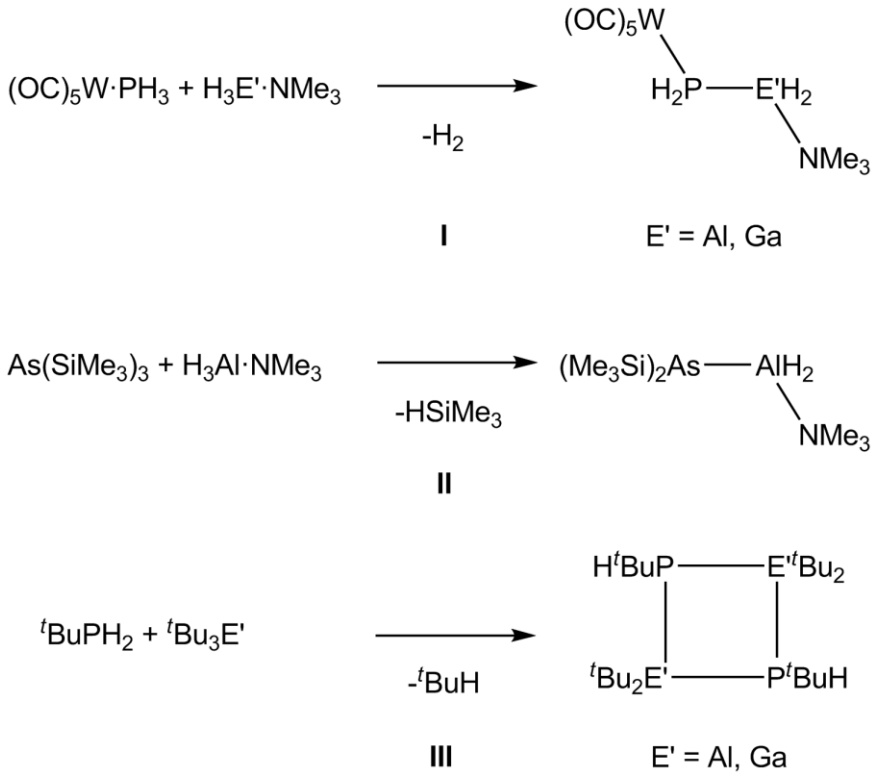

Figure 9. Synthesis of group 13/15 compounds via elimination reactions.

Additionally monomeric group 13/15 compounds can be obtained by cleavage of oligomeric and polymeric species. *Manners* and coworkers reported on the cleavage of PABs with N-heterocyclic carbenes (NHC)s, resulting in the formation of the monomeric $H_2N–BH_2·NHC$,[59] which could only be characterized by NMR spectroscopy and mass spectrometry. *Rivard* and coworkers reported on the synthesis and characterization of LA/LB stabilized $H_2B–NH_2$ which was generated by treating *μ*-aminodiborane, $H_2NB_2H_5$ with the strong LB dmap.[60] Preliminary results from *Adolf* in the *Scheer* group showed, that cleavage of poly(phenylphosphinoborane) can be achieved by strong LBs like dmap or NHCs.[61]

1.5 Heavier Congeners

The research in the field of heavier elements of group 13 and 15 is mainly dominated by solid state chemistry and utilization of III-V materials as semiconductors. However, it has to be emphasized, that current research also focuses on heavier group 13/15 molecular compounds. Over the last years compounds containing most of the combinations of group 13/15 elements could be synthesized. The combination of P and Al/Ga or As and B, respectively prepared in the *Scheer* group will be described in the following chapter. Examples for the combination of As/Al and Ga are the trimeric arsinoalane $[Ph_2As–AlMe_2]_3·(C_7H_8)_2$[62] and the dimeric arsinogalane $[Ph_2As–GaMe_2]_2$

(Figure 10, **I**).[63] The combinations Sb/Bi and Al/Ga are described by *Schulz et al.*. In [(nacnac)E'(EEt_2)$_2$] (E' = Al, Ga; E = Sb, Bi) those compounds are stabilized by a nacnac-ligand with two 2,6-diisopropylphenyl groups (Figure 10, **II**, nacnac = *β*-diketiminate).[64] Besides the three LA/LB adducts of the type $(SiMe_3)_3Sb{\cdot}BX_3$ (X = Cl, Br or I)[65] no compounds are known containing a covalent Sb–B bond. Very recently, *Jones et al.* reported on the synthesis of a boryl-dibismuthene containing a boron-bismuth bond (Figure 10, **III**).[66]

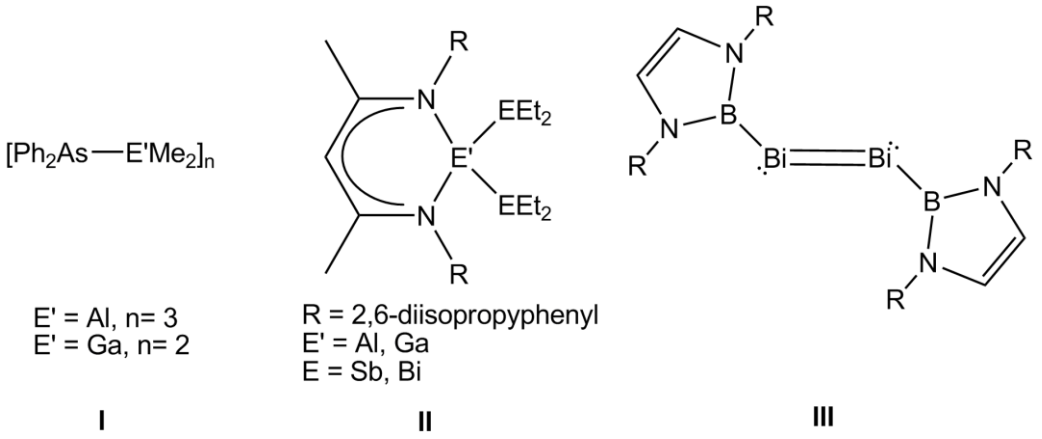

Figure 10. Examples for compounds containing combinations of heavier group 13/15 elements.

1.6 Syntheses and studies of the reactivity of only hydrogen-substituted Pnictogenyltrielanes

In 2001, our group was able to generate the highly sensitive and elusive monomeric parent compound of the phosphanylalanes and -galanes by LA/LB stabilization in $(OC)_5W{\cdot}H_2P–E'H_2{\cdot}NMe_3$ (Figure 11, **I**) by H_2 elimination of $(OC)_5W{\cdot}PH_3$ and $H_3E'{\cdot}NMe_3$ (E' = Al, Ga).[56] The monomeric LA/LB stabilized phosphanylalanes could also be transformed into dimers, trimers and tetramers in a controlled manner via oligomerisation of the monomers.[67] Some years later, stabilization of the monomeric parent compound of the phosphanyl- and arsanylboranes $(OC)_5W{\cdot}H_2E–BH_2{\cdot}NMe_3$ (Figure 11, **II**) could be realized by salt metathesis of $[(OC)_5W{\cdot}EH_2Li]$ and $ClH_2B{\cdot}NMe_3$ (E = P, As).[68] Finally, the only LB stabilized parent compound of $H_2P–BH_2{\cdot}NMe_3$ was prepared by photolytic treatment of a solution of $(OC)_5W{\cdot}H_2E–BH_2{\cdot}NMe_3$ and $P(OMe)_3$ (Figure 11, **IV**, E = P).[69] Subsequently, several examples of different LA/LB stabilized phosphanylboranes were prepared.[70] A new, convenient salt metathesis with $[(Me_3Si)_2ELi{\cdot}2thf]$ and $ClH_2B{\cdot}NMe_3$ afforded $(Me_3Si)_2E–BH_2{\cdot}NMe_3$ (E = P, As; Figure 11, **III**). The silylated compounds can easily be transferred into the only LB stabilized monomeric parent phosphanylborane and for the first time the access to the only LB stabilized arsanylboranes $H_2E–BH_2{\cdot}NMe_3$ (E = P, As) has been achieved (Figure 11, **IV**). This new route allowed to study the

reactivity of the only LB stabilized pnictogenylboranes in detail, since they can be prepared on gram scale.[71] The oligomerization of $H_2P–BH_2·NMe_3$ by titanocene was achieved, forming B/P containing compounds with up to 12 B/P atoms.[72] Preliminary studies by *Schwan* in the *Scheer* group on the thermolysis of $H_2P–BH_2·NMe_3$ led to the elimination of NMe_3 and the resulting intermediate phosphinoborane [$H_2P–BH_2$] readily polymerized to give the parent polymer of the PPBs.[73] Those studies were continued by *Stauber* of our group and transferred to the monoalkyl-substituted phosphanylborane $MeHP–BH_2·NMe_3$.[74] It was shown, that reaction with iodo-boranes can also lead to smaller cationic oligomeric units. Also for the first time anionic species were observed in NMR spectroscopy and mass spectrometry experiments.

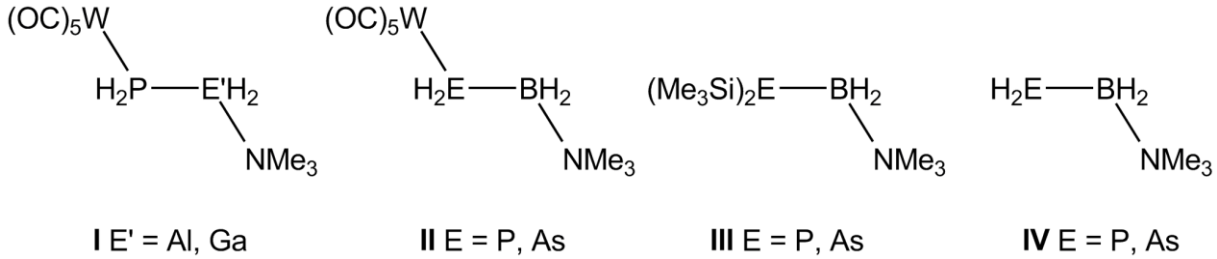

Figure 11. Selected examples of pnictogenyltrielanes.

1.7 References

[1] J. L. Gay-Lussac, J. L. Thénard, *Mem. de. Phys. et de.Chim. de la Soc. d'Arcueil* **1809**, *2*, 210 as cited in V. Jonas, G. Frenking, *J. Chem. Soc., Chem. Commun.* **1994**, 1489–1490.

[2] A. Besson, *Comptes Rendus* **1890**, 516.

[3] for example: A. Staubitz, A.P.M. Robertson, M.E. Sloan, I. Manners, *Chem. Rev.* **2010**, *110*, 4023–4078; A. Staubitz, A.P.M. Robertson, I. Manners, *Chem. Rev.* **2010**, *110*, 4079–4124.

[4] S. Schulz, *Adv. Organomet. Chem.* **2003**, *49*, 225–317, and references cited therein.

[5] a) F. Maury, *Adv. Mater.* **1991**, *3*, 542–548; b) R. L. Wells, W. L. Gladfelter, *J. Cluster Sci.* **1997**, *8*, 217–237.

[6] H. M. Manasevit, *Appl. Phys. Lett.* **1968**, *12*, 156–159.

[7] C. W. Hamilton, R. T. Baker, A. Staubitz, I. Manners, *Chem. Soc. Rev.* **2009**, *38*, 279–293.

[8] A. F. Hollemann, E.Wiberg, *Lehrbuch der Anorganischen Chemie, Vol. 102*, Walter de Gruyter Verlag, Berlin-New York, **2007**.

[9] H. Umeyama, K. Morokuma, *J. Am. Chem. Soc.* **1976**, *98*, 7208–7220.

[10] A. Stock, E. Pohland, *Ber. Dtsch. Chem. Ges.* **1926**, *59*, 2215–2223.

[11] X. Feng, M. M. Olmstead, P. P. Power, *Inorg. Chem.* **1986**, *25*, 4615–4616.

[12] A. B. Burg, H. I. Schlesinger, *J. Am. Chem. Soc.* **1937**, *59*, 780–787.

[13] Y. D. Blum, R. M. Laine, U.S. Pat. 4801439, **1989**.

[14] H. Dorn, R. A. Singh, J. A. Massey, A. J. Lough, I. Manners, *Angew. Chem. Int. Ed.* **1999**, 38, 3321–3323, *Angew. Chem.* **1999**, *111*, 3540–3543.

[15] C.A. Jaska, K. Temple, A. J. Lough, I. Manners, *Chem. Commun.* **2001**, 962–963.

[16] C.A. Jaska, K. Temple, A. J. Lough, I. Manners, *J. Am. Chem. Soc.* **2003**, *125*, 9424–9434.

[17] N. Blaquiere, S. Diallo-Garcia, S. I. Gorelsky, D. A. Black, K. Fagnou, *J. Am. Chem. Soc.* **2008**, *130*, 14034–14035.

[18] D. Pun, E. Lobkovsky, P. J. Chirik, *Chem. Commun.* **2007**, 3297–3299.

[19] M. C. Denney, V. Pons, T. J. Hebden, D. M. Heinekey, K. I. Goldberg, *J. Am. Chem. Soc.* **2006**, *128*, 12048–12049.

[20] A. Staubitz, A. P. Soto, I. Manners, *Angew. Chem. Int. Ed.* **2008**, *47*, 6212–6215, *Angew. Chem.* **2008**, *120*, 6308–6311.

[21] B. L. Dietrich, K. I. Goldberg, D. M. Heinekey, T. Autrey, J.C. Linehan, *Inorg. Chem.* **2008**, *47*, 8583–8585.

[22] a) A. P. M. Robertson, E. M. Leitao, and I. Manners, *J. Am. Chem. Soc.* **2011**, *133*, 19322–19325; b) E. M. Leitao, N. E. Stubbs, A. P. M. Robertson, H. Helten, R. J. Cox, G. C. Lloyd-Jones, I. Manners, *J. Am. Chem. Soc.* **2012**, *134*, 16805−16816.

[23] J.-M. Denis, H. Forintos, H. Szelke, L. Toupet, T.-N. Pham, P.-J. Madec, A.-C. Gaumont, *Chem. Commun.* **2003**, 54−55.

[24] H. Dorn, R. A. Singh, J. A. Massey, J. M. Nelson, C. A. Jaska, A. J. Lough, I. Manners, *J. Am. Chem. Soc.* **2000**, *122*, 6669−6678.

[25] H. Dorn, J. M. Rodezno, B. Brunnhöfer, E. Rivard, J. A. Massey, I. Manners, *Macromolecules* **2003**, *36*, 291−297.

[26] T. J. Clark, K. Lee, I. Manners, *Chem. Eur. J.* **2006**, *12*, 8634–8648.

[27] a) A. Schäfer, T. Jurca, J. Turner, J. R. Vance, K. Lee, V. A. Du, M. F. Haddow, G. R. Whittell, I. Manners, *Angew. Chem. Int. Ed.* **2015**, *54*, 4836–4841; *Angew. Chem.* **2015**, *127*, 4918–4923; b) J. R. Vance, A. Schäfer, A. P. M. Robertson, K. Lee, J. Turner, G. R. Whittell, I. Manners, *J. Am. Chem. Soc.* **2014**, *136*, 3048–3064.

[28] a) A. N. Marziale, A. Friedrich, I. Klopsch, M. Drees, V. R. Celinski, Schmedt auf der Günne, Jörn, S. Schneider, *J. Am. Chem. Soc.* **2013**, *135*, 13342–13355, b) D. F. Schreiber, C. O'Connor, C. Grave, Y. Ortin, H. Müller-Bunz, A. D. Phillips, *ACS Catal.* **2012**, *2*, 2505–2511, c) H. Ma, C. Na, *ACS Catal.* **2015**, *5*, 1726–1735.

[29] M. Roselló-Merino, J. López-Serrano, S. Conejero, *J. Am. Chem. Soc.* **2013**, *135*, 10910–10913.

[30] D. J. Nelson, B. J. Truscott, J. D. Egbert, S. P. Nolan, *Organometallics* **2013**, *32*, 3769–3772.

[31] L. Yang, W. Luo, G.-Z. Cheng, *Catal. Lett.* **2013**, *143*, 873–880.

[32] C. Li, J. Zhou, W. Gao, J. Zhao, J. Liu, Y. Zhao, M. Wei, D. G. Evans, X. Duan, *J. Mater. Chem. A* **2013**, *1*, 5370–5376.

[33] a) M. Zahmakiran, S. Özkar, *Top. Catal.* **2013**, *56*, 1171–1183. b) G. Xin, J. Yang, W. Li, J. Zheng, X. Li, *Eur. J. Inorg. Chem.* **2012**, 5722–5728.

[34] a) M. A. Huertos, A. S.Weller, *Chem. Commun.* **2012**, *48*, 7185 –7187; b) M. A. Huertos, A. S. Weller, *Chem. Sci*. **2013**, *4*, 1881 –1888; c) T. N. Hooper, M. A. Huertos, T. Jurca, S. D. Pike, A. S.Weller, I. Manners, *Inorg. Chem.* **2014**, *53*, 3716 – 3729; d) H. C. Johnson, T. N. Hooper, A. S. Weller, *Top. Organomet. Chem.* **2015**, *49*, 153 – 220.

[35] W. M. Haynes, ed., *CRC Handbook of Chemistry and Physics, 95thEdition (Internet Version 2015)*, CRC Press/Taylor and Francis, Boca Raton, FL, **2015**.

[36] S. Pandey, P. Lönnecke, E. Hey-Hawkins, *Eur. J. Inorg.Chem.* **2014**, 2456 – 2465

[37] Y. Kumashiro, *J. Mater. Res.* **1990**, *5*, 2933–2947.

[38] T. J. Clark, J. M. Rodezno, S. B. Clendenning, S. Aouba, P. M. Brodersen, A. J. Lough, H. E. Ruda, I. Manners, *Chem.Eur. J.* **2005**, *11*, 4526–4534.

[39] G. N. Lewis, *Valence and the Structure of Atoms and Molecules*, Chemical Catalogue Company, New York, **1923**.

[40] a) H. C. Brown, H. I. Schlesinger, S. Z. Cardon, *J. Am. Chem. Soc.* **1942**, *64*, 325–329. b) H. C. Brown, B. Kanner, *J. Am. Chem. Soc.* **1966**, *88*, 986–992.

[41] a) G. Wittig, E. Benz, *Chem. Ber.* **1959**, *92*, 1999–2013. b) W. Tochtermann, *Angew. Chem. Int. Ed.* **1966**, *5*, 351–371; *Angew. Chem.* **1966**, *78*, 355–375.

[42] G. C. Welch, R. R. S. Juan, J. D. Masuda, D. W. Stephan, *Science* **2006**, *314*, 1124–1126.

[43] G. C. Welch, D.W. Stephan, *J. Am. Chem. Soc.* **2007**, *129*, 1880–1881.

[44] P. Spies, G. Erker, G. Kehr, K. Bergander, R. Fröhlich, S. Grimme, D.W. Stephan, *Chem. Commun.* **2007**, 5072–5074.

[45] a) D. W. Stephan, G. Erker, *Angew. Chem. Int. Ed.* **2015**, *54*, 6400–6441, *Angew. Chem.* **2015**, *127*, 6498–6541; b) D. W. Stephan, G. Erker, *Angew. Chem. Int. Ed.* **2010**, 49, 46–76, *Angew. Chem.* **2010**, *122*, 50–81.

[46] F. Bertini, V. Lyaskovskyy, B. J. J. Timmer, F. J. J. de Kanter, M. Lutz, A. W. Ehlers, J. C. Slootweg, K. Lammertsma, *J. Am. Chem.Soc.* **2012**, *134*, 201−204.

[47] a) W. Uhl, C. Appelt, J. Backs, H. Westenberg, A. Wollschläger, J. Tannert, *Organometallics* **2014**, *33*, 1212−1217; b) C. Appelt, J. C. Slootweg, K. Lammertsma, W. Uhl, *Angew. Chem. Int. Ed.* **2013**, *52*, 4256–4259; *Angew. Chem.* **2013**, *125*, 4350–4353; c) W. Uhl, C. Appelt, A. Wollschläger, A. Hepp, E.-U. Würthwein, *Inorg. Chem.* **2014**, *53*, 8991−8999; d) W. Uhl, P. Wegener, M. Layh, A. Hepp, E.-U. Würthwein, *Organometallics* **2015**, *34*, 2455–2462; e) W. Uhl, C. Appelt, *Organometallics* **2013**, *32*, 5008−5014; f) W. Uhl, C. Appelt, M. Lange, *Z. Anorg. Allg. Chem.* **2015**, *641,* 311–315; g) T. Holtrichter-Rößmann, J. Isermann, C. Rösener, B. Cramer, C.-G. Daniliuc, J. Kösters, M. Letzel, E.-U. Würthwein, W. Uhl, *Angew. Chem. Int. Ed.* **2013**, *52*, 7135–7138; *Angew. Chem.* **2013**, *125*, 7275–7278; h) F. Bertini, F. Hoffmann, C. Appelt, W. Uhl, A. W. Ehlers, J. C. Slootweg, K. Lammertsma, *Organometallics* **2013**, *32*, 6764−6769.

[48] M.-A. Courtemanche, A. P. Pulis, É. R., M.-A. Légaré, D.W. Stephan, F.-G. Fontaine, *Chem. Commun.* **2015**, *51*, 9797–9800.

[49] J.A. Bailey, P.G. Pringle, *Coord. Chem. Rev.* **2015**, 77–90.

[50] J.M. Breunig, A. Hübner, M. Bolte, M. Wagner, H.-W. Lerner, *Organometallics* **2013**, *32*, 6792–6799.

[51] M. Kaaz, J. Bender, D. Forster, W. Frey, M. Nieger, D. Gudat, *Dalton Trans.* **2014**, *43*, 680–689.

[52] J.A. Bailey, M.F. Haddow, P.G. Pringle, *Chem. Commun.* **2014**, *50*, 1432–1434.

[53] J.A. Bailey, M. Ploeger, P.G. Pringle, *Inorg. Chem.* **2014**, *53*, 7763–7769.

[54] A.M. Spokoyny, C.D. Lewis, G. Teverovskiy, S.L. Buchwald, *Organometallics* **2012**, *31*, 8478–8481.

[55] A. Tsurusaki, T. Sasamori, A. Wakamiya, S. Yamaguchi, K. Nagura, S. Irle, N.Tokitoh, *Angew. Chem. Int. Ed.* **2011**, *50*, 10940–10943; *Angew. Chem.* **2011**, *123*, 11132–11135.

[56] U. Vogel, A. Y. Timoshkin, M. Scheer, *Angew. Chem. Int. Ed.* **2001**, *40*, 4409–4412; *Angew. Chem.* **2001**, *113*, 4541–4544.

[57] J. F. Janik, R. L. Wells, P. S. White, *Inorg. Chem.* **1998**, *37*, 3561–3566.

[58] D. A. Atwood, A. H. Cowley, P. R. Harris, R. A. Jones, S. U. Koschmieder, C. M. Nunn, *J. Organomet. Chem.* **1993**, *449*, 61–67.

[59] N. E. Stubbs, T. Jurca, E. M. Leitao, C. H. Woodall, I. Manners, *Chem. Commun.* **2013**, *49*, 9098–9100.

[60] A. C. Malcolm, K. J. Sabourin, R. McDonald, M. J. Ferguson, E. Rivard, *Inorg. Chem.* **2012**, *51*, 12905−12916.

[61] A. Adolf, PhD-thesis, University of Regensburg, **2007**.

[62] J. A. Laske Cooke, A. P. Purdy, R. L. Wells, P. S. White, *Organometallics* **1996**, *15*, 84–90.

[63] A. H. Cowley, R. A. Jones, *Angew. Chem. Int. Ed. Engl.* **1989**, *28*, 1208–1215; *Angew. Chem.* **1989**, *101*, 1235–1243.

[64] a) C. Ganesamoorthy, D. Bläser, C. Wölper, S. Schulz, *Angew. Chem. Int. Ed.* **2014**, *53*, 11587–11591; *Angew. Chem.* **2014**, *126*, 11771–11775; b) C. Ganesamoorthy, D. Bläser, C. Wölper, S. Schulz, *Chem. Commun.* **2014**, *50*, 12382–12384.

[65] M. S. Lube, R. L. Wells, P. S. White, *Dalton Trans*. **1997**, 285–286.

[66] D. Dange, A. Davey, J. A. B. Abdalla, S. Aldridge, C. Jones, *Chem. Commun.* **2015**, *51*, 7128–7131.

[67] M. Bodensteiner, U. Vogel, A. Y. Timoshkin, M. Scheer, *Angew. Chem. Int. Ed.* **2009**, *48*, 4629–4633; *Angew. Chem.* **2009**, *121*, 4700-4704.

[68] U. Vogel, P. Hoemensch, K. Schwan, A. Y. Timoshkin, M. Scheer, *Chem. Eur. J.* **2003**, *9*, 515–519.

[69] K. Schwan, A. Timoshkin, M. Zabel, M. Scheer, *Chem. Eur. J.* **2006**, *12*, 4900–4908.

[70] a) A. Adolf, M. Zabel, M. Scheer, *Eur. J. Inorg. Chem.* **2007**, 2136–2143; b) A. Adolf, U. Vogel, M. Zabel, A. Y. Timoshkin, M. Scheer, *Eur. J. Inorg. Chem.* **2008**, 3482–3492.

[71] C. Marquardt, A. Adolf, A. Stauber, M. Bodensteiner, A. V. Virovets, A. Y. Timoshkin, M. Scheer, *Chem. Eur. J.* **2013**, *19*, 11887–11891.

[72] a) C. Thoms, C. Marquardt, A. Y. Timoshkin, M. Bodensteiner, M. Scheer, *Angew. Chem. Int. Ed.* **2013**, *52*, 5150–5154; *Angew. Chem*. **2013**, *125,* 5254–5259; b) C. Thoms, PhD-thesis, University of Regensburg, **2012**.

[73] K.-C. Schwan, PhD-thesis, University of Regensburg, **2006**.

[74] A. Stauber, PhD-thesis, University of Regensburg, **2014**.

2. Research Objectives

Since the simple thermolysis of the parent compound $H_2P–BH_2·NMe_3$ appears to be a promising route for the synthesis of PPBs, this type of polymerization should be reinvestigated within the scope of this thesis. The new method would represent a scarce example of an addition-polymerization. To allow a proper characterization of the obtained products, substituents should be introduced on the phosphorus atom to increase the solubility. The polymerization of new alkyl- and aryl-substituted phosphanylboranes should be investigated in close collaboration with the *Manners* group (Bristol, UK). To accomplish this goal, following tasks arise:

- Synthesis of organo-substituted phosphanylboranes $R_1R_2P–BH_2·NMe_3$ (R_1, R_2 = H, alkyl, aryl).
- Polymerization/oligomerization of the parent and organo-substituted phosphanylboranes and characterization of the obtained products.
- Investigation of the reactivity of the substituted phosphanylboranes to ensure the comparability with the parent compound (e.g. oxidation with chalcogens and coordination of main group LAs).

Another goal of this work was the synthesis of small oligomeric units containing PB chains. Smaller oligomeric units are expected to show a higher solubility than the corresponding PPBs and enable a proper characterization. To achieve this, other research objectives of this work are:

- Generation of suitable BH_2^+ building blocks which allow the synthesis of cationic compounds containing linear BE-chains (E = P, As).
- Experiments on the displacement of the LB by a variety of anionic phosphanides which should result in the formation of compounds exhibiting linear, anionic PB chains.

A new and convenient one-pot reaction was developed allowing the generation of $H_2As–BH_2·NMe_3$ in gram scale. The pnictogenylboranes of the heavier congeners antimony and bismuth however remain unknown to date. Therefore another important aspect of this work was:

- Development of a new method which allows the bond formation between Sb and B or Bi and B, respectively.
- Isolation and characterization of the parent compounds $H_2E–BH_2·LB$ (E = Sb, Bi).

The major parts of the investigations on the pnictogenylboranes are based on reactions with main group compounds or early transition metals. In the reaction with Cu(I)I novel clusters were obtained. To study if reaction with monovalent – especially late transition - metal cations, allows the generation of new coordination compounds following investigations have to be made:

- Reactivity studies of the pnictogenylboranes towards Cu(I), Ag(I) and Tl(I) cations.
- Synthesis of homoleptic complexes and coordination polymers with weakly coordinating anions**.**

3. Metal-Free Addition/Head-to-Tail Polymerization of Transient Phosphinoboranes, RPH-BH_2: A Route to Poly(alkylphosphinoborane)s

C. Marquardt, T. Jurca, K.-C. Schwan, A. Stauber, A. V. Virovets, G. R. Whittell, I. Manners and M. Scheer

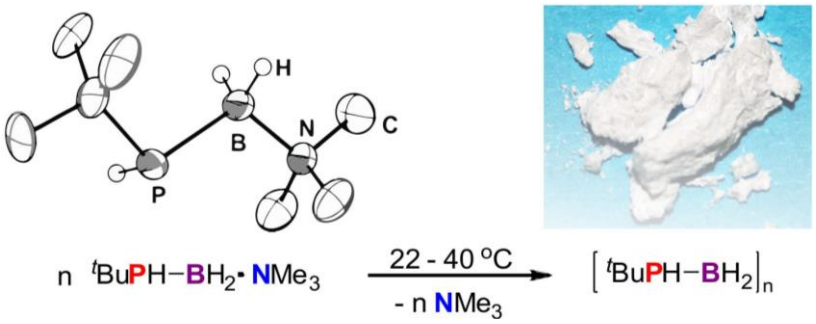

Abstract: Mild thermolysis of Lewis base-stabilized phosphinoborane monomers $R_1R_2P{-}BH_2{\cdot}NMe_3$ (R_1, R_2 = H, Ph or tBu/H) at room temperature to 100 °C provides a convenient new route to oligo- and poly(phosphinoborane)s $[R_1R_2P{-}BH_2]n$. The polymerization appears to proceed via the addition/head-to-tail polymerization of short-lived free phosphinoborane monomers, $R_1R_2P{-}BH_2$. This method offers access to high molar mass materials, as exemplified by poly(t-butylphosphinoborane), that are currently inaccessible using other routes (e.g. catalytic dehydrocoupling).

The terms phosphinoborane and phosphanylborane are equal, as poly(phosphinoborane)s is the commonly used term for PB polymers, phosphinoborane will be used throughout this chapter.

3.1 Introduction

Polymers based on main group elements other than carbon represent attractive materials as a result of their uses as elastomers, lithographic resists, biomaterials, polyelectrolytes, ceramic precursors and in optoelectronics.[1,2] Current routes to main group macromolecules generally involve either polycondensation or ring-opening polymerization pathways. Metal-catalyzed polycondensation processes, such as cross-coupling and dehydrocoupling, have also attracted recent attention.[1p,3] In contrast to the situation with organic polymer synthesis, the use of addition polymerization methods is rare, partly due to challenges associated with the generation of suitable multiply bonded monomers. Nevertheless, *Gates* and coworkers have shown that kinetically stable phosphaalkenes (MesP=C(Ar)Ph, Ar = Ph, C_6H_4OMe) undergo an addition-rearrangement polymerization in the presence of radical or anionic initiators.[1q,4] Furthermore, *Baines* and coworkers have utilized anion-initiated addition polymerization of germenes, and silenes ($Mes_2E=CHCH_2{}^tBu$, E = Ge, Si) to form polygermenes and poly(silylenemethylene)s respectively,[5] demonstrating the use of addition polymerization as a promising approach for the synthesis of main group polymers.[6,7]

Compounds with bonds between elements of Groups 13 and 15 are formally isoelectronic to their carbon analogues. However, due to electronegativity differences, the bonds are polar and lead to different physical and chemical properties.[8,9,10] The analogy has nevertheless stimulated the synthesis of a range of new molecules and materials such as BN analogues of pyrene[11], carbon nanotubes,[12] and fullerene-like BN hollow spheres.[13] Counterparts of organic macromolecules have also attracted much attention and polymers based on poly(p-phenylene)-like cyclolinear structures involving borazines (polyborazylenes) have been studied in detail and, more recently, analogs of polyolefins, poly(aminoborane)s $[RNH\text{-}BH_2]_n$, have been isolated.[14]

Poly(phosphinoborane)s $[RPH\text{-}BH_2]_n$ have been prepared over the past decade as high molar mass materials by the rhodium- and iron-catalyzed dehydrogenation of primary phosphine-boranes $RPH_2{\cdot}BH_3$.[15] Studies of the coordination chemistry of phosphine-borane ligands at d-block metal centers have allowed the elucidation of the fundamental P-B bond formation processes leading to dehydrogenative oligomerization and polymerization.[16] These have revealed a two-fold role for P-H bonds; activation of P-H bond by metal centers to form metal-phosphidoborane intermediates, and promotion of dehydrogenative coupling of P-H (protic H) with B-H (hydridic H) to release H_2 and form a P-B bond.[15g,16] However, as P-H bonds are effectively non-polar (electronegativity: P = 2.19, H = 2.20),[9] catalytic dehydrocoupling routes have relied on

electron withdrawing effects from aryl groups on phosphorus to promote the reaction. This has resulted in relatively limited substrate scope. Thus, the only examples of poly(alkylphosphinoborane)s are of modest molar mass and have been prepared by the slow dehydrocoupling of $^{i}BuPH_2{\cdot}BH_3$[15c] and $FcCH_2PH_2{\cdot}BH_3$[15e] at 110-120 °C over 13 - 18 h in the presence of Rh catalysts in reactions that generally lead to appreciable chain branching and crosslinking, resulting in a very high polydispersity index (PDI) value (e.g. > 5).[15c]

A potential avenue to broaden substrate scope and circumvent the shortcomings of metal-catalyzed dehydropolymerization routes to poly(phosphinoborane)s would be the implementation of an addition polymerization strategy. This would require access to suitable monomeric precursors. Significantly, recent progress by Scheer and coworkers has allowed the facile, gram-scale preparation of $H_2P{-}BH_2{\cdot}NMe_3$ (**1a**), a Lewis base-stabilized monomeric phosphinoborane.[17,18] Elimination of the Lewis base should yield a reactive monomeric phosphinoborane [$H_2P{-}BH_2$] that might be expected to oligomerize and/or polymerize.

3.2 Results and Discussion

In order to explore the potential of this new polymerization strategy in detail we also targeted the aryl-substituted analogue $Ph_2P{-}BH_2{\cdot}NMe_3$ (**1b**) and the alkyl-substituted $^{t}BuPH{-}BH_2{\cdot}NMe_3$ (**1c**), respectively. We therefore developed a salt metathesis route as a novel and convenient method for the generation of substituted phosphanylboranes stabilized only by a Lewis base (Scheme 1). Deprotonation of the corresponding phosphines and subsequent reaction with $IBH_2{\cdot}NMe_3$ afforded the desired phosphanylboranes in good yield and with high purity. Adducts **1b** and **1c** were obtained as white solids that are soluble in THF, toluene, Et_2O and MeCN and, in the case of **1c,** also *n*-hexane. Characterization was achieved by multinuclear NMR spectroscopy and single crystal X-ray diffraction studies (Figure 1).

$$R_1R_2PH \xrightarrow[-\ NH_3]{+\ NaNH_2} NaPR_1R_2 \xrightarrow[-\ NaI]{+\ IBH_2{\bullet}NMe_3} R_1R_2PBH_2{\bullet}NMe_3$$

1b, $R_1 = R_2 = Ph$ (71%) **1c**, $R_1 = {}^{t}Bu$, $R_2 = H$ (55%)

Scheme 1. Synthesis of Lewis base stabilized organosubstituted phosphanylboranes (**1b**,**c**).

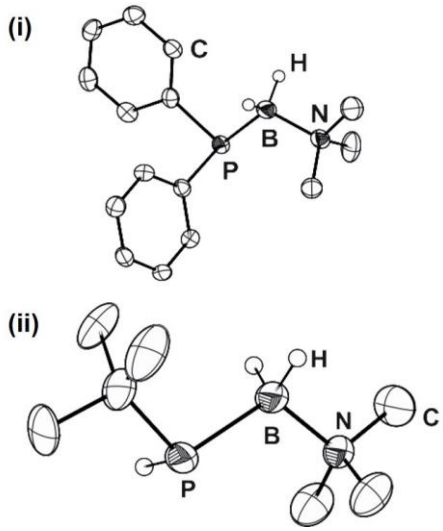

Figure 1. Solid state structure of **1b** (i) and **1c** (ii), (ellipsoids at the 50% probability level). Hydrogen atoms bound to carbon atoms are omitted for clarity. Selected bond lengths [Å] and angles [°] (i); P–B 1.975(2), B-N 1.619(3), P–B–N 112.4(2); (ii) P–B 1.985(2), N–B 1.621(2), B–P–C 102.7(1), P–B–N 108.9(1).

Attempts to thermally-induce oligomerization and polymerization (Scheme 2) were initially made for **1a** and involved reactions at 80°C both in the presence and absence of solvent. However, irrespective of the conditions, in case of this precursor the major fraction of the product (**3a**) was insoluble in common solvents and the soluble fraction appeared to consist of low molar mass, potentially branched oligomers with multiple phosphorus and boron environments.

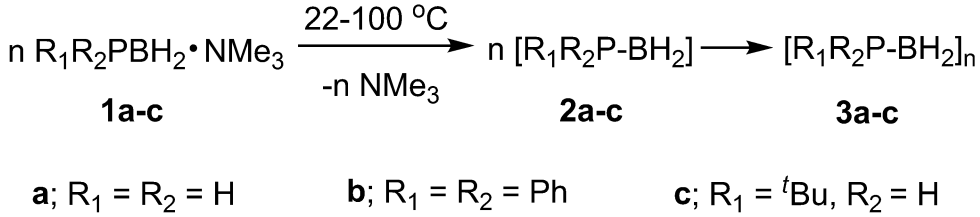

Scheme 2. Polymerization/oligomerization of Lewis base stabilized phosphanylboranes (**1a-c**).

For example, thermolysis of **1a** in toluene (80 °C, 20 h) gave a white, wax-like product. The soluble extract in dilute C_6D_6[20] gave a $^{31}P\{^1H\}$ NMR spectrum that featured a set of three broad signals at δ = -110, -116 and -133 ppm, which showed further broadening in the ^1H coupled ^{31}P NMR spectrum. These resonances are in a similar chemical shift range to those reported for $[H_2P{-}BH_2]_x$ prepared via $B(C_6F_5)_3$-catalyzed dehydro-coupling of $H_3P{\cdot}BH_3$ ($\delta(^{31}P)$ = -95 to -120 ppm), where a mixture of oligomers and low molar mass polymer (M_n < 2000 g mol^{-1}) was formed.[19] Furthermore, one of the peaks has a chemical shift similar to that for the borane complex of **1a**, $BH_3{-}H_2P{-}BH_2{\cdot}NMe_3$ (^{31}P NMR: δ = -116.0),[17a] in which the phosphorus center would exist in a similar environment. The $^{11}B\{^1H\}$ spectrum showed a set of three overlapping

triplets at *ca.* δ = -38, -40 and -41 ppm as major peaks ($^1J_{BP}$ *ca.* 65 Hz) which further split into triplets on ^{1}H coupling ($^1J_{BH}$ = *ca.* 105 Hz, typical for BH_2 groups). The ^{11}B NMR chemical shifts were similar to those reported for internal BH_2 groups in phosphinoborane polymers and oligomers; $[H_2P{-}BH_2]_x$ ^{11}B δ = - 32 ppm[19], $[PhPH{-}BH_2]_n$ ^{11}B δ = - 34.7 ppm.[15a] Several signals at δ = -8 to -10 ppm were tentatively assigned to the NMe_3-coordinated BH_2 end groups (cf. NMe_3-capped terminal BH_2 group in **1a** at $\delta(^{11}B)$ = - 6.7 ppm).[17a] Analysis of the soluble fraction of **3a** by mass spectrometry (MS) and dynamic light scattering (DLS) was also consistent with the presence of oligomers. For example, electrospray ionization (ESI) MS showed a pattern with intervals of 46 m/z, expected for a $[H_2P{-}BH_2]$ moiety, up to 1700 Da, corresponding to up to *ca.* 37 repeat units (see Figure S12).

As a result of the insolubility of the poly(phosphinoborane) **3a** formed from heating **1a**, next we turned our attention to the analogous thermally-induced polymerization of phosphanylboranes with organic substituents at phosphorus (**1b**,**c**) (Scheme 2). Thermolysis of phosphanylborane **1b** was conducted in toluene solution at 100 ^{o}C for 18 h. The ^{1}H, ^{31}P, and ^{11}B NMR resonances of the isolated product **3b** were consistent with the formation of oligomeric species $[Ph_2P{-}BH_2]_x$ and occurred at a similar chemical shift to those reported for $[Ph_2P{-}BH_2]_3$ and $[Ph_2P{-}BH_2]_4$.[15b] ESI-MS analysis of **3b** indicated the presence of linear NMe_3-capped oligomers with a maximum detectable mass up to 1200 g mol^{-1} corresponding to *ca.* 6 repeat units (Figure S15), slightly greater than for the reports of Rh^I-catalyzed dehydrocoupling of $Ph_2PH{\cdot}BH_3$.[15b] In addition, the ESI-mass spectrum of **3b** displayed several peaks corresponding to small, NMe_3 capped oligomeric units, $[Me_3N{\cdot}BH_2{-}Ph_2P{-}BH_2{\cdot}NMe_3]^+$ and $[Me_3N{\cdot}BH_2{-}Ph_2P{-}BH_2{-}Ph_2P{-}BH_2{\cdot}NMe_3]^+$. These represent a class of highly stable cationic phosphinoborane chains, whose preparation has recently been reported.[18f] Analysis by DLS was also consistent with the formation of oligomeric products that undergo facile aggregation (see supporting information for further details).

Finally, we explored the thermolysis of the ^{t}Bu-substituted phosphanylborane **1c** using three methods: heating **1c** at 40 °C for 48 h in the absence of solvent, stirring a toluene solution of **1c** at room temperature (22 ^{o}C), and performing the latter experiment at 40 °C for 48 h. After complete consumption of the starting material (and removal of the solvent for reactions conducted in toluene), the crude product was dissolved in *n*-hexane and precipitated by adding the resulting solution slowly to vigorously stirred acetonitrile. All three methods led to the isolation of the product **3c** as a fine white powder (Figure 3, *inset*) with similar NMR spectra. The $^{11}B\{^1H\}$ NMR featured a single very broad signal at δ = -38 ppm. The $^{31}P\{^1H\}$ NMR spectrum featured a set of 3 broad signals at δ = -19, -21 and -24 ppm. Further broadening and splitting into poorly defined doublets was observed

in the ^{1}H coupled ^{31}P NMR spectrum. We attribute the overlapping resonances to tacticity; the tentative assignment of rm, mr, rr, and mm triads is based on statistical probability (Figure 2). Similar features have been observed in poly(methylenephosphine) polymers.[4a] Overall, the observed NMR spectra for **3c** were similar to those for $[RHP{-}BH_2]_n$ (R = Ph, ^{i}Bu, *p*-nBuC$_6$H$_4$, *p*-dodecylC$_6$H$_4$).[15a,b,c,g]

The ESI-MS of acetonitrile solutions of **3c** (reaction in toluene, 22 ^{o}C, 48 h) showed patterns corresponding to the successive loss of 102 m/z, characteristic of a single unit of [^{t}BuPH–BH$_2$] (Figure S19). Samples obtained from the three methods were analyzed by DLS at optimized concentrations in CH_2Cl_2. The range of values obtained for R_h of 4.4 – 5.5 nm correspond to molar masses of 26 800 – 39 900 g mol^{-1} for monodisperse polystyrene samples in THF (Figure S20).[21] GPC analysis of the samples with $CHCl_3$ as eluent, also using polystyrene standards, was consistent with these results within experimental error and showed the presence of polymer with molar masses (M_n) of 27 800 – 35 000 g mol^{-1} with polydispersity indices, (PDI)s of 1.6-1.9 (Figures 3 and S22).

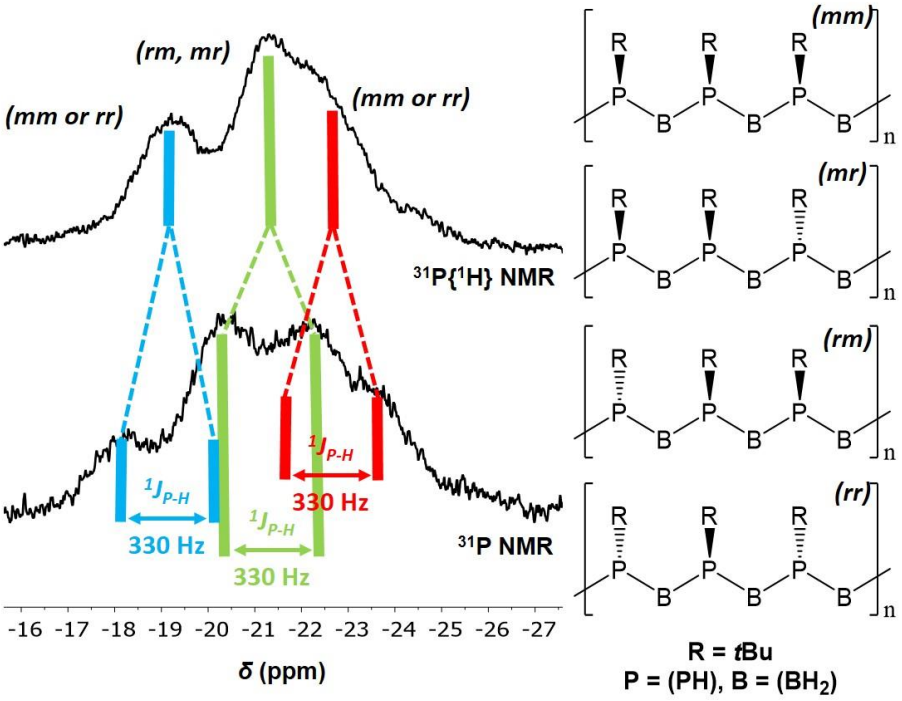

Figure 2. ^{31}P and $^{31}P\{^{1}H\}$ NMR spectra of $[^{t}BuPH\text{-}BH_2]_n$ (**3c**) in $CDCl_3$ with proposed tacticity resulting in overlapped resonances.

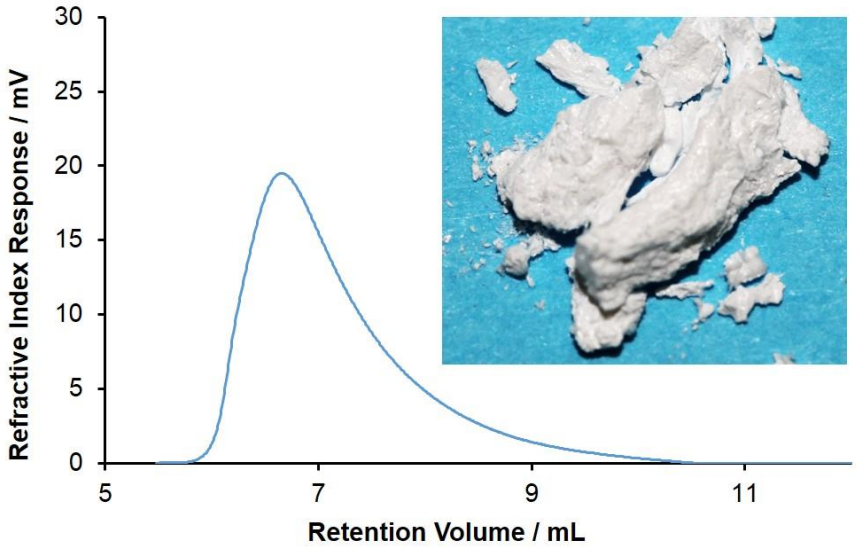

Figure 3. GPC trace for [^{t}BuPH-BH_2]$_n$ (**3c**, from polymerization in toluene, 22 ^{o}C, 48 h) in $CHCl_3$; *inset:* photograph of a purified sample of **3c**.

We propose that polymerization of **1a**-**c** is triggered by initial thermolysis of Lewis base stabilized phosphanylboranes **1a**-**c**, leading to elimination of NMe_3 to form the unprotected monomeric phosphinoborane intermediate **2a**-**c**. The resulting absence of the Lewis base leads to a lack of electronic stabilization for **2a**-**c**. As a result, the lone-pair at phosphorus together with a vacant p-orbital at boron, in conjunction with the aforementioned electronic destabilization, appears to promote a head-to-tail addition oligomerization/polymerization sequence which ultimately affords **3a**-**c**, although the full mechanistic details are not yet clear (Scheme 2). We attribute the difference in product distribution to the reactivity of **2a**-**c** and the solubility of the polymer products **3a**-**c**. Sterically unencumbered **2a** is likely to be highly reactive and forms the insoluble material which may be of high molar mass, together with soluble oligomers. In contrast, **2b**, which contains two bulky phenyl groups at phosphorus, appears to afford only oligomers. Presumably the steric bulk hinders polymer formation both kinetically, and possibly thermodynamically as well. In contrast, the *t*-butyl-substituted species **3c** affords soluble, high molecular weight polymer.

High molar mass poly(phenylphosphinoborane) free of crosslinked material has been recently prepared using an iron-based dehydrocoupling catalyst in toluene solution, a reaction significantly more efficient that the previously reported Rh-catalyzed process performed in the absence of solvent.[15g] We were intrigued whether alkyl-substituted polymer **3c** would be accessible by a similar route. For comparison we prepared poly(phenylphosphinoborane) from $PhPH_2{\cdot}BH_3$ and 1 mol% of $Cp(CO)_2Fe(OSO_2CF_3)$ (100 °C, 24 h) and isolated the material with M_n = 59 000 g mol^{-1}, and a PDI = 1.6.[15g] When ^{t}BuPH$_2{\cdot}$BH$_3$ was treated with $Cp(CO)_2Fe(OSO_2CF_3)$ under the same conditions

(Scheme 3) near complete consumption of $^{t}BuPH_2{\cdot}BH_3$ required 176 h by ^{31}P and ^{11}B NMR. Subsequent precipitation into, and washes with cold pentane afforded a dark amber wax-like product. $^{31}P\{^{1}H\}/^{31}P$ and $^{11}B\{^{1}H\}$ NMR featured multiple broad overlapping resonances ($\delta^{11}B$ -40 ppm, $\delta^{31}P$ ca. -20 ppm). Although ESI MS showed peaks separated by Δ(m/z) = 102, attributed to units of [$^{t}BuPH\text{-}BH_2$], masses up to only 1100 Da were detected. Moreover, GPC analysis of the products with $CHCl_3$ as eluent revealed no high molar mass component and the product appears to be an oligomer of about 10 units or less. This is in stark contrast to the high molar mass polymer (**3c**) obtained via the thermally-induced polymerization of phosphanylborane **1c**.

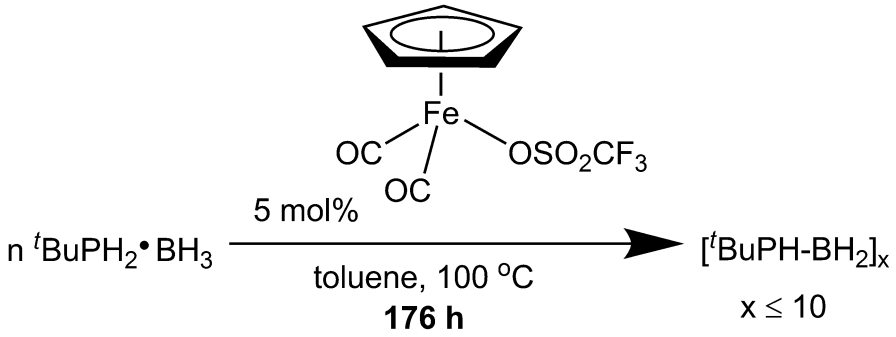

Scheme 3. Attempted synthesis of [tBuPH-BH_2]n (3c) via catalytic dehydrocoupling of $tBuPH_2{\cdot}BH_3$.

3.3 Conclusion

In summary, a straightforward synthesis of organosubstituted monomeric phosphanylboranes stabilized only by a Lewis base has been developed to obtain compounds **1b** and **1c**. Simple thermal treatment of the monomeric Lewis base stabilized phosphinoboranes **1a-c** led to the formation of oligomeric and polymeric compounds **3a-c**. Due to the low solubility of **3a**, characterization of this polymer was limited. Polymerization of **1b** led to short chain oligomers **3b** which could be characterized by multinuclear NMR, and mass spectrometry. However, polymerization of **1c** afforded **3c** with high molar mass (M_n = 27 800 – 35 000 g mol^{-1}) and reasonably low PDI (1.6-1.9) characteristic of a mainly linear material. In contrast, previous work with Rh-catalysts has given lower molar mass, branched materials (M_n < ca. 10,000 g mol^{-1}) under forcing thermal conditions in the melt where the yields have been limited by gel formation.[15c] In addition, poly(phosphinoborane) **3c** could not be accessed via the recently reported Fe-catalyzed catalytic dehydrocoupling route, presumably also due to the deactivated P-H bond in the alkylphosphinoborane monomer.

Based on these results, the new metal-free polymerization method described offers considerable promise for the preparation of a range of new poly(phosphinoborane)s with

alkyl substituents on phosphorus that are of interest as elastomers, flame retardant materials, and as ceramic precursors. Expansion of substrate/polymer scope, reaction optimization, and the detailed elucidation of the reaction mechanism, which appears to involve the addition/head-to-tail polymerization of transient phosphinoborane monomers, are currently under investigation.

3.4 References

[1] a) M. Liang, I. Manners, *J. Am. Chem. Soc.* **1991**, *113*, 4044–4045; b) H. R. Allcock, *Chem. Mater.* **1994**, *6*, 1476–1491; c) C. H. Honeyman, I. Manners, C. T. Morrissey, H. R. Allcock, *J. Am. Chem. Soc.* **1995**, *117*, 7035–7036; d) R. D. Archer, *Inorganic and Organometallic Polymers*, Wiley-VCH, New York, **2001**; e) I. Manners, *Angew. Chem. Int. Ed.* **1996**, *35*, 1602–1621; *Angew. Chem.* **1996**, *108*, 1712–1731; f) S. J. Clarson, J. A. Semlyen*, Siloxane Polymers*, Prentice Hall, Englewood Cliffs, **1993**; g) R. H. Neilson, P. Wisian-Neilson, *Chem. Rev.* **1988**, *88*, 541–562; h) R. D. Miller, J. Michl*, Chem. Rev.* **1989**, *89*, 1359–1410; i) R. De Jaeger, M. Gleria, *Prog. Polym. Sci.* **1998**, *23*, 179–276; j) R. West, *J. Organomet. Chem.* **1986**, *300*, 327–346; k) T. Imori, V. Lu, H. Cai, T. D. Tilley, *J. Am. Chem. Soc.* **1995**, *117*, 9931–9940; l) X. He, T. Baumgartner, *RSC Adv.* **2013**, *3*, 11334–11350; m) S. Wilfert, H. Henke, W. Schoefberger, O. Brüggemann, I. Teasdale, *Macromol. Rapid Commun.* **2014**, *35*, 1135–1141; n) W. Cao, Y. Gu, M. Meineck, T. Li, H. Xu, *J. Am. Chem. Soc.* **2014**, *136*, 5132–5137; o) F. Choffat, S. Käser, P. Wolfer, D. Schmid, R. Mezzenga, P. Smith, W. Caseri, *Macromolecules* **2007**, *40*, 7878–7889; p) J. Linshoeft, E. J. Baum, A. Hussain, P. J. Gates, C. Näther, A. Staubitz, *Angew. Chem. Int. Ed.* **2014**, *53*, 12916 – 12920; *Angew. Chem.* **2014**, *126*, 13130– 13134; q) B. W. Rawe, C. P. Chun, D. P. Gates, *Chem. Sci.* **2014**, *5*, 4928–4938.

[2] a) P. J. Fazen, J. S. Beck, A. T. Lynch, E. E. Remsen, L. G. Sneddon, *Chem. Mater.* **1990**, *2*, 96–97; b) F. Jäkle, *Chem. Rev.* **2010**, *110*, 3985–4022; c) H. Kuhtz, F. Cheng, S. Schwedler, L. Böhling, A. Brockhinke, L. Weber, K. Parab, F. Jäkle, *ACS Macro Lett*. **2012**, *1*, 555–559; d) Z. M. Hudson, D. J. Lunn, M. A. Winnik, I. Manners, *Nat. Commun.* **2014**, *5*, 3372; e) A. Lorbach, M. Bolte, H. Li, H.-W. Lerner, M. C. Holthausen, F. Jäkle, M. Wagner, *Angew. Chem. Int. Ed.* **2009**, *48*, 4584–4588; *Angew. Chem.* **2009**, *121*, 4654–4658; f) A. Hübner, Z.-W. Qu, U. Englert, M. Bolte, H.-W. Lerner, M. C. Holthausen, M. Wagner, *J. Am. Chem. Soc*. **2011**, *133*, 4596–4609; g) G. Zhang, G. M. Palmer, M.W. Dewhirst, C. L. Fraser, *Nat. Mater.* **2009**, *8*, 747–751.

[3] a) E. M. Leitao, T. Jurca, I. Manners, *Nat. Chem*. **2013**, *5*, 817–829; b) G. He, L. Kang, W. T. Delgado, O. Shynkaruk, M. J. Ferguson, R. McDonald, E. Rivard, *J. Am. Chem. Soc*. **2013**, *135*, 5360–5363; c) M. Heeney, W. Zhang, D. J. Crouch, M. L. Chabinyc, S. Gordeyev, R. Hamilton, S. J. Higgins, I. McCulloch, P. J. Skabara, D. Sparrowe, S. Tierney, *Chem. Commun*, **2007**, 5061–5063; d) B. W. Rawe, D. P. Gates, *Angew. Chem. Int. Ed.* **2015**, *54*, 11438–11442; *Angew. Chem.* **2015**, *127*, 11600–11604.

[4] a) C.-W. Tsang, M. Yam, D. P. Gates, *J. Am. Chem. Soc.* **2003**, *125*, 1480–1481; b) C.-W. Tsang, B. Baharloo, D. Riendl, M. Yam, D. P. Gates, *Angew. Chem. Int. Ed.* **2004**, *43*, 5682-5685; *Angew. Chem.* **2004**, *116*, 5800–5803; c) P. W. Siu, S. C. Serin, I. Krummenacher, T. W. Hey, D. P. Gates, *Angew. Chem. Int. Ed.* **2013**, *52*, 6967–6970; *Angew. Chem.* **2013**, *125*, 7105–7108.

[5] a) L. C. Pavelka, S. J. Holder, K. M. Baines, *Chem. Commun*. **2008**, 2346–2348; b) L. C. Pavelka, K. K. Milnes, K. M. Baines, *Chem. Mater*. **2008**, *20*, 5948–5950.

[6] As an additional example, reaction of $Tip_2Si{=}SiTip\text{-}pC_6H_4\text{-}SiTip{=}SiTip_2$ (Tip = 2,4,6-$^{i}Pr_3C_6H_2$) with tetrasiladiene resulted in the formation of σ-π conjugated organosilicon hybrid polymers; M. Majumdmar, I. Bejan, V. Huch, A. J. P. White, G. R. Whittell, A. Schäfer, I. Manners, D. Scheschkewitz, *Chem. Eur. J.* **2014**, *20*, 9225–9229.

[7] Anionic polymerization of masked disilenes has also been reported; a) K. Sakamoto, K. Obata, H. Hirata, M. Nakajima, H. Sakurai, *J. Am. Chem. Soc.* **1989**, *111*, 7641–7643; b) K. Skamoto, M. Yoshida, H. Sakurai, *Polymer* **1994**, *35*, 4990–4997.

[8] Z. Liu, T. B. Marder, *Angew. Chem. Int. Ed.* **2007**, *47*, 242–244; *Angew. Chem.* **2007**, *120*, 248–250.

[9] Electronegativities on the Pauling scale, B = 2.04, N = 3.04, P = 2.19; W. M. Haynes, ed., *CRC Handbook of Chemistry and Physics, 95thEdition (Internet Version 2015)*, CRC Press/Taylor and Francis, Boca Raton, FL, **2015**.

[10] A. Staubitz, A. P. M. Robertson, M. E. Sloan, I. Manners, *Chem. Rev.* **2010**, *110*, 4023–4078.

[11] M. J. D. Bosdet, W. E. Piers, T. S. Sorensen, M. Parvez, *Angew. Chem. Int. Ed.* **2007**, *46*, 4940–4943; *Angew. Chem.* **2007**, *119*, 5028–5031.

[12] M. Terrones, J. M. Romo-Herrera, E. Cruz-Silva, F. López-Uríaz, E. Muñoz-Sandoval, J. J. Velázquez-Salazar, H. Terrones, Y. Bando, D. Goldberg, *Mater. Today* **2007**, *10*, 30–38.

[13] X. Wang, Y. Xie, Q. Guo, *Chem. Commun.* **2003**, 2688–2689.

[14] a) M. E. Bluhm, M. G. Bradley, R. Butterick III, U. Kusari, L. G. Sneddon, *J. Am. Chem. Soc.* **2006**, *128*, 7748–7749; b) D. W. Himmelberger, C. W. Yoon, M. E.

Bluhm, P. J. Carroll, L. G. Sneddon, *J. Am. Chem. Soc.* **2009**, *131*, 14101–14110; c) L. G. Sneddon, M. G. L. Mirabelli, A. T. Lynch, P. J. Fazen, K. Su, J. S. Beck, *Pure & Appl. Chem.* **1991**, *63*, 407–410; d) T. Wideman, P. J. Fazen, K. Su, E. E. Remsen, G. A. Zank, L. G. Sneddon, *Appl. Organometal. Chem.* **1998**, *12*, 681–693; e) A. Staubitz, A. Presa Soto, Ian Manners, *Angew. Chem. Int. Ed.* **2008**, *47*, 6212–6215; *Angew. Chem.* **2008**, *120*, 6308–6311; f) A. Staubitz, M. E. Sloan, A. P. M. Robertson, A. Friedrich, S. Schneider, P. J. Gates, J. S. Auf der Günne, I. Manners, *J. Am. Chem. Soc.* **2010**, *132*, 13332–13345; g) A. N. Marziale, A. Friedrich, I. Klopsch, M. Drees, V. R. Celinski, S. Schmedt auf der Günne, S. Schneider, *J. Am. Chem. Soc.* **2013**, *135*, 13342–13355; h) R. Dallanegra, A. P. M. Robertson, A. B. Chaplin, I. Manners, A. S. Weller, *Chem. Commun.* **2011**, *47*, 3763–3765.

[15] a) H. Dorn, R. A. Singh, J. A. Massey, A. J. Lough, I. Manners, *Angew. Chem. Int. Ed.* **1999**, *38*, 3321–3323; *Angew. Chem.* **1999**, *111*, 3540–3543; b) H. Dorn, R. A. Singh, J. A. Massey, J. M. Nelson, C. A. Jaska, A. J. Lough, I. Manners, *J. Am. Chem. Soc.* **2000**, *122*, 6669–6678; c) H. Dorn, J. M. Rodezno, B. Brunnhöfer, E. Rivard, J. A. Massey, I. Manners, *Macromolecules* **2003**, *36*, 291–297; d) T. J. Clark, J. M. Rodezno, S. B. Clendenning, S. Aouba, P. M. Brodersen, A. J. Lough, H. E. Ruda, I. Manners, *Chem. Eur. J.* **2005**, *11*, 4526–4534; e) S. Pandey, P. Lönnecke, E. Hey-Hawkins, *Eur. J. Inorg.Chem.* **2014**, 2456–2465; f) D. Jacquemin, C. Lambert, E. A. Perpète, *Macromolecules* **2004**, *37*, 1009–1015; g) A. Schäfer, T. Jurca, J. Turner, J. R. Vance, K. Lee, V. A. Du, M. F. Haddow, G. R. Whittell, I. Manners, *Angew. Chem. Int. Ed.* **2015**, *54*, 4836–4841; *Angew. Chem.* **2015**, *127*, 4918–4923.

[16] a) M. A. Huertos, A. S.Weller, *Chem. Commun.* **2012**, *48*, 7185–7187; b) M. A. Huertos, A. S. Weller, *Chem. Sci*. **2013**, *4*, 1881–1888; c) T. N. Hooper, M. A. Huertos, T. Jurca, S. D. Pike, A. S.Weller, I. Manners, *Inorg. Chem.* **2014**, *53*, 3716–3729; d) H. C. Johnson, T. N. Hooper, A. S. Weller, *Top. Organomet. Chem.* **2015**, *49*, 153–220; e) Thoms, C.; Marquardt, C.; Timoshkin, A. Y.; Bodensteiner, M.; Scheer, M. *Angew. Chem. Int. Ed.* **2013**, *52*, 5150–5154; *Angew. Chem.* **2013**, *125*, 5254–5259.

[17] a) K.-C. Schwan, A. Y. Timoshkin, M. Zabel, M. Scheer, *Chem. Eur. J*. **2006**, *12*, 4900–4908; b) C. Marquardt, A. Adolf, A. Stauber, M. Bodensteiner, A. V. Virovets, A.Y. Timoshkin, M. Scheer, *Chem. Eur. J.* **2013***, 19*, 11887–11891.

[18] (i) For the formation of stable monomeric phosphinoboranes with bulky substituents see: a) X. Feng, M. M. Olmstead, P. P. Power, *Inorg. Chem.* **1986**, *25*, 4615–4616; b) A. M. Spokoyny, C. D. Lewis, G. Teverovskiy, S. L. Buchwald, *Organometallics*, **2012**, *31*, 8478–8481; c) J. A. Bailey, P. G. Pringle, *Coord. Chem.*

Rev. **2015**, *297*, 77–90; (ii) For examples of the analogous stabilization of other group 13-15 species see: (P-Al, P-Ga) d) U. Vogel, A. Y. Timoshkin, M. Scheer, *Angew. Chem. Int. Ed.* **2001**, *40*, 4409–4412; *Angew. Chem.* **2001**, *113*, 4541–4544; (As-B) e) M. A. Mardones, A. H. Cowley, L. Contreras, R. A. Jones, C. J. Carrano, *J. Organomet. Chem.* **1993**, *455*, C1-C2; f) C. Marquardt, C. Thoms. A. Stauber, G. Balázs, M. Bodensteiner, M. Scheer, *Angew. Chem. Int. Ed.* **2014**, *53*, 3727–3730; *Angew. Chem.* **2014**, *126*, 3801–3804; (B-N) g) N. E. Stubbs, T. Jurca, E. M. Leitao, C. H. Woodall, I. Manners, *Chem. Commun*. **2013**, *49*, 9098–9100; h) H. Braunschweig, W. C. Ewing, K. Geetharani, M. Schafer, *Angew. Chem. Int. Ed.* **2015**, *54*, 1662–1665; *Angew. Chem.* **2015**, *127*, 1682–1685; i) A. K. Swarnakar, C. Hering-Junghans, K. Nagata, M. J. Ferguson, R. McDonald, N. Tokitoh, E. Rivard, *Angew. Chem. Int. Ed.* **2015**, *54*, 10666–10669; *Angew. Chem.* **2015**, *127*, 10812–10816; (iii) For the successful stabilization of phosphinoborane monomers at metal centers see: j) A. Amgoune, S. Ladeira, K. Miqueu, D. Bourissou, *J. Am. Chem. Soc.* **2012**, *134*, 6560–6563.

[19] J.-M. Denis, H. Forintos, H. Szelke, L. Toupet, T.-N. Pham, P.-J. Madec, A.-C. Gaumont, *Chem. Commun.* **2003**, 54–55.

[20] Attempted dissolution of reaction products (**3a**) in *n*-hexane, benzene, toluene, Et_2O, THF, CH_2Cl_2, $CHCl_3$, MeCN, and 1,4-dioxane was not successful.

[21] L. J. Fetters, N. Hadjichristidis, J. S. Lindner, J. W. Mays, *J. Phys. Chem. Ref. Data*. **1994**, *23*, 619–640.

3.5 Supporting Information

General Experimental:

Unless otherwise noted, all manipulations were performed under an atmosphere of dry argon using standard glove-box and Schlenk techniques. All solvents were degassed and purified by standard procedures. The compounds $IBH_2{\cdot}NMe_3$,[1] $H_2PBH_2{\cdot}NMe_3$ (**1a**),[2] and $^tBuPH_2$[3] were prepared according to literature procedures. Other chemicals were obtained from Sigma-Aldrich ($NaNH_2$) or STREM Chemicals, INC. (PPh_2H). The NMR spectra for the monomers **1b, 1c** and for the compounds **3b** and **3c** were recorded on an Avance 400 spectrometer (^1H: 400.13 MHz, ^{31}P: 161.976 MHz, ^{11}B: 128.378 MHz, $^{13}C\{^1H\}$: 100.623 MHz) with δ [ppm] referenced to external $SiMe_4$ (^1H, ^{13}C), H_3PO_4 (^{31}P), $BF_3{\cdot}Et_2O$ (^{11}B). Other NMR spectra were recorded using Oxford Jeol Eclipse 300 and 400 MHz spectrometers. ^1H NMR spectra were calibrated using residual proton signals of the solvent: (δ $^1H(CHCl_3)$ = 7.24; δ $^1H(C_6D_5H)$ = 7.20). ^{13}C NMR spectra were calibrated using the solvent signals (δ $^{13}C(CDCl_3)$ = 77.0; δ $^{13}C(C_6D_6)$ = 128.0). ^{11}B and

^{31}P NMR spectra were calibrated against external standards (^{31}P: 85% H_3PO_4(aq) (δ ^{31}P = 0.0); ^{11}B: $BF_3{\cdot}OEt_2$ (δ ^{11}B = 0.0)). IR spectra were measured on a DIGILAB (FTS 800) FT-IR spectrometer. Mass spectra were recorded on a ThermoQuest Finnigan TSQ 7000 (ESI-MS) or a Finnigan MAT 95 (FD-MS and EI-MS) or a Bruker Daltonics Apex IV Fourier transform Ion Cyclotron mass spectrometer. The C, H, N analyses were measured on an Elementar Vario EL III apparatus. Gel permeation chromatography (GPC) was performed on a Viscotek RImax chromatograph, equipped with an automatic sampler, a pump, an injector and inline degasser. The columns were contained within an oven (35°C) and consisted of styrene/divinyl benzene gels with pore sizes ranging from 500 Å to 100,000 Å. THF containing 0.1 % w/w [nBu$_4$N]Br and 1% v/v toluene was used as the eluent at a flow rate of 1.0 mL min^{-1}. All samples analysed by GPC were dissolved in the eluent (2 mg mL^{-1}), stirred for 1 h at room temperature and passed through a membrane filter (200 nm pores) before analysis. The calibration was conducted using a series of monodisperse polystyrene standards obtained from Aldrich. Dynamic Light Scattering (DLS) was performed on a Malvern Instruments Zetasizer Nano S using a 5mW He-Ne laser (633 nm). The correlation function was collected in real time and fitted with a function capable of modelling polymodal size distributions.

The single crystal X-ray structure analysis was performed on a Gemini R Ultra CCD diffractometer from Agilent Technologies (formerly Oxford Diffraction) applying Cu-K_α radiation (λ = 1.54178 Å) at 123 K. Crystallographic data are given in Table S1. Absorption corrections were applied semi-empirically from equivalent reflections or analytically (SCALE3/ABSPACK algorithm implemented in CrysAlis PRO software by Agilent Technologies Ltd).[4] All structures were solved using SIR97[5], and refined using SHELXL-14.[6] The hydrogen positions of the methyl groups were located geometrically and refined riding on the carbon atoms. Hydrogen atoms belonging to BH_2 and PH_2 groups were located from the difference Fourier map and refined without constraints. Due to the bad displacement parameters of the heavily disordered ^{t}Bu-moiety in **1c**, the carbon atoms were refined applying ISOR restraints. Figures were created with OLEX 2.[7] All cif-files are available online from the Cambridge Crystallographic Data Centre.

Synthesis of Ph_2P-$BH_2{\cdot}NMe_3$ (1b):

1.740 mL (1.866 g, 10 mmol) Ph_2PH was added to a suspension of 390 mg (10 mmol) $NaNH_2$ in 20 ml THF at -40 °C. The mixture was allowed to reach room temperature and was stirred for an additional 2 h, until a clear red solution was obtained. After cooling to -80 °C, the $NaPPh_2$ solution was added to a solution of 1.990 g (10 mmol) $IBH_2{\cdot}NMe_3$ in 20 mL THF at -80 °C. After warming up to room temperature, the mixture was stirred for an additional 18 h. All volatiles were removed under vacuum and the remaining solids

were suspended in 50 mL of toluene and filtered over diatomaceous earth. The toluene was removed, and the resulting white solid washed 5 times with 10 mL of Et_2O at 0 °C to remove NaI. The remaining white solid was dissolved in 20 mL of toluene and filtered over diatomaceous earth. After removing the toluene the resulting **1b** was washed 3 times with 10 mL of *n*-hexane and dried under vacuum. **1b** is a white powder at room temperature. Crystals of **1b** were obtained by dissolving a small amount of **1b** in *n*-hexane and storing the solution at 3°C. Yield of (**1b**): 1.833 g (71 %); ^{1}H NMR (400 MHz, C_6D_6): δ = 1.92 (s, 9H, NMe_3), 2.84 (q, $^{1}J_{H,B}$ = 107 Hz, 2H, BH_2), 7.07 (m, 2H, *p*-Ph), 7.20 (m, 4H, *m*-Ph) 7.87 (m, 4H, *o*-Ph). ^{31}P NMR (162 MHz, C_6D_6): δ = –39.5 (m, br, PPh_2). ^{31}P{^{1}H} NMR (162 MHz, C_6D_6): δ = –39.5 (m, br, PPh_2). ^{11}B NMR (128 MHz, C_6D_6): δ = –1.7 (td, $^{1}J_{B,P}$ = 45 Hz, $^{1}J_{B,H}$ = 107 Hz, BH_2). ^{11}B{^{1}H} NMR (128 MHz, C_6D_6): δ = –1.7 (d, $^{1}J_{B,P}$ = 45 Hz, BH_2). ^{13}C NMR (101 MHz, C_6D_6): δ = 52.4 (d, $^{3}J_{P,C}$ = 11 Hz, NMe_3), 126.44 (s, *p*-Ph), 128.13 (d, $^{3}J_{P,C}$ = 6 Hz, *m*-Ph) 134.80 (d, $^{2}J_{P,C}$ = 16 Hz, *o*-Ph), 143.78 (d, $^{1}J_{P,C}$ = 16 Hz, *i*-Ph). IR (KBr): $\tilde{\nu}$ = 3061 (w), 3040 (w), 3010 (w), 2994 (w), 2943 (w), 2918 (w), 2361 (s, br, BH), 2290 (w, br, BH), 1580 (w), 1478 (s), 1465 (s), 1442 (s), 1430 (m), 1403 (w), 1315 (w), 1252 (m), 1155 (m), 1123 (s), 1078 (m), 1058 (s), 1027 (m), 1015 (w), 850 (s), 747 (s), 699 (s), 639 (w), 510 (m), 473 (w). EI-MS (toluene): *m/z* = 257 (22.5 %, $[M]^+$), 108 (100 %, $[M - Me_3N{\cdot}BH_2 - Ph]^+$), 72 (42 %, $[M\text{-}PPh_2]^+$). Elemental analysis (%) calculated for $C_{15}H_{21}BNP$ (**1b**): C: 70.07, H: 8.23, N: 5.45; found: C: 70.05, H: 8.11, N: 5.41.

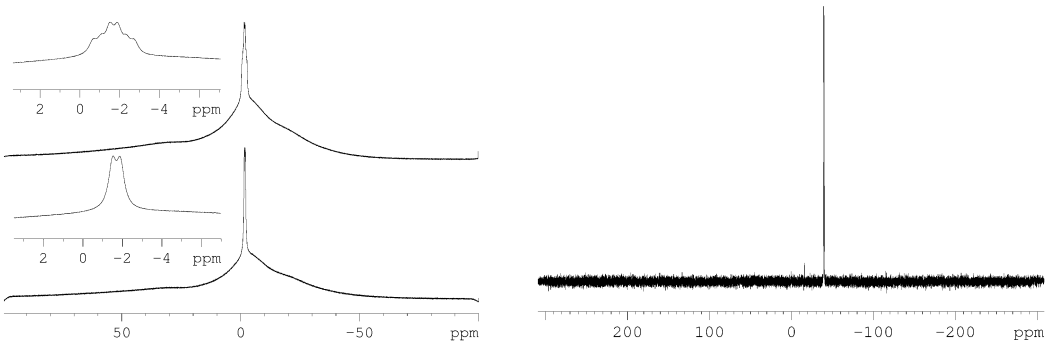

Figure S1: (*bottom left*) ^{11}B{^{1}H} (128 MHz), (*top left*) ^{11}B (128 MHz), (*right)* ^{31}P (162 MHz) NMR spectra of **1b** in in C_6D_6.

Synthesis of ^{t}BuHP-$BH_2{\cdot}NMe_3$ (1c):

2.550 mL (1.802 g, 20 mmol) $^{t}BuPH_2$ was added to a suspension of 780 mg (20 mmol) $NaNH_2$ in 20 ml THF at -40 °C. The mixture was allowed to reach room temperature and was stirred for an additional 2 h, until a clear yellow solution was obtained. After cooling to -80 °C, the Na^{t}BuPH solution was added to a solution of 3.980

g (20 mmol) $IBH_2{\cdot}NMe_3$ in 20 mL THF at -80 °C. After warming up to room temperature, the mixture was stirred for an additional 18 h. All volatiles were removed under vacuum and the remaining solids suspended in 20 mL of *n*-hexane and filtered over diatomaceous earth. The *n*-hexane was removed, and then **1c** was purified by sublimation at 45 °C ($1{\cdot}10^{-3}$ mbar). **1c** is a white powder at room temperature. Crystals of **1c** were obtained by dissolving a small amount of **1c** in *n*-hexane and storing the solution at -28 °C. Yield of (**1c**): 1.767 g (55 %); ^{1}H NMR (400 MHz, C_6D_6): δ = 1.50 (dm, $^{3}J_{H,P}$ = 11 Hz, 9H, P^{t}Bu), 1.94 (s, 9H, NMe_3), 2.60 (d, $^{1}J_{H,P}$ = 197 Hz, 1H, PH^{t}Bu), 2.67 (q, BH_2). ^{31}P NMR (162 MHz, C_6D_6): δ = –67.6 (d, br $^{1}J_{H,P}$ = 197 Hz, PH). ^{31}P{^{1}H} NMR (162 MHz, C_6D_6): δ = –67.6 (q, $^{1}J_{B,P}$ = 48 Hz, PH). ^{11}B NMR (128 MHz, C_6D_6): δ = –6.0 (td, $^{1}J_{B,P}$ = 48 Hz, $^{1}J_{B,H}$ = 104 Hz, BH_2). ^{11}B{^{1}H} NMR (128 MHz, C_6D_6): δ = –6.0 (d, $^{1}J_{B,P}$ = 48 Hz, BH_2). ^{13}C NMR (101 MHz, C_6D_6): δ = 26.4 (s, C), 33.3 (d, $^{2}J_{C,P}$ = 11 Hz, ^{t}Bu), 52.0 (d, $^{3}J_{C,P}$ = 11 Hz, NMe_3). IR (KBr): $\tilde{\nu}$ = 2993 (m), 2962 (m), 2939 (s), 2892 (m), 2854 (m), 2388 (s, br, BH), 2295 (w, br, BH), 2244 (m, PH), 1482 (s), 1464 (s), 1403 (w), 1358 (m), 1252 (m), 1189 (w), 1154 (s), 1124 (s), 1067 (s), 1012 (w), 984 (w), 872 (m), 847 (s), 846 (s), 693 (w), 545 (w), 599 (w), 475 (w). EI-MS (solid): *m/z* = 161 (6.4 %, $[M]^+$), 104 (1.8 %, $[M\text{-}^{t}Bu]^+$), 72 (100 %, $[M\text{-}PH^{t}Bu]^+$), 58 (11 %, $[M$ -H -$H_2BPH^{t}Bu]^+$). Elemental analysis (%) calculated for $C_7H_{21}BNP$ (**1c**): C: 52.13, H: 13.13, N: 8.69; found: C: 52.32, H: 13.06, N: 8.70.

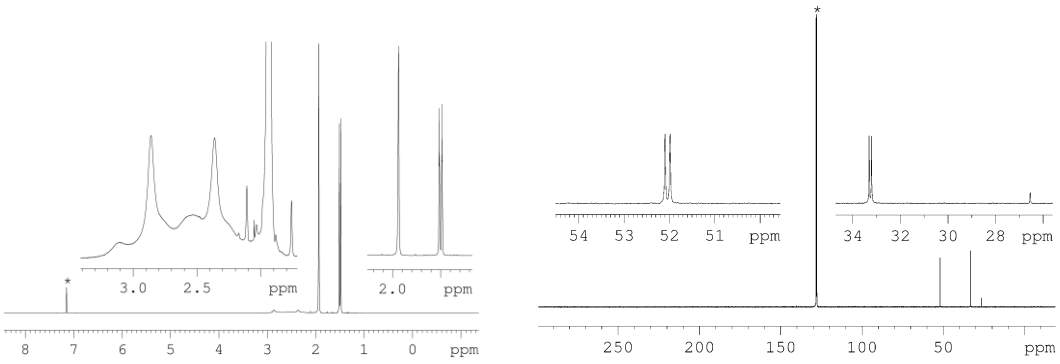

Figure S2: (*left*) ^{1}H (400 MHz); (*right)* ^{13}C{^{1}H} (101 MHz) NMR spectra of **1c** in in C_6D_6.* = solvent (C_6D_6)

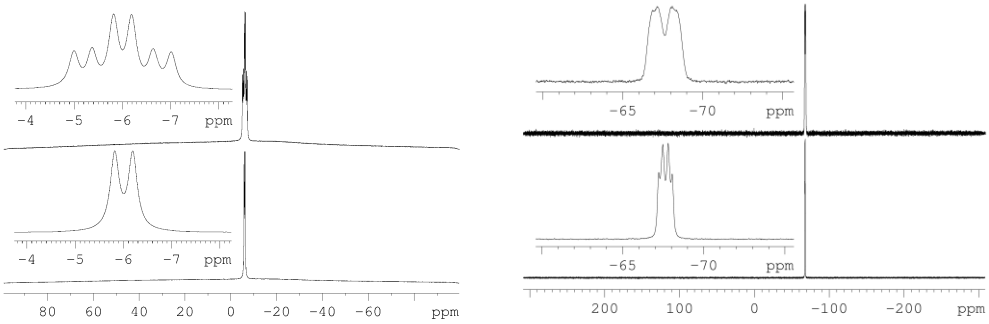

Figure S3: (*bottom left*) $^{11}B\{^1H\}$ (128 MHz), (*top left*) ^{11}B (128 MHz), (*bottom right*) $^{31}P\{^1H\}$ (162 MHz), (*top right*) ^{31}P (162 MHz) NMR spectra of **1c** in in C_6D_6.

Synthesis of ^{t}BuPH$_2$·BH$_3$:

Under flow of N_2, a solution of ^{t}Bu$_2$PCl$_2$ (1.09 g, 6.8 mmol) in dibutyl ether (5 mL) was added dropwise to a dibutyl ether (20 mL) suspension of $LiBH_4$ (0.30 g, 14 mmol) cooled to 5 ^{o}C with an ice bath. The mixture became cloudy immediately and was allowed to stir for 30 min. The reaction flask was then assembled into a short-path distillation setup and reaction solution held at -5 ^{o}C while the receiving flask was held at -196 ^{o}C in liquid N_2. Upon placing the system under static vacuum, ^{t}BuPH$_2$·BH$_3$ was transferred to the receiving flask as a clear oil. The resulting lower yield of 437 mg (62 %) is a result of loss of volatile product under vacuum. ^{1}H NMR (300 MHz, toluene-d8): δ = 3.75 (br doublet of quartets, P*H*, $^1J_{P,H}$ = 350 Hz), 0.85 (d, ^{t}Bu*H,* $^3J_{P,H}$ = 15 Hz), 0.4-1.8 (br m, B*H*); ^{31}P NMR (121 MHz, toluene-d8): δ -11.5 (br triplet of multiplets, *P*H$_2$, $^1J_{P,H}$ = 350 Hz; $^{31}P\{^1H\}$, (q, $^1J_{P,B}$ = 34 Hz); $^{11}B\{^1H\}$ NMR (96 MHz, toluene-d8): δ -44.3 (br d, *B*H$_3$, $^1J_{B,P}$ = 33 Hz). The resulting product was used for catalytic dehydrocoupling experiments without further purification.

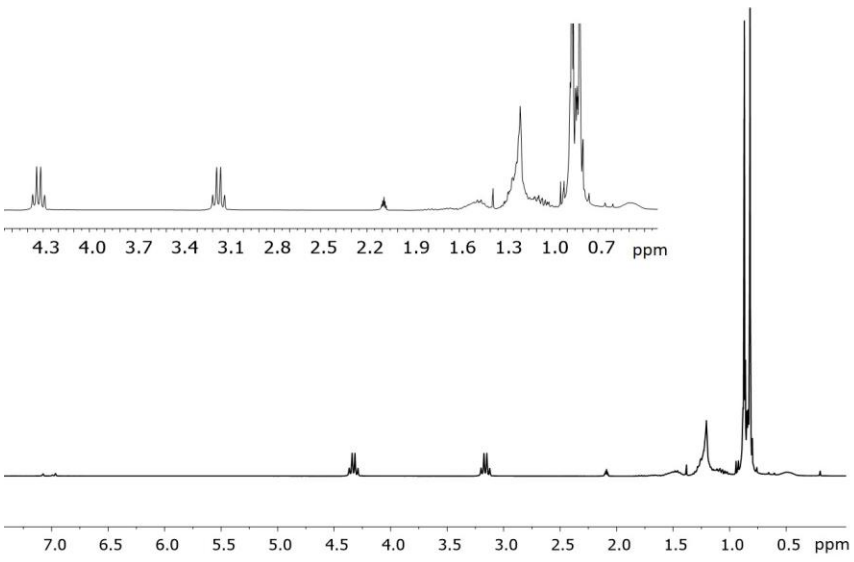

Figure S4: ^{1}H (300 MHz) NMR spectra of ^{t}BuPH$_2$·BH$_3$ in toluene-d8.

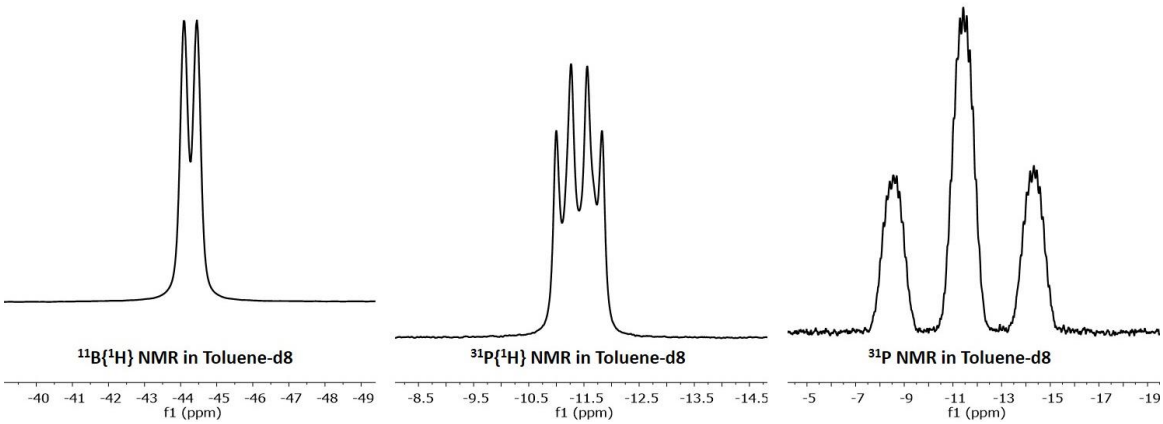

Figure S5: (*left*) $^{11}B\{^1H\}$ (96 MHz), *(middle)* $^{31}P\{^1H\}$ (121 MHz), *(right)* ^{31}P (121 MHz) NMR spectra of $^tBuPH_2{\cdot}BH_3$ in toluene-d8.

Polymerization Experiments:

Polymerization of H_2P-$BH_2{\cdot}NMe_3$ (1a) to form $[H_2P–BH_2]_n$ (3a)

a) 0.300 mL (262 mg, 2.5 mmol) of H_2P-$BH_2{\cdot}NMe_3$ was dissolved in 10 mL of toluene and heated at 80 °C for 20 h. All volatiles were removed under vacuum to give a white residue with an oily to wax like consistency which was nearly insoluble in all common solvents. Efforts were carried out to purify $[PH_2–BH_2]_n$ by extraction with different solvents but were not successful. Extracts in different solvents were analysed by ESI-MS, EI-MS, NMR and DLS. Yield of (**3a**): no reliable determination was possible, as the polymer contains solvent and trace starting material. $^{31}P\{^1H\}$ NMR (121 MHz, C_6D_6): δ = –109.7 (br), –115 (br), –132.5 (br). ^{11}B NMR (96 MHz, C_6D_6): δ = –38 to –41 (m, br, BH_2), –8 to –10 (td, br, BH_2). $^{11}B\{^1H\}$ NMR (96 MHz, C_6D_6): δ = –38 to –41 (m, br, BH_2), –8 to –10 (d, br, BH_2).

b) 0.300 mL (262 mg, 2.5 mmol) of H_2P-$BH_2{\cdot}NMe_3$ was heated at 80 °C for 70 h, affording a white waxy residue which was nearly insoluble in all common solvents. Efforts to purify $[PH_2–BH_2]_n$ by extraction with different solvents were not successful. Analysis of **3a** was conducted by ESI-MS, EI-MS, NMR and DLS. Yield of (**3a**): 86 mg (75 %) ^1H NMR (300 MHz, C_6D_6): δ = 1.8 (br, BH_2), 3.6 (br, PH_2). $^{31}P\{^1H\}$ NMR (121 MHz, C_6D_6): δ = –112 to –105 (br), –125 to –120 (br), –132 (br), –142 (br). ^{11}B NMR (96 MHz, C_6D_6): δ = –34 to –42 (m, br, BH_2), –6 to –12 (td, br, BH_2). $^{11}B\{^1H\}$ NMR (96 MHz, C_6D_6): δ = –34 to –42 (m, br, BH_2), –6 to –12 (d, br, BH_2).

ESI-MS of **3a** (obtained from polymerization reaction in toluene, 80 ^oC, 20 h) in acetonitrile showed signals up to 1700 Da. A systematic loss of 46 m/z, consistent with [H_2P-BH_2] was observed (Figure S12). The polymer consists of at least 37 repeat units, however no exact end groups could be determined by ESI-MS.

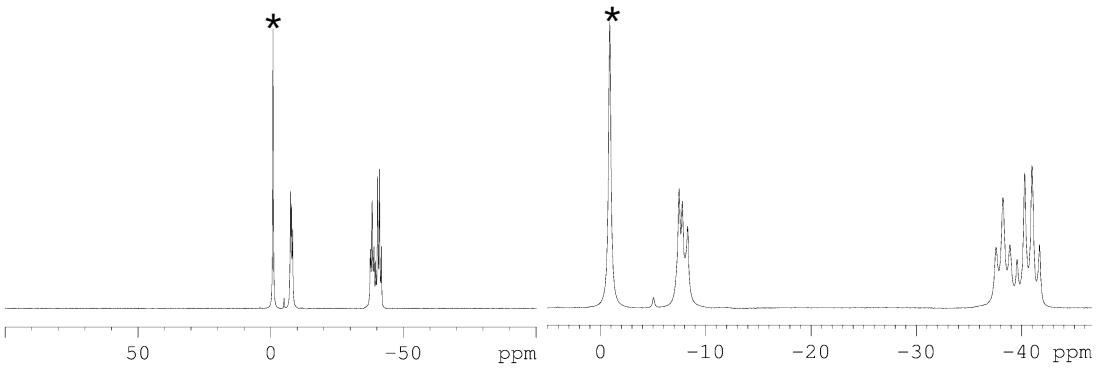

Figure S6: $^{11}B\{^{1}H\}$ (96 MHz) NMR spectra of **3a** (from polymerization reaction in toluene, 80 ^{o}C, 20 h) in C_6D_6; * = $ClBH_2{\cdot}NMe_3$ (starting material for **1a**).

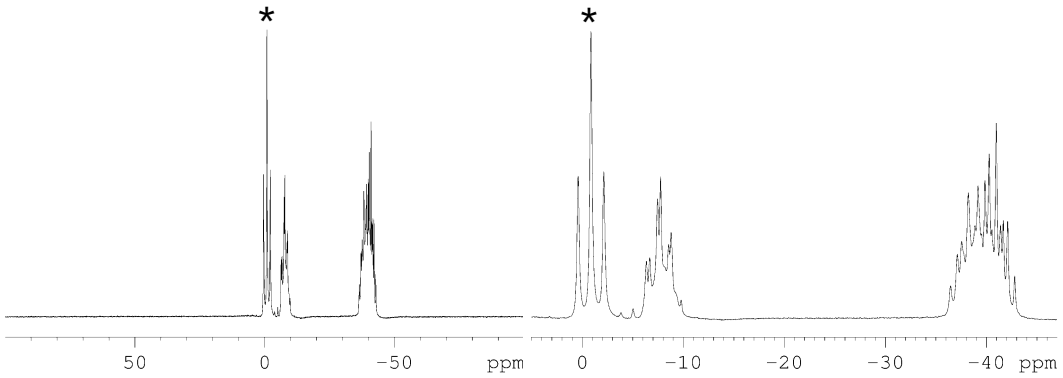

Figure S7: ^{11}B (96 MHz) NMR spectra of **3a** (from polymerization reaction in toluene, 80 ^{o}C, 20 h) in C_6D_6; * = $ClBH_2{\cdot}NMe_3$ (starting material for **1a**).

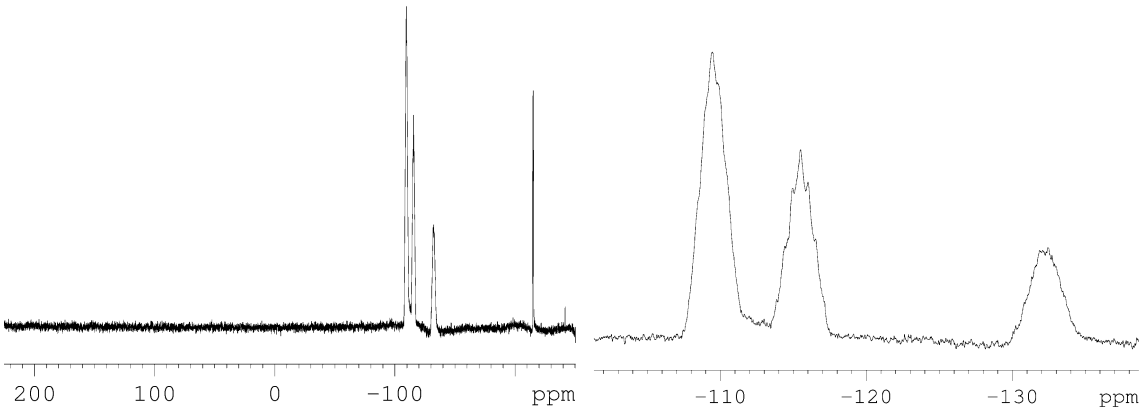

Figure S8: $^{31}P\{^{1}H\}$ (121 MHz) NMR spectra of **3a** (from polymerization reaction in toluene, 80 ^{o}C, 20 h) in C_6D_6.

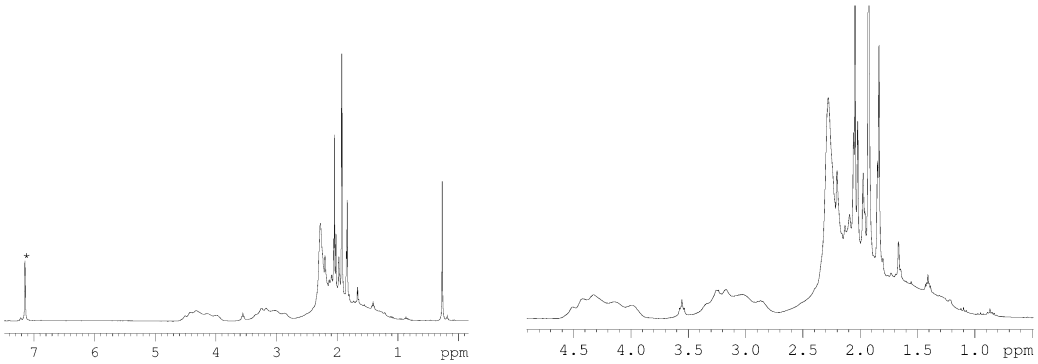

Figure S9: ^{1}H (300 MHz) NMR spectra of **3a** (from neat polymerization reaction, 80 ^{o}C, 70 h) in C_6D_6; * = solvent (C_6D_6).

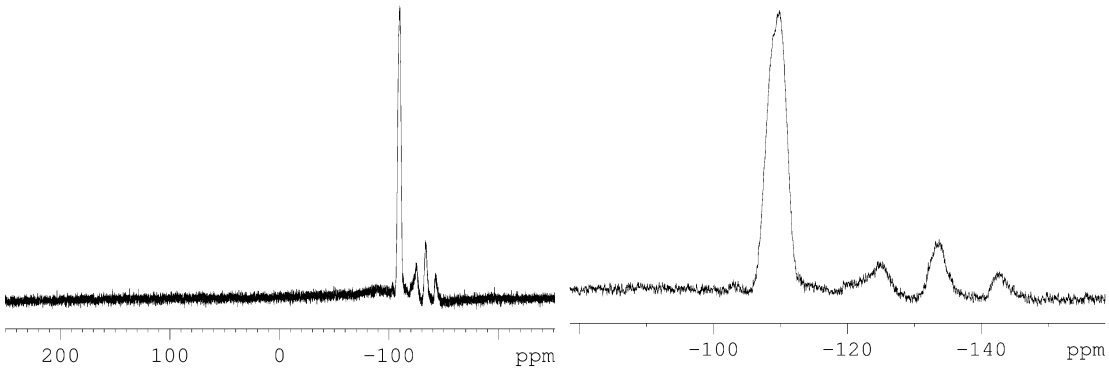

Figure S10: $^{31}P\{^{1}H\}$ (121 MHz) NMR spectra of **3a** (from neat polymerization reaction, 80 ^{o}C, 70 h) in C_6D_6.

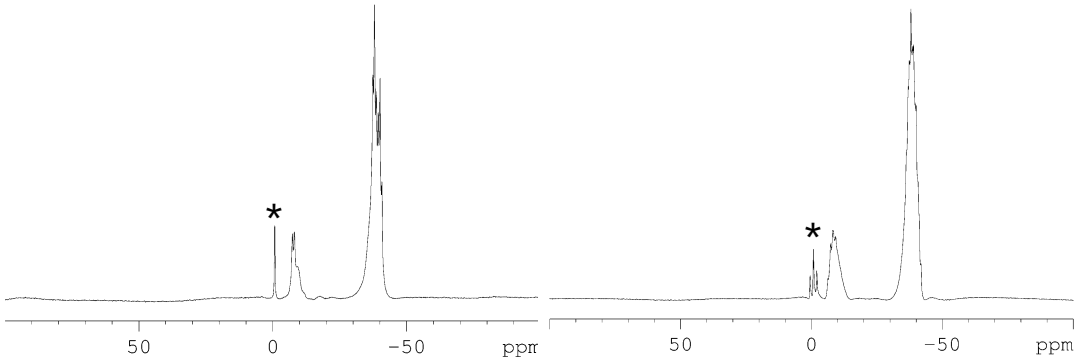

Figure S11: (*left*) $^{11}B\{^{1}H\}$ (96 MHz), (*right*) ^{11}B (96 MHz) NMR spectra of **3a** (from neat polymerization reaction, 80 ^{o}C, 70 h) in C_6D_6; * = $ClBH_2{\cdot}NMe_3$ (starting material for **1a**).

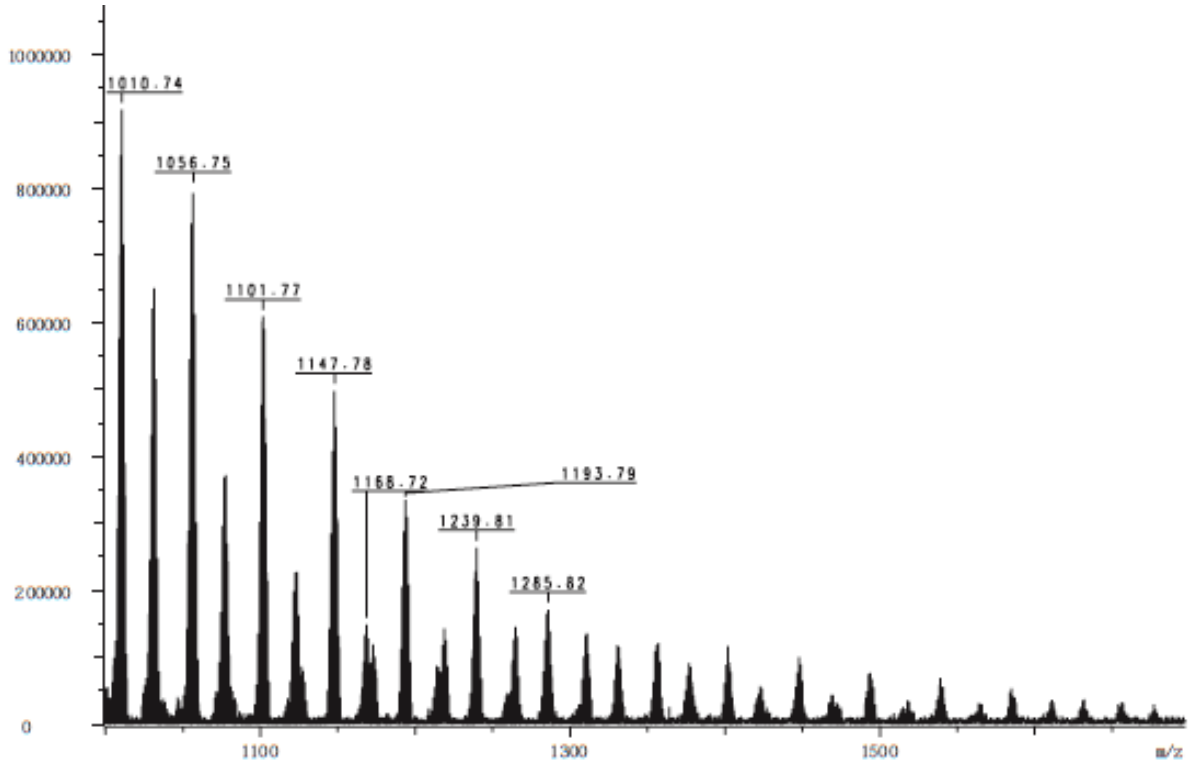

Figure S12: ESI – mass spectrum of **3a** (from polymerization reaction in toluene, 80 ^{o}C, 20 h) in acetonitrile.

Attempted Polymerization of Ph_2P-BH_2·NMe_3 (1b) to form $[Ph_2P–BH_2]_n$ (3b)

600 mg (2.33 mmol) of Ph_2P-BH_2·NMe_3 was dissolved in 20 mL toluene and heated to 100 °C for 18 h. All volatiles were removed under vacuum affording a fine white powder (**3b**). NMR measurement of a sample showed that the reaction proceeded cleanly, so no further purification was conducted prior to analysis. Yield of (**3b**): 402 mg (86 %) ^{31}P NMR (162 MHz, THF-d8): δ = –18.5 (s, br, P). $^{31}P\{^{1}H\}$ NMR (162 MHz, THF-d8): δ = –18.5 (s, br, P). ^{11}B NMR (128 MHz, THF-d8): δ = –33.7 (br, BH_2). $^{11}B\{^{1}H\}$ NMR (128 MHz, THF-d8): δ = –33.7 (br, BH_2).

Thermolysis of **1b** in toluene at 100 °C for 18 h led to complete consumption of the starting material and formation of **3b**. The $^{31}P\{^{1}H\}$ NMR featured a very broad signal at δ = -18 ppm, which showed further broadening in the ^{31}P NMR spectrum. Generation of a small amount of free phosphine Ph_2PH was also observed. The $^{11}B\{^{1}H\}$ NMR spectrum featured a very broad uniform signal at δ = -34 ppm, suggestive of either a low molecular weight cyclic oligomeric species or a high molecular weight polymer whose end-groups cannot be detected. The observed NMR signals were similar to those reported for $[Ph_2P–BH_2]_3$ and $[Ph_2P–BH_2]_4$.[7] ESI-MS of **3b** in both THF and toluene revealed a fragmentation pattern which featured loss of units with 198 m/z (representative of

[Ph_2P─BH_2]), and a maximum detectable mass in the region of 1200 Da (Figure S15). This was indicative of NMe_3-capped oligomers with no greater than 6 repeat units.

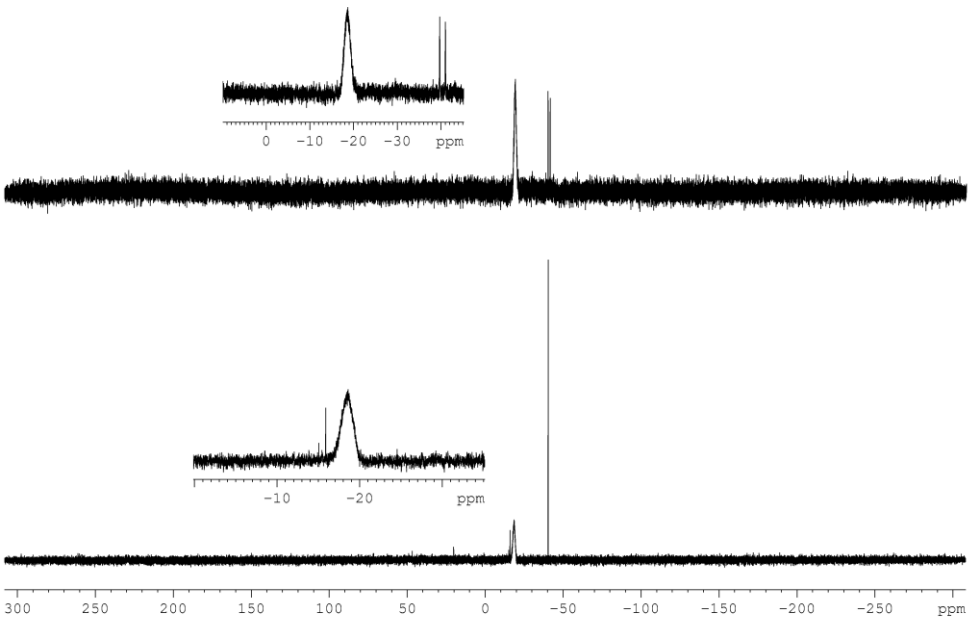

Figure S13: (*bottom*) $^{31}P\{^1H\}$ (162 MHz), (*top*) ^{31}P (162 MHz) NMR spectra of **3b** (from polymerization reaction in toluene, 100 ^oC, 18 h) in THF-d8.

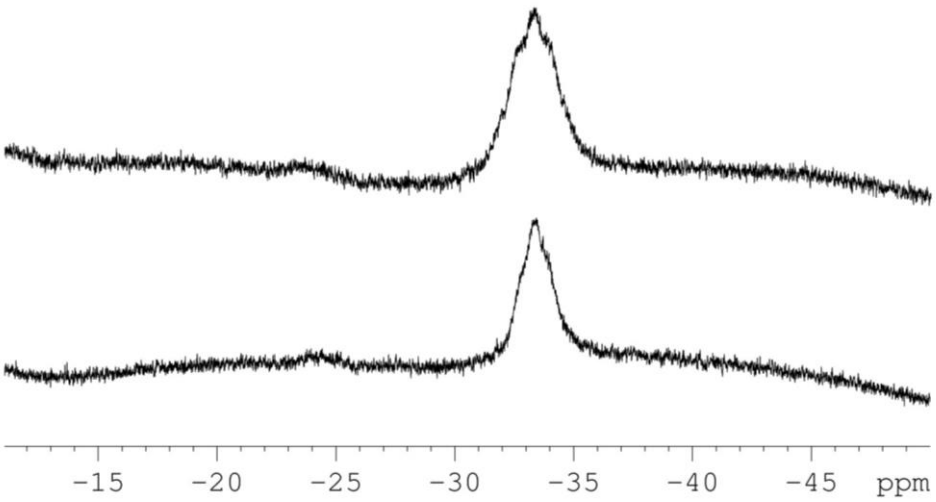

Figure S14: (*bottom*) $^{11}B\{^1H\}$ (128 MHz), (*top*) ^{11}B (128 MHz) NMR spectra of **3b** (from polymerization reaction in toluene, 100 ^oC, 18 h) in THF-d8.

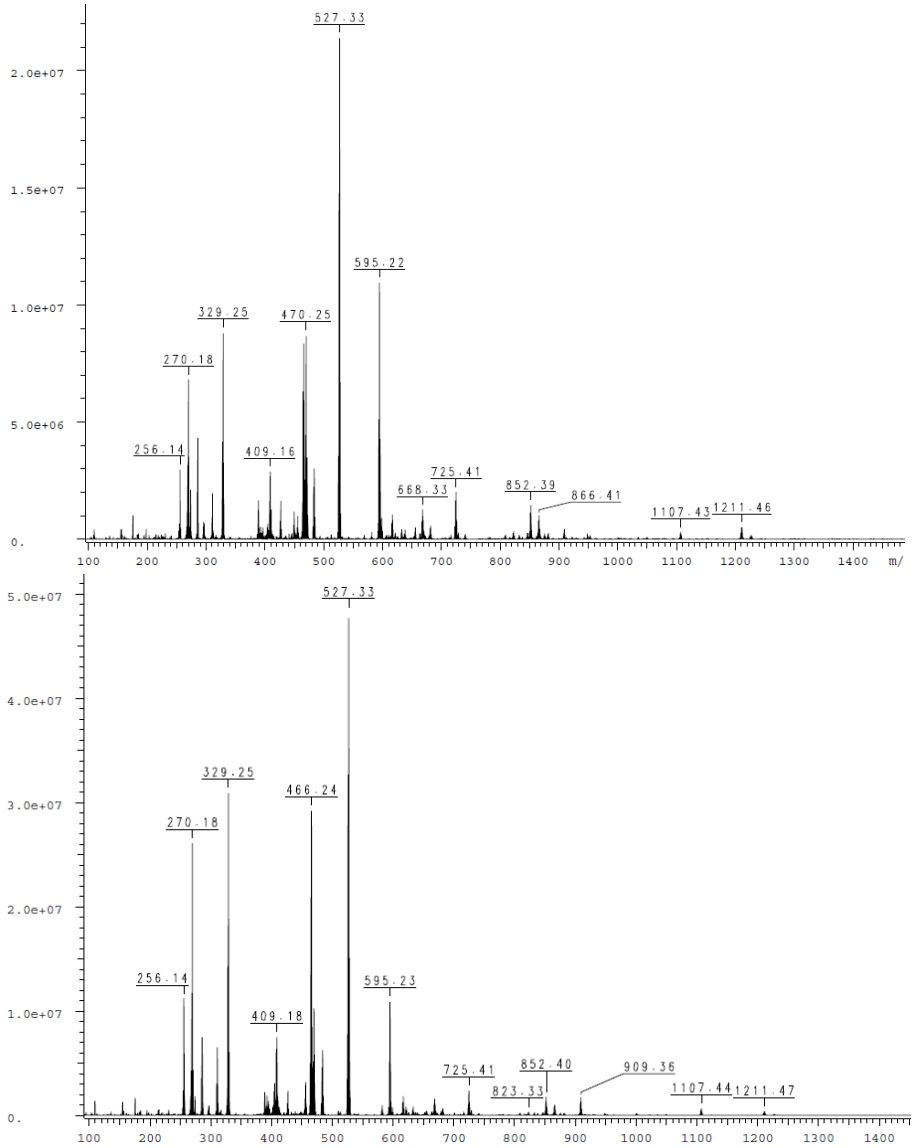

Figure S15: ESI – mass spectra of **3b** (from polymerization reaction in toluene, 100 ^{o}C, 18 h) in THF (*top*), and toluene (*bottom*).

Poly(phosphinoborane) **3b** was analysed by DLS. All samples were characterised by correlation function with a high *y*-intercept, which is indicative of the presence of particles within the measurable size range (1nm – 5µm). It proved impossible, however, to satisfactorily fit the decay of these functions, therefore suggesting that they result from the sum of multiple exponentials and the samples were ultimately too polydisperse for analysis.

Polymerization of ^{t}BuHP-BH$_2$·NMe$_3$ (1c) to form [^{t}BuHP-BH$_2$]$_n$ (3c)

Three methods were employed:

a) 100 mg (0.62 mmol) of ^{t}BuHP-BH$_2$·NMe$_3$ was heated at 40°C for 48 h.

b) 410 mg (2.55 mmol) of ^{t}BuHP-BH$_2$·NMe$_3$ was dissolved in 10 mL toluene and heated at 40°C for 48 h.

c) 500 mg (3.11 mmol) of ^{t}BuHP-BH_2·NMe_3 was dissolved in 10 mL toluene and stirred at room temperature (22 ^{o}C) for 48 h.

After removing all the volatiles under vacuum, the remaining polymer was dissolved in a minimum amount of toluene (*ca.* 1.5 mL). The viscous solution was added drop wise to vigorously stirred acetonitrile (*ca.* 200 mL) and a white rubber-like solid precipitated. The solid was filtered off and dried under vacuum.

Yield of (**3c**): a) 125 mg (40 %)
b) 120 mg (46 %)
c) 250 mg (80 %)

The NMR shifts and corresponding spectra from the polymerization reaction in toluene, 22 ^{o}C, 48 h (c), are shown below. The NMR spectra obtained from the 48 h polymerization reactions in the absence of solvent (a), and in toluene (b) at 40 ^{o}C are similar.

^{1}H NMR (400 MHz, $CDCl_3$): δ = 0.6 -1.6 (s, v br, BH_2), 1.18 (s, br, P^{t}Bu), 3.73 (d, br, $^1J_{H,P}$ = 330 Hz PH). ^{31}P NMR (162 MHz, $CDCl_3$): δ = –18 to –25 (br, PH). ^{31}P{^{1}H} NMR (162 MHz, $CDCl_3$): δ = –18 to –25 (br, PH). ^{11}B NMR (128 MHz, $CDCl_3$): δ = –38 (br, BH_2). ^{11}B{^{1}H} NMR (128 MHz, $CDCl_3$): δ = –38 (br, BH_2). ^{13}C NMR (101 MHz, $CDCl_3$) δ = 26.9 (s, ^{t}Bu), 27.5 – 29.2 (m, v br, ^{t}Bu).

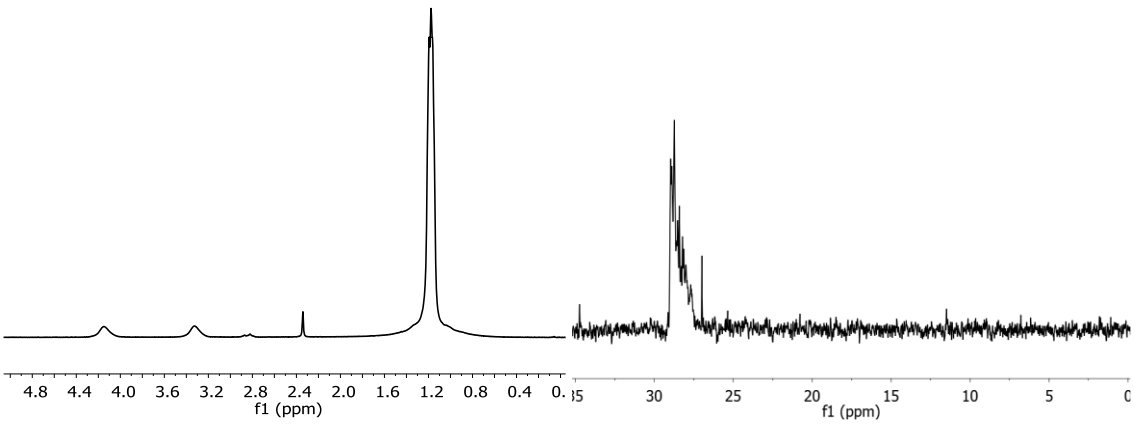

Figure S16: (*left*) ^{1}H (400 MHz), (*right*) ^{13}C (101 MHz) NMR spectra of **3c** (from polymerization reaction in toluene, 22 ^{o}C, 48 h) in $CDCl_3$.

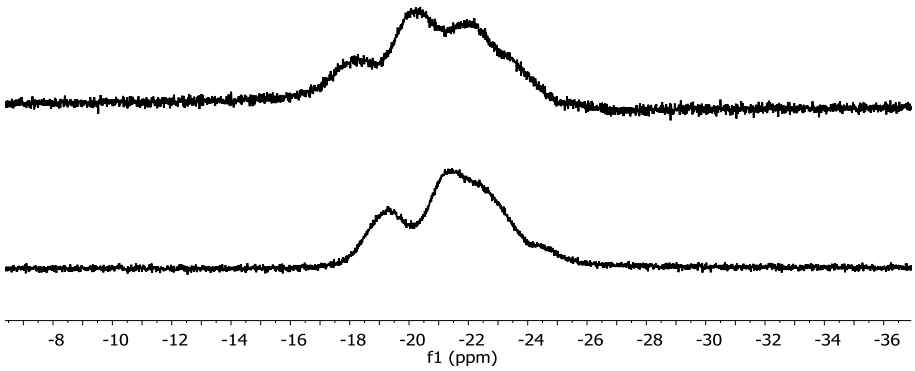

Figure S17: (*bottom*) $^{31}P\{^{1}H\}$ (121 MHz), (*top*) ^{31}P (121 MHz) NMR spectra of **3c** (from polymerization reaction in toluene, 22 ^{o}C, 48 h) in $CDCl_3$.

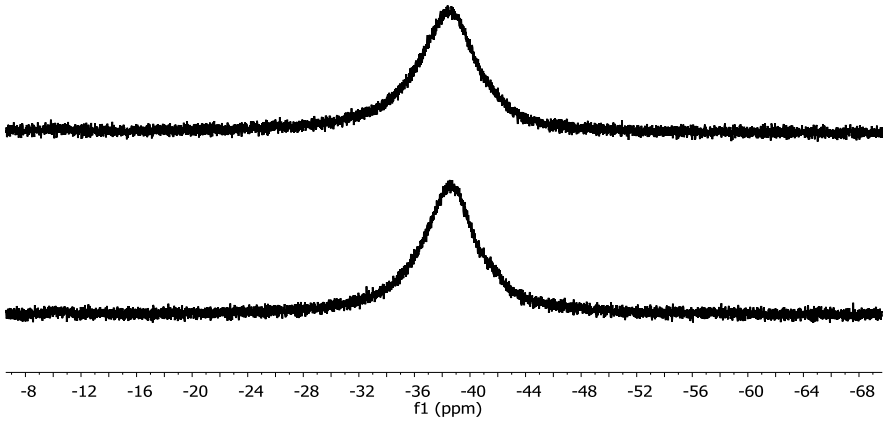

Figure S18: (*bottom*) $^{11}B\{^{1}H\}$ (96 MHz), (*top*) ^{11}B (96 MHz) NMR spectra of **3c** (from polymerization reaction in toluene, 22 ^{o}C, 48 h) in $CDCl_3$.

GPC analysis conducted with THF as eluent resulted in two peaks. A lower molecular weight component ranging from M_n = 17 000 to 22 400 g mol^{-1}, and an apparent higher molecular weight component ranging from M_n = 197 000 to 220 000 g mol^{-1} (Figure S21). The lower molecular weight component is consistent with DLS data (see manuscript, and Figure S20). The absence of a size population by DLS that corresponds to the high molecular weight component is suggestive that the presence of this species is dependent on the conditions applied, and most probably larger aggregates form in diluted THF solutions but not in solutions of CH_2Cl_2. Similar phenomena have been observed for poly(phenylphosphinoborane)[7], where the concentration of aggregates decreases with time and is effectively zero after stirring at room temperature for one day.

Repeated GPC analysis on samples stirred at room temperature for one day showed no significant difference to those analyzed immediately after dissolving in THF. This suggests that if aggregates are present then they are either kinetically more stable than those of the phenyl analogue, or THF is only a marginal solvent for the material (**3c**) prepared in this study.

GPC analysis was then conducted with $CHCl_3$ as eluent. The results are discussed in the main text. See Figures 3 and S22. The results were consistent with DLS data and indicated that these were true values for unimolecularly dissolved polymer chains in solution.

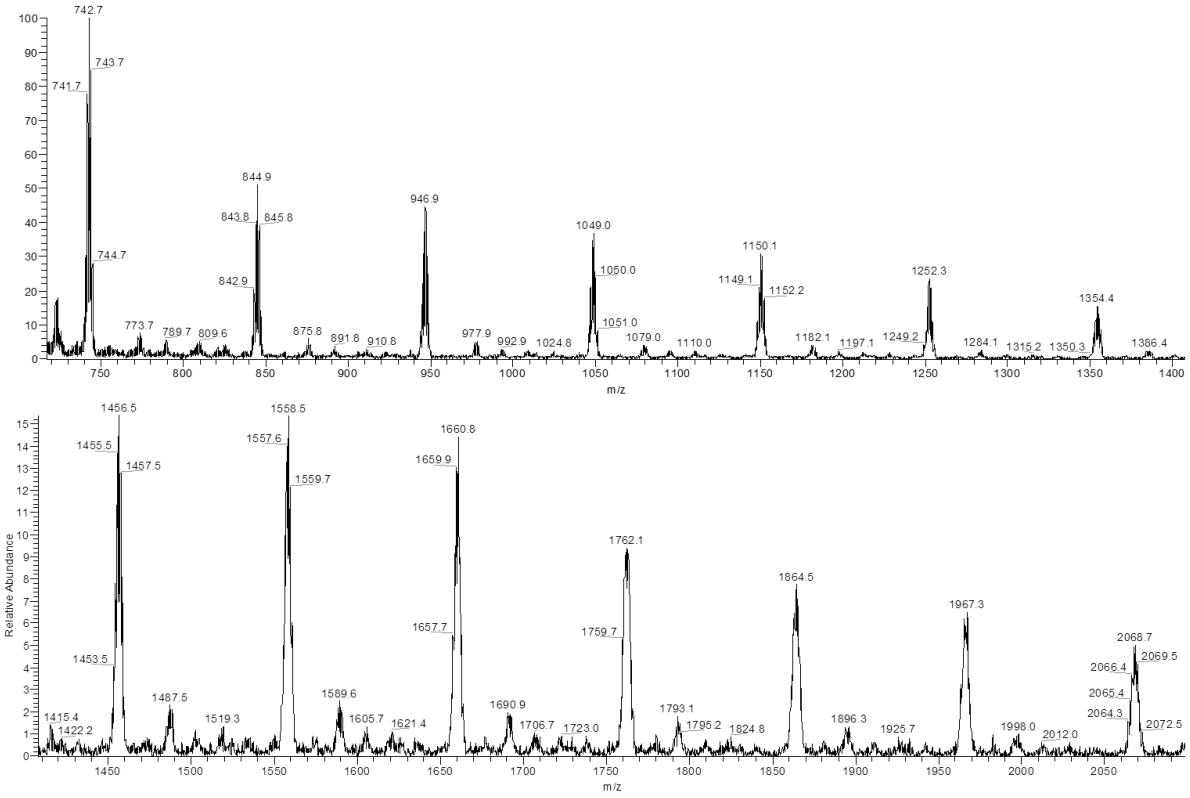

Figure S19: ESI – mass spectra of **3c** (from polymerization reaction in toluene, 22 ^{o}C, 48 h) in acetonitrile.

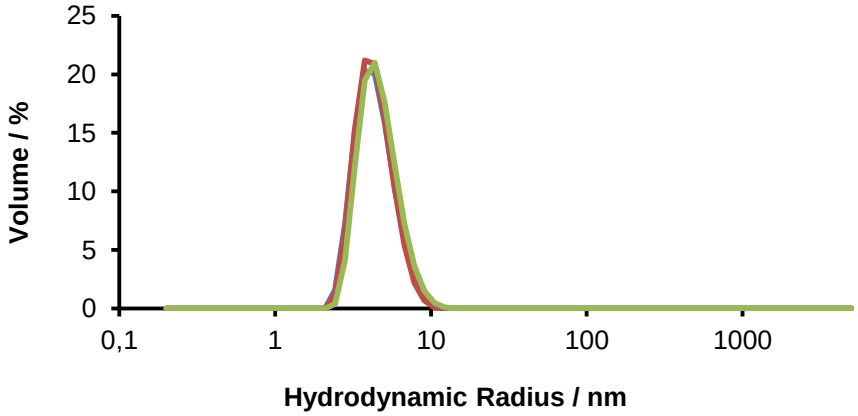

Figure S20: DLS chromatogram of **3c** in $CHCl_3$ isolated from: *blue* (neat, 40 ^{o}C, 48 h) R_h = 5.5 nm; *green* (in toluene, 40 ^{o}C, 48 h) R_h = 4.4 nm; *red* (in toluene, 22 ^{o}C, 48 h) R_h = 5.1 nm.

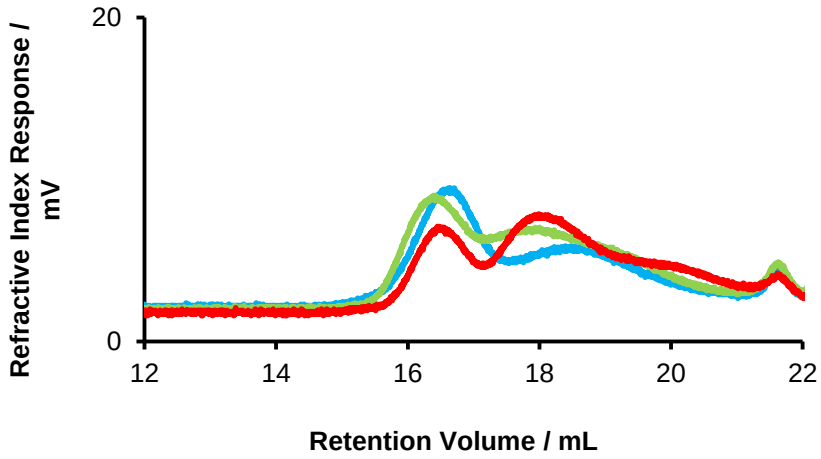

Figure S21: GPC chromatogram of **3c** in THF: *blue* (neat, 40 °C, 48 h); *green* (in toluene, 40 °C, 48 h); *red* (in toluene, 22 °C, 48 h).

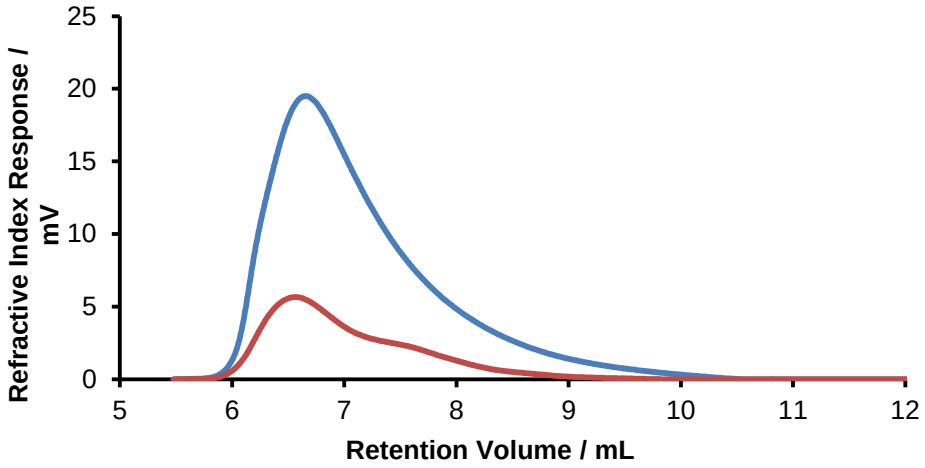

Figure S22: GPC chromatogram of **3c** in $CHCl_3$ isolated from: *red* (neat, 40 °C, 48 h) M_n = 27 800 g mol^{-1}, PDI = 1.9; *blue* (in toluene, 22 °C, 48 h) M_n = 35 000 g mol^{-1}, PDI = 1.6.

Catalytic dehydrocoupling of $^{t}BuPH_2{\cdot}BH_3$ by $Cp(CO)_2Fe(OSO_2CF_3)$ (5 mol%).

To a 1.0 M solution of $^{t}BuPH_2{\cdot}BH_3$ (83 mg, 0.80 mmol), in 0.8 mL of anhydrous toluene was added 5 mol% of $Cp(CO)_2Fe(OSO_2CF_3)$ (12.8 mg, 0.04 mmol). The solution was then charged into a quartz J. Young NMR tube, which was subsequently sealed and allowed to react at 100 °C. The solution turned from dark red to bright yellow within the first hour, and remained so throughout the duration of the reaction. Progress was monitored *in situ* by $^{31}P\{^{1}H\}$ (121 MHz) and $^{11}B\{^{1}H\}$ (96 MHz) NMR spectroscopy for the formation of poly(phosphinoborane) (Figure S23). After consumption of $^{t}BuPH_2{\cdot}BH_3$ (176 h), the reaction solution was transferred into a beaker of cold pentane (-78 °C), which resulted in the precipitation of product. The solution was filtered and washed several

times (3 x 2 mL) with cold pentane and dried under vacuum to afford an amber gum (38 mg, 47% yield). $^{31}P\{^1H\}/^{31}P$ (121 MHz) and $^{11}B\{^1H\}$ (96 MHz) NMR spectroscopy of isolated product in toluene are identical to *in situ* experiments and indicate the presence of multiple broad, ill-defined components ($\delta^{11}B$ -40 ppm, $\delta^{31}P$ -11 ppm).

Catalytic dehydrocoupling of $^tBuPH_2{\cdot}BH_3$ by $Cp(CO)_2Fe(OSO_2CF_3)$ (5 mol%), large scale.

To a 1.0 M solution of $^tBuPH_2{\cdot}BH_3$ (400 mg, 3.80 mmol), in 3.8 mL of anhydrous toluene was added 5 mol% of $Cp(CO)_2Fe(OSO_2CF_3)$ (61 mg, 0.19 mmol). The solution was then charged into a J. Young reaction vessel, which was subsequently sealed and allowed to react at 100 ^oC for 176 h. The solution turned from dark red to bright yellow within the first hour, and remained so throughout the reaction. After 176 h, the reaction solution was then quickly transferred into a beaker of cold pentane (-78 ^oC), which resulted in the immediate precipitation of product. The solution was filtered and washed several times (3 x 2 mL) with cold pentane and dried under vacuum to afford an amber gum (134 mg, 34% yield). $^{31}P\{^1H\}/^{31}P$ (121 MHz) and $^{11}B\{^1H\}$ (96 MHz) NMR spectroscopy of the isolated compound in toluene are identical to *in situ* experiments (*vide supra*) and indicate the presence of multiple, ill-defined components (see Figures S23 and S24). ESI-MS revealed multiple components, with weights no higher than ~1100 g/mol, but with anticipated fragmentation patterns for loss of 102 m/z, corresponding to $[^tBuPH{\cdot}BH_2]$ (Figure S25). GPC analysis of a 2 mg/mL $CHCl_3$ solution of the dark amber gum with $CHCl_3$ as eluent revealed no components within the calibrated range (i.e. greater than ca. 1000 g mol^{-1}). The absence of a peak corresponding to high molar mass material from GPC analysis, in conjuction with the results from ESI-MS indicated a polydisperse mixture of low molecular weight oligomers (~10 units or less as detected).

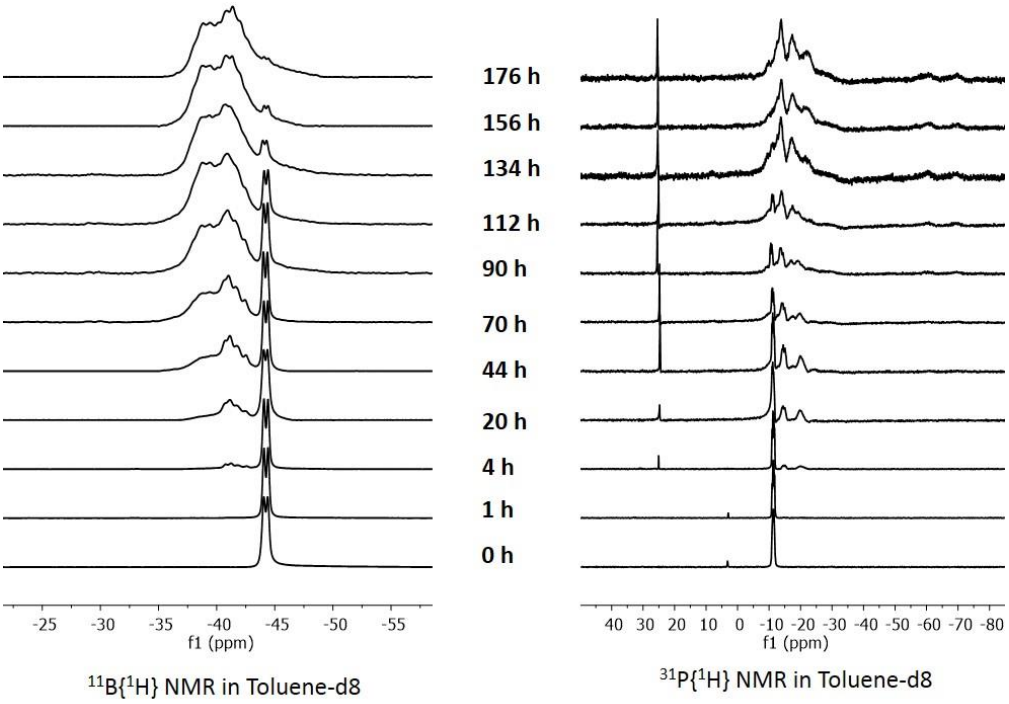

Figure S23: (*left*) $^{11}B\{^1H\}$ (96 MHz), (*right*) $^{31}P\{^1H\}$ (121 MHz) NMR reaction profiles for the dehydrocoupling reaction of $^tBuPH_2{\cdot}BH_3$ to oligomers of $[^tBuPH\text{-}BH_2]_n$ with 5 mol% $Cp(CO)_2Fe(OSO_2CF_3)$ as catalyst in toluene d-8 at 100 ^oC.

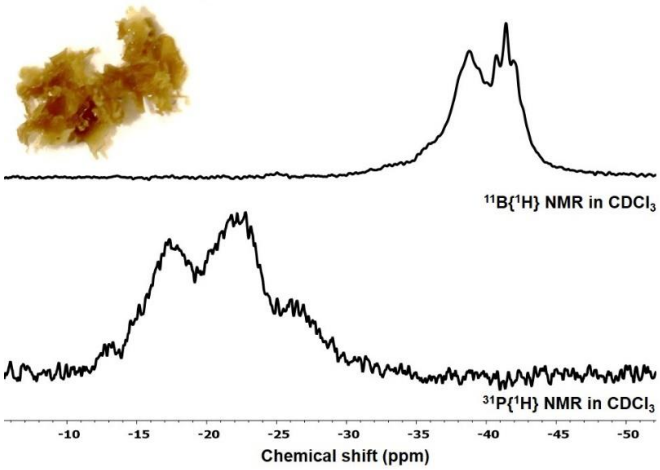

Figure S24: (*bottom*) $^{31}P\{^1H\}$ (121 MHz), (*top*) $^{11}B\{^1H\}$ (96 MHz) NMR spectra of $[^tBuPH\text{-}BH_2]_n$ oligomers in $CDCl_3$; isolated from the large scale reaction of $^tBuPH_2{\cdot}BH_3$ with 5 mol% $Cp(CO)_2Fe(OSO_2CF_3)$ as catalyst in toluene (100 ^oC, 176 h); (*inset*) photo of isolated oligomers.

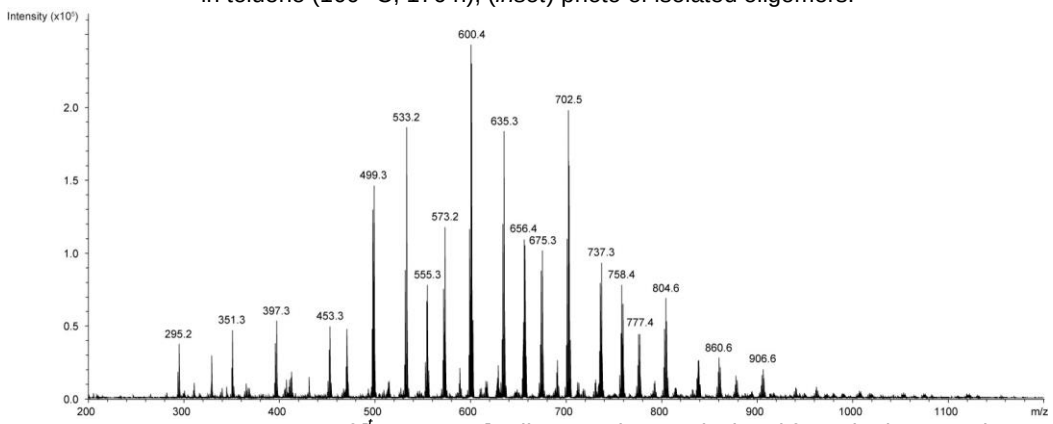

Figure S25: ESI – mass spectrum of $[^tBuPH\text{-}BH_2]_n$ oligomers in THF, isolated from the large scale reaction of $^tBuPH_2{\cdot}BH_3$ with 5 mol% $Cp(CO)_2Fe(OSO_2CF_3)$ as catalyst in toluene (100 ^oC, 176 h).

Crystallographic details

Table S1. Crystallographic data for compounds **1b** and **1c**.

	1b	**1c**
Empirical formula	$C_{15}H_{21}BNP$	$C_7H_{21}BNP$
Formula weight *M*	257.11 g/mol	161.03 g/mol
Crystal	colourless block	colourless block
Crystal size [mm^3]	0.15 x 0.08 x 0.07	0.38 x 0.14 x 0.06
Temperature *T*	123(1) K	123(1) K
Crystal system	orthorhombic	orthorhombic
Space group	*Pca*2_1	*Pnma*
Unit cell dimensions	*a* = 16.5779(2) Å	*a* = 10.1552(2) Å
	b = 6.2048(1) Å	*b* = 10.1654(3) Å
	c = 14.2632(1) Å	*c* = 11.0614(2) Å
	α = 90°	*α* = 90°
	β = 90°	*β* = 90°
	γ = 90°	*γ* = 90°
Volume *V*	1467.15(3) $Å^3$	1141.89(5) $Å^3$
Formula units *Z*	4	4
Absorption coefficient $\mu_{Cu\text{-}K\alpha}$	1.488 mm^{-1}	1.660 mm^{-1}
Density (calculated) ρ_{calc}	1.164 g/cm^3	0.937 g/cm^3
F(000)	552	360
Theta range $\theta_{min}/\theta_{max}$	5.336 / 66.511°	5.912 / 67.044°
Absorption correction	analytical	multi-scan
Index ranges	–18 < *h* < 19	–11 < *h* < 12
	–5 < *k* < 7	–13 < *k* < 12
	–16 < *l* < 16	–13 < *l* < 13
Reflections collected	6445	8996
Independent reflections [$I > 2\sigma(I)$]	2317 (R_{int} = 0.0236)	831 (R_{int} = 0.0480)
Completeness to full *θ*	0.970	0.988
Transmission T_{min} / T_{max}	0.860 / 0.925	0.848 / 1.000
Data / restraints / parameters	2364 / 1 / 214	1074 / 18 / 110
Goodness-of-fit on F^2 *S*	1.031	1.014
Final *R*-values [$I > 2\sigma(I)$]	R_1 = 0.0261	R_1 = 0.0344
	wR_2 = 0.0695	wR_2 = 0.1022
Final *R*-values (all data)	R_1 = 0.0268	R_1 = 0.0453
	wR_2 = 0.0706	wR_2 = 0.1087
Largest difference hole	–0.140	–0.117
and peak *Δρ*	0.233 $eÅ^{-3}$	0.208 $eÅ^{-3}$
Flack parameter	0.007(9)	-

All crystal manipulations were performed under mineral oil or perfluorinated oil. The diffraction experiments were performed at 123 K on an Agilent Technologies Gemini R Ultra diffractometer or an Agilent SuperNova diffractometer with Cu-K_α or Mo- K_α radiation. Crystallographic data together with the details of the experiments are given in Table 1. The cell determination, data reduction and absorption correction for all compounds were performed with the help of the CrysAlis PRO software by Agilent Technologies Ltd. The full-matrix least-square refinement against F^2 was done with ShelXL. During the refinement several restraints and constraints had to be applied. For the description of the refinement strategy we list the commonly used syntax for the ShelXL program (DFIX, SADI, SIMU, ISOR, EADP). All atoms except hydrogen were refined anisotropically if not described otherwise. The H atoms were calculated geometrically and a riding model was used during refinement process. Graphical material was created with the free software Olex2. CCDC-1415883 (**1b**) and CCDC-1415884 (**1c**) contain the supplementary crystallographic data for this paper. These data can be obtained free of charge from The Cambridge Crystallographic Data Centre via www.ccdc.cam.ac.uk/data_request/cif.

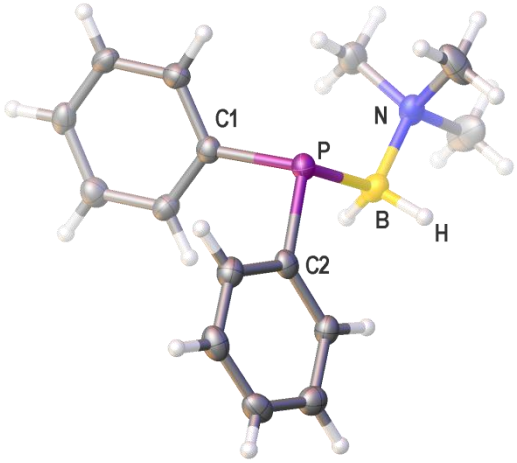

Figure S26. Molecular structure of compound **1b** determined by single crystal X-ray structure analysis (thermal ellipsoids drawn at 50% probability level). Selected bond lengths [Å] and angles [°]: P–B 1.975(2), P-C1 1.849(2), P-C2 1.847(2), B-N 1.619(3), C1–P–C2 99.3(8), C1–P–B 105.7(1), C2–P–B 102.1(1), P–B–N 112.4(2).

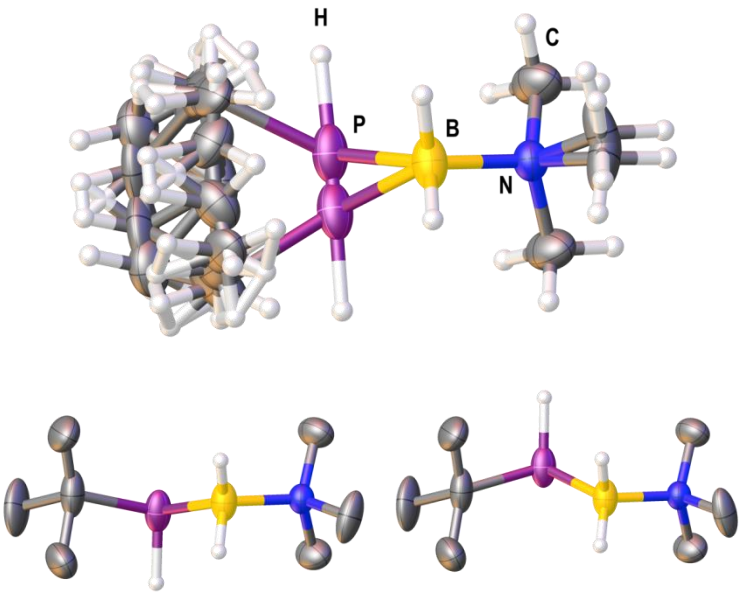

Figure S27. Molecular structure of compound **1c** determined by single crystal X-ray structure analysis (thermal ellipsoids drawn at 50% probability level). (*top*) heavily disordered structure, (*bottom*) the two enantiomers present. Selected bond lengths [Å] and angles [°]: P–B 1.985(2), P–C 1.890(2), N–B 1.621(2), B–P–C 102.7(1), P–B–N 108.9(1).

References

[1] C. Marquardt, C. Thoms, A. Stauber, G. Balazs, M. Bodensteiner, M. Scheer, *Angew. Chem. Int. Ed.* **2014**, *53*, 3727–3730; *Angew. Chem.* **2014**, *126*, 3801–3804.

[2] C. Marquardt, A. Adolf, A. Stauber, M. Bodensteiner, A. V. Virovets, A. Y. Timoshkin, M. Scheer, *Chem. Eur. J.* **2013***, 19*, 11887–11891.

[3] W. A. Herrmann, G. Brauer, *Synthetic Methods of Organometallic and Inorganic Chemistry*, *Vol.* 3 *,* **1996** *,* Thieme Publishers*,* Stuttgart.

[4] Agilent Technologies **2006-2011**, CrysAlisPro Software system, different versions, Agilent Technologies UK Ltd, Oxford, UK.

[5] A. Altomare, M. C.Burla, M. Camalli, G. L. Cascarano, C. Giacovazzo, A. Guagliardi, A.G. G. Moliterni, G. Polidori, R. Spagna, *J. Appl. Cryst.* **1999**, *32*, 115–119.

[6] G. M. Sheldrick, *Acta Cryst.* **2008**, *A64*, 112–122.

[7] O.V. Dolomanov, L.J. Bourhis, R.J. Gildea, J.A.K. Howard, H. Puschmann, OLEX2: A complete structure solution, refinement and analysis program, *J. Appl. Cryst*. **2009**, *42*, 339–341.

[7] H. Dorn, R. A. Singh, J. A. Massey, J. M. Nelson, C. A. Jaska, A. J. Lough, I. Manners, *J. Am. Chem. Soc.* **2000**, *122*, 6669–6678.

3.6 Author Contributions

The syntheses and characterization of compounds **1b** and **1c** were performed by Christian Marquardt.

X-ray structural analyses of **1b** and **1c** were performed by Christian Marquardt and Dr. Alexander V. Virovets.

The syntheses and characterization of compounds **3a** was performed by Dr. Karl-Christian Schwan (reported in his PhD-thesis, Regensburg, **2006**), Dr. Andreas Stauber (reported in his PhD-thesis, Regensburg, **2014**) and Christian Marquardt. Prof. Dr. Anne Staubitz (University of Bremen) and Dr. Holger Helten (RWTH Aachen University) are gratefully acknowledged for helpful discussion.

The syntheses of compounds **3b** and **3c** were performed by Christian Marquardt.

The characterization of compounds **3b** and **3c** were performed by Christian Marquardt (NMR spectroscopy, ESI-MS) and Dr. Titel Jurca (NMR spectroscopy, ESI-MS, GPC- and DLS-experiments; University of Bristol).

Syntheses, characterization, catalytic dehydrocoupling of $^{t}BuPH_2 \cdot BH_3$, and resulting products were performed by Dr. Titel Jurca (University of Bristol).

The GPC- and DLS-experiments were evaluated and interpreted by Dr. Titel Jurca, Dr. George R. Whittell and Prof. Dr. Ian Manners (University of Bristol).

The manuscript (including supporting information, figures, schemes and graphical abstract) was written by Christian Marquardt and Dr. Titel Jurca with equal contributions.

We thank Dr. F. H. Schacher (Friedrich-Schiller-University Jena) for access to GPC equipment that uses $CHCl_3$ as eluent and Dr. P. Gates (University of Bristol) for MS data.

4. Cationic Chains of Phosphanyl- and Arsanylboranes

C. Marquardt, C. Thoms, A. Stauber, G. Balázs, M. Bodensteiner and M. Scheer

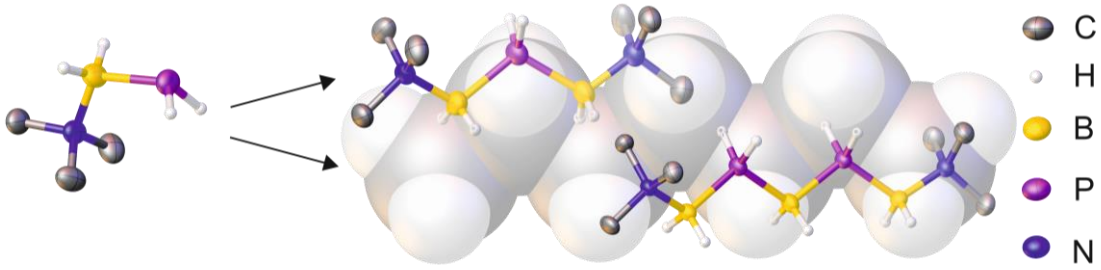

Abstract: Whilst catena-phosphorus cations have been intensively studied in the last years, mixed group 13/15 element cationic chains have not been reported so far. Reaction of the pnictogenylboranes $H_2EBH_2{\cdot}NMe_3$ (E = P, As) with monohalideboranes lead to the cationic chain compounds $[Me_3N{\cdot}BH_2EH_2BH_2{\cdot}NMe_3][X]$ (E = P, As; X= $AlCl_4$, I) and $[Me_3N{\cdot}BH_2PH_2BH_2PH_2BH_2{\cdot}NMe_3][X]$ (X = I, $VCl_4(THF)_2$), respectively. All compounds have been characterized by X-ray structure analysis, NMR spectroscopy, IR spectroscopy and mass spectrometry. DFT calculations elucidate the reaction pathway, the high thermodynamic stability, the charge distribution within the chain and confirm the observed solid-state structures.

4.1 Introduction

Over the last years, efforts at catenation of non-carbon elements have gained increasing attention. Whereas several chains of polyphosphines and polyphosphorus anions have been reported,[1-6] only recently the chemistry of *catena*-phosphorus cations has been discovered by *Burford et al.,* leading to a wide variety of new *catena*-phosphorus species (cf. **A**-**C**).[7] Besides linear chains, other structural motifs were found. Particularly cationic cycles[8,9] like **D** and cages such as **E** are known, and their reactivity has been studied.[10]

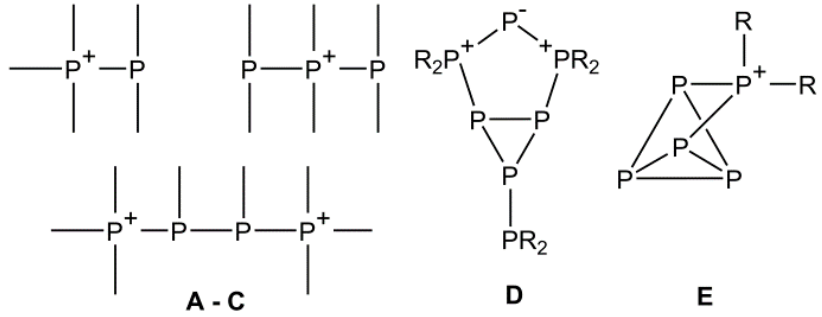

Otherwise boron compounds tend to form higher aggregated clusters rather than linear chains.[11] Although hints were given for the existence of a linear $B_8(NMe_2)_{10}$ compound,[12] the only structural characterized longer derivatives are $B_4(NMe_2)_6$[13] and a cyclic $B_6(NMe_2)_6$.[14] Recently, a B_4R_4 chain was stabilized in the coordination sphere of a transition metal.[15] All examples reveal the requirement of organic substituents for catenation. A similar need was found for a reported In_6 chain.[16]

Lewis acid/base adduct compounds for group 13/15 elements of the type $R_3E{\cdot}E'R_3$ (E = group 15 element, E' = group 13 element) are electronically and structurally related to hydrocarbons. The poly(amino- and poly(phosphinoborane)s are mainly obtained by dehydrogenation/dehydrocoupling reactions mediated by metal catalysts and represents the inorganic analogues of polymers like polyolefins.[17,18]

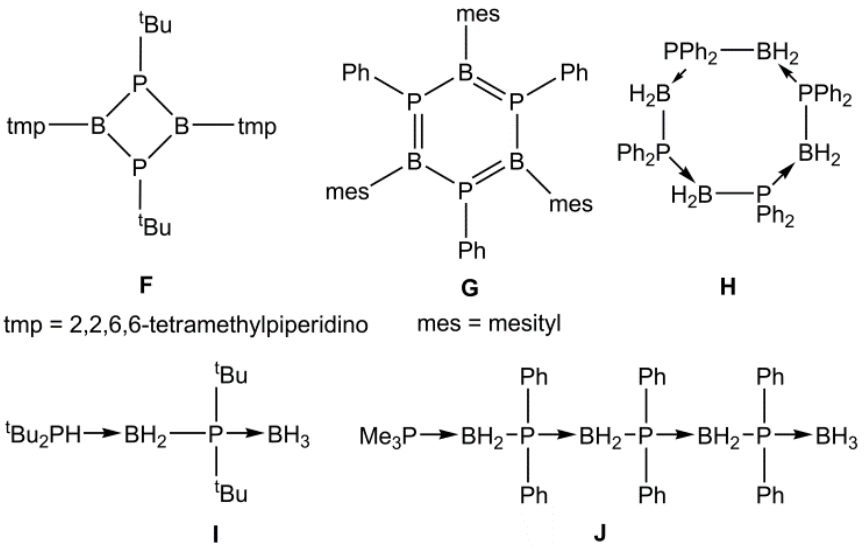

Among the different structural motifs of oligo(phosphinoborane)s only the ring systems (**F**,[19] **G**[19c] and **H**[20]) and the short 4-membered chain **I**[21] have been characterized by X-ray structural analysis for which the presence of organic substituents is very helpful. Longer chain molecules like **J**[22] were only characterized by spectroscopy.

We are especially interested in the synthesis of *parent* 13/15 compounds containing E–H bonds,[23] and reported recently the high yield synthesis of the pnictogenylboranes $H_2EBH_2{\cdot}NMe_3$ (E = P, As).[24] Since they possess a Lewis basic lone pair, they are an ideal starting material for the synthesis of oligomeric compounds containing mixed group 13/15 element chains by NMe_3 elimination. For instance, dehydro-oligomerization by titanocene leads to unprecedented phosphinoborane chain complexes.[25] Since only neutral and complex-bound chain compounds have been reported so far,[25,23b] the quest for cationic chain molecules remains open. Herein we report the synthesis and characterization of the first cationic chain compounds containing mixed group 13/15 elements, including the first arsenic-containing chain molecules.

4.2 Results and Discussion

The reaction of the phosphanyl- or the arsanylborane $H_2EBH_2{\cdot}NMe_3$ (E = P, As) with one equivalent of $AlCl_3$ and $ClBH_2{\cdot}NMe_3$ leads to the formation of **1** revealing the cationic chain $[Me_3N{\cdot}BH_2{-}EH_2{-}BH_2{\cdot}NMe_3]^+$ (**1a**: E = P, **1b**: E = As) (Scheme 1, i).

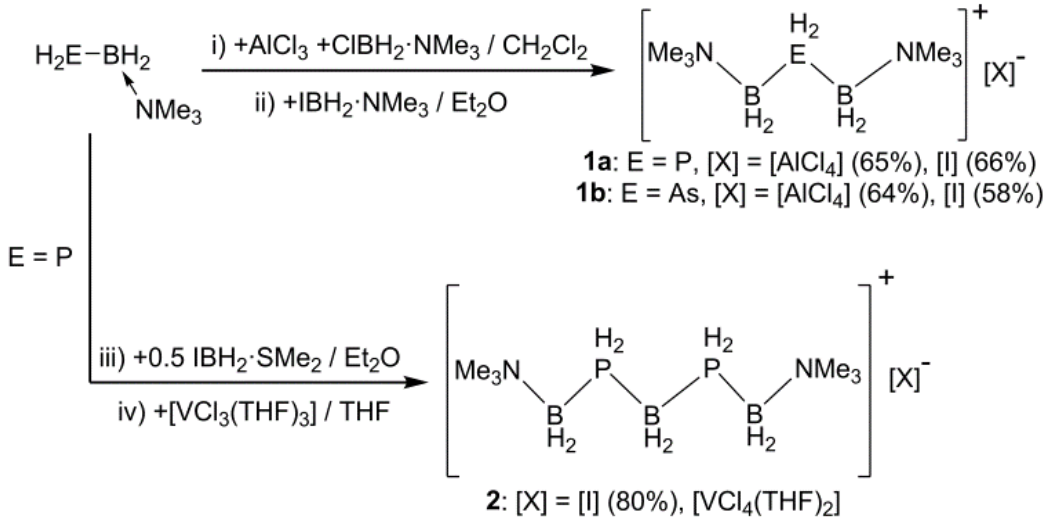

Scheme 1. Synthesis of cationic phosphanylborane chain compounds (yields in parentheses): i) +$AlCl_3$ +$ClBH_2{\cdot}NMe_3$ in CH_2Cl_2; ii) +$IBH_2{\cdot}NMe_3$ in Et_2O; iii) +0.5 $IBH_2{\cdot}SMe_2$ in Et_2O; iv) +$[VCl_3(THF)_3]$ in THF.

According to ^{31}P NMR investigations, the reaction proceeds without any formation of side products, and the compounds **1a,b** can be isolated as crystalline solids in good yields (**1a**[$AlCl_4$]: E = P 65%, **1b**[$AlCl_4$]: E = As 64%). For **1a**[$AlCl_4$], the ^{31}P NMR spectrum shows a very broad triplet at $\delta = -135.0$ ppm. The ^{11}B NMR spectra of **1a**[$AlCl_4$] and **1b**[$AlCl_4$] show similar chemical shifts at $\delta = -11.7$ ppm (**1a**[$AlCl_4$]) and $\delta = -9.1$ ppm (**1b**[$AlCl_4$]). In the solid state **1a** adopts a zigzag conformation, with all substituents being in an antiperiplanar position (Figure 1). The P–B bond length of 1.957(3) Å is slightly shortened compared to the starting material (1.976(2) Å for $H_2PBH_2{\cdot}NMe_3$[23b]). The dihedral-angle defined by the two B–P–B units is only 6.4(1)° indicating an almost ideal zigzag conformation. In the solid state, weak H···Cl interactions between the PH_2 groups of the cation and $AlCl_4$ are observed (H···Cl distances 2.83 Å) which are slightly below the sum of the van der Waals radii of chlorine and hydrogen ($\sum r_{vdW\ H,Cl} = 2.85$ Å).[26]

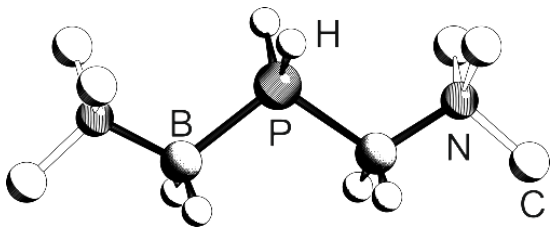

Figure 1. Molecular structure of the cation in **1a**[$AlCl_4$] and **1a**[I] in the solid state. Hydrogen atoms at the methyl groups are omitted for clarity. Selected bond lengths [Å] and angles [°]: **1a**[$AlCl_4$]: P–B 1.957(2), N–B 1.594(2)-1.600(2); B–P–B 107.5(8), N–B–P 114.6(1)–114.7(1); **1a**[I]: P–B 1.959(5)-1.966(5), N–B 1.601(6)–1.608(6); B–P–B 111.5(8), N–B–P 113.0(3)–113.8(3).

Interestingly, **1b** shows a distorted zigzag chain in the solid state (Figure 2) with two nearly identical As–B bond lengths (2.076(3) - 2.086(3) Å, 2.071(4) Å for

$H_2AsBH_2{\cdot}NMe_3$[24]). One of the two B–As units adopts an antiperiplanar conformation, whereas the second one shows a synclinal conformation, leading to a dihedral angle of 58.5(2)°. According to DFT calculations, the conformation with two antiperiplanar B–As units is more stable by 3.5 $kJ{\cdot}mol^{-1}$ in solution. Hence, the conformation found in the solid state of **1b** is probably a result of packing effects. It is noteworthy that for **1b**[$AlCl_4$] no H···Cl interactions are observed in the solid state.

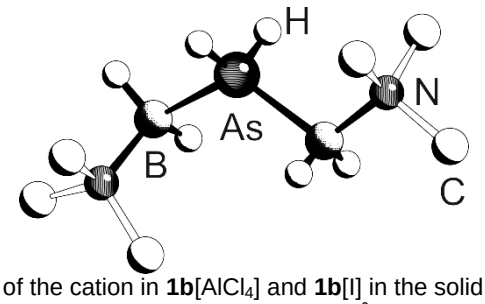

Figure 2. Molecular structure of the cation in **1b**[$AlCl_4$] and **1b**[I] in the solid state. The hydrogen atoms at the methyl groups are omitted for clarity. Selected bond lengths [Å] and angles [°]: **1b**[$AlCl_4$]: As–B 2.076(3)-2.086(4), N–B 1.590(4)-1.595(5); B–As–B 123.0(1), N–B–As 113.3(2)-113.8(2); **1b**[I]: As–B 2.076(5)-2.077(6), N–B 1.587(6)-1.591(6); B–As–B 123.3(2), N–B–As 112.2(4)-112.8(3).

To elucidate the formation pathway, different experiments were carried out. Reacting $H_2EBH_2{\cdot}NMe_3$ (E = P, As) with $AlCl_3$ results in the formation of the Lewis acid/base adduct $AlCl_3{\cdot}H_2EBH_2{\cdot}NMe_3$ (E = P, As). The subsequent addition of $ClBH_2{\cdot}NMe_3$ in CH_2Cl_2 neatly yields **1**[$AlCl_4$], probably via the intermediary hyper-coordinated Al species $Me_3N{\cdot}BH_2Cl{\cdot}AlCl_3{\cdot}H_2EBH_2{\cdot}NMe_3$ (E = P, As). If $ClBH_2{\cdot}NMe_3$ is first treated with $AlCl_3$, followed by $H_2EBH_2{\cdot}NMe_3$ (E = P, As), the yield of the reaction decreases significantly. This is probably a consequence of the less stable intermediate boranylium cation [$Me_3N{\cdot}BH_2$][$AlCl_4$]. Note that no change of reactivity is observed if $AlCl_3$ is added to a mixture of the corresponding pnictogenylborane and $ClBH_2{\cdot}NMe_3$.

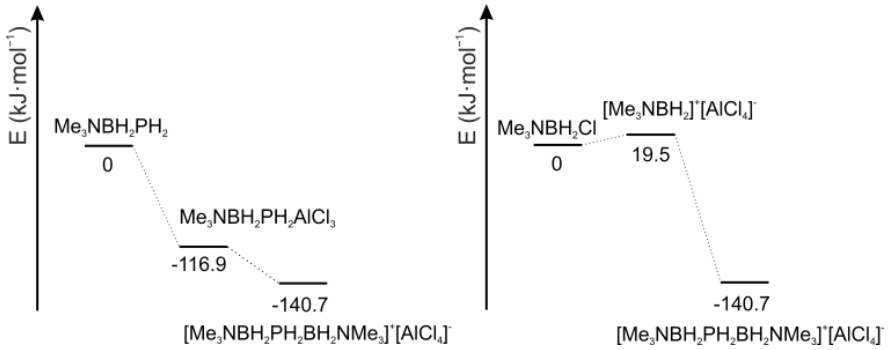

Figure 3. Energy profile of the reaction of $PH_2BH_2{\cdot}NMe_3$, $AlCl_3$ and $ClBH_2{\cdot}NMe_3$, starting from: a) $PH_2BH_2{\cdot}NMe_3$ and b) $ClBH_2{\cdot}NMe_3$

This reaction pathway is further supported by DFT calculations. The overall reaction of $H_2PBH_2{\cdot}NMe_3$ with $AlCl_3$ and $ClBH_2{\cdot}NMe_3$ to form [**1a**][$AlCl_4$] is endothermic by 95.9

kJ·mol^{-1} in the gas phase. However, it becomes exothermic by −140.7 kJ·mol^{-1} when the solvent effects are incorporated. The initial step towards the Lewis acid/base adduct $Me_3N{\cdot}BH_2PH_2{\cdot}AlCl_3$ is exothermic by -116.9 kJ·mol^{-1}, whereas the formation of the boranylium cation $Me_3N{\cdot}BH_2^+$ is endothermic by 19.5 kJ·mol^{-1}, but followed by the strongly exothermic addition of the second phosphanylborane unit (Figure 3). Hence, both energy profiles are feasible and in a good agreement with the experimental observations.

When $IBH_2{\cdot}NMe_3$, is treated with $H_2EBH_2{\cdot}NMe_3$ (E = As, P), no halogen abstracting agent is necessary to form **1**[I] (**1a**: E = P, **1b**: E = As) in good yields, due to the much better leaving group iodine (Scheme 1; ii). The spectroscopic data and geometric parameters of **1** are essentially identical with the compounds **1**[$AlCl_4$]. In the solid state **1a**[I] and **1b**[I] are isostructural to their [$AlCl_4$] derivatives. Even the weak interactions between the hydrogen atoms of the EH_2 groups and the counter ion are present.

The Natural Population Analysis (NPA) shows a relatively strong charge separation within the cationic chain of **1**, the positive charge being accumulated on the central P (+0.52e) and As (+0.53e) atom, whereas the B atoms are negatively charged (−0.22e and −0.18e for **1a** and **1b**, respectively). Based on the charge distribution the B–E–B unit (E = P, As) can formally be described as a phosphonium or arsonium cation.

Furthermore, we tried to create more extended B–P frameworks by combining the good leaving group iodide with an even more labile Lewis base. The corresponding reaction of $IBH_2{\cdot}SMe_2$ with $H_2PBH_2{\cdot}NMe_3$ leads to the formation of $[Me_3N{\cdot}BH_2{-}PH_2{-}BH_2{-}PH_2{-}BH_2{\cdot}NMe_3]^+[I]^-$ (**2**[I], Scheme 1, iii) in high yields. Interestingly, when $H_2PBH_2{\cdot}NMe_3$ is reacted with [$VCl_3(THF)_3$], **2**[$VCl_4(THF)_2$] is obtained (Scheme 1 , iv). However, the exact yield of the reaction could not be determined, as [$HNMe_3$][$VCl_4(THF)_2$] co-crystallizes with **2**[$VCl_4(THF)_2$]. We attribute the formation of **2**[$VCl_4(THF)_2$] to the presence of $ClBH_2{\cdot}NMe_3$ in the starting material $H_2PBH_2{\cdot}NMe_3$.[24] [$VCl_3(THF)_3$] acts as halide abstractor leading to the formation of the boranylium cation $BH_2{\cdot}NMe_3^+$ which reacts with $H_2PBH_2{\cdot}NMe_3$ to give **2**[$VCl_4(THF)_2$]. The NMR spectra of **2**[$VCl_4(THF)_2$] and **2**[I] show similar chemical shifts. The solid-state structures of **2**[I] and **2**[$VCl_4(THF)_2$] show the cation **2** in an *all*-antiperiplanar conformation in **2**[$VCl_4(THF)_2$] featuring an ideal zigzag chain whereas in **2**[I] the arrangement along the two central B–P bonds is synclinal (Figures 4 and 5). According to DFT calculations, the energy difference between the both alignments in solution is only 5.8 kJ·mol^{-1}, favoring the *all*-antiperiplanar conformation. Hence, the observed different conformations of **2** probably originate from the size of the counter ion and packing effects.

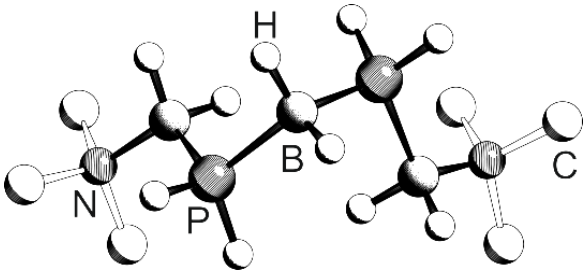

Figure 4. Molecular structure of the cation of **2**[I] in the solid state. The hydrogen atoms at the methyl groups are omitted for clarity. Selected bond lengths [Å] and angles [°]: P–B 1.948(3) - 1.949(5), N–B 1.595(6); B–P–B 110.6(2), P–B–P 108.2(1), N–B–P 116.9(3), B–P–B–P 51.7(2).

An NPA analysis for **2** shows a more accentuated charge separation comparing to **1**. The positive charge is equally localized on the two phosphorus atoms (+0.58e), whereas the negative charge is considerably higher on the central boron atom (−0.74e) relative to the peripheral boron atoms (−0.23e). Hence, the charge distribution again shows the pronounced ionicity of the B–P–B–P–B chains.

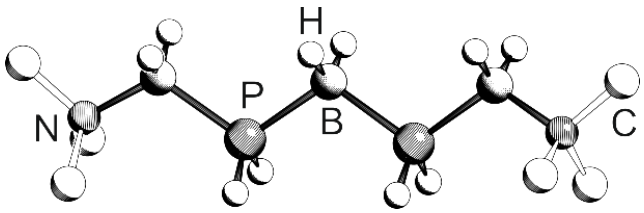

Figure 5. Molecular structure of the cation of **2**[$VCl_4(THF)_2$]. The hydrogen atoms at the methyl groups are omitted for clarity. Selected bond lengths [Å] and angles [°]: P–B 1.930(3) - 1.954(3), N–B 1.600(3) - 1.604(4), B–P–B 109.7(1)-110.5(1), P–B–P 111.4(1), N–B–P 114.6(2) – 115.5(2), B–P–B–P 171.3(2) – 174.6(2).

4.3 Conclusion

The results show the advantages of use of the parent phosphinoborane $H_2PBH_2{\cdot}NMe_3$ as a remarkable monomer to build-up unprecedented cationic chain compounds in a stepwise manner, and in high yields, which are structurally and electronically related to *n*-alkanes. These first phosphanylborane chains are unique representatives of the cationic class of group 13/15 catena compounds, and they are the longest X-ray structural characterized 13/15 chain-compounds. The first arsenic-containing chain compound has now also been isolated. The chains show excellent thermodynamic stability, and the presented concepts will allow the formation of more extended chain molecules and also of more complex hydrocarbon-related structures. This will contribute to our knowledge about the C/PB relationship, and in future the chemical behavior will be investigated in more detail.

4.4 Referenecs

[1] M. Baudler, *Angew. Chem. Int. Ed.* **1982**, *21*, 492–512; *Angew. Chem.* **1982**, *94*, 520–539.

[2] M. Baudler, *Angew. Chem. Int. Ed.* **1987**, *26*, 419–441; *Angew. Chem.* **1987**, *99*, 429–451.

[3] M. Baudler, K. Glinka, *Chem. Rev.* **1993**, *93*, 1623–1667.

[4] M. Baudler, K. Glinka, *Chem. Rev.* **1994**, *94*, 1273–1297.

[5] H. G. von Schnering, W. Hönle, *Chem. Rev.* **1988**, *88*, 243–273.

[6] I. Jevtovikj, P. Lönnecke, E. Hey-Hawkins, *Chem. Commun.* **2013**, *49*, 7355–7357.

[7] C. A. Dyker, N. Burford, *Chem. Asian J.* **2008**, *3*, 28–36.

[8] M. Baudler, Y. Aktalay, K.-F. Tebbe, T. Heinlein, *Angew. Chem. Int. Ed.* **1981**, *20*, 967–969; *Angew. Chem.* **1981**, *93*, 1020–1022.

[9] K.-O. Feldmann, J. J. Weigand, *Angew. Chem. Int. Ed.* **2012**, *51*, 7545–7549; *Angew. Chem*. **2012**, *124*, 7663–7667.

[10] M. H. Holthausen, A. Hepp, J. J. Weigand, *Chem. Eur. J.* **2013**, *19*, 9895–9907.

[11] a) E. Osorio, J. K. Olson, W. Tiznado, A. I. Boldyrev, *Chem. Eur. J.* **2012**, *18*, 9677–9681; b) H. Braunschweig, R. D. Dewhurst, *Angew. Chem. Int. Ed.* **2013**, *52*, 3574–3583; *Angew. Chem.* **2013**, *125*, 3658–3667.

[12] K. H. Hermersdörfer, E. Metejcikova, H. Nöth, *Chem. Ber*. **1970**, *103*, 516–527.

[13] G. Linti, D. Loderer, H. Nöth, K. Polborn, W. Rattay, *Chem Ber*. **1994**, *127*, 1909-1922. In the same paper the structure of a linear [B-N-B-B-B-B] chain compound was given.

[14] H. Nöth, H. Pommerening, *Angew. Chem. Int. Ed.* **1980**, *19*, 482–483; *Angew. Chem*. **1980**, *92*, 481–482.

[15] H. Braunschweig, Q. Ye, A. Vargas, R. D. Dewhurst, K. Radacki, A. Damme. *Nat. Chem*. **2012**, *4*, 563–567.

[16] M. S. Hill, P. B. Hitchcock, R. Pongtavornoinyo, *Science* **2006**, *311*, 1904–1907.

[17] A. Staubitz, A. P. M. Robertson, M. E. Sloan, I. Manners*, Chem. Rev.*, **2010**, *110*, 4023–4078.

[18] A. Staubitz, A. P. M. Robertson, I. Manners*, Chem. Rev.* **2010**, *110*, 4079–4124.

[19] a) B. Kaufmann, H. Nöth, R. T. Paine, K. Polborn, M. Thomann, *Angew. Chem. Int. Ed.* **1993**, *32*, 1446–1448; *Angew. Chem.* **1993**, *105*, 1534–1536; b) B. Kaufmann, H. Nöth, R. T. Paine, *Chem. Ber.* **1996,** *129*, 557–560; c) H. V. Rasika Dias, P. P. Power, *J. Am. Chem. Soc.* **1989**, *111*, 144–148.

[20] a) H. Dorn, R. A. Singh, J. A. Massey, A. J. Lough, I. Manners, *Angew. Chem. Int. Ed*. **1999**, *38*, 3321–3323; *Angew. Chem.* **1999**, *111*, 3540–3543; b) H. Dorn, R. A. Singh, J. A. Massey, J. M. Nelson, C. A. Jaska, A. J. Lough, I. Manners, *J. Am. Chem. Soc.* **2000**, *122,* 6669–6678.

[21] M. E. Sloan, T. J. Clark, I. Manners, *Inorg. Chem.* **2009**, *48*, 2429–2435.

[22] T. Oshiki, T. Imamoto, *Bull. Chem. Soc. Jpn.* **1990**, *63*, 2846–2849.

[23] a) U. Vogel, A. Y. Timoshkin, M. Scheer, *Angew. Chem. Int. Ed*. **2001**, *40*, 4409–4412; *Angew. Chem*. **2001**, *113*, 4541–4544; b) K.-Ch. Schwan, A. Timoshkin, M. Zabel, M. Scheer, *Chem. Eur. J*. **2006**, *12*, 4900–4908; c) U. Vogel, A. Y. Timoshkin, K.-Ch. Schwan, M. Bodensteiner, M. Scheer, *J. Organomet. Chem*. **2006**, *691*, 4556–4564.

[24] C. Marquardt, A. Adolf, A. Stauber, M. Bodensteiner, A. V. Virovets, A. Y. Timoshkin, M. Scheer, *Chem. Eur. J.* **2013***, 19*, 11887–11891.

[25] C. Thoms, C. Marquardt, M. Bodensteiner, M. Scheer, *Angew. Chem. Int. Ed.* **2013**, *52*, 5150–5154; *Angew. Chem*. **2013**, *125*, 5254–5259.

[26] M. Mantina, A. C. Chamberlin, R. Valero, C. J. Cramer, D. G. Truhlar, *J. Phys. Chem.* A **2009,** *113*, 5806–5812.

4.5 Supporting Information

General Experimental:

All manipulations were performed under an atmosphere of dry argon using standard glove-box and Schlenk techniques. All solvents are degassed and purified by standard procedures. The compounds $H_2EBH_2{\cdot}NMe_3$ (E = P, As),[1] $ClBH_2{\cdot}NMe_3$[2] and $[VCl_3(THF)_3]$[3] were prepared according to literature procedures. Other chemicals were obtained from Sigma-Aldrich ($AlCl_3$, I_2) or STREM Chemicals, INC. ($BH_3{\cdot}SMe_2$, $BH_3{\cdot}NMe_3$). The NMR spectra were recorded on either an Avance 400 spectrometer (^1H: 400.13 MHz, ^{31}P: 161.976 MHz, ^{11}B: 128.378 MHz, $^{13}C\{^1H\}$: 100.623 MHz, ^{27}Al: 104.261 MHz) with δ [ppm] referenced to external $SiMe_4$ (^1H, ^{13}C), H_3PO_4 (^{31}P), $BF_3{\cdot}Et_2O$ (^{11}B), $CFCl_3$ (^{19}F) or $Al(NO_3)_3{\cdot}9\ H_2O$ (^{27}Al). IR spectra were measured on a DIGILAB (FTS 800) FT-IR spectrometer. All mass spectra were recorded on a ThermoQuest Finnigan TSQ 7000 (ESI-MS). The C, H, N analyses were measured on an Elementar Vario EL III apparatus.

Synthesis of $[Me_3N{\cdot}BH_2{-}PH_2{-}BH_2{\cdot}NMe_3]^+[AlCl_4]^-$ (1a[$AlCl_4$])

A solution of 52 mg (0.5 mmol) $H_2PBH_2{\cdot}NMe_3$ in 1 mL toluene is added to a suspension of 67 mg (0.5 mmol) $AlCl_3$ in 10 ml CH_2Cl_2. After stirring the mixture for 10 minutes, 53 mg (0.5 mmol) $ClBH_2{\cdot}NMe_3$ in 5 ml of CH_2Cl_2 is added. The mixture is stirred for 18 hours. After filtration the solution is layered with 30 mL of *n*-hexane. **1a**[$AlCl_4$] crystallises at 4 °C as colourless needles. The crystals are separated and washed with cold *n*-hexane (0°C, 3×5 mL). Yield of **1a**[$AlCl_4$]: 95 mg (55 %). ^1H NMR (CD_2Cl_2, 25 °C): δ = 2.22 (q, $^1J_{H,B}$ = 113 Hz, 4H, BH_2), 2.81 (s, 18H, NMe_3), 3.74 (dm, $^1J_{H,P}$ = 342 Hz, 2H, PH_2). ^{31}P NMR (CD_2Cl_2, 25 °C): δ = –135.0 (t, $^1J_{H,B}$ = 342 Hz, br, PH_2). $^{31}P\{^1H\}$ NMR (CD_2Cl_2, 25 °C): δ = –135.0 (s, br, PH_2). ^{11}B NMR (CD_2Cl_2, 25 °C): δ = –11.7 (td, $^1J_{B,P}$ = 62 Hz, $^1J_{B,H}$ = 113 Hz, BH_2). $^{11}B\{^1H\}$ NMR (CD_2Cl_2, 25 °C): δ = –11.7 (d, $^1J_{B,P}$ = 62 Hz, BH_2). ^{27}Al NMR (CD_2Cl_2, 25 °C): δ = 102.9 (s, $AlCl_4$) ^{13}C NMR (CD_2Cl_2, 25 °C): δ = 54.5 (d, $^3J_{C,P}$ = 6 Hz, NMe_3). IR (KBr): $\tilde{\nu}$ = 3382 (m, vbr, $AlCl_4$), 3013 (m), 2960 (m), 2920 (m), 2840 (m), 2446 (s, br, BH), 2413 (s, br, BH), 2303 (w, PH), 1638 (w), 1486 (s), 1470 (s), 1415 (w), 1245 (m), 1156 (m), 1127 (s), 1087 (s), 1056 (m), 1015 (m), 976 (m), 872 (m), 795 (s), 711 (w), 605 (w), 496 (vs), 483 (vs). ESI-MS (CH_2Cl_2): *m/z* = 177 (100 %, $[Me_3N{\cdot}BH_2{-}PH_2{-}BH_2{\cdot}NMe_3]^+$). Elemental analysis (%) calculated for $C_6H_{24}AlB_2Cl_4N_2P$ (**1a**[$AlCl_4$]): C: 20.85, H: 7.00, N: 8.10; found: C: 19.43, H: 6.90, N: 7.53.

Synthesis of $[Me_3N{\cdot}BH_2{-}AsH_2{-}BH_2{\cdot}NMe_3]^+[AlCl_4]^-$ (1b[$AlCl_4$]):

A solution of 74 mg (0.5 mmol) $H_2AsBH_2{\cdot}NMe_3$ in 1 mL toluene is added to a suspension of 67 mg (0.5 mmol) $AlCl_3$ in 10 ml CH_2Cl_2. After stirring the mixture for 10 minutes, 53 mg (0.5 mmol) $ClBH_2{\cdot}NMe_3$ in 5 ml of CH_2Cl_2 is added. The mixture is stirred for 18h hours. After filtration the solution is layered with 30 mL of *n*-hexane. **1b**[$AlCl_4$] crystallises at room temperature as colourless needles. The crystals are separated and washed with cold *n*-hexane (0°C, 3×5 mL). Yield of **1b**[$AlCl_4$]: 125 mg (64 %); ^{1}H NMR (CD_2Cl_2, 25 °C): δ = 2.48 (q, $^1J_{H,B}$ = 115 Hz, 4H, BH_2), 2.82 (s, 18H, NMe_3). ^{11}B NMR (CD_2Cl_2, 25 °C): δ = –9.1 (t, $^1J_{B,H}$ = 115 Hz, BH_2). ^{11}B{^{1}H} NMR (CD_2Cl_2, 25 °C): δ = –9.1 (s, BH_2). ^{27}Al NMR (CD_2Cl_2, 25 °C): δ = 102.9 (s, $AlCl_4$) ^{13}C NMR (CD_2Cl_2, 25 °C): δ = 54.5 (s, NMe_3). IR (KBr): $\tilde{\nu}$ = 3350 (m, vbr, $AlCl_4$), 3059 (m), 2958 (m), 2458 (s, br, BH), 2420 (s, br, BH), 2312 (w), 2177 (m, AsH), 1638 (w), 1485 (s), 1469 (s), 1420 (w), 1243 (m), 1161 (m), 1123 (s), 1072 (s), 1011 (m), 978 (m), 869 (m), 736 (w), 680 (m), 612 (m), 496 (vs). ESI-MS (CH_2Cl_2): *m/z* = 221 (100 %, $[Me_3N{\cdot}BH_2{-}AsH_2{-}BH_2{\cdot}NMe_3^+$). Elemental analysis (%) calculated for $C_6H_{24}AlAsB_2Cl_4N_2$ (**1b**[$AlCl_4$]): C: 18.50, H: 6.21, N: 7.19; found: C: 18.21, H: 5.89, N: 6.89.

Synthesis of $Me_3N{\cdot}BH_2I$:

To a solution of 5 g (68.5 mmol) $BH_3{\cdot}NMe_3$ in 100 mL of Et_2O 8.6 g (33.9 mmol) I_2 is added in 5 portions. After stirring the mixture for 18 hours, all volatiles are removed under reduced pressure. The remaining white solid is washed 5 times with 30 mL of *n*-hexane, and dried under reduced pressure. Yield of [$Me_3N{\cdot}BH_2I$]: 13.1 g (95 %); ^{1}H NMR ($CDCl_3$, 25 °C): δ = 2.83 (s, 9H, NMe), 2.90 (q, $^1J_{H,B}$ = 128 Hz, 4H, BH_2). ^{11}B NMR ($CDCl_3$, 25 °C): δ = –9.4 (t, $^1J_{B,H}$ = 130 Hz, BH_2). ^{11}B{^{1}H} NMR ($CDCl_3$, 25 °C): δ = –9.4 (s, BH_2).

Synthesis of $[Me_3N{\cdot}BH_2{-}PH_2{-}BH_2{\cdot}NMe_3]^+$ $[I]^-$ (1a[I]):

To a solution of 252 mg (2.40 mmol) $H_2PBH_2{\cdot}NMe_3$ in 80 mL of Et_2O, 508 mg $IBH_2{\cdot}NMe_3$ (2.55 mmol) are added in 3 portions. After stirring for 16 h at room temperature, all volatiles are removed under reduced pressure. The remaining solid is washed several times with toluene. **1a**[I] remains as a white solid. Crystals of **1a**[I] are obtained as colourless blocks by layering a solution in a 3:1 mixture of THF/acetonitrile with of *n*-hexane. Yield of **1a**[I]: 480 mg (66 %); ^{1}H NMR (CD_3CN, 25 °C): δ = 2.14 (q, $^1J_{H,B}$ = 111 Hz, 4H, BH_2), 2.74 (s, 18H, NMe_3), 3.77 (dm, $^1J_{H,P}$ = 350 Hz, 2H, PH_2). ^{31}P NMR (CD_3CN, 25 °C): δ = –136.0 (tm, $^1J_{H,B}$ = 350 Hz, br, PH_2). ^{31}P{^{1}H} NMR (CD_3CN, 25 °C): δ = –136.0 (m, br, PH_2). ^{11}B NMR (CD_3CN, 25 °C): δ = –11.0 (td, $^1J_{B,P}$ = 63 Hz, $^1J_{B,H}$ = 111 Hz, BH_2). ^{11}B{^{1}H} NMR (CD_3CN, 25 °C): δ = –11.0 (d, $^1J_{B,P}$ = 63 Hz). IR (KBr):

$\tilde{\nu}$ = 3008 (w, CH), 2992 (w, CH), 2953 (w, CH), 2904 (w, CH), 2804 (w), 2739 (w), 2442 (s, br, BH), 2411 (s, br, BH), 2363 (w, PH), 2312 (w, PH), 2301 (w), 1483 (m, sh), 1473 (s), 1443 (w), 1412 (w), 1252 (w, sh), 1244 (s), 1157 (m), 1129 (s), 1084 (s), 1055 (w), 1011 (s), 973 (m), 946 (w), 874 (w), 809 (vs), 709 (m), 412 (w). ESI-MS (CD_3CN): *m/z* = 177 (100 %, $[Me_3N{\cdot}BH_2{-}PH_2{-}BH_2{\cdot}NMe_3]^+$). Elemental analysis (%) calculated for $C_6H_{24}B_2IN_2P$ (**1a**[I]): C: 23.72, H: 7.96, N: 9.22; found: C: 23.51, H: 7.22, N: 9.25.

Synthesis of $[Me_3N{\cdot}BH_2{-}AsH_2{-}BH_2{\cdot}NMe_3]^+[I]^-$ (1b[I]):

To a solution of 74 mg (0.5 mmol) $H_2AsBH_2{\cdot}NMe_3$ in 20 mL of Et_2O, 100 mg $IBH_2{\cdot}NMe_3$ (0.5 mmol) are added in 3 portions at -80°C. After stirring for 16 h at room temperature, all volatiles are removed under reduced pressure. The remaining solid is washed several times with 10 mL *n*-hexane. **1b**[I] remains as a white solid. Crystals of **1b**[I] form already during the reaction. Yield of **1b**[I]: 100 mg (58 %); ^{1}H NMR (CD_2Cl_2, 25 °C): δ = 2.45 (q, $^1J_{H,B}$ = 116 Hz, 4H, BH_2), 2.89 (s, 18H, NMe_3), 3.26 (m, 2H, AsH_2). ^{11}B NMR (CD_2Cl_2, 25 °C): δ = –9.11 (t, $^1J_{B,H}$ = 116 Hz, BH_2). ^{11}B{^{1}H} NMR (CD_2Cl_2, 25 °C): δ = –9.11 (s). ^{13}C NMR (CD_2Cl_2, 25 °C): δ = 54.7 (s, NMe_3). IR (KBr): $\tilde{\nu}$ = 3009 (m), 3003 (m), 2949 (m), 2840 (m), 2807 (m), 2739 (m), 2455 (s, br, BH), 2418 (s, br, BH), 2320 (w), 2155 (m, AsH), 2120 (m, AsH), 1470 (s), 1413 (m), 1243 (m), 1164 (m), 1126 (s), 1067 (s), 1011 (m), 978 (m), 956 (m), 871 (m), 843 (m), 796 (m), 731 (w), 686 (m), 641 (m), 473 (w). ESI-MS (CH_2Cl_2): *m/z* = 220.9 (25%, $[Me_3N{\cdot}BH_2{-}AsH_2{-}BH_2{\cdot}NMe_3]^+$), 294.8 (27%, $[Me_3N{\cdot}BH_2{-}AsH_2{-}BH_2{\cdot}NMe_3]^+{\cdot}OEt_2$), 367.9 (100%, $[Me_3N{\cdot}BH_2{-}AsH_2{-}BH_2{\cdot}NMe_3]^+{\cdot}2OEt_2$). Elemental analysis (%) calculated for $C_6H_{24}AsB_2IN_2$ (**1b**[I]): C: 20.73, H: 6.96, N: 8.06; found: C: 20.59, H: 6.48, N: 7.70.

Synthesis of $Me_2S{\cdot}BH_2I$:

To a solution of 1.519 g (20 mmol) of $BH_3{\cdot}SMe_2$ in 50 mL of benzene 2.5 g (9.9 mmol) I_2 is added in 5 portions. After stirring the mixture for 18 hours, all volatiles are removed under reduced pressure. The remaining colourless liquid is filtrated and stored at -28°C. Yield of [$Me_2S{\cdot}BH_2I$]: 3.45 g (86 %); ^{1}H NMR ($CDCl_3$, 25 °C): δ = 1.4 (s, 6H, SMe), 2.98 (q, $^1J_{H,B}$ = 136 Hz, 2H, BH_2). ^{11}B NMR ($CDCl_3$, 25 °C): δ = –20.9 (t, $^1J_{B,H}$ = 136 Hz, BH_2). ^{11}B{^{1}H} NMR ($CDCl_3$, 25 °C): δ = –20.9 (s, BH_2).

Synthesis of $[Me_3N{\cdot}BH_2{-}PH_2{-}BH_2{-}PH_2{-}BH_2{\cdot}NMe_3]^+[I]^-$ (2[I]):

104 mg (1 mmol) $H_2PBH_2{\cdot}NMe_3$ in 2 mL of toluene is added to 20 ml of Et_2O. At -80 °C 0.5 mL (0.5 mmol) of a 1M solution of $Me_2S{\cdot}BH_2I$ in toluene is added. After 2 h a white solid precipitates. After stirring the mixture for additional 18 h, the Et_2O solution is

decanted and the remaining solid is washed 3 times with 10 mL of *n*-hexane. Crystals of **2**[I] are obtained as colourless blocks by storing an acetonitrile solution at -28°C for several days. Yield of **2**[I]: 140 mg (80 %). ^{1}H NMR (CD_2Cl_2, 25 °C): δ = 1.28 (q, $^{1}J_{H,B}$ = 107 Hz, 2H, BH_2), 2.23 (q, $^{1}J_{H,B}$ = 118 Hz, 4H, BH_2), 2.85 (s, 18H, NMe_3), 3.92 (dm, $^{1}J_{H,P}$ = 352 Hz, 4H, PH_2). ^{31}P NMR (CD_2Cl_2, 25 °C): δ = –120.0 (t, br $^{1}J_{H,P}$ = 355 Hz, PH_2). ^{31}P{^{1}H} NMR (CD_2Cl_2, 25 °C): δ = –120.0 (s, br, PH_2). ^{11}B NMR (CD_2Cl_2, 25 °C): δ = –11.0 (td, $^{1}J_{B,P}$ = 67 Hz, $^{1}J_{B,H}$ = 111 Hz, BH_2), –40.6 (tt, $^{1}J_{B,P}$ = 64 Hz, $^{1}J_{B,H}$ = 118 Hz, BH_2). ^{11}B{^{1}H} NMR (CD_2Cl_2, 25 °C): δ = –11.0 (d, $^{1}J_{B,P}$ = 67 Hz, BH_2), –40.6 (t, $^{1}J_{B,P}$ = 64 Hz, BH_2). ^{13}C NMR (CD_2Cl_2, 25 °C): δ = 54.5 (m, NMe_3). IR (KBr): $\tilde{\nu}$ = 2997 (m), 2949 (m), 2904 (w), 2807 (w), 2739 (w), 2433 (s, br, BH), 2407 (s, br, BH), 2305 (w, PH), 1473 (s), 1411 (m), 1244 (s), 1156 (m), 1132 (s), 1097 (s), 1061 (m), 1014 (m), 977 (m), 928 (w), 862 (m), 816 (s), 801 (s), 715 (w), 659 (w), 592 (w). ESI-MS (CH_2Cl_2): *m/z* = 223.2 (100 %, $[Me_3N{\cdot}BH_2{-}PH_2{-}BH_2{-}PH_2{-}BH_2{\cdot}NMe_3]^+$). Elemental analysis (%) calculated for $C_6H_{28}B_3IN_2P_2$ (**2**[I^-]): C: 20.61, H: 8.07, N: 8.01; found: C: 20.55, H: 8.07, N: 7.53.

Synthesis of $[Me_3N{\cdot}BH_2{-}PH_2{-}BH_2{-}PH_2{-}BH_2{\cdot}NMe_3]^+[VCl_4(THF)_2]^-$ (2[$VCl_4(THF)_2$]):

To a solution of 306 mg (0.819 mmol) [$VCl_3(THF)_3$] in 5 ml THF a solution of 86 mg (0.819 mmol) $H_2PBH_2{\cdot}NMe_3$ in 2 ml THF is added drop wise under stirring. The mixture is stirred for 6 hours. The volume is reduced to the half and the concentrated solution is slowly added to 30 ml *n*-hexane when **2**[$VCl_4(THF)_2$] precipitates. For complete precipitation the solution is stored for an hour at –28 °C. After filtration the precipitate is dried in vacuum. **2**[$VCl_4(THF)_2$] is obtained as a pale pink solid. Crystals of **2**[$VCl_4(THF)_2$] can be obtained by layering the concentrated solution with the double amount of *n*-hexanes. Yield of **2**[$VCl_4(THF)_2$]: -- mg (--%); ^{1}H NMR (CD_3CN, 25 °C): δ = silent, due to the paramagnetic counter ion $[VCl_4(THF)_2]^-$. ^{31}P NMR (CD_3CN, 25 °C): δ = –119.7 (t, $^{1}J_{H,P}$ = 341 Hz, br, PH_2). ^{31}P{^{1}H} NMR (CD_2Cl_2, 25 °C): δ = –119.7 (s, br, PH_2). ^{11}B NMR (CD_2Cl_2, 25 °C): δ = –10.6 (td, $^{1}J_{B,P}$ = 64 Hz, $^{1}J_{B,H}$ = 109 Hz, BH_2), –40.9 (tt, $^{1}J_{B,P}$ = 68 Hz, $^{1}J_{B,H}$ = 107 Hz, BH_2). ^{11}B{^{1}H} NMR (CD_2Cl_2, 25 °C): δ = –10.6 (d, $^{1}J_{B,P}$ = 64 Hz, BH_2), –40.9 (t, $^{1}J_{B,P}$ = 68 Hz, BH_2). IR (KBr): $\tilde{\nu}$ = 2467 (m, br, BH); 2433 (m, sh, BH); 2402 (m, sh, PH); 2358 (w, sh, PH). ESI-MS (CD_3CN): cation: *m/z* = 223.0 (100 %, $[Me_3N{\cdot}BH_2{-}PH_2{-}BH_2{-}PH_2{-}BH_2{\cdot}NMe_3]^+$); anion: *m/z* = 190.7 (80 %, $[VCl_4]^-$).

X-ray diffraction analysis

The X-ray diffraction experiments were performed on either a Gemini R Ultra CCD diffractometer (**1a**[$AlCl_4$], **1a**[I], **1b**[I], **2**[$VCl_4(THF)_2$], **2**[I]) or a SuperNova A CCD diffractometer (**1b**[$AlCl_4$]) from Agilent Technologies (formerly Oxford Diffraction)

applying Cu-K_α radiation (λ = 1.54178 Å). **2**[I] was measured with Mo-K_α radiation (λ = 0.71073 Å). The measurements were performed at 123 K. Crystallographic data together with the details of the experiments are given in the Tables 1 - 3 (see below). Absorption corrections were applied semi-empirically from equivalent reflections or analytically (SCALE3/ABSPACK algorithm implemented in CrysAlis PRO software by Agilent Technologies Ltd).[4] All structures were solved using SIR97[5], except **2**[$VCl_4(THF)_2$], which was solved by SUPERFLIP,[6] Refinements against F^2 in anisotropic approximation were done using SHELXL-97.[7] The hydrogen positions of the methyl groups were located geometrically and refined riding on the carbon atoms. Hydrogen atoms belonging to BH_2, PH_2 and AsH_2 groups were located from the difference Fourier map and refined without constraints (**1a**[$AlCl_4$], **1b**[$AlCl_4$], **2**[$VCl_4(THF)_2$]) or with restrained E–H (E = P, As) distances (**1a**[I], **1b**[I], **2**[I]). Figures were created with SCHAKAL99, DIAMOND 3 and OLEX.[8] CCDC-974446 (**1a**[$AlCl_4$]), CCDC-974447 (**1a**[I]), CCDC-974448 (**1b**[AlCl4]), CCDC-974449 (**1b**[I]), CCDC-974450 (**2**[I]), and CCDC-974451 (**2**[VCl4(THF)2]) contain the supplementary crystallographic data for this paper. These data can be obtained free of charge from the Cambridge Crystallographic Data Centre via www.ccdc.cam.ac.uk/data_request/cif.

Crystal Structures

$[Me_3N{\cdot}BH_2{-}PH_2{-}BH_2{\cdot}NMe_3]^+[AlCl_4]^-$ (1a[$AlCl_4$]):

1a[$AlCl_4$] crystallizes from a CH_2Cl_2 solution layered by twice the amount of *n*-hexane at room temperature as colourless needles in the orthorhombic space group $Pna2_1$. Figure S1 shows the structure of **1a**[$AlCl_4$] in the solid state.

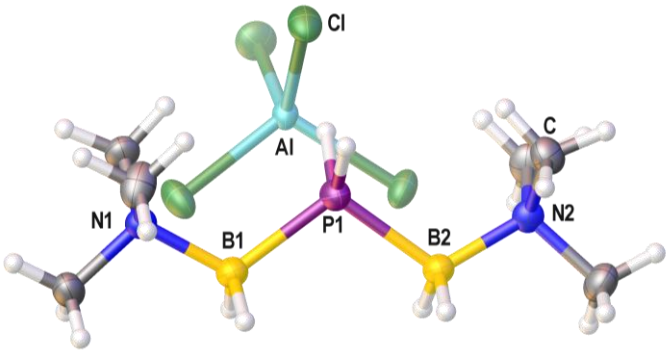

Figure S1. Left: molecular structure **1a**[$AlCl_4$] in the solid state. Selected bond lengths [Å] and angles [°]: P1–B1 1.957(2), P1–B2 1.957(2), N1–B 1.594(2), N2–B2 1.600(2), B1–P1–B2 107.5(1), P1–B1–N1 114.7(1), P1–B2–N2 114.7(1).

$[Me_3N{\cdot}BH_2{-}AsH_2{-}BH_2{\cdot}NMe_3]^+[AlCl_4]^-$ (1b[$AlCl_4$]):

1b[$AlCl_4$] crystallizes from a CH_2Cl_2 solution layered by twice the amount of *n*-hexane at room temperature as colourless needles in the orthorhombic space group $P2_12_12_1$. Figure S2 shows the structure of **1b**[$AlCl_4$] in the solid state.

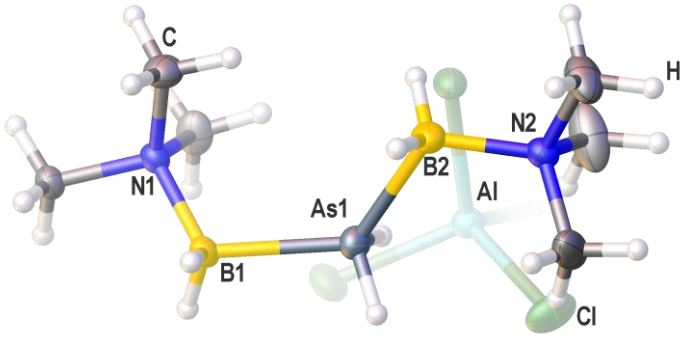

Figure S2. Molecular structure of **1b**[$AlCl_4$] in the solid state. Selected bond lengths [Å] and angles [°]: As1–B1 2.086(4), As1–B2 2.076(3), N1–B1 1.590(4), N2–B2 1.595(5), B1–As1–B2 123.02(14), As1–B1–N1 113.3(2), As1– B2–N2 113.8(2).

$[Me_3N{\cdot}BH_2{-}PH_2{-}BH_2{\cdot}NMe_3]^+[I]^-$ (1a[I]):

1a[I] crystallizes in form of colourless blocks in the monoclinic space group $P2_1n$. Figure S3 shows the structure of **1a**[I] in the solid state.

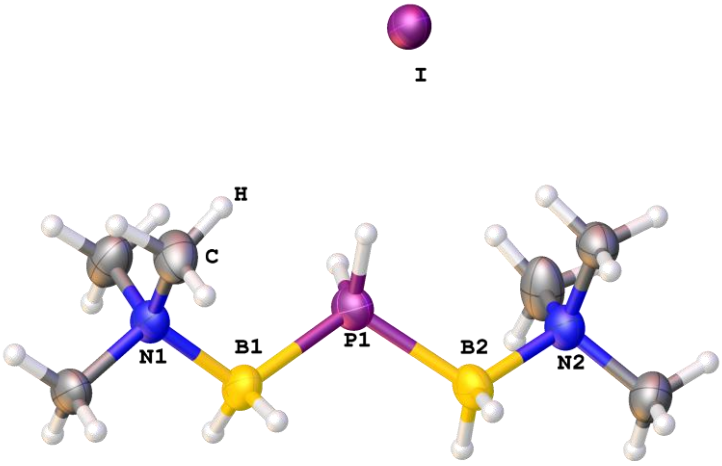

Figure S3. Molecular structure of **1a**[I] in the solid state. Selected bond lengths [Å] and angles [°]: P1–B1 1.966(5), P1–B2 1.959(5), N1–B1 1.608(6), N2–B2 1.601(6), B1–P1–B2 111.5(2), P1–B1–N1 113.0(3), P1–B2–N2 113.8(3).

$[Me_3N{\cdot}BH_2{-}AsH_2{-}BH_2{\cdot}NMe_3]^+[I]^-$ (1b[I]):

1b[I] crystallizes in form of colourless blocks in the monoclinic space group C_2c. Figure S4 shows the structure of **1b**[I] in the solid state.

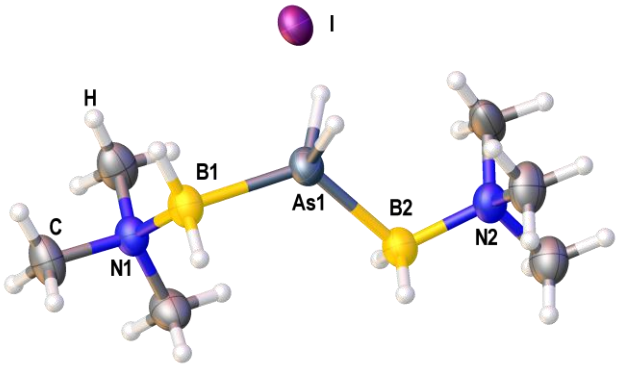

Figure S4. Molecular structure of **1b**[I] in the solid state. Selected bond lengths [Å] and angles [°]: As1–B1 2.077(5), As1–B2 2.076(6), N1–B1 1.587(6), N2–B2 1.591(6), N2–C5 1.495(7), N2–C6 1.495(6), B1–As1–B2 123.3(2), As1–B1–N1 112.8(3), As1–B2–N2 112.2(4).

$[Me_3N{\cdot}BH_2{-}PH_2{-}BH_2{-}PH_2{-}BH_2{\cdot}NMe_3]^+[I]^-$ (2[I]):

2[I] crystallises by storing a acetonitrile of **2**[I] solution at -28°C in form of colourless blocks in the monoclinic space group *P*2/*c.* Figure S5 shows the structure of **2**[I] in the solid state.

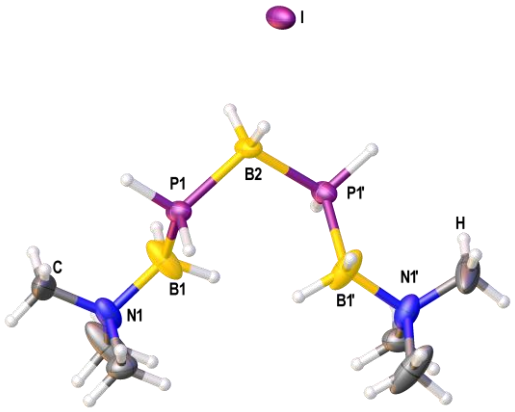

Figure S5. Molecular structure of **2**[I] in the solid state. Selected bond lengths [Å] and angles [°]: P1–B1 1.949(5), P1–B2 1.948(3), N1–B1 1.595(6), B1–P1–B2 110.63(18), P1–B1–N1 116.9(3), P1–B2–P1 108.2(2).

$[Me_3N{\cdot}BH_2{-}PH_2{-}BH_2{-}PH_2{-}BH_2{\cdot}NMe_3]^+[VCl_4(THF)_2]^-$ (2[$VCl_4(THF)_2$]):

2[$VCl_4(THF)_2$] crystallises in form of yellow plates in the monoclinic space group *P* 2_1/c by layering a concentrated solution in THF with *n*-hexanes. Figure S6 shows the structure of **2**[$VCl_4(THF)_2$] in the solid state.

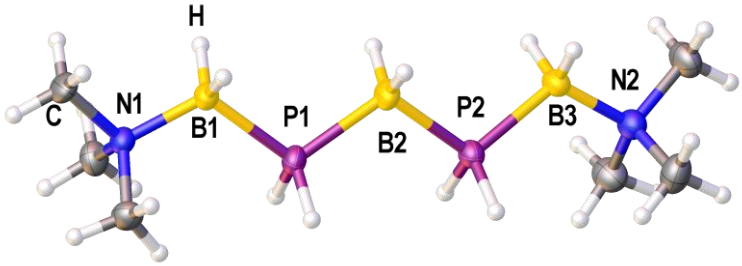

Figure S6: Molecular structure of the cation of **2**[$VCl_4(THF)_2$]$^-$ in the solid state. Selected bond lengths [Å] and angles[°]: P1–B1 1.954(3), P1–B2 1.945(3), P2–B2 1.930(3), P2–B3 1.950(3), N1–B1 1.600(3), N2–B3 1.604(4), N1–B1– P1 114.62(19), B1–P1–B2 110.49(13), P1–B2–P3 111.36(17), B2–P2–B3 109.74(14), P2–B3–N2 115.5(2).

Crystallographic information

Table S1. Crystallographic data for compounds **1a**[$AlCl_4$] and **1b**[$AlCl_4$].

	1a[$AlCl_4$]	**1b**[$AlCl_4$]
Empirical formula	$C_6H_{24}AlB_2Cl_4N_2P$	$C_6H_{24}AlAsB_2Cl_4N_2$
Formula weight *M*	345.64 g/mol	389.59 g/mol
Crystal	colourless needle	colourless block
Crystal size [mm^3]	0.74 x 0.16 x 0.09	0.24 x 0.23 x 0.14
Temperature *T*	123(1) K	123(1) K
Crystal system	orthorhombic	orthorhombic
Space group	$Pna2_1$	$P2_12_12_1$
Unit cell dimensions	*a* = 13.9502(1) Å	*a* = 9.6860(2) Å
	b = 21.2715(2) Å	*b* = 11.3287(2) Å
	c = 6.0802(1) Å	*c* = 16.4121(2) Å
	α = 90°	*α* = 90°
	β = 90°	*β* = 90°
	γ = 90°	*γ* = 90°
Volume *V*	1804.25(4) $Å^3$	1800.90(5) $Å^3$
Formula units *Z*	4	4
Absorption coefficient $\mu_{Cu\text{-}K\alpha}$	7.104 mm^{-1}	8.319 mm^{-1}
Density (calculated) ρ_{calc}	1.273 g/cm^3	1.437 g/cm^3
F(000)	720	792
Theta range $\theta_{min}/\theta_{max}$	3.79 / 73.80°	4.74 / 73.45°.
Absorption correction	analytical	analytical
Index ranges	–17 < *h* < 17	–10 < *h* < 11
	–26 < *k* < 26	–13 < *k* < 10
	–7 < *l* < 7	–20 < *l* < 20
Reflections collected	29533	7537
Independent reflections [$I > 2\sigma(I)$]	3591 (R_{int} = 0.0468)	3438 (R_{int} = 0.0298)
Completeness to full *θ*	0.997	0.990
Transmission T_{min} / T_{max}	0.073 / 0.612	0.258 / 0.438
Data / restraints / parameters	3628 / 1 / 176	3485 / 0 / 175
Goodness-of-fit on F^2 *S*	1.017	1.037
Final *R*-values [$I > 2\sigma(I)$]	R_1 = 0.0237,	R_1 = 0.0301,
	wR_2 = 0.0668	wR_2 = 0.0784
Final *R*-values (all data)	R_1 = 0.0239,	R_1 = 0.0305,
	wR_2 = 0.0670	wR_2 = 0.0788
Largest difference hole	–0.291,	–0.374,
and peak *Δρ*	0.283 $eÅ^{-3}$	0.626 $eÅ^{-3}$
Flack parameter	0.06(1)	0.03(2)

Table S2. Crystallographic data for compounds **1a**[I] and **1b**[I].

	1a[I]	**1b**[I]
Empirical formula	$C_6H_{24}B_2IN_2P$	$C_6H_{24}B_2AsN_2P$
Formula weight *M*	303.76 g/mol	347.71 g/mol
Crystal	colourless block	colourless block
Crystal size [mm^3]	0.14 x 0.08 x 0.08	0.21 x 0.15 x 0.09
Temperature *T*	123(1) K	123(1) K
Crystal system	monoclinic	monoclinic
Space group	$P2_1n$	C_2c
Unit cell dimensions	a = 9.4332(2) Å	a = 20.2158(4) Å
	b = 6.8542(1) Å	b = 13.5649(2) Å
	c = 22.3341(3) Å	c = 11.7771(2) Å
	α = 90°	α = 90°
	β = 92.300(2)°	β = 115.707(2)°
	γ = 90°	γ = 90°
Volume *V*	1442.89(4) Å^3	2909.93(11) Å^3
Formula units *Z*	4	8
Absorption coefficient $\mu_{Cu\text{-}K\alpha}$	18.174 mm^{-1}	19.512 mm^{-1}
Density (calculated) ρ_{calc}	1.398 g/cm^3	1.587 g/cm^3
F(000)	608	1360
Theta range $\theta_{min}/\theta_{max}$	3.96 / 66.44°	4.02 / 66.63°.
Absorption correction	analytical	analytical
Index ranges	–11 < h < 11	–23 < h < 24
	–8 < k < 5	–16 < k < 12
	–26 < l < 26	–13 < l < 14
Reflections collected	9440	20347
Independent reflections [$I > 2\sigma(I)$]	2159 (R_{int} = 0.0664)	2326 (R_{int} = 0.0842)
Completeness to full θ	0.996	0.998
Transmission T_{min} / T_{max}	0.214 / 0.402	0.103 / 0.354
Data / restraints / parameters	2530 / 5 / 133	2566 / 7 / 139
Goodness-of-fit on F^2 *S*	1.064	1.106
Final *R*-values [$I > 2\sigma(I)$]	R_1 = 0.0479,	R_1 = 0.0321,
	wR_2 = 0.1113	wR_2 = 0.0912
Final *R*-values (all data)	R_1 = 0.0479,	R_1 = 0.0351,
	wR_2 = 0.1033	wR_2 = 0.0925
Largest difference hole	–1.130,	–0.746,
and peak $\Delta\rho$	1.258 eÅ^{-3}	0.108 eÅ^{-3}

Table S3. Crystallographic data for compounds **2**[I] and **2**[$VCl_4(THF)_2$].

	2[I]	**2**[$VCl_4(THF)_2$]
Empirical formula	$C_6H_{28}B_3I_1N_2P_2$	$C_{14}H_{44}B_3Cl_4N_2O_2P_2V$
Formula weight *M*	349.57 g/mol	559.62 g/mol
Crystal	colourless block	yellow plate
Crystal size [mm^3]	0.23 x 0.13 x 0.08	0.29 x 0.21 x 0.06
Temperature *T*	123(1) K	123(1) K
Crystal system	monoclinic	monoclinic
Space group	*P* 2/*c*	*P* 2_1/c
Unit cell dimensions	*a* = 10.8435(3) Å	*a* = 18.6430(3) Å
	b = 7.1547(1) Å	*b* = 10.3593(2) Å
	c = 11.9395(4) Å	*c* = 15.7607(2) Å
	α = 90°	*α* = 90°
	β = 112.021(4)°	*β* = 111.880(2)°
	γ = 90°	*γ* = 90°
Volume *V*	858.71(5) $Å^3$	2824.60(8) $Å^3$
Formula units *Z*	2	4
Absorption coefficient $\mu_{Cu\text{-}K\alpha}$	2.025 mm^{-1}	7.588 mm^{-1}
Density (calculated) ρ_{calc}	1.352 g/cm^3	1.316 g/cm^3
F(000)	352	1176
Theta range $\theta_{min}/\theta_{max}$	3.39 / 30.05°	4.98 / 72.84°
Absorption correction	analytical	multi-scan
Index ranges	–14 < *h* < 14	–22 < *h* < 19
	–9 < *k* < 9	–12 < *k* < 9
	–16 < *l* < 16	–18 < *l* < 19
Reflections collected	8573	10304
Independent reflections [$I > 2\sigma(I)$]	2024 (R_{int} = 0.0262)	3998 (R_{int} = 0.0448)
Completeness to full *θ*	0.999	0.999
Transmission T_{min} / T_{max}	0.724 / 0.904	0.209 / 1.000
Data / restraints / parameters	2284 / 5 / 88	5459 / 0 / 299
Goodness-of-fit on F^2 *S*	1.057	0.956
Final *R*-values [$I > 2\sigma(I)$]	R_1 = 0.0332,	R_1 = 0.0461,
	wR_2 = 0.0789	wR_2 = 0.1033
Final *R*-values (all data)	R_1 = 0.0384,	R_1 = 0.0632,
	wR_2 = 0.0825	wR_2 = 0.1128
Largest difference hole	–0.679,	–0.710,
and peak *Δρ*	0.937 $eÅ^{-3}$	0.796 $eÅ^{-3}$

NMR spectroscopy

$[Me_3N{\cdot}BH_2{-}PH_2{-}BH_2{\cdot}NMe_3]^+[AlCl_4]^-$ (1a[$AlCl_4$]):

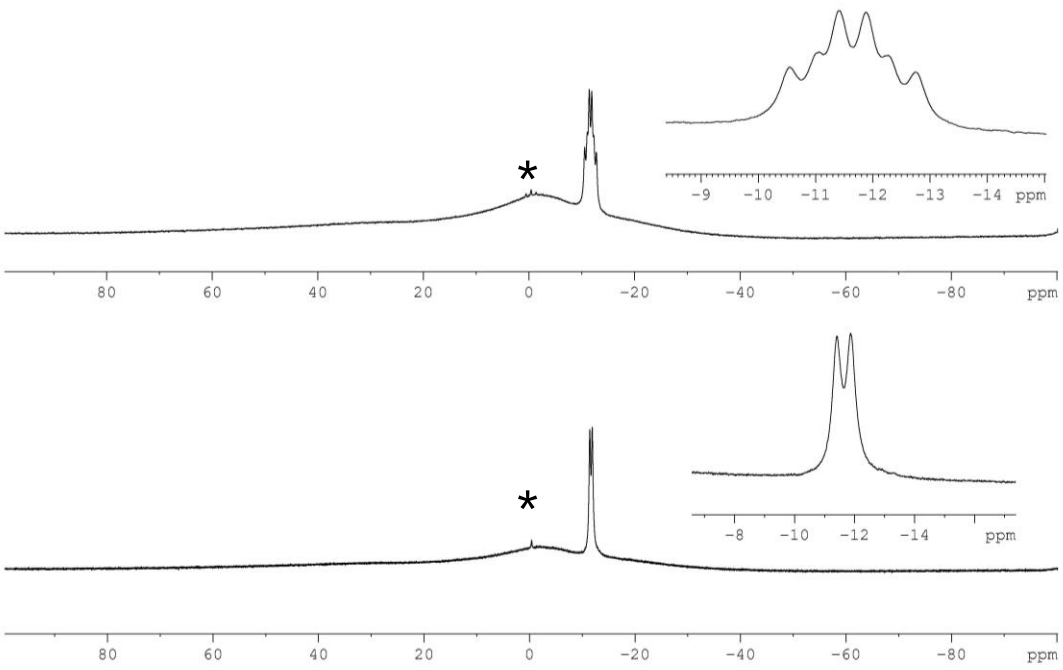

Figure S7: $^{11}B\{^1H\}$ (bottom) and ^{11}B NMR spectrum (top) of **1a**[$AlCl_4$] in CD_2Cl_2. * = decomposition product $ClBH_2{\cdot}NMe_3$.

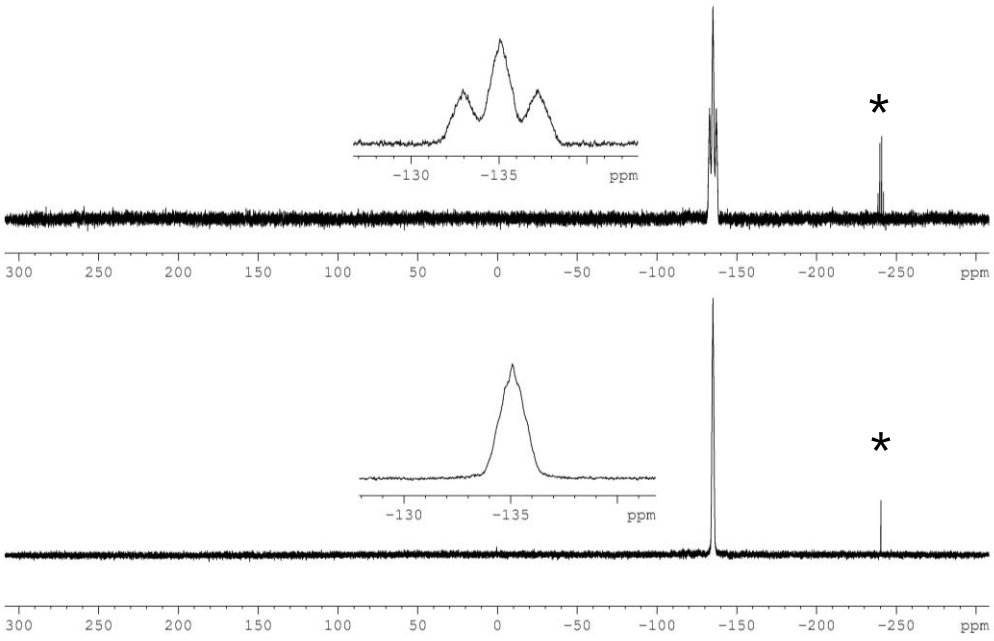

Figure S8: $^{31}P\{^1H\}$ (bottom) and ^{31}P NMR spectrum (top) of **1a**[$AlCl_4$] in CD_2Cl_2. * = decomposition product PH_3.

$[Me_3N{\cdot}BH_2{-}AsH_2{-}BH_2{\cdot}NMe_3]^+[AlCl_4]^-$ (1b[$AlCl_4$]):

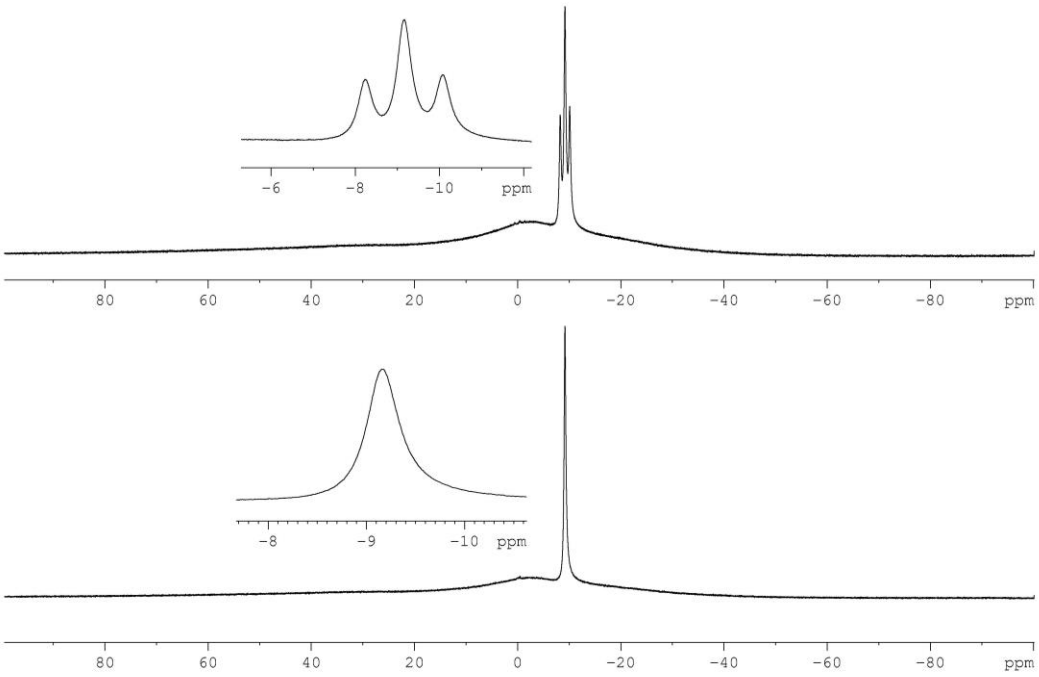

Figure S9: $^{11}B\{^1H\}$ (bottom) and ^{11}B NMR spectrum (top) of **1b**[$AlCl_4$] in CD_2Cl_2.

$[Me_3N{\cdot}BH_2{-}PH_2{-}BH_2{\cdot}NMe_3]^+[I]^-$ (1a[I]):

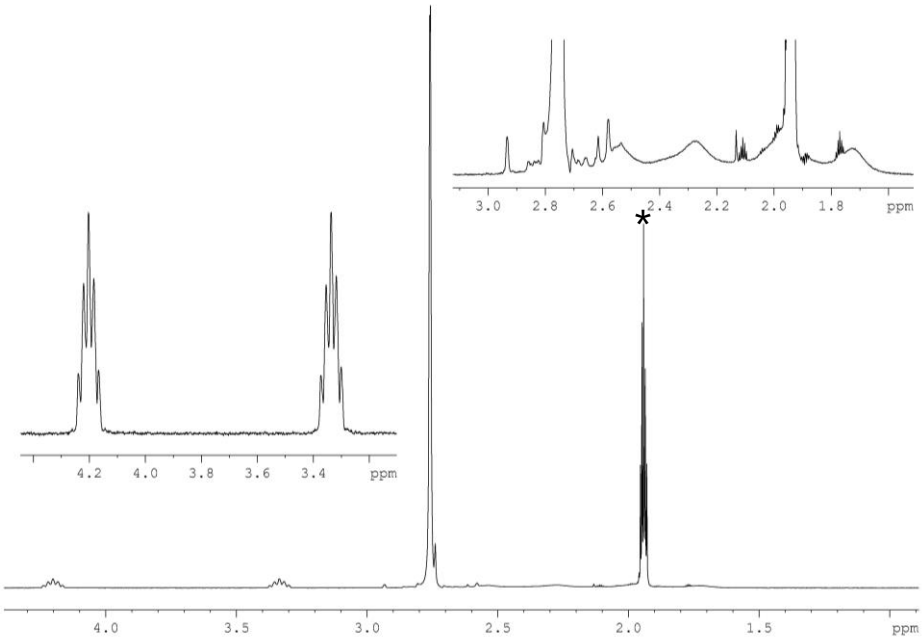

Figure S10: ^1H NMR spectrum of **1a**[I] in CD_3CN. * = solvent (CH_3CN)

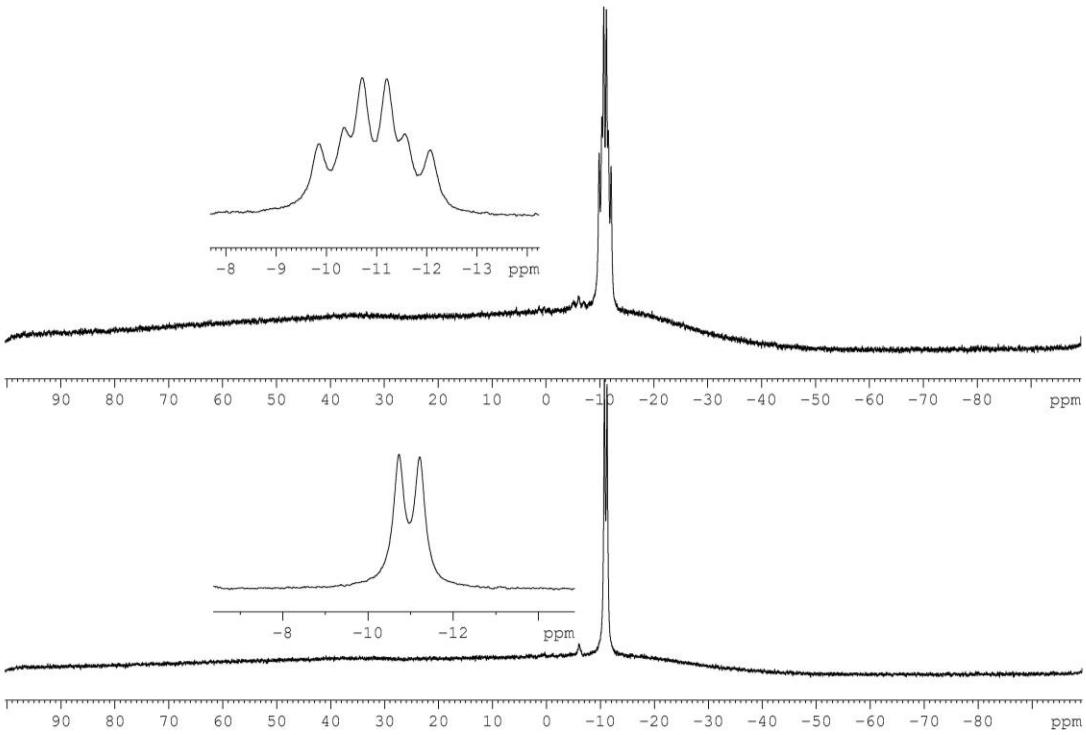

Figure S11: $^{11}B\{^{1}H\}$ (bottom) and ^{11}B NMR spectrum (top) of **1a**[I] in CD_3CN.

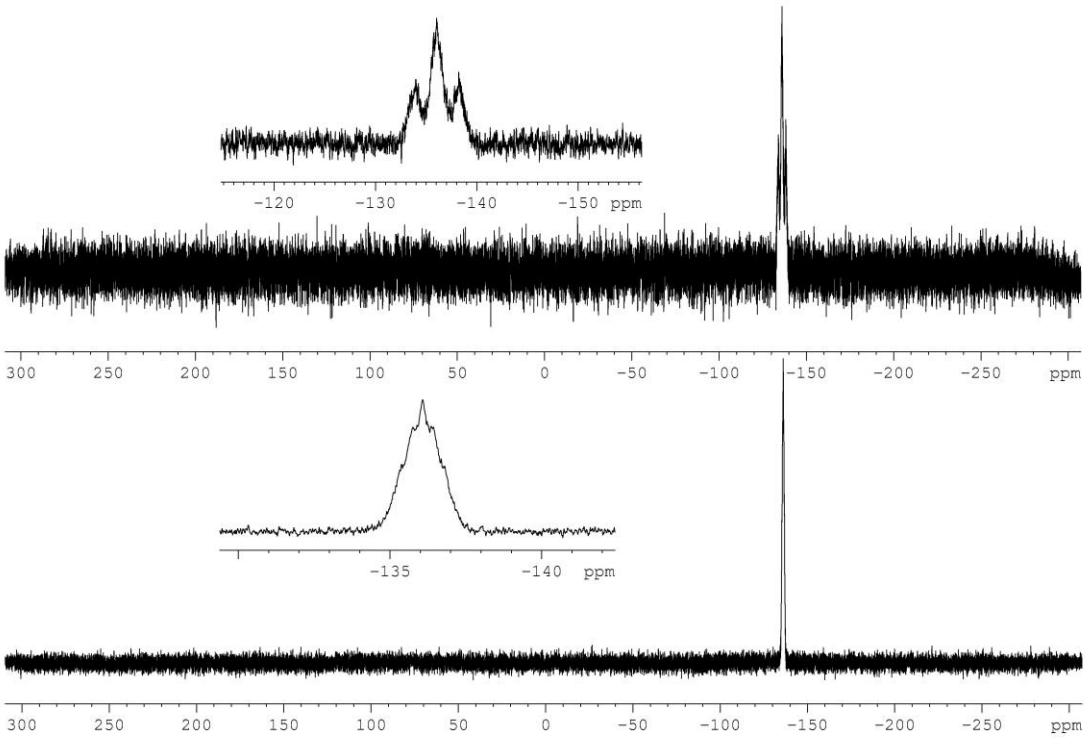

Figure S12: $^{31}P\{^{1}H\}$ (bottom) and ^{31}P NMR spectrum (top) of **1a**[I] in CD_3CN

$[Me_3N{\cdot}BH_2{-}AsH_2{-}BH_2{\cdot}NMe_3]^+[I]^-$ (1b[I]):

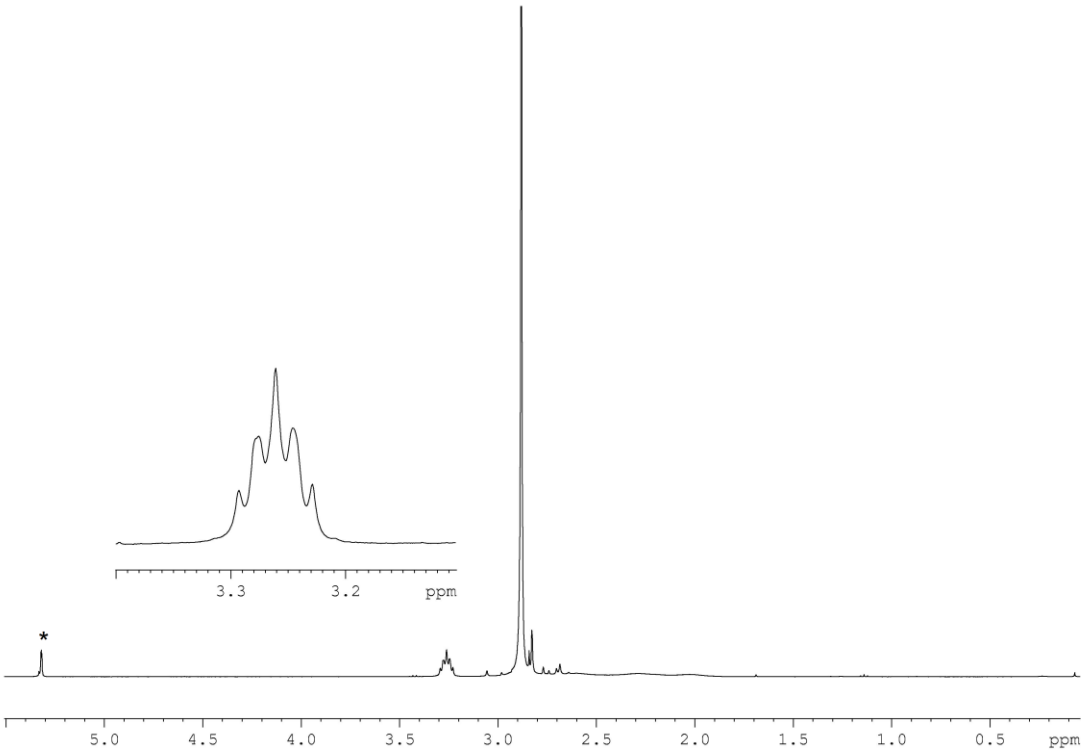

Figure S13: ^{1}H NMR spectrum of **1a**[I] in CD_2Cl_2. * = solvent (*)

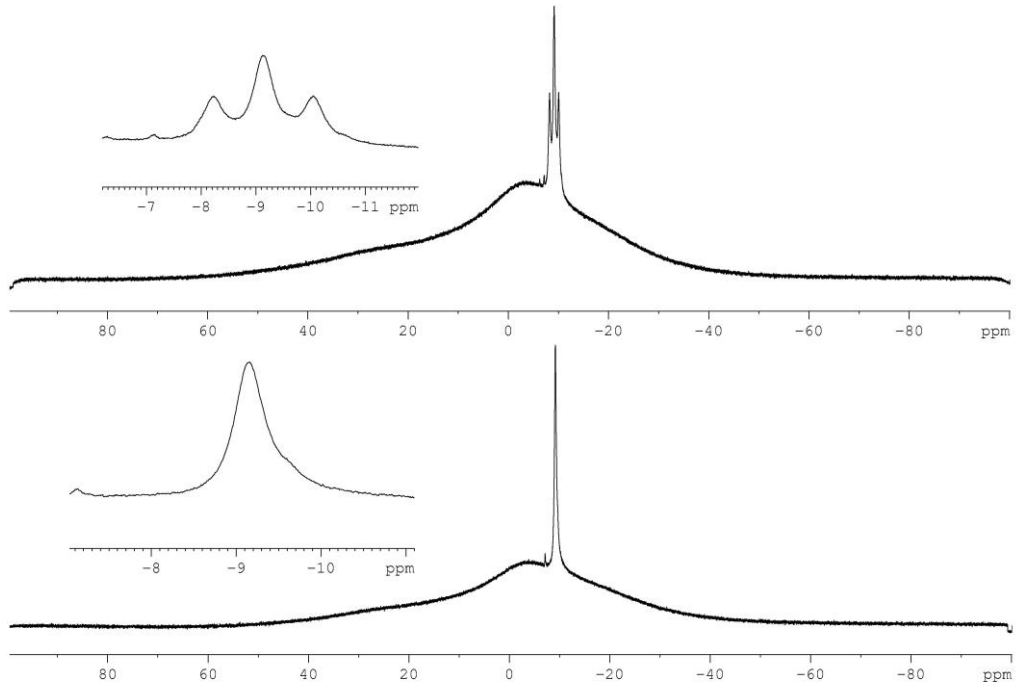

Figure S14: $^{11}B\{^1H\}$ (bottom) and ^{11}B NMR spectrum (top) of **1b**[I] in CD_2Cl_2.

$[Me_3N{\cdot}BH_2{-}PH_2{-}BH_2{-}PH_2{-}BH_2{\cdot}NMe_3]^+[I]^-$ (2[I]):

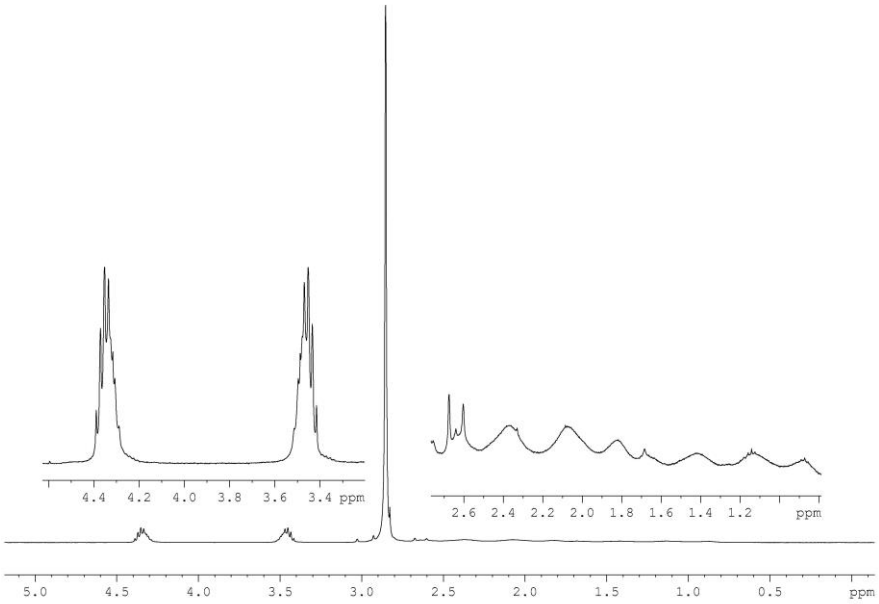

Figure S15: ^{1}H NMR spectrum of **2**[I] in CD_2Cl_2.

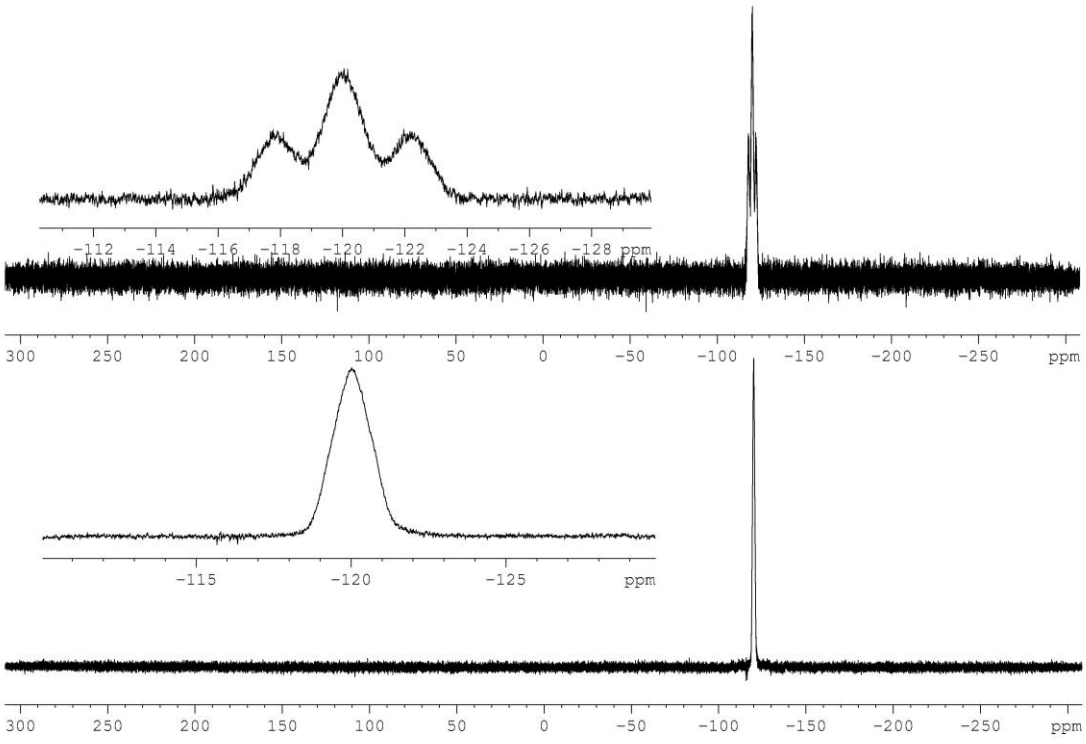

Figure S16: $^{11}B\{^1H\}$ (bottom) and ^{11}B NMR spectrum (top) of **2**[I] in CD_2Cl_2.

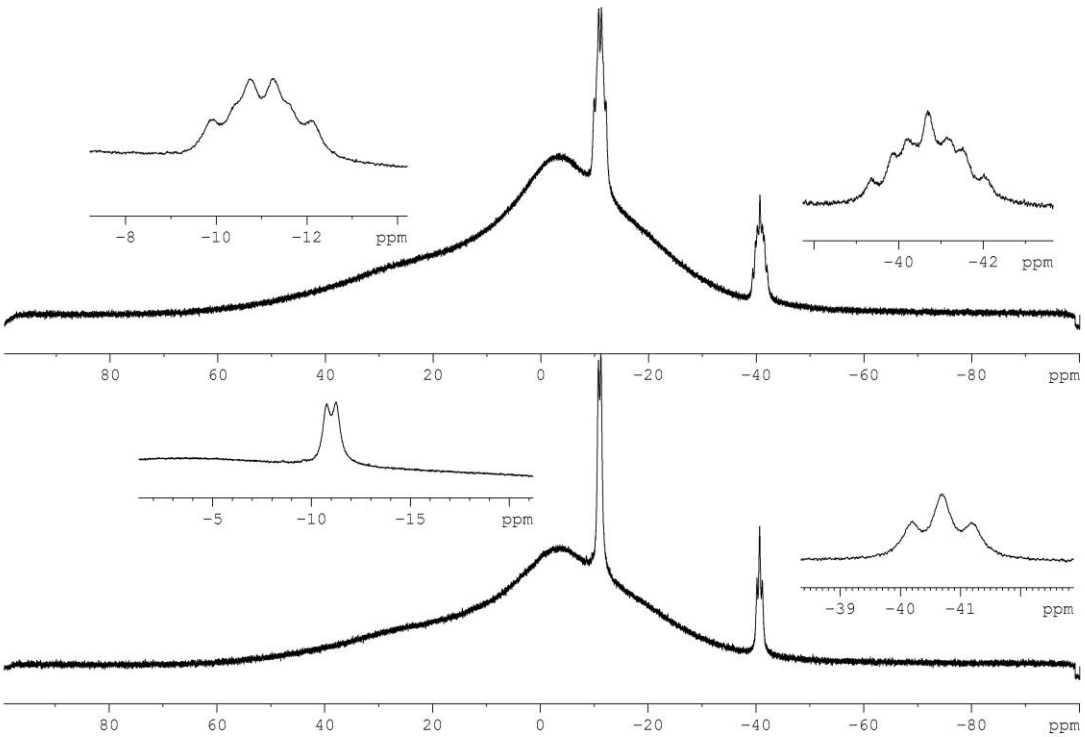

Figure S17: $^{31}P\{^{1}H\}$ (bottom) and ^{31}P NMR spectrum (top) of **2**[I] in CD_2Cl_2.

Computational Details

All calculations have been performed with the TURBOMOLE program package[9] at the B3LYP[10]/def2-TZVP[11] level of theory. The nature of the stationary point was checked by the absence of imaginary frequencies. For the calculation of the energy profile and relative energies the solvent effects were incorporated via the Conductor-like Screening Model (COSMO)[12] using the dielectric constant of CH_2Cl_2 (ε = 8.930). The natural population analysis[13] was performed as implemented in TURBOMOLE on the geometries optimized in the gas phase.

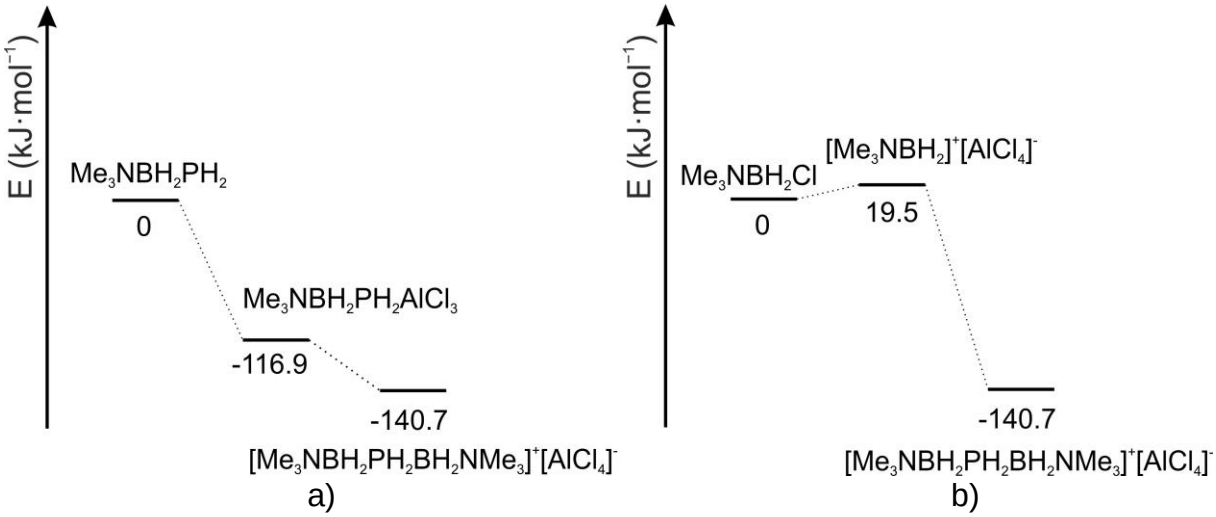

Figure S18. Energy profile of the reaction of $PH_2BH_2NMe_3$, $AlCl_3$ and $ClBH_2NMe_2$, starting from: a) $PH_2BH_2NMe_3$ and b) $ClBH_2NMe_3$. Relative energies calculated at the B3LYP/def2-TZVP level.

Table S4. Calculated reaction enthalpies at the B3LYP/def2-TZVP level of theory.

Reaction	Reaction enthalpy ($kJ \cdot mol^{-1}$)
$H_2PBH_2NMe_3 + ClBH_2NMe_3 + AlCl_3 = [Me_3NBH_2PH_2BH_2NMe_3]^+ + [AlCl_4]^-$	−140.65
$H_2PBH_2NMe_3 + AlCl_3 = Me_3NBH_2PH_2AlCl_3$	−116.94
$Me_3NBH_2PH_2AlCl_3 + ClBH_2NMe_3 = [Me_3NBH_2PH_2BH_2NMe_3]^+ + [AlCl_4]^-$	−23.71
$AlCl_3 + ClBH_2NMe_3 = [Me_3NBH_2]^+ + [AlCl_4]^-$	19.47
$H_2PBH_2NMe_3 + [Me_3NBH_2]^+ = [Me_3NBH_2PH_2BH_2NMe_3]^+$	−160.12

Cartesian coordinates of the optimized geometry (xyz) can be obtained from http://dx.doi.org/10.1002/anie.201310519.

References

[1] C. Marquardt, A. Adolf, A. Stauber, M. Bodensteiner, A. V. Virovets, A. Y. Timoshkin, M. Scheer, *Chem. Eur. J.* **2013***, 19*, 11887–11891.

[2] G. E. Ryschkewitsch, J. W. Wiggins, *Inorg. Synth.,* **1970**, *12*, 116.

[3] A. Gansäuer, B. Rinker, *Tetrahedron* 2002, *58*, 7017–7026

[4] Agilent Technologies **2006-2011**, CrysAlisPro Software system, different versions, Agilent Technologies UK Ltd, Oxford, UK.

[5] A. Altomare, M. C.Burla, M. Camalli, G. L. Cascarano, C. Giacovazzo, A. Guagliardi, A.G. G. Moliterni, G. Polidori, R. Spagna, J. Appl. Cryst. **1999**, *32*, 115–119

[6] L. Palatinus, G. Chapuis, *J. Appl. Cryst.* **2007**, *40*, 786–790.

[7] G. M. Sheldrick, *Acta Cryst.* **2008**, *A64*, 112–122.

[8] a) E. Keller, **1997**, SCHAKAL99, Freiburg. b) K. Brandenburg, H. Putz, **2005**, DIAMOND 3, Crystal Impact GbR, Postfach 1251, D-53002 Bonn. c) O.V. Dolomanov, L.J. Bourhis, R.J. Gildea, J.A.K. Howard, H.Puschmann, OLEX2: A complete structure solution, refinement and analysis program, *J. Appl. Cryst*. **2009**, *42*, 339–341.

[9] a) R. Ahlrichs, M. Bär, M. Häser, H. Horn, C. Kölmel, *Chem. Phys. Lett.***1989**, *162*, 165–169; b) O. Treutler, R. Ahlrichs, *J. Chem. Phys.* **1995**, *102*, 346–354.

[10] a) P. A. M. Dirac, *Proc. Royal Soc.A*,**1929**, *123*, 714; b) J. C. Slater, *Phys. Rev.***1951**, *81*, 385; c) S. H. Vosko, L. Wilk, M. Nusair, *Can. J. Phys.***1980**, *58*, 1200. d) A. D. Becke, *Phys. Rev. A*, **1988**, *38*, 3098. e) C. Lee, W. Yang, R. G. Parr, *Phys. Rev. B*,**1988**, *37*, 785. f) A. D. Becke, *J. Chem. Phys.* **1993**, *98*, 5648.

[11] a) A. Schäfer, C. Huber, R. Ahlrichs, *J. Chem. Phys.***1994**, *100*, 5829; b) K. Eichkorn, F. Weigend, O. Treutler, R. Ahlrichs, *Theor. Chem. Acc.***1997**, *97*, 119.

[12] A. Klamt, G. Schüürmann, *J. Chem. Soc. Perkin Trans. 2*, **1993**, 799–805; A. Schäfer, A. Klamt, D. Sattel, J. C. W. Lohrenz, F. Eckert, *Phys. Chem. Chem. Phys.* **2000**, *2*, 2187–2193.

[13] A. E. Reed, R. B. Weinstock, F. Weinhold, *J. Chem. Phys.* **1985**, *83*, 735–746.

4.6 Author Contributions

The syntheses and characterization of compounds **1a**[$AlCl_4$], **1b**[$AlCl_4$], **1b**[I] and **2**[I] were performed by Christian Marquardt.

The syntheses and characterization of compound **1a**[I] was performed by Dr. Andreas Stauber (reported in his PhD-thesis, Regensburg, **2014**) and of compound **2**[$VCl_4(THF)_2$] by Dr. Christine Thoms (reported in her PhD-thesis, Regensburg, **2012**).

X-ray structural analyses of all compounds were performed by Christian Marquardt, except of **2**[$VCl_4(THF)_2$] which was performed by Dr. Michael Bodensteiner.

All DFT-calculations were performed by Dr. Gábor Balázs.

The manuscript (including supporting information, figures, schemes and graphical abstract) was written by Christian Marquardt.

5. Cationic chains of Arsanylboranes and substituted Phosphanylboranes

C. Marquardt, G. Balázs, A.V. Virovets and M. Scheer

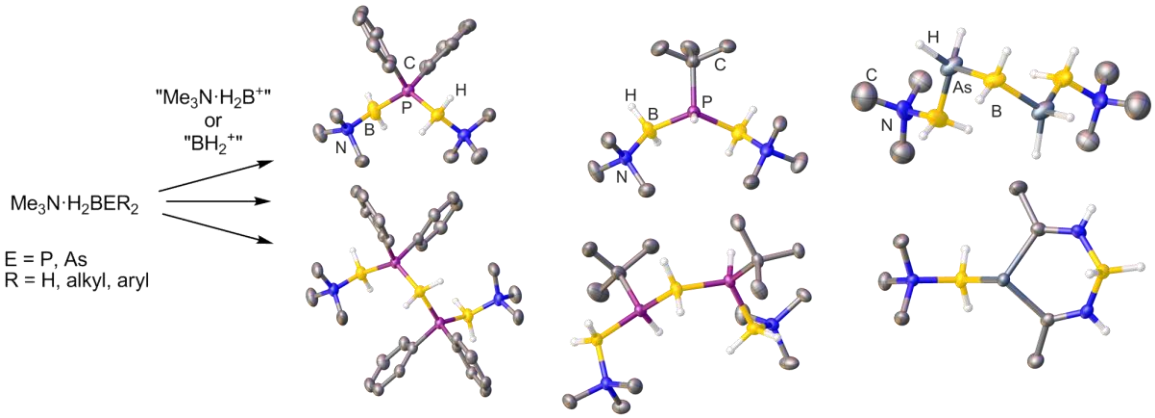

Abstract: The substituted monomeric phosphanylboranes $Ph_2P–BH_2·NMe_3$ and $^tBuHP–BH_2·NMe_3$, have been used for the synthesis of cationic chain compounds buildup by $R_2E–BH_2$ units. The products $[Me_3N·H_2B–PR_1R_2–BH_2·NMe_3]^+I^-$ and $[Me_3N·H_2B–PR_1R_2–BH_2–PR_1R_2–BH_2·NMe_3]^+I^-$ (R_1 = R_2 = Ph; R_1 = H, R_2 = ^{t}Bu) were studied by X-ray structure analysis, NMR, IR spectroscopy and mass spectrometry. DFT calculations show the relatively high charge separation within the cation. The reaction of $H_2As–BH_2·NMe_3$ with $IBH_2·SMe_2$ leads to the formation of $[Me_3N·H_2B–AsH_2–BH_2–AsH_2–BH_2·NMe_3]^+I^-$ (**3a**), which was fully characterized. Compound **3a** reacts with acetonitrile via a formal hydroarsination reaction to [*cyclo*-{$As(BH_2·NMe_3)(CMe=NH)_2(BH_2)$}$]^+[I]^-$ (**3b**). The reported synthetic strategy proved to be a general way for the formation of small, cationic oligomeric units.

5.1 Introduction

In the last years phosphine-borane adducts of the type $H_3B{\cdot}PH_2R$ (R = aryl, alkyl) gained increasing interest, as they are valuable precursors for the synthesis of inorganic polymers via metal catalyzed dehydrocoupling reactions.[1] Very recently a new earth abundant polymerization catalyst was reported for the synthesis of poly(phosphinoborane)s.[2] In addition the ferrocenyl substituted phosphine-borane adduct $H_3B{\cdot}PH^tBuFc$ (Fc = ferrocen) was dimerized by a dehydrocoupling reaction.[3] Besides the linear poly(phosphinoborane)s, the homocatenation of non-carbon elements is also in the focus of current research. Whereas several chains of polyphosphines and polyphosphorus anions have been reported some decades ago,[4] only recently the chemistry of *catena*-phosphorus cations was extensively studied by *Burford,* leading to a variety of new *catena*-phosphorus species.[5] Besides homoatomic species, mixed group 13/15 element cations are of high interest. Boronium cations of the formula $[H_2B(EMe_3)_2]^+$ (E = P, As) are already known for some decades.[6] Dications, where 3 phosphorus donors coordinate to a formally BH^{2+} dication (*i.e.* $[BH(PMe_3)_3]^{2+}$) have been reported, as well.[7] In addition to linear species many examples of cyclic species are known (**I**, **II**).[8] The diphosphinoboronium cations can be used for the facile synthesis of highly congested diphosphinobenzene derivatives,[9] deprotonation of $[H_2B(PMe_3)_2]^+$ with MeLi, leads to the ylide **III** which was used as chelating ligands for transition metals (**IV**).[10] The application of diphosphinoboronium cations as precursors for chiral ligands for Rh-catalyzed asymmetric hydrogenation has also been reported.[11]

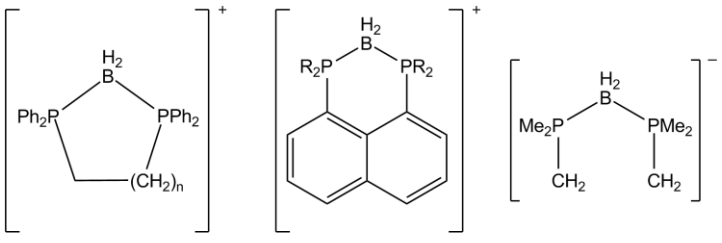

I n = 1 - 3 **II** R = Me, Ph **III**

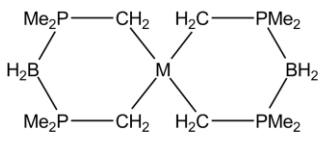

IV M = Ni, Pd, Pt

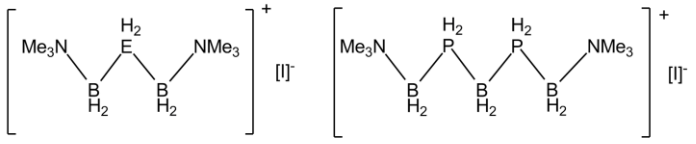

V (E = P, As) **VI**

Our group is especially interested in the synthesis and reactivity of group 13/15 compounds bearing only hydrogen substituents at the group 13/15 elements. We reported the high-yield synthesis of the pnictogenylboranes $H_2EBH_2{\cdot}NMe_3$ (E = P, As),[12] which are excellent building blocks for the generation of oligomeric[13] and polymeric[14] compounds. Furthermore, this enabled the preparation of compounds containing cationic chains of phosphanyl- and arsanylboranes of type **V** and **VI**, which are relatives of alkanes.[15] For the arsenic derivative, only **V** containing the shorter cationic chain $[Me_3N{\cdot}H_2B–AsH_2–BH_2{\cdot}NMe_3]^+$ was obtained. In the case of phosphorus as the group 15 element the cationic species $[Me_3N{\cdot}H_2B–[PH_2–BH_2]_n{\cdot}NMe_3]^+$ (**V**: n = 1; **VI**: n = 2) could be isolated and characterized. Interestingly, in the electron impact mass spectrometry experiments of polymers obtained by thermolysis experiments of $Ph_2P–BH_2{\cdot}NMe_3$ (**1**) and ^{t}BuHP–$BH_2{\cdot}NMe_3$ (**2**), cationic chains of the type **V** and **VI** were observed and are supposed to play an important role during the polymerization.[14] Motivated from our recent results in the field of poly(phosphinoborane)s and cationic chain-like compounds of the unsubstituted phosphanylborane, we aimed for a selective approach and investigated the reactivity of **1** and **2** towards $IBH_2{\cdot}NMe_3$ as well as $IBH_2{\cdot}SMe_2$.

5.2 Results and Discussion

The reaction of **1** and **2** with $IBH_2{\cdot}NMe_3$ leads quantitatively (according to ^{31}P NMR) to the formation of $[Me_3N{\cdot}H_2B–PR_1R_2–BH_2{\cdot}NMe_3]^+[I]^-$ (**1a** $R_1 = R_2$ = Ph, **2a** R_1 = H, R_2 = ^{t}Bu) and can be isolated in good crystalline yields (Scheme 1). By reacting $IBH_2{\cdot}SMe_2$, containing the more labile Lewis base SMe_2 with **1** and **2** the compounds $[Me_3N{\cdot}H_2B–PR_1R_2–BH_2–PR_1R_2–BH_2{\cdot}NMe_3]$ (**1b** $R_1 = R_2$ = Ph, **2b** R_1 = H, R_2 = ^{t}Bu), with a longer cationic chains are formed quantitatively and can be isolated in good crystalline yields (Scheme 1). All obtained ionic compounds are white solids which are well soluble in polar solvents like CH_2Cl_2, MeCN or THF. Similar to the cationic chains of the parent compound **I** and **II**, they are not sensitive towards oxygen or moisture.

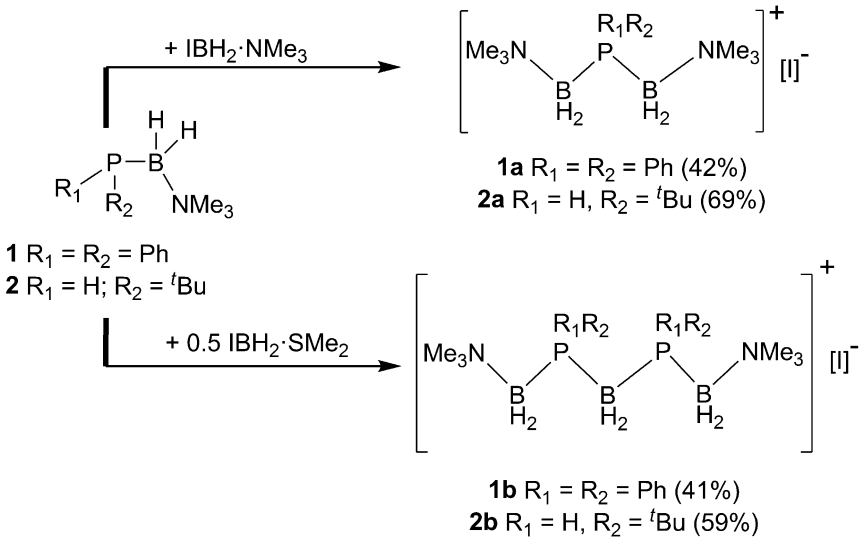

Scheme 1. Synthesis of **1a**, **1b**, **2a** and **2b**. Crystalline yields are given in parentheses.

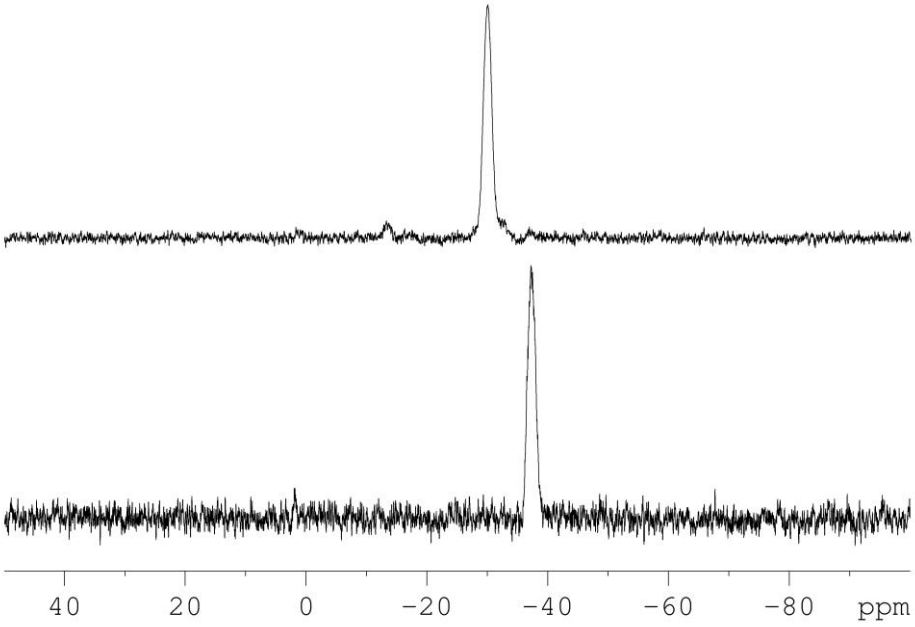

Figure 1. ^{31}P NMR spectra of **1a** (bottom) and **1b** (top) in CD_2Cl_2.

The ^{31}P NMR spectra reveal a broad singlet at δ = –37.3 ppm for **1a** and at δ = –30.0 ppm for **1b**, respectively. In the ^{11}B NMR spectrum of **1a** a broad signal can be detected at δ = –8.0 ppm. The ^{11}B NMR spectrum of **1b** shows a broad triplet at δ = –30.5 ppm for the central boron atom and a broad signal at δ = –7.6 ppm for the terminal boron atoms. Due to broadness of the signals, a fine splitting could not be resolved. The IR spectra of **1a** and **1b** show absorptions for the B–H valence stretches between 2452 cm^{-1} and 2395 cm^{-1} and in the ESI-MS spectra of **1a,b** and **2a,b** the molecular ion peak is detected.

Single crystals of **1a** and **1b** are obtained by layering a CH_2Cl_2 solution of the compounds with *n*-hexane. In the solid state **1a** reveals a B–P–B chain in which all substituents adopt a staggered conformation along the P-B axis. The P–B bond lengths of **1a** are 1.981(4) and 1.981(3) Å and the B–P–B angle measures 123.04(16)°. Compound **1b** crystallizes with two independent cations in the asymmetric unit. Again along the P-B axis of the B–P–B–P–B chain all substituents are in a staggered conformation. All P–B bond lengths are similar, the peripheral P1–B2 and P2–B3 bonds range from 1.971(4) to 1.975(4) Å whilst the inner P1–B2 and P2–B2 bonds are slightly shorter with 1.945(4) to 1.962(4) Å. The B1–P1–B2 and B2–P2–B3 angles range from 123.39(18) to 124.30(18)° and P1–B2–P2 from 119.12(19) to 119.32(19)°. Compared to the starting material **1** the P–B bond lengths do not change essentially for the cationic compounds **1a** and **1b** (1.975(2) Å for $Ph_2P–BH_2·NMe_3$).[14]

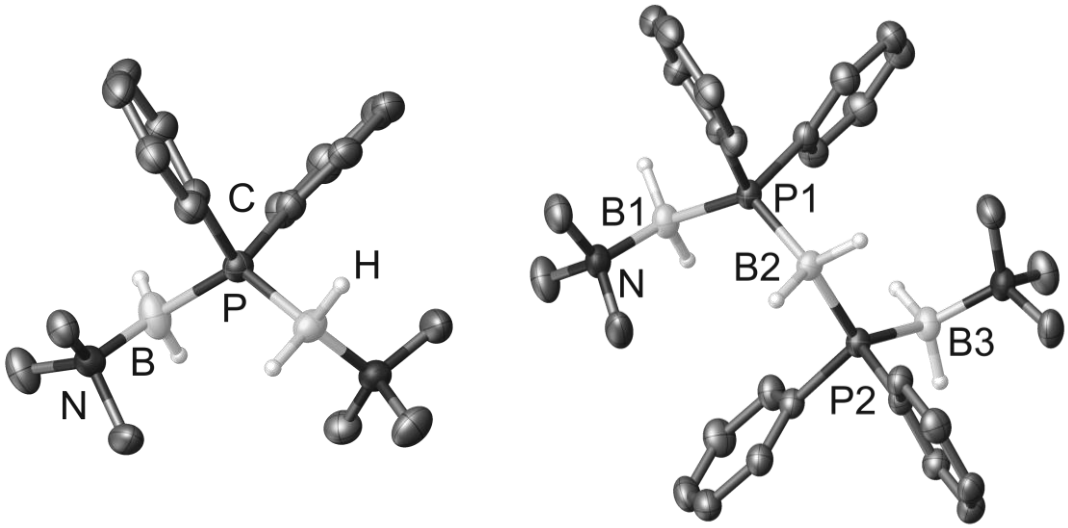

Figure 2. Molecular structures of the cations in **1a** (left) and **1b** (right) in the solid state. Hydrogen atoms bond to carbon atoms are omitted for clarity. Thermal ellipsoids are drawn with 50% probability. Selected bond lengths [Å] and angles [°]: **1a** P–B 1.981(4) – 1.983(4), B–P–B 123.04(16); **1b** P1–B1 1.971(4) – 1.972(4), P1–B2 1.948(4) – 1.962(4), P2–B2 1.945(4), P2–B3 1.971(4) – 1.975(4), B1–P1–B2 123.94(18) - 124.30(18), P1–B2–P2 119.12(19) – 119.32(19), B2–P2–B3 123.39(18) – 123.71(18).

Like the parent compounds $[Me_3N·H_2B–[PH_2–BH_2]_n·NMe_3]^+I^-$ (n = 1, 2) **1a** shows a high thermodynamic stability. However, in one case we were able to structurally characterize $[Me_3N·H_2B–PPh_2–CH_2CH_2CH_2CH_2OH]^+I^-$ (**1c**) which seems to be a decomposition product of **1a** in which THF is involved. Interestingly, it could not be detected in the reaction mixture by NMR spectroscopy or mass spectrometry even after storage of **1a** for several months in THF solution. However it was unambiguously identified in two single-crystal X-ray experiments (**1c**, **1c**thf).[16] DFT calculations show, that the isomer of **1c** in which the oxygen bonds to phosphorus is thermodynamically

more stable by 46.78 kJ·mol^{-1} then the isomer with the carbon atom bonded to phosphorus.

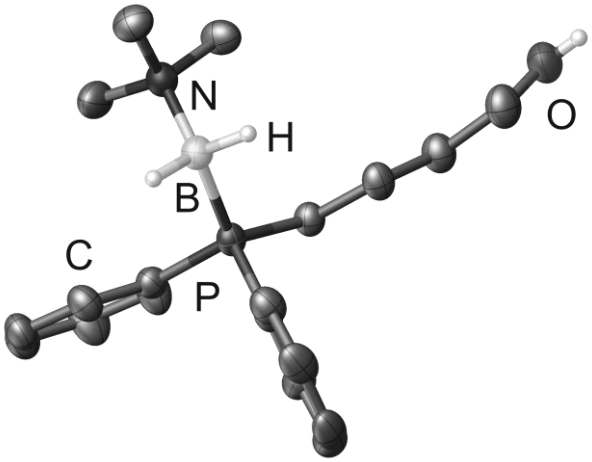

Figure 3. Molecular structures of the cation in **1c** in the solid state. Hydrogen atoms bond to carbon atoms are omitted for clarity. Thermal ellipsoids are drawn with 50% probability. Selected bond lengths [Å] and angles [°]: **1c** P–B 1.981(4) – 1.983(4), B–P–B 123.04(16).

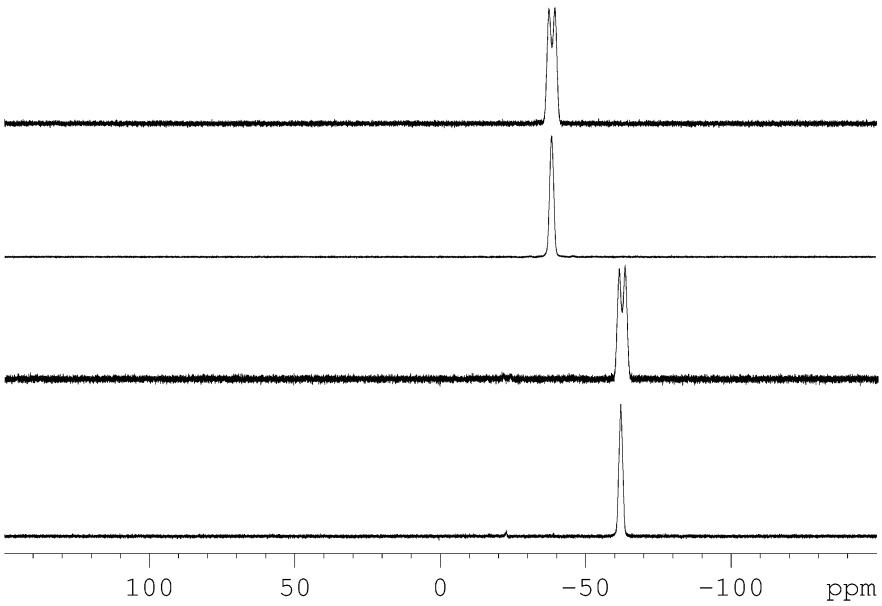

Figure 4. NMR spectra of **2a** ($^{31}P\{^{1}H\}$,^{31}P) and **2b** ($^{31}P\{^{1}H\}$,^{31}P; bottom to top) in CD_2Cl_2.

The ^{31}P NMR spectra reveal a doublet at δ = –62.0 ppm for **2a** ($^{1}J_{P,H}$ = 326 Hz) and at δ = –38.0 ppm for **2b** ($^{1}J_{P,H}$ = 332 Hz), respectively. In the ^{11}B NMR spectrum of **2a** a broad multiplett is be detected at δ = –9.1 ppm. The ^{11}B NMR spectrum of **2b** shows a broad multiplett at δ = –38.1 ppm for the central boron atom and a broad signal at δ = –9.8 ppm for the terminal boron atoms. With four different substituents on the two phosphorus atoms **2b** possesses two chirality centres. Therefore three different isomers

(*D*-, *L*- and *meso*-**2b**, Scheme 2) are possible. ^{31}P and ^{11}B NMR spectra of **2b** show only one set of signals, since presumably the signals of the isomers are overlapping/superimposed. However in the ^{1}H NMR spectrum two set of signals can be found, one for *meso*-**2b** and one for the D-/L-**2b** isomers, with a ratio of 4:1. The IR spectra of **2a** and **2b** show absorptions for the B–H valence stretches between 2444 cm^{-1} and 2405 cm^{-1} and for the P–H valence stretches between 2313 cm^{-1} and 2287 cm^{-1}.

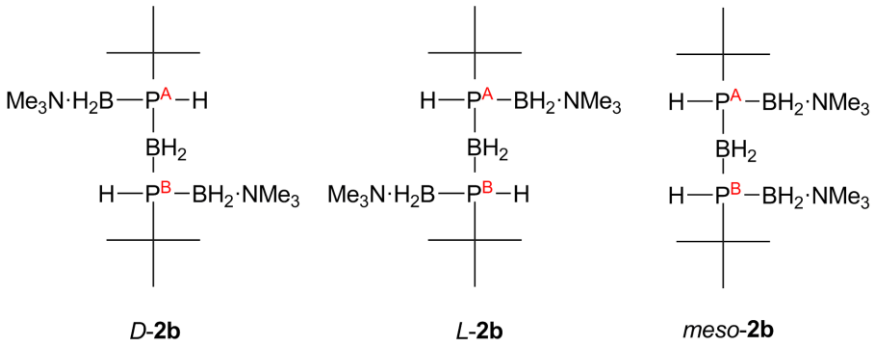

D-**2b** *L*-**2b** *meso*-**2b**

Scheme 2. *D*-/*L*- and *meso*- forms of **2b**.

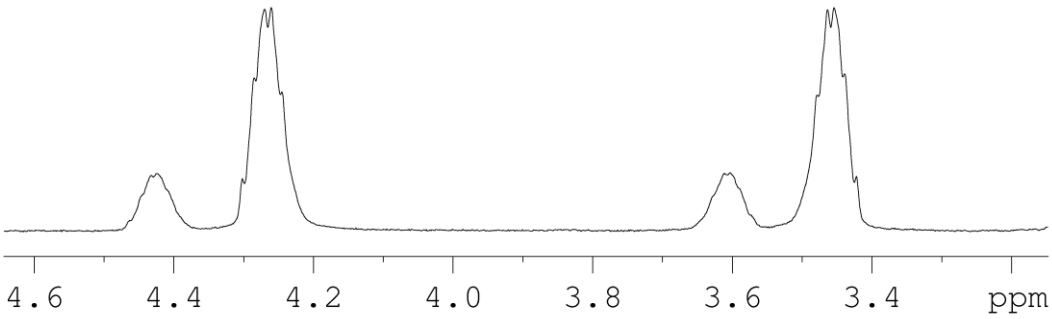

Figure 5. P-H-Region of the ^{1}H NMR spectrum of **2b** in CD_2Cl_2 showing the resonance signals of the P-H-groups of the *meso*- and the D-/L-form.

In the solid state **2a** reveals a B–P–B chain in which all substituents are in an eclipsed, anticlinal conformation along the P–B axis. The P–B bond lengths of compound **2a** are 1.977(5) and 1.979(4) Å and the B–P–B angle measures 112.4(2)°. For **2b** single crystal X-ray structure determination could only be performed for *meso*-**2b**. However the ^{1}H NMR spectrum suggests that also the D-/L-compounds are present. Despite many attempts it could not be separated or crystallized and seems to be an oily adhesive on the crystals. In the solid state **2b** shows a five membered B–P–B–P–B chain. Along the P1–B1- and the P2–B2-axis the substituents adopt an antiperiplanar conformation, whilst along the P1–B2 axis a synclinal and along the P2–B3- axis an anticlinal arrangement can be found. Compound **2b** reveals similar P–B bond lengths, the outer P1–B2 and P2–

B3 bonds are 1.975(3) and 1.981(3) Å, respectively, whilst the inner P1–B2 and P2–B2 bonds are slightly shorter with 1.940(3) and 1.946(3) Å, respectively. The B1–P1–B2 and B2–P2–B3 angles range from 113.54(11) to 114.41(11)° and the P1–B2–P2 angle is 116.43(13)°. Compared to the starting material **2** the P–B bond lengths are a little shortened (1.985(2) Å for ^{t}BuHP–BH_2·NMe_3).[14]

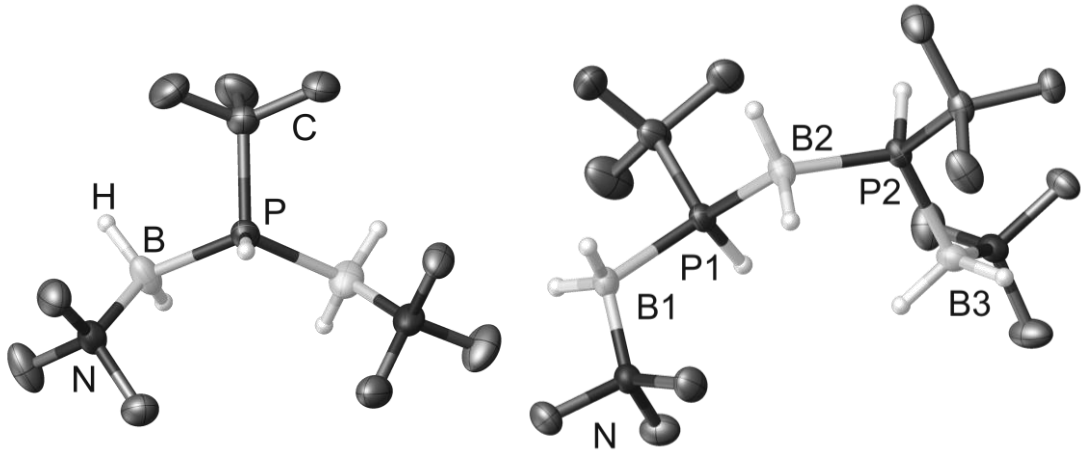

Figure 6. Molecular structures of the cations in **2a** (left) and **2b** (right) in the solid state. Hydrogen atoms bond to carbon atoms are omitted for clarity. Thermal ellipsoids are drawn with 50% probability. Selected bond lengths [Å] and angles [°]: **2a** P–B 1.977(5) – 1.979(4), B–P–B 112.4(2); **2b** P1–B1 1.981(3), P1–B2 1.940(3), P2–B2 1.946(3), P2–B3 1.975(3), B1–P1–B2 114.41(11), P1–B2–P2 116.43(13), B2–P2–B3 113.54(11).

DFT calculations show that the *meso*-isomer of **2b** is thermodynamically favoured by 2.45 kJ·mol^{-1}.

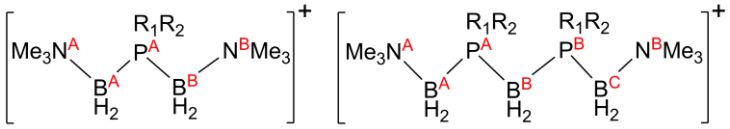

I $R_1 = R_2 = H$
1a $R_1 = R_2 = Ph$
1b $R_1 = H$, $R_2 = {}^{t}Bu$

II $R_1 = R_2 = H$
2a $R_1 = R_2 = Ph$
2b $R_1 = H$, $R_2 = {}^{t}Bu$

Natural population analysis (NPA) shows a charge separation within the cationic chain in **1a,b** and **2a,b**, similar to that observed in **I** and **II** (Table1). Generally, the phenyl substituted phosphorus atoms are more positive compared to the ^{t}Bu substituted ones. In **1b** and **2b** the central boron atom bears a considerably higher negative charge than the peripheral boron atoms.

Table 1. Distribution of NPA charges in **I**, **II**, **1a**, **1b**, **2a**, **2b**.

	N^A	B^A	P^A	B^B	P^B	B^C	N^B
I	-0.34	-0.22	0.52	-0.22	-	-	-0.34
1a	-0.35	-0.22	1.04	-0.22	-	-	-0.35
2a	-0.34	-0.21	0.75	-0.22	-	-	-0.34
II	-0.34	-0.23	0.58	-0.74	0.58	-0.23	-0.34
1b	-0.35	-0.22	1.09	-0.77	1.09	-0.22	-0.35
2b	-0.34	-0.22	0.83	-0.77	0.83	-0.22	-0.34

If $H_2As–BH_2·NMe_3$ is reacted with $IBH_2·SMe_2$, $[Me_3N·H_2B–AsH_2–BH_2–AsH_2–BH_2·NMe_3]^+I^-$ (**3a**) is formed, according to ^1H and ^{11}B NMR studies of the reaction mixture. Despite the surprising thermal stability of the phosphorus derivative **II** the longer cationic arsenic derivative $[Me_3N·H_2B–AsH_2–BH_2–AsH_2–BH_2·NMe_3]^+I^-$ (**3a**) initially only could be characterised in solution by NMR spectroscopy. Due to its instability compound **3a** readily undergoes reaction with solvents. However, **3a** can be obtained in good crystalline yields (79%, scheme 2) from layering a CH_2Cl_2 solution with *n*-hexane at -28°C. Storage of a CH_2Cl_2 solution at room temperature leads to fast decomposition. Attempts to isolate **3a** from other solvents (Et_2O, THF, MeCN) failed as side reactions take place.

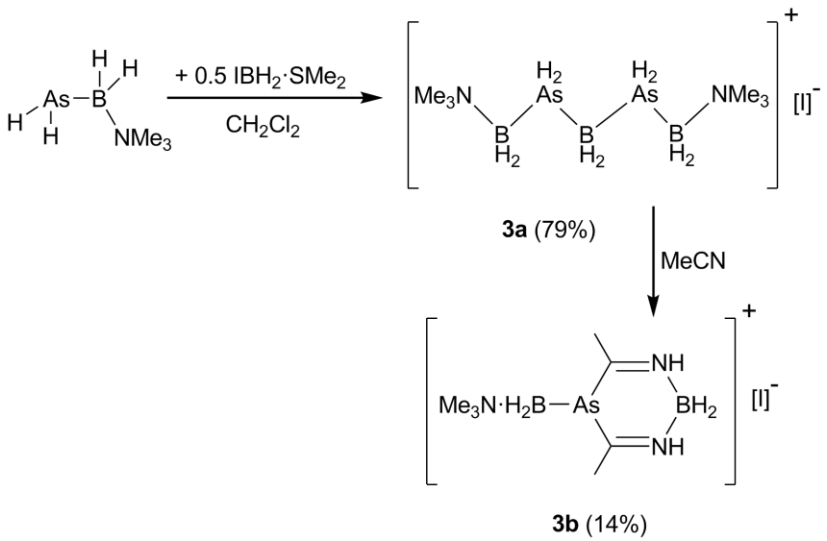

Scheme 2. Synthesis of **3a** and its decomposition to **3b**. Crystalline yields are given in parentheses.

In the $^{11}B\{^1H\}$ NMR spectrum of **3a** a broad signal can be found at δ = –35.7 ppm for the central B atom, and for the NMe_3 coordinated boron atom at δ = –8.6 ppm. In the ^{11}B NMR spectrum both signals split into triplets with typical $^1J_{B,H}$ coupling constants ($^1J_{B,H}$ = 114 Hz). The IR spectrum of **3a** shows absorptions for the B–H valence stretches

between 2448 cm^{-1} and 2425 cm^{-1} and for the As–H valence stretches at 2310 cm^{-1}. Whilst the parent compounds of the phosphorus derivatives are stable, **3a** is in solution very prone towards decomposition. Storing a solution of **3a** in acetonitrile leads to the heterocycle **3b**, which could be fully characterized. DFT calculations reveal that this process is exothermic by 109.8 $kJ \cdot mol^{-1}$. Stirring **3a** in CH_2Cl_2 leads to decomposition with the formation of an insoluble red solid, for which the reaction solution shows only the resonances for $ClBH_2 \cdot NMe_3$ in the ^{11}B NMR spectrum. However, dissolving of solid **3a** in CH_2Cl_2 followed by immediate filtration and over layering of the solution with *n*-hexane leads to crystalline **3a** at -28°C. In the $^{11}B\{^1H\}$ NMR spectrum of **3b** a broad signal is found at δ = –10.6 ppm for the B atom of the heterocycle, the resonance signal of the arsenic bond boron atom is assigned at δ = –2.3 ppm. In the ^{11}B NMR spectrum both signals split into triplets with typical $^1J_{B,H}$ coupling constants ($^1J_{B,H}$ = 112 Hz and $^1J_{B,H}$ = 122 Hz for only arsenic bond boron). The IR spectrum of **3b** shows absorptions for the B–H valence stretches between 2456 cm^{-1} and 2428 cm^{-1}. In the ESI-MS spectra the molecular ion peak is detected for **3a** and **3b**.

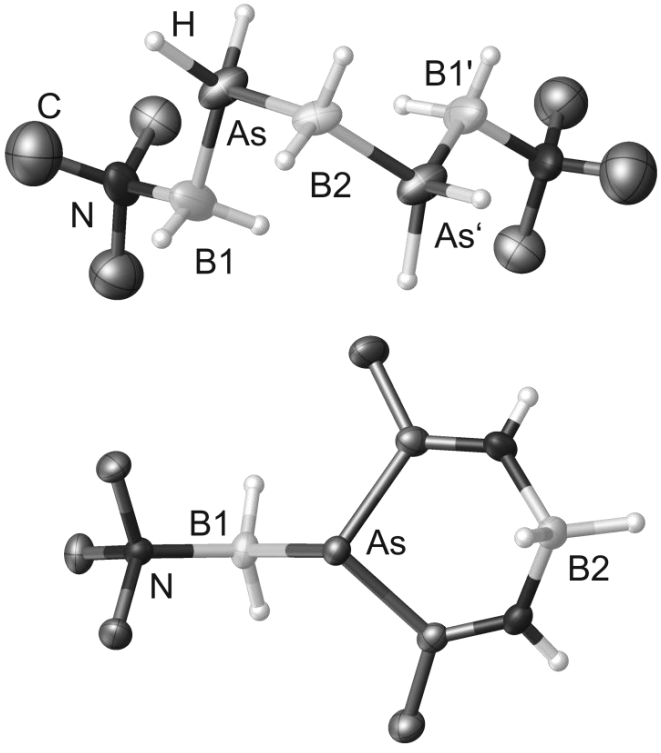

Figure 7. Molecular structures of the cations in **3a** (top) and **3b** (bottom) in the solid state. Hydrogen atoms bond to carbon atoms are omitted for clarity. Thermal ellipsoids are drawn with 50% probability. Selected bond lengths [Å] and angles [°]: **3a** As–B1 2.070(9), As–B2 2.048(6), B1–As–B2 111.4(3), As–B2–As 107.0(5); **3b** As–B1 2.1123(19) – 2.1377(13), As–C 1.9435(16) – 1.9521(16).

In the solid state **3a** reveals similar As–B bond lengths, with 2.070(9) Å for the peripheral As–B1 bond and slightly shorter As–B2 bonds lengths (2.048(6) Å). The B1–

As–B2 angle measures 111.4(3) and the As–B1–As' angle 107.0(5)°. The As-B bond lengths are shorter compared to $[Me_3N{\cdot}H_2B–AsH_2–BH_2{\cdot}NMe_3]^+$ (**I**, 2.076(5) – 2.086(4)Å)[11] and similar to the starting material $H_2As–BH_2{\cdot}NMe_3$ (2.071(4)Å).[12] Similar to compound **II**, antiperiplanar arrangement on the outer As-B1-axis and synclinal arrangement on the central As-B2-axis leads to an u-shaped structural motif.[11] For **3b** a boat shaped conformation is observed in the solid state.

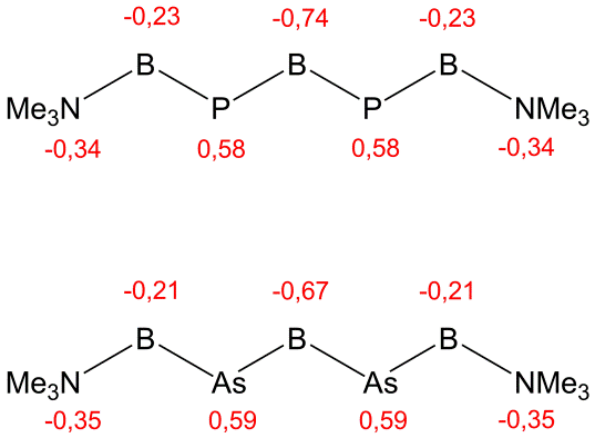

Figure 8. Charge distribution according to NPA of **II** and **3a**.

Like in the case of **II,** NPA for **3a** shows a positive charge which is equally localized on the two arsenic atoms (+0.59e). The negative charge is considerably higher on the central boron atom (–0.67e) relative to the peripheral boron atoms (–0.21e). Compared to the phosphorus derivative **II** the charge distribution in **3a** is similar.[11]

5.3 Conclusion

The reaction of monomeric phosphanyl- and arsanylboranes with Lewis Base adducts of a monoiodoborane has demonstrated to be an easy way for the generation of small oligomeric units. The products are obtained in good yields and were fully characterized. Those compounds were observed in the electron impact mass spectrometry experiments of polymers obtained by thermolysis experiments of **1** and **2**, demonstrating their high thermodynamic stability. Whilst the parent compounds of the phosphorus derivatives are stable decomposition was observed for the diphenyl substituted derivative. Furthermore, the so far longest arsenic-boron containing chain could be isolated and was completely characterized. The presented reaction is a versatile way for the synthesis of cationic oligomers based on phosphorus- and arsenic-donors.

5.4 References

[1] A. Staubitz, A. P. M. Robertson, M. E. Sloan, I. Manners, *Chem. Rev.* **2010**, *110,* 4023–4078; T. J. Clark, K. Lee, I. Manners, *Chem. Eur. J.* **2006**, *12*, 8634–8648.

[2] A. Schäfer, T. Jurca, J. Turner, J. R. Vance, K. Lee, V. A. Du, M. F. Haddow, G. R. Whittell, I. Manners, *Angew. Chem. Int. Ed.* **2015**, *54*, 4836–4841; *Angew. Chem.* **2015**, *127*, 4918–4923.

[3] S. Pandey, P. Lönnecke, E. Hey-Hawkins, *Inorg. Chem.* **2014**, *53*, 8242−8249.

[4] M. Baudler, *Angew. Chem. Int. Ed.* **1982**, *21*, 492–512; *Angew. Chem.* **1982**, *94*, 520–539; M. Baudler, *Angew. Chem. Int. Ed.* **1987**, *26*, 419–441; *Angew. Chem.* **1987**, *99*, 429–451; M. Baudler, K. Glinka, *Chem. Rev.* **1993**, *93*, 1623–1667; M. Baudler, K. Glinka, *Chem. Rev.* **1994**, *94*, 1273–1297; H. G. von Schnering, W. Hönle, *Chem. Rev.* **1988**, *88*, 243–273; I. Jevtovikj, P. Lönnecke, E. Hey-Hawkins, *Chem. Commun.* **2013**, *49*, 7355–7357.

[5] C. A. Dyker, N. Burford, *Chem. Asian J.* **2008**, *3*, 28–36.

[6] N. E. Miller, E. L. Muetterties, *J. Am. Chem. Soc.* **1964**, 86, 1033–1038.

[7] H. Schmidbaur, T. Wimmer, G. Reber, G. Müller, *Angew. Chem. Int. Ed.* **1988**, *27*, 1071–1074; *Angew. Chem.* **1988**, *100*, 1135–1138; M. Sigl, A. Schier, H. Schmidbaur, *Chem. Ber./Recueil* **1997**, *130*, 1411–1416.

[8] D. R. Martin, C. M. Merkel, J. P. Ruiz, *Inorg. Chim. Acta* **1985**, *100*, 293–297; K. Owsianik, R. Chauvin, A. Balińska, M. Wieczorek, M. Cypryk, M. Mikołajczyk, *Organometallics* **2009**, *28*, 4929–4937; T. Costa, H. Schmidbaur, *Chem. Ber.* **1982,** *115*, 1374–1378.

[9] Y. Yamamoto, T. Koizumi, K. Katagiri, Y. Furuya, H. Danjo, T. Imamoto, K. Yamaguchi, *Org. Lett.* **2006**, *26*, 6103–6106.

[10] G. Müller, U. Schubert, O. Orama, H. Schmidbaur, Chem. Ber. **1979**, *112*, 3302–3310.

[11] T. Miyazaki, M. Sugawara, H. Danjo, T. Imamoto, *Tetrahedron Lett.* **2004**, 45, 9341–9344.

[12] C. Marquardt, A. Adolf, A. Stauber, M. Bodensteiner, A. V. Virovets, A. Y. Timoshkin, M. Scheer, *Chem. Eur. J.* **2013**, *19*, 11887–11891.

[13] C. Thoms, C. Marquardt, M. Bodensteiner, M. Scheer, *Angew. Chem. Int. Ed.* **2013**, *52*, 5150–5154; *Angew. Chem.* **2013**, *125*, 5254–5259.

[14] C. Marquardt, T. Jurca, K.-C. Schwan, A. Stauber, A. V. Virovets, G. R. Whittell, I. Manners, M. Scheer, *Angew. Chem. Int. Ed.* **2015**, *54*, 13782–13786; *Angew. Chem.* **2015**, *127*, 13986–13991.

[15] C. Marquardt, C. Thoms, A. Stauber, G. Balazs, M. Bodensteiner, M. Scheer, *Angew. Chem. Int. Ed.* **2014**, *53*, 3727–3730; *Angew. Chem.* **2014**, *126*, 3801–3804.

[16] Bond lengths, r-values and Hirshfeld Rigid-Bond Test supports correct assignment of C atom on Phosphorus atom, F.L.Hirshfeld, *Acta Cryst.* **1976**, A32, 239–244.

5.5 Supporting Information

General Experimental:

All manipulations were performed under an atmosphere of dry argon using standard glove-box and Schlenk techniques. All solvents are degassed and purified by standard procedures. The compounds $Ph_2P–BH_2·NMe_3$, $^tBuHP–BH_2·NMe_3$,[1] $H_2As–BH_2·NMe_3$,[2] $IBH_2·NMe_3$ and $IBH_2·SMe_2$[3] were prepared according to literature procedures. The NMR spectra were recorded on an Avance 400 spectrometer (^1H: 400.13 MHz, ^{31}P: 161.976 MHz, ^{11}B: 128.378 MHz, $^{13}C\{^1H\}$: 100.623 MHz) with δ [ppm] referenced to external $SiMe_4$ (^1H, ^{13}C), H_3PO_4 (^{31}P), $BF_3·Et_2O$ (^{11}B). IR spectra were recorded on a DIGILAB (FTS 800) FT-IR spectrometer. All mass spectra were recorded on a ThermoQuest Finnigan TSQ 7000 (ESI-MS). The C, H, N analyses were measured on an Elementar Vario EL III apparatus.

Synthesis of $[Me_3N·BH_2–PPh_2–BH_2·NMe_3]^+[I]^-$ (1a):

To a solution of 130 mg (0.5 mmol) $Ph_2PBH_2·NMe_3$ in 20 mL of Et_2O 100 mg (0.5 mmol) $BH_2I·NMe_3$ are added as a solid at -40°C. The mixture is stirred for 50h, and a white solid precipitates. All volatiles are removed under reduced pressure. The remaining solid is washed 3 times with 5 mL of Et_2O. After dissolving in 5 ml of CH_2Cl_2, the solution is filtrated and over layered by 25 mL of *n*-hexane. **1a** crystallizes at room temperature in form of colorless needles. The solution is decanted off and the crystals are washed 3 times with 5 mL of *n*-hexane. The resulting crystals are dried under reduced pressure. Yield of **1a**: 96 mg (42 %). ^1H NMR (CD_2Cl_2, 25 °C): δ = 2.61 (d, $^4J_{P,H}$ = 1 Hz, 18H, NMe_3), 2.7 (m, br, 4H, BH_2), 7.51 (m, 6H, *m*-H and *p*-H, Ph), 7.70 (m, 4H, *o*-H, Ph). ^{31}P NMR (CD_2Cl_2, 25 °C): δ = -37.3 (s, br). $^{31}P\{^1H\}$ NMR (CD_2Cl_2, 25 °C): δ = -37.3 (s, br). ^{11}B NMR (CD_2Cl_2, 25 °C): δ = -8.0 (m, br). $^{11}B\{^1H\}$ NMR (CD_2Cl_2, 25 °C): δ = -8.0 (m, br). $^{13}C\{^1H\}$ NMR (CD_2Cl_2, 25 °C): δ = 55.0 (d, $^3J_{C,P}$ = 5 Hz, NMe_3), 128.3 (d, $^1J_{C,P}$ = 47 Hz, *i*-Ph), 129.7 (d, $^4J_{C,P}$ = 9 Hz, *p*-Ph), 131.3 (d, $^3J_{C,P}$ = 3 Hz, *m*-Ph), 133.5 (d, $^2J_{C,P}$ = 7 Hz, *o*-Ph). IR (KBr): $\tilde{\nu}$ = 3050, 3020, 2998 (m, CH), 2949 (m, CH), 2433 (s, BH), 2398 (s,BH), 1483 (vs), 1468 (s), 1438 (s),1410 (m),1313(w), 1243 (m), 1157 (m), 1125 (s), 1072 (vs), 1017 (m), 970 (m), 863 (s), 749 (s), 703 (s), 513 (m), 430 (w). ESI-MS (CH_2Cl_2): *m/z* =

785.5 (1%, $[Me_3N{\cdot}BH_2{-}PPh_2{-}BH_2{\cdot}NMe_3]^+{}_2I^-$), 329.2 (100%, $[Me_3N{\cdot}BH_2{-}PPh_2{-}BH_2{\cdot}NMe_3]^+$). Elemental analysis (%) calculated for $C_{18}H_{32}B_2IN_2P{\cdot}(CH_2Cl_2)$ (**1a**$\cdot(CH_2Cl_2)$): C: 42.21, H: 6.34, N: 5.19; found: C: 42.57, H: 6.28, N: 5.01.

Decomposition of $[Me_3N{\cdot}BH_2{-}PPh_2{-}BH_2{\cdot}NMe_3]^+[I]^-$ (1c):

If $[Me_3N{\cdot}BH_2{-}PPh_2{-}BH_2{\cdot}NMe_3]^+[I]^-$ (**1c**) is stored in THF slow decomposition to $[Me_3N{\cdot}BH_2{-}PPh_2{-}(CH_2)_4{-}OH]^+[I]^-$ (**1c**) is observed. Several crystals were examined by X-Ray diffraction, however compound **1c** could not be observed in NMR spectroscopy or mass spectrometry experiments. Yield of **1c**: few crystals.

Synthesis of $[Me_3N{\cdot}BH_2{-}PPh_2{-}BH_2{-}PPh_2{-}BH_2{\cdot}NMe_3]^+[I]^-$ (1b):

To a solution of 130 mg (0.5 mmol) $Ph_2PBH_2{\cdot}NMe_3$ in 20 mL of Et_2O 101 mg (0.25 mmol) $BH_2I{\cdot}SMe_2$ in toluene are added at 0°C. The mixture is stirred for 1 day, and a white solid precipitates. The Et_2O solution is decanted off and all volatiles are removed under reduced pressure. After dissolving in 5 ml of CH_2Cl_2, the solution is filtrated and over layered by 25 mL of *n*-hexane. **1b** crystallizes at room temperature in form of colorless blocks. The solution is decanted off and the crystals are washed 3 times with 5 mL of *n*-hexane. The resulting crystals are dried under reduced pressure. Yield of **1b**: 70 mg (42 %). ^{1}H NMR (CD_2Cl_2, 25 °C): δ = 2.33 (NMe_3), 2.5 (br, BH_2), 7.3 (*m*-H, Ph), 7.40 (*p*-H, Ph), 7.5 (*o*-H, Ph). ^{31}P NMR (CD_2Cl_2, 25 °C): δ = -30.0 (s, br). ^{31}P{^{1}H} NMR (CD_2Cl_2, 25 °C): δ = -30.0 (s, br). ^{11}B NMR (CD_2Cl_2, 25 °C): δ = -30.5 (m, br, $PPh_2{-}BH_2{-}PPh_2$), -7.6 (m, br, $Me_3N{\cdot}BH_2{-}PPh_2$). ^{11}B{^{1}H} NMR (CD_2Cl_2, 25 °C): δ = -30.5 (m, br, $PPh_2{-}BH_2{-}PPh_2$), -7.6 (m, br, $Me_3N{\cdot}BH_2{-}PPh_2$). ^{13}C{^{1}H} NMR (CD_2Cl_2, 25 °C): δ = 54.9 (d, $^3J_{C,P}$ = 5 Hz, NMe_3), 129.0 (d, $^4J_{C,P}$ = 9 Hz, *p*-Ph), 128.3 (d, $^1J_{C,P}$ = 53 Hz, *i*-Ph), 130.8 (d, $^3J_{C,P}$ = 2 Hz, *m*-Ph), 133.9 (d, $^2J_{C,P}$ = 8 Hz, *o*-Ph). IR (KBr): $\tilde{\nu}$ = 3070 (w), 3050 (w), 3021 (w), 3003 (w), 2935 (w), 2920 (w), 2844 (w), 2801 (w), 2452 (m, BH), 2395 (s,BH), 2314 (w), 1978 (vw), 1910 (vw), 1842 (vw), 1481 (vs), 1469 (s), 1434 (s),1411 (w),1312 (w), 1252 (m), 1158 (m), 1127 (s), 1099 (m), 1080 (vs), 1020 (m), 985 (m), 866 (m), 782 (m), 761 (m), 741 (m), 699 (vs), 654 (m), 513 (m), 476 (m), 432 (w). ESI-MS (CH_2Cl_2): *m/z* = 527.3 (100%, $[Me_3N{\cdot}BH_2{-}PPh_2{-}BH_2{-}PPh_2{-}BH_2{\cdot}NMe_3]^+$), 466.2 (51%, $[Me_3N{\cdot}BH_2{-}PPh_2{-}BH_2{-}PPh_2{-}B]^+$), 409.0 (15%, $[BH_2{-}PPh_2{-}BH_2{-}PPh_2{-}BH_2]^+$). Elemental analysis (%) calculated for $C_{30}H_{44}B_3IN_2P_2{\cdot}(CH_2Cl_2)_{0.33}$ (**1b**$\cdot(CH_2Cl_2)_{0.33}$): C: 53.37, H: 6.60, N: 4.11; found: C: 53.36, H: 6.58, N: 3.86.

Synthesis of $[Me_3N{\cdot}BH_2{-}P^tBuH{-}BH_2{\cdot}NMe_3]^+[I]^-$ (2a):

A solution of 160 mg (1 mmol) ^{t}BuHP$BH_2{\cdot}NMe_3$ in 5 mL of CH_2Cl_2 is added to 199 mg (1 mmol) $BH_2I{\cdot}NMe_3$ in 5 mL of CH_2Cl_2 at -80°C. The mixture is stirred for 8h, and a

white solid precipitates. The solution is filtrated and over layered by 40 mL of *n*-hexane. **2a** crystallizes at room temperature in form of colorless needles. The solution is decanted of and the crystals are washed 3 times with 5 mL of *n*-hexane. The resulting crystals are dried under reduced pressure. Yield of **2a**: 250 mg (69 %). ^{1}H NMR (CD_2Cl_2, 25 °C): δ = 1.25 (d, $^{2}J_{P,H}$ = 7 Hz, 9H, ^{t}Bu), 2.26 (m, br, 4H, BH_2), 2.90 (d, $^{4}J_{P,H}$ = 1 Hz, 18H, NMe_3), 5.32 (d, $^{1}J_{P,H}$ = 326 Hz, 1H, PH). ^{31}P NMR (CD_2Cl_2, 25 °C): δ = -62.0 (d, br, $^{1}J_{P,H}$ = 326 Hz). ^{31}P{^{1}H} NMR (CD_2Cl_2, 25 °C): δ = -62.0 (s, br). ^{11}B NMR (CD_2Cl_2, 25 °C): δ = -9.12 (m, br). ^{11}B{^{1}H} NMR (CD_2Cl_2, 25 °C): δ = -9.12 (s, $^{1}J_{B,P}$ = 65 Hz). ^{13}C{^{1}H} NMR (CD_2Cl_2, 25 °C): δ = 27.4 (d, $^{1}J_{C,P}$ = 34 Hz, **C**$(CH_3)_3$), 28.0 (s, C(**C**$H_3)_3$), 55.1 (d, $^{3}J_{C,P}$ = 5 Hz, NMe_3). IR (KBr): $\tilde{\nu}$ = 3019 (m), 2998 (m, CH), 2970(m), 2948 (m, CH), 2807, 2780(w), 2755(w), 2444 (m, BH), 2400 (m,BH), 2287 (s, PH), 2217 (w), 2177 (w), 1701 (m), 1474 (m), 1410 (m),1363(m), 1249 (m), 1198 (m), 1164 (m), 1134 (m), 1089 (m), 1023 (m), 976 (m), 853 (m), 829 (m), 710 (w), 636 (w), 482 (w), 426 (w). ESI-MS (CH_2Cl_2): *m/z* = 233 (100%, $[Me_3N{\cdot}BH_2{-}P^{t}BuH{-}BH_2{\cdot}NMe_3]^+$). Elemental analysis (%) calculated for $C_{10}H_{32}B_2IN_2P$ (**2a**): C: 33.31, H: 8.95, N: 7.77; found: C: 33.46, H: 8.97, N: 7.67.

Synthesis of $[Me_3N{\cdot}BH_2{-}P^{t}BuH{-}BH_2{-}P^{t}BuH{-}BH_2{\cdot}NMe_3]^+[I]^-$ (2b):

To a solution of 160 mg (1 mmol) $^{t}BuHPBH_2{\cdot}NMe_3$ in 10 mL of Et_2O a solution of 202 mg (0.5 mmol) $BH_2I{\cdot}SMe_2$ in toluene is added at -80°C. The mixture is stirred for 8h, after which all volatiles are removed under reduced pressure and the resulting white solid is dissolved in 5 mL of CH_2Cl_2. The solution is filtrated and over layered by 20 mL of *n*-hexane. **2b** crystallizes at room temperature in form of colorless needles. The solution is decanted of and the crystals are washed 3 times with 5 mL of *n*-hexane. The resulting crystals are dried under reduced pressure. Yield of **2b**: 137 mg (59 %). ^{1}H NMR (CD_2Cl_2, 25 °C): δ = 1.23 (d, $^{2}J_{P,H}$ = 14 Hz, 18H, ^{t}Bu), 1.50 – 2.80 (m, br, 6H, BH_2), 2.87 (s, 18H, NMe_3), 3.86 (dm, $^{1}J_{P,H}$ = 323 Hz, 0.8 H, PH), 4.02 (dm, $^{1}J_{P,H}$ = 329 Hz, 0.2 H, PH). ^{31}P NMR (CD_2Cl_2, 25 °C): δ = -38.0 (d, br, $^{1}J_{P,H}$ = 332 Hz). ^{31}P{^{1}H} NMR (CD_2Cl_2, 25 °C): δ = -38.0 (s, br). ^{11}B NMR (CD_2Cl_2, 25 °C): δ = -38.1 (m, $P^{t}BuH{-}BH_2{-}P^{t}BuH$), -9.8 (m, $Me_3N{\cdot}BH_2{-}P^{t}BuH$). ^{11}B{^{1}H} NMR ($CD_2Cl_2$, 25 °C): δ = -38.1 (t, $^{1}J_{B,P}$ = 72 Hz, m, br, $P^{t}BuH{-}BH_2{-}P^{t}BuH$), -9.8 (d, $^{1}J_{B,P}$ = 43 Hz, $Me_3N{\cdot}BH_2{-}P^{t}BuH$). ^{13}C{^{1}H} NMR ($CD_2Cl_2$, 25 °C): δ = 27.8 (d, $^{1}J_{C,P}$ = 39 Hz, **C**$(CH_3)_3$), 28.3 (s, C(**C**$H_3)_3$), 54.8 (m, NMe_3). IR (KBr): $\tilde{\nu}$ = 2970 (s), 2944 (s, CH), 2901 (s), 2865 (s), 2810 (w), 2714 (w), 2417 (s, BH), 2340 (m,BH), 2313 (m, PH), 2219 (w), 2175 (w), 1474 (m), 1412 (m),1393(m), 1364 (s), 1247 (s), 1191 (m), 1160 (m), 1133 (s), 1088 (s), 1023 (m), 979 (m), 945 (w), 855 (s), 839 (s), 820 (m), 752 (w), 718 (w), 691 (w), 652 (w), 606 (w), 569 (w), 477 (w), 427 (w). ESI-MS (CH_2Cl_2): *m/z* = 335.2 (100%, $[Me_3N{\cdot}BH_2{-}P^{t}BuH{-}BH_2{-}P^{t}BuH{-}BH_2{\cdot}NMe_3]^+$). Elemental

analysis (%) calculated for $C_{14}H_{44}B_3IN_2P_2$ (**2b**): C: 36.35, H: 9.59, N: 6.06; found: C: 36.46, H: 9.51, N: 6.06.

Synthesis of $[Me_3N{\cdot}BH_2{-}AsH_2{-}BH_2{-}AsH_2{-}BH_2{\cdot}NMe_3]^+[I]^-$ (3a):

To a solution of 150 mg (1.0 mmol) $H_2AsBH_2{\cdot}NMe_3$ in 20 mL CH_2Cl_2 100 mg (0.5 mmol) $BH_2I{\cdot}SMe_2$ in toluene are added drop by drop. After stirring the mixture for 18 h, all volatiles are removed under reduced pressure. The remaining solid is dissolved in 10 mL of CH_2Cl_2 and filtrated over diatomaceous earth. The solvent is removed under reduced pressure and the remaining solid is washed 4 times with 50 ml *n*-hexane. The white solid is dried under reduced pressure. Crystals of **3a** are obtained by storing a solution of **3a** in CH_2Cl_2, over layered by the 5 fold amount of *n*-hexane at -28°C. Yield of **3a**: 175 mg (79 %). ^{1}H NMR (CD_2Cl_2, 25 °C): δ = 1.76 (q, 2H, $(AsH_2)_2B\mathbf{H}_2$), 2.43 (q, 4H, $Me_3N{\cdot}B\mathbf{H}_2$), 2.86 (s, 18H, NMe_3), 2.94 (q, $^3J_{H,H}$ = 6.6 Hz, 4H, AsH_2). ^{11}B NMR (CD_2Cl_2, 25 °C): δ = –8.60 (t, $^1J_{B,H}$ = 114 Hz, $Me_3N{\cdot}\mathbf{B}H_2$), –35.73 (t, $^1J_{B,H}$ = 114 Hz, $(AsH_2)_2\mathbf{B}H_2$). ^{11}B{^{1}H} NMR (CD_2Cl_2, 25 °C): δ = –8.60 (s, $Me_3N{\cdot}\mathbf{B}H_2$), –35.73 (s, $(AsH_2)_2\mathbf{B}H_2$). ^{13}C{^{1}H} NMR (CD_2Cl_2, 25 °C): δ = 54.46 (s). IR (KBr): $\tilde{\nu}$ = 2997 (w), 2948 (w), 2806(vw), 2739 (vw), 2448 (s, br, BH), 2415 (s, br, BH), 2310 (w, AsH), 2180 (m), 1483 (s), 1470 (s), 1410 (m), 1245 (m), 1241 (m), 1159 (m), 1125 (s), 1076 (s), 1010 (m), 977 (m), 973 (m), 970 (m), 867 (s), 817 (w), 739 (m), 700 (m), 639 (w), 562 (w), 465 (w), 419 (w). ESI-MS (CH_2Cl_2): *m/z* = 311.0 (100 %, $[Me_3N{\cdot}BH_2{-}AsH_2{-}BH_2{-}AsH_2{-}BH_2{\cdot}NMe_3]^+$). Elemental analysis (%) calculated for $C_6H_{28}As_2B_3I_1N_2$ (**3a**): C: 16.47, H: 6.45, N: 6.40; found: C: 16.57, H: 6.37, N: 6.30.

Synthesis of [*cyclo*-{$As(BH_2{\cdot}NMe_3)(CMe{=}NH)_2(BH_2)$}]$^+$[I]$^-$ (3b):

To a solution of 105 mg (0.67 mmol) $H_2AsBH_2{\cdot}NMe_3$ in 20 mL Et_2O, 75 mg (0.375 mmol) $BH_2I{\cdot}SMe_2$ in toluene are added drop by drop. A yellow-orange precipitate is formed. After decanting off the supernatant the remaining solid is dried under reduced pressure and is dissolved in 5 mL of MeCN. The yellow supernatant is filtrated of the red solid and concentrated to 2 mL. **3b** crystallizes -28 °C as colorless blocks. The crystals are separated and washed three times with *n*-hexane. Yield of **3b**: 20 mg (14%). ^{1}H NMR (CD_3CN, 25 °C): δ = 2.57 (s, 6H, CH_3CN), 2.86 (s, 9H, NMe_3), 10.32 (s, br, 2H, NH). ^{11}B NMR (CD_3CN, 25 °C): δ = –2.28 (t, $^1J_{B,H}$ = 122 Hz, BH_2), –10.62 (t, $^1J_{B,H}$ = 112 Hz, BH_2). ^{11}B{^{1}H} NMR (CD_3CN, 25 °C): δ = –2.28 (s, BH_2), –10.62 (s, BH_2). ^{13}C{^{1}H} NMR (CD_3CN, 25 °C): δ = 27.7 (C-$\mathbf{Me}_3$), 54.3 (N-$\mathbf{Me}_3$), 203 (As-**C**=C). IR (KBr): $\tilde{\nu}$ = 3091 (s), 3055 (s), 3004(s), 2964 (s), 2899 (w), 2817 (w), 2456 (s, br, BH), 2428 (s, br, BH), 2357 (w), 2302 (m), 2248 (w), 1623 (s), 1580 (w), 1478 (m), 1465 (m), 1407 (w), 1370 (w), 1263 (w), 1163 (w), 1117 (m), 1057 (s), 1009 (m), 971 (w), 919 (w), 851(m), 704 (w), 508 (w), 482

(w), 410 (w). ESI-MS (CH_3CN): *m/z* = 243.9 (100 %, $[Me_3N{\cdot}BH_2{-}(As(CH_3C{=}NH)_2BH_2)]^+$), 170.7 (67 %, $[As(CH_3C{=}NH)_2BH]^+$). Elemental analysis (%) calculated for $C_7H_{21}As_1B_2I_1N_3$ (**3b**): C: 22.64, H: 5.70, N: 11.32; found: C: 22.61, H: 5.70, N: 11.15.

X-ray diffraction analysis

The single crystal X-ray diffraction experiments were performed on either a Gemini R Ultra CCD diffractometer (**1a**, **1b**, **1c**, **1c**thf, **3a**, **3b)**, a SuperNova A CCD diffractometer (**2a**) or a GV1000 diffractometer (**2b**) from Agilent Technologies (formerly Oxford Diffraction) applying Cu-K_α radiation (λ = 1.54178 Å) or Mo-K_α radiation (λ = 0.71073 Å). The measurements were performed at 123 K. Crystallographic data together with the details of the experiments are given below. Absorption corrections were applied semi-empirically from equivalent reflections or analytically (SCALE3/ABSPACK algorithm implemented in CrysAlis PRO software by Agilent Technologies Ltd).[4] All structures were solved using SIR97,[5] SHELXS[6] and OLEX 2.[7] Refinements against F^2 in anisotropic approximation were done using SHELXL.[6] The hydrogen positions of the methyl groups were located geometrically and refined riding on the carbon atoms. Hydrogen atoms belonging to BH_2 and PH_2 groups were located from the difference Fourier map and refined without constraints (**1a**, **2a**, **2b**, **3b**) or with restrained E–H distances (**1c**thf, **1b**, **3a**). Figures were created with OLEX 2.[7] The CIF files are deposited on the provided DVD.

Table S1: Crystallographic data for **1a** and **1b**.

Compound	**1a**	**1b**
empirical formula	$C_{19}H_{34}B_2Cl_2IN_2P$	$C_{31.87}H_{47.73}B_3Cl_{3.73}IN_2P_2$
formula weight	540.87	812.33
temperature [K]	123(1)	123(1)
crystal system	triclinic	monoclinic
space group	*P*-1	$P2_1/c$
a [Å]	9.3937(3)	16.8246(3)
b [Å]	10.5965(4)	31.1660(3)
c [Å]	13.3900(3)	16.9956(2)
α [°]	84.367(2)	90
β [°]	74.705(3)	115.3135(18)
γ [°]	83.602(3)	90
Volume [Å^3]	1274.34(7)	8056.0(2)
Z	2	8
ρ_{calc} [g/cm^3]	1.410	1.340
μ [mm^{-1}]	12.433	9.444
F (000)	548.0	3315.0
crystal size [mm^3]	0.3406×0.2804×0.204	0.4249×0.2534×0.0678
radiation	CuK*α* (*λ* = 1.54178)	CuK*α* (*λ* = 1.54178)
absorption correction	analytical	multi-scan
T_{min} / T_{max}	0.071 / 0.231	0.284/ 1.000
2*Θ* range [°]	6.862 to 133.424	6.466 to 148.296
completeness	0.990	0.989
index ranges	-11 ≤ *h* ≤ 11 -12 ≤ *k* ≤ 12 -15 ≤ *l* ≤ 13	-20 ≤ *h* ≤ 19 -24 ≤ *k* ≤ 38 -20 ≤ *l* ≤ 16
reflections collected	15976	26811
independent reflections	4468 [R_{int} = 0.0390, R_{sigma} = 0.0281]	15588 [R_{int} = 0.0295, R_{sigma} = 0.0430]
data / restraints / parameters	4468/0/297	15588/33/886
GOF on F^2	1.064	0.977
R_1/wR_2 [I≥2σ(*I*)]	R_1 = 0.0331, wR_2 = 0.0863	R_1 = 0.0561, wR_2 = 0.1516
R_1/wR_2 [all data]	R_1 = 0.0339, wR_2 = 0.0871	R_1 = 0.0649, wR_2 = 0.1567
max/min $\Delta\rho$ [e·Å^{-3}]	0.64/-1.14	1.83/-1.23

Table S2: Crystallographic data for **2a** and **2b**.

Compound	**2a**	**2b**
empirical formula	$C_{10}H_{32}B_2IN_2P$	$C_{14}H_{44}B_3IN_2P_2$
formula weight	359.86	461.78
temperature [K]	123(1)	125(3)
crystal system	orthorhombic	monoclinic
space group	*Pca*2_1	*P*2_1/*c*
a [Å]	11.77706(14)	15.5144(3)
b [Å]	13.37507(17)	11.91050(18)
c [Å]	11.92904(13)	13.6793(2)
α [°]	90	90
β [°]	90	97.9693(19)
γ [°]	90	90
Volume [Å^3]	1879.05(4)	2503.32(8)
Z	4	4
ρ_{calc} [g/cm^3]	1.272	1.225
μ [mm^{-1}]	14.035	11.220
F (000)	736.0	960.0
crystal size [mm^3]	0.2154×0.1908×0.1672	0.2576×0.1118×0.076
radiation	CuK*α* (*λ* = 1.54178)	CuK*α* (*λ* = 1.54178)
absorption correction	analytical	analytical
T_{min} / T_{max}	0.127 / 0.268	0.198 / 0.566
2*Θ* range [°]	10.008 to 143.98	5.752 to 147.638
completeness	0.999	0.996
index ranges	-14 ≤ *h* ≤ 14 -16 ≤ *k* ≤ 11 -14 ≤ *l* ≤ 14	-13 ≤ *h* ≤ 18 -14 ≤ *k* ≤ 14 -16 ≤ *l* ≤ 17
reflections collected	11823	17673
independent reflections	3456 [R_{int} = 0.0411, R_{sigma} = 0.0319]	4921 [R_{int} = 0.0435, R_{sigma} = 0.0280]
data / restraints / parameters	3456/1/174	4921/0/235
GOF on F^2	1.019	1.056
R_1/wR_2 [I≥2*σ(I)*]	R_1 = 0.0214, wR_2 = 0.0542	R_1 = 0.0308, wR_2 = 0.0824
R_1/wR_2 [all data]	R_1 = 0.0226, wR_2 = 0.0553	R_1 = 0.0317, wR_2 = 0.0836
max/min Δ*ρ* [e·Å^{-3}]	0.44/-0.47	0.62/-0.88
flack parameter	-0.022(4)	-

Table S3: Crystallographic data for **1c** and **1c**thf.

Compound	**1c**	**1c**thf
empirical formula	$C_{19}H_{30}BINOP$	$C_{23}H_{38}BINO_2P$
formula weight	457.12	529.22
temperature [K]	123(1)	123(1)
crystal system	monoclinic	triclinic
space group	$P2_1/n$	$P1$
a [Å]	9.12890(10)	8.379(5)
b [Å]	10.08680(10)	9.515(5)
c [Å]	23.3859(3)	9.941(5)
α [°]	90	67.031(5)
β [°]	94.2550(10)	67.658(5)
γ [°]	90	64.058(5)
Volume [Å^3]	2147.47(4)	634.9(6)
Z	4	1
ρ_{calc} [g/cm^3]	1.414	1.384
μ [mm^{-1}]	12.447	10.632
F (000)	928.0	272.0
crystal size [mm^3]	0.2676×0.1801×0.1795	0.0993×0.0819×0.0673
radiation	CuKα (λ = 1.54178)	CuKα (λ = 1.54178)
absorption correction	analytical	multi-scan
T_{min} / T_{max}	0.163 / 0.296	0.853 / 1.000
2Θ range [°]	7.582 to 148.352	9.988 to 133.222
completeness	0.995	0.996
index ranges	-10 ≤ h ≤ 11 -12 ≤ k ≤ 11 -25 ≤ l ≤ 29	-9 ≤ h ≤ 9 -11 ≤ k ≤ 11 -10 ≤ l ≤ 11
reflections collected	11545	6369
independent reflections	4230 [R_{int} = 0.0344, R_{sigma} = 0.0367]	3333 [R_{int} = 0.0259, R_{sigma} = 0.0376]
data / restraints / parameters	4230/0/238	3333/16/277
GOF on F^2	1.075	1.044
R_1/wR_2 [I≥2σ(I)]	R_1 = 0.0302, wR_2 = 0.0786	R_1 = 0.0208, wR_2 = 0.0481
R_1/wR_2 [all data]	R_1 = 0.0329, wR_2 = 0.0816	R_1 = 0.0210, wR_2 = 0.0482
max/min $\Delta\rho$ [e·Å^{-3}]	0.50/-0.85	0.42/-0.24
flack parameter	-	-0.005(4)

Table S4: Crystallographic data for **3a** and **3b**.

Compound	**3a**	**3b**
empirical formula	$C_6H_{28}As_2B_3IN_2$	$C_{16}H_{45}As_2B_4I_2N_7$
formula weight	437.47	782.47
temperature [K]	123(1)	123(1)
crystal system	monoclinic	triclinic
space group	*P*2/*c*	*P*-1
a [Å]	10.9397(3)	10.0086(2)
b [Å]	7.29831(14)	13.1830(3)
c [Å]	11.9091(4)	13.2350(3)
α [°]	90	79.410(2)
β [°]	113.112(4)	70.016(2)
γ [°]	90	79.674(2)
Volume [Å^3]	874.52(5)	1600.31(7)
Z	2	2
ρ_{calc} [g/cm^3]	1.661	1.624
μ [mm^{-1}]	18.366	4.034
F (000)	424.0	764.0
crystal size [mm^3]	0.242×0.1566×0.1331	0.518×0.4334×0.3068
radiation	CuK*α* (*λ* = 1.54178)	MoK*α* (*λ* = 0.71073)
absorption correction	multi-scan	multi-scan
T_{min} / T_{max}	0.090 / 1.000	0.630 / 1.000
2*Θ* range [°]	8.788 to 131.962	5.71 to 69.936
completeness	0.999	0.999
index ranges	-12 ≤ *h* ≤ 12 -8 ≤ *k* ≤ 7 -14 ≤ *l* ≤ 14	-15 ≤ *h* ≤ 15 -21 ≤ *k* ≤ 21 -21 ≤ *l* ≤ 21
reflections collected	6614	30756
independent reflections	1525 [R_{int} = 0.0468, R_{sigma} = 0.0277]	12999 [R_{int} = 0.0232, R_{sigma} = 0.0445]
data / restraints / parameters	1525/17/83	12999/0/339
GOF on F^2	1.081	0.901
R_1/wR_2 [I≥2*σ(I)*]	R_1 = 0.0450, wR_2 = 0.1221	R_1 = 0.0226, wR_2 = 0.0449
R_1/wR_2 [all data]	R_1 = 0.0462, wR_2 = 0.1240	R_1 = 0.0350, wR_2 = 0.0457
max/min Δρ [e·Å^{-3}]	1.34/-0.78	1.39/-0.77

Computational Details

All calculations have been performed with the TURBOMOLE program package[8] at the RI[9]-B3LYP[10]/def2-TZVP[11] level of theory. The solvent effects were incorporated via the Conductor-like Screening Model (COSMO)[12] using the dielectric constant of THF (ε = 7.250). The natural population analysis[13] was performed as implemented in TURBOMOLE. For reaction energies the SCF energies were used without corrections. The *meso* isomer $[\{Me_3NBH_2PH(^tBu)\}_2BH_2]^+$ is with 2.45 kJ·mol^{-1} more stable than the *d,l* isomer. Cartesian coordinates for optimized geometries (xyz) are deposited on the provided DVD.

References

[1] C. Marquardt, T. Jurca, K.-C. Schwan, A. Stauber, A. V. Virovets, G. R. Whittell, I. Manners, M. Scheer, *Angew. Chem. Int. Ed.* **2015**, *54*, 13782–13786; *Angew. Chem.* **2015**, *127*, 13986–13991.

[2] C. Marquardt, A. Adolf, A. Stauber, M. Bodensteiner, A. V. Virovets, A. Y. Timoshkin, M. Scheer, *Chem. Eur. J.* **2013**, *19*, 11887–11891.

[3] C. Marquardt, C. Thoms, A. Stauber, G. Balazs, M. Bodensteiner, M. Scheer, *Angew. Chem. Int. Ed.* **2014**, *53*, 3727–3730; *Angew. Chem.* **2014**, *126*, 3801–3804.

[4] Agilent Technologies **2006-2015**, CrysAlisPro Software system, different versions, Agilent Technologies UK Ltd, Oxford, UK.

[5] A. Altomare, M. C.Burla, M. Camalli, G. L. Cascarano, C. Giacovazzo, A. Guagliardi, A.G. G. Moliterni, G. Polidori, R. Spagna, J. Appl. Cryst. **1999**, *32*, 115–119.

[6] G. M. Sheldrick, *Acta Cryst.* **2008**, *A64*, 112–122.

[7] O.V. Dolomanov, L.J. Bourhis, R.J. Gildea, J.A.K. Howard, H.Puschmann, OLEX2: A complete structure solution, refinement and analysis program, *J. Appl. Cryst*. **2009**, *42*, 339–341.

[8] a) F. Furche, R. Ahlrichs, C. Hättig, W. Klopper, M. Sierka, F. Weigend, *WIREs Comput. Mol. Sci.* **2014**, *4*, 91–100; b) R. Ahlrichs, M. Bär, M. Häser, H. Horn, C. Kölmel, *Chem. Phys. Lett.***1989**, *162*, 165–169; c) O. Treutler, R. Ahlrichs, *J. Chem. Phys.***1995**, *102*, 346–354.

[9] a) M. Sierka, A. Hogekamp, R. Ahlrichs, *J. Chem. Phys.* **2003**, *118*, 9136; c) K. Eichkorn, O. Treutler, H. Oehm, M. Häser, R. Ahlrichs, *Chem. Phys. Lett.* **1995**, *242*, 652–660; b) K. Eichkorn, F. Weigend, O. Treutler, R. Ahlrichs, *Theor. Chem. Acc.* **1997**, *97*, 119.

[10] a) P. A. M. Dirac, *Proc. Royal Soc.A*, **1929**, *123*, 714. b) J. C. Slater, *Phys. Rev.***1951**, *81*, 385. c) S. H. Vosko, L. Wilk, M. Nusair, *Can. J. Phys.***1980**, *58*, 1200.

d) A. D. Becke, *Phys. Rev. A*, **1988**, *38*, 3098. e) C. Lee, W. Yang, R. G. Parr, *Phys. Rev. B*,**1988**, *37*, 785. f) A. D. Becke, *J. Chem. Phys.* **1993**, *98*, 5648.

[11] a) A. Schäfer, C. Huber, R. Ahlrichs, *J. Chem. Phys.***1994**, *100*, 5829; b) K. Eichkorn, F. Weigend, O. Treutler, R. Ahlrichs, *Theor. Chem. Acc.***1997**, *97*, 119.

[12] a) A. Klamt, G. Schüürmann *J. Chem. Soc. Perkin Trans. 2* **1993**, 799–805; b) A. Schäfer, A. Klamt, D. Sattel, J. C. W. Lohrenz, F. Eckert *Phys. Chem. Chem. Phys.* **2000**, *2*, 2187–2193.

[13] A. E. Reed, R. B. Weinstock, F. Weinhold, *J. Chem. Phys.* **1985**, *83*, 735–746.

5.6 Author Contributions

The syntheses and characterization of all compounds were performed by Christian Marquardt.

Josef Baumann is gratefully acknowledged for contributions to the syntheses of **1a** and **1c** during his bachelor thesis (Regensburg, **2013**) under supervision of Christian Marquardt.

X-ray structural analyses of all compounds were performed by Christian Marquardt and Dr. A. V. Virovets.

All DFT-calculations were performed by Dr. Gábor Balázs.

The manuscript (including supporting information, figures, schemes and graphical abstract) was written by Christian Marquardt.

6. Anionic Chains of Parent Phosphanylboranes

C. Marquardt, A. Stauber, G. Balázs, M. Bodensteiner, A. V. Virovets, A. Y. Timoshkin and M. Scheer

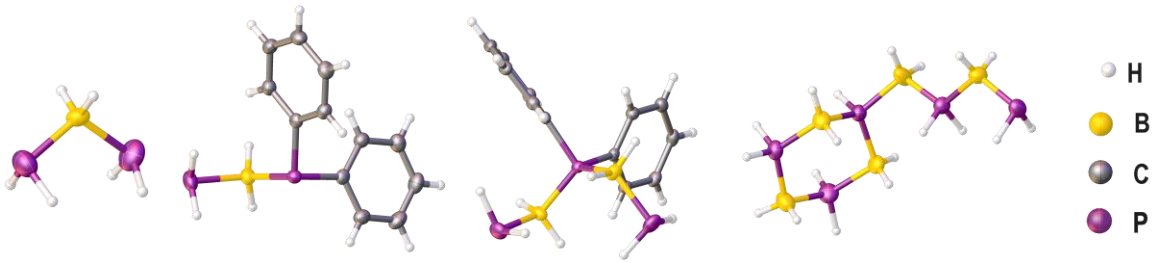

Abstract: We report on the synthesis and structural characterization of unprecedented anionic parent compounds of mixed group 13/15 elements. The reactions of the phosphanylborane $H_2PBH_2{\cdot}NMe_3$ (**1**) with sodium salts of PH_2^-, ^{t}BuPH$^-$ and Ph_2P^-, respectively leads to the formation of $[Na]^+[H_2P–BH_2–PH_2]^-$ (**2**), $[Na]^+[H_2P–BH_2–P^tBuH]^-$ (**3**) and $[Na]^+[H_2P–BH_2–PPh_2]^-$ (**4**), respectively, containing anionic phosphorus-boron chain-like units. Using a different stoichiometry and reaction conditions the longer 5-membered species $[Na]^+[H_2P–BH_2–PPh_2–BH_2–PH_2]^-$ (**5**) can be obtained. The cyclic compound $[NHC^{dipp}{\cdot}H_2B–PH_2–BH_2{\cdot}NHC^{dipp}]^+[P_5B_5H_{19}]^-$ (**6**) containing a *n*-butylcyclohexane-like anion was also synthesized. All compounds have been characterized by X-ray structure analysis, multinuclear NMR spectroscopy, IR spectroscopy, and mass spectrometry. DFT calculations elucidate the high thermodynamic stability and give insight into the reaction pathway.

6.1 Introduction

The interest of catenation of non-carbon atoms increased significantly over the last years. Current research focuses especially on the catenation of group 15 elements. Whereas chains of polyphosphines and polyphosphorus anions have already been studied thoroughly in the last decades,[1] the chemistry of catena-phosphorus cations has been discovered recently and was investigated for example intensively by the groups *Burford*[2] and *Weigand*.[3] Recently, amine- and phosphine-borane adducts gained increasing interest as hydrogen storage materials as well as precursors for novel inorganic polymers.[4] Poly(amino- and poly(phosphinoborane)s are primarily obtained by dehydrogenation/dehydrocoupling reactions of the corresponding compounds $RR'HE{\cdot}BH_3$ (E = N, P) mediated by metal catalysts and can be viewed as inorganic analogues of organic polymers such as polyolefins.[4] Recently, a breakthrough for a non-catalytic addition polymerization of Lewis base stabilized phosphanylborane monomers was achieved.[5] In contrast, only a few short chains of neutral oligo(phosphinoborane)s have been characterized by X-ray structure analysis,[6] compounds containing longer chains were only characterized by spectroscopic methods.[7] In all of the reported compounds the P–B core is protected by organic substituents. We are especially interested in the synthesis and reactivity of parent group 13/15 compounds containing E–H bonds.[8] Recently, we reported the high-yield synthesis of pnictogenylboranes $H_2EBH_2{\cdot}NMe_3$ (E = P (**1**), As),[9] which are excellent building blocks for the formation of oligomeric[10] and polymeric[5] compounds. Moreover, by using them as starting materials we succeeded in the synthesis of the first cationic chains of phosphanyl- and arsanylboranes.[11]

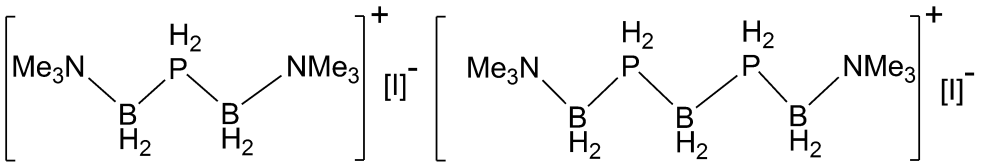

I **II**

The cationic species $[Me_3N{\cdot}H_2B{-}[PH_2{-}BH_2]_n{\cdot}NMe_3]^+$ (**I**: n = 1; **II**: n = 2) are thermodynamically sufficiently stable to be isolated, whereas compounds containing an anionic P–B–P core are unknown so far. In contrast to other cationic[12] and neutral[13] compounds containing a P–B–P backbone,[11] the parent anionic species are almost exclusively restricted to branched examples, like compound of type **III**[14] and **IV**[15] demonstrate. Shorter anionic compounds with BH_3 end groups (type **V**[16] and **VI**)[17] e.g.

are obtained by deprotonation of the corresponding phosphine-borane adduct. The only linear anionic chains (type **VII**) contain electron withdrawing CF_3 groups to distribute the charge appropriate. However, they were only obtained as mixtures and were solely studied by NMR spectroscopy.[18] Therefore, the quest for alternative approaches to linear chains of parent phosphanylboranes was still open. Herein we present a general synthetic approach and the structural characterization of the first mainly H-substituted, parent anionic phosphanylborane chains.

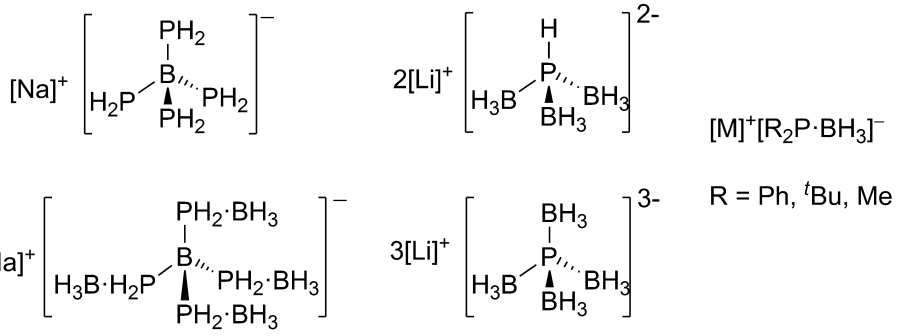

III **IV** **V**

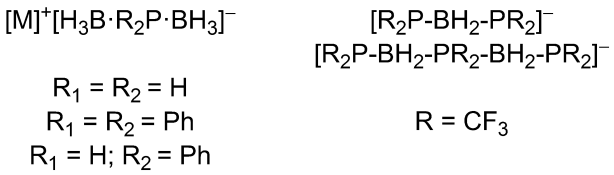

VI **VII**

6.2 Results and Discussion

Sonication of a solution of phosphanylborane $H_2PBH_2{\cdot}NMe_3$ (**1**) with one equivalent of $NaPH_2$ in THF leads to the substitution of NMe_3 by PH_2^- and the formation of $[Na]^+[H_2P–BH_2–PH_2]^-$ (Scheme 1). According to ^{31}P NMR spectroscopy, the reaction proceeds efficiently, without the formation of side products. After addition of 18-crown-6 the compound **2**$(thf)_2$ can be isolated as a crystalline solid in 56% yield. In the ^{31}P NMR spectrum of **2**$(thf)_2$ a very broad triplet at $\delta = –175.0$ ppm with a $^1J_{PH}$ coupling of 172 Hz is observed, without further resolved coupling. The ^{11}B NMR spectrum of **2**$(thf)_2$ shows a triplet of triplets at $\delta = –34.7$ ppm ($^1J_{BP}$ = 26 Hz, $^1J_{BH}$ = 99 Hz). The X-ray structure of **2**$(thf)_2$ shows the $[H_2P–BH_2–PH_2]^-$ anion in an *all*-antiperiplanar conformation (Figure 1), without any contacts to the cation. The P–B bond lengths of 1.961(3) and 1.964(3) Å are

slightly shortened compared to the starting material $H_2PBH_2{\cdot}NMe_3$ (1.976(2) Å)[8b] but to a lower extent than in the cationic species $[Me_3N{\cdot}H_2B{-}PH_2{-}BH_2{\cdot}NMe_3]^+$ (1.957(3) Å).[11]

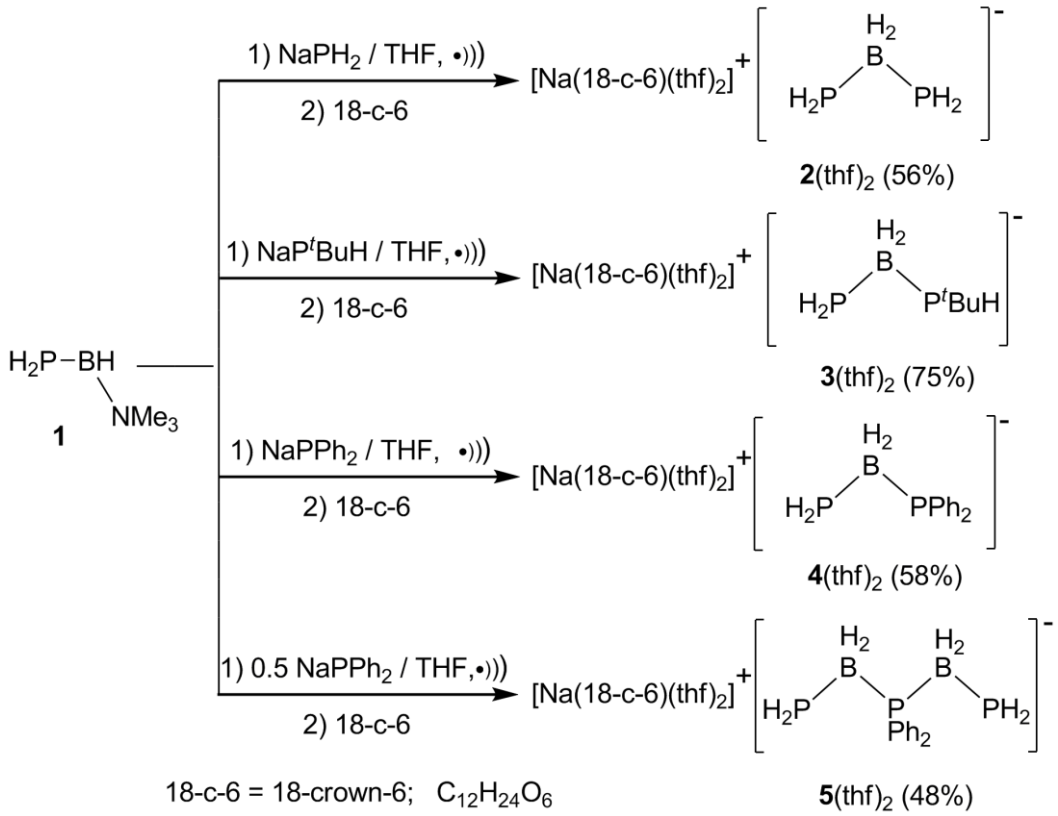

Scheme 1. Reaction of **1** with phosphorus centered nucleophiles. Isolated yields are given in parentheses.

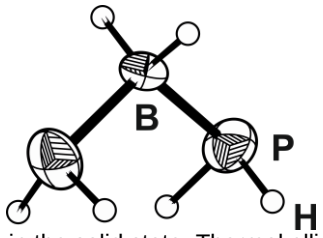

Figure 1. Molecular structure of **2**$(thf)_2$ in the solid state. Thermal ellipsoids are drawn with 50% probability. The counterion [Na(18-crown-6)thf_2)] is omitted for clarity. Selected bond lengths [Å] and angles [°]: P–B 1.961(3) and 1.964(3), P–B–P 110.4(2).

Since the phosphanides containing organic substituents attached to phosphorus are expected to be stronger nucleophiles than PH_2^-, they also should be able to substitute NMe_3 in **1**. Indeed, the reaction of $H_2PBH_2{\cdot}NMe_3$ with NaP^tBuH or $NaPPh_2$ selectively leads to the organic substituted anionic chain compounds $[Na]^+[H_2P{-}BH_2{-}P^tBuH]^-$ and $[Na]^+[H_2P{-}BH_2{-}PPh_2]^-$, respectively (Scheme 1).[19] Again, according to ^{31}P NMR spectroscopy, the reactions proceed without any side products in good isolated yields.[20] After addition of 18-crown-6 to the reaction mixture **3**$(thf)_2$ or **4**$(thf)_2$ can be isolated as crystalline solids. In the ^{31}P NMR spectrum a triplet for the PH_2 group of **3**$(thf)_2$ can be

found at δ = –219.4 ppm ($^1J_{PH}$ = 173 Hz) and at δ = –203.3 ppm ($^1J_{PH}$ = 173 Hz) for **4**(thf)$_2$, respectively. The P^{t}BuH group of **3**(thf)$_2$ arises as a doublet at δ = –32.9 ppm ($^1J_{PH}$ = 178 Hz) and the PPh$_2$ group of **4**(thf)$_2$ is detected as a broad singlet at δ = –15.2 ppm. The ^{11}B NMR spectra of **3**(thf)$_2$ reveals a triplet of triplets at δ = –33.8 ppm ($^1J_{BP}$ = 97 Hz, $^1J_{BH}$ = 98 Hz) and for **4**(thf)$_2$ at δ = –29.2 ppm ($^1J_{BH}$ = 98 Hz). The compounds **3**(thf)$_2$ and **4**(thf)$_2$ reveal in the solid state P1–B bond lengths of 1.973(3) Å (**3**(thf)$_2$) and 1.973(4) Å (**4**(thf)$_2$), respectively, which remain essentially unchanged compared to the starting material $H_2PBH_2{\cdot}NMe_3$ (1.976(2) Å)[8b] (Figure 2). The P2–B bond lengths are found to be 1.951(4) Å for (**3**(thf)$_2$) and 1.965(2) Å for (**4**(thf)$_2$) (figure 2).[21] Both P2–B bond lengths are slightly shorter compared to the P–B bond lengths of the neutral species H^{t}BuPBH$_2{\cdot}$NMe$_3$ (1.985(2) Å) and Ph$_2$PBH$_2{\cdot}$NMe$_3$(1.975(2) Å).[5]

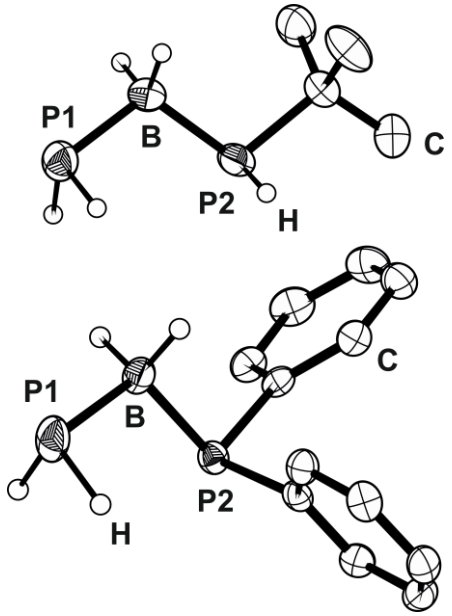

Figure 2. Molecular structures of the anions in **3**(thf)$_2$ (top) and **4**(thf)$_2$ (bottom) in the solid state. Thermal ellipsoids are drawn with 50% probability. Hydrogen atoms bond to carbon atoms are omitted for clarity. Selected bond lengths [Å] and angles [°]: **3**(thf)$_2$ P1–B 1.973(3); 1.976(2), P2–B 1.951(4); 1.953(4), P1–B–P2 107.8(2) – 112.4(1);[22] **4**(thf)$_2$ P1–B 1.973(4), P2–B 1.965(2), P1–B–P2 111.3(1).

The natural population analysis (NPA) reveal that the main part of the negative charge in the chain $[H_2P–BH_2–PH_2]^-$ is localized on the B atom (−0.70e) whereas the P atoms are almost neutral (−0.06e). The introduction of organic substituents on one phosphorus atom in $[H_2P–BH_2–PH_2]^-$ does not change the charge distribution on the boron atom (−0.72e for **3**(thf)$_2$ and −0.71e for **4**(thf)$_2$) but induces a gain of positive charge on the phosphorus atoms (+0.22e for **3**(thf)$_2$ and +0.58e for **4**(thf)$_2$) to which the organic groups are attached, while the other phosphorus atom stay almost neutral (−0.04e for **3**(thf)$_2$ and −0.01e for **4**(thf)$_2$). The remaining negative charge is dissipated on the organic groups. According to the NPA charge distribution the anions in **2**-**4** can be best described as

boranate anions. In these anions the highest molecular orbital (HOMO) represent a combination of the lone pairs of phosphorus atoms. At the organic substituted derivatives $[H_2P–BH_2–PRR']^-$ the lone pair of the phosphorus atom bearing the organic substituent(s) represent the HOMO.

The availability of the lone pair of electrons of the phosphorus atoms in the anions **2**, **3** and **4** for further reactions prompted us to investigate their reactivity towards $H_2PBH_2{\cdot}NMe_3$ (**1**). While for compound **2** no reaction was observed, the reaction of **1** with **4** leads to the formation of **5**$(thf)_2$, containing the 5-membered anionic chain $[H_2P–BH_2–PPh_2–BH_2–PH_2]^-$ (Scheme 1). The same reaction product is obtained if $H_2PBH_2{\cdot}NMe_3$ is reacted with 0.5 equivalents of $NaPPh_2$. NMR spectra of the reaction mixture show that the reaction proceeds very selectively; only traces of **4** and an excess **1** are found. After addition of 18-crown-6 **5**$(thf)_2$ can be isolated in good crystalline yields (48%). Surprisingly the reaction of **3** with **1** or NaP^tBuH with 2 equivalents of **1** leads to a mixture of different products. Despite many attempts the separation of the reaction products and their undoubtful identification was not successful. In the ^{31}P NMR spectrum of isolated **5**$(thf)_2$ a broad triplet at δ = –219.4 ppm with $^1J_{PH}$ = 180 Hz for the PH_2 group is observed, the PPh_2 group is detected as a broad singlet at δ = –0.2 ppm. The ^{11}B NMR spectrum of **5**$(thf)_2$ reveals a broad multiplet at δ = –34.4.

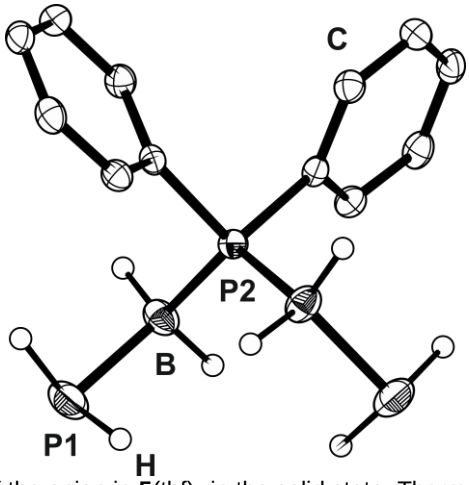

Figure 3. Molecular structure of the anion in **5**$(thf)_2$ in the solid state. Thermal ellipsoids are drawn with 50% probability. Hydrogen atoms bond to carbon are omitted for clarity. Selected bond lengths [Å] and angles [°]: P1–B 1.965(2), P1–B 1.940(2), P1–B–P2 113.1(1), B–P2–B 121.1(1).

NPA charge distribution of the anion of **5**$(thf)_2$ shows a positive charge accumulation on the P2 atom (+1.14e) whereas the negative charge remains on the boron atoms (−0.73e). In order to gain a deeper insight in the energetics of the substitution reactions of $H_2PBH_2{\cdot}NMe_3$ (**1**) with phosphorus centered nucleophiles DFT calculations have been performed.[23] Accordingly, the reaction of **1** with PH_2^- leading to $[H_2P–BH_2–PH_2]^-$ is

exothermic by −39.4 kJ·mol^{-1}. Similarly, an exothermic reaction is predicted by the reaction of tBuHP$^-$ and Ph_2P^- with **1** by −63.4 kJ·mol^{-1} and −35.5 kJ·mol^{-1}, respectively. The reaction of $[H_2P–BH_2–PPh_2]^-$ with **1** leading to $[H_2P–BH_2–PPh_2–BH_2–PH_2]^-$ is only slightly exothermic by −19.1 kJ·mol^{-1}. Although the reaction of **2** with **1** is predicted to be exothermic by −18.6 kJ·mol^{-1}, experimentally no reaction was observed, likely due to kinetic effects (see Figure 4).

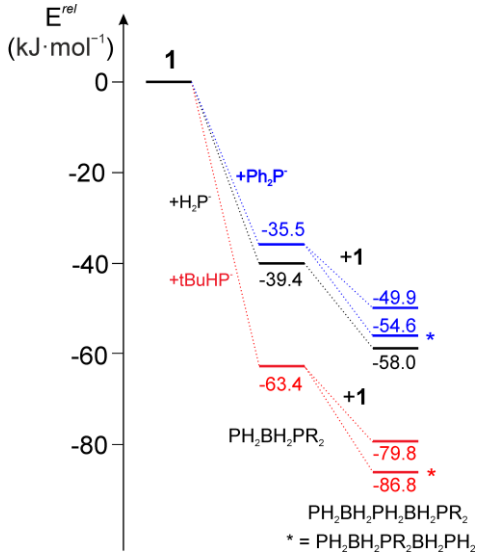

Figure 4. Energy profile of the reaction of $H_2PBH_2·NMe_3$ (**1**) with P centered nucleophiles. Relative energies calculated at the B3LYP/def2-TZVP level.

Since N-heterocyclic carbenes (NHCs) are known to be nucleophiles, the reaction of $H_2PBH_2·NMe_3$ (**1**) with NHC^{dipp} was also investigated. At room temperature no reaction was observed. Refluxing in toluene affords the ionic group 13/15 compound **6** (Scheme 2) as the only isolated product in minor yields. The formation of **6** is rather unexpected. Probably, during the reaction NMe_3 is eliminated leading to the transient H_2PBH_2 which aggregates and in the presence of NHC^{dipp} rearranges to **6**. The formation of the cationic part in **6** may also be the result of the presence of $ClBH_2·NMe_3$ in the starting material,[24] or fragmentation of **1**.

DFT computations indicate that gas phase reactions leading to the contact ion pair **6** are exothermic by -215 and -200 kJ mol^{-1} for the reactions 1 and 2, respectively:

6x**1** + 3 NHC^{dipp} + $ClBH_2·NMe_3$ = $[NHC^{dipp}H]^+Cl^-$ + 7 NMe_3 + $[NHC^{dipp}·BH_2PH_2BH_2·NHC^{dipp}]^+ \cdots [P_5B_5H_{19}]^-$ (1)

7x**1** + 2 NHC^{dipp} = 7 NMe_3 + PH_3 + $[NHC^{dipp}·BH_2PH_2BH_2·NHC^{dipp}]^+ \cdots [P_5B_5H_{19}]^-$ (2)

In the $^{11}B\{^1H\}$ and $^{31}P\{^1H\}$ NMR spectra of **6** many broad and overlapping signals are observed. An accurate assignment of the signals is not possible due to the broadness of the signals and the very complex spin system leading to sophisticated coupling pattern. In the ESI mass spectrum the molecular ion peak for both the anion $[P_5B_5H_{19}]^-$ (negative mode) and the cation $[NHC^{dipp}{\cdot}BH_2{-}PH_2{-}BH_2{\cdot}NHC^{dipp}]^+$ (positive mode) was observed.

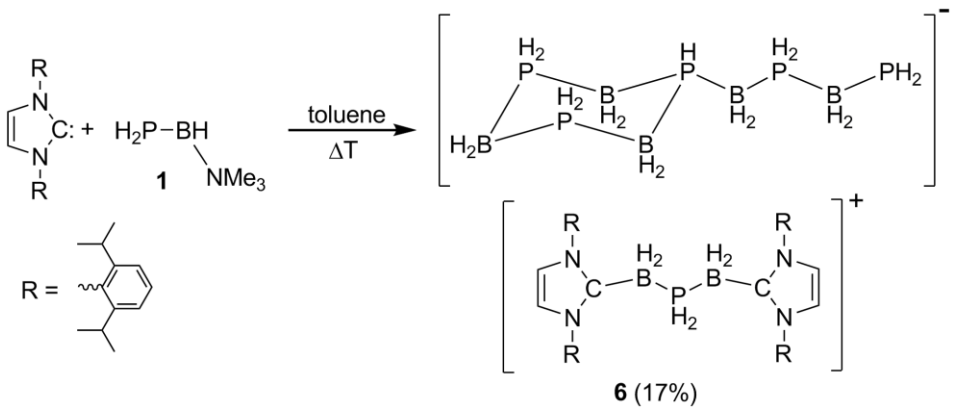

Scheme 2. Synthesis of **6.** Yield in parentheses.

The solid state structure of **6** shows a cation featuring a B–P–B unit which is stabilized by two NHC ligands. The anion is a *n*-butylcyclohexane-like unit built up from alternating BH_2 and PH_2 units. The cationic part of **6** shows P–B bond lengths of 1.929(2) and 1.947(2) Å. Similar B-P bond lengths have been found in the anion of **6** (exocyclic part: 1.927(3) - 1.964(3) Å and within the ring 1.930(3) -1.952(2) Å). A comparable structural motif was recently reported by *Baker et al.* for the cyclic aminoborane tetramer, B-(cyclotriborazanyl)-amine-borane.[25]

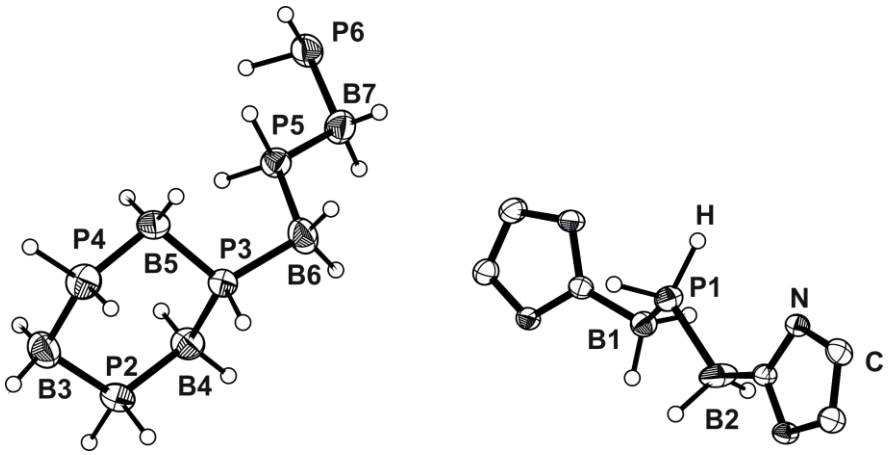

Figure 5. Molecular structure of **6** in the solid state. Thermal ellipsoids are drawn with 50% probability. The hydrogen atoms at the carbon atoms and the dipp groups at the carbenes are omitted for clarity. Selected bond lengths [Å] and angles [°]: P–B 1.929(2) - 1.964(3), B–P–B 104.0(1) - 119.0(1), P–B–P 106.0(2) - 114.6(1).

6.3 Conclusion

The results show that the parent phosphanylborane $H_2PBH_2{\cdot}NMe_3$ is a valuable precursor for the generation of mixed anionic group 13/15 chains. For the first time a rational synthetic approach together with the structural characterization of the unprecedented linear, anionic compounds was possible. These unique 13/15 compounds represent the anionic counterparts of the recently reported cationic species.[11] The compounds **2** - **6** are stable under inert conditions and represent promising starting materials for the preparation of extended group 13/15 chains, cycles and polymers.

6.4 References

[1] a) M. Baudler, *Angew. Chem. Int. Ed.* **1982**, *21*, 492–512; *Angew. Chem.* **1982**, *94*, 520–539; b) M. Baudler, *Angew. Chem. Int. Ed.* **1987**, *26*, 419–441; *Angew. Chem.* **1987**, *99*, 429–451; c) M. Baudler, K. Glinka, *Chem. Rev.* **1993**, *93*, 1623–1667; d) M. Baudler, K. Glinka, *Chem. Rev.* **1994**, *94*, 1273–1297; e) H. G. von Schnering, W. Hönle, *Chem. Rev.* **1988**, *88*, 243–273; f) R. Wolf, S. Gomez-Ruiz, J. Reinhold, W. Boehlmann, E. Hey-Hawkins, *Inorg. Chem.* **2006**, *45*, 9107–9113; g) R. Wolf, E. Hey-Hawkins, *Z. anorg. allg. Chem*. **2006**, 727–734; h) R. Wolf, E. Hey-Hawkins, *Chem. Comm.* **2004**, *22*, 2626–2627; i) R. Wolf, A. Schisler, P. Loennecke, C. Jones, E. Hey-Hawkins, *Eur. J. Inorg. Chem.* **2004**, *16*, 3277–3286; j) I. Jevtovikj, P. Lönnecke, E. Hey-Hawkins, *Chem. Commun.* **2013**, *49*, 7355–7357.

[2] a) C.A. Dyker, N. Burford, *Chem. Asian J.* **2008**, *3*, 28–36; b) A.P.M. Robertson, P.A. Gray, N. Burford, *Angew. Chem. Int. Ed.* **2014**, *53*, 6050–6069, *Angew. Chem.* **2014**, 126, 6162–6182; c) S.S. Chitnis, E. MacDonald, N. Burford, U. Werner-Zwanziger, R. McDonald, *Chem. Commun.* **2012**, *48*, 7359–7361; d) Y-Y. Carpenter, C.A. Dyker, N. Burford, M.D. Lumsden, A. Decken, *J. Am. Chem. Soc.* **2008**,*130*, 15732–15741; e) J.J. Weigand, N. Burford and A. Decken, *Eur. J. Inorg. Chem.* **2007**, 4868–4872; f) S. D. Riegel, N. Burford, M.D. Lumsden, A. Decken, *Chem. Commun*, **2007**, *44*, 4668–4670; g) C. A. Dyker, S. D. Riegel, N. Burford, M. D. Lumsden, A. Decken, *J. Am. Chem. Soc.* **2007**, *129*, 7464–7474; h) C. A. Dyker, N. Burford, M. D. Lumsden, A. Decken, *J. Am. Chem. Soc.* **2006**,*128*, 9632–9633; i) N. Burford, C.A. Dyker, M. Lumsden, A. Decken, *Angew. Chem. Int. Ed.* **2005**; *44*, 6196–6199, *Angew. Chem.* **2005**, *117*, 6352–6355; j) N. Burford, C. A. Dyker, A. Decken, *Angew. Chem. Int. Ed.* **2005**, *44*, 2364–2367; *Angew. Chem.* **2005**, *117*, 2416–2419.

[3] a) M. Donath, M. Bodensteiner, J. J. Weigand, *Chem. Eur. J* **2014**, *20*, 17306–17310; b) M. H. Holthausen, J. J. Weigand, *Chem. Soc. Rev.* **2014**, 43, 6639–6657; c) K.-O. Feldmann, J. J. Weigand, *Angew. Chem. Int. Ed.* **2012**, 51, 7545–7549; *Angew. Chem.* **2012**, 124, 7663–7667; d) M. Donath, E. Conrad, P. Jerabek, G. Frenking, R. Fröhlich, N. Burford, J. J. Weigand, *Angew. Chem. Int. Ed.* **2012**, *51*, 2964–2967; *Angew. Chem.* **2012**, *124*, 3018–3021; e) J. J. Weigand, N. Burford, M. D. Lumsden, A. Decken, *Angew. Chem. Int. Ed.* **2006**, *45*, 6733–6736; *Angew. Chem.* **2006**, *118*, 6885–6889; f) J. J. Weigand, N. Burford, R. J. Davidson, T. S. Cameron, P. Seelheim, *J. Am. Chem. Soc.* **2009**, *131*, 17943–17953, g) J. J. Weigand, M. Holthausen, *J. Am. Chem. Soc.* **2009**, *131*, 14210–14211; h) J. J. Weigand, M. Holthausen, R. Fröhlich, *Angew. Chem. Int. Ed.*, **2009**, *48*, 295–298; *Angew. Chem.* **2009**, *121*, 301–304; i) J. J. Weigand, N. Burford, S. Riegel, A. Decken, *J. Am. Chem. Soc.* **2007**, *129*, 7969–7976.

[4] A. Staubitz, A. P. M. Robertson, M. E. Sloan, I. Manners, *Chem. Rev.* **2010**, *110*, 4023–4078; A. Staubitz, A. P. M. Robertson, I. Manners, *Chem. Rev.* **2010**, *110*, 4079–4124.

[5] C. Marquardt, T. Jurca, K.-C. Schwan, A. Stauber, A. V. Virovets, G. R. Whittell, I. Manners, M. Scheer, *Angew. Chem. Int. Ed.* **2015**, *54*, 13782–13786; *Angew. Chem.* **2015**, *127*, 13986–13991.

[6] B. Kaufmann, H. Nöth, R. T. Paine, K. Polborn, M. Thomann, *Angew. Chem. Int. Ed.* **1993**, *32*, 1446–1448; *Angew. Chem.* **1993**, *105*, 1534–1536;b) H. V. Rasika Dias, P. P. Power, *J. Am. Chem. Soc.* **1989**, *111*, 144–148. c) H. Dorn, R. A. Singh, J. A. Massey, A. J. Lough, I. Manners, *Angew. Chem. Int. Ed*. **1999**, *38*, 3321–3323; *Angew. Chem.* **1999**, *111*, 3540–3543; d) H. Dorn, R. A. Singh, J. A. Massey, J. M. Nelson, C. A. Jaska, A. J. Lough, I. Manners, *J. Am. Chem. Soc.* **2000**, *122,* 6669–6678. e) M. E. Sloan, T. J. Clark, I. Manners, *Inorg. Chem.* **2009**, *48*, 2429–2435.

[7] T. Oshiki, T. Imamoto, *Bull. Chem. Soc. Jpn.* **1990**, *63*, 2846–2849.

[8] a) U. Vogel, A. Y. Timoshkin, M. Scheer, *Angew. Chem. Int. Ed.* **2001**, *40*, 4409–4412; Angew. Chem. **2001**, *113*, 4541–4544; b) K.-C. Schwan, A. Timoshkin, M. Zabel, M. Scheer, *Chem. Eur. J.* **2006**, *12*, 4900–4908; c) U. Vogel, A. Y. Timoshkin, K.-C. Schwan, M. Bodensteiner, M. Scheer*, J. Organomet. Chem.* **2006**, *691*, 4556–4564.

[9] C. Marquardt, A. Adolf, A. Stauber, M. Bodensteiner, A. V. Virovets, A. Y. Timoshkin, M. Scheer, *Chem. Eur. J.* **2013**, *19*, 11887–11891.

[10] C. Thoms, C. Marquardt, M. Bodensteiner, M. Scheer, *Angew. Chem. Int. Ed.* **2013**, *52*, 5150–5154; Angew. Chem. **2013**, *125*, 5254–5259.

[11] C. Marquardt, C. Thoms, A. Stauber, G. Balazs, M. Bodensteiner, M. Scheer, *Angew. Chem. Int. Ed.* **2014**, *53*, 3727–3730; *Angew. Chem.* **2014**, *126*, 3801–3804; and references cited herein.

[12] a) T. Costa, H. Schmidbaur, *Chem. Ber.* **1982**, *115*, 1374–1378; b) T. Miyazaki, M. Sugawara, H. Danjo, T. Imamoto, *Tetrahedron Lett.* **2004**, *45*, 9341–9344; c) D. R. Martin, C. M. Merkel, J. P. Ruiz, *Inorg. Chim. Acta* **1985**, *100*, 293–297; d) K. Owsianik, R. Chauvin, A. Balińska, M. Wieczorek, M. Cypryk, M. Mikołajczyk, *Organometallics* **2009**, *28*, 4929–4937; e) H. Schmidbaur, T. Wimmer, G. Reber, G. Müller, *Angew. Chem. Int. Ed.* **1988**, *27*, 1071–1074; *Angew. Chem.* **1988**,*100*, 1135–1138.

[13] B. Kaufmann, R. Jetzfellner, E. Leissring, K. Issleib, H. Noeth, M. Schmidt, *Chem. Ber./Recueil* **1997**,130, 1677–1692.

[14] a) M. Baudler, C. Block, *Z. anorg. allg. Chem*. **1988**, *567*, 7–12. b) M. Baudler, C. Block, H. Budzikiewicz, H. Münster, *Z. anorg. allg. Chem*. **1989**, *569*, 7–15.

[15] E. Mayer, *Angew. Chem. Int. Ed.* **1971**, *10*, 416–417; *Angew. Chem.* **1971**, *83*, 446–447.

[16] a) F. Dornhaus, M. Bolte, H.-W. Lerner, M. Wagner, *Eur. J. Inorg. Chem.* **2006**, *24*, 5138–3147, b) H. C. Miller, E. L. Muetterties, US 2999864, **1961**.

[17] a) R. E. Hester, E. Mayer, *Spectrochim. Acta Mol. and Biomol. Spectrosc.* **1967**, *23*, 2218–2220. b) M. R. Anstey, M. T. Corbett, E. H. Majzoub, J. G. Cordaro, *Inorg. Chem.* **2010**, *49*, 8197–8199; c) E. Mayer, A. W. Laubengayer, *Monatsh. Chem.* **1970**, *101*, 1138–1144; d) F. Dornhaus, M. Bolte, H.-W. Lerner, M. Wagner, *Eur. J. Inorg. Chem.* **2006**, *24*, 1777–1785.

[18] A. B. Burg, *Inorg. Chem.* **1978**, *17*, 593–599.

[19] The reaction of **1** with $KPPh_2$ leads to $[K]^+[H_2P–BH_2–PPh_2]^-$. Basically the analytical data of the potassium salt **4b** is in good agreement with the sodium compound **4**$(thf)_2$. However during X-Ray analysis oxidation process takes place, and a partly oxidized species is determined in the solid state. See SI for further information.

[20] ^{31}P NMR spectrum of reaction mixture of **3** and **4** shows small amounts of corresponding phosphines $^tBuPH_2$ and $HPPh_2$, respectively, and of **1**. Traces of **5** can rarely be observed in the spectrum of **4**.

[21] The asymmetric unit contains two molecules. Only one bond length is given, see Figure 2 or SI for further information.

[22] Compound **3**$(thf)_2$ shows disorder in the solid state. Bond lengths are given for the main component. The component with the lower occupied species, shows elongated P2–B bond length.

[23] See SI for further Information.

[24] $ClBH_2{\cdot}NMe_3$ is a starting material for $H_2PBH_2{\cdot}NMe_3$ (see ref. 7). Reaction with $H_2PBH_2{\cdot}NMe_3$ generated without $ClBH_2{\cdot}NMe_3$ does not yield **6**. Though many attempts with different stoichiometries were made, a rational synthesis of **6** could not be achieved and is bound by $ClBH_2{\cdot}NMe_3$ generated $H_2PBH_2{\cdot}NMe_3$.

[25] H. A. Kalviri, F. Gärtner, G. Ye, I. Korobkova, R. Tom Baker, *Chem. Sci.* **2015**, *6*, 618–624.

6.5 Supporting Information

General Experimental:

All manipulations were performed under an atmosphere of dry argon using standard glove-box and Schlenk techniques. All solvents are degassed and purified by standard procedures. The compounds $H_2PBH_2{\cdot}NMe_3$,[1] $ClBH_2{\cdot}NMe_3$,[2] $NaPH_2$,[3] NHC^{dipp}[4] and $^tBuPH_2$[5] were prepared according to literature procedures. Other chemicals were obtained from STREM Chemicals, INC. (PPh_2H). The NMR spectra were recorded on either an Avance 400 spectrometer (^1H: 400.13 MHz, ^{31}P: 161.976 MHz, ^{11}B: 128.378 MHz, $^{13}C\{^1H\}$: 100.623 MHz) with δ [ppm] referenced to external $SiMe_4$ (^1H, ^{13}C), H_3PO_4 (^{31}P), $BF_3{\cdot}Et_2O$ (^{11}B). IR spectra were recorded on a DIGILAB (FTS 800) FT-IR spectrometer. All mass spectra were recorded on a ThermoQuest Finnigan TSQ 7000 (ESI-MS) or a Finnigan MAT 95 (FD-MS and EI-MS). The C, H, N analyses were measured on an Elementar Vario EL III apparatus.

General remarks for C, H, N analyses:

C, H, N analyses were carried out repeatedly. Different amounts of coordinating THF have been found in nearly all cases. Total removal of the THF was not always possible, however C, H, N analyses are in good agreement with the expected values considering a varying THF-content (0.2 % tolerance).

Synthesis of $[Na(C_{12}H_{24}O_6)(thf)_2]^+[HP_2{-}BH_2{-}PH_2]^-$ (2(thf)$_2$):

A solution of 53 mg (0.50 mmol) $H_2PBH_2{\cdot}NMe_3$ in 1 mL toluene is added to a suspension of 30 mg (0.53 mmol) $NaPH_2$ in 20 ml THF. After sonication of the mixture for 2.5 h, the solution is filtrated onto 132 mg (0.5 mmol) solid $C_{12}H_{24}O_6$ (18-crown-6). The solution is layered with 60 mL of *n*-hexane. **2**$(thf)_2$ crystallises at 4 °C as colourless blocks. The crystals are separated and washed with cold *n*-hexane (0°C, 3×5 mL). Yield of **2**: 103 mg (56 %). ^1H NMR (THF-d_8, 25 °C): δ = 0.93 (d, $^1J_{H,P}$ = 172 Hz, 4H, PH_2), 1.09

(qt, $^{1}J_{H,B}$ = 99 Hz, 2H, BH_2), 3.64 (s, 24H, $C_{12}H_{24}O_6$). ^{31}P NMR (THF-d_8, 25 °C): δ = –175.0 (tm, $^{1}J_{H,P}$ = 172 Hz, br, PH_2). $^{31}P\{^{1}H\}$ NMR (THF-d_8, 25 °C): δ = –175.0 (q, $^{1}J_{B,P}$ = 26 Hz, PH_2). ^{11}B NMR (THF-d_8, 25 °C): δ = –34.7 (tt, $^{1}J_{B,P}$ = 26 Hz, $^{1}J_{B,H}$ = 99 Hz, BH_2). $^{11}B\{^{1}H\}$ NMR (THF-d_8, 25 °C): δ = –34.7 (t, $^{1}J_{B,P}$ = 26 Hz, BH_2). $^{13}C\{^{1}H\}$ NMR (THF-d_8, 25 °C): δ = 70.6 (s, $C_{12}H_{24}O_6$). IR (KBr): $\tilde{\nu}$ = 2900 (vs, CH), 2870 (s, CH), 2825 (m), 2796 (m), 2747 (w), 2747 (w), 2712 (w), 2690 (w), 2326 (s, br, BH), 2311 (s, br, BH), 2270 (s, PH), 2253 (s, PH), 2141 (w), 1979 (w), 1931 (w), 1887 (w), 1839 (vw), 1471 (m), 1455 (m), 1435 (w), 1410 (vw), 1352 (s), 1283 (m), 1250 (m), 1237 (m), 1109 (vs, CO), 1075 (m), 1058 (w), 966 (vs), 841 (m), 765 (w), 711 (w), 652 (w), 531 (w). ESI-MS (THF): anion: *m/z* = 79 (100 %, $[HP_2–BH_2–PH_2]^-$). ESI-MS (THF) cation: *m/z* = 653 (8% $[Na(C_{12}H_{24}O_6)]^+_2[HP_2–BH_2–PH_2]^-$); 287 (100 %, $[Na(C_{12}H_{24}O_6)]^+$). Elemental analysis (%) calculated for $C_{12}H_{30}B_1NaO_6P_2$ (**2**): C: 39.32, H: 8.26; found: C: 39.30, H: 8.40.

Synthesis of [NaP^{t}BuH]:

1.2 mL (900 mg, 10 mmol) ^{t}BuPH_2 is added to a suspension of 390 mg (10 mmol) $NaNH_2$ in 10 mL THF at -50°C. The solution is stirred for 5 h at room temperature, until all $NaNH_2$ is consumed. A clear yellow solution is obtained which is degassed 3 times to remove NH_3. The solution is used as a 1 M stock solution of NaP^{t}BuH in THF. Yield of [NaP^{t}BuH]: (100 %, according to ^{31}P NMR). ^{31}P NMR (C_6D_6, 25 °C): δ = –81.4 (dm, $^{1}J_{H,P}$ = 157 Hz, P^{t}BuH). $^{31}P\{^{1}H\}$ NMR (C_6D_6, 25 °C): δ = –81.4 (s, P^{t}BuH).

Synthesis of $[Na(C_{12}H_{24}O_6)(thf)_2]^+[H^tBuP–BH_2–PH_2]^-$ (3(thf)$_2$):

A solution of 106 mg (1 mmol) $H_2PBH_2{\cdot}NMe_3$ in 1 mL toluene is added to a solution of 112 mg (1 mmol) NaP^{t}BuH in 20 ml THF. After sonication of the mixture for 2.5 h, the solution is filtrated onto 264 mg (1 mmol) solid $C_{12}H_{24}O_6$ (18-crown-6). The solution is layered with 60 mL of *n*-hexane. **3**(thf)$_2$ crystallises at 4 °C as colourless blocks. The crystals are separated and washed with cold *n*-hexane (0°C, 3×5 mL). Yield of $[Na(C_{12}H_{24}O_6)(thf)_{0.15}]^+[H^tBuP–BH_2–PH_2]^-$: 374 mg (75 %). ^{1}H NMR (THF-d_8, 25 °C): δ = 0.72 (ddm, $^{1}J_{H,P}$ = 173 Hz, $^{3}J_{H,P}$ = 60 Hz, 2H, PH_2), 1.07 (d, $^{3}J_{H,P}$ = 9 Hz, ^{t}Bu), 1.22 (m, 2H, BH_2), 1.76 (dm, $^{1}J_{H,P}$ = 177 Hz, 1H, PH^{t}Bu), 3.64 (s, 24H, $C_{12}H_{24}O_6$). ^{31}P NMR (THF-d_8, 25 °C): δ = –188.0 (t, br, $^{1}J_{H,P}$ = 173 Hz, PH_2), –32.9 (d, br, $^{1}J_{H,P}$ = 178 Hz, P^{t}BuH). $^{31}P\{^{1}H\}$ NMR (THF-d_8, 25 °C): δ = –188.8 (m, PH_2), –32.9 (m, P^{t}BuH). ^{11}B NMR (THF-d_8, 25 °C): δ = –33.8 (tt, $^{1}J_{B,P}$ = 97 Hz, $^{1}J_{B,H}$ = 99 Hz, BH_2). $^{11}B\{^{1}H\}$ NMR (THF-d_8, 25 °C): δ = –33.8 (t, $^{1}J_{B,P}$ = 27 Hz, BH_2). $^{13}C\{^{1}H\}$ NMR (THF-d_8, 25 °C): δ = 27.3 (dd, $^{1}J_{C,P}$ =15 Hz, $^{3}J_{C,P}$ = 5 Hz, $\underline{C}(CH_3)_3$), 33.8 (d, $^{2}J_{C,P}$ = 10 Hz, CH_3), 70.6 (s, $C_{12}H_{24}O_6$). IR (KBr): $\tilde{\nu}$ = 2902 (vs, CH), 2316 (s, br, BH), 2240 (s, PH), 1975 (w), 1627 (br, w), 1471 (m), 1464 (m), 1353 (s), 1285 (m), 1251 (s), 1109 (vs, CO), 962 (s), 837 (m), 711 (w), 530

(w). ESI-MS (THF): anion: *m/z* = 227 (15%, $[H^tBuP–BH_2–PH_2–BH_2–PH_2–BH_2–PH_2]^-$), 181 (100 %, $[H^tBuP–BH_2–PH_2–BH_2–PH_2]^-$), 135 (48 %, $[H^tBuP–BH_2–PH_2]^-$). Elemental analysis (%) calculated for $C_{16}H_{38}B_1NaO_6P_2(thf)_{0.15}$ (**3**$thf_{0.15}$): C: 46.00, H: 9.12; found: C: 46.06, H: 9.02.

Synthesis of $[NaPPh_2]$:

1.74 mL (1.860 g, 10 mmol) Ph_2PH is added to a suspension of 390 mg (10 mmol) $NaNH_2$ in 10 mL THF at -50°C. The solution is stirred for 5 h at room temperature, until all $NaNH_2$ is consumed. A clear red solution is obtained which is degassed 3 times to remove NH_3. The solution is used as a 1 M stock solution of $NaPPh_2$ in THF. Yield of $[NaPPh_2]$: (100 %, according to ^{31}P NMR). ^{31}P NMR (C_6D_6, 25 °C): δ = –27.2 (s, PPh_2). $^{31}P\{^1H\}$ NMR (C_6D_6, 25 °C): δ = –27.2 (s, PPh_2).

Synthesis of $[Na(C_{12}H_{24}O_6)(thf)_2]^+[Ph_2P–BH_2–PH_2]^-$ (4$(thf)_2$):

A solution of 106 mg (1.00 mmol) $H_2PBH_2{\cdot}NMe_3$ in 1 mL toluene is added to a solution of 208 mg (1.00 mmol) $NaPPh_2$ in 20 ml THF. After sonication of the mixture for 2.5 h, the solution is filtrated onto 264 mg (1.00 mmol) solid $C_{12}H_{24}O_6$ (18-crown-6). After removal of all volatiles under reduced pressure **4** is dissolved in 5 mL of THF and filtrated again. The solvent is removed and 20 mL of *n*-hexane are added to the white solid. Then THF is added drop wise until a clear colourless solution is obtained. **4**$(thf)_2$ crystallises at -28 °C as colourless blocks. The crystals are separated and washed with cold *n*-hexane (0°C, 3×5 mL). At room temperature **4**$(thf)_2$ is a colourless waxy solid/oil. Yield of $[Na(C_{12}H_{24}O_6)(thf)_{1.1}]^+[Ph_2P–BH_2–PH_2]^-$: 310 mg (58 %). ^1H NMR (THF-d_8, 25 °C): δ = 0.71 (d, $^1J_{H,P}$ = 173 Hz, 2H, PH_2), 1.50 (q, $^1J_{H,B}$ = 100 Hz, 2H, BH_2). 3.56 (s, 24H, $C_{12}H_{24}O_6$), 6.86 (m, 2H, *p*-Ph), 6.97 (m, 4H, *m*-Ph), 7.44 (m, 4H, *o*-Ph). ^{31}P NMR (THF-d_8, 25 °C): δ = –203.3 (t, $^1J_{H,P}$ = 173 Hz, br, PH_2), –15.2 (s, PPh). $^{31}P\{^1H\}$ NMR (THF-d_8, 25 °C): δ = –203.3 (PH_2), –15.2 (s, PPh). ^{11}B NMR (THF-d_8, 25 °C): δ = –29.17 (tt, $^1J_{B,H}$ = 98 Hz, BH_2). $^{11}B\{^1H\}$ NMR (THF-d_8, 25 °C): δ = –29.17 (t, BH_2). $^{13}C\{^1H\}$ NMR (THF-d_8, 25 °C): δ = 70.6 (s, $C_{12}H_{24}O_6$), 124.1 (s, *p*-Ph), 126.8 (d, *m*-Ph, $^2J_{P,C}$ = 5 Hz), 134.7 (d, *o*-Ph, $^2J_{P,C}$ = 14 Hz), 150.8 (dd, *i*-Ph, $^1J_{P,C}$ = 26 Hz, $^3J_{P,C}$ = 4 Hz). IR (film, NaCl):): $\tilde{\nu}$ = 2910 (vs, CH), 2876 (vs, CH), 2320 (s, br, BH), 2267 (s, PH), 1959 (w), 1894 (w), 1821 (vw), 1620 (w), 1579 (m), 1474 (s), 1455 (m), 1431 (m), 1353 (s), 1297 (m), 1250 (m), 1107 (vs, CO), 1027 (m), 957 (s), 835 (m), 741 (m), 700 (s), 591 (m), 542 (w), 507 (w), 417 (w). ESI-MS (THF): anion: *m/z* = 277 (12 %, $[H_2P–BH_2–Ph_2P–BH_2–PH_2]^-$), 231 (100%, $[Ph_2P–BH_2–PH_2]^-$), 185 (34%, Ph_2P^-). Elemental analysis (%) calculated for $C_{25}H_{38}BNaO_6P_2(thf)_{1.1}$ (**4**$(thf)_{1.1}$): C: 57.04, H: 7.89; found: C: 57.11, H: 7.79.

Synthesis of $[Na(C_{12}H_{24}O_6)(thf)_2]^+[H_2P–BH_2–Ph_2P–BH_2–PH_2]^-$ (5(thf)$_2$):

A solution of 53 mg (0.50 mmol) $H_2PBH_2{\cdot}NMe_3$ in 1 mL toluene is added to a solution of 52 mg (0.25 mmol) $NaPPh_2$ in 20 ml THF. After sonication of the mixture for 5 h, the solution is filtrated onto 66 mg (0.25 mmol) solid $C_{12}H_{24}O_6$ (18-crown-6). After removal of all volatiles under reduced pressure the remaining solid is dissolved in 5 mL of THF and filtrated again. The solvent is removed and 20 mL of *n*-hexane are added to the white solid. THF is added drop wise until a clear colourless solution is obtained. **5**(thf)$_2$ crystallises at -28 °C as colourless plates. The crystals are separated and washed with cold *n*-hexane (0°C, 3×5 mL). Yield of **5**: 70 mg (48 %). ^{1}H NMR (THF-d$_8$, 25 °C): δ = 0.74 (dm, $^1J_{H,P}$ = 181 Hz, 4H, PH_2), 1.51 (q, $^1J_{H,B}$ = 105 Hz, 4H, BH_2), 3.60 (s, 24H, $C_{12}H_{24}O_6$), 7.08 -7.19 (m, 6H, *m*- & *p*-Ph) 7.69 (m, 4H, *o*-Ph). ^{31}P NMR (THF-d$_8$, 25 °C): δ = –219.4 (tm, $^1J_{H,P}$ = 181 Hz, 2P, PH_2), 0.1 (s, br, 1P, PPh_2). ^{31}P{^{1}H} NMR (THF-d$_8$, 25 °C): δ = –219.4 (m, 2P, PH_2), 0.1 (s, br, 1P, PPh_2). ^{11}B NMR (THF-d$_8$, 25 °C): δ = –34.4 (m, BH_2). ^{11}B{^{1}H} NMR (THF-d$_8$, 25 °C): δ = –34.4 (m, BH_2). ^{13}C{^{1}H} NMR (THF-d$_8$, 25 °C): δ = 70.6 (s, $C_{12}H_{24}O_6$), 127.3 (d, *m*-Ph, $^2J_{P,C}$ = 8 Hz), 127.7 (d, *p*-Ph, $^2J_{P,C}$ = 2 Hz), 134.59 (d, *o*-Ph, $^2J_{P,C}$ = 6 Hz), 139.81 (d, *i*-Ph, $^2J_{P,C}$ = 36 Hz). IR (KBr): $\tilde{\nu}$ = 2902 (vs, CH), 2826 (s, CH), 2747 (w), 2375 (s, br, BH), 2356 (s, br, BH), 2332 (s, PH), 2279 (s, PH), 1622 (vw), 1479 (w), 1477 (w) 1453 (m), 1434 (w), 1352 (s), 1284 (w), 1251 (m), 1113 (vs, CO), 1028 (w), 965 (s), 837 (m), 791 (w), 775 (vw), 742 (m), 723 (w), 702 (m), 615 (vw), 531 (w), 496 (w), 466 (w), 435 (vw). ESI-MS (THF): anion: *m/z* = 323 (100 %, $[Ph_2P(BH_2–PH_2)_n]^-$ (n = 3)), 277 (100 %, $[Ph_2P(BH_2–PH_2)_n]^-$ (n = 2)), 230 (75%, $[Ph_2P(BH_2–PH_2)_n]^-$ (n = 1)). Elemental analysis (%) calculated for $C_{24}H_{42}B_2NaO_6P_3$ (**5**): C: 51.04, H: 7.50; found: C: 51.14, H: 7.56.

Synthesis of $[K(C_{12}H_{24}O_6)]^+[Ph_2P–BH_2–PH_2]^-$ (4b):

A solution of 50 mg (0.45 mmol) $H_2PBH_2{\cdot}NMe_3$ in 1 mL toluene is added to a solution of 106 mg (0.5 mmol) $KPPh_2$ in 20 ml THF. After sonication of the mixture for 2.5 h, the solution is filtrated onto 132 mg (0.50 mmol) $C_{12}H_{24}O_6$ (18-crown-6). The solution is layered with 60 mL of *n*-hexane. **4b** crystallises at -30 °C as colourless blocks. The crystals are separated and washed with cold *n*-hexane (-30°C, 3×5 mL). Yield of $[K(C_{12}H_{24}O_6)]^+[Ph_2P–BH_2–PH_2]^-$: 130 mg (54 %). ^{1}H NMR (THF-d$_8$, 25 °C): δ = 0.71 (d, $^1J_{H,P}$ = 173 Hz, 2H, PH_2), 1.50 (q, $^1J_{H,B}$ = 100 Hz, 2H, BH_2). 3.56 (s, 24H, $C_{12}H_{24}O_6$), 6.86 (m, 2H, *p*-Ph), 6.97 (m, 4H, *p*-Ph), 7.44 (m, 4H, *o*-Ph). ^{31}P NMR (THF-d$_8$, 25 °C): δ = –204.8 (t, $^1J_{H,P}$ = 173 Hz, br, PH_2), –15.66 (s, PPh). ^{31}P{^{1}H} NMR (THF-d$_8$, 25 °C): δ = –204.8 (PH_2), –15.66 (s, PPh). ^{11}B NMR (THF-d$_8$, 25 °C): δ = –31.04 (tt, $^1J_{B,H}$ = 98 Hz, BH_2). ^{11}B{^{1}H} NMR (THF-d$_8$, 25 °C): δ = –31.04 (t, BH_2). ^{13}C{^{1}H} NMR (THF-d$_8$, 25 °C): δ = 71.0 (s, $C_{12}H_{24}O_6$), 124.1 (s, *p*-Ph), 126.8 (d, *m*-Ph, $^2J_{P,C}$ = 5 Hz), 134.7 (d, *o*-

Ph, $^{2}J_{P,C}$ = 14 Hz), 150.7 (dd, *i*-Ph, $^{1}J_{P,C}$ = 26 Hz, $^{3}J_{P,C}$ = 4 Hz). IR (KBr): $\tilde{\nu}$ = 3062 (w, CH), 3004 (vs, CH), 2896 (vs, CH), 2823 (s, CH), 2794 (w, CH), 2743 (w, CH), 2718 (w, CH), 2681 (w, CH), 2337 (s, br, BH), 2297 (s, br, BH), 2272 (s, PH), 2234 (s, PH), 1974 (w), 1604 (w), 1579 (m), 1472 (s), 1453 (m), 1431 (m), 1351 (s), 1284 (m), 1248 (m), 1108 (vs, CO), 1028 (w), 963 (s), 838 (m), 758 (m), 739 (m), 701 (m), 559 (w), 529 (w), 493 (w), 475 (w), 432 (w). ESI-MS (THF): anion: *m/z* = 323 (5 %, $[H_2P–BH_2–Ph_2P–BH_2–PH_2–BH_2–PH_2]^-$), 277 (100 %, $[H_2P–BH_2–Ph_2P–BH_2–PH_2]^-$), 247 (20%, $[H_2P–BH_2–Ph_2PO]^-$), 231 (20%, $[H_2P–BH_2–Ph_2P]^-$). Elemental analysis (%) calculated for $C_{25}H_{38}BKO_6P_2(O)_{0.8}$ (**4b**): C: 52.65, H: 7.00; found: C: 52.59, H: 7.11.

Synthesis of $[NHC^{dipp}·BH_2–PH_2–BH_2·NHC^{dipp}]^+[B_5P_5H_{19}]^-$(6):

To a solution of 400 mg NHC^{dipp} (1.03 mmol) in 20 ml toluene, a solution of 105 mg (1 mmol) $H_2PBH_2·NMe_3$ in 10 mL toluene is added drop wise at room temperature. After the mixture was stirred for 30 min, it is refluxed for further 3 h. After cooling to room temperature the solution is layered with n-pentane. Colourless needles of **6** can be obtained by storing the solution for 4 months. Yield of **6**: 30 mg (17%); ^{31}P NMR (CD_3CN, 25 °C): δ = –125.0 (t, br, cation). $^{31}P\{^1H\}$ NMR (CD_3CN, 25 °C): δ = –125.0 (s, br, cation). In the $^{11}B\{^1H\}$ and $^{31}P\{^1H\}$ NMR spectra many broad and overlapping signals are observed. An accurate assignment of the signals is not possible due to the broadness of the signals and the very complex spin system leading to sophisticated coupling pattern. ESI-MS (CD_3CN): cation: *m/z* = 835.6 [100%, $NHC^{dipp}·BH_2–PH_2–BH_2·NHC^{dipp}]^+$); anion: *m/z* = 227.9 $[100\%, B_5P_5H_{19}]^-$).

X-ray diffraction analysis

The X-ray diffraction experiments were performed on either a Gemini R Ultra CCD diffractometer (**4**$(thf)_2$, **5**$(thf)_2$,**4b**), SuperNova A CCD diffractometer (**2**$(thf)_2$, **6**) or a GV1000 diffractometer (**3**$(thf)_2$) from Agilent Technologies (formerly Oxford Diffraction) applying Cu-K_α radiation (λ = 1.54178 Å). The measurements were performed at 123 K. Crystallographic data together with the details of the experiments are given in the Tables S1 - S3 (see below). Absorption corrections were applied semi-empirically from equivalent reflections or analytically (SCALE3/ABSPACK algorithm implemented in CrysAlis PRO software by Agilent Technologies Ltd).[6] All structures were solved using SIR97[7], and OLEX 2.[9c] Refinements against F^2 in anisotropic approximation were done using SHELXL-97.[8] The hydrogen positions of the methyl groups were located geometrically and refined riding on the carbon atoms. Hydrogen atoms belonging to BH_2 and PH_2 groups were located from the difference Fourier map and refined without

constraints (**2**(thf)$_2$, **6**) or with restrained P–H distances (**3**(thf)$_2$, **4**(thf)2, **5**(thf)$_2$,**4b**). Figures were created with OLEX 2.[9] The CIF files are deposited on the provided DVD.

Crystal Structures

[Na($C_{12}H_{24}O_6$)(thf)$_2$]$^+$[HP_2–BH_2–PH_2]$^-$ (2(thf)$_2$)]):

Compound **2**(thf)$_2$ crystallizes from a THF solution layered by *n*-hexane at 4° C as colourless blocks in the monoclinic space group *P*2/*c*. Figure S1 shows the structure of **2**(thf)$_2$ in the solid state.

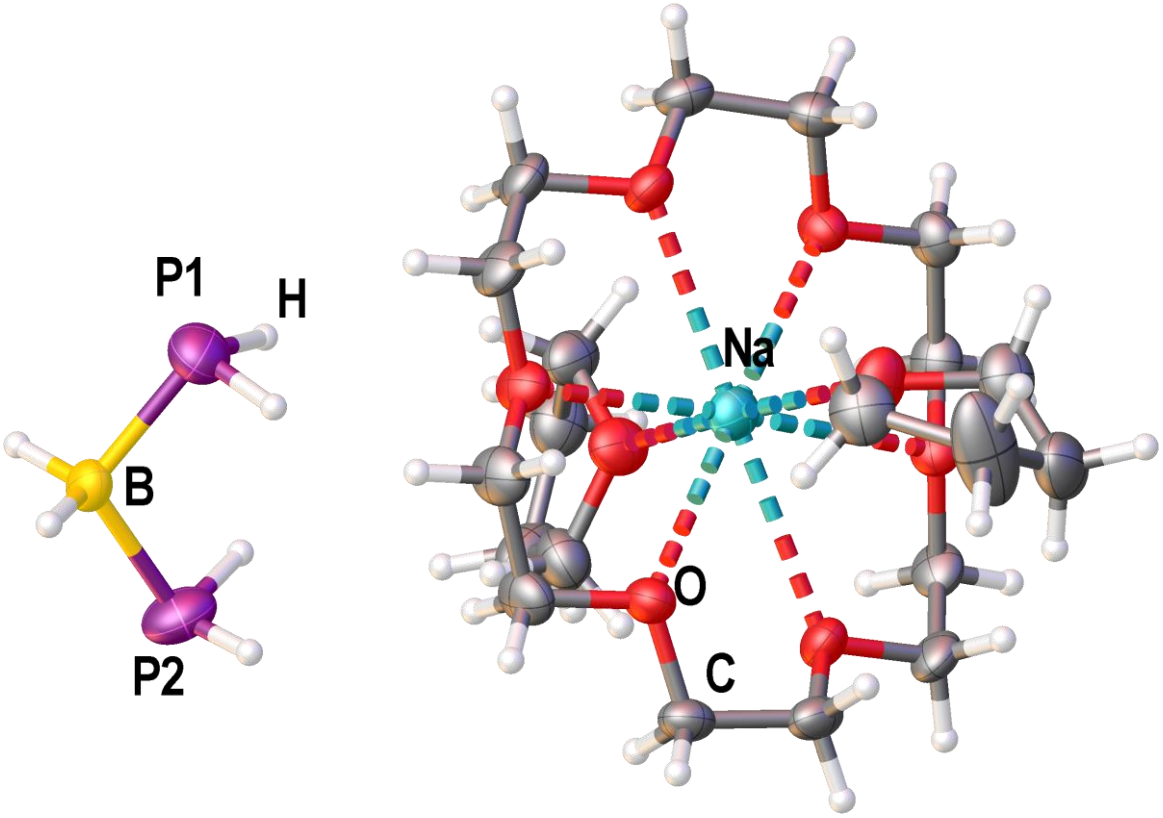

Figure S1. Molecular structure of **2**(thf)$_2$ in the solid state. Selected bond lengths [Å] and angles [°]: P1–B 1.961(3), P2–B 1.961(4), P1–B–P2 110.5(1).

[Na($C_{12}H_{24}O_6$)(thf)$_2$]$^+$[H^{t}BuP–BH_2–PH_2]$^-$ (3(thf)$_2$):

Compound **3**(thf)$_2$ crystallizes from a THF solution layered by *n*-hexane at 4° C as colourless blocks in the monoclinic space group $P\bar{1}$. Figure S2 shows the structure of **3**(thf)$_2$ in the solid state.

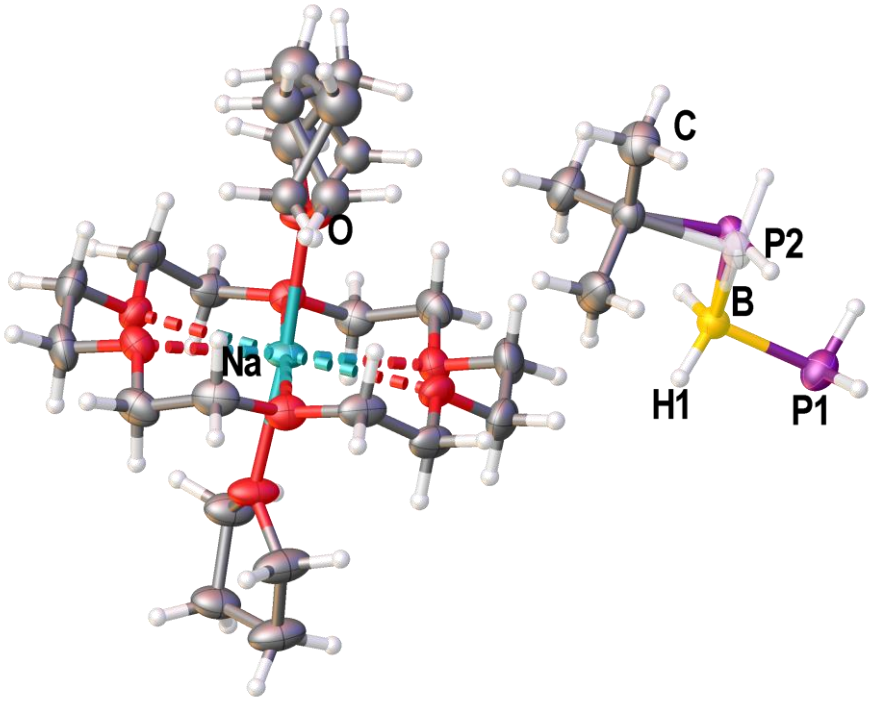

Figure S2. Molecular structure of **3**$(thf)_2$ in the solid state. Selected bond lengths [Å] and angles [°]: P1–B 1.974(2)–1.980(2), P2–B 1.958(2)–1.962(2), P2–C 1.886(2)–1.888(2), P1–B–P2 109.1(1)–111.9(1), P2–B–C 106.5(8)–107.0(1).

$[Na(C_{12}H_{24}O_6)(thf)_2]^+[Ph_2P–BH_2–PH_2]^-$ (4$(thf)_2$):

Compound **4**$(thf)_2$ crystallizes from a THF/*n*-hexane mixture at -28° C as colourless blocks in the orthorhombic space group *Pccn*. Figure S3 shows the structure of **4**$(thf)_2$ in the solid state.

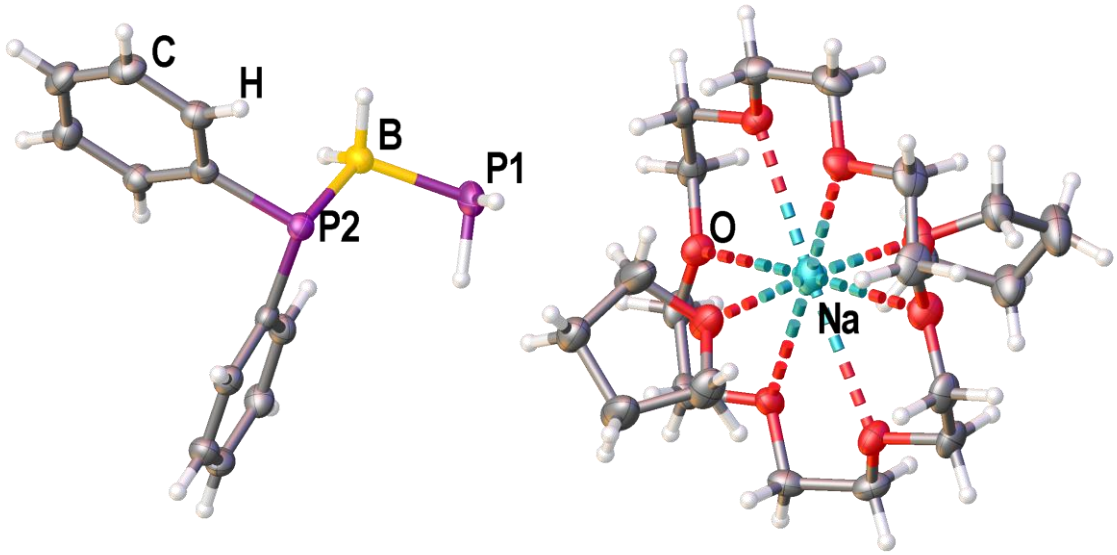

Figure S3. Molecular structure of **4**$(thf)_2$ in the solid state. Selected bond lengths [Å] and angles [°]: P1–B 1.9734(16) , P2–B 1.9650(16), P2–C 1.8405(13)–1.8474(13), P1–B–P2 109.1(1)–111.9(1), P2–B–C 111.4(1).

$[Na(C_{12}H_{24}O_6)(thf)_2]^+[H_2P–BH_2–Ph_2P–BH_2–PH_2]^-$ ($5(thf)_2$):

Compound **5**$(thf)_2$ crystallizes from a THF/*n*-hexane mixture at -28° C as colourless plates in the monoclinic space group C_2c. Figure S4 shows the structure of **5**$(thf)_2$ in the solid state.

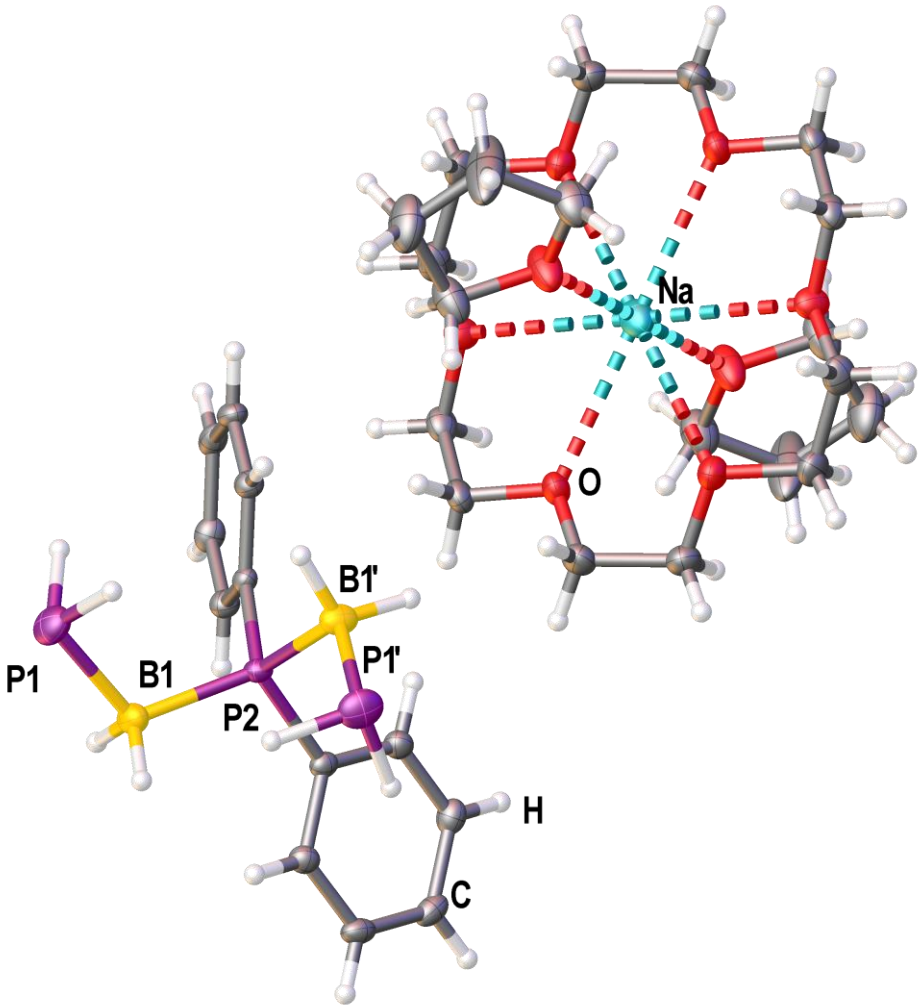

Figure S4. Molecular structure of **5**$(thf)_2$ in the solid state. Selected bond lengths [Å] and angles [°]: P1–B 1.965(2) , P2–B 1.940(2), P2–C 1.826(2), P1–B–P2 113.1(1), B–P2–B 121.1(1).

$[K(C_{12}H_{24}O_6)]^+[Ph_2PO_{0.5}–BH_2–PH_2]^-$ (4b):

Compound **4b** crystallises by layering a THF solution of **4b** with *n*-hexane at -28°C in form of colourless blocks in the tetragonal space group $P4_1$. The molecule is partly oxidized with occupancy of 50% for the oxygen atom. Figure S5 shows the structure of **4b** in the solid state.

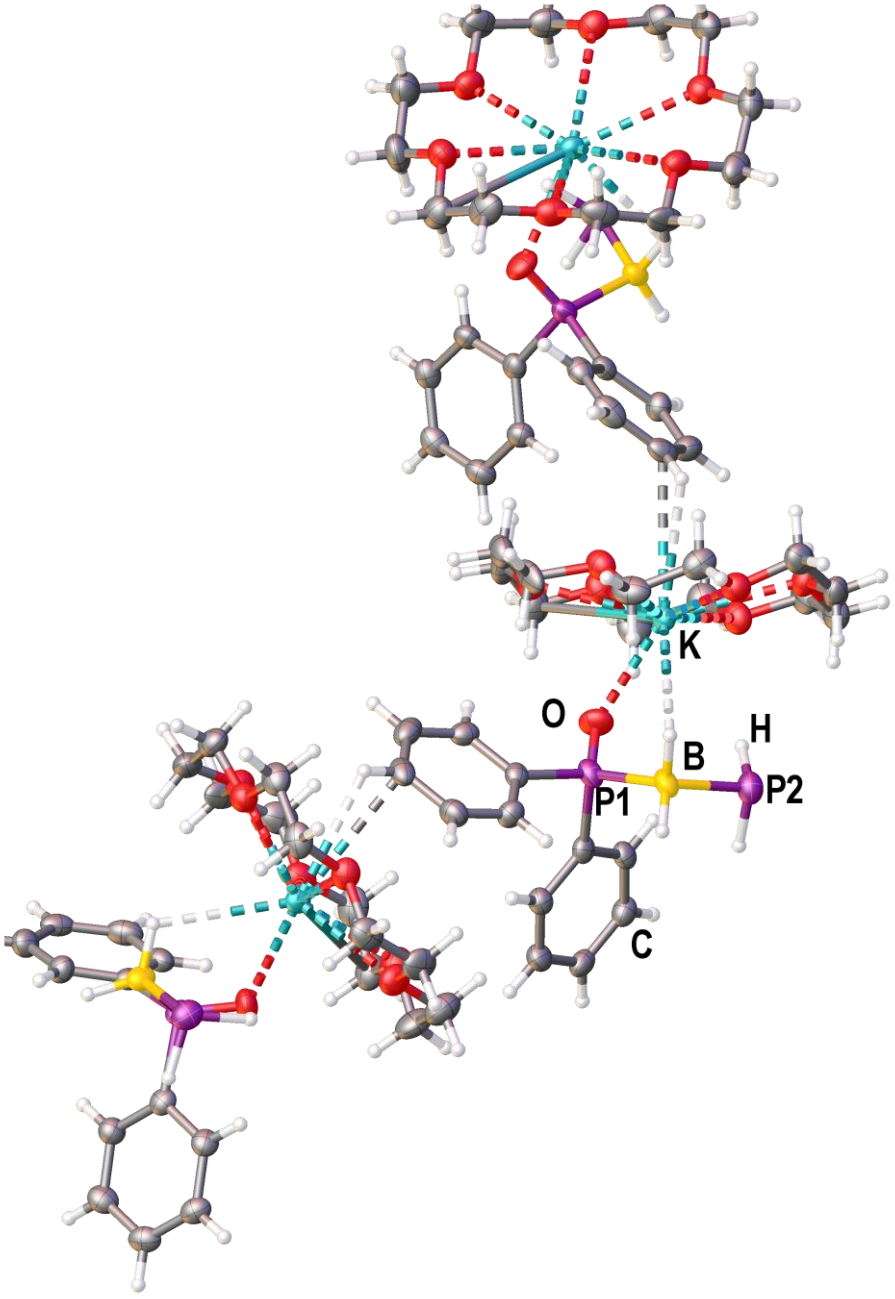

Figure S5. Molecular structure of **4b** in the solid state. Selected bond lengths [Å] and angles [°]: P1–B 1.979(5), P2–B 1.968(6), P1–O 1.372(7), P1–B2–P2 111.1 (3).

$[NHC^{dipp}{\cdot}BH_2{-}PH_2{-}BH_2{\cdot}NHC^{dipp}]^+[B_5P_5H_{19}]^-$ (6):

Compound **6** crystallizes from a toluene solution layered *n*-hexane at room temperature as colourless blocks in the triclinic space group $P\bar{1}$. The Figures S6 and S7 show the structure of **6** in the solid state.

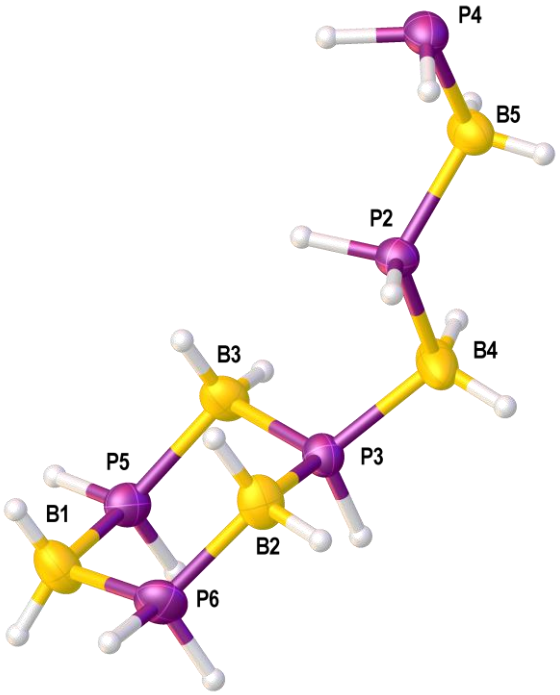

Figure S6: Molecular structure of the anion of **6** in the solid state. Selected bond lengths [Å] and angles [°]: P2–B4 1.939(3), P2–B5–1.928(3), P3–B4 1.948(3), P3–B3 1.952(3), P3–B2 1.941(3), P4–B5 1.964(3), P5–B1 1.941(3), P5–B3 1.945(2), P6–B1 1.930(3), P6–B2 1.930(3), B4–P2–B5 119.05(13), B2–P3–B3 112.18(12), B2–P3–B4 114.49(13), B3–P3–B4 111.25(12), B1–P5–B3 117.74(12), B1–P6–B2 118.64(13), P5–B1–P6 106.96(16), P3–B2–P6 107.75(12), P3–B3–P5 106.66(11), P2–B4–P3 108.94(15), P2–B5–P4 114.65(16).

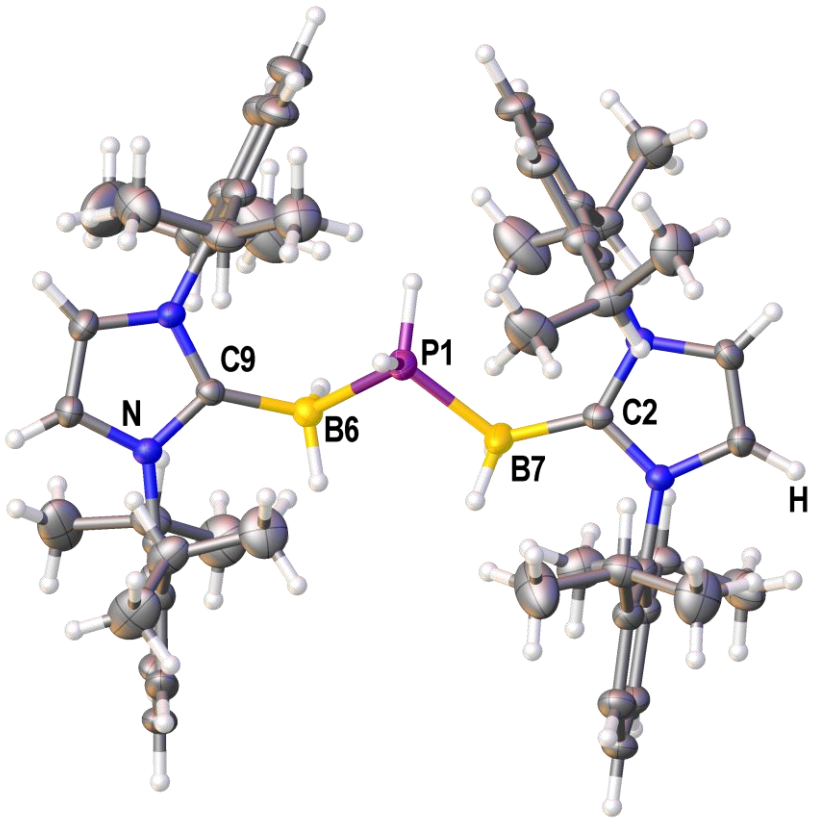

Figure S7: Molecular structure of the cation of **6** in the solid state. Selected bond lengths [Å] and angles [°]: P1–B6 1.948(2), P1–B7 1.929(2), C2–B7 1.589(3), C9–B6 1.592(3), B6–P1–B7 104.03(10), P1–B6–C9 118.41(14), P1–B7–C2 124.65(15.

Crystallographic information

Table S1. Crystallographic data for compounds **2**$(thf)_2$ and **3**$(thf)_2$.

	2$(thf)_2$	**3**$(thf)_2$
Empirical formula	$C_{20}H_{46}BNaO_8P_2$	$C_{24}H_{54}BNaO_8P_2$
Formula weight *M*	510.31 g/mol	566.41 g/mol
Crystal	colourless block	colourless block
Crystal size [mm^3]	0.24 x 0.12 x 0.11	0.20 x 0.14 x 0.12
Temperature *T*	123(1) K	123(2) K
Crystal system	monoclinic	triclinic
Space group	$P\,2_1/c$	$P\bar{1}$
Unit cell dimensions	a = 11.0550(3) Å	a = 9.1081(2) Å
	b = 13.4206(3) Å	b = 18.5819(5) Å
	c = 19.7417(5) Å	c = 19.5284(5) Å
	α = 90°	α = 88.080(2)°
	β = 102.592(2)°	β = 85.232(2)°
	γ = 90°	γ = 79.598(2)°
Volume *V*	2858.52(13) $Å^3$	3238.96(14) $Å^3$
Formula units *Z*	4	4
Absorption coefficient $\mu_{Cu\text{-}K\alpha}$	1.847 mm^{-1}	1.679 mm^{-1}
Density (calculated) ρ_{calc}	1.186 g/cm^3	1.162 g/cm^3
F(000)	1104	1232
Theta range $\theta_{min}/\theta_{max}$	4.01 / 67.08°	2.42 / 73.74°
Absorption correction	gaussian	gaussian
Index ranges	$-12 < h < 12$	$-9 < h < 11$
	$-15 < k < 16$	$-17 < k < 22$
	$-23 < l < 23$	$-22 < l < 24$
Reflections collected	31100	20740
Independent reflections [$I > 2\sigma(I)$]	3927 (R_{int} = 0.0554)	8962 (R_{int} = 0.0377)
Completeness to full θ	0.986	0.985
Transmission T_{min} / T_{max}	0.740 / 0.852	0.805 / 0.866
Data / restraints / parameters	5036 / 0 / 313	12383 / 0 / 705
Goodness-of-fit on F^2 *S*	1.032	1.004
Final *R*-values [$I > 2\sigma(I)$]	R_1 = 0.0463,	R_1 = 0.0619,
	wR_2 = 0.1110	wR_2 = 0.1679
Final *R*-values (all data)	R_1 = 0.0635,	R_1 = 0.0779,
	wR_2 = 0.1215	wR_2 = 0.1796
Largest difference hole	–0.349,	–0.426,
and peak $\Delta\rho$	0.422 $eÅ^{-3}$	0.669 $eÅ^{-3}$

Table S2. Crystallographic data for compounds **4**$(thf)_2$ and **5**$(thf)_2$.

	4$(thf)_2$	**5**$(thf)_2$
Empirical formula	$C_{32}H_{54}BNaO_8P_2$	$C_{20}H_{40}B_2NaO_8P_3$
Formula weight *M*	662.49 g/mol	708.30 g/mol
Crystal	colourless needle	colourless plate
Crystal size [mm^3]	0.55 x 0.15 x 0.12	0.33 x 0.17 x 0.13
Temperature *T*	123(1) K	123(1) K
Crystal system	orthorhombic	monoclinic
Space group	*Pccn*	C_2c
Unit cell dimensions	*a* = 19.8641(2) Å	*a* = 18.1267(4) Å
	b = 19.2682(2) Å	*b* = 9.1422(1) Å
	c = 19.2347(2) Å	*c* = 26.0012(6) Å
	α = 90°	*α* = 90°
	β = 90°	*β* = 115.213(3)°
	γ = 90°	*γ* = 90°
Volume *V*	7361.98(12) $Å^3$	3898.34(7) $Å^3$
Formula units *Z*	8	4
Absorption coefficient $\mu_{Cu\text{-}K\alpha}$	1.552 mm^{-1}	1.868 mm^{-1}
Density (calculated) ρ_{calc}	1.195 g/cm^3	1.207 g/cm^3
F(000)	2848	1520
Theta range $\theta_{min}/\theta_{max}$	3.92 / 66.96°	3.73/ 66.84°
Absorption correction	analytical	analytical
Index ranges	–19 < *h* < 23	–21 < *h* < 20
	–20 < *k* < 22	–8 < *k* < 10
	–21 < *l* < 22	–30 < *l* < 31
Reflections collected	42140	8588
Independent reflections [$I > 2\sigma(I)$]	6023 (R_{int} = 0.0302)	3120 (R_{int} = 0.0219)
Completeness to full *θ*	0.996	0.984
Transmission T_{min} / T_{max}	0.582 / 0.884	0.692 / 0.824
Data / restraints / parameters	6546 / 4 / 413	3421 / 4 / 226
Goodness-of-fit on F^2 *S*	1.036	1.027
Final *R*-values [$I > 2\sigma(I)$]	R_1 = 0.0321,	R_1 = 0.0361,
	wR_2 = 0.0847	wR_2 = 0.0976
Final *R*-values (all data)	R_1 = 0.0349,	R_1 = 0.0400,
	wR_2 = 0.0871	wR_2 = 0.0941
Largest difference hole	–0.310,	–0.347,
and peak *Δρ*	0.340 $eÅ^{-3}$	0.370 $eÅ^{-3}$

Table S3. Crystallographic data for compounds **4b** and **6**.

	4b	**6**
Empirical formula	$C_{48}H_{76}B_2K_2O_{13}P_4$	$C_{54}H_{97}B_7N_4P_6$
Formula weight *M*	1084.78 g/mol	1063.84 g/mol
Crystal	colourless block	colourless block
Crystal size [mm^3]	0.28 x 0.21 x 0.15	0.23 x 0.20 x 0.18
Temperature *T*	123(1) K	123(1) K
Crystal system	tetragonal	triclinic
Space group	$P\,4_1$	$P\bar{1}$
Unit cell dimensions	a = 10.10742(18) Å	a = 10.7534(4) Å
	b = 10.10742(18) Å	b = 16.4085(4) Å
	c = 27.2611(7) Å	c = 19.562(5) Å
	α = 90°	α = 81.297(2)°
	β = 90°	β = 75.959(2)°
	γ = 90°	γ = 89.987(2)°
Volume *V*	2785.00(12) Å^3	3307.68(15) Å^3
Formula units *Z*	2	2
Absorption coefficient $\mu_{Cu\text{-}K\alpha}$	3.068 mm^{-1}	1.764 mm^{-1}
Density (calculated) ρ_{calc}	1.294 g/cm^3	1.068 g/cm^3
F(000)	1152	1148
Theta range $\theta_{min}/\theta_{max}$	4.35 / 66.69°	3.32 / 70.78°
Absorption correction	analytical	analytical
Index ranges	$-11 < h < 12$	$-12 < h < 13$
	$-8 < k < 10$	$-19 < k < 16$
	$-31 < l < 32$	$-23 < l < 23$
Reflections collected	11742	24139
Independent reflections [$I > 2\sigma(I)$]	4259 (R_{int} = 0.0390)	9745 (R_{int} = 0.0255)
Completeness to full θ	0.974	0.987
Transmission T_{min} / T_{max}	0.583 / 0.742	0.751 / 0.930
Data / restraints / parameters	4642 / 5 / 332	12250 / 0 / 756
Goodness-of-fit on F^2 *S*	1.022	1.068
Final *R*-values [$I > 2\sigma(I)$]	R_1 = 0.0389,	R_1 = 0.0461,
	wR_2 = 0.0899	wR_2 = 0.1310
Final *R*-values (all data)	R_1 = 0.0437,	R_1 = 0.0572,
	wR_2 = 0.0926	wR_2 = 0.1364
Largest difference hole	–0.179,	–0.456
and peak $\Delta\rho$	0.346 eÅ^{-3}	0.878 eÅ^{-3}

NMR spectroscopy

$[Na(C_{12}H_{24}O_6)(thf)_2]^+[HP_2–BH_2–PH_2]^-$ ($2(thf)_2$)]):

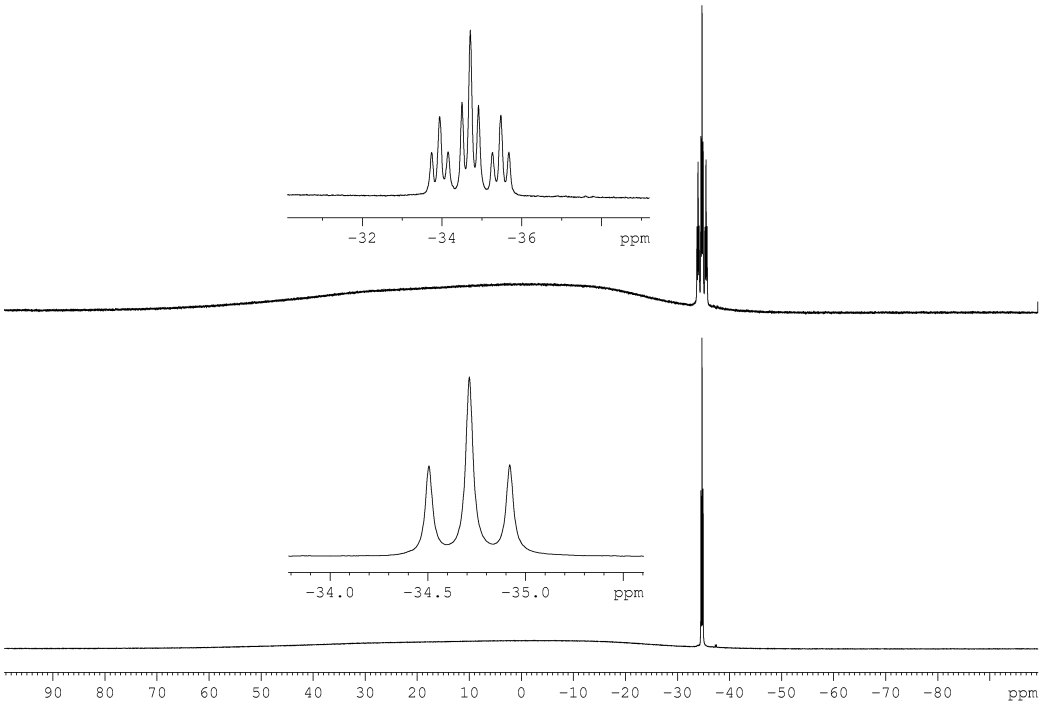

Figure S8: $^{11}B\{^1H\}$ (bottom) and ^{11}B NMR spectrum (top) of **2** in THF-d_8.

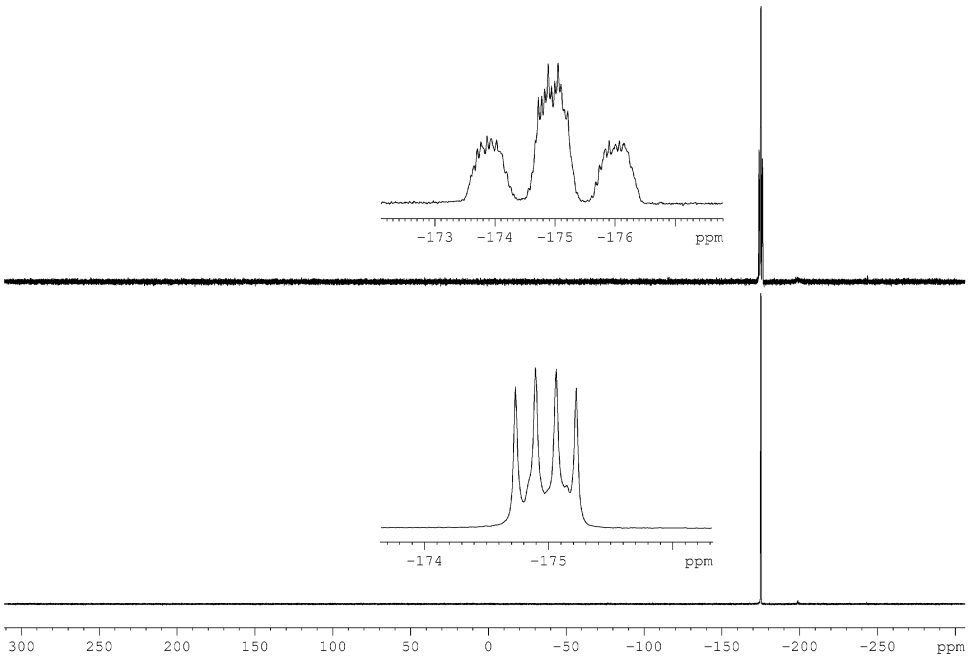

Figure S9: $^{31}P\{^1H\}$ (bottom) and ^{31}P NMR spectrum (top) of **2** in THF-d_8.

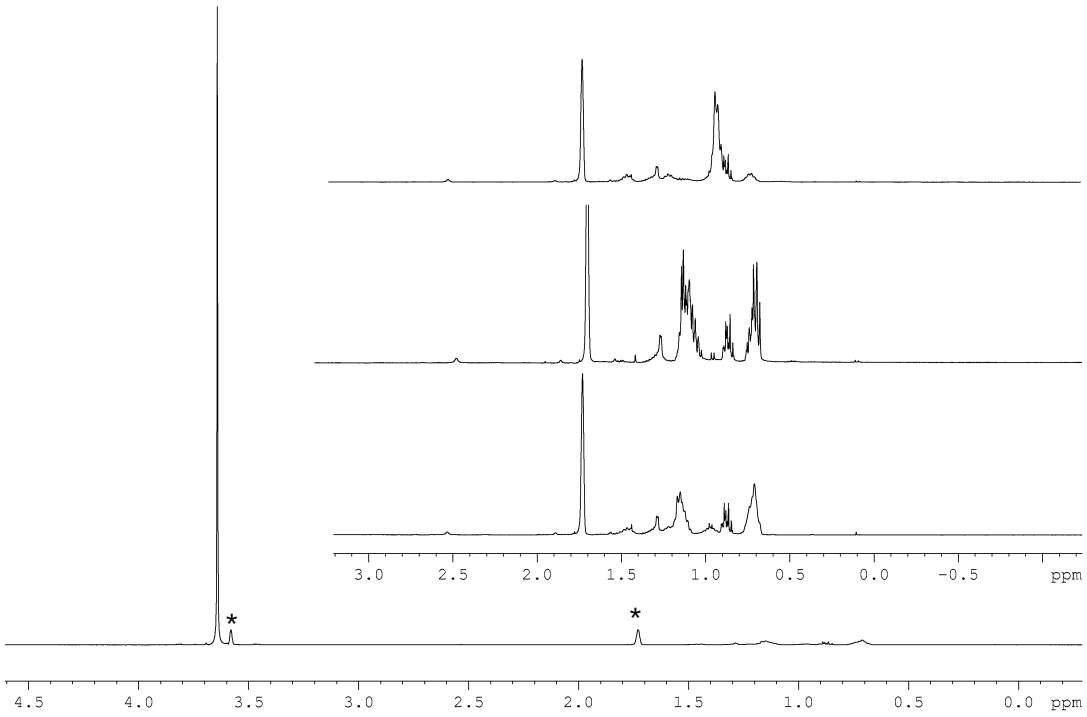

Figure S10: ^{1}H NMR spectrum of **2** in THF-d_8. * = solvent (THF-d_8). Magnified part shows ^{1}H, ^{1}H{^{11}B}, ^{1}H{^{31}P} NMR (from bottom to top) of the anion.

$[Na(C_{12}H_{24}O_6)(thf)_2]^+[H^tBuP–BH_2–PH_2]^-$ (3(thf)$_2$):

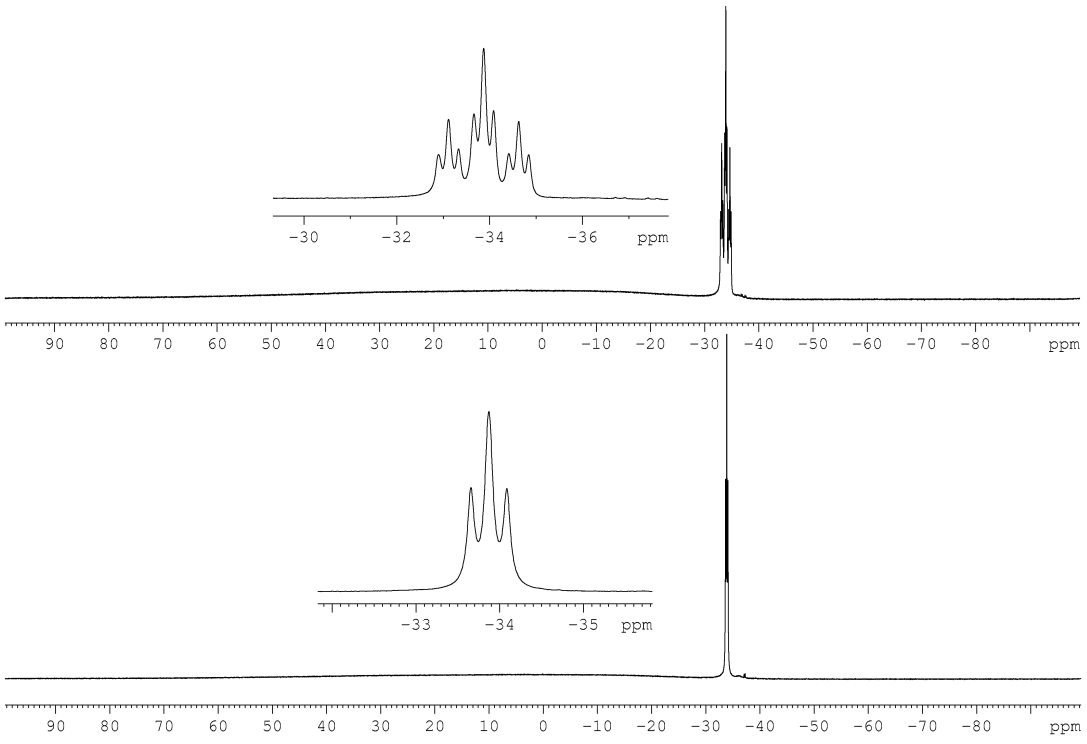

Figure S11: ^{11}B{^{1}H} (bottom) and ^{11}B NMR spectrum (top) of **3** in THF-d_8.

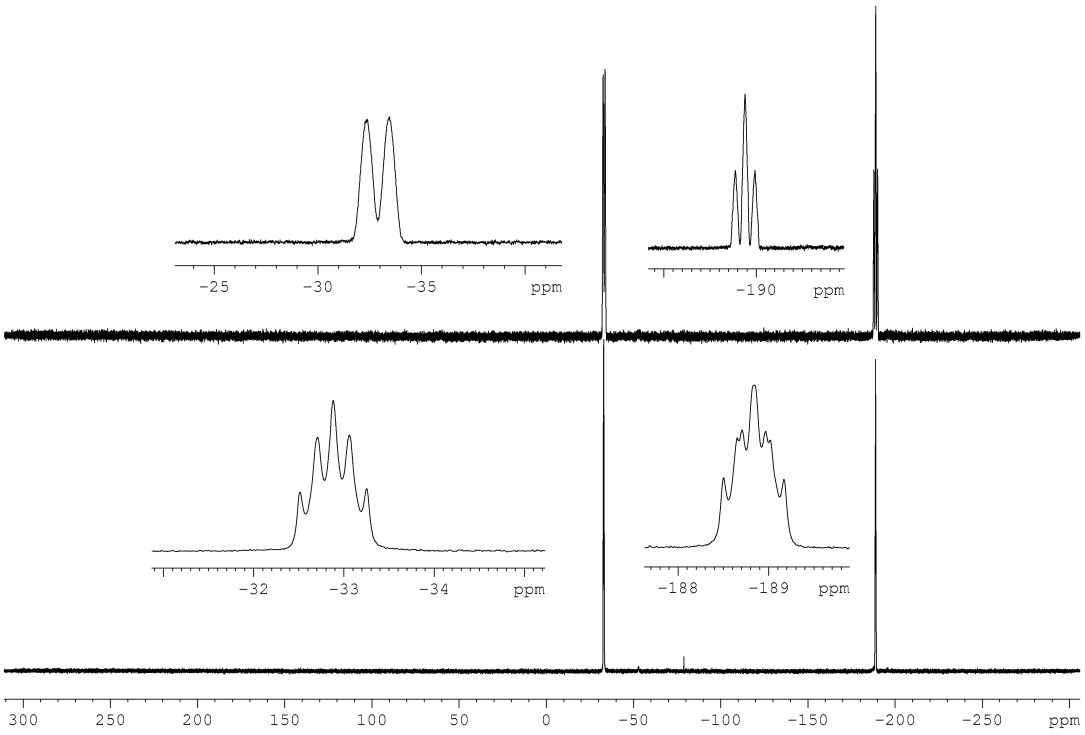

Figure S12: $^{31}P\{^{1}H\}$ (bottom) and ^{31}P NMR spectrum (top) of **3** in THF-d8.

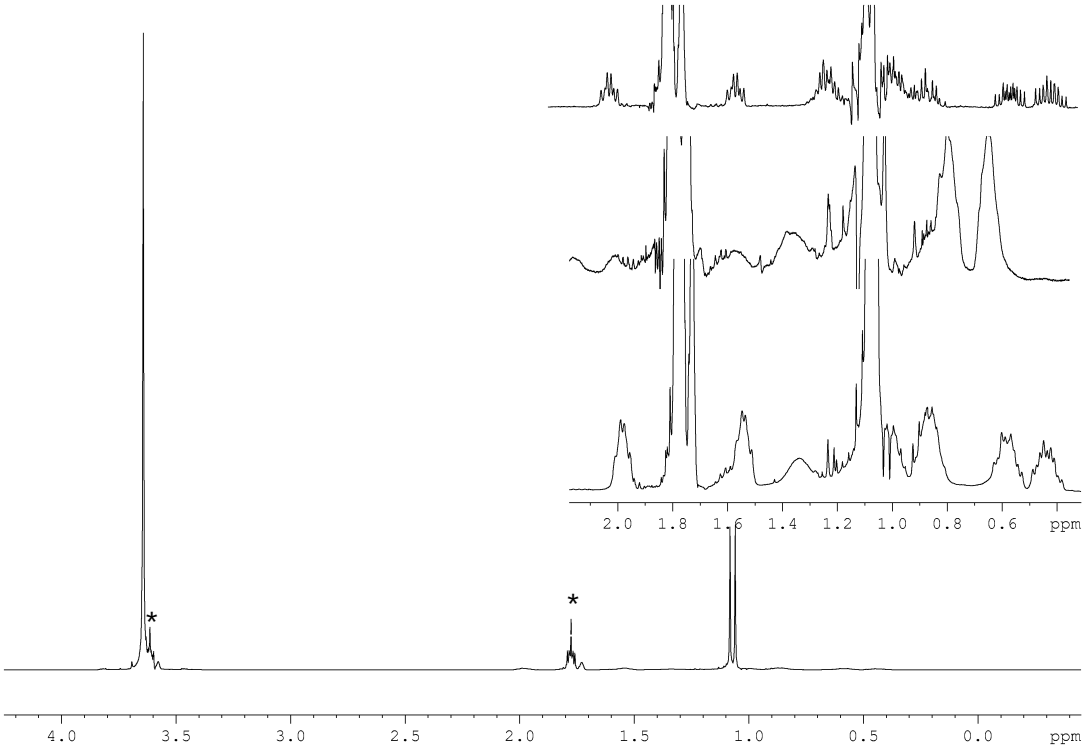

Figure S13: ^{1}H NMR spectrum of **3** in THF-d_8. * = solvent (THF-d_8). Magnified part shows ^{1}H, $^{1}H\{^{31}P\}$, $^{1}H\{^{11}B\}$ NMR (from bottom to top) of the anion.

$[Na(C_{12}H_{24}O_6)(thf)_2]^+[Ph_2P–BH_2–PH_2]^-$ ($4(thf)_2$):

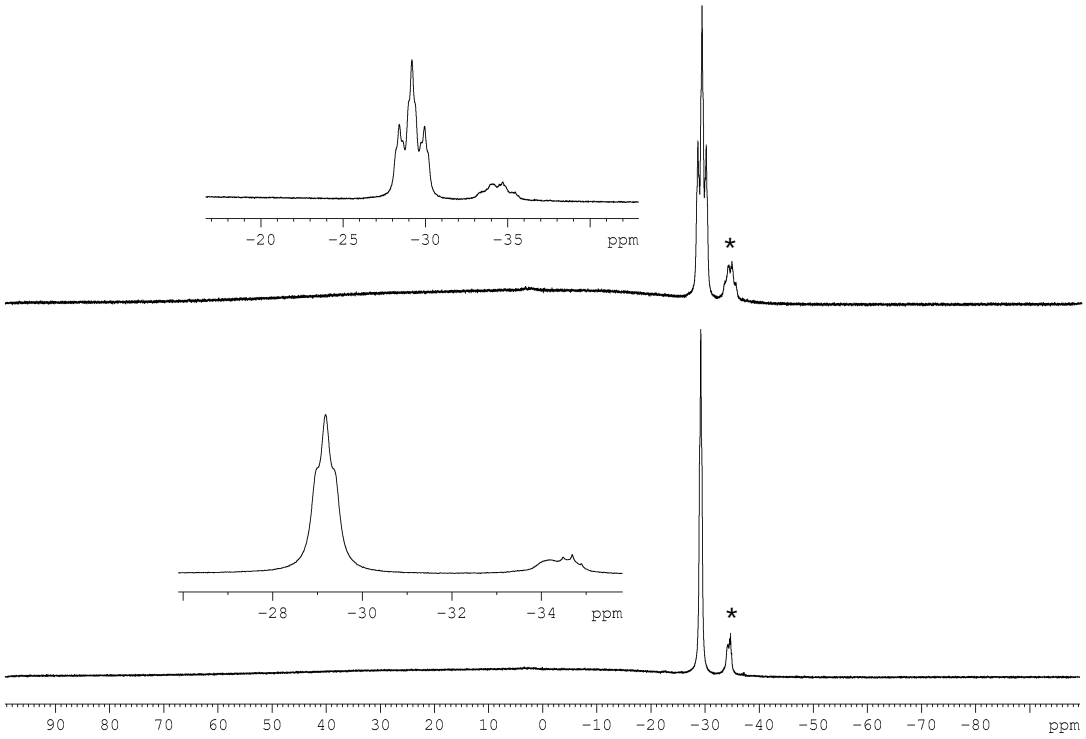

Figure S14: $^{11}B\{^1H\}$ (bottom) and ^{11}B NMR spectrum (top) of **4** in THF-d_8. * = **5**

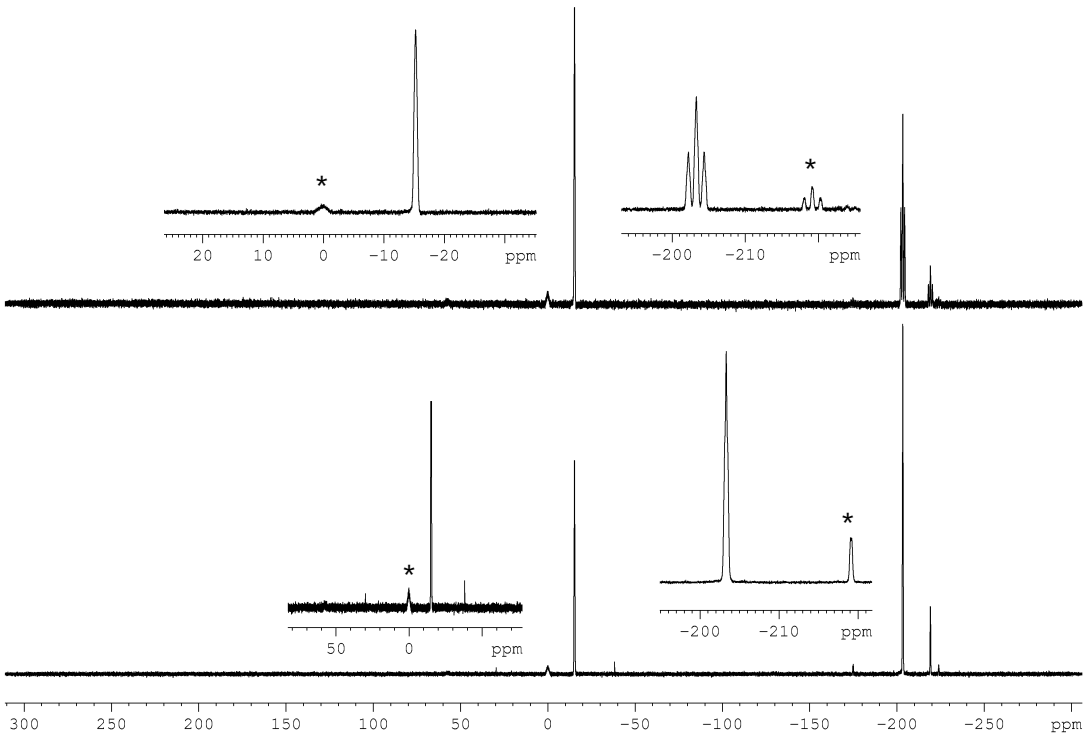

Figure S15: $^{31}P\{^1H\}$ (bottom) and ^{31}P NMR spectrum (top) of **4** in THF-d_8. * = **5**

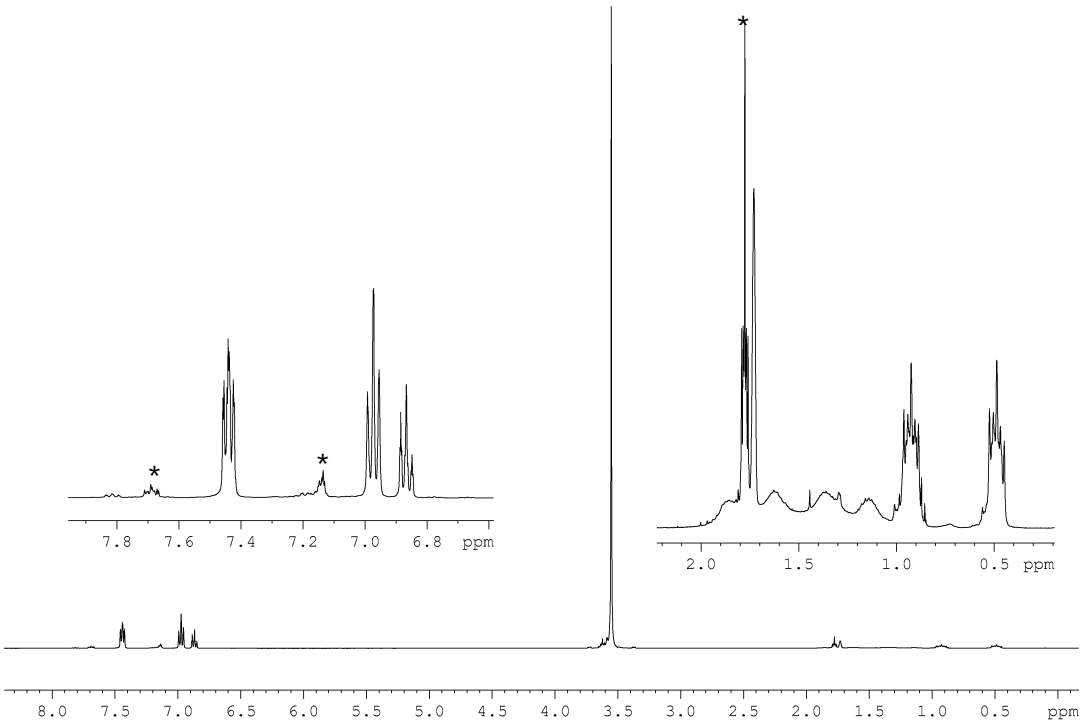

Figure S16: ^{1}H NMR spectrum of **4** in THF-d_8. * = **5** ** = solvent (THF-d_8).

$[Na(C_{12}H_{24}O_6)(thf)_2]^+[H_2P–BH_2–Ph_2P–BH_2–PH_2]^-$ **(5(thf)$_2$):**

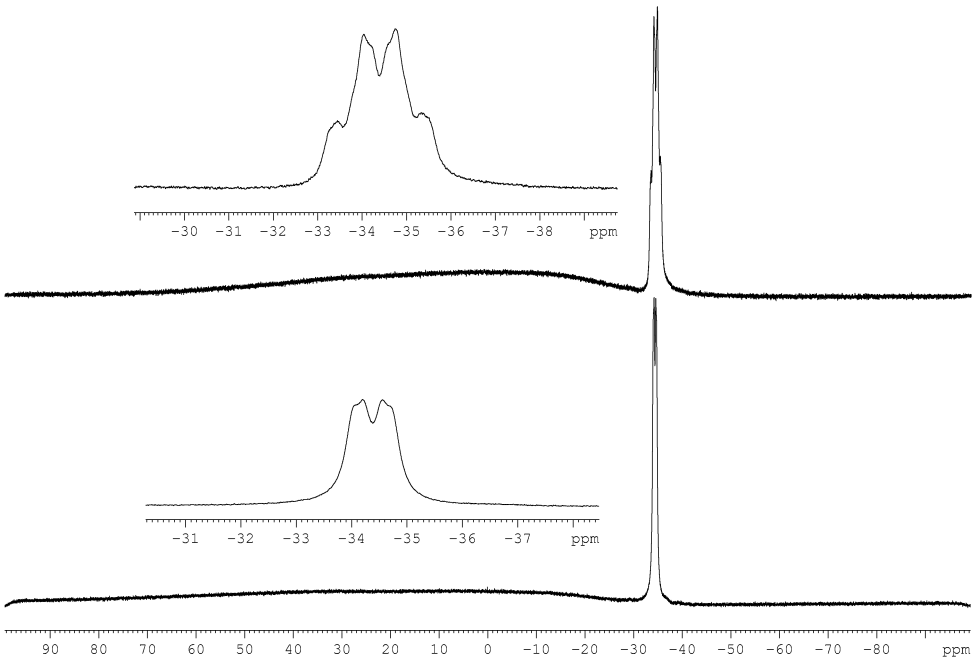

Figure S17: ^{11}B{^{1}H} (bottom) and ^{11}B NMR spectrum (top) of **5** in THF-d_8.

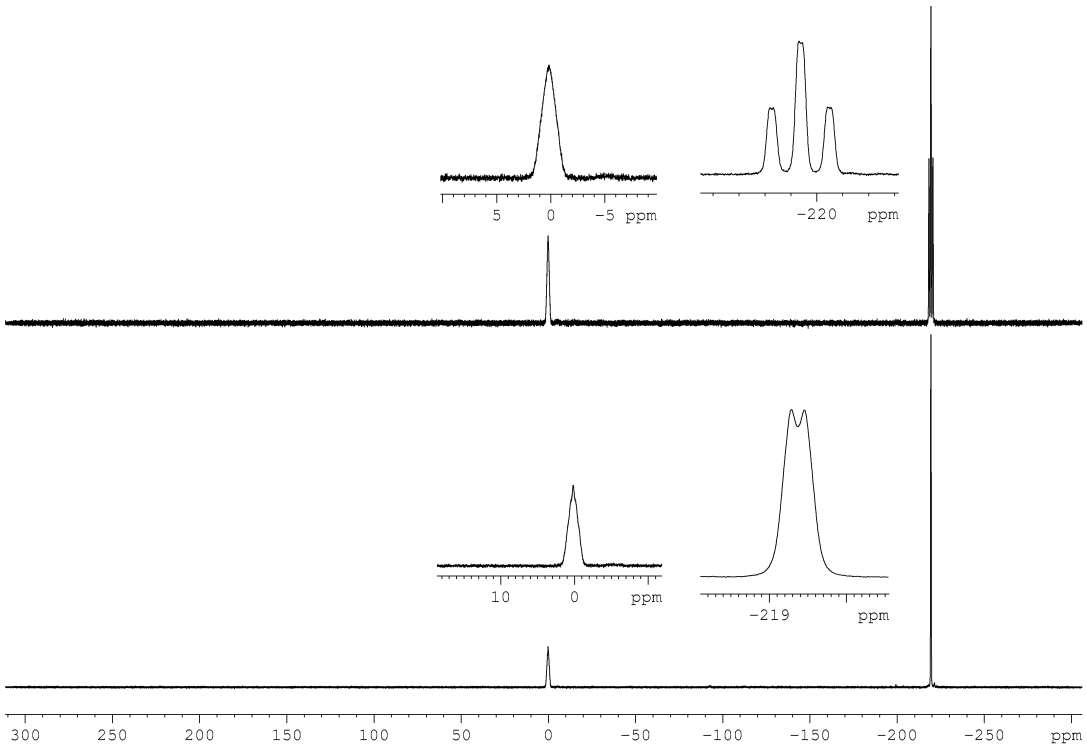

Figure S18: $^{31}P\{^{1}H\}$ (bottom) and ^{31}P NMR spectrum (top) of **5** in THF-d_8.

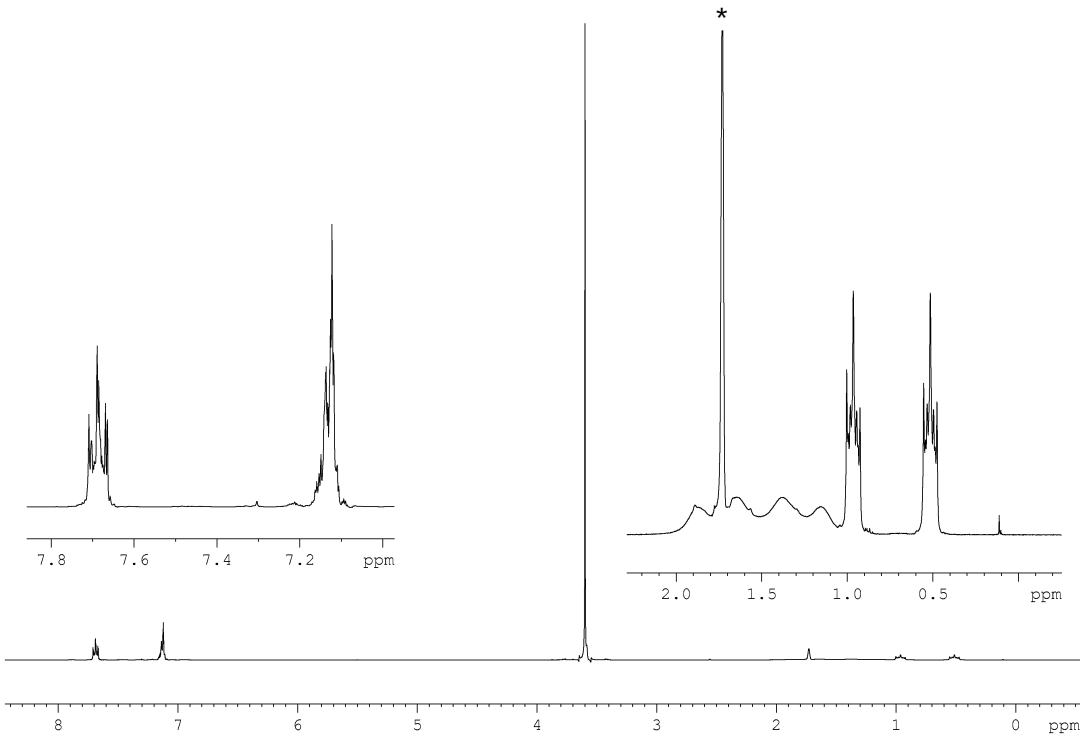

Figure S19: ^{1}H NMR spectrum of **5** in THF-d_8. * = solvent (THF-d_8).

Computational Details

All calculations have been performed with the TURBOMOLE program package[10] at the B3LYP[11]/def2-TZVP[12] level of theory. The solvent effects were incorporated via the Conductor-like Screening Model (COSMO)[13] using the dielectric constant of CH_2Cl_2 (ε = 8.930). The nature of the stationary point was checked by the absence of imaginary frequencies. A numerical frequency analysis has been performed with the module NumForce of the TURBOMOLE program package. The natural population analysis[14] was performed as implemented in TURBOMOLE. Computations for the reactions leading to **6** have been performed at B3LYP/def2-TZVP level of theory using Gaussian[15] program package.

Table S4. Reaction energies calculated at the B3LYP/def2-TZVP level of theory. The solvent effects have been incorporated via the COSMO formalism (ε = 7.250). Energies are not corrected from ZPE.

Reaction	Reaction energy ($kJ \cdot mol^{-1}$)
$PH_2BH_2NMe_3 + [PH_2]^- = [PH_2BH_2PH_2]^- + NMe_3$	−39.40
$PH_2BH_2NMe_3 + [PhPH]^- = [PH_2BH_2PHPh]^- + NMe_3$	−37.56
$PH_2BH_2NMe_3 + [tBuPH]^- = [PH_2BH_2PHtBu]^- + NMe_3$	−63.44
$PH_2BH_2NMe_3 + [Ph_2P]^- = [PH_2BH_2PPh_2]^- + NMe_3$	−35.47
$PH_2BH_2NMe_3 + [tBu_2P]^- = [PH_2BH_2PtBu_2]^- + NMe_3$	−67.88
$[PH_2BH_2PH_2]^- + PH_2BH_2NMe_3 = [PH_2BH_2PH_2BH_2PH_2]^- + NMe_3$	−18.60
$[PH_2BH_2PHPh]^- + PH_2BH_2NMe_3 = [PH_2BH_2PH_2BH_2PHPh]^- + NMe_3$	−12.96
$[PH_2BH_2PHPh]^- + PH_2BH_2NMe_3 = [PH_2BH_2PHPhBH_2PH_2]^- + NMe_3$	−19.43
$[PH_2BH_2PHtBu]^- + PH_2BH_2NMe_3 = [PH_2BH_2PH_2BH_2PHtBu]^- + NMe_3$	−16.41
$[PH_2BH_2PHtBu]^- + PH_2BH_2NMe_3 = [PH_2BH_2PHtBuBH_2PH_2]^- + NMe_3$	−23.36
$[PH_2BH_2PPh_2]^- + PH_2BH_2NMe_3 = [PH_2BH_2PH_2BH_2PPh_2]^- + NMe_3$	−14.36
$[PH_2BH_2PPh_2]^- + PH_2BH_2NMe_3 = [PH_2BH_2PPh_2BH_2PH_2]^- + NMe_3$	−19.13
$[PH_2BH_2PtBu_2]^- + PH_2BH_2NMe_3 = [PH_2BH_2PH_2BH_2PtBu_2]^- + NMe_3$	−22.44
$[PH_2BH_2PtBu_2]^- + PH_2BH_2NMe_3 = [PH_2BH_2PtBu_2BH_2PH_2]^- + NMe_3$	−20.29

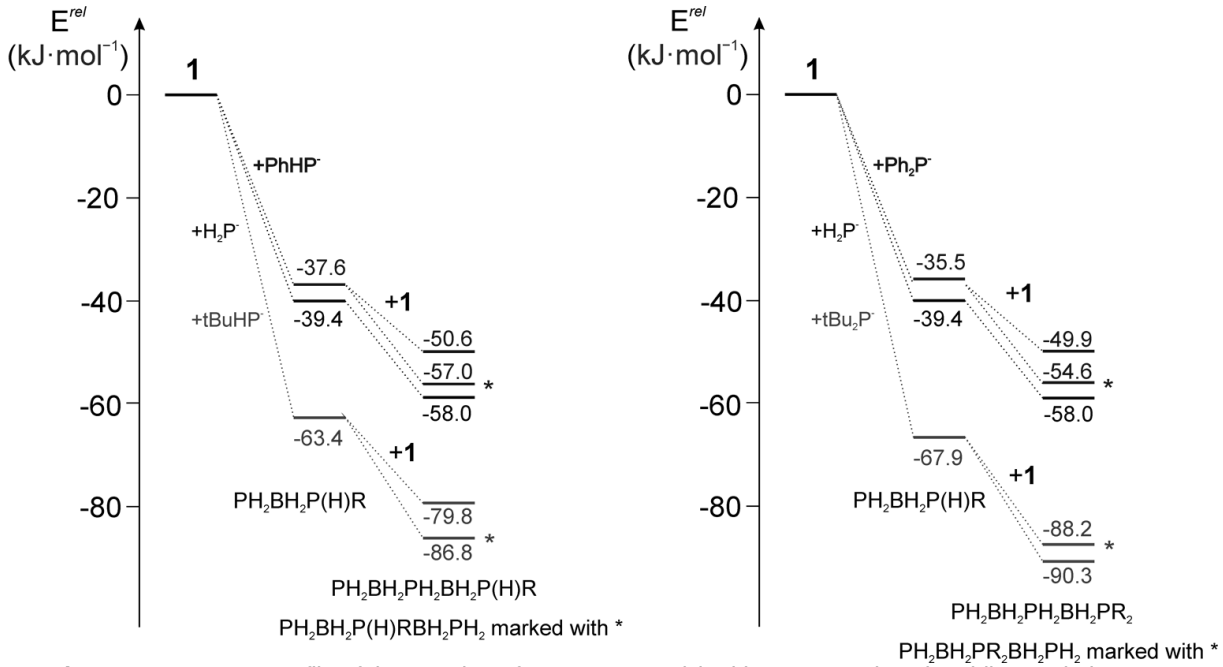

Figure S20: Energy profile of the reaction of $PH_2BH_2NMe_3$ (**1**) with P centered nucleophiles. Relative energies calculated at the B3LYP/def2-TZVP level.

Cartesian coordinates of the optimized geometries (xyz) are deposited on the provided DVD.

References

[1] C. Marquardt, A. Adolf, A. Stauber, M. Bodensteiner, A. V. Virovets, A. Y. Timoshkin, M. Scheer, *Chem. Eur. J.* **2013***, 19*, 11887–11891.

[2] G. E. Ryschkewitsch, J. W. Wiggins, *Inorg. Synth.* **1970**, *12*, 116.

[3] H. Jacobs, K. M. Hassiepen, *Z. Anorg. Allg. Chem.* **1985**, *531*, 108–118.

[4] L. Hintermann, *Beilstein J. Org. Chem*. **2007**, *3*, No.22.

[5] W. A. Herrmann, G. Brauer, *Synthetic Methods of Organometallic and Inorganic Chemistry*, *Vol.* 3 *,* **1996** *,* Thieme Publishers*,* Stuttgart.

[6] Agilent Technologies **2006-2011**, CrysAlisPro Software system, different versions, Agilent Technologies UK Ltd, Oxford, UK.

[7] A. Altomare, M. C.Burla, M. Camalli, G. L. Cascarano, C. Giacovazzo, A. Guagliardi, A.G. G. Moliterni, G. Polidori, R. Spagna, *J. Appl. Cryst.* **1999**, *32*, 115–119

[8] G. M. Sheldrick, *Acta Cryst.* **2008**, *A64*, 112–122.

[9] a) E. Keller, **1997**, SCHAKAL99, Freiburg. b) K. Brandenburg, H. Putz, **2005**, DIAMOND 3, Crystal Impact GbR, Postfach 1251, D-53002 Bonn; c) O.V. Dolomanov, L.J. Bourhis, R.J. Gildea, J.A.K. Howard, H.Puschmann, OLEX2: A complete structure solution, refinement and analysis program, **2009**. *J. Appl. Cryst*., *42*, 339–341.

[10] a) R. Ahlrichs, M. Bär, M. Häser, H. Horn, C. Kölmel, *Chem. Phys. Lett.***1989**, *162*, 165–169; b) O. Treutler, R. Ahlrichs, *J. Chem. Phys.***1995**, *102*, 346–354.

[11] a) P. A. M. Dirac, *Proc. Royal Soc.A*,**1929**, *123*, 714; b) J. C. Slater, *Phys. Rev.***1951**, *81*, 385; c) S. H. Vosko, L. Wilk, M. Nusair, *Can. J. Phys.***1980**, *58*, 1200; d) A. D. Becke, *Phys. Rev. A*, **1988**, *38*, 3098; e) C. Lee, W. Yang, R. G. Parr, *Phys. Rev. B*,**1988**, *37*, 785; f) A. D. Becke, *J. Chem. Phys.* **1993**, *98*, 5648.

[12] a) A. Schäfer, C. Huber, R. Ahlrichs, *J. Chem. Phys.***1994**, *100*, 5829; b) K. Eichkorn, F. Weigend, O. Treutler, R. Ahlrichs, *Theor. Chem. Acc.***1997**, *97*, 119.

[13] A. Klamt, G. Schüürmann *J. Chem. Soc. Perkin Trans. 2*, **1993**, 799–805; A. Schäfer, A. Klamt, D. Sattel, J. C. W. Lohrenz, F. Eckert *Phys. Chem. Chem. Phys.*, **2000**, *2*, 2187–2193.

[14] A. E. Reed, R. B. Weinstock, F. Weinhold, *J. Chem. Phys.*, **1985**, *83*, 735–746.

[15] M. J. Frisch, G. W. Trucks, H. B. Schlegel, G. E. Scuseria, M. A. Robb, J. R. Cheeseman, J. A. Montgomery, Jr., T. Vreven, K. N. Kudin, J. C. Burant, J. M. Millam, S. S. Iyengar, J. Tomasi, V. Barone, B. Mennucci, M. Cossi, G. Scalmani, N. Rega, G. A. Petersson, H. Nakatsuji, M. Hada, M. Ehara, K. Toyota, R. Fukuda, J. Hasegawa, M. Ishida, T. Nakajima, Y. Honda, O. Kitao, H. Nakai, M. Klene, X. Li, J. E. Knox, H. P. Hratchian, J. B. Cross, V. Bakken, C. Adamo, J. Jaramillo, R. Gomperts, R. E. Stratmann, O. Yazyev, A. J. Austin, R. Cammi, C. Pomelli, J. W. Ochterski, P. Y. Ayala, K. Morokuma, G. A. Voth, P. Salvador, J. J. Dannenberg, V. G. Zakrzewski, S. Dapprich, A. D. Daniels, M. C. Strain, O. Farkas, D. K. Malick, A. D. Rabuck, K. Raghavachari, J. B. Foresman, J. V. Ortiz, Q. Cui, A. G. Baboul, S. Clifford, J. Cioslowski, B. B. Stefanov, G. Liu, A. Liashenko, P. Piskorz, I. Komaromi, R. L. Martin, D. J. Fox, T. Keith, M. A. Al-Laham, C. Y. Peng, A. Nanayakkara, M. Challacombe, P. M. W. Gill, B. Johnson, W. Chen, M. W. Wong, C. Gonzalez, and J. A. Pople, Gaussian03, revision B.05. Gaussian, Inc., Wallingford CT, 2004.

6.6 Author Contributions

The syntheses and characterization of compounds **2**$(thf)_2$, **3**$(thf)_2$, **4**$(thf)_2$, **4b**, **5**$(thf)_2$, were performed by Christian Marquardt.

The syntheses and characterization of compound **6** was performed by Dr. Andreas Stauber. Compound **2** was synthesized and characterized by NMR spectroscopy and mass spectrometry by Dr. Andreas Stauber for the first time. Both compounds have been reported in his PhD-thesis (Regensburg, **2014**)

X-ray structural analyses of all compounds were performed by Christian Marquardt and Dr. A. V. Virovets, except for compound **6** which was performed by Dr. Michael Bodensteiner.

All DFT-calculations were performed by Dr. Gábor Balázs, except for compound **6** which was performed by Prof. Dr. Alexey Y. Timoshkin.

The manuscript (including supporting information, figures, schemes and graphical abstract) was written by Christian Marquardt.

7. Coordination of Boron centered Lewis Acids by organosubstituted Phosphanylboranes

C. Marquardt and M. Scheer

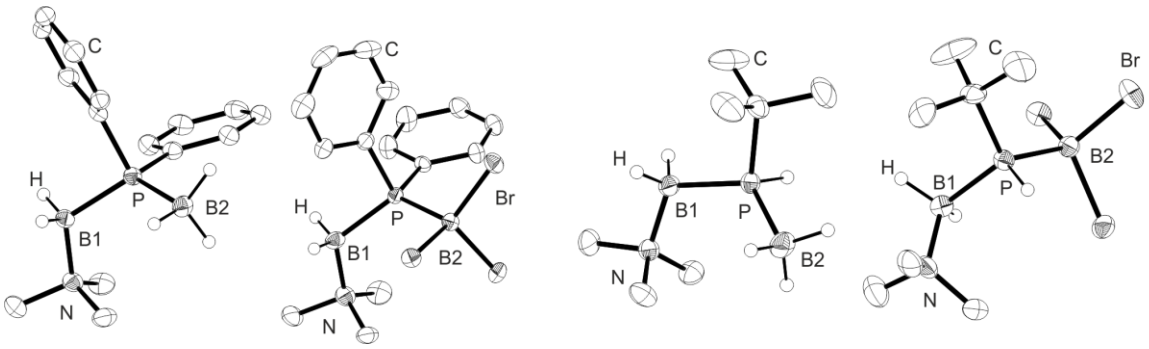

Abstract: The reaction of the monomeric phosphanylboranes $Ph_2P–BH_2·NMe_3$ (**1a**) and $^tBuHP–BH_2·NMe_3$ (**1b**) with the main group Lewis Acids BH_3 and BBr_3 yield the adducts $H_3B·Ph_2P–BH_2·NMe_3$ (**2a**) and $H_3B·^tBuHP–BH_2·NMe_3$ (**2b**), $Br_3B·Ph_2P–BH_2·NMe_3$ (**3a**) and $Br_3B·^tBuHP–BH_2·NMe_3$ (**3b**). All compounds have been characterized completely by single crystal X-ray structure analysis, NMR and IR spectroscopy as well as mass spectrometry. The secondary and tertiary phosphines **1a** and **1b** behave as classical Lewis bases and we were able to attach BX_3 (X = H, Br) end groups to them.

7.1 Introduction

Phosphine-borane adducts are a widely used class of compounds, which are used for the synthesis of polymers via dehydrocoupling reactions.[1] Especially Rh(I)-based catalysts turned out to be very effective for this kind of dehydrocoupling reactions.[2] Recently an earth-abundant Fe-catalyst was reported by the *Manners* group, which allows the control of the molecular weight of the poly(phosphinoborane)s.[3] With the P–B bonds being isoelectronic to C–C single bonds, polymers with a P–B backbone can be viewed as an inorganic analogue of polyolefins. Besides the synthetic and academic interest, those compounds also have potential applications. E.g. it was shown, that the poly(phosphinoborane) $[RHP–BH_2]_n$ (R = *p*-$CF_3C_6H_4$) can be used as an electron beam resist for lithographic applications.[1,4] Our group is especially interested in the synthesis and reactivity of phosphanylboranes of the type $R_2P–BH_2·NMe_3$ (R = H, alkyl, aryl),[5] which are Lewis base stabilized relatives to alkenes. Those compounds can be viewed as donor-stabilized monomers of poly(phosphinoborane)s and thus are potentially candidates for polymerization. Mild thermolysis triggers the elimination of NMe_3. The absence of the Lewis base leads to a lack of electronic stabilization (lone-pair at phosphorus together with a vacant p-orbital at boron) resulting in head-to-tail polymerization or oligomerization, respectively. As the polymer of the parent compound $H_2P–BH_2·NMe_3$ showed low solubility and could not be characterized completely oligomers generated by the use of Ti-complexes were studied initially.[6] Introduction of alkyl- and aryl-substituents increased the solubility of the polymers. Those phosphanylboranes are excellent starting materials for poly(phosphinoborane)s via mild thermolysis.[7] A new high molecular weight polymer $[^tBuHP–BH_2]_n$ which was not accessible by catalytic dehydrocoupling reactions could be generated by this method. Moreover a series of oligomeric compounds containing unprecedented cationic and anionic chains of pnictogenylboranes could be obtained.[8] To study the reactivity of the monomeric building blocks $Ph_2P–BH_2·NMe_3$ (**1a**) and $^tBuHP–BH_2·NMe_3$ (**1b**) the coordination behavior towards boron centered Lewis acids was investigated. Herein we report about the coordination of boron centered Lewis Acid by the phosphanylboranes **1a** and **1b**.

7.2 Results and Discussion

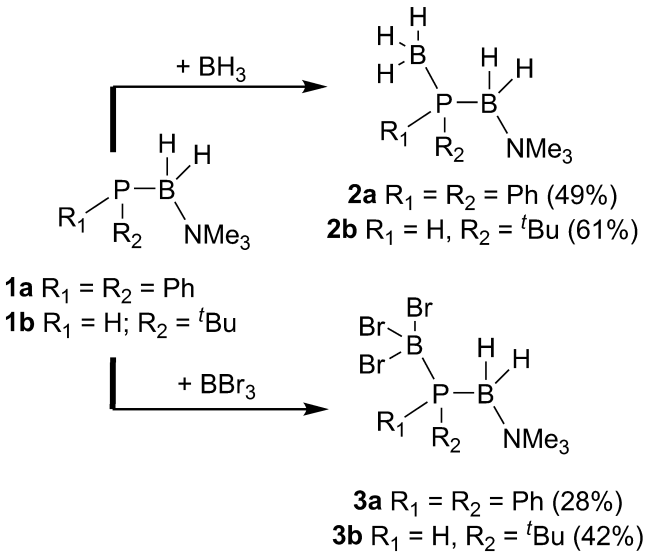

Scheme 1: Synthesis of Lewis Acid/ Base adducts. Yields are given in parentheses.

Reactions of $Ph_2P–BH_2·NMe_3$ (**1a**) or $^tBuHP–BH_2·NMe_3$ (**1b**) with $H_3B·LB$ (LB = THF, SMe_2) yield the adducts $H_3B·Ph_2P–BH_2·NMe_3$ (**2a,** 49% yield) and $H_3B·^tBuHP–BH_2·NMe_3$ (**2b**, 28% yield), respectively. In the reaction of **1a** or **1b** with BBr_3 the adducts $Br_3B·Ph_2P–BH_2·NMe_3$ (**3a**, 61% yield) and $Br_3B·^tBuHP–BH_2·NMe_3$ (**3b**, 42% yield) are obtained (Scheme 1). The BH_3-adducts **2a** and **2b** are formed selectively. The reaction can be monitored by ^{31}P NMR spectroscopy. The resonance signals for **2a** arise at δ = −23.5 ppm and for **2b** at δ = −26.8 ppm. After crystallization compounds **2a** and **2b** can be isolated in moderate crystalline yields.[9] The BBr_3-adducts **3a** and **3b**, however precipitate upon addition of BBr_3 to **1a** and **1b**. After removal of the supernatant, the solids are dissolved in MeCN, filtrated and crystalized from saturated MeCN solutions. The low solubility of BBr_3-compounds leads to a loss of the products during filtration resulting in low crystalline yields. For compound **3a** a signal arises at δ = −24.4 ppm and for **3b** at δ = −32.1 ppm. The resonance signals of all compounds are shifted to lower fields in the ^{31}P NMR spectra compared to **1a** (δ = −39.5 ppm) and **1b** (δ = −67.6 ppm, Figure 1). The same behavior was observed for the parent compound and its adducts $X_3B·H_2P–BH_2·NMe_3$ (X = Cl, H).[10]

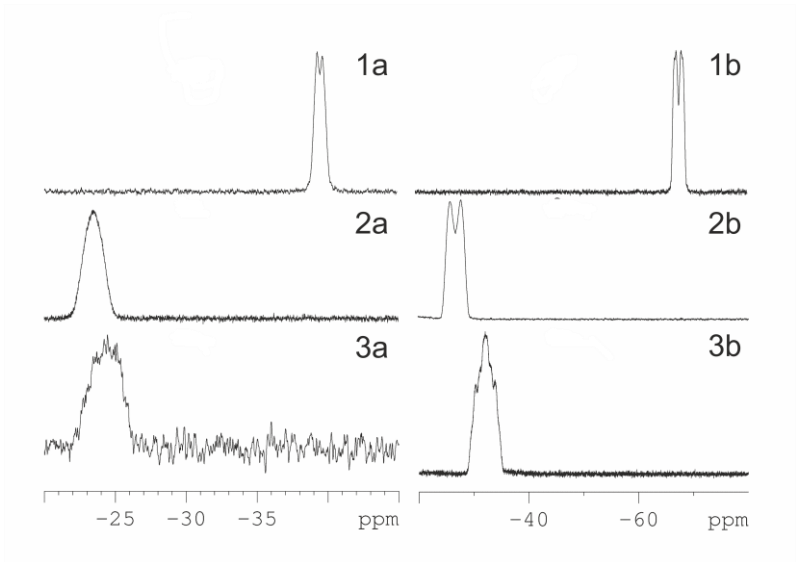

Figure 1: ^{31}P NMR spectra of **1a, 2a** and **3a** (left) **1b, 2b** and **2b** (right).

The BH_3 adducts are well soluble in non-polar solvents (**2a:** toluene, **3a:** *n*-hexane), while the BBr_3-adducts (**2b**, **3b**) are only soluble in polar solvents like MeCN. Crystals of **2a**–**3b** are obtained by storing solutions of the adducts in the above mentioned solvents at -28°C. The obtained compounds are stable in the solid state as well as in solution. In the solid state **2a** and **3a** reveal a P–B1 bond length of 1.9657(17) Å (**2a**) and 1.978(4) Å for **3a**, respectively (Figure 2), which is similar to **1a** (1.975(2) Å). The P–B2 bond lengths, between the phosphorus atoms and the boron atoms of the Lewis acids are with 1.9422(18) Å for **2a** shorter than in **3a** (1.974(4) Å), probably due to the slightly higher steric demand of BBr_3.

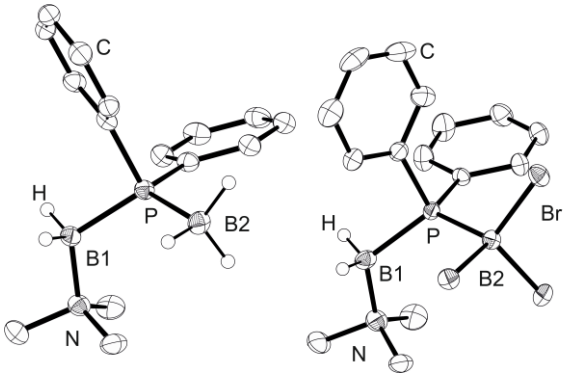

Figure 2: Molecular structure of **2a** (left) and **3a** (right). Hydrogen atoms bond to carbon atoms are omitted for clarity. Thermal ellipsoids are drawn with 50% probability. Selected bond lengths [Å] and angles [°]: **2a** P–B1 1.9657(17), P–B2 1.9422(18), B1–P–B2 119.68(8); **3a** P–B1 1.978(4), P–B2 1.974(4), B1–P–B2 120.00(16).

Compound **2b** and **3b** reveal in the solid state a P–B1 bond length of 1.9644(19) Å (**2b**) and 1.992(8) Å (**3b**), which are essentially similar compared to **1b** (1.985(2) Å). The P–B2 bond lengths show the same tendencies as observed for **2a** and **3a**. Again, a

shorter P–B2 bond length is observed for the BH_3-complex **2a** 1.946(2) Å compared to **3b** (1.987(9) Å, Figure 3). We attribute this small difference to the higher steric demand of the Br atoms of the BBr_3.

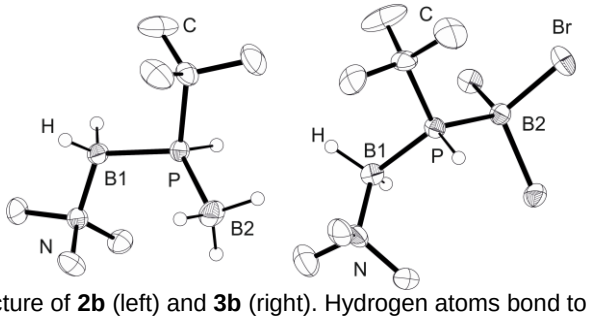

Figure 3: Molecular structure of **2b** (left) and **3b** (right). Hydrogen atoms bond to carbon atoms are omitted for clarity. Thermal ellipsoids are drawn with 50% probability. Selected bond lengths [Å] and angles [°]: **2b** P–B1 1.9644(19), P–B2 1.946(2), B1–P–B2 122.61(9); **3b** P–B1 1.992(8), P–B2 1.987(9), B1–P1–B2 109.5(3).

The same behavior was observed for the parent compound. The adducts $X_3B{\cdot}H_2P–BH_2{\cdot}NMe_3$ (X = Cl, H) reveal also nearly no change of the P–B1 bond length compared to $H_2P–BH_2{\cdot}NMe_3$.[10]

All compounds exhibit a staggered arrangement along the P–B- and N–B-axis, despite of **3b** which shows an eclipsed conformation along the P–B1-axis. In the IR spectra absorptions are observed in the expected range for the B–H and P–H valence stretches. Electron impact mass spectrometry shows peaks for the compounds with elimination of H^- (**2a**, **2b**, **3b**) or Br^- (**3a**, **3b**).

7.3 Conclusion

We have shown, that the reactions of the monomeric phosphanylboranes **1a** and **1b** with the main group Lewis Acids BH_3 and BBr_3 lead to the adducts **2a**–**3b**. The secondary and tertiary phosphines **1a** and **1b** behave as classical Lewis bases and we were able to attach BX_3 (X = H, Br) end groups to them. The compounds are stable in solution and solid state and could be characterized completely. The organo-substituted phosphanylboranes **1a** and **1b**, show the same coordination behavior compared to the parent compound $H_2P–BH_2{\cdot}NMe_3$.

7.4 References

[1] A. Staubitz, A. P. M. Robertson, M. E. Sloan, I. Manners, *Chem. Rev.* **2010**, *110,* 4023–4078; T. J. Clark, K. Lee, I. Manners, *Chem. Eur. J.* **2006**, *12*, 8634–8648.

[2] H. Dorn, R. A. Singh, J. A. Massey, A. J. Lough, I. Manners, *Angew. Chem. Int. Ed.* **1999**, *38*, 3321–3323, *Angew. Chem.* **1999**, *111*, 3540–3543.

[3] A. Schäfer, T. Jurca, J. Turner, J. R. Vance, K. Lee, V. A. Du, M. F. Haddow, G. R. Whittell, I. Manners, *Angew. Chem. Int. Ed.* **2015**, *54*, 4836–4841; *Angew. Chem.* **2015**, *127*, 4918–4923.

[4] Y. Xia, G. M. Whitesides, *Angew. Chem. Int. Ed*. **1998**, *37*, 550–575; *Angew. Chem.* **1998**, *110*, 568–594; M. Geissler, Y. Xia, *Adv. Mater.* **2004**, *16*, 1249–1269; T. J. Clark, J. M. Rodezno, S. B. Clendenning, S. Aouba, P. M Brodersen, A. J. Lough, H. E. Ruda, I. Manners, *Chem. Eur. J.* **2005**, *11*, 4526–4534.

[5] C. Marquardt, A. Adolf, A. Stauber, M. Bodensteiner, A. V. Virovets, A. Y. Timoshkin, M. Scheer, *Chem. Eur. J.* **2013**, *19,* 11887–11891.

[6] C. Thoms, C. Marquardt, M. Bodensteiner, M. Scheer, *Angew. Chem. Int. Ed.* **2013**, *52*, 5150–5154; *Angew. Chem.* **2013**, *125*, 5254–5259.

[7] C. Marquardt, T. Jurca, K.-C. Schwan, A. Stauber, A. V. Virovets, G. R. Whittell, I. Manners, M. Scheer, *Angew. Chem. Int. Ed.* **2015**, *54*, 13782–13786; *Angew. Chem.* **2015**, *127*, 13986–13991.

[8] C. Marquardt, C. Thoms, A. Stauber, G. Balazs, M. Bodensteiner, M. Scheer, *Angew. Chem. Int. Ed.* **2014**, *53*, 3727–3730; *Angew. Chem.* **2014**, *126*, 3801–3804; unpublished results, please see chapter 5 and 6.

[9] Compound **2b** shows a high solubility, even in *n*-hexane at low temperatures. Due to the high solubility only a low crystalline yield was obtained.

[10] K.-C. Schwan, A. Y. Timoskin, M. Zabel, M. Scheer, *Chem. Eur. J.* **2006**, *12*, 4900–4908.

7.5 Supporting Information

General Experimental:

All manipulations were performed under an atmosphere of dry argon using standard glove-box and Schlenk techniques. All solvents are degassed and purified by standard procedures. The compounds $Ph_2P–BH_2·NMe_3$ (**1a**) and $^tBuHP–BH_2·NMe_3$ (**1b**) were prepared according to literature procedures.[1] $H_3B·thf$, $H_3B·SMe_2$ and BBr_3 were obtained from ABCR. The NMR spectra were recorded on an Bruker Avance 400 spectrometer (^1H: 400.13 MHz, ^{31}P: 161.976 MHz, ^{11}B: 128.378 MHz, $^{13}C\{^1H\}$: 100.623 MHz) with δ [ppm] referenced to external $SiMe_4$ (^1H, ^{13}C), H_3PO_4 (^{31}P), $BF_3·Et_2O$ (^{11}B). IR spectra were measured on a DIGILAB (FTS 800) FT-IR spectrometer. All mass spectra were recorded on a Finnigan MAT 95 (EI-MS). The C, H, N analyses were measured on an Elementar Vario EL III apparatus.

Synthesis of $H_3B{\cdot}Ph_2P{-}BH_2{\cdot}NMe_3$ (2a):

To a solution of 130 mg (0.5 mmol) $Ph_2P{-}BH_2{\cdot}NMe_3$ in 20 mL of toluene 0.5 mL (0.5 mmol) of a 1M solution of $H_3B{\cdot}$thf in thf is added at -80°C. After stirring the mixture for 18h at r.t., the clear solution is concentrated under reduced pressure. **2a** crystallises at -28°C as colourless blocks. The supernatant is decanted off; the resulting crystals are washed two times with *n*-hexane and dried under reduced pressure. Yield of $H_3B{\cdot}Ph_2P{-}BH_2{\cdot}NMe_3$ (**2a**): 66 mg (49 %). ^{1}H NMR (C_6D_6, 25 °C): δ = 1.79 (s, 9H, NMe_3), 2.02 (q, $^1J_{H,B}$ = 95 Hz, 3H, BH_3), 2.72 (q, $^1J_{H,B}$ = 104 Hz, 2H, BH_2), 7.03 (m, *p*-Ph, 2H), 7.12 (m, *m*-Ph, 4H), 8.12 (m, *o*-Ph, 4H). ^{31}P NMR (C_6D_6, 25 °C): δ = –23.5 (s, br). ^{31}P{^{1}H} NMR (C_6D_6, 25 °C): δ = –23.5 (s, br). ^{11}B NMR (C_6D_6, 25 °C): δ = –35.8 (dq, $^1J_{B,P}$ = 52 Hz, $^1J_{B,H}$ = 95 Hz, 1B, BH_3), –6.9 (m, 1B, BH_2). ^{11}B{^{1}H} NMR (C_6D_6, 25 °C): δ = –35.8 (d, $^1J_{B,P}$ = 52 Hz, 1B, BH_3), –6.9 (d, $^1J_{B,P}$ = 83 Hz, 1B, BH_2). ^{13}C{^{1}H} NMR (C_6D_6, 25 °C): δ = 53.6 (d, $^3J_{P,C}$ = 5 Hz, NMe_3), 128.4 (s, *p*-Ph), 129.2 (d, $^3J_{P,C}$ = 2 Hz, *m*-Ph), 133.5 (d, $^2J_{P,C}$ = 7 Hz, *o*-Ph), 135. 6 (d, $^1J_{P,C}$ = 44 Hz, *i*-Ph). IR (KBr): $\tilde{\nu}$ = 3070 (w, CH), 3052 (w, CH), 3013 (w, CH), 3000 (w, CH), 2948 (w, CH), 2920 (w, CH), 2434 (s, BH), 2397 (s), 2370 (s, BH), 2368 (s), 2288 (m, BH), 2270 (m), 2222 (w), 2130 (w), 2108 (w), 2000 (w), 1971 (w), 1918 (w), 1900 (w), 1840 (w), 1831 (w), 1795 (w), 1780 (w), 1585 (w), 1570 (w), 1480 (s), 1463 (s), 1455 (m), 1435 (s), 1415 (w), 1311 (w), 1249 (m), 1180 (w), 1153 (m), 1124 (s), 1100 (m), 1081 (s), 1057 (vs), 1023 (w), 1014 (m), 1000 (w), 976 (m), 865 (s), 790 (w), 767 (m), 749 (s), 704 (s), 646 (m), 575 (m), 507 (s), 488 (w), 463 (w), 422 (w). EI-MS (toluene): *m/z* = 270 (3%, $[M{-}H]^+$), 257 (100%, $[M{-}BH_3]^+$). Elemental analysis (%) calculated for $C_{15}H_{24}B_2N_1P_1$ (**2a**): C: 66.49; H: 8.93; N: 5.17; found: C: 66.52; H: 8.68; N: 5.12.

Synthesis of $Br_3B{\cdot}Ph_2P{-}BH_2{\cdot}NMe_3$ (3a):

To a solution of 125 mg (0.5 mmol) $Ph_2P{-}BH_2{\cdot}NMe_3$ in 20 mL of toluene 123 mg (0.05 mL, 0.5 mmol) of BBr_3 is added at -80°C. Upon addition a white precipitate is formed. After stirring the mixture for 18 h at r.t., the supernatant is decanted off and the remaining solid is dissolved in MeCN. The solution is filtrated and concentrated until crystallisation begins. **3a** crystallises at -28°C as colourless blocks. The supernatant is decanted off; the resulting crystals are washed two times with *n*-hexane and dried under reduced pressure. Yield of $Br_3B{\cdot}Ph_2P{-}BH_2{\cdot}NMe_3$ (**3a**): 70 mg (28 %). ^{1}H NMR (CD_3CN, 25 °C): δ = 2.77 (d, $^4J_{P,H}$ = 1 Hz, 9H, NMe_3), 2.86 (q, $^1J_{H,B}$ ~ 100 Hz, 2H, BH_2), 7.44 (m, *m*-Ph, 4H), 7.52 (m, *p*-Ph, 2H), 7.88 (m, *o*-Ph, 4H). ^{31}P NMR (CD_3CN, 25 °C): δ = –24.4 (s, br). ^{31}P{^{1}H} NMR (CD_3CN, 25 °C): δ = –24.4 (s, br). ^{11}B NMR (CD_3CN, 25 °C): δ = –12.0 (d, $^1J_{B,P}$ = 125 Hz, 1B, BBr_3), –7.8 (m, 1B, BH_2). ^{11}B{^{1}H} NMR (CD_3CN, 25 °C): δ = –12.0 (d, $^1J_{B,P}$ = 125 Hz, 1B, BBr_3), –7.8 (d, $^1J_{B,P}$ = 69 Hz, 1B, BH_2). ^{13}C{^{1}H} NMR (CD_3CN,

25 °C): δ = 55.6 (d, $^{3}J_{P,C}$ = 5 Hz, NMe_3), 128.9 (d, $^{1}J_{P,C}$ = 51 Hz, *i*-Ph), 129.2 (d, $^{2}J_{P,C}$ = 9 Hz *o*-Ph), 131.8 (d, $^{4}J_{P,C}$ = 2 Hz, *p*-Ph), 136.6 (d, $^{3}J_{P,C}$ = 9 Hz, *m*-Ph). IR (KBr): $\tilde{\nu}$ = 3081 (w, CH), 3061 (w, CH), 3000 (w, CH), 2993 (w, CH), 2947 (w, CH), 2919 (w, CH), 2481 (m, BH), 2421 (m, BH), 1957 (w), 1895 (w), 1815 (w), 1483 (s), 1463 (s), 1435 (s), 1242 (w), 1198 (w), 1165 (w), 1126 (s), 1090 (s), 1084 (s), 1070 (s), 1022 (m), 998 (w), 974 (w), 958(w), 869 (s), 744 (vs), 692 (vs), 607 (vs), 598 (vs), 512 (s), 478 (s), 447 (w), 405 (w). EI-MS (MeCN): *m/z* = 508 (1%, $[M–H]^+$), 428 (70%, $[M–Br]^+$), 257 (97%, $[M–BBr_3]^+$), 72 (100 %, $[M–BBr_3–PPh_2]^+$). Elemental analysis (%) calculated for $C_{15}H_{21}B_2Br_3N_1P_1$ (**3a**): C: 35.49; H: 4.17; N: 2.76; found: C: 35.50; H: 4.08; N: 2.89.

Synthesis of $H_3B·^{t}BuHP–BH_2·NMe_3$ (2b):

To a solution of 160 mg (1.0 mmol) $^{t}BuHP–BH_2·NMe_3$ in 10 mL of *n*-hexane 0.1 mL (1 mmol) of $H_3B·SMe_2$ 10 M in excess SMe_2 are added at -80°C. After stirring the mixture for 18h, the solution is filtrated and concentrated under reduced pressure. **2b** crystallises at -28°C as colourless blocks. The supernatant is decanted off; the resulting crystals are washed two times with small amounts of -80°C cold *n*-hexane and dried under reduced pressure. Yield of $H_3B·^{t}BuHP–BH_2·NMe_3$ (**2b**): 106 mg (61 %). ^{1}H NMR (C_6D_6, 25 °C): δ = 1.31 (d, $^{3}J_{P,H}$ = 13 Hz, 9H, ^{t}Bu), 1.42 (q, $^{1}J_{B,H}$ = 96 Hz, 3H, BH_3), 2.03 (s, 9H, NMe_3), 2.34 (q, $^{1}J_{B,H}$= 2H, BH_2), 3.49 (dm, $^{1}J_{P,H}$= 311 Hz, 1H, PH). ^{31}P NMR (C_6D_6, 25 °C): δ = –26.8 (d, $^{1}J_{H,P}$ = 311 Hz). $^{31}P\{^{1}H\}$ NMR (C_6D_6, 25 °C): δ = –26.8 (s, br). ^{11}B NMR (C_6D_6, 25 °C): δ = –39.4 (dq, $^{1}J_{B,H}$= 96 Hz, $^{1}J_{P,B}$= 47 Hz, BH_3), –10.0 (m, BH_2). $^{11}B\{^{1}H\}$ NMR (C_6D_6, 25 °C): δ = –39.4 (d, $^{1}J_{P,B}$= 47 Hz, BH_3), –9.97 (d, $^{1}J_{P,B}$= 80 Hz, BH_2). $^{13}C\{^{1}H\}$ NMR (C_6D_6, 25 °C): δ = 26.2 (d, $^{1}J_{P,C}$ = 34 Hz, **C**Me_3), 28.6 (d, $^{2}J_{P,C}$ = 1 Hz, C**Me**$_3$), 53.2 (d, $^{3}J_{P,C}$ = 5 Hz, NMe_3). IR (KBr): $\tilde{\nu}$ = 3022(w), 2998(w), 2976(s), 2953(s), 2923(m), 2898(m), 2864(m), 2425(s, BH), 2410 (s), 2396(s), 2353 (s), 2341(vs, BH), 2284(m, PH), 2263(m), 1485(s), 1474(s), 1410(m), 1392(m), 1365(s), 1248(m), 1194(w), 1161(s), 1130(vs), 1088(vs), 1063(vs), 1020(s), 978(m), 964(w), 909(s), 862(vs), 824(m), 785(m), 742 (w), 720 (w), 668 (w), 623 (w), 607 (w), 546 (w), 480 (w). EI-MS (toluene): *m/z* = 174.2 (5%, $[M–H]^+$), 161 (64%, $[M–BH_3]^+$), 72 (98%, $[M–BH_3·^{t}BuHP]^+$). Elemental analysis (%) calculated for $C_7H_{24}B_2N_1P_1$ (**2b**): C: 47.95, H: 13.81, N: 7.99; found: C: 48.02, H 13.79, N 7.86.

Synthesis of $Br_3B·^{t}BuHP–BH_2·NMe_3$ (3b):

To a solution of 160 mg (1.0 mmol) $^{t}BuHP–BH_2·NMe_3$ in 10 mL of *n*-hexane 246 mg (0.1 mL, 1 mmol) of BBr_3 are added at r.t.. Upon the addition a white precipitate is formed. After stirring the mixture for 18h, the supernatant is decanted off and all volatiles are removed under reduced pressure. **3b** is dissolved in 10 mL of MeCN, whereby a

white solid remains. After filtration, the solution is concentrated until crystallisation begins. **3b** crystallises at -28°C as colourless blocks. The supernatant is decanted off; the resulting crystals are washed two times with *n*-hexane and dried under reduced pressure. Yield of $Br_3B{\cdot}^tBuHP{-}BH_2{\cdot}NMe_3$ (**3b**): 170 mg (42 %). ^{1}H NMR (CD_3CN, 25 °C): δ = 1.44 (d, $^3J_{P,H}$ = 14 Hz, 9H, ^{t}Bu), 2.32 (q, BH_2), 2.81 (d, $^4J_{P,H}$ = 1 Hz, 9H, NMe_3), 4.45 (dt, $^1J_{P,H}$ = 342 Hz, $^3J_{H,H}$ = 3 Hz 1H, PH). ^{31}P NMR (CD_3CN, 25 °C): δ = –32.1 (m, br). ^{31}P{^{1}H} NMR (CD_3CN, 25 °C): δ = –32.1 (m, br). ^{11}B NMR (CD_3CN, 25 °C): δ = –14.2 (d, $^1J_{B,P}$ = 130 Hz, 1B, BBr_3), –9.6 (m, 1B, BH_2). ^{11}B{^{1}H} NMR (CD_3CN, 25 °C): δ = –14.2 (d, $^1J_{B,P}$ = 130 Hz, 1B, BBr_3), –9.6 (d, $^1J_{B,P}$ = 69 Hz, 1B, BH_2). ^{13}C NMR (CD_3CN, 25 °C): δ = 30.1 (s, C**Me**$_3$), 32.2 (d, $^1J_{P,C}$ = 28 Hz, **C**Me_3), 55.6 (d, $^3J_{P,C}$ = 5 Hz, NMe_3). IR (KBr): $\tilde{\nu}$ = 3020 (m), 3010 (m), 3000 (m), 2986(s), 2957(vs), 2903(s), 2868(s), 2725 (w), 2462(vs, BH), 2428(vs, BH), 2349(m, PH), 2331(m, PH), 2258 (w), 2214 (w), 2175(w), 1480 (s), 1469(vs), 1450 (s), 1410(s), 1369(s), 1252 (s), 1243(s), 1172(s), 1131(vs), 1089(vs), 1017(s), 978(vs), 957(m), 940(m), 873(s), 860 (s), 810(s), 774(w), 734(s), 712(vs), 634(s), 589(vs), 569(vs), 476(s), 416(s). EI-MS (MeCN): *m/z* = 332 (14%, [*M*–Br]$^+$), 161 (46%, [*M*–BBr_3]$^+$), 72 (100%, [*M*–$BBr_3{\cdot}^tBuHP$]$^+$). Elemental analysis (%) calculated for $C_7H_{21}B_2Br_3N_1P_1$ (**3b**): C: 20.54, H: 5.17, N: 3.42; found: C: 20.86, H: 5.04, N: 3.42.

X-ray diffraction analysis

All X-ray diffraction experiments were performed on a Gemini R Ultra CCD diffractometer from Agilent Technologies (formerly Oxford Diffraction) applying Cu-K_α radiation (λ = 1.54178 Å). The measurements were performed at 123 K. Crystallographic data together with the details of the experiments are given below. Absorption corrections were applied semi-empirically from equivalent reflections or analytically (SCALE3/ABSPACK algorithm implemented in CrysAlis PRO software by Agilent Technologies Ltd).[2] All structures were solved using OLEX 2[3] and SHELXT.[4] Refinements against F^2 in anisotropic approximation were done using SHELXL.[4] The hydrogen positions of the methyl groups were located geometrically and refined riding on the carbon atoms. Hydrogen atoms belonging to BH_2 and PH_2 groups were located from the difference Fourier map and refined without constraints. Figures were created with OLEX 2.[3] CIF files are deposited on the provided DVD.

Table S1: Crystallographic data for compounds **2a** and **2b**

Compound	**2a**	**2b**
empirical formula	$C_{15}H_{24}B_2NP$	$C_7H_{24}B_2NP$
formula weight	270.94	174.86
crystal system	monoclinic	monoclinic
space group	$P2_1/c$	$P2_1/c$
a [Å]	10.2441(2)	8.4405(3)
b [Å]	9.1036(2)	14.6830(3)
c [Å]	17.4754(3)	10.6969(3)
α [°]	90	90
β [°]	99.674(2)	112.073(4)
γ [°]	90	90
Volume [Å^3]	1606.55(6)	1228.51(6)
Z	4	4
ρ_{calc} [g/cm^3]	1.120	0.945
μ [mm^{-1}]	1.369	1.557
F (000)	584.0	392.0
crystal size [mm^3]	0.40 × 0.20 × 0.15	0.31 × 0.25 × 0.12
absorption correction	multi-scan	analytical
T_{min} / T_{max}	0.888 / 1.000	0.717 / 0.889
2*Θ* range [°]	8.756 to 147.83	10.768 to 134.27
completeness	0.986	0.996
index ranges	-12 ≤ *h* ≤ 12 -9 ≤ *k* ≤ 11 -19 ≤ *l* ≤ 21	-10 ≤ *h* ≤ 10 -17 ≤ *k* ≤ 17 -12 ≤ *l* ≤ 12
reflections collected	7563	13966
independent reflections	3099 [R_{int} = 0.0259, R_{sigma} = 0.0314]	2177 [R_{int} = 0.0536, R_{sigma} = 0.0277]
data/restraints/parameters	3099/0/195	2177/0/130
GOF on F^2	1.111	1.056
R_1/wR_2 [I≥2σ(*I*)]	R_1 = 0.0327 wR_2 = 0.0885	R_1 = 0.0390 wR_2 = 0.1077
R_1/wR_2 [all data]	R_1 = 0.0376 wR_2 = 0.1012	R_1 = 0.0438 wR_2 = 0.1134
max/min $\Delta\rho$ [e·Å^{-3}]	0.31/-0.28	0.47/-0.28

Table S2: Crystallographic data for compounds **3a** and **3b**

Compound	**3a**	**3b**
empirical formula	$C_{15}H_{21}B_2Br_3NP$	$C_7H_{21}B_2Br_3NP$
formula weight	507.65	411.57
crystal system	orthorhombic	orthorhombic
space group	*Pbca*	$P2_12_12_1$
a [Å]	13.9030(2)	8.9233(2)
b [Å]	14.5499(2)	10.9770(3)
c [Å]	19.2931(2)	15.5922(4)
α [°]	90	90
β [°]	90	90
γ [°]	90	90
Volume [Å^3]	3902.75(9)	1527.27(6)
Z	8	4
ρ_{calc} [g/cm^3]	1.728	1.790
μ [mm^{-1}]	8.383	10.523
F (000)	1984.0	800.0
crystal size [mm^3]	0.35 × 0.26 × 0.20	0.26 × 0.15 × 0.09
absorption correction	analytical	analytical
T_{min} / T_{max}	0.180 / 0.361	0.270 / 0.517
2*Θ* range [°]	9.922 to 148.274	9.854 to 134.144
completeness	0.987	0.993
index ranges	-17 ≤ *h* ≤ 15	-10 ≤ *h* ≤ 9
	-17 ≤ *k* ≤ 11	-13 ≤ *k* ≤ 13
	-15 ≤ *l* ≤ 23	-18 ≤ l ≤ 13
reflections collected	7874	7313
independent reflections	3792 [R_{int} = 0.0299,	2623 [R_{int} = 0.0495,
	R_{sigma} = 0.0343]	R_{sigma} = 0.0528]
data/restraints/parameters	3792/0/209	2623/0/145
GOF on F^2	1.143	1.062
R_1/wR_2 [I≥2*σ(I)*]	R_1 = 0.0332	R_1 = 0.0326,
	wR_2 = 0.0870	wR_2 = 0.0649
R_1/wR_2 [all data]	R_1 = 0.0384	R_1 = 0.0367
	wR_2 = 0.1100	wR_2 = 0.0674
max/min Δ*ρ* [e·Å^{-3}]	0.71/-0.84	0.34/-0.42
flack parameter	-	0.01(5)

References

[1] C. Marquardt, T. Jurca, K.-C. Schwan, A. Stauber, A. V. Virovets, G. R. Whittell, I. Manners, M. Scheer, *Angew. Chem. Int. Ed.* **2015**, *54*, 13782–13786; *Angew. Chem.* **2015**, *127*, 13986–13991.

[2] Agilent Technologies **2006-2011**, CrysAlisPro Software system, different versions, Agilent Technologies UK Ltd, Oxford, UK.

[3] O.V. Dolomanov, L.J. Bourhis, R.J. Gildea, J.A.K. Howard, H.Puschmann, OLEX 2: A complete structure solution, refinement and analysis program, *J. Appl. Cryst*. **2009**, 42, 339–341

[4] G. M. Sheldrick, *Acta Cryst.* **2008**, *A64*, 112–122.

7.6 Author Contributions

The syntheses and characterization of all compounds were performed by Christian Marquardt.

Josef Baumann is gratefully acknowledged for contributions to the syntheses of **2a** and **3a** during his bachelor-thesis (**2013**) under the supervision of Christian Marquardt.

Tobias Kahoun is gratefully acknowledged for contributions to the syntheses of **2b** and **3b** during a research course under the supervision of Christian Marquardt.

X-ray structural analyses of all compounds were performed by Christian Marquardt.

The manuscript (including supporting information, figures, schemes and graphical abstract) was written by Christian Marquardt.

8. Oxidation of the substituted Phosphanylboranes $Ph_2P–BH_2·NMe_3$ and $^tBuHP–BH_2·NMe_3$ with chalcogens

C. Marquardt, O. Hegen and M. Scheer

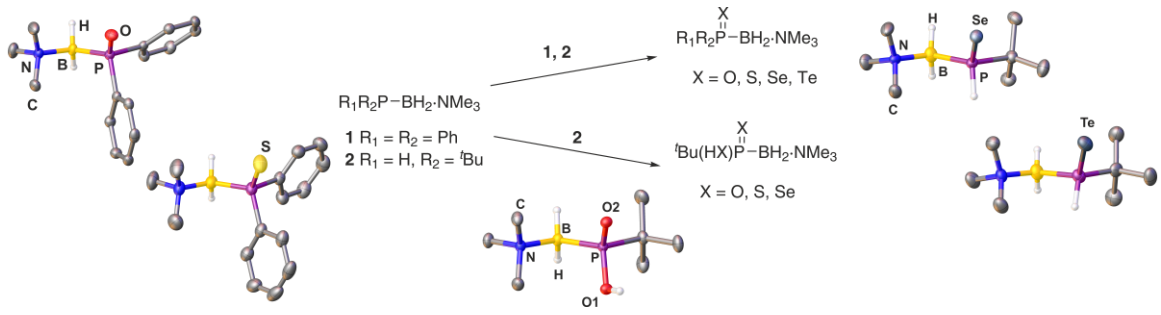

Abstract: The elemental chalcogens sulfur, selenium, tellurium and bis(trimethylsilyl)peroxide as an oxygen source are applied for the oxidation of the phosphanylboranes $Ph_2P–BH_2·NMe_3$ (**1**) and $^tBuHP–BH_2·NMe_3$ (**2**). The corresponding mono-oxidation products $Ph_2P(X)–BH_2·NMe_3$ (X = O – Te, **3a-d**) and $^tBuHP(X)–BH_2·NMe_3$ (X = O – Te, **4a-d**) were obtained in good yields and have been characterized completely by single crystal X-ray structure analysis, NMR, IR spectroscopy and mass spectrometry. While the first oxidation step proceeds very selectively for all chalcogenides, further oxidation is observed for the ^{t}Bu derivative with O_2, S_8 and Se - yielding $^tBu(HX)P(X)–BH_2·NMe_3$ (X = O, S, Se, **5a-c**) - which, however does not proceed selective. The telluride compounds presented herein are the first examples for neutral Te-substituted phosphanylboranes.

8.1 Introduction

In the last two decades phosphine-borane (PB) adducts - especially of the form $RH_2P{\cdot}BH_3$ (R = alkyl, aryl) - gained increasing attention, particularly as reagents for the synthesis of polymers via dehydrocoupling reactions.[1,2] The coordination chemistry of PB adducts, mainly for secondary phosphines, was investigated as well, to gain further insight into the mechanistic details of those dehydrocoupling reactions.[3] The donor part of the adducts, the phosphines are of general interest because of their importance as ligands, starting materials or active intermediates in many reactions.[4] In the laboratory they can also easily be oxidized using elemental chalcogens or organic oxidants.[5] Phosphorus-chalcogen containing compounds have become valuable tools for organic synthesis. Compounds of the type R_2HPO can be used as chiral preligands for enatioselective catalysis.[6] A very well-known example is the Lawesson's reagent $[(4\text{-}MeOC_6H_4)PS(\mu\text{-}S)]_2$ which is a widely used reagent in organic chemistry, for the conversion of C=O to C=S groups.[7] The selenium analog $[PhPSe(\mu\text{-}Se)]_2$, which is also known as the Woollins' reagent, was similarly applied in a great variety of transformations.[8] Due to the lability of terminal P=Te groups, phosphine-tellurides can be applied as tellurium-transfer reagents that are soluble and highly reactive compared to elemental tellurium as starting material.[9] Moreover, organophosphorus-chalcogen compounds can be used as pesticides, as precursors for metal chalcogenide thin films or nanoparticles and as lubricant additives.[10] The oxidation of phosphino-borane adducts or phosphinoboranes however has not been studied so thoroughly yet. Although boranylphosphine oxides and sulfides are well known, examples for the selenide[11] (Scheme 1, **A** and **C**) and telluride[12,13] derivatives are very rare. The telluride compounds are only known for anionic species (Scheme 1, **B** and **C**).

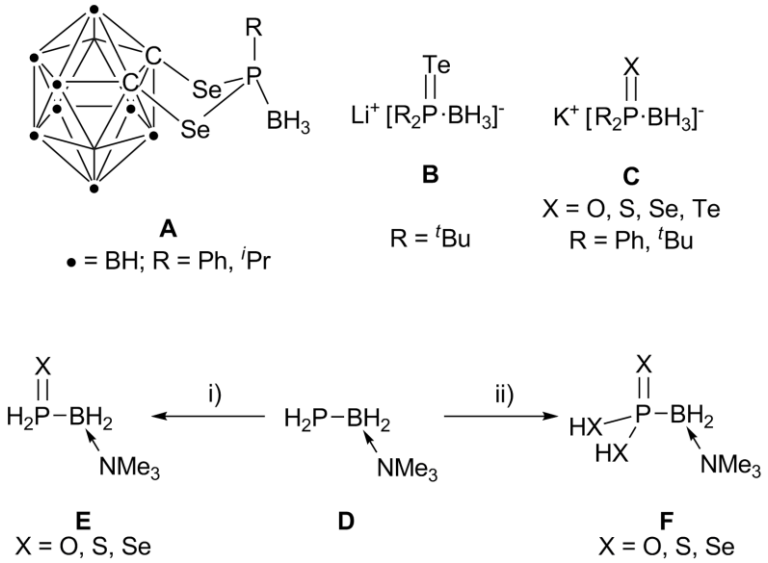

Scheme 1. Chalcogen derivatives of phosphinoboranes (**A**-**C**) and oxidation of the phosphanylborane $H_2P–BH_2·NMe_3$ (**D**-**F**). i) X = O, $+Me_3NO$; X = S, Se, +1/8 X_8; ii) X = O, $+O_2$ (exc.); X = S, Se, +1/8 X_8 (exc.).

We are especially interested in the parent compound of the phosphanylboranes $H_2P–BH_2·NMe_3$, which is readily available at gram scale[14] and can be used for the synthesis of oligomeric and polymeric compounds.[15]

Several attempts were made to selectively oxidize this special primary phosphine.[16] However only the boranylphosphine chalcogenide compounds $H_2P(X)–BH_2·NMe_3$ (**E:** X = S, Se; scheme 1) could be isolated. The formation of the boranylphosphine oxide $H_2P(O)–BH_2·NMe_3$ was postulated based on NMR experiments, since several attempts of its isolation failed. While the reaction of **D** with an excess of O_2 leads to the formation of the boranyl phosphonic acid $(HO)_2P(O)–BH_2·NMe_3$ (**F**: X=O; Scheme 1),[16] the reactions with an excess of sulfur or selenium lead to a mixture of products. Spectroscopic studies provided evidence for the presence of the trithioboranylphosphonates and triselenoboranylphosphonates (**F**; X = S, Se; Scheme 1).

Inspired by the oxidation of the phosphanylborohydrides $[R_2P·BH_3]^-$ (R = Ph, ^{t}Bu; scheme 1, **C**), and the unsatisfying characterization of the mono-oxidation products of $H_2P–BH_2·NMe_3$ (**E**) with O_2, we aimed to get a series of boranylphosphine chalcogenides starting from the tertiary phosphine $Ph_2P–BH_2·NMe_3$ (**1**) and the secondary phosphine ^{t}BuHP–$BH_2·NMe_3$ (**2**), which was recently used for the efficient synthesis of poly(phosphinoboranes).[15b]

8.2 Results and Discussion

Reaction of **1** and **2** with bis(trimethylsilyl)peroxide and elemental sulfur, selenium and tellurium yield the corresponding monochalcogenide compounds **3a**–**3d** and **4a**–**4d**, respectively (Scheme 2).

During the reaction of **1** and the chalcogenides a yellowish to brown precipitate is formed which was insoluble in all common solvents and could not be further characterized. The ^{31}P NMR spectra of the supernatant crude reaction mixtures of **3a** – **3d** show, that almost no soluble side products are formed.

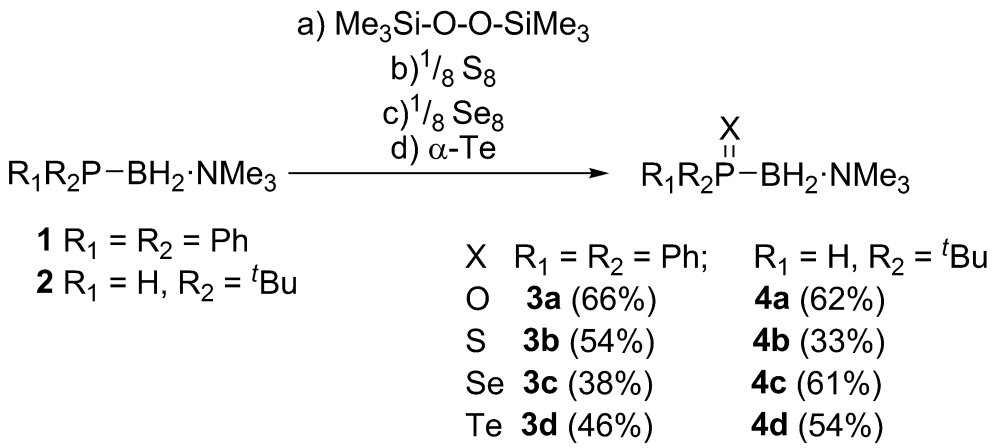

Scheme 2. Oxidation of the substituted phosphanylboranes **1** and **2**.

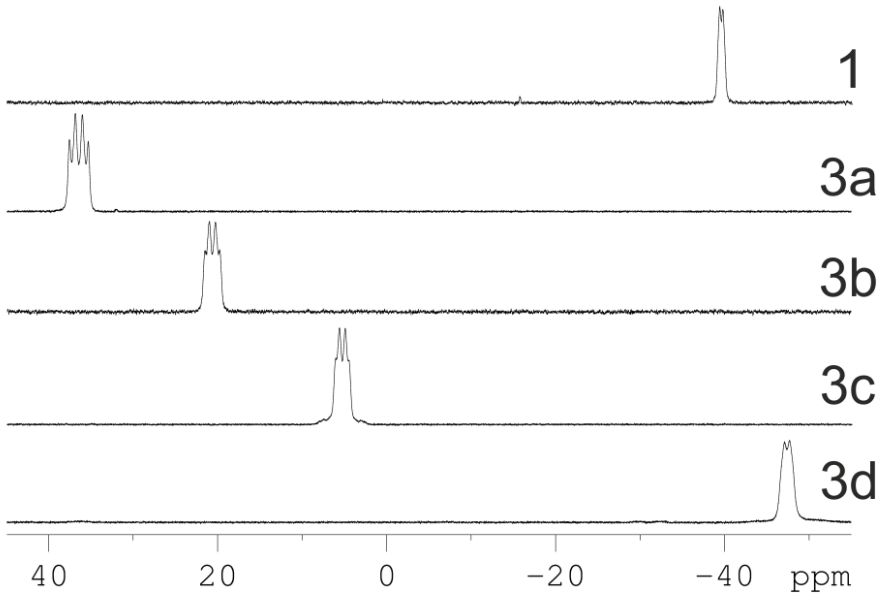

Figure 1. ^{31}P NMR spectra of **1** and **3a** - **3d** in CD_2Cl_2.

In each of the ^{31}P NMR spectra a *pseudo*-quartet arises, for **3a** (δ = 36.4 ppm), **3b** (δ = 20.7 ppm) and **3c** (δ = 5.3 ppm) which are shifted stronger to lower field with rising electronegativity of the chalcogen substituent X compared to the starting material **1**. Only **3d** (δ = −47.3 ppm) is slightly high field shifted compared to **1** (Figure 1). In the ^{31}P{^{1}H} NMR spectrum of **3c** the ^{77}Se-satellites are observed with a $^1J_{P,Se}$ coupling constant of approximately 600 Hz. For **3d** no signals of the ^{125}Te satellites can be resolved.[17]

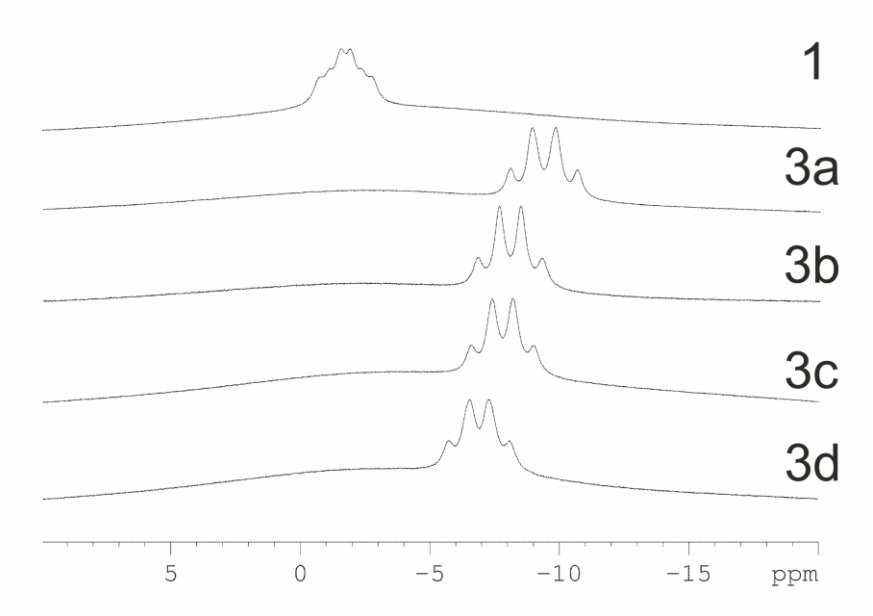

Figure 2. ^{11}B NMR spectra of **1** and **3a-3d** in CD_2Cl_2.

In the ^{11}B NMR spectra a *pseudo*-quartet can be found for all four compounds (**3a** (δ = −9.4 ppm), **3b** (δ = −8.0 ppm), **3c** (δ = −7.8 ppm) and **3d** (δ = −6.9 ppm)), which are high field shifted compared to **1** (δ = −1.7 ppm).

Table 1. NMR parameters for compounds **1**, **3a** - **3d**

compound (X)	^{31}P δ [ppm]	^{11}B δ [ppm]	$^{1}J_{B,P}$ [Hz]	$^{1}J_{B,H}$ [Hz]
1	−39.5	−1.7	45	107
3a (O)	+36.4	−9.4	125	110
3b (S)	+20.7	−8.0	102	106
3c (Se)	+5.3	−7.8	93	103
3d (Te)	−47.3	−6.9	86	103

Table 1 shows that with decreasing electronegativity of the chalcogenide (**3a**–**3d**) the resonance signals are shifted to higher fields in the ^{31}P NMR spectra and the boron-phosphorus coupling constants are also decreasing. In the ^{11}B NMR spectra the opposite effect is observed; decreasing electronegativity leads to a low field shift. In the EI-MS spectra the molecular ion peak is detected for all compounds. The IR spectra for **3a**–**3d** show absorptions for the B–H valence stretches between 2392 cm^{-1} and 2438 cm^{-1}, which are clearly at higher wavenumbers than the starting material **1** (2290 cm^{-1} and 2361 cm^{-1}). Unfortunately, the unambiguous assignment of the band corresponding to the P-X valence stretches in the IR spectra was not possible. Problems with assignment

of the P-X stretches have also been reported for the oxidation of the phosphanylborohydrides $[R_2P{\cdot}BH_3]^-$ (R = Ph, ^{t}Bu; scheme 1, **C**).[13]

Table 2. IR Data for compounds **1**, **3a** - **3d**

compound (X)	$\tilde{\nu}$ (B-H) [cm^{-1}]	$\tilde{\nu}$ (B-H) [cm^{-1}]
1	2361	2290
3a (O)	2414	2392
3b (S)	2438	2407
3c (Se)	2436	2408
3d (Te)	2433	2407

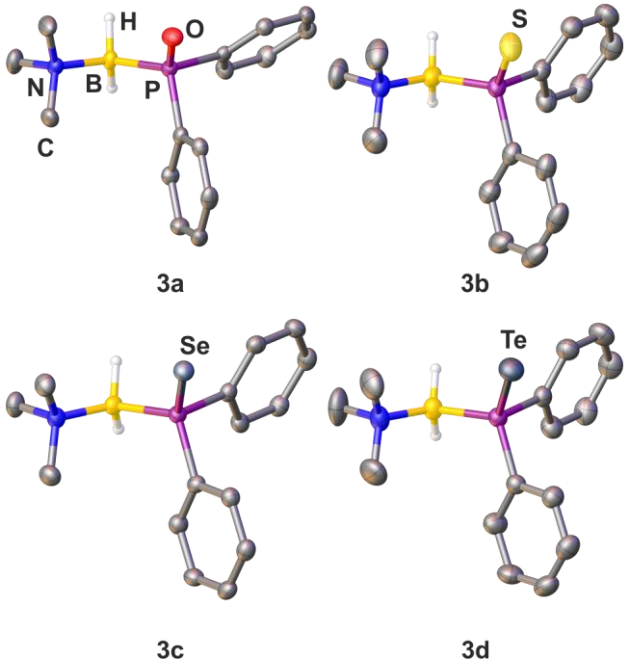

Figure 3. Molecular structures of **3a** - **3d** in the solid state. Hydrogen atoms bonded to carbon are omitted for clarity. Thermal ellipsoids are drawn with 50% probability. Selected bond lengths [Å] and angles [°]: **3a**: P–B 1.954(3), P–O 1.5027(19), O–P–B 118.75(13), P–B–N 115.08(19); **3b**: P–B 1.965(3), P–S 1.9864(9), S–P–B 118.34(10), P–B–N 118.44(19); **3c**: P–B 1.964(4), P–Se 2.1477(9), Se–P–B 118.70(10), P–B–N 119.3(2); **3d**: P–B 1.972(3), P–Te 2.3941(7), Te–P–B 118.80(10), P–B–N 120.03(19).

Single crystals suitable for X-ray structure analysis are obtained by storing a saturated CH_2Cl_2 solution at -28°C. All compounds adopt in the solid state a synclinal arrangement. The P–X bond lengths increases in accordance with the increase of covalent radii of X, moving down the group from oxygen to tellurium (**3a**: P–O 1.5027(19), **3b**: P–S 1.9864(9), **3c**: P–Se 2.1477(9), **3d**: P–Te 2.3941(7)). The determined bond lengths are similar to the corresponding bond lengths reported for the compounds obtained by the

oxidation of the phosphanylborohydrides [K(18-c-6)][$XPPh_2BH_3$].[13] The P–B bond length in **3a**–**3d** is slightly shorter than in the starting material (**1**: 1.974(3), **3a**: 1.954(3), **3b**: P–B 1.965(3), **3c**: P–B 1.964(4), **3d**: P–B 1.972(3)). The same trend was also observed for the phosphanylborohydrides. A comparison of the discussed bond lengths with those related ionic compounds is given in table 3.

Table 3. Comparison of P–B- and P–X-bond length [Å] of **1**, **3a** - **3d** with related phosphanylborohydrides

	P–B [Å]	P–X [Å]		P–B [Å]	P–X [Å]
1	1.974(3)		**$[PPh_2BH_3]^-$**	1.960(6)	
3a	1.954(3)	1.5027(19)	**$[OPPh_2BH_3]^-$**	1.908(2)	1.514(1)
3b	1.965(3)	1.9864(9)	**$[SPPh_2BH_3]^-$**	1.972(5)	1.987(4)
3c	1.964(4)	2.1477(9)	**$[SePPh_2BH_3]^-$**	1.907(6)	2.182(1)
3d	1.972(3)	2.3941(7)	**$[TePPh_2BH_3]^-$**	1.921(6)	2.398(1)

As shown in table 3 the P–B- and P–X-bond length of **3a**–**3d** ($Ph_2P(X)–BH_2·NMe_3$) are very similar to the structural related, ionic compounds [K(18-c-6)][$XPPh_2BH_3$] (X = O, S, Se, Te), and the same changes of the bond lengths upon oxidation are observed.

The ^{31}P NMR spectra of the reaction mixtures of **4a** – **4d** show, that for **4a** and **4d** no side products are formed. Some traces of the bis-oxidation-product $^tBu(HX)P(X)–BH_2·NMe_3$ (X = S, Se) can be observed for the oxidation with elemental sulfur and selenium. During the reaction with *α*-Te a precipitate is formed which could not be further characterized.

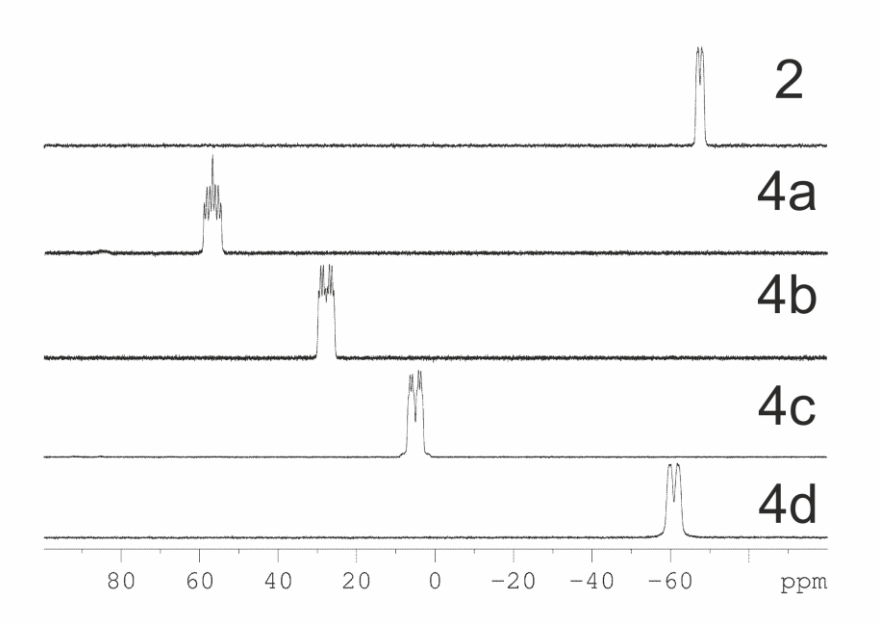

Figure 4. ^{31}P NMR spectra of **2** and **4a** - **4d** in C_6D_6.

The ^{31}P NMR spectra show multiplets (which result from the superposition of a doublet of quartets) for **4a** (δ = +57.1 ppm), **4b** (δ = +27.9 ppm), **4c** (δ = +4.9 ppm) and **4d** (δ = −60.9 ppm). All signals are low field shifted with rising electronegativity of the chalcogenide substituent X, compared with the starting material **2** (δ = −67.6 ppm) (figure 4). Similar to the compounds **3c** and **3d** the ^{31}P{^{1}H} NMR spectra show ^{77}Se satellites for **4c** ($^{1}J_{P,Se}$ ~ 582 Hz) and for **4d** no signals for ^{125}Te satellites can be resolved.[17]

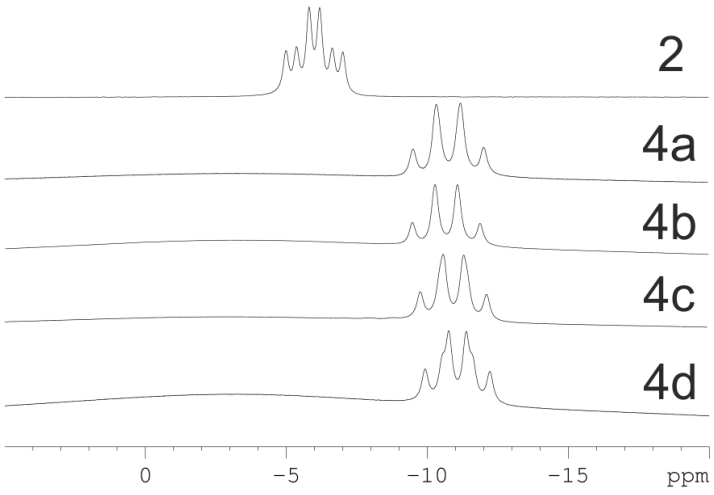

Figure 5. ^{11}B NMR spectra of **2**, **4a** - **4d** in C_6D_6.

In the ^{11}B NMR spectra all four compounds **4a** (δ = −10.8 ppm), **4b** (δ = −10.7 ppm), **4c** (δ = −11.0 ppm) and **4d** (δ = −11.1 ppm) show a *pseudo*-quartet. All signals are high field shifted compared to **2** (δ = −6.0 ppm).

Table 4. NMR Parameters for compounds **2, 4a - 4d**

compound (X)	^{31}P δ [ppm]	^{11}B δ [ppm]	$^{1}J_{B,P}$ [Hz]	$^{1}J_{H,P}$ [Hz]	$^{1}J_{B,H}$ [Hz]
2	−67.6	−6.0	48	197	104
4a (O)	+57.1	−10.8	115	344	103
4b (S)	+27.9	−10.7	96	355	106
4c (Se)	+4.9	−11.0	87	352	108
4d (Te)	−60.9	−11.1	76	345	109

Table 4 reveals that decreasing electronegativity of the chalcogenide leads to a high field shift for the signals in the ^{31}P NMR spectra for **4a**-**4d**. The boron-phosphorus

coupling constants are decreasing as well. In the ^{11}B NMR spectra the signals remain essentially similar. In the ^{1}H NMR spectrum the resonance signal for the PH group can be found as doublet of doublet of doublets. The signal pattern is caused by the $^{1}J_{P,H}$ coupling and additionally $^{3}J_{H,H}$ couplings to the two diastereotopic hydrogen atoms on the boranyl group. For the BH_2 group a set of two *pseudo*-quartets is found.

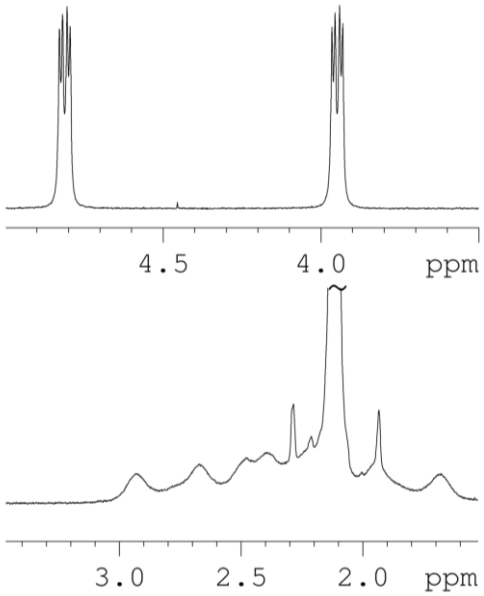

Figure 6. Sections of ^{1}H NMR spectrum of **4d** in C_6D_6. Top: PH resonance. Bottom: BH_2-region.

In the EI-MS spectra the molecular ion peak is detected for all compounds. The IR spectra for **4a** – **4d** show absorptions for the B–H valence stretches between 2381 cm^{-1} and 2425 cm^{-1}, which are at slightly higher wavenumbers than the starting material **2** (2388 cm^{-1} and 2295 cm^{-1}). The P–H valence stretches of **4b – 24** between 2281 cm^{-1} and 2304 cm^{-1} appear at slightly higher wavenumbers compared to **2** (2244 cm^{-1}). The stretches for compound **4a** remain nearly unchanged. Similarly to **3a** – **3d** unambiguously assignment of the P-X valence stretches in the IR spectra was not possible.

Table 5. IR Data for compounds **2**, **4a** - **4d**

compound (X)	$\tilde{\nu}$ (B-H) [cm^{-1}]	$\tilde{\nu}$ (B-H) [cm^{-1}]	$\tilde{\nu}$ (P-H) [cm^{-1}]
2	2388	2295	2244
4a (O)	2400/2381	2300	2242/2209
4b (S)	2431	2391	2281
4c (Se)	2419	2385	2298
4d (Te)	2425	2392	2304

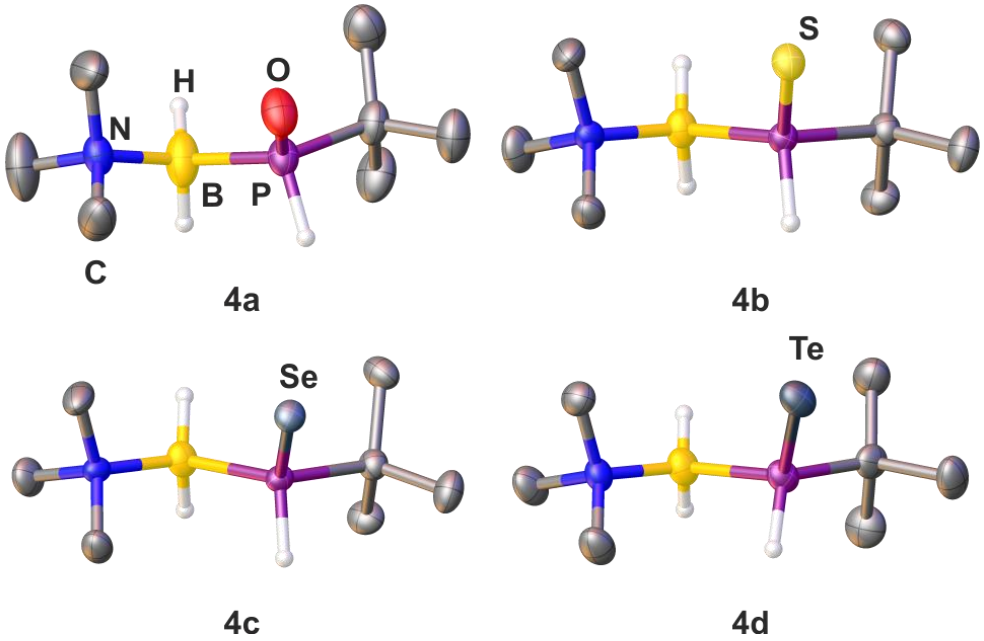

Figure 7. Molecular structure of **4a**, **4b**, **4c** and **4d** in the solid state. Hydrogen atoms bond to carbon are omitted for clarity. Thermal ellipsoids are drawn with 50% probability. Selected bond lengths [Å] and angles [°]: **4a**: P–B 1.944(3), P–O 1.5010(15), O–P–B 118.47(11), P–B–N 111.51(16); **4b**: P–B 1.966(2), P–S 1.9945(8), S–P–B 119.37(7), P–B–N 113.07(11); **4c**: P–B 1.971(2), P–Se 2.1467(5), Se–P–B 119.47(7), P–B–N 113.20(13); **4d**: P–B 1.980(12), P–Te 2.400(3), Te–P–B 122.1(4), P–B–N 115.1(7).

Single crystals suitable for X-ray structure analysis are obtained by dissolving **4a**-**d** in a small amount of toluene and addition of *n*-hexane and storing the solution at -28°C (Figure 7). To maximize the distance between the sterically demanding ^{t}Bu moiety and the NMe_3 group compounds **4a**-**d** adopt in the solid state a synclinal arrangement. The P–X bond lengths increases moving down the group from oxygen to tellurium (**4a**: P–O 1.5010(15), **4b**: P–S 1.9945(8), **4c**: P–Se 2.1467(5), **4d**: P–Te 2.400(3)) and are nearly identical compared to **3a** – **3d**. The P–B bond length is slightly shorter than in the starting material (**2**: 1.985(2), **4a**: 1.944(3), **4b**: P–B 1.966(2), **4c**: P–B 1.971(2), **4d**: P–B 1.980(12)). The P–X and P–B bond lengths of the products obtained by oxidation of **2**, show the same trends as observed for **3a**-**3d**. First attempts to crystallize **4a**-**4d** from CH_2Cl_2 solution yielded crystals of the decomposition product $[^{t}BuH_2P–BH_2{\cdot}NMe_3]^{+}Cl^{-}$ (**2z**), which was only characterized by single crystal X-ray diffraction analysis (Figure 8).

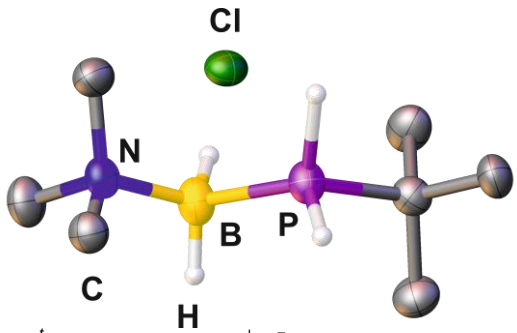

Figure 8. Molecular structure of $[^{t}BuH_2P–BH_2{\cdot}NMe_3]^{+}Cl^{-}$ (**2z**) in the solid state. Thermal ellipsoids are drawn with 50% probability. Hydrogen atoms bond to carbon are omitted for clarity. Selected bond lengths [Å] and angles [°]:P–B 1.966(4), B–N 1.577(5), P–B–N 114.5(2), C–P–B 110.86(16).

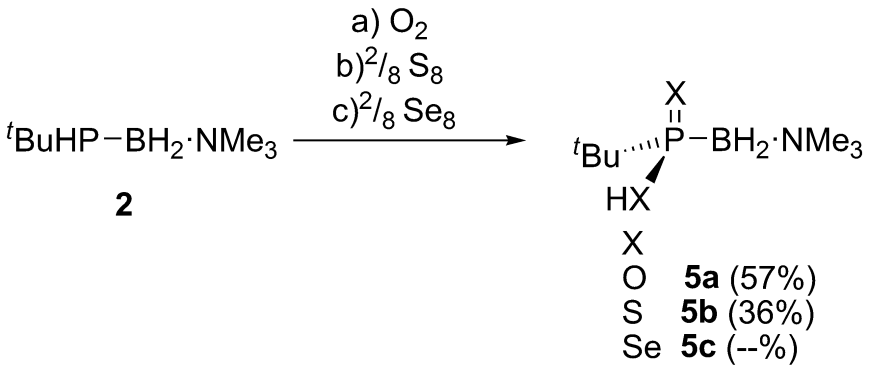

Scheme 3. Further oxidation of the substituted phosphanylborane **2**.

To investigate if the double oxidized species ^{t}Bu(HX)P(X)–BH_2·NMe_3 (X = O, S, Se, Te) are also accessible, **2** was reacted with 2 equivalents of bis(trimethylsilyl)peroxide, elemental sulfur, selenium and tellurium (Scheme 3). While the oxidation with bis(trimethylsilyl)peroxide stops at **4a**, further addition of pure O_2 leads to the formation of ^{t}Bu(HO)P(O)–BH_2·NMe_3 **(5a)**. The same reaction is observed when **2** is reacted only with O_2. Reaction of **2** with elemental sulfur leads selectively to ^{t}Bu(HS)P(S)–BH_2·NMe_3 (**5b**). In the case of selenium the second oxidation step proceeds very unselective and a mixture of several products is obtained. Isolation of compound **5c** was not successful, but a signal in ^{31}P NMR can be tentatively assigned to **5c**. Overall it is notable, that the first oxidation steps proceeds very smoothly, whereas the second step is very unselective. Even with a large excess of *α*-Te and prolonged reaction times, the oxidation stops at the stage of **4d** which remains stable in the reaction mixture. The ^{31}P NMR spectra show a broad multiplet (Figure 9) for **5a** (*δ* = +90.7 ppm), **5b** (*δ* = +83.3 ppm) and **5c** (*δ* = +59.6 ppm) which are low field shifted with increasing electronegativity of the chalcogenide X compared to **2**.

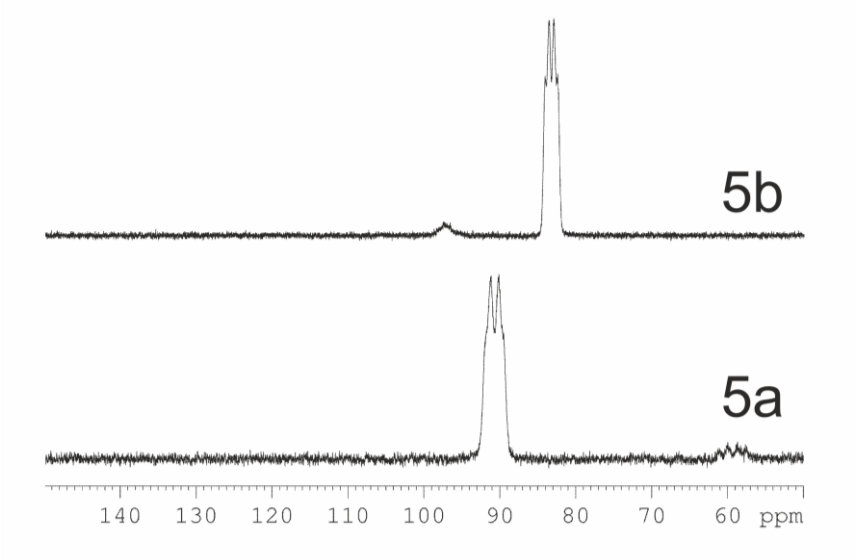

Figure 9. ^{31}P NMR spectra of **5a** in $CDCl_3$ and **5b** in C_6D_6.

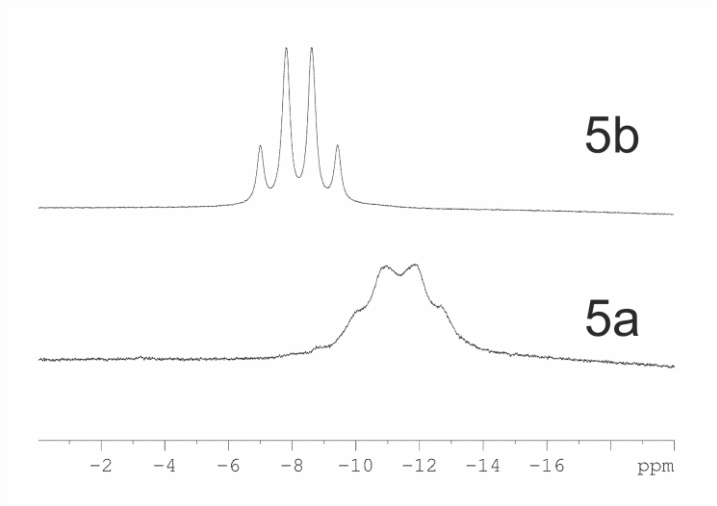

Figure 10. ^{11}B NMR spectra of **5a** in $CDCl_3$ and **5b** in C_6D_6.

In the ^{11}B NMR spectra (Figure 10) a *pseudo*-quartet arise for all compounds (**5a** δ = −11.4 ppm, **5b** δ = −8.2 ppm). All signals are high field shifted compared to **2** δ = −6.0 ppm. The ^{11}B NMR chemical shift of **5c** could not be clearly assigned, since the obtained mixture of products showed multiple overlapping signals. In the ^{1}H NMR spectrum of **5a** the OH-group arises as a broad singlet at δ = 11.74 ppm whilst the SH-group of **5b** can be found as a broad signal at δ = 1.82 ppm (Figure 11).

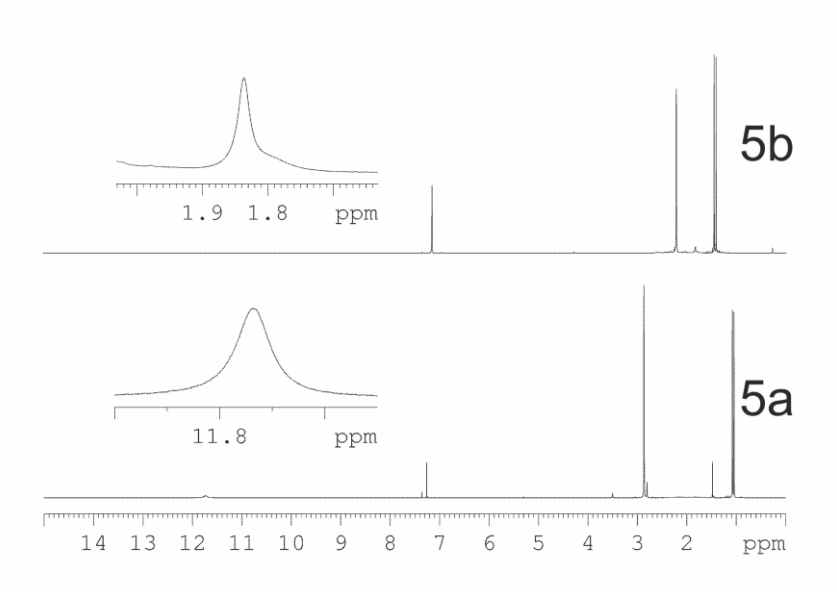

Figure 11. ^{1}H NMR spectrum of **5a** in $CDCl_3$ and **5b** in C_6D_6. XH (X =O, S) signals are magnified.

Decreasing electronegativity of the chalcogenide of the compounds (**5a–5b**) leads to a high field shift of the resonance signals in the ^{31}P NMR spectra. In the ^{11}B NMR spectra the opposite effect is observed; the decreasing electronegativity leads to a low field shift. In the FD-MS spectra of **5a–5c** the molecular ion peak is detected. For sulfur and

selenium, compounds with an increased amount of the chalcogenides are observed $[(^{t}Bu(HX)P(X)–BH_2·NMe_3)(X)_n]^+$ (n = 1-6). The IR spectra for **5a–5b** show absorptions for the B–H valence stretches between 2441 cm^{-1} and 2386 cm^{-1}, which are at higher wavenumbers than the starting material **2** (2295 cm^{-1} and 2388 cm^{-1}). Like for the compounds mentioned before an unambiguous assignment of the P-X valence stretches in the IR spectra was not possible. For **5a** single crystals were obtained by slow evaporation of the solvent from a CH_2Cl_2 solution and were characterized by single crystal X-ray structure analysis (Figure 12). In the solid state **5a** can be found as a dimer, forming hydrogen bridges between O1–H and O2. All substituents along the N–B–P–C backbone of compound **5a** adopt a staggered arrangement. The P–O bond lengths of **5a** (P–O1 1.5855(8), P–O2 1.5209(8) Å) remains similar to **4a** (1.5010(15) Å). The P–B bond length is slightly shorter than in the starting material but essentially unchanged compared to the mono-oxidized species **4a** (2: 1.985(2) Å, **4a**: 1.944(3) Å, **5a**: 1.9436(14) Å).

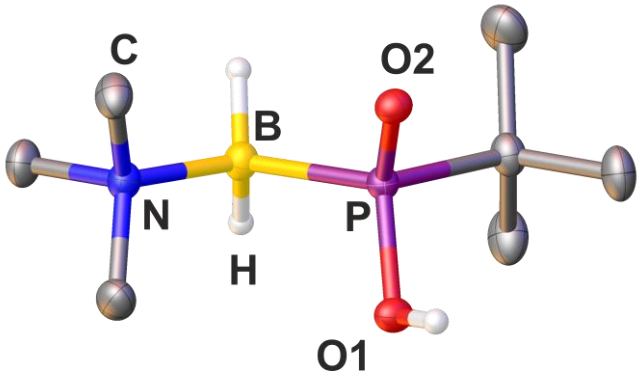

Figure 12. Molecular Structure of **5a** in the solid state. Hydrogen atoms bond to carbon are omitted for clarity. Thermal ellipsoids are drawn with 50% probability. Selected bond lengths [Å] and angles [°]:P–B 1.9436(14), O1–P 1.5855(8), O2–P 1.5209(8), B–N 1.6099(15), P–B–N 113.93(8), O1–P–B 108.74(5), O2–P–B 114.71(5), O1–P–O2 111.04(4).

8.3 Conclusion

Oxidation of the phosphanylboranes $Ph_2P–BH_2·NMe_3$ and $^{t}BuHP–BH_2·NMe_3$ could easily be achieved by the reaction with elemental chalcogens and bis(trimethylsilyl)peroxide, respectively. The first oxidation steps proceeds very cleanly and all obtained compounds were fully characterized. For $^{t}BuHP–BH_2·NMe_3$ the formation of the doubly oxidized product $^{t}Bu(HX)P(X)–BH_2·NMe_3$ was observed and could be spectroscopically characterized. This reaction proceeds cleanly only for elemental oxygen and sulfur. $Ph_2P(Te)–BH_2·NMe_3$ and $^{t}BuHP(Te)–BH_2·NMe_3$ are the first examples for neutral compounds with a B–P–Te unit, which may represent interesting new ligands. Currently the coordination chemistry of $Ph_2P(X)–BH_2·NMe_3$, $^{t}BuHP(X)–$

$BH_2{\cdot}NMe_3$ (X = O, S, Se, Te), ^{t}BuP(XH)(X)–$BH_2{\cdot}NMe_3$ and the corresponding anions $[^t Bu(X)_2P–BH_2{\cdot}NMe_3]^-$ (X = O, S) are under investigation.

8.4 References

[1] A. Staubitz, A. P. M. Robertson, M. E. Sloan, I. Manners, *Chem. Rev.* **2010,** *110,* 4023–4078.

[2] a) T. J. Clark, K. Lee, I. Manners, *Chem. Eur. J.* **2006**, *12*, 8634–8648; b) A. Schäfer, T. Jurca, J. Turner, J. R. Vance, K. Lee, V. A. Du, M. F. Haddow, G. R. Whittell, I. Manners, *Angew. Chem. Int. Ed.* **2015**, *54*, 4836–4841; *Angew. Chem.* **2015**, *127*, 4918–4923.

[3] H. Helten, B. Dutta, J. R. Vance, M. E. Sloan, M. F. Haddow, S. Sproules, D. Collison, G. R. Whittell, G. C. Lloyd-Jones, I. Manners, *Angew. Chem. Int. Ed.* **2013**, *52*, 437–444; *Angew. Chem.* **2013**, *125*, 455–458; M. A. Huertos, A. S. Weller, *Chem. Commun.* **2012**, *48*, 7185–7187; M. A. Huertos, A. S. Weller, *Chem. Sci.* **2013**, *4*, 1881–1888; C. Johnson, T. N. Hooper, A. S. Weller, *Top. Organomet. Chem.* **2015**, *49*, 153–220, T. N. Hooper, M. A. Huertos, T. Jurca, S. D. Pike, A. S. Weller, I. Manners, *Inorg. Chem.* **2014**, *53*, 3716–3729.

[4] M. Brynda, *Coord. Chem. Rev.* **2005**, *249*, 2013–2034.

[5] F. Uhlig, E. Herrmann, D. Schädler, G. Ohms, G. Großmann, S. Besser, R. Herbst-Irmer, *Z. Anorg. Allg. Chem.* **1993**, *619*, 1962–1970.

[6] N. V. Dubrovina, A. Börner, *Angew. Chem. Int. Ed.* **2004**, *43*, 5883–5886, *Angew. Chem.* **2004**, *116*, 6007–6010.

[7] a) M. Jesberger, T. P. Davis, L. Barner, *Synthesis* **2003**, *13*, 1929–1958; b) M. S. Foreman, J. D. Woollins, *J. Chem. Soc., Dalton Trans.* **2000**, 1533–1543; c) M. P. Cava, M. I. Levinson, *Tetrahedron* **1985**, *41*, 5061–5087; d) R. A. Cherkasov, G. A. Kutyre, A. N. Pudovik, *Tetrahedron* **1985**, *41*, 2567–2624.

[8] a) J. D. Woollins, *Synlett.* **2012**, 1154–1169, and references cited therein; b) G. Hua, J. D. Woollins, *Selenium and Tellurium Chemistry: From Small Molecules to Biomolecules and Materials*, Springer, Heidelberg, **2011**, Ch.1, 1–39; c) L. Ascherl, A. Nordheider, K. S. Athukorala Arachchige, A. M. Z. Slawin, J. D. Woollins, *Chem. Commun.* **2014**, *50*, 6214–6216.

[9] a) I. D. Sadekov, A. A. Maksimenko, V. L. Nivorozhkin, *Russ. Chem. Rev.* **1998**, *67*, 193–208; b) W.-W. du Mont, *Angew. Chem. Int. Ed.* **1980**, *19*, 554–555; *Angew. Chem.* **1980**, *92*, 562–563; c) T. Chivers, *J. Chem. Soc., Dalton Trans.* **1996**, 1185–1194; d) M. L. Steigerwald, T. Siegrist, S. M. Stuczynski, Y.-U. Kwon, *J. Am. Chem. Soc.* **1992**, *114*, 3155–3156; e) M. L. Steigerwald, T. Siegrist, S. M. Stuczynski,

Inorg. Chem. **1991**, *30*, 2256–2257; f) M. L. Steigerwald, T. Siegrist, S. M. Stuczynski, *Inorg. Chem.* **1991**, *30*, 4940–4945.

[10] R. Davies, L. Patel, *Handbook of Chalcogen Chemistry: New Perspectives in Sulfur, Selenium and Tellurium",* 2nd Edn., *RSC Publishing*, **2013**, Vol.1, Ch. 5, 238–306.

[11] B. Wrackmeyer, E. V. Klimkina; W. Milius, *Eur. J. Inorg. Chem.* **2014**, 4865–4876

[12] B. Bildstein, F. Sladky, *Phosphorus, Sulfur, and Silicon* **1990,** *47*, 341–347.

[13] F. Dornhaus, M. Bolte, H.-W. Lerner, M. Wagner, *Eur. J. Inorg. Chem.* **2006**, 5138–5147.

[14] C. Marquardt, A. Adolf, A. Stauber, M. Bodensteiner, A. V. Virovets, A.Y. Timoshkin, M. Scheer, *Chem. Eur. J.* **2013***, 19*, 11887–11891.

[15] a) C. Marquardt, C. Thoms, A. Stauber, G. Balázs, M. Bodensteiner, M. Scheer, *Angew. Chem. Int. Ed.* **2014**, *53*, 3727–3730; *Angew. Chem.* **2014**, *126*, 3801–3804; b) C. Marquardt, T. Jurca, K.-C. Schwan, A. Stauber, A. V. Virovets, G. R. Whittell, I. Manners, M. Scheer, *Angew. Chem. Int. Ed.* **2015**, *54*, 13782–13786; *Angew. Chem.* **2015**, *127*, 13986–13991; c) unpublished results, see chapter 6.

[16] K.-C. Schwan, A. Y. Timoskin, M. Zabel, M. Scheer, *Chem. Eur. J.* **2006**,*12*, 4900-4908.

[17] A broad base for the resonance signal is observed indicative for a phosphorus bound tellurium atom.

8.5 Supporting Information

General Experimental:

All manipulations were performed under an atmosphere of dry argon using standard glove-box and Schlenk techniques. All solvents are degassed and purified by standard procedures. The compounds $Ph_2P–BH_2·NMe_3$ and $^tBuHP–BH_2·NMe_3$ were prepared according to literature procedures.[1] S_8, Se_{red}, α-Te and $Me_3Si–O–O–SiMe_3$ were obtained from STREM Chemicals, INC. The NMR spectra were recorded on a Bruker Avance 400 spectrometer (^1H: 400.13 MHz, ^{31}P: 161.976 MHz, ^{11}B: 128.378 MHz, $^{13}C\{^1H\}$: 100.623 MHz) with δ [ppm] referenced to external $SiMe_4$ (^1H, ^{13}C), H_3PO_4 (^{31}P), $BF_3·Et_2O$ (^{11}B). IR spectra were measured on a DIGILAB (FTS 800) FT-IR spectrometer. All mass spectra were recorded on a Finnigan MAT 95 (EI-MS). The C, H, N analyses were measured on an Elementar Vario EL III apparatus.

Synthesis of $Ph_2P(O)–BH_2·NMe_3$ (3a):

To a solution of 130 mg (0.5 mmol) $Ph_2P–BH_2·NMe_3$ in 10 mL of CH_2Cl_2 0.11 mL (0.5 mmol) of $Me_3Si–O–O–SiMe_3$ are added at r.t. After stirring the mixture for one day, all volatiles are removed under reduced pressure. The remaining solid is dissolved in ca. 5mL of CH_2Cl_2 and over layered by 30 mL of *n*-hexane. **3a** crystallizes at r.t. as colourless blocks. The supernatant is decanted off; the resulting crystals are washed two times with *n*-hexane and dried under reduced pressure. Yield of $Ph_2P(O)–BH_2·NMe_3$ (**3a**): 98 mg (66 %). ^{1}H NMR (CD_2Cl_2, 25 °C): δ = 2.45 (q, $^1J_{H,B}$ ~ 110 Hz, 2H, BH_2), 2.78 (s, 9H, NMe_3), 7.30-7.40 (m, *m*-Ph & *p*-Ph, 6H), 7.70-7.80 (m, *o*-Ph, 4H). ^{31}P NMR (CD_2Cl_2, 25 °C): δ = 36.44 (q, $^1J_{B,P}$ = 125 Hz, PPh_2). ^{31}P{^{1}H} NMR (CD_2Cl_2, 25 °C): δ = 36.44 (q, $^1J_{B,P}$ = 125 Hz, PPh_2). ^{11}B NMR (CD_2Cl_2, 25 °C): δ = –9.36 (pseudo-q, $^1J_{B,P}$ = 125 Hz, BH_2, $^1J_{B,H}$ ~ 110 Hz, BH_2). ^{11}B{^{1}H} NMR (CD_2Cl_2, 25 °C): δ = –9.36 (d, $^1J_{B,P}$ = 125 Hz, BH_2). ^{13}C{^{1}H} NMR (CD_2Cl_2, 25 °C): δ = 54.7 (d, $^3J_{P,C}$ = 7 Hz, NMe_3), 128.34 (d, $^3J_{P,C}$ = 10 Hz, *m*-Ph), 129.78 (d, $^4J_{P,C}$ = 2 Hz, *p*-Ph), 130.38 (d, $^2J_{P,C}$ = 9 Hz, *o*-Ph), 141.46 (d, $^1J_{P,C}$ = 62 Hz, *i*-Ph). IR (KBr): $\tilde{\nu}$ = 3069 (w, CH), 3042 (w, CH), 3013 (w, CH), 2998 (w, CH), 2942 (w, CH), 2918 (w, CH), 2414 (s, BH), 2392 (s, BH), 2298 (vw), 1483 (s), 1462 (s), 1445 (m), 1435 (s), 1406 (vw), 1302 (vw), 1252 (w), 1150 (s), 1140 (vs), 1127 (vs), 1102 (s), 1070 (s), 1061 (s), 1020 (w), 1008 (w), 990 (w), 970 (w), 867 (s), 765 (w), 744 (vs), 730 (m), 706 (vs), 645 (m), 542 (vs), 499 (s), 471 (w), 441 (w). EI-MS (toluene): *m/z* = 273 (4.8 %, $[M]^+$), 258 (1.7 %, $[M\text{-Me}]^+$). Elemental analysis (%) calculated for $C_{15}H_{21}B_1N_1O_1P_1$ (**3a**): C: 65.90, H: 7.75, N: 5.13; found: C: 65.60, H: 7.61, N: 5.02.

Synthesis of $Ph_2P(S)–BH_2·NMe_3$ (3b):

To a solution of 257 mg (1 mmol) $Ph_2P–BH_2·NMe_3$ in 10 mL of CH_2Cl_2 32 mg (1 mmol) of S_8 are added at r.t.. After stirring the mixture for one day, the solution is filtrated and the solution is concentrated under reduced pressure until the first crystals appear. The solution is allowed to reach r.t. again. **3b** crystallises at -28°C as colourless blocks. The supernatant is decanted off; the resulting crystals are washed two times with *n*-hexane and dried under reduced pressure. Yield of $Ph_2P(S)–BH_2·NMe_3$ (**3b**): 157 mg (54 %). ^{1}H NMR (CD_2Cl_2, 25 °C): δ = 2.66 (q, $^1J_{H,B}$ ~ 106 Hz, 2H, BH_2), 2.82 (d, $^4J_{H,P}$ ~ 2 Hz 9H, NMe_3), 7.32-7.40 (m, *m*-Ph & *p*-Ph, 6H), 7.90-7.99 (m, *o*-Ph, 4H). ^{31}P NMR (CD_2Cl_2, 25 °C): δ = 20.72 (q, $^1J_{B,P}$ = 102 Hz, PPh_2). ^{31}P{^{1}H} NMR (CD_2Cl_2, 25 °C): δ = 20.72 (q, $^1J_{B,P}$ = 102 Hz, PPh_2). ^{11}B NMR (CD_2Cl_2, 25 °C): δ = –8.04 (pseudo-q, $^1J_{B,P}$ = 102 Hz, BH_2, $^1J_{B,H}$ ~ 106 Hz, BH_2). ^{11}B{^{1}H} NMR (CD_2Cl_2, 25 °C): δ = –8.04 (d, $^1J_{B,P}$ = 102 Hz, BH_2). ^{13}C{^{1}H} NMR (CD_2Cl_2, 25 °C): δ = 54.4 (d, $^3J_{P,C}$ = 6 Hz, NMe_3), 128.30 (d, $^3J_{P,C}$ = 11 Hz, *m*-Ph), 129.85 (d, $^4J_{P,C}$ = 2 Hz, *p*-Ph), 131.50 (d, $^2J_{P,C}$ = 9 Hz, *o*-

Ph), 138.30 (d, $^1J_{P,C}$ = 52 Hz, *i*-Ph). IR (KBr): $\tilde{\nu}$ = 3065 (w, CH), 3042 (w, CH), 3018 (w, CH), 2999 (w, CH), 2945 (w, CH), 2438 (s, BH), 2407 (s, BH), 2292 (vw), 1977 (vw), 1927 (vw), 1838 (vw), 1690 (vw), 1617 (vw), 1567 (vw), 1479 (vs), 1464 (s), 1435 (vs), 1406 (w), 1309 (w), 1247 (m), 1179 (w), 1151 (m), 1121 (vs), 1091 (s), 1069 (vs), 1010 (m), 973 (m), 867 (s), 761 (s), 750 (s), 702 (vs), 660 (vs), 574 (vs), 517 (s), 490 (s), 460 (m), 417 (w), 430 (m). EI-MS (toluene): *m/z* = 289 (69.6 %, $[M]^+$), 257 (2.9 %, $[M\text{-S}]^+$), 185 (18.2 %, $[M\text{-S-BH}_2\cdot\text{NMe}_3]^+$), 72 (100 %, $[M\text{-Ph}_2\text{PS}]^+$). Elemental analysis (%) calculated for $C_{15}H_{21}B_1N_1S_1P_1$ (**3b**): C: 62.26, H: 7.32, N: 4.84; found: C: 61.95, H: 7.26, N: 4.62.

Synthesis of $Ph_2P(Se)–BH_2\cdot NMe_3$ (3c):

To a solution of 130 mg (0.5 mmol) $Ph_2P–BH_2\cdot NMe_3$ in 10 mL of CH_2Cl_2 40 mg (0.5 mmol) of Se_{red} are added at r.t. After stirring the mixture for one day, the solution is filtrated and the solution is concentrated under reduced pressure until the first crystals appear. The solution is allowed to reach r.t. again. **3c** crystallises at -28°C as colourless blocks. The supernatant is decanted off; the resulting crystals are washed two times with *n*-hexane and dried under reduced pressure. Yield of $Ph_2P(Se)–BH_2\cdot NMe_3$ (**3c**): 65 mg (38 %). ^{1}H NMR (CD_2Cl_2, 25 °C): δ = 2.79 (q, $^1J_{H,B}$ ~ 103 Hz, 2H, BH_2), 2.82 (d, $^4J_{H,P}$ ~ 1 Hz 9H, NMe_3), 7.32-7.39 (m, *m*-Ph & *p*-Ph, 6H), 7.91-8.01 (m, *o*-Ph, 4H). ^{31}P NMR (CD_2Cl_2, 25 °C): δ = 5.30 (q, $^1J_{B,P}$ = 93 Hz, $^1J_{P,Se}$ = 600 Hz, PPh_2). $^{31}P\{^1H\}$ NMR (CD_2Cl_2, 25 °C): δ = 5.30 (q, $^1J_{B,P}$ = 93 Hz, $^1J_{P,Se}$ = 600 Hz, PPh_2). ^{11}B NMR (CD_2Cl_2, 25 °C): δ = –7.76 (pseudo-q, $^1J_{B,P}$ = 93 Hz, $^1J_{B,H}$ ~ 103 Hz, BH_2). $^{11}B\{^1H\}$ NMR (CD_2Cl_2, 25 °C): δ = –7.76 (d, $^1J_{B,P}$ = 93 Hz, BH_2). $^{13}C\{^1H\}$ NMR (CD_2Cl_2, 25 °C): δ = 54.54 (d, $^3J_{P,C}$ = 6 Hz, NMe_3), 128.31 (d, $^3J_{P,C}$ = 10 Hz, *m*-Ph), 129.95 (d, $^4J_{P,C}$ = 3 Hz, *p*-Ph), 132.38 (d, $^2J_{P,C}$ = 9 Hz, *o*-Ph), 136.13 (d, $^1J_{P,C}$ = 49 Hz, *i*-Ph). IR (KBr): $\tilde{\nu}$ = 3046 (w, CH), 3015 (w, CH), 2998 (w, CH), 2945 (w, CH), 2921 (w, CH), 2584 (vw, CH), 2436 (s, BH), 2408 (m, BH), 2290 (vw), 1978 (vw), 1921 (vw), 1835 (vw), 1631 (vw), 1479 (vs), 1465 (s), 1435 (vs), 1406 (w), 1308 (w), 1248 (m), 1179 (m), 1150 (m), 1121 (s), 1067 (vs), 1009 (m), 974 (m), 867 (s), 759 (s), 751 (s), 700 (vs), 636 (m), 520 (vs), 489 (s). LIFDI-MS (toluene): *m/z* = 337 (100 %, $[M]^+$). Elemental analysis (%) calculated for $C_{15}H_{21}B_1N_1Se_1P_1$ (**3c**): C: 53.40, H: 6.28, N: 4.15; found: C: 53.60, H: 6.28, N: 4.04.

Synthesis of $Ph_2P(Te)–BH_2\cdot NMe_3$ (3d):

To a solution of 130 mg (0.5 mmol) $Ph_2P–BH_2\cdot NMe_3$ in 10 mL of CH_2Cl_2 65 mg (0.5 mmol) of α-Te are added at r.t. After stirring the mixture for three days, the solution is filtrated and the volume of the solvent is evaporated under reduced pressure until the first crystals appear. The solution is allowed to reach r.t. again and over layered by 30

mL of *n*-hexane. **3d** crystallises at r.t. as yellow blocks. The supernatant is decanted off; the resulting crystals are washed two times with *n*-hexane and dried under reduced pressure. Yield of $Ph_2P(Te)–BH_2·NMe_3$ (**3d**): 90 mg (46 %). ^{1}H NMR (CD_2Cl_2, 25 °C): δ = 2.81 (d, $^4J_{H,P}$ ~ 2 Hz 9H, NMe_3), 2.94 (q, $^1J_{H,B}$ ~ 103 Hz, 2H, BH_2), 7.30-7.40 (m, *m*-Ph & *p*-Ph, 6H), 7.86-7.98 (m, *o*-Ph, 4H). ^{31}P NMR (CD_2Cl_2, 25 °C): δ = –47.36 (m, PPh_2). $^{31}P\{^1H\}$ NMR (CD_2Cl_2, 25 °C): δ = –47.36 (m, PPh_2). ^{11}B NMR (CD_2Cl_2, 25 °C): δ = –6.94 (pseudo-q, $^1J_{B,P}$ = 86 Hz, BH_2, $^1J_{B,H}$ ~ 103 Hz, BH_2). $^{11}B\{^1H\}$ NMR (CD_2Cl_2, 25 °C): δ = –9.36 (d, $^1J_{B,P}$ = 86 Hz, BH_2). $^{13}C\{^1H\}$ NMR (CD_2Cl_2, 25 °C): δ = 55.03 (d, $^3J_{P,C}$ = 6 Hz, NMe_3), 128.37 (d, $^3J_{P,C}$ = 10 Hz, *m*-Ph), 130.07 (d, $^4J_{P,C}$ = 3 Hz, *p*-Ph), 133.70 (d, $^2J_{P,C}$ = 9 Hz, *o*-Ph), 134.16 (d, $^1J_{P,C}$ = 43 Hz, *i*-Ph). IR (KBr): $\tilde{\nu}$ = 3044 (w, CH), 3014 (w, CH), 2998 (w, CH), 2944 (w, CH), 2433 (s, BH), 2407 (s, BH), 1971 (vw), 1917 (vw), 1828 (vw), 1777 (vw), 1681 (vw), 1610 (vw), 1582 (vw), 1478 (vs), 1464 (s), 1434 (vs), 1404 (m), 1309 (m), 1247 (m), 1180 (m), 1150 (m), 1121 (s), 1066 (vs), 1011 (m), 971 (m), 867 (s), 754 (s), 749 (s), 698 (vs), 630 (m), 512 (vs), 488 (m), 470 (m), 450 (s), 425 (w). EI-MS (toluene): *m/z* = 387 (8.1 %, $[M]^+$), 257 (50.1 %, $[M\text{-Te}]^+$), 72 (100 %, $[M\text{-}Ph_2PTe]^+$). Elemental analysis (%) calculated for $C_{15}H_{21}B_1N_1Te_1P_1$ (**3d**): C: 46.50, H: 5.46, N: 3.61; found: C: 46.78, H: 5.47, N: 3.57.

Synthesis of ^{t}BuHP(O)–BH_2·NMe_3 (4a):

To a solution of 80 mg (0.5 mmol) ^{t}BuHP–BH_2·NMe_3 in 10 mL of CH_2Cl_2 0.11 mL (0.5 mmol) of $Me_3Si–O–SiMe_3$ are added at r.t. After stirring the mixture for one day, all volatiles are removed under reduced pressure. The remaining solid is dissolved in a mixture of ca. 2mL toluene and over layered by 20 mL of *n*-hexane. After filtration **4a** crystallises at -28°C as colourless blocks. The supernatant is decanted off; the resulting crystals are washed two times with *n*-hexane and dried under reduced pressure. Yield of ^{t}BuHP(O)–BH_2·NMe_3 (**4a**): 55 mg (62 %). ^{1}H NMR (C_6D_6, 25 °C): δ = 1.26 (d, $^3J_{H,P}$ = 14 Hz, 9H ^{t}Bu), 2.06 (m, 2H, BH_2), 2.23 (s, 9H, NMe_3), 6.77 (dd, $^1J_{H,P}$ = 344 Hz, $^3J_{H,H}$ = 5 Hz, 1H, PH). ^{31}P NMR (C_6D_6, 25 °C): δ = 57.14 (m, $^1J_{B,P}$ = 115 Hz, $^1J_{H,P}$ = 344 Hz, P^{t}BuH). $^{31}P\{^1H\}$ NMR (C_6D_6, 25 °C): δ = 57.14 (q, $^1J_{B,P}$ = 115 Hz, P^{t}BuH). ^{11}B NMR (C_6D_6, 25 °C): δ = –10.77 (pseudo-q, $^1J_{B,P}$ = 115 Hz, $^1J_{B,H}$ ~ 103 Hz, BH_2). $^{11}B\{^1H\}$ NMR (C_6D_6, 25 °C): δ = –10.77 (d, $^1J_{B,P}$ = 115 Hz, BH_2). $^{13}C\{^1H\}$ NMR (C_6D_6, 25 °C): δ = 24.67 (d, $^2J_{P,C}$ = 2 Hz, C**Me**$_3$), 31.46 (d, $^1J_{P,C}$ = 48 Hz, **C**Me$_3$), 53.27 (d, $^3J_{P,C}$ = 6 Hz, NMe_3). IR (KBr): $\tilde{\nu}$ = 3011 (m, CH), 2960 (s, CH), 2944 (s, CH), 2900 (s, CH), 2863 (s, CH), 2400 (s, BH), 2381 (s, BH), 2300 (m, BH), 2242 (s, PH), 2209 (s, PH), 2090 (w), 1810 (w), 1650 (w), 1489 (s), 1474 (s), 1461 (s), 1407 (m), 1389 (m), 1361 (s), 1253 (s), 1204 (w), 1155 (s), 1138 (s), 1107 (s), 1076 (s), 1026 (s), 1014 (s), 986 (s), 946 (m), 906 (s), 867 (s), 817 (s), 736 (m), 718 (m), 645 (s), 611 (s), 487 (s), 448 (w), 425 (w). EI-MS

(toluene): *m/z* = 176 (1.5 %, $[M]^+$), 160 (0.4 %, $[M\text{-O}]^+$), 120 (100 %, $[M\text{-}^t\text{Bu}]^+$), 72 (32.9 %, $[M\text{-}^t\text{BuHPO}]^+$). Elemental analysis (%) calculated for $C_7H_{21}B_1N_1O_1P_1$ (**4a**): C: 47.42, H: 11.95, N: 7.90; found: C: 47.48, H: 11.79, N: 7.89.

Synthesis of ^{t}BuHP(S)–BH$_2$·NMe$_3$ (4b):

To a solution of 80 mg (0.5 mmol) ^{t}BuHP–BH$_2$·NMe$_3$ in 10 mL of CH_2Cl_2 16 mg (0.05 mmol) of S_8 are added at r.t. After stirring the mixture for one day, all volatiles are removed under reduced pressure. The remaining solid is dissolved in a mixture of ca. 2mL toluene and over layered by 20 mL of *n*-hexane. After filtration, **4b** crystallises at -28°C as colourless blocks. The supernatant is decanted off; the resulting crystals are washed two times with *n*-hexane and dried under reduced pressure. Yield of ^{t}BuHP(S)–BH$_2$·NMe$_3$ (**4b**): 32 mg (33 %). ^{1}H NMR (C_6D_6, 25 °C): δ = 1.32 (d, $^3J_{H,P}$ = 15 Hz, 9H, ^{t}Bu), 2.08 (m, 2H, BH$_2$), 2.18 (s, 9H, NMe$_3$), 5.80 (ddd, $^1J_{H,P}$ = 355 Hz, $^3J_{H,H}$ = 9 Hz, $^3J_{H,H}$ = 3 Hz, 1H, PH). ^{31}P NMR (C_6D_6, 25 °C): δ = 27.91 (dq, $^1J_{B,P}$ = 96 Hz, $^1J_{H,P}$ = 355 Hz, P^{t}BuH). ^{31}P{^{1}H} NMR (C_6D_6, 25 °C): δ = 27.91 (q, $^1J_{B,P}$ = 96 Hz, P^{t}BuH). ^{11}B NMR (C_6D_6, 25 °C): δ = –10.70 (pseudo-q, $^1J_{B,P}$ = 96 Hz, $^1J_{B,H}$ ~ 106 Hz, BH$_2$). ^{11}B{^{1}H} NMR (C_6D_6, 25 °C): δ = –10.70 (d, $^1J_{B,P}$ = 96 Hz, BH$_2$). ^{13}C{^{1}H} NMR (C_6D_6, 25 °C): δ = 25.93 (d, $^2J_{P,C}$ = 2 Hz, C**Me**$_3$), 31.43 (d, $^1J_{P,C}$ = 38 Hz, **C**Me$_3$), 52.85 (d, $^3J_{P,C}$ = 6 Hz, NMe$_3$). IR (KBr): $\tilde{\nu}$ = 3003 (w, CH), 2973 (m, CH), 2942 (s, CH), 2924 (m, CH), 2898 (m, CH), 2862 (m, CH), 2431 (s, BH), 2391 (m, BH), 2281 (m, PH), 1488 (m), 1473 (s), 1458 (m), 1408 (w), 1398 (w), 1390 (w), 1361 (m), 1249 (m), 1194 (w), 1157 (m), 1123 (vs), 1076 (vs), 1017 (s), 976 (m), 956 (w), 911 (s), 863 (vs), 813 (m), 706 (w), 669 (s), 610 (w), 554 (s), 483 (w). EI-MS (toluene): *m/z* = 193 (43.4 %, $[M]^+$), 136 (11,5 %, $[M\text{-}^t\text{Bu}]^+$), 72 (100 %, $[M\text{-}\ ^t\text{BuHPS}]^+$). Elemental analysis (%) calculated for $C_7H_{21}B_1N_1P_1S_1$ (**4b**): C: 43.50, H: 10.96, N: 7.25; found: C: 43.53, H: 10.79, N: 7.21.

Synthesis of ^{t}BuHP(Se)–BH$_2$·NMe$_3$ (4c):

To a solution of 80 mg (0.5 mmol) ^{t}BuHP–BH$_2$·NMe$_3$ in 10 mL of CH_2Cl_2 40 mg (0.5 mmol) of Se_{red} are added at r.t. After stirring the yellow solution for one day, all volatiles are removed under reduced pressure. The remaining solid is dissolved in a mixture of ca. 2mL toluene and over layered by 20 mL of *n*-hexane. After filtration **4c** crystallises at -28°C as colourless blocks. The supernatant is decanted off; the resulting crystals are washed two times with *n*-hexane and dried under reduced pressure. Yield of ^{t}BuHP(Se)–BH$_2$·NMe$_3$ (**4c**): 61 mg (51 %). ^{1}H NMR (C_6D_6, 25 °C): δ = 1.33 (dd, $^3J_{H,P}$ = 16 Hz, $^4J_{H,H}$ = 1 Hz, 9H, ^{t}Bu), 2.20 (m, 2H, BH$_2$), 2.21 (s, 9H, NMe$_3$), 5.12 (ddd, $^1J_{H,P}$ = 352 Hz, $^3J_{H,H}$ = 9 Hz, $^3J_{H,H}$ = 3 Hz, 1H, PH). ^{31}P NMR (C_6D_6, 25 °C): δ = 4.92 (dq, $^1J_{B,P}$ = 87 Hz, $^1J_{H,P}$ = 352 Hz, P^{t}BuH). ^{31}P{^{1}H} NMR (C_6D_6, 25 °C): δ = 4.92 (q, $^1J_{P,Se}$ = 582 Hz, $^1J_{B,P}$ =

87 Hz, P^{t}BuH). ^{11}B NMR (C_6D_6, 25 °C): δ = –10.95 (pseudo-q, $^1J_{B,P}$ = 87 Hz, $^1J_{B,H}$ ~ 108 Hz, BH_2). $^{11}B\{^1H\}$ NMR (C_6D_6, 25 °C): δ = –10.95 (d, $^1J_{B,P}$ = 87 Hz, BH_2). $^{13}C\{^1H\}$ NMR (C_6D_6, 25 °C): δ = 26.60 (d, $^2J_{P,C}$ = 2 Hz, C**Me**$_3$), 29.43 (d, $^1J_{P,C}$ = 33 Hz, **C**Me$_3$), 52.99 (d, $^3J_{P,C}$ = 6 Hz, NMe_3). IR (KBr): $\tilde{\nu}$ = 3009 (m, CH), 2998 (w, CH), 2973 (m, CH), 2964 (s, CH), 2942 (s, CH), 2925 (m, CH), 2898 (m, CH), 2862 (m, CH), 2825 (w, CH), 2797 (w, CH), 2419 (s, BH), 2400 (s, BH), 2385 (s, BH), 2298 (s, PH), 2187 (w), 2138 (w), 2080 (w), 2027 (w), 1485 (s), 1474 (s), 1462 (s), 1434 (m), 1404 (s), 1388 (w), 1361 (s), 1248 (s), 1207 (w), 1179 (w), 1154 (s), 1119 (s), 1073 (s), 1016 (s), 975 (s), 957 (w), 942 (w), 887 (s), 861 (s), 829 (w), 811 (s), 697 (w), 639 (s), 599 (m), 467 (s), 440 (w), 420 (w), 406 (w). EI-MS (toluene): *m/z* = 241 (27.3 %, $[M]^+$), 72 (100 %, $[M-{}^t\text{BuHPSe}]^+$). Elemental analysis (%) calculated for $C_7H_{21}B_1N_1P_1Se_1$ (**4c**): C: 34.84, H: 8.78, N: 5.81; found: C: 35.19 H: 8.75, N: 5.79.

Synthesis of ^{t}BuHP(Te)–BH_2·NMe_3 (4d):

To a solution of 80 mg (0.5 mmol) ^{t}BuHP–BH_2·NMe_3 in 10 mL of toluene 65 mg (0.5 mmol) of α-Te are added at r.t. The yellow solution is stirred for one day and a green solid precipitates. All volatiles are removed under reduced pressure. The remaining solid is dissolved in a mixture of ca. 2mL toluene and over layered by 20 mL of *n*-hexane. **4d** crystallises at -28°C as colourless plates. The supernatant is decanted off; the resulting crystals are washed two times with *n*-hexane and dried under reduced pressure. Yield of ^{t}BuHP(Te)–BH_2·NMe_3 (**4d**): 74 mg (54 %). ^{1}H NMR (C_6D_6, 25 °C): δ = 1.33 (d, $^3J_{H,P}$ = 16 Hz, 9H, ^{t}Bu), 2.11 (s, 9H, NMe_3), 2.30 (m, 2H, BH_2), 4.30 (ddd, $^1J_{H,P}$ = 345 Hz, $^3J_{H,H}$ = 10 Hz, $^3J_{H,H}$ = 4 Hz, 1H, PH). ^{31}P NMR (C_6D_6, 25 °C): δ = -60.87 (m, $^1J_{H,P}$ = 345 Hz, P^{t}BuH). $^{31}P\{^1H\}$ NMR (C_6D_6, 25 °C): δ = -60.87 (m, P^{t}BuH). ^{11}B NMR (C_6D_6, 25 °C): δ = –11.06 (pseudo-q, $^1J_{B,P}$ = 76 Hz, $^1J_{B,H}$ ~ 109 Hz, BH_2). $^{11}B\{^1H\}$ NMR (C_6D_6, 25 °C): δ = –11.06 (d, $^1J_{B,P}$ = 76 Hz, BH_2). $^{13}C\{^1H\}$ NMR (C_6D_6, 25 °C): δ = 26.74 (d, $^1J_{P,C}$ = 28 Hz, **C**Me$_3$), 27.61 (d, $^2J_{P,C}$ = 3 Hz, C**Me**$_3$), 53.25 (d, $^3J_{P,C}$ = 6 Hz, NMe_3). IR (KBr): $\tilde{\nu}$ = 3015 (w, CH), 2999 (w, CH), 2976 (m, CH), 2942 (m, CH), 2922 (m, CH), 2897 (m, CH), 2861 (m, CH), 2425 (s, BH), 2392 (s, BH), 2304 (m, PH), 1637 (w), 1485 (m), 1466 (m), 1458 (m), 1408 (w), 1388 (w), 1360 (m), 1251 (m), 1194 (w), 1156 (m), 1122 (s), 1074 (vs), 1017 (m), 978 (w), 957 (w), 859 (s), 842 (s), 810 (w), 680 (w), 630 (w), 591 (w), 480 (w), 438 (w). EI-MS (solid): *m/z* = 291 (9.5 %, $[M]^+$), 232 (1.1 %, $[M-{}^t\text{BuH}]^+$), 161 (20.5 %, $[M\text{-Te}]^+$), 72 (100 %, $[M-{}^t\text{BuHPTe}]^+$). Elemental analysis (%) calculated for $C_7H_{21}B_1N_1P_1Te_1$ (**4d**): C: 28.86, H: 7.27, N: 4.81; found: C: 29.02, H: 7.10, N: 4.74.

Synthesis of ^{t}Bu(HO)P(O)–BH$_2$·NMe$_3$ (5a):

To a solution of 80 mg (0.5 mmol) ^{t}BuHP–BH$_2$·NMe$_3$ in 5 mL of toluene 0.22 mL (1 mmol) of Me$_3$Si–O–O–SiMe$_3$ are added at r.t. After stirring the mixture for one day, only **4a** is obtained. All volatiles are removed under reduced pressure. The remaining solid is dissolved in 5 mL toluene and freezed with liquid N_2. The flask is evacuated and flooded with pure O_2. After stirring the mixture for 1h, the procedure is repeated. The turbid solution is stirred for 18 h. After removal of all volatiles under reduced pressure **5a** is obtained as a white powder.

Alternatively **5a** can also be obtained from the direct reaction of **2** with pure O_2 according to the procedure mentioned above. The remaining white solid is dissolved in CH_2Cl_2 and after filtration **5a** crystallises at r.t. as colourless blocks by slow evaporation of the solvent. The supernatant is decanted off; the resulting crystals are washed two times with *n*-hexane and benzene and dried under reduced pressure. Yield of ^{t}Bu(HO)P(O)–BH$_2$·NMe$_3$ (**5a**): 55 mg (57 %). ^{1}H NMR ($CDCl_3$, 25 °C): δ = 1.06 (d, $^{3}J_{H,P}$ = 14 Hz, 9H ^{t}Bu), 1.97 (m, 2H, BH$_2$), 2.87 (s, 9H, NMe$_3$), 11.74 (s, br, 1H, OH). ^{31}P NMR ($CDCl_3$, 25 °C): δ = 90.7 (m, br, P^{t}BuH). ^{31}P{^{1}H} NMR ($CDCl_3$, 25 °C): δ = 90.7 (q, br, P^{t}BuH). ^{11}B NMR ($CDCl_3$, 25 °C): δ = –11.4 (m, BH$_2$). ^{11}B{^{1}H} NMR ($CDCl_3$, 25 °C): δ = –11.4 (d, $^{1}J_{B,P}$ = 142 Hz, BH$_2$). ^{13}C{^{1}H} NMR (C_6D_6, 25 °C): δ = 24.0 (d, $^{2}J_{P,C}$ = 2 Hz, C**Me**$_3$), 33.9 (d, $^{1}J_{P,C}$ = 57 Hz, **C**Me$_3$), 54.3 (d, $^{3}J_{P,C}$ = 7 Hz, NMe$_3$). IR (KBr): $\tilde{\nu}$ = 3015 (w, CH), 2970 (s, CH), 2954 (m, CH), 2925 (w, CH), 2901 (w, CH), 2885 (w, CH), 2417 (s, BH), 2386 (m, BH), 2304(w), 1715 (m, br), 1472 (m), 1410 (w), 1388 (w), 1358 (w), 1251 (m), 1198 (vw), 1157 (s), 1139 (m), 1102 (s), 1075 (s), 1012 (m), 978 (m), 913 (s), 863 (s), 818 (s), 732 (m), 653 (s), 623 (s), 519 (s), 478 (w), 441 (w). FD-MS (CH_2Cl_2): *m/z* = 193 (100 %, [*M*]$^{+}$). Even after several reproductions the compounds could not be obtained analytically pure. Elemental analysis (%) calculated for $C_7H_{21}B_1N_1O_2P_1$ (**5a**): C: 43.49, H: 10.96, N: 7.25; found: C: 42.31, H: 10.44, N: 7.14.

Synthesis of ^{t}Bu(HS)P(S)–BH$_2$·NMe$_3$ (5b):

To a solution of 80 mg (0.5 mmol) ^{t}BuHP–BH$_2$·NMe$_3$ in 10 mL of toluene 32 mg (1.0 mmol) of S_8 are added at r.t.. After stirring the mixture for 18 h, all volatiles are removed under reduced pressure. The obtained viscous oil is dissolved in 20 mL of *n*-hexane and filtrated over diatomaceous earth. Storing of the solution at –80°C leads to precipitation as a white solid. The supernatant is decanted off and the resulting white powder is washed two times with –80°C cold *n*-hexane and dried under reduced pressure. **5b** is obtained as colourless oil at room temperature. Yield of ^{t}Bu(HS)P(S)–BH$_2$·NMe$_3$ (**5b**): 40 mg (36 %). ^{1}H NMR (C_6D_6, 25 °C): δ = 1.44 (d, $^{3}J_{H,P}$ = 17 Hz, 9H, ^{t}Bu), 1.84 (s, 1H, SH), 2.20 (m, 2H, BH$_2$), 2.22 (s, 9H, NMe$_3$). ^{31}P NMR (C_6D_6, 25 °C): δ = 83.3 (m, br,

P^{t}BuH). ^{31}P{^{1}H} NMR (C_6D_6, 25 °C): δ = 83.3 (q, $^1J_{B,P}$ = 97 Hz, P^{t}BuH). ^{11}B NMR (C_6D_6, 25 °C): δ = –8.2 (pseudo-q, $^1J_{B,P}$ = 97 Hz, BH_2). ^{11}B{^{1}H} NMR (C_6D_6, 25 °C): δ = –8.2 (d, $^1J_{B,P}$ = 97 Hz, BH_2). ^{13}C{^{1}H} NMR (C_6D_6, 25 °C): δ = 24.5 (d, $^2J_{P,C}$ = 3 Hz, C**Me**$_3$), 38.0 (d, $^1J_{P,C}$ = 29 Hz, **C**Me$_3$), 52.7 (d, $^3J_{P,C}$ = 6 Hz, NMe$_3$). IR (KBr): $\tilde{\nu}$ = 2966 (m), 2945 (m), 2921 (m), 2898 (w), 2864 (w), 2805 (vw), 2441 (s, BH), 2411 (m, BH), 2307 (w), 2202 (vw), 2153 (vw), 1487 (m), 1456 (m), 1409 (w), 1386 (w), 1359 (m), 1253 (m), 1187 (w), 1159 (m), 1127 (s), 1080 (vs), 1017 (m), 976 (w), 872 (m), 804 (w), 746 (w), 664 (s), 604 (m), 560 (vs), 488 (w), 472 (w), 428 (w). FD-MS (CH_2Cl_2): *m/z* = 225 (100 %, [*M*]$^+$), 448 (60 %, [*M*-H]$_2^+$), 480 (16 %, [(*M*-H)$_2$S]$^+$). Elemental analysis (%) calculated for $C_7H_{21}B_1N_1P_1S_2$ (**5b**): C: 37.31, H: 9.40, N: 6.22, S: 28.4; found: C: 37.01, H: 9.10, N: 6.15, S 28.65.

Attempted Synthesis of ^{t}Bu(HSe)P(Se)–BH$_2$·NMe$_3$ (5c):

I) To a solution of 80 mg (0.5 mmol) ^{t}BuHP–BH_2·NMe_3 in 10 mL of toluene 80 mg (1.0 mmol) of Se_{red} are added at r.t.. After stirring the orange solution for 18 h, all volatiles are removed under reduced pressure.

II) To a solution of 50 mg (0.31 mmol) ^{t}BuHP–BH_2·NMe_3 in 7 mL of toluene 24 mg (0.3 mmol) of Se_{grey} are added at r.t.. After stirring the colourless solution for 18h, all volatiles are removed under reduced pressure. The isolated **4c** (46 mg, 0.2 mmol) is dissolved again in 7 mL of toluene and added to 15 mg (0.2 mmol) of Se_{grey}, the solution is stirred for 18 h upon which it turns slightly yellow.

III) To a solution of 50 mg (0.31 mmol) ^{t}BuHP–BH_2·NMe_3 in 7 mL of toluene 24 mg (0.3 mmol) of Se_{red} are added at r.t.. After stirring the colourless solution for 18 h another 24 mg (0.2 mmol) of Se_{red} are added. The solution is stirred for 18 h upon which it turns yellow.

All approaches give essentially the same results. However, route II) and III) in which the second equivalent of Se were added to **4c** yield most of the desired product **5c**.
Yield of ^{t}Bu(HSe)P(Se)–BH$_2$·NMe$_3$ (**5c**): 51% by ^{31}P NMR. ^{31}P NMR (C_6D_6, 25 °C): δ = 59.6 (m, br). ^{31}P{^{1}H} NMR (C_6D_6, 25 °C): δ = 59.6 (q, $^1J_{B,P}$ = 82 Hz, P^{t}BuH). FD-MS (CH_2Cl_2): *m/z* = 320 (27%, [*M*]$^+$), 636 (100 %, [*M*-H]$_2^+$), 716 (19 %, [(*M*-H)$_2$Se] $^+$), 954 (8 %, [M_2Se_4] $^+$).

X-ray diffraction analysis

The X-ray diffraction experiments were performed on either a Gemini R Ultra CCD diffractometer (**3a**, **3c**, **4d**, **4z, 5c)**, GV1000 (**4a-4c**) or a SuperNova(Mo) EOS CCD diffractometer (**3b, 3d**) from Agilent Technologies (formerly Oxford Diffraction) applying

Cu-K_α radiation (λ = 1.54178 Å) or Mo-K_α radiation (λ = 0.71073 Å). Crystallographic data together with the details of the experiments are given below. Data collection, cell refinement, data reduction and absorption corrections were performed with the CrysAlis PRO software by Agilent Technologies Ltd).[2] All structures were solved using OLEX 2[9c], SHELXT and SHELXS.[3] Refinements against F^2 in anisotropic approximation were done using SHELXL.[3] The hydrogen positions of the methyl groups were located geometrically and refined riding on the carbon atoms. Hydrogen atoms belonging to BH_2 and PH_2 groups were located from the difference Fourier map and refined without constraints (**3a, 3c, 4b, 2z, 5a**) or with restrained B–H and P–H distances (**3b, 3d, 4a, 4c, 4d**) or SADI for disorder in **4a**. All crystals of **3c** showed twinning, they were refined applying hklf5 refinement. Figures were created with OLEX 2.[4] CIF files are deposited on the provided DVD.

Table S1. Crystallographic data for compounds **3a** and **3b**

Compound	**3a**	**3b**
empirical formula	$C_{15}H_{21}BNOP$	$C_{15}H_{21}BNPS$
formula weight	273.11	289.17
temperature [K]	123(1)	253(1)
crystal system	monoclinic	orthorhombic
space group	*Cc*	$P2_12_12_1$
a [Å]	14.1159(2)	8.8629(4)
b [Å]	8.94230(10)	10.2958(5)
c [Å]	11.7656(2)	17.4692(7)
α [°]	90	90
β [°]	90.997(2)	90
γ [°]	90	90
Volume [Å^3]	1484.93(4)	1594.08(12)
Z	4	4
ρ_{calc} [g/cm^3]	1.222	1.205
μ [mm^{-1}]	1.552	0.290
F (000)	584.0	616.0
crystal size [mm^3]	0.3601 × 0.3132 × 0.2066	0.3631 × 0.3115 × 0.1901
radiation	CuK_α (λ = 1.54178)	MoK_α (λ = 0.71073)
absorption correction	analytical	analytical
T_{min} / T_{max}	0.723 / 0.803	0.919 / 0.953
2Θ range [°]	11.714 to 133.142	6.066 to 64.734
completeness	0.989	0.998
index ranges	-16 ≤ *h* ≤ 16 -7 ≤ *k* ≤ 10 -14 ≤ *l* ≤ 10	-12 ≤ *h* ≤ 13 -15 ≤ *k* ≤ 15 -26 ≤ *l* ≤ 12
reflections collected	2841	13253
independent reflections	1768 [R_{int} = 0.0262, R_{sigma} = 0.0331]	5238 [R_{int} = 0.0361, R_{sigma} = 0.0529]
data/restraints/ parameters	1768/2/183	5238/2/183
GOF on F^2	1.055	1.061
R_1/wR_2 [I≥2σ(*I*)]	R_1 = 0.0314, wR_2 = 0.0823	R_1 = 0.0467, wR_2 = 0.0896
R_1/wR_2 [all data]	R_1 = 0.0320, wR_2 = 0.0828	R_1 = 0.0650, wR_2 = 0.1013
max/min $\Delta\rho$ [e·Å^{-3}]	0.21 / -0.27	0.31 / -0.21
flack parameter	-0.03(2)	-0.02(5)

Table S2. Crystallographic data for compounds **3c** and **3d**

Compound	**3c**	**3d**
empirical formula	$C_{15}H_{21}BNPSe$	$C_{15}H_{21}BNPTe$
formula weight	336.07	384.71
temperature [K]	123(1)	253(1)
crystal system	monoclinic	monoclinic
space group	$P2_1/c$	$P2_1/c$
a [Å]	10.125(5)	10.3229(3)
b [Å]	8.995(5)	9.1162(2)
c [Å]	17.632(5)	18.1336(4)
α [°]	90.000	90
β [°]	99.393(5)	97.753(2)
γ [°]	90.000	90
Volume [Å^3]	1584.3(13)	1690.87(7)
Z	4	4
ρ_{calc} [g/cm^3]	1.409	1.511
μ [mm^{-1}]	4.029	1.841
F (000)	688.0	760.0
crystal size [mm^3]	0.23 × 0.18 × 0.17	0.29 × 0.24 × 0.19
radiation	CuK_α (λ = 1.54178)	MoK_α (λ = 0.71073)
absorption correction	analytical	analytical
T_{min} / T_{max}	0.531 / 0.618	0.683 / 0.760
2Θ range [°]	8.852 to 134.176	5.986 to 65.05
completeness	0.996	0.999
index ranges	-12 ≤ *h* ≤ 11 -10 ≤ *k* ≤ 10 -20 ≤ *l* ≤ 20	-15 ≤ *h* ≤ 14 -13 ≤ *k* ≤ 13 -27 ≤ *l* ≤ 26
reflections collected	4888	20261
independent reflections	4888 [R_{int} = 0.0397, R_{sigma} = 0.0144]	5676 [R_{int} = 0.0445, R_{sigma} = 0.0459]
data/restraints/parameters	4888/0/184	5676/2/183
GOF on F^2	1.043	1.064
R_1/wR_2 [I≥2σ(*I*)]	R_1 = 0.0387, wR_2 = 0.1117	R_1 = 0.0391, wR_2 = 0.0721
R_1/wR_2 [all data]	R_1 = 0.0406, wR_2 = 0.1135	R_1 = 0.0641, wR_2 = 0.0853
max/min $\Delta\rho$ [e·Å^{-3}]	0.87 / -0.91	0.84 / -0.97

Table S3. Crystallographic data for compounds **4a** and **4b**

Compound	**4a**	**4b**
empirical formula	$C_7H_{21}BNOP$	$C_7H_{21}BNPS$
formula weight	177.03	193.09
temperature [K]	123(1)	123(1)
crystal system	monoclinic	monoclinic
space group	$P2_1/c$	$P2_1/c$
a [Å]	11.5762(8)	14.142(5)
b [Å]	9.3826(4)	7.505(5)
c [Å]	11.7519(8)	11.223(5)
α [°]	90	90.000
β [°]	117.018(9)	92.886(5)
γ [°]	90	90.000
Volume [Å^3]	1137.11(15)	1189.7(10)
Z	4	4
ρ_{calc} [g/cm^3]	1.034	1.078
μ [mm^{-1}]	1.773	3.264
F (000)	392.0	424.0
crystal size [mm^3]	0.28 × 0.20 × 0.13	0.33 × 0.11 × 0.05
radiation	CuK_α (λ = 1.54178)	CuK_α (λ = 1.54178)
absorption correction	analytical	analytical
T_{min} / T_{max}	0.744 / 0.814	0.556 / 0.847
2Θ range [°]	8.574 to 147.708	6.258 to 146.578
completeness	0.992	0.988
index ranges	-14 ≤ *h* ≤ 13 -10 ≤ *k* ≤ 11 -12 ≤ *l* ≤ 14	-17 ≤ *h* ≤ 16 -6 ≤ *k* ≤ 8 -13 ≤ *l* ≤ 11
reflections collected	5040	3725
independent reflections	2205 [R_{int} = 0.0258, R_{sigma} = 0.0318]	2269 [R_{int} = 0.0284, R_{sigma} = 0.0385]
data /restraints/parameters	2205/4/132	2269/0/118
GOF on F^2	1.068	1.044
R_1/wR_2 [I≥2σ(*I*)]	R_1 = 0.0523, wR_2 = 0.1435	R_1 = 0.0310, wR_2 = 0.0774
R_1/wR_2 [all data]	R_1 = 0.0600, wR_2 = 0.1531	R_1 = 0.0369, wR_2 = 0.0820
max/min $\Delta\rho$ [e·Å^{-3}]	0.34 / -0.32	0.38 / -0.24

Table S4. Crystallographic data for compounds **4c** and **4d**

Compound	**4c**	**4d**
empirical formula	$C_7H_{21}BNPSe$	$C_7H_{21}BNPTe$
formula weight	239.99	288.63
temperature [K]	123(1)	123(1)
crystal system	monoclinic	orthorhombic
space group	$P2_1/c$	$Pca2_1$
a [Å]	14.2187(3)	15.8116(3)
b [Å]	7.58340(13)	7.08283(14)
c [Å]	11.3458(2)	22.3794(6)
α [°]	90	90
β [°]	93.5571(17)	90
γ [°]	90	90
Volume [Å^3]	1221.02(4)	2506.28(9)
Z	4	8
ρ_{calc} [g/cm^3]	1.305	1.530
μ [mm^{-1}]	4.992	19.547
F (000)	496.0	1136.0
crystal size [mm^3]	0.24 × 0.20 × 0.14	0.73 × 0.14 × 0.03
radiation	CuK_α (λ = 1.54178)	CuK_α (λ = 1.54178)
absorption correction	analytical	gaussian
T_{min} / T_{max}	0.477 / 0.615	0.051 / 0.0549
2Θ range [°]	6.228 to 147.3	6.844 to 133.73
completeness	1.000	0.995
index ranges	-14 ≤ *h* ≤ 17 -9 ≤ *k* ≤ 9 -14 ≤ *l* ≤ 9	-18 ≤ *h* ≤ 11 -8 ≤ *k* ≤ 8 -26 ≤ *l* ≤ 26
reflections collected	6816	16595
independent reflections	2401 [R_{int} = 0.0303, R_{sigma} = 0.0288]	4243 [R_{int} = 0.0519, R_{sigma} = 0.0414]
data/restraints/ parameters	2401/3/118	4243/7/220
GOF on F^2	1.062	1.031
R_1/wR_2 [I≥2σ(*I*)]	R_1 = 0.0272, wR_2 = 0.0714	R_1 = 0.0399, wR_2 = 0.1000
R_1/wR_2 [all data]	R_1 = 0.0293, wR_2 = 0.0736	R_1 = 0.0502, wR_2 = 0.1080
max/min $\Delta\rho$ [e·Å^{-3}]	0.53 / -0.38	1.21 / -0.99
flack parameter	-	-0.002(10)

Table S5. Crystallographic Data for compounds **2z** and **5a**

Compound	**2z**	**5a**
empirical formula	$C_{17}H_{50}B_2Cl_8N_2P_2$	$C_7H_{21}BNO_2P$
formula weight	649.75	193.03
temperature [K]	123(1)	123(1)
crystal system	monoclinic	monoclinic
space group	$P2_1/c$	$P2_1/c$
a [Å]	17.6626(7)	11.1493(3)
b [Å]	9.5940(3)	10.02901(16)
c [Å]	22.0625(9)	11.2694(2)
α [°]	90	90
β [°]	109.812(4)	114.171(3)
γ [°]	90	90
Volume [Å^3]	3517.3(3)	1149.62(4)
Z	4	4
ρ_{calc} [g/cm^3]	1.227	1.115
μ [mm^{-1}]	6.786	1.860
F (000)	1368.0	424.0
crystal size [mm^3]	0.27 × 0.13 × 0.05	0.41 × 0.2 × 0.19
radiation	CuK_α (λ = 1.54178)	CuK_α (λ = 1.54184)
absorption correction	multi-scan	gaussian
T_{min} / T_{max}	0.254 / 1.000	0.600 / 0.786
2Θ range [°]	8.376 to 134.352	8.694 to 133.474
completeness	0.960	0.991
index ranges	-16 ≤ *h* ≤ 20 -11 ≤ *k* ≤ 11 -25 ≤ *l* ≤ 26	-13 ≤ *h* ≤ 13 -11 ≤ *k* ≤ 11 -13 ≤ *l* ≤ 13
reflections collected	16640	8282
independent reflections	6029 [R_{int} = 0.0609, R_{sigma} = 0.0604]	2019 [R_{int} = 0.0232, R_{sigma} = 0.0184]
data/restraints/parameters	6029/0/331	2019/0/124
GOF on F^2	1.008	1.078
R_1/wR_2 [I≥2σ(*I*)]	R_1 = 0.0488, wR_2 = 0.1188	R_1 = 0.0270, wR_2 = 0.0776
R_1/wR_2 [all data]	R_1 = 0.0683, wR_2 = 0.1328	R_1 = 0.0294, wR_2 = 0.0787
max/min $\Delta\rho$ [e·Å^{-3}]	0.33 / -0.54	0.43 / -0.24

References

[1] C. Marquardt, T. Jurca, K.-C. Schwan, A. Stauber, A. V. Virovets, G. R. Whittell, I. Manners, M. Scheer, *Angew. Chem. Int. Ed.* **2015**, *54*, 13782–13786; *Angew. Chem.* **2015**, *127*, 13986–13991.

[2] Agilent Technologies **2006-2011**, CrysAlisPro Software system, different versions, Agilent Technologies UK Ltd, Oxford, UK.

[3] G. M. Sheldrick, *Acta Cryst.* **2008**, *A64*, 112–122.

[4] O.V. Dolomanov, L.J. Bourhis, R.J. Gildea, J.A.K. Howard, H.Puschmann, OLEX2: A complete structure solution, refinement and analysis program, *J. Appl. Cryst*. **2009**, 42, 339–341.

8.6 Author Contributions

The syntheses and characterization of **3a-3d** and **4a-4d**, as well as **2z** were performed by Christian Marquardt.

Tobias Kahoun is gratefully acknowledged for contributions to the syntheses of **4a**-**4d** during a research course under the supervision of Christian Marquardt.

The syntheses and characterization of **5a-5c** were performed by Oliver Hegen.

X-ray structural analyses of all compounds were performed by Christian Marquardt.

The manuscript (including supporting information, figures, schemes and graphical abstract) was written by Christian Marquardt.

9. Isolation and characterization of Lewis Base stabilized monomeric parent Stibanylboranes

C. Marquardt, O. Hegen, M. Hautmann, G. Balázs, M. Bodensteiner, A. V. Virovets, A. Y. Timoshkin and M. Scheer

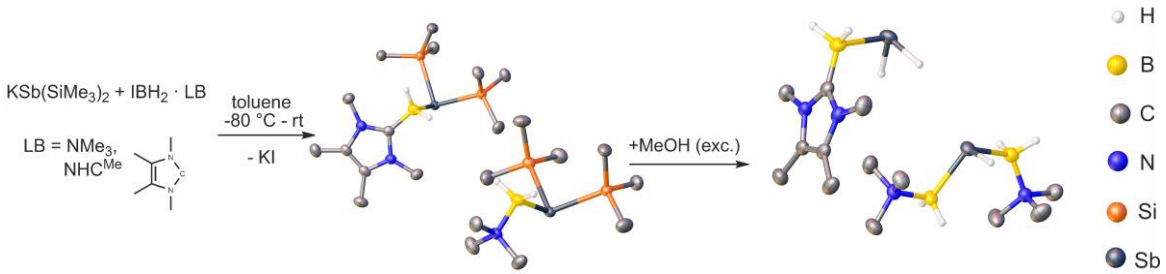

Abstract: The synthesis of the Lewis base stabilized monomeric parent compound of stibanylboranes, "$H_2Sb–BH_2$", is reported. Through a salt metathesis route the silyl-substituted compounds $(Me_3Si)_2Sb–BH_2·LB$ (LB = NMe_3, NHC^{Me}) were synthesized as representatives of derivatives with a Sb-B σ-bond. Under very mild conditions, they could be transformed into the target compounds $Me_3N·H_2B–HSb–BH_2·NMe_3$ and $H_2Sb–BH_2·NHC^{Me}$, respectively. The products were characterized by X-ray structure analysis, NMR spectroscopy, IR spectroscopy and mass spectrometry. DFT calculations give further insight into the stability and bonding of these unique compounds.

9.1 Introduction

Binary group 13/15 compounds have been extensively investigated in recent decades owing to their interesting physical properties, particularly their semiconducting properties. Because of their narrow direct bandgaps (from 0.17 eV for InSb to 3.44 eV for GaN), they are potential candidates for applications in micro- and optoelectronic devices. Combination with even more group 13/15 elements facilitates tuning of the band gaps, thereby leading to ternary and quarternary materials.[1] The hitherto unknown BSb compound in particular might possess some interesting features for optoelectric devices.[2,3,4] However, examples for compounds with a direct Sb–B bond are very rare. Besides the three Lewis acid/base adducts of the type $X_3B{\cdot}Sb(SiMe_3)_3$ (X = Cl, Br or I)[5] and the stibaborane cluster *closo*-1,1-$(Me_2PPh)_2$-1,2,3-$PdSb_2B_9H_9$[6] no well-defined molecular stibaboranes have been isolated so far. The published $(H_3C)_2Sb\text{-}BH_2$,[7] obtained by reaction of $(H_3C)_2SbBr$ with $NaBH_4$, later proved to be a mixture of $(H_3C)_3Sb$, $(H_3C)_2SbH$ and B_5H_9.[8] Reactive main-group compounds like the elusive $H_2N–BH_2$ can be stabilized applying donor-acceptor complexation,[9] in the coordination sphere of transition metals,[10] or with support of strong donors like N-Heterocyclic carbenes.[11] In our group we are especially interested in the stabilization of the monomeric parent compounds of the type $H_2E–E'H_2$ (E = group 15 atom, E' = group 13 atom). We initially discovered the synthesis of the Lewis base stabilized phosphanylborane $H_2P–BH_2{\cdot}NMe_3$[12] through the photochemically induced elimination of $W(CO)_5$ from $(CO)_5W{\cdot}H_2P–BH_2{\cdot}NMe_3$ in the presence of $P(OMe)_3$. Subsequently, we found that a salt metathesis reaction between $LiE(SiMe_3)_2{\cdot}2thf$ (E = P, As) and $ClBH_2{\cdot}NMe_3$ in boiling *n*-hexane yielded $(Me_3Si)_2E–BH_2{\cdot}NMe_3$, which could then be transformed into the parent compounds by methanolysis, thereby enabling the generation of $H_2As–BH_2{\cdot}NMe_3$ for the first time.[13] The first route is restricted to the phosphanylborane while the second route can also be used for the arsanylborane but could not be transferred to the heavier stibanylborane analogue. In this context, the extreme thermal instability of primary stibines containing small substituents is well known.[14] Simple primary stibines (Scheme 1, **A**)[15,16] decompose within minutes or hours at room temperature.[17] Primary stibines, which are sufficiently stable at ambient temperatures require sterically demanding substituents like neopentyl (Me_3CCH_2)[18] or $CH(SiMe_3)_2$[19] (Scheme 1, **B**), and have to be stored in the dark. For $(Me_3Si)_2CHSbH_2$ it was possible to investigate its coordination behavior.[20] Sterically crowded substituents like 9-Trypticenyl (Scheme 1, **C**)[21] or terphenyl (Scheme 1, **D**)[22] lead to primary stibines which are stable up to 195°C. Herein we present a selective synthesis of the stibanylboranes $H_2Sb–BH_2{\cdot}LB$ as the first stable

primary stibines without a bulky substituent and the first stibanylboranes with a σ-bond between the two elements.

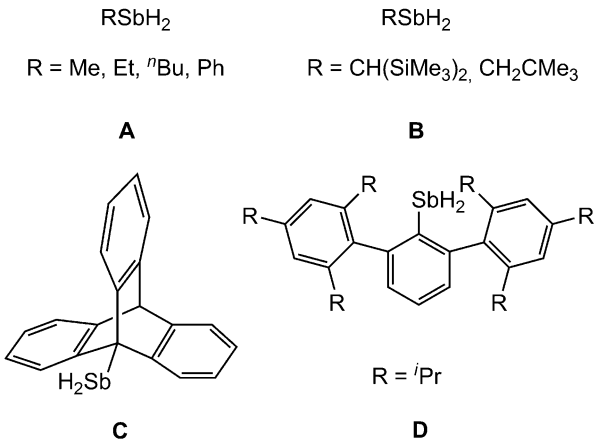

Scheme 1. Examples of primary stibines.

9.2 Results and Discussion

DFT calculations[23] (Table 1) show, that stronger donors significantly weaken the E–B bond (E = group 15 element) of the pnictogenylboranes. This is in part a reflection of a greater stabilization of radical BH_2 species by stronger Lewis bases. The B–Sb bond energy of approximately 162-264 kJ mol^{-1} is sufficiently strong for compounds containing this bond to be isolable. However, the monomeric parent compound $H_2Sb–BH_2·LB$ has not yet been obtained.

Table 1. Standard dissociation enthalpies ΔH^o_{298} in kJ mol^{-1} for homolytic B-E bond breaking processes. B3LYP/def2-TZVPP level of theory.

process	N	P	As	Sb	Bi
$H_2EBH_2 = H_2E•+•BH_2$	576	355	314	264	234
$H_2EBH_2·NMe_3 = H_2E•+•BH_2·NMe_3$	441	300	271	231	207
$H_2EBH_2·NHC^{Me} = H_2E•+•BH_2·NHC^{Me}$	309	210	189	162	155

(NHC^{Me} = 1,3,4,5-tetramethylimidazolylidene)

When the iodo-derivative is used instead of $ClBH_2·NMe_3$ in the reaction with $KSb(SiMe_3)_2$, the salt metathesis occurs already at low temperatures (Scheme 2). Therefore, by using $IBH_2·NMe_3$ and $IBH_2·NHC^{Me}$ (NHC^{Me} = 1,3,4,5-tetramethyl-imidazolylidene), respectively, the silylated stibanylboranes $(Me_3Si)_2Sb–BH_2·LB$ (**1**: LB = NMe_3 (63%), **2**: LB = NHC^{Me} (57%)) were obtained in good yields. Compound **1** and **2** can easily be isolated by extraction with *n*-hexane, followed by crystallization at -28°C.

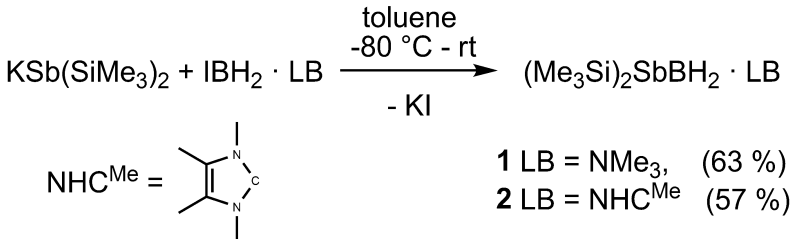

Scheme 2. Synthesis of silylated stibanylboranes **1** and **2**. Yield in parentheses.

Apart from the already mentioned Lewis acid/base adducts,[65] compounds **1** and **2** are the first examples for compounds with a well-defined 2-center-2-electron-σ-bond between antimony and boron. In the EI-MS spectra the molecular ion peak is detected for **1** and **2**. The IR spectra of **1** and **2** show absorptions for the B–H stretches between 2306 cm^{-1} and 2406 cm^{-1}. The ^{11}B NMR spectra reveal signals at δ = –8.5 ppm (**1**) and –39.0 ppm (**2**), which split into triplets with typical $^{1}J_{B,H}$ coupling constants (**1**: $^{1}J_{B,H}$ = 114 Hz, **2**: $^{1}J_{B,H}$ = 103 Hz). The solid state structures of the stibanylboranes (Figure 1) show a bond length of 2.295(6) Å for the Sb–B-bonds of **1** and 2.350(2) Å for those of **2**. The values are in good agreement with the calculated sum of the covalent radii of boron and antimony ($\sum r_{cov}$(Sb,B) = 2.29 Å).[24] Compound **1** shows a similar E–B–N bond angle to that of $(Me_3Si)_2E–BH_2·NMe_3$ (E = P, As)[13] and also adopts a *syn-periplanar* arrangement (for $SiMe_3$- and H-substituents, view along Sb–B-axis), whereas **2** deviates slightly from the *syn-periplanar* arrangement.

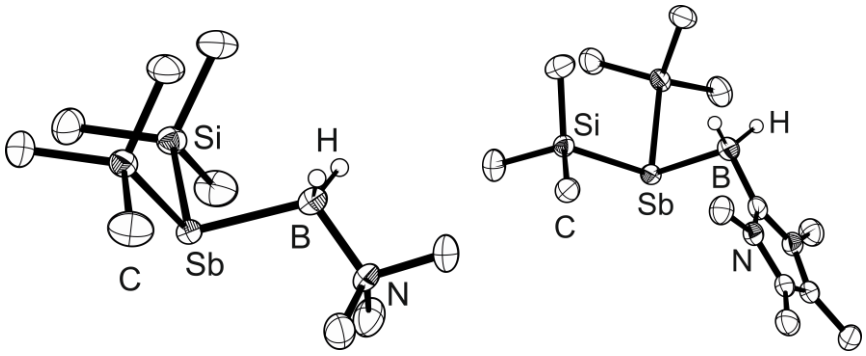

Figure 1. Molecular structure of **1** (left) and **2** (right) in the solid state. Thermal ellipsoids are drawn with 50% probability. Hydrogen atoms on methyl groups are omitted for clarity.[25]

Subsequent methanolysis of **1** and **2**, at low temperatures, however, leads to the monomeric parent compound of the stibanylboranes, $H_2Sb–BH_2·LB$ (Scheme 3).

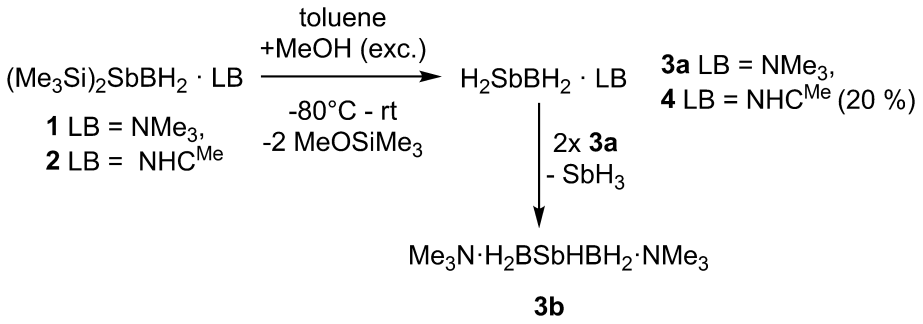

Scheme 3. Methanolyis of the silylated stibanylboranes **1** and **2**. Yield in parentheses.

In the case of **1** even with a large excess of methanol and a long reaction time, complete cleavage of the $SiMe_3$ groups does not occur, although DFT studies suggest that methanolysis reactions of both **1** and **2** are highly exothermic and exergonic (by more than 180 kJ mol^{-1} at 298 K). The stibanylborane $H_2Sb–BH_2·NMe_3$ (**3a**) can be observed in the ^1H and ^{11}B NMR spectra ($\delta(^1H)$ = –0.78 ppm, SbH_2), however only about 50% of the $SiMe_3$ groups of **1** are cleaved and a mixture of **1, 3a** and other not assignable reaction products are obtained. All attempts to isolate **3a** from the reaction mixture failed because decomposition occurs. Numerous attempts were made to isolate **3a**. Instead, a few crystals of $Me_3N·H_2B–HSb–BH_2·NMe_3$ (**3b**) were obtained and characterized by X-ray structure analysis. The decomposition pathway of **3a** is not known, but we suppose, that **3a** is generated concomitantly with the elimination of SbH_3 to yield the secondary stibine **3b**. This assumption is further supported by precipitation of elemental antimony. Computations show that reaction 2 **3a** (sol) = SbH_3 (g) + **3b** (sol) in toluene is exergonic by 12 kJ mol^{-1} at 298 K. In the ^1H NMR spectrum of the mixture a signal centered at δ = –2.45 ppm was tentatively attributed to the SbH-group in **3b**. The central structural motif of **3b** is the B–Sb–B-backbone. In the solid state structure of **3b** one of the two Sb–B subunits adopts an *antiperiplanar* conformation, whereas the second subunit shows a *synclinal* conformation, leading to a dihedral angle defined by the two N–Sb–B units of 32.3(3)°. The Sb–B bond lengths of 2.291(4) Å and 2.297(4) Å are identical to the starting material **1** (2.295(6) Å). Compound **3b** is a neutral species and is reminiscent of the recently discovered cationic chains of pnictogenylboranes.[26]

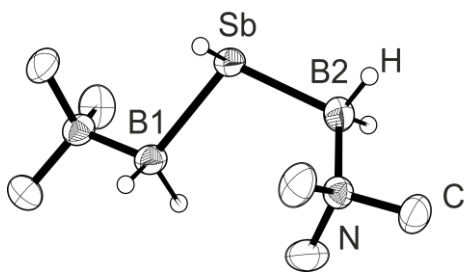

Figure 2. Structure of **3b** in the solid state. Thermal ellipsoids are drawn with 50% probability. Hydrogen atoms on methyl groups are omitted for clarity.[25]

Reacting the NHC^{Me} stabilized species **2** with an excess of methanol leads to the formation of the monomeric parent compound $H_2Sb–BH_2·NHC^{Me}$ (**4**), which can be isolated as a colourless solid in 20% yield. Compound **4** is highly unstable and decomposes already during crystallization into elemental antimony (most likely through SbH_3 elimination)[27] and the borane adduct $BH_3·NHC^{Me}$. Besides the high sensitivity towards moisture and oxygen, decomposition of **4** is readily induced by exposure to light and temperatures above -30°C. DFT computations show that reaction **4**(g) = Sb (s) + $BH_3·NHC^{Me}$ (g) + ½H_2 (g) is exergonic by 133 kJ mol^{-1} at 298 K. The stibanylborane **4** represents the first example of Lewis Base stabilized monomeric parent compound of a stibanylborane. In the ^{1}H NMR spectrum of **4** the signal for the SbH_2 group arises at δ = –0.96 ppm as a pseudo-triplet due to the coupling to the boranyl moiety which arises as a broad quartet at δ = 2.44 ppm. This was further confirmed by ^{1}H,^{1}H COSY NMR experiments, which clearly indicate cross-peaks for the $^3J_{H,H}$ coupling between the H atoms of the SbH_2 and BH_2 groups. The ^{11}B NMR spectrum of **4** shows a signal at δ = –38.6 ppm, which splits into a triplet ($^1J_{B,H}$ = 103 Hz). In the EI-MS spectra the molecular ion peak can be detected for **4**. The IR spectra of **4** reveals absorptions for the B–H stretches between 2395 cm^{-1} and 2281 cm^{-1} and a very prominent absorption for the Sb–H stretches at 1818 cm^{-1} (1870 cm^{-1} for $Me_3CCH_2SbH_2$[18] and 1860 cm^{-1} for $(Me_3Si)_2CHSbH_2$[19]). Crystals of **4** were obtained by storing a *n*-hexane solution at -28°C. In the solid state, stibanylborane **4** shows (Figure 3) a staggered arrangement for the substituents around the Sb–B moiety (lone pair at the Sb atom is in an *antiperiplanar* conformation respective to NHC^{Me}). The parent compounds $H_2E–BH_2·NMe_3$ (E = P, As) show the same conformation of the lone pair at the pnictogen-atom and the Lewis base.[12,13] Calculations on stabilized pnictogenylboranes have shown, that the energy difference to the *synperiplanar* conformation calculated for the gas phase are very small (6 – 7 kJ mol^{-1}), and that the found conformation originates most probably from packing effects in the solid state.[28] The Sb–B bond distance is 2.318(2) Å and therefore within the expected range for a Sb–B single bond ($\sum r_{cov}$(Sb,B) = 2.29 Å,[24] calculated Sb–B bond length for compound **4** is 2.3448 Å[23]). It is slightly shorter compared to the starting material **2** (2.350(2) Å) and similar to the Sb–B bond distances of **1** (2.295(6) Å) and the adducts $X_3B·Sb(SiMe_3)_3$ (X = Cl, Br or I, 2.257(8) – 2.268(17) Å).[65]

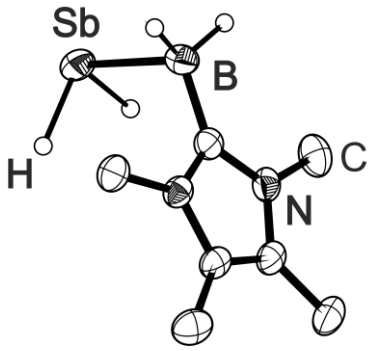

Figure 3. Molecular structure of **4** in the solid state. Thermal ellipsoids are drawn with 50% probability. Hydrogen atoms on methyl groups are omitted for clarity.[29]

9.3 Conclusion

In summary, by using $IBH_2{\cdot}LB$ (LB = NMe_3, NHC^{Me}), a direct synthesis and isolation of a series of stable stibanylboranes was achieved. The silylsubstituted compounds **1** and **2** are unique representatives with a well-defined 2-center-2-electron-σ-bond between antimony and boron. Furthermore, it was possible for the first time to synthesize, isolate and comprehensively characterize the Lewis base stabilized monomeric parent compound **4** of the stibanylboranes, "H_2SbBH_2". This compound represents a unique primary stibine without a bulky substituent as usually needed for stable primary stibines. Furthermore, the diboranylstibine **3b** was obtained as a decomposition product of the primary stibine, revealing a first longer neutral B-Sb-B chain.

9.4 References

[1] S. Schulz, *Adv. Organomet. Chem.* **2003**, *49,* 225–316.

[2] E. Deligoz, K. Colakoglu, Y.O. Ciftci, *J. Ph. Chem. Solids* **2007**, *68*, 482–489.

[3] S. Bağci, S. Duman, H. M. Tütüncü, G. P. Srivastava*, Phys. Rev. B* **2009**, *79*, 125326.

[4] H. L. Zhuang, R. G. Hennig, *Appl. Phys. Lett.* **2012**, *101*, 153109.

[5] M. S. Lube, R. L. Wells, P. S. White, *Dalton Trans*. **1997**, 285–286.

[6] S. A. Jasper, Jr., S. Roach, J. N. Stipp, J. C. Huffman, L. J. Todd, *Inorg. Chem.* **1993**, *32,* 3072–3080.

[7] A. B. Burg, L. R. Grant, *J. Am. Chem. Soc.* **1959**, *81*, 1–5.

[8] A. B. Burg, *Inorg. Chem.* **1977**, *16*, 217–218.

[9] A. C. Malcolm, K. J. Sabourin, R. McDonald, M. J. Ferguson, E. Rivard, *Inorg. Chem.* **2012**, *51*, 12905−12916.

[10] G. Alcaraz, S. Sabo-Etienne, *Angew. Chem. Int. Ed.* **2010**, *49*, 7170–7179; *Angew. Chem.* **2010**, *122*, 7326–7335.

[11] a) N. E. Stubbs, T. Jurca, E. M. Leitao, C. H. Woodall, I. Manners, *Chem. Commun.* **2013**, *49*, 9098–9100, stabilization of reactive main group compounds by NHCs see for examples b) Y. Wang, G. H. Robinson, *Inorg. Chem.* **2014**, *53*, 11815–11832; c) Y. Wang, G. H. Robinson, *Dalton Trans.* **2012**, *41*, 337–345; d) Y. Wang, G. H. Robinson, *Inorg. Chem.* **2011**, *50*, 12326–12337; e) R. C. Fischer, P. P. Power, *Chem. Rev.* **2010**, *110*, 3877–3923; f) Y. Wang, M. Chen,Y. Xie, P. Wei, H. F. Schaefer III, P. von R. Schleyer, G. H. Robinson, *Nat. Chem.* **2015**, *7*, 509–513.

[12] K.-C. Schwan, A. Y. Timoskin, M. Zabel, M. Scheer, *Chem. Eur. J.* **2006**, *12*, 4900–4908.

[13] C. Marquardt, A. Adolf, A. Stauber, M. Bodensteiner, A. V. Virovets, A. Y. Timoshkin, M. Scheer, *Chem. Eur. J.* **2013**, *19*, 11887–11891.

[14] M. Brynda, *Coord. Chem. Rev.* **2005**, *249*, 2013–2034.

[15] A. L. Rheingold, P. Choudhury, M. F. El-Shazly, *Synth. React. Inorg. Met.-Org. Chem.,* **1978**, 8(5&6), 453–465.

[16] E. Wiberg, K. Mödritzer, *Z. Naturforschg.* **1957**, *12 b*, 128–130.

[17] M. Wieber, *Gmelin Handbook of Inorganic Chemistry*; Springer-Verlag: Berlin, **1981**; Sb Organoantimony Compounds.

[18] D. G. Hendershot, J. C. Pazik, A. D. Berry, *Chem. Mater.* **1992**, *4*, 833–837.

[19] G. Balázs, H. J. Breunig, E. Lork, W. Offermann, *Organometallics* **2001**, *20,* 2666–2668.

[20] G. Balázs, H. J. Breunig, E. Lork, S. Mason, *Organometallics* **2003**, *22,* 576–585.

[21] R. J. Baker, M. Brym, C. Jones, M. Waugh, *J. Organomet. Chem.* **2004**, *689*, 781–790.

[22] B. Twamley, C.-S. Hwang, N. J. Hardman, P. P. Power, *J. Organomet. Chem.* **2000**, *609*, 152–160.

[23] *cf.* SI for details.

[24] A. F. Hollemann, E. Wiberg, N. Wiberg, Lehrbuch der anorganischen Chemie, 102. Auflage, *de Gruyter*, Berlin, New York, **2007**.

[25] Hydrogen atoms at B and Sb atom were located from the difference Fourier map and refined freely (**2**, **3b**) or with restrained B-H-distances (**1**). See SI for further information.

[26] C. Marquardt, C. Thoms, A. Stauber, G. Balazs, M. Bodensteiner, M. Scheer, *Angew. Chem. Int. Ed.* **2014**, *53*, 3727–3730; *Angew. Chem.* **2014**, *126*, 3801–3804.

[27] Appearance of H_2 was detected in ^{1}H NMR spectrum at δ = 4.46 ppm in C_6D_6. See: G. R. Fulmer, A. J. M. Miller, N. H. Sherden, H. E. Gottlieb, A. Nudelman, B. M. Stoltz, J. E. Bercaw, K. I. Goldberg, *Organometallics* **2010**, *29*, 2176–2179.

[28] K.-C. Schwan, A. Adolf, C. Thoms, M. Zabel, Al. Y. Timoshkin, M. Scheer, *Dalton Trans.* **2008**, 5054–5058.

[29] The antimony atom is disordered over two positions. Only the major component (80%) is shown here; the second component shows a slightly shorter Sb-B bond length. Hydrogen atoms at Sb atom were located from the difference Fourier map and refined with restrained Sb-H-distances.See SI for further information.

9.5 Supporting Information

General Experimental:

All manipulations were performed under an atmosphere of dry argon using standard glove-box and Schlenk techniques. All solvents are degassed and purified by standard procedures. The compounds $IBH_2{\cdot}NMe_3$,[1] $IBH_2{\cdot}NHC^{Me}$[2] and $Sb(SiMe_3)_3$[3] were prepared according to literature procedures. Other chemicals were obtained from STREM Chemicals, INC. (KO^tBu) and Sigma-Aldrich (MeOH, dried over molecular sieve). Due to the high sensitive towards light all reaction vessels were covered in aluminium-foil. The NMR spectra were recorded on an Avance 400 spectrometer (^1H: 400.13 MHz, ^{11}B: 128.378 MHz, $^{13}C\{^1H\}$: 100.623 MHz) with δ [ppm] referenced to external $SiMe_4$ (^1H, ^{13}C) and $BF_3{\cdot}Et_2O$ (^{11}B). IR spectra were measured on a DIGILAB (FTS 800) FT-IR spectrometer. All mass spectra were recorded on a Finnigan MAT 95 (EI-MS). The C, H, N analyses were measured on an Elementar Vario EL III apparatus.

Synthesis of $(Me_3Si)_2SbK$:

To a solution of 7.3 g (21.4 mmol) $Sb(SiMe_3)_3$ in 60 mL of THF 2.4 g (21.2 mmol) of KO^tBu are added at -65°C over 20 minutes. The slightly brown solution turns orange as the solution is allowed to reach 0°C. The mixture is stirred for further 4 h, whereupon the solution turns further dark red. After removal of all volatiles under reduced pressure, the resulting solid is washed two times with *n*-hexanes and dried under reduced pressure. Yield of $(Me_3Si)_2SbK$: 5.8 g (89%): ^1H NMR (CD_3CN, 25 °C): δ = 0.25 (s, $SiMe_3$).^{13}C NMR (CD_3CN, 25 °C): δ = 10.15 (s, $SiMe_3$).

Synthesis of $(Me_3Si)_2SbBH_2{\cdot}NMe_3$ (1):

A solution of 199 mg (1.00 mmol) $IBH_2{\cdot}NMe_3$ in 10 mL toluene is added to a suspension of 305 mg (1.00 mmol) $KSb(SiMe_3)_2$ in 10 ml toluene at -80°C. The suspension is stirred for 18 h and allowed to reach temperature. After removal of all volatiles under reduced pressure, the remaining solid is extracted with 3 x 20 mL of of *n*-hexane and filtrated over diatomaceous earth. The solution is concentrated to 5 mL. At -28°C **1** crystallises as colourless needles. After removal of the mother liquor, the crystals are dissolved again in 5 mL of *n*-hexane and recrystallized again. Yield of $(Me_3Si)_2SbBH_2{\cdot}NMe_3$: 212 mg (63 %). ^1H NMR (C_6D_6, 25 °C): δ = 0.63 (s, 18H, $SiMe_3$), 1.97 (s, 9H, NMe_3), 3.00 (q, $^1J_{H,B}$ = 114 Hz, 2H, BH_2). ^{11}B NMR (C_6D_6, 25 °C): δ = –8.5 (t, $^1J_{B,H}$ = 114 Hz, BH_2). $^{11}B\{^1H\}$ NMR (C_6D_6, 25 °C): δ = –8.5 (s, BH_2). ^{13}C NMR (C_6D_6, 25 °C): δ = 4.30 (s, $SiMe_3$), 53.48 (s, NMe_3). IR (KBr): $\tilde{\nu}$ = 3003 (m, CH), 2999 (m, CH), 2955 (m, CH), 2943 (m, CH), 2885 (m, CH), 2388 (m, br, BH), 2363 (m, br, BH), 2293 (m), 2265 (w), 1637 (w, br), 1492 (m), 1463 (w), 1460 (vw), 1402 (w), 1239 (m), 1235 (m), 1135(m), 1111 (m), 1026 (s), 974 (w), 840 (vs, br), 743 (m),

686 (m), 617 (m), 540 (w), 460 (vw). EI-MS (solid): *m/z* = 339 (11%, $[M]^+$), 324 (1%, $[M–Me]^+$), 72 (100 %, $[M–Sb(SiMe_3)_2]^+$). Elemental analysis (%) calculated for $(Me_3Si)_2SbBH_2{\cdot}NMe_3$ (**1**): C: 31.85, H: 8.61, N: 4.12; found: C: 31.85, H: 8.57, N: 4.03.

Synthesis of $(Me_3Si)_2SbBH_2{\cdot}NHC^{Me}$ (2):

A solution of 264 mg (1.00 mmol) $IBH_2{\cdot}$ NHC^{Me} in 10 mL toluene is added to a suspension of 305 mg (1.00 mmol) $KSb(SiMe_3)_2$ in 10 ml toluene at -80°C. The suspension is stirred for 18 h and allowed to reach temperature. After removal of all volatiles under reduced pressure, the remaining solid is extracted with 5 x 10 mL of *n*-hexane and filtrated over diatomaceous earth. The solution is concentrated to 5 mL. At -28°C **2** crystallises as colourless blocks. After removal of the mother liquor, the crystals are washed 2 times with 5 mL of *n*-hexane at -28°C. The crystals are dissolved again in 5 mL of *n*-hexane and recrystallized again. Yield of $(Me_3Si)_2SbBH_2{\cdot}NHC^{Me}$: 230 mg (57 %). ^{1}H NMR (C_6D_6, 25 °C): δ = 0.67 (s, 18H, $SiMe_3$), 1.18 (s, 6H, C=C-Me_3), 2.45 (q, $^1J_{H,B}$ = 103Hz, 2H, BH_2), 3.08 (s, 6H, NMe). ^{11}B NMR (C_6D_6, 25 °C): δ = –39.03 (t, $^1J_{B,H}$ = 104 Hz, BH_2). $^{11}B\{^1H\}$ NMR (C_6D_6, 25 °C): δ = –39.03 (s, BH_2). ^{13}C NMR (C_6D_6, 25 °C): δ = 4.9 (s, $SiMe_3$), 8.8 (s, C=C-**Me**), 32.0 (s, N-**Me**) 122.8 (s, C=C), 170.9 (s, C-BH_2). IR (KBr): $\tilde{\nu}$ = 2944 (m, CH), 2887 (m, br), 2406 (m, br, BH), 2404 (m, BH), 2351 (m), 2306 (m), 1656 (m), 1471 (m), 1439 (m), 1397 (m), 1237 (s), 1160 (m), 1111 (w), 1066 (w), 922 (s), 828 (vs), 745 (m), 685 (s), 617 (s), 570 (w). EI-MS (solid): *m/z* = 404 (4%, $[M]^+$), 137 (100 %, $[M\text{-}Sb(SiMe_3)_2]^+$), 73 (47 %, $[SiMe_3]^+$). Elemental analysis (%) calculated for $(Me_3Si)_2SbBH_2{\cdot}NHC^{Me}$ (**2**): C: 38.60, H: 7.98, N: 6.93; found: C: 38.73, H: 8.09, N: 7.03.

Methanolysis of $(Me_3Si)_2SbBH_2{\cdot}NMe_3$ (1) – Generation of 3a and 3b:

A solution of 398 mg (2.00 mmol) $IBH_2{\cdot}NMe_3$ in 10 mL toluene is added to a suspension of 612 mg (2.00 mmol) $KSb(SiMe_3)_2$ in 20 ml toluene at -80°C. The suspension is stirred for 18 h and allowed to reach temperature. The suspension is cooled down again to -80°C and 1 mL (25 mmol) of MeOH is added. The mixture is allowed to reach room temperature and another 0.2 mL (5 mmol) of MeOH are added. After stirring for 20 minutes all volatiles are removed under reduced pressure and the remaining solid is extracted with 5 x 10 mL of *n*-hexane and filtrated over diatomaceous earth. Yield of **3a** and **3b**: isolation of **3a** and **3b** as a pure product and the determination of the yields was not possible. ^{1}H NMR (C_6D_6, 25 °C): δ = –0.78 (t, $^3J_{H,H}$ = 5 Hz, SbH_2, **3a**), –2.48 (t, $^3J_{H,H}$ = 7 Hz, SbH, **3b**), other signals overlap. ^{11}B NMR (C_6D_6, 25 °C): δ = –8.0 (t, $^1J_{B,H}$ = 113 Hz, BH_2, **3a**). $^{11}B\{^1H\}$ NMR (C_6D_6, 25 °C): δ = –8.0 (m, **3a**). The NMR spectras are inconclusive due to overlap of signals.

Synthesis of $H_2SbBH_2{\cdot}NHC^{Me}$ (4):

A solution of 528 mg (2.00 mmol) $IBH_2{\cdot}$ NHC^{Me} in 10 mL toluene is added to a suspension of 612 mg (2.00 mmol) $KSb(SiMe_3)_2$ in 20 ml toluene at -80°C. The suspension is stirred for 18 h and allowed to reach room temperature. The suspension is cooled down again to -80°C and 1 mL (25 mmol) of MeOH is added. The mixture is allowed to reach room temperature and another 0.2 mL (5 mmol) of MeOH are added. After stirring for 20 minutes all volatiles are removed under reduced pressure and the remaining solid is extracted with 5 x 10 mL of *n*-hexane and filtrated over diatomaceous earth. The solution is concentrated to 25 mL. At -28°C **4** crystallises as colourless blocks. After removal of the mother liquor, the crystals are washed 2 times with 5 mL of *n*-hexane at -40°C. Yield of $H_2SbBH_2{\cdot}NHC^{Me}$: 105 mg (20 %). ^{1}H NMR (C_6D_6, 25 °C): δ = –0.96 (t, $^3J_{H,H}$ = 7 Hz, 2H), 1.75 (s, 6H, C=C-Me_3), 2.44 (q, $^1J_{H,B}$ = 103 Hz, 2H, BH_2), 2.96 (s, 6H, NMe). ^{11}B NMR (C_6D_6, 25 °C): δ = –38.57 (t, $^1J_{B,H}$ = 103 Hz, BH_2). $^{11}B\{^1H\}$ NMR (C_6D_6, 25 °C): δ = –38.57 (s, BH_2). ^{13}C NMR (C_6D_6, 25 °C): δ = 7.8 (s, C=C-**Me**), 31.5 (s, N-**Me**) 122.7 (s, C=C). IR (KBr): $\tilde{\nu}$ = 2980 (w, CH), 2939 (m, CH), 2922 (m, CH), 2856 (w, CH), 2789 (w, CH), 2395 (s, br, BH), 2349 (m), 2281 (s, br, BH), 1818 (vs, SbH), 1654 (s), 1741 (vs), 1436 (vs), 1395 (vs), 1367 (m), 1226 (m), 1210 (m), 1157 (m), 1141 (s), 1103 (s), 1033 (w), 935 (s), 911 (m), 800 (m), 703 (w), 584 (w), 538 (w), 471 (w), 414 (w). EI-MS (solid): *m/z* = 260 (0.61%, $[M]^+$), 137 (100%, $[M\text{-}SbH_2]^+$),. Elemental analysis (%) calculated for $(C_7H_{16}N_2BSb)_{0.8}(C_7H_{15}N_2B)_{0.2}$ (**3**): C: 35.59, H: 6.74, N: 11.85; found: C: 35.88, H: 6.69, N: 11.46.

X-ray diffraction analysis

The single crystal X-ray diffraction experiments were performed on either a Gemini R Ultra CCD diffractometer (**1**, **2)**, SuperNova A CCD diffractometer (**3b**) or a SuperNova(Mo) Eos CCD diffractometer (**4**) from Agilent Technologies (formerly Oxford Diffraction) applying Cu-K_α radiation (λ = 1.54178 Å) or applying Mo-K_α radiation (λ = 0.71073 Å). All measurements were performed at 123 K. Crystallographic data together with the details of the experiments are given in the Tables 1 and 2 (see below). Absorption corrections were applied semi-empirically from equivalent reflections or analytically (SCALE3/ABSPACK algorithm implemented in CrysAlis PRO software by Agilent Technologies Ltd).[4] All structures were solved using SIR97[5], and OLEX 2.[9] Refinements against F^2 in anisotropic approximation were done using SHELXL.[6] The hydrogen positions of the methyl groups were located geometrically and refined riding on the carbon atoms. Hydrogen atoms belonging to BH_2 and SbH_2 groups were located from the difference Fourier map and refined without constraints (**2**, **3b**) or with restrained B–H distances (**1**) or SADI for Sb–H distances (**4**). Figures were created with OLEX 2.[7] CCDC-1406968-1406971 contain the supplementary crystallographic data for this publication. These data can be obtained free of

charge at www.ccdc.cam.ac.uk/conts/retrieving.html (or from the Cambridge Crystallographic Data Centre, 12 Union Road, Cambridge CB2 1EZ, UK; Fax: + 44-1223-336-033; e-mail: deposit@ccdc.cam.ac.uk).

Crystal Structures

$(Me_3Si)_2SbBH_2 \cdot NMe_3$ (1):

1 crystallizes from a *n*-hexane solution -28° C as colourless needles in the orthorhombic space group $Cmc2_1$. Figure S1 shows the structure of **1** in the solid state.

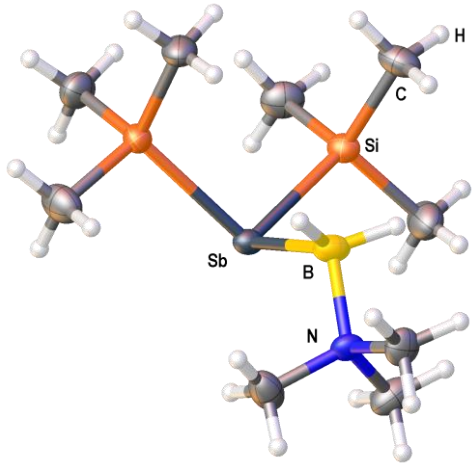

Figure S1. Molecular structure of **1** in the solid state. Selected bond lengths [Å] and angles [°]: Sb–Si 2.5394(13), Sb–B 2.296(9), N–B 1.645(11), Si–Sb–Si 102.89(7), B–Sb–Si 98.27(16), N–B–Sb 111.1(5).

$(Me_3Si)_2SbBH_2 \cdot NHC^{Me}$ (2):

2 crystallizes from a *n*-hexane solution -28° C as colourless blocks in the monoclinic space group $P2_1/c$. Figure S2 shows the structure of **2** in the solid state.

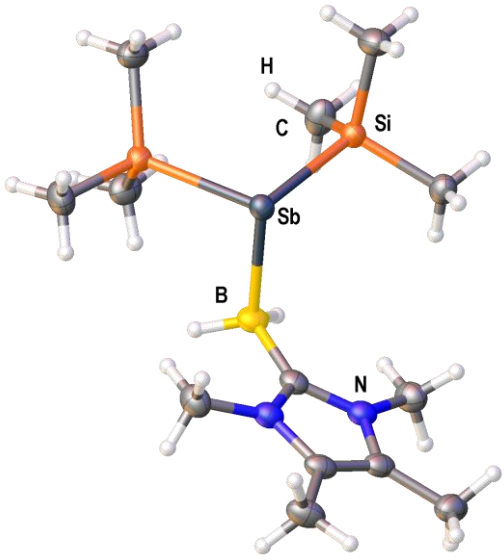

Figure S2. Molecular structure of **2** in the solid state. Selected bond lengths [Å] and angles [°]: Sb–Si 2.5520(6) - 2.5532(5), Sb–B 2.350(2), C–B 1.593(3), Si2 Sb1 Si1 98.513(18), B–Sb–Si 100.86(7), B–Sb–Si 92.32(6), C–B–Sb 107.34(14).

$Me_3N{\cdot}H_2BSbHBH_2{\cdot}NMe_3$ (3b):

3b crystallizes from a *n*-hexane solution at -28° C as colourless plates in the orthorhombic space group *Pbca*. Figure S3 shows the structure of **3b** in the solid state.

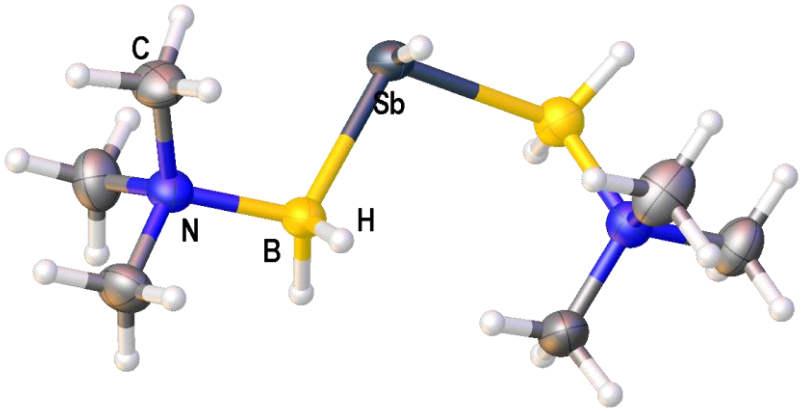

Figure S3. Molecular structure of **3b** in the solid state. Selected bond lengths [Å] and angles [°]: Sb–B 2.291(4) - 2.297(4), B–N 1.607(5) - 1.625(5), B–Sb–B 107.74(15), N–B–Sb 111.5(2) - 118.4(2).

$H_2SbBH_2{\cdot}NHC^{Me}$ (4):

4 crystallizes from a *n*-hexane mixture at -28° C as colourless blocks in the triclinic space group $P\bar{1}$ The antimony atom is disordered over two positions. Figure S4 shows the structure of **4** in the solid state.

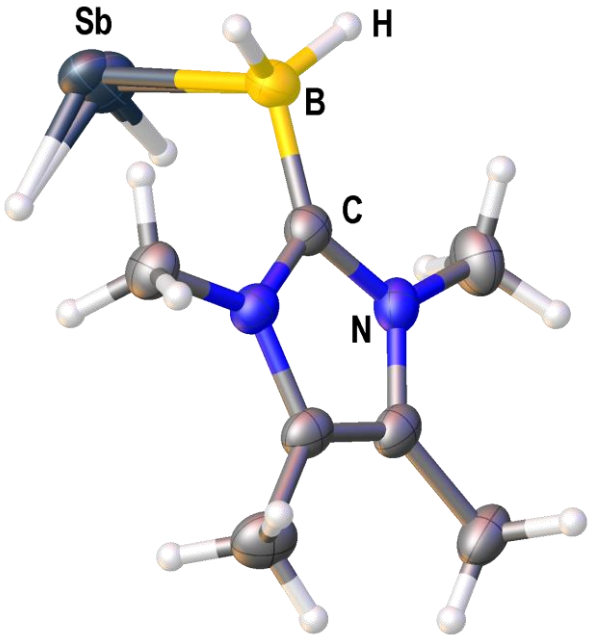

Figure S4. Molecular structure of **4** in the solid state. Selected bond lengths [Å] and angles [°]:Sb1–B 2.318(2), Sb2–B 2.267(5), B–C 1.570(3), C–B–Sb1 109.22(11), C–B–Sb2 106.31(15).

In the solid state, the antimony atom is disordered over two positions. A second, shorter Sb–B bond length is found. A possible explanation would be the oxidation of a small

percentage of compound **4** during the preparation of the crystals for the X-ray measurement. NMR spectroscopy, mass spectrometry and other analytical methods involved in the characterization do not show any evidence for the presence of an oxidized product. The bond length of the major compound (**4**) is in good agreement with calculated values (2.3448 Å). DFT calculations for an oxidized species [$H_2(O)SbBH_2{\cdot}NHC^{Me}$] would exhibit a shorter bond length of 2.3070 Å. The found shorter Sb–B bond length of 2.267(5) of the minor component (occupation of Sb by 20%), could be either assigned to a disordering or a partial oxidation. However, we were unable to locate a reasonable electron density for a possible O atom occupied its position by 20% near the antimony atom.

Crystallographic Information

Table S1. Crystallographic data for compounds **1** and **2**.

	1	**2**
Empirical formula	$C_9H_{29}BNSbSi_2$	$C_{13}H_{32}BN_2SbSi_2$
Formula weight *M*	340.07 g/mol	405.14 g/mol
Crystal	colourless needle	colourless block
Crystal size [mm^3]	0.64 × 0.23 × 0.17	0.43 × 0.36 × 0.21
Temperature *T*	123(1) K	123(1) K
Radiation	Cu-K_α (λ = 1.54178 Å)	Cu-K_α (λ = 1.54178 Å)
Crystal system	orthorhombic	monoclinic
Space group	$Cmc2_1$	$P2_1/c$
Unit cell dimensions	*a* = 14.9980(3) Å	*a* = 12.1336(1) Å
	b = 10.4896(2) Å	*b* = 12.9385(1) Å
	c = 11.0167(2) Å	*c* = 12.8885(1) Å
	α = 90°	*α* = 90°
	β = 90°	*β* = 96.222(1)°
	γ = 90°	*γ* = 90°
Volume *V*	1733.18(6) $Å^3$	2011.45(3) $Å^3$
Formula units *Z*	4	4
Absorption coefficient $\mu_{Cu\text{-}K\alpha}$	13.728 mm^{-1}	11.935 mm^{-1}
Density (calculated) ρ_{calc}	1.303 g/cm^3	1.138 g/cm^3
F(000)	696	832
Theta range $\theta_{min}/\theta_{full}/\theta_{max}$	5.16 /66.51/66.51°	3.66 /66.58/66.58°
Absorption correction	analytical	analytical
Index ranges	$-17 < h < 17$	$-14 < h < 13$
	$-9 < k < 12$	$-15 < k < 14$
	$-13 < l < 11$	$-15 < l < 13$
Reflections collected	3540	11324
Independent reflections [$I > 2\sigma(I)$]	1418 (R_{int} = 0.0398)	3533 (R_{int} = 0.0288)
Completeness to full *θ*	0.988	0.995
Transmission T_{min} / T_{max}	0.048 / 0.295	0.074 / 0.273
Data / restraints / parameters	1418 / 2 / 85	3533 / 0 / 190
Goodness-of-fit on F^2 *S*	1.046	1.082
Final *R*-values [$I > 2\sigma(I)$]	R_1 = 0.0242,	R_1 = 0.0222,
	wR_2 = 0.0551	wR_2 = 0.0536
Final *R*-values (all data)	R_1 = 0.0245,	R_1 = 0.0234,
	wR_2 = 0.0554	wR_2 = 0.0542
Largest difference hole	–0.58,	–0.58,
and peak *Δρ*	0.36 $eÅ^{-3}$	0.43 $eÅ^{-3}$
Flack parameter	–0.015(8)	–

Table S2. Crystallographic data for compounds **3b** and **4**.

	3b	**4**
Empirical formula	$C_6H_{23}B_2N_2Sb$	$C_7H_{16}BN_2Sb$
Formula weight *M*	266.63 g/mol	260.78 g/mol
Crystal	colourless plate	colourless blocks
Crystal size [mm^3]	0.24 × 0.17 × 0.03	0.22 × 0.12 × 0.06
Temperature *T*	123(1) K	123(1) K
Radiation	Cu-K_α (λ = 1.54178 Å)	Mo-K_α (λ = 0.71073 Å)
Crystal system	orthorhombic	triclinic
Space group	*Pbca*	$P\bar{1}$
Unit cell dimensions	*a* = 20.2849(10) Å	*a* = 8.2625(2) Å
	b = 11.6491(6) Å	*b* = 8.2880(2) Å
	c = 10.5383(4) Å	*c* = 8.6339(2) Å
	α = 90°	*α* = 101.745(2) °
	β = 90°	*β* = 96.091(2) °
	γ = 90°	*γ* = 111.755(2) °
Volume *V*	2490.2(2) $Å^3$	526.81(2) $Å^3$
Formula units *Z*	8	2
Absorption coefficient $\mu_{Cu\text{-}K\alpha}$	17.182 mm^{-1}	2.575 mm^{-1}
Density (calculated) ρ_{calc}	1.422 g/cm^3	1.644 g/cm^3
F(000)	1072	256
Theta range $\theta_{min}/\theta_{full}/\theta_{max}$	4.36/ 67.05/74.06°	3.17 /26.00/30.57°
Absorption correction	analytical	gaussian
Index ranges	–25 < *h* < 24	–11< *h* < 11
	–13 < *k* < 14	–11 < *k* < 11
	–8 < *l* < 12	–12 < *l* < 12
Reflections collected	9073	26995
Independent reflections [$I > 2\sigma(I)$]	2483 (R_{int} = 0.0381)	3223 (R_{int} = 0.0291)
Completeness to θ_{full}	0.981	0.996
Transmission T_{min} / T_{max}	0.170 / 0.664	0.719 / 0.884
Data / restraints / parameters	2483 / 0 / 125	3223 / 2 / 129
Goodness-of-fit on F^2 *S*	1.054	1.062
Final *R*-values [$I > 2\sigma(I)$]	R_1 = 0.0370,	R_1 = 0.0211,
	wR_2 = 0.1053	wR_2 = 0.0597
Final *R*-values (all data)	R_1 = 0.0477,	R_1 = 0.0246,
	wR_2 = 0.1115	wR_2 = 0.0605
Largest difference hole	–1.11,	–0.24,
and peak $\Delta\rho$	1.06 $eÅ^{-3}$	0.75 $eÅ^{-3}$

NMR spectroscopy

$(Me_3Si)_2SbBH_2 \cdot NMe_3$ (1):

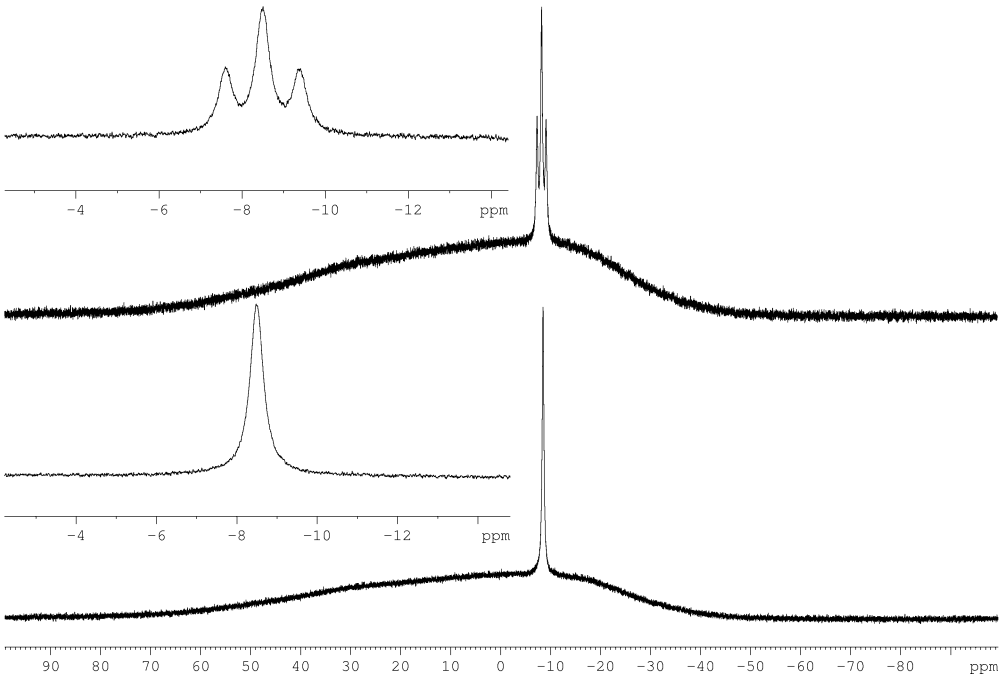

Figure S5: $^{11}B\{^1H\}$ (bottom) and ^{11}B NMR spectrum (top) of **1** in C_6D_6.

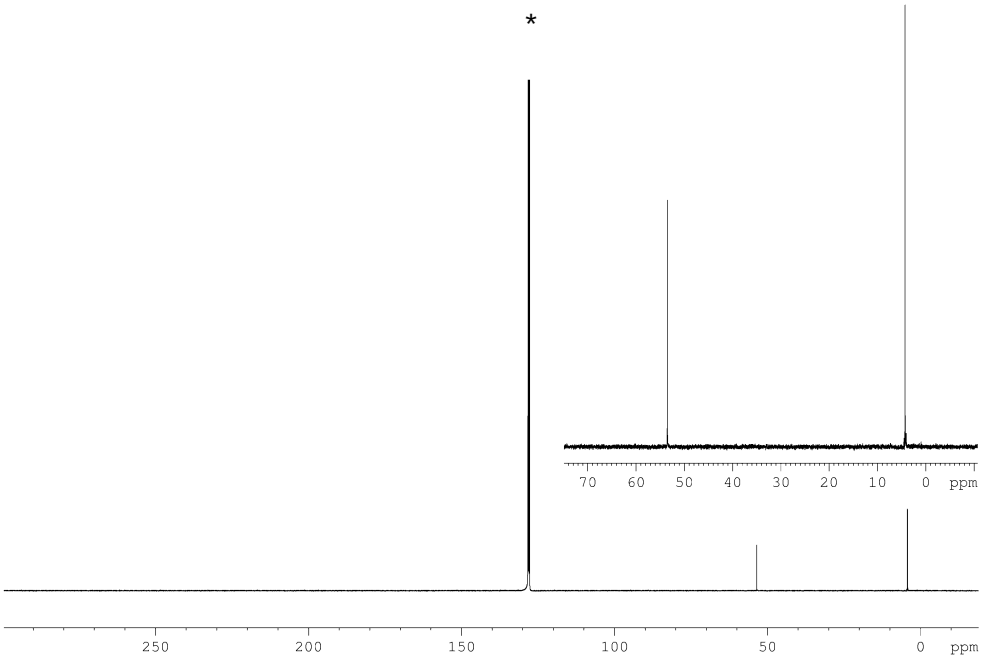

Figure S6: $^{13}C\{^1H\}$ of **1** in C_6D_6. * = C_6D_6

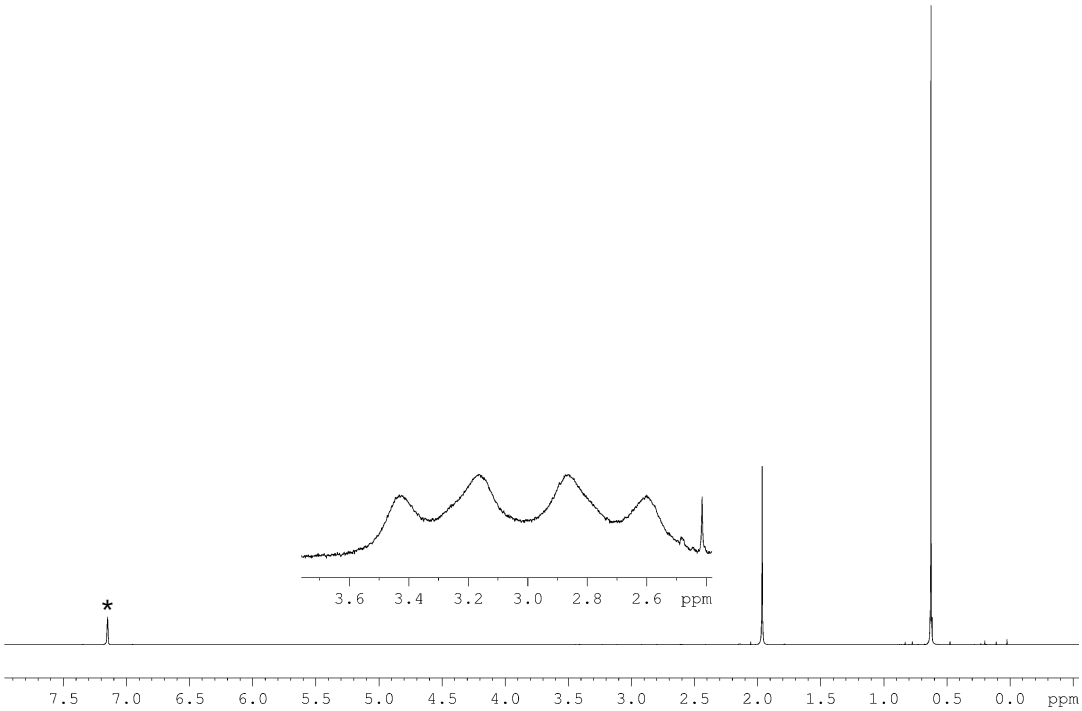

Figure S7: ^{1}H NMR spectrum of **1** in C_6D_6. * = C_6D_6 Magnified part shows BH_2.

$(Me_3Si)_2SbBH_2 \cdot NHC^{Me}$ (2):

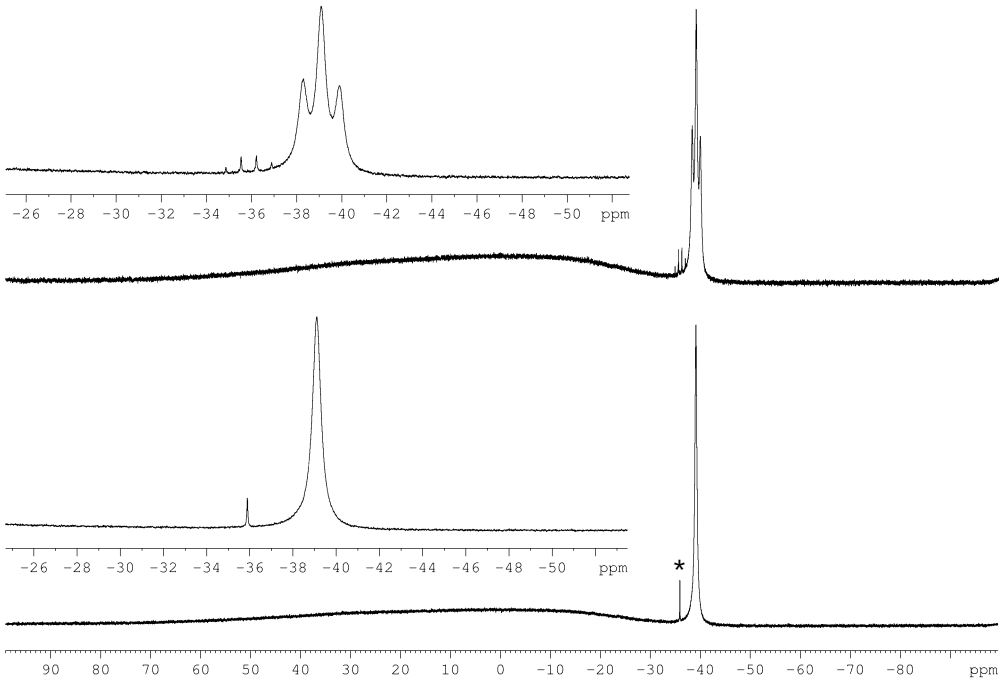

Figure S8: $^{11}B\{^{1}H\}$ (bottom) and ^{11}B NMR spectrum (top) of **2** in C_6D_6. * = $NHC^{Me} \cdot BH_3$

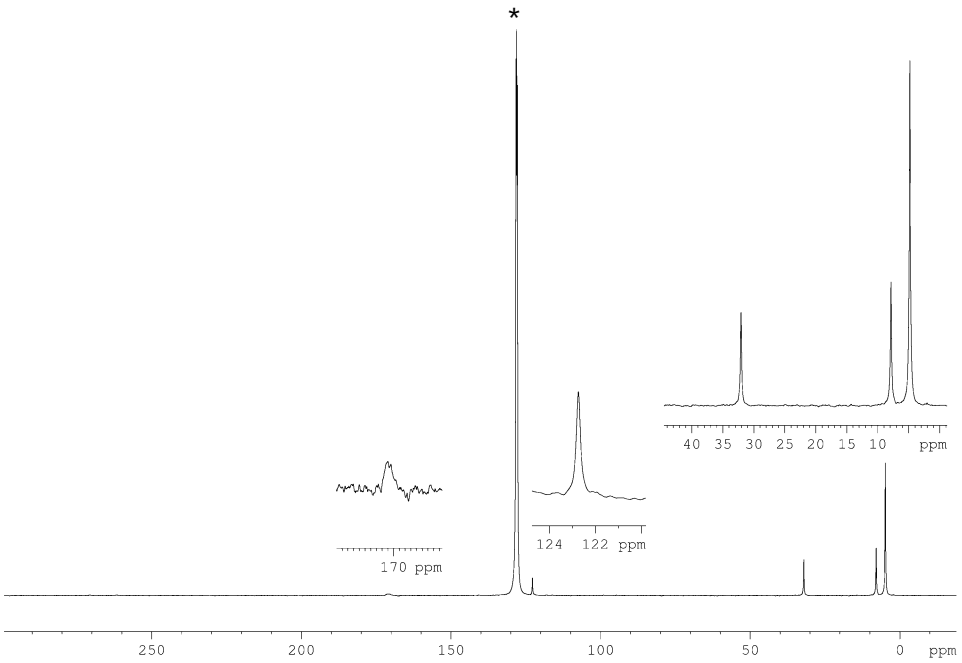

Figure S9: $^{13}C\{^{1}H\}$ of **2** in C_6D_6. * = C_6D_6

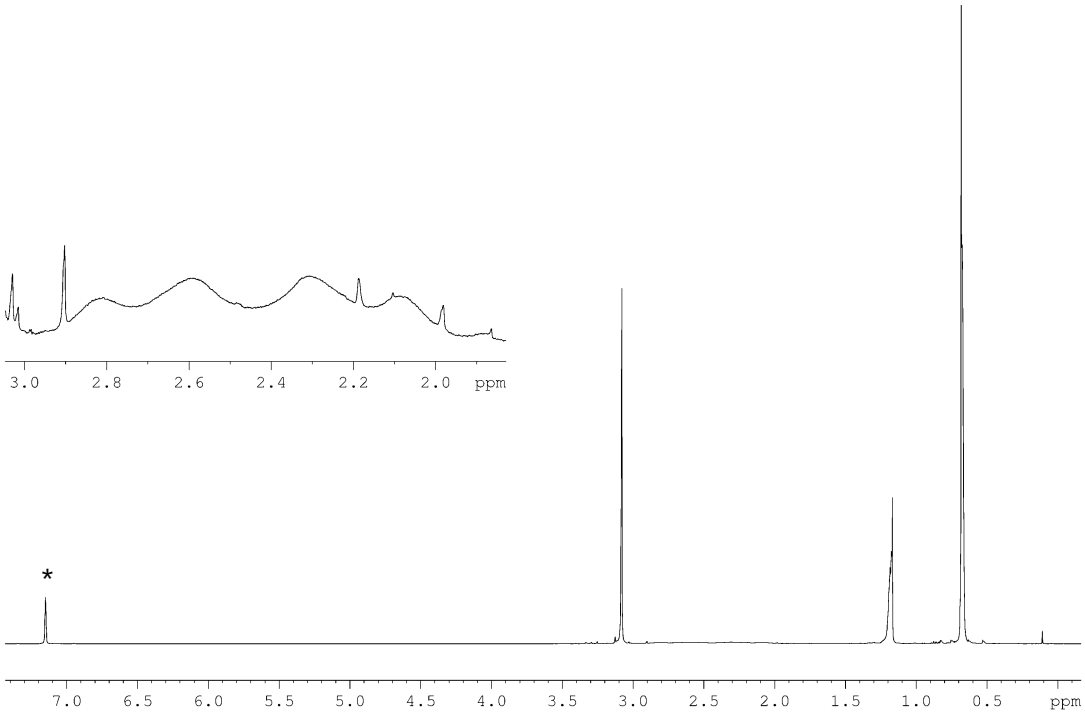

Figure S10: ^{1}H NMR spectrum of **2** in C_6D_6. * = solvent (C_6D_6) Magnified part shows BH_2.

Methanolysis of $(Me_3Si)_2SbBH_2 \cdot NMe_3$ (1):

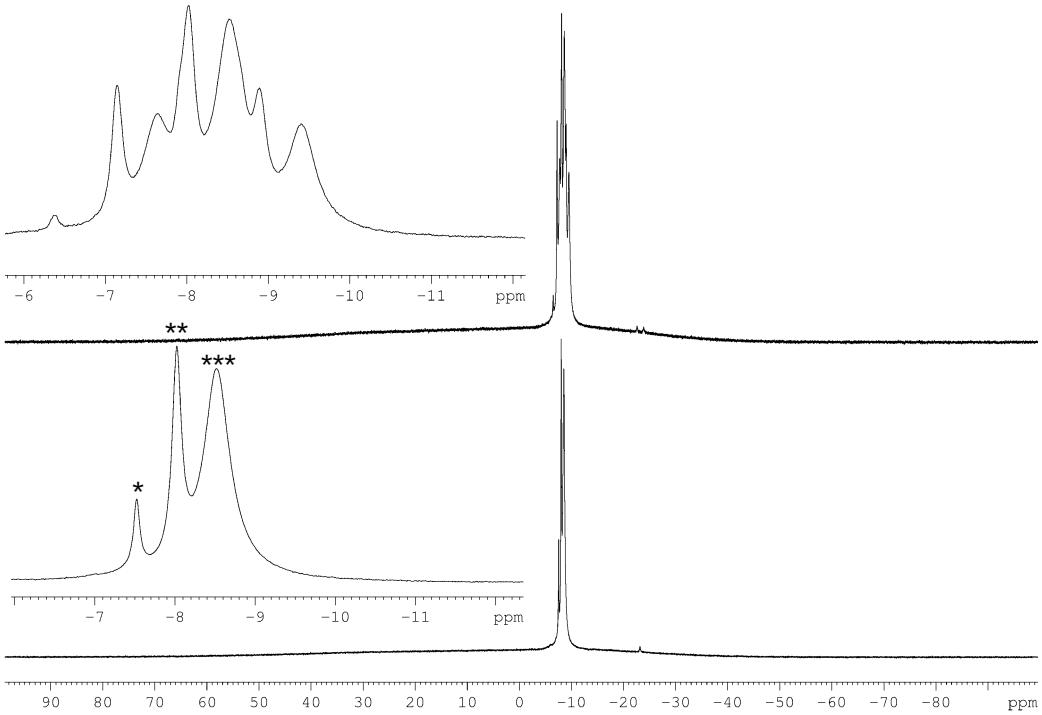

Figure S11: $^{11}B\{^1H\}$ (bottom) and ^{11}B NMR spectrum (top) of products of methanolysis in C_6D_6. * = $Me_3N \cdot BH_3$, ** = $Me_3N \cdot BH_2SbH_2$, *** = $Me_3N \cdot BH_2Sb(SiMe_3)_2$ (**1**).

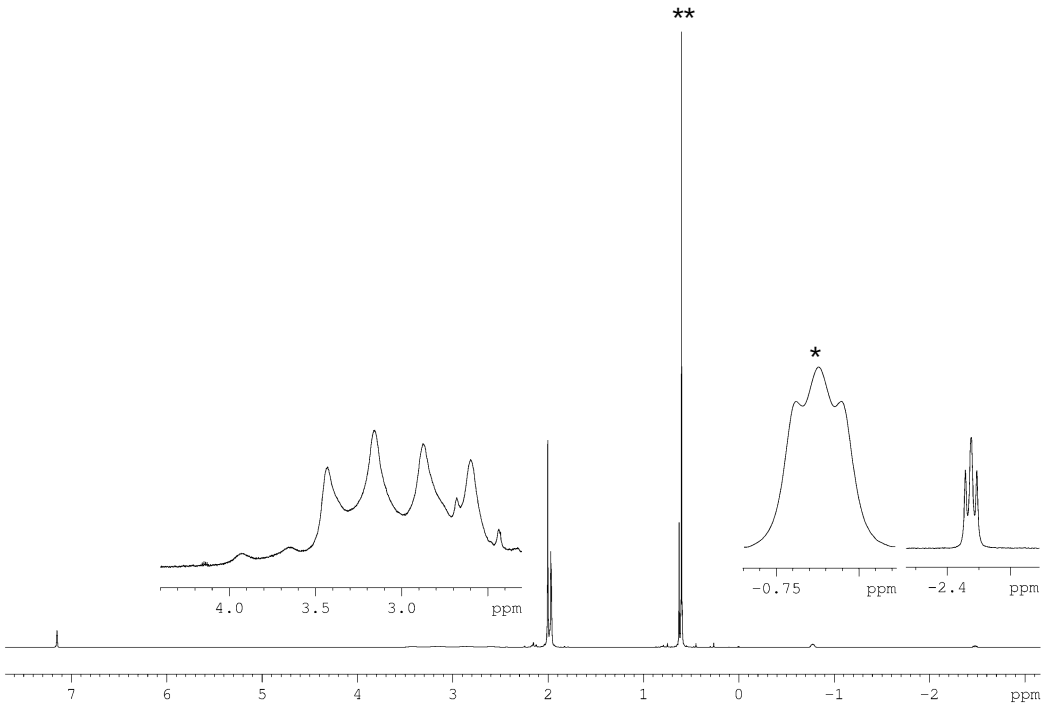

Figure S12: ^1H NMR spectrum of products of methanolysis in C_6D_6. * = $Me_3N \cdot BH_3$, ** = $Me_3N \cdot BH_2SbH_2$, *** = $Me_3N \cdot BH_2Sb(SiMe_3)_2$ (**1**).

$H_2SbBH_2 \cdot NHC^{Me}$ (4):

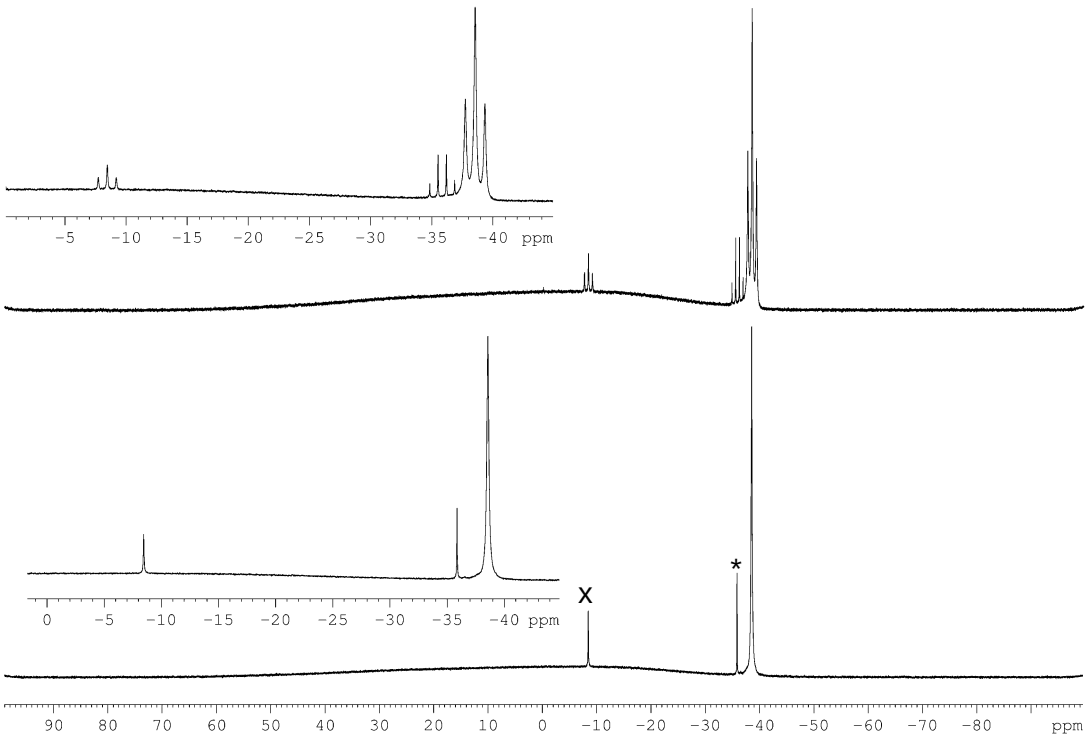

Figure S13: $^{11}B\{^1H\}$ (bottom) and ^{11}B NMR spectrum (top) of **4** in C_6D_6. x = decomposition product, * = $NHC^{Me} \cdot BH_3$.

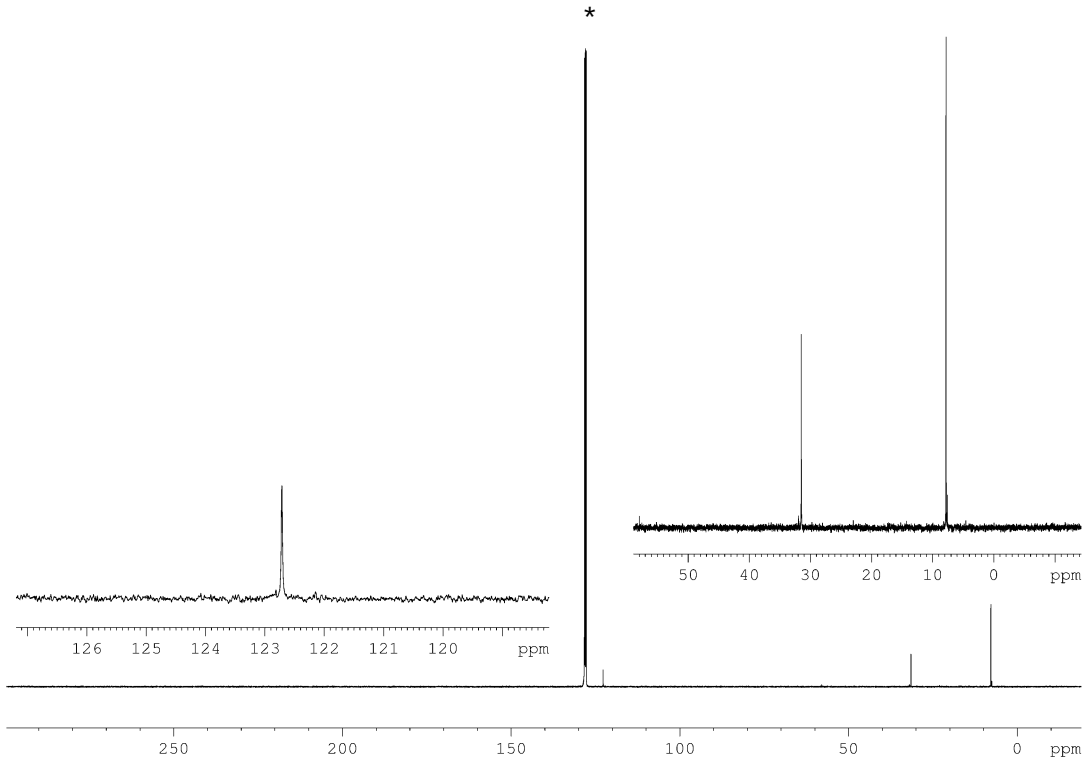

Figure S14: $^{13}C\{^1H\}$ NMR spectrum (top) of **4** in C_6D_6. * = C_6D_6.

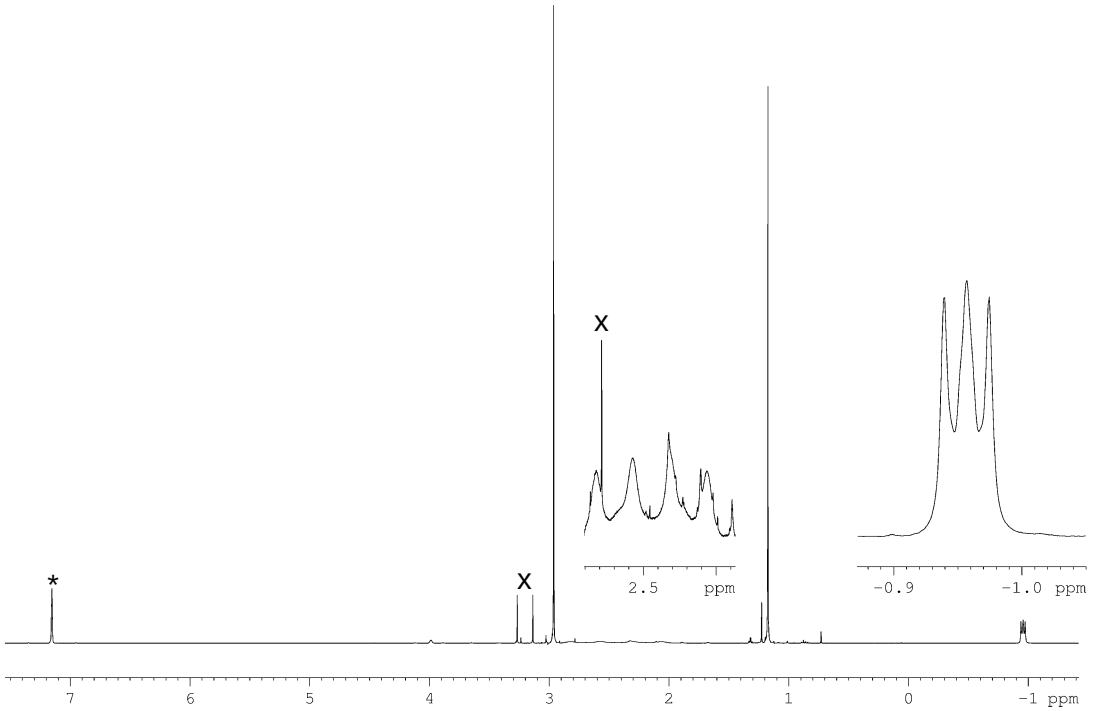

Figure S15: ^{1}H NMR spectrum of **4** in C_6D_6. x = decomposition product, * = C_6D_6

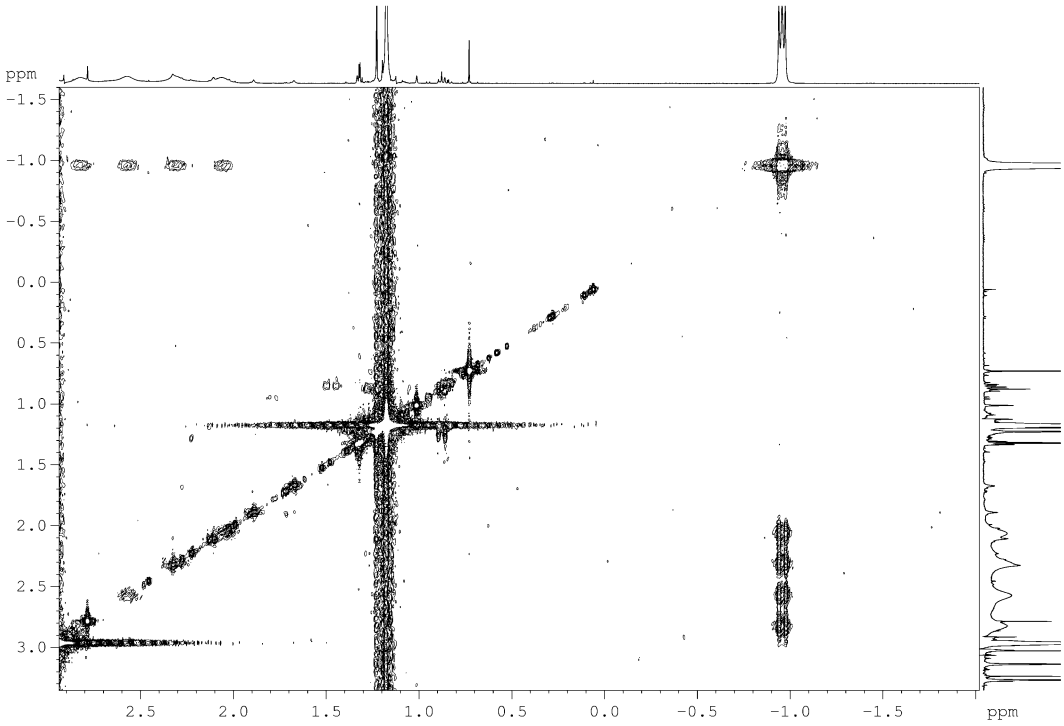

Figure S16: ^{1}H ^{1}H COSY NMR spectrum of **4** in C_6D_6.

Computational Details

The DFT calculations have been performed by using the standard Gaussian 09 program suite.[8] B3LYP functional[9] has been used together with Ahlrichs def2-TZVPP basis set (all electron for H,B,C,N,P,As , effective core potentials for Sb,Bi).[10] All structures were fully

optimized with subsequent vibrational analysis and correspond to minima on their respective potential energy surfaces.

The geometry of $H_2SbBH_2{\cdot}NHC^{Me}$ (**4**), $H_2(O)SbBH_2{\cdot}NHC^{Me}$ and *meso*-$NHC^{Me}{\cdot}H_2BSb(H)O$-$O(H)SbBH_2{\cdot}NHC^{Me}$ was optimized using the Turbomole program package.[11] The B3LYP functional, as implemented in Turbomole together with the def2-TZVP[12] basis set for all atoms was used. Through the geometry optimization steps the RI[13] and the Multipole Accelerated Resolution of Identity (MARI-J)[14] approximation was used.

Table S3. Total energies E^o_0, sum of electronic and thermal enthalpies H^o_{298} (Hartree) and standard entropies S^o_{298} (cal $mol^{-1}K^{-1}$) for studied compounds. B3LYP/def2-TZVPP level of theory. (NHC^{Me}-1,3,4,5-tetramethylimidazoline)

Compound	E^o_0	H^o_{298}	S^o_{298}
BH_2	-25.9465549	-25.928327	47.731
BH_2NMe_3	-200.554448	-200.403613	79.204
BH_2NHC^{Me}	-409.6648966	-409.447597	108.102
BH_3NMe_3	-201.2250556	-201.062851	75.87
BH_3NHC^{Me}	-410.2962624	-410.068594	107.459
NH_2	-55.9066	-55.88384	46.503
PH_2	-342.5377771	-342.520624	50.785
AsH_2	-2237.083886	-2237.067891	53.834
SbH_2	-241.5050968	-241.490642	56.03
BiH_2	-215.881183	-215.867332	57.989
NH_2BH_2	-82.0838608	-82.031731	54.528
PH_2BH_2	-368.6263217	-368.583966	60.827
AsH_2BH_2	-2263.156092	-2263.115621	64.176
SbH_2BH_2	-267.557488	-267.519336	67.097
BiH_2BH_2	-241.921893	-241.884875	70.223
$NH_2BH_2NMe_3$	-256.6373323	-256.455412	84.902
$PH_2BH_2NMe_3$	-543.2122712	-543.038323	90.162
$AsH_2BH_2NMe_3$	-2437.746829	-2437.574568	92.594
$SbH_2BH_2NMe_3$ (**3a**)	-442.152569	-441.982396	95.41
$BiH_2BH_2NMe_3$	-416.519098	-416.349910	99.27
$NH_2BH_2NHC^{Me}$	-465.6968576	-465.449288	112.641
$PH_2BH_2NHC^{Me}$	-752.2880911	-752.04821	117.146
$AsH_2BH_2NHC^{Me}$	-2646.825525	-2646.587395	121.562
$SbH_2BH_2NHC^{Me}$ (**4**)	-651.236018	-650.999970	122.929
$BiH_2BH_2NHC^{Me}$	-625.609034	-625.373867	125.079

MeOH	-115.778606	-115.723207	57.03
$SiMe_3OMe$	-524.578230	-524.414248	98.837
$NMe_3BH_2Sb(SiMe_3)_2$ (**1**)	-1259.691527	-1259.295437	175.528
$NHC^{Me}BH_2Sb(SiMe_3)_2$ (**2**)	-1468.771532	-1468.309690	199.624
H_2	-1.180004	-1.166631	31.133
N_2	-109.573262	-109.564369	45.733
P_4	-1365.569033	-1365.55744	66.862
As_4	-8943.773456	-8943.763289	78.221
Sb	-240.293793	-240.291432	43.039
Bi	-214.68486	-214.6825	44.67
SbH_3	-242.11865	-242.095873	55.612
$SbH(BH_2NMe_3)_2$ (**3b**)	-642.18393	-641.866515	128.283

Table S4. Reaction energies ΔE^o_0, standard enthalpies ΔH^o_{298}, Gibbs energies ΔG^o_{298} in kJ mol^{-1} and standard entropies ΔS^o_{298} in J mol^{-1} K^{-1} for decomposition processes. B3LYP/def2-TZVPP level of theory. (NHC^{Me}-1,3,4,5-tetramethylimidazoline)

Process	ΔE^o_0	ΔH^o_{298}	ΔS^o_{298}	ΔG^o_{298}
$H_2NBH_2NMe_3 = ½N_2 + BH_3NMe_3 + ½H_2$	93.6	71.0	123.0	34.4
$H_2PBH_2NMe_3 = ¼P_4 + BH_3NMe_3 + ½H_2$	13.0	7.3	75.3	-15.1
$H_2AsBH_2NMe_3 = ¼As_4 + BH_3NMe_3 + ½H_2$	-30.4	-32.6	77.0	-55.6
$H_2SbBH_2NMe_3 = Sb + BH_3NMe_3 + ½H_2$	114.8	117.6	163.5	68.9
$H_2SbBH_2NMe_3 = Sb$ (solid) $+ BH_3NMe_3 + ½H_2$		-150.6[a]	28.1[a]	-158.9[a]
$H_2BiBH_2NMe_3 = Bi + BH_3NMe_3 + ½H_2$	50.4	55.8	154.1	9.8
$H_2BiBH_2NMe_3 = Bi$ (solid) $+ BH_3NMe_3 + ½H_2$		-153.4[a]	24.1[a]	-160.6[a]
$H_2NBH_2NHC^{Me} = ½N_2 + BH_3NHC^{Me} + ½H_2$	62.9	39.9	139.1	-1.6
$H_2PBH_2NHC^{Me} = ¼P_4 + BH_3NHC^{Me} + ½H_2$	25.1	18.2	94.5	-10.0
$H_2AsBH_2NHC^{Me} = ¼As_4 + BH_3NHC^{Me} + ½H_2$	-10.8	-14.0	87.9	-40.2
$H_2SbBH_2NHC^{Me} = Sb + BH_3NHC^{Me} + ½H_2$	146.9	148.7	180.5	94.9
$H_2SbBH_2NHC^{Me} = Sb$ (solid) $+ BH_3NHC^{Me} + ½H_2$		-119.5[a]	45.1[a]	-133.0[a]
$H_2BiBH_2NHC^{Me} = Bi + BH_3NHC^{Me} + ½H_2$	99.5	103.6	178.3	50.4
$H_2BiBH_2NHC^{Me} = Bi$ (solid) $+ BH_3NHC^{Me} + ½H_2$		-105.6[a]	48.3[a]	-120.0[a]

[a] Data for the reactions including solid compounds are calculated using experimental values of sublimation enthalpies of 268.2 and 209.2 kJ mol^{-1} for solid Sb and Bi, respectively, and sublimation entropies of 134.5 and 130.0 J mol^{-1} K^{-1} for solid Sb and Bi, respectively.[15]

Thermodynamic stability with respect to decomposition (Table S4) lowers in order N>P>As>Sb>Bi; thus, compounds formed by heavier group 15 elements (P-Bi) are thermodynamically unstable with respect to decomposition (Gibbs energies for the decomposition are exergonic).

Table S5. Reaction energies ΔE^o_0, standard enthalpies ΔH^o_{298}, Gibbs energies ΔG^o_{298} in kJ mol^{-1} and standard entropies ΔS^o_{298} in J mol^{-1} K^{-1} for methanolysis processes and SbH_3 elimination reactions. B3LYP/def2-TZVPP level of theory.

Process	ΔE^o_0	ΔH^o_{298}	ΔS^o_{298}	ΔG^o_{298}
$(SiMe_3)_2SbBH_2NMe_3$ + 2 MeOH =				
$H_2SbBH_2NMe_3$ + $SiMe_3OMe$	-158.3	-181.3	14.6	-185.6
$(SiMe_3)_2SbBH_2NHC^{Me}$ + 2 MeOH =				
$H_2SbBH_2NHC^{Me}$ + $SiMe_3OMe$	-167.3	-190.0	28.9	-198.6
2 $SbH_2BH_2NMe_3$ =	6.7	6.3	-29.0	
SbH_3 + $SbH(BH_2NMe_3)_2$				15.0
2 $SbH_2BH_2NMe_{3(soln)}$ =				
SbH_3 (g) + $SbH(BH_2NMe_3)_{2\ (soln)}$		6.3	61.0[b]	-11.9[b]

(NHC^{Me}-1,3,4,5-tetramethylimidazoline) [b] Estimated by taking into account the solvation entropy as -90 J mol^{-1} K^{-1}.[15]

Table S6. Calculated bond lengths in the optimized geometries of 4, SbO and SbO-OSb. B3LYP/def2-TZVP level of theory.

Distance / [Å]	$H_2SbBH_2{\cdot}NHC^{Me}$ (**4**)	$H_2(O)SbBH_2{\cdot}NHC^{Me}$	*meso*-$NHC^{Me}{\cdot}H_2BSb(H)O$-$O(H)SbBH_2{\cdot}NHC^{Me}$
B-Sb	2.3448	2.3070	2.3186
Sb-H	1.7280	1.7334	1.7365
C-B	1.5723	1.5809	1.5727
Sb-O	-	1.8385	2.0322
O-O	-	-	1.4830

Cartesian coordinates of the optimized geometries (xyz) can be obtained from http://dx.doi.org/10.1002/anie.201505773.

References

[1] C. Marquardt, C. Thoms, A. Stauber, G. Balazs, M. Bodensteiner, M. Scheer, *Angew. Chem. Int. Ed.* **2014**, *53*, 3727–3730; *Angew. Chem.* **2014**, *126*, 3801–3804.

[2] A. Stauber, PhD thesis, University of Regensburg (Germany), **2014**.

[3] E. Amberger, R. W. Salazar G., *J. Organomet. Chem.* **1967**, *8*, 111–114.

[4] Agilent Technologies **2006-2011**, CrysAlisPro Software system, different versions, Agilent Technologies UK Ltd, Oxford, UK.

[5] A. Altomare, M. C.Burla, M. Camalli, G. L. Cascarano, C. Giacovazzo, A. Guagliardi, A.G. G. Moliterni, G. Polidori, R. Spagna, J. Appl. Cryst. **1999**, *32*, 115–119

[6] G. M. Sheldrick, *Acta Cryst.* **2008**, *A64*, 112–122.

[7] O.V. Dolomanov, L.J. Bourhis, R.J. Gildea, J.A.K. Howard, H.Puschmann, OLEX2: A complete structure solution, refinement and analysis program, *J. Appl. Cryst*. **2009**, *42*, 339–341.

[8] M. J. Frisch, G. W. Trucks, H. B. Schlegel, G. E. Scuseria, M. A. Robb, J. R. Cheeseman, G. Scalmani, V. Barone, B. Mennucci, G. A. Petersson, H. Nakatsuji, M. Caricato, X. Li, H. P. Hratchian, A. F. Izmaylov, J. Bloino, G. Zheng, J. L. Sonnenberg, M. Hada, M. Ehara, K. Toyota, R. Fukuda, J. Hasegawa, M. Ishida, T. Nakajima, Y. Honda, O. Kitao, H. Nakai, T. Vreven, J. A. Montgomery, Jr., J. E. Peralta, F. Ogliaro, M. Bearpark, J. J. Heyd, E. Brothers, K. N. Kudin, V. N. Staroverov, T. Keith, R. Kobayashi, J. Normand, K. Raghavachari, A. Rendell, J. C. Burant, S. S. Iyengar, J. Tomasi, M. Cossi, N. Rega, J. M. Millam, M. Klene, J. E. Knox, J. B. Cross, V. Bakken, C. Adamo, J. Jaramillo, R. Gomperts, R. E. Stratmann, O. Yazyev, A. J. Austin, R. Cammi, C. Pomelli, J. W. Ochterski, R. L. Martin, K. Morokuma, V. G. Zakrzewski, G. A. Voth, P. Salvador, J. J. Dannenberg, S. Dapprich, A. D. Daniels, O. Farkas, J. B. Foresman, J. V. Ortiz, J. Cioslowski, D. J. Fox, Gaussian 09, Revision D.01, Gaussian, Inc., Wallingford CT, 2013.

[9] a) A. D. Becke, *J. Chem. Phys*., **1993**, *98*, 5648–5652; b) C. Lee, W. Yang, R. G. Parr, *Phys. Rev. B*., **1988**, *37*, 785–789.

[10] F. Weigend, R. Ahlrichs, *Phys.Chem.Chem.Phys.*, **2005**, *7*, 3297–3305.

[11] a) R. Ahlrichs, M. Bär, M. Häser, H. Horn, C. Kölmel, *Chem. Phys. Lett.***1989**, *162*, 165–169; b) O. Treutler, R. Ahlrichs, *J. Chem. Phys.***1995**, *102*, 346–354.

[12] a) A. Schäfer, C. Huber, R. Ahlrichs, *J. Chem. Phys.***1994**, *100*, 5829; b) K. Eichkorn, F. Weigend, O. Treutler, R. Ahlrichs, *Theor. Chem. Acc.***1997**, *97*, 119.

[13] a) K. Eichkorn, O. Treutler, H. Oehm, M. Häser, R. Ahlrichs, *Chem. Phys. Lett.***1995**, *242*, 652–660; b) K. Eichkorn, F. Weigend, O. Treutler, R. Ahlrichs, *Theor. Chem. Acc.***1997**, *97*, 119.

[14] M. Sierka, A. Hogekamp, R. Ahlrichs, *J. Chem. Phys.***2003**, *118*, 9136.

[15] A. S. Lisovenko, A. Y. Timoshkin, *Inorg. Chem.*, **2010**, *49*, 10357–10369. Database "Thermal Constants of Substances", Ed. V.S. Iorish, V.S. Yungman, Internet:http://www.chem.msu.su/cgi-bin/tkv.pl

9.6 Author Contributuions

The syntheses and characterization of all compounds were performed by Christian Marquardt.

Oliver Hegen contributed to the syntheses of the compounds **1** and **2** during a research

course under the supervision of Christian Marquardt.

The syntheses and characterization of $Sb(SiMe_3)_3$ and $KSb(SiMe_3)_2$ were performed by Matthias Hautmann under supervision of Dr. Gábor Balázs.

X-ray structural analyses of all compounds were performed by Christian Marquardt, Dr. A. V. Virovets and Dr. Michael Bodensteiner.

All DFT-calculations were performed by Dr. Gábor Balázs and Prof. Dr. Alexey Y. Timoshkin.

The manuscript (including supporting information, figures, schemes and graphical abstract) was written by Christian Marquardt.

10. Coordination of Pnictogenylboranes towards monovalent coinage metal cations

C. Marquardt, M. Fleischmann, O. Hegen, L. Dütsch and M. Scheer

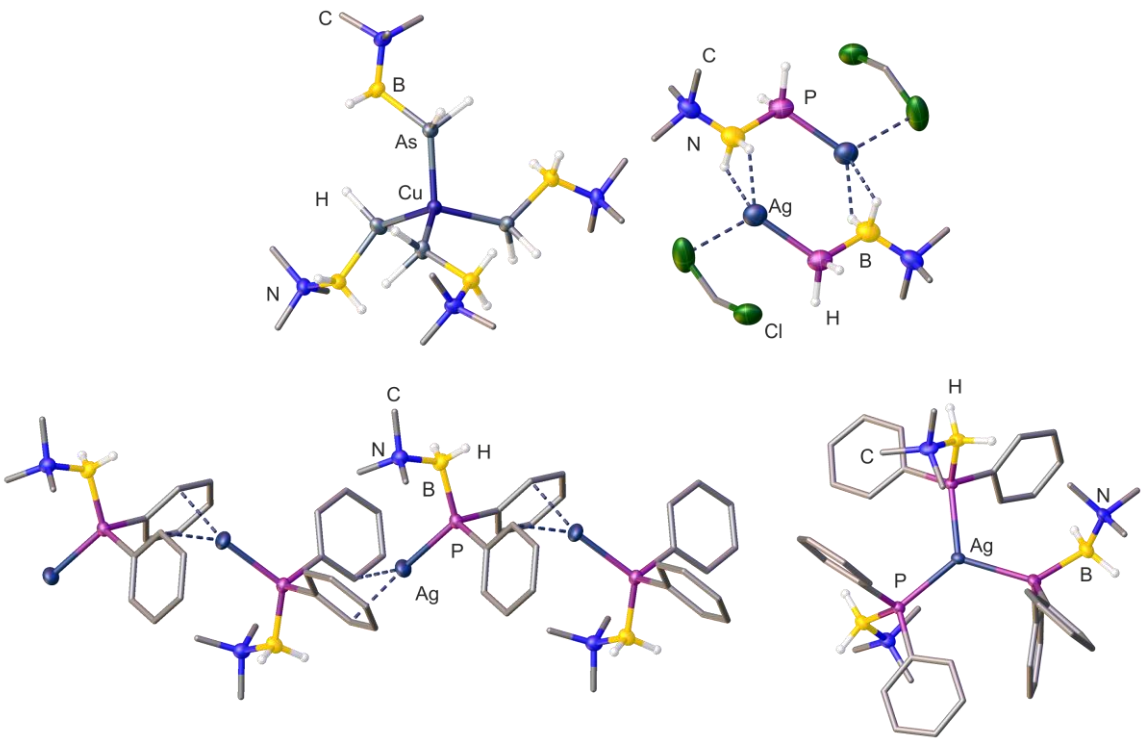

Abstract: Reactions of the pnictogenylboranes $H_2E–BH_2·NMe_3$ (**A1:** E = P; **A2:** E = As) and $Ph_2P–BH_2·NMe_3$ (**A3)** with $[Cu(MeCN)_4][BF_4]$ afford the homoleptic complexes $[Cu(H_2E–BH_2·NMe_3)_4(BF_4)]$ (**1:** E = P, **2:** E = As) and $[Cu(Ph_2P–BH_2·NMe_3)_3][BF_4]$ (**3**). Compound **2** represents the first structurally characterized complex of a primary arsine coordinated to a Cu center. Reactions of **A3** with [Ag][X] (X = BF_4, FAl ($[FAl\{OC_6F_{10}(C_6F_5)\}_3]$)) selectively afford a one-dimensional polymer (for $[BF_4]$) and the coordination compounds $[Ag(Ph_2P–BH_2·NMe_3)(MeCN)]^+[FAl]^-$ (**7**) and $[Ag(Ph_2P–BH_2·NMe_3)_n]^+[FAl]^-$ (**8:** n = 2; **9:** n = 3) for [FAl]. All complexes were characterized by single-crystal X-ray structure analysis, multinuclear NMR spectroscopy, IR spectroscopy and mass spectrometry.

10.1 Introduction

Although the coordination chemistry of phosphines towards the coinage metals Cu^+ and Ag^+ is very well studied, complexes including primary phosphines (RPH_2) remain scarce.[1,2] In contrast to phosphines, Cu[3] and Ag[4] complexes of arsines are less common and they have only been investigated by theoretical methods[5] for primary arsines ($RAsH_2$). Reports on complexes of primary arsines are restricted to heteroleptic complexes of the type $[M(L)_n(AsH_2R)]$ (M = Cr, Mo, W, Fe, Co, Ni, L = CO; M = Ti, L = Cl; M = Y, L = CH_4Me).[6] Recently, phosphine-copper-catalysts with chiral phosphorus-ligands have been used for a variety of transformations of organic substrates, including asymmetric hydrogenations.[7] Chiral phosphine-silver(I) complexes are very useful tools for organic synthesis, and various different asymmetric carbon-carbon bond forming reactions have been reported.[8] Monomeric Lewis base stabilized pnictogenylboranes of the type $R_2E–BH_2·NMe_3$ (E = P, As; R = H, alkyl, aryl) are special phosphines and arsines containing one electropositive boranyl group. They represent easily accessible building blocks for neutral polymeric[9] and ionic[10] oligomeric compounds, with a backbone of alternating group 13 and group 15 elements. The oxidation with the chalcogens (O, S, Se, Te) as well as their reactivity towards mainly main group Lewis acids has been studied thoroughly.[11] The reaction behavior towards transition metal complexes has not been studied so thoroughly yet. The reaction of $H_2P–BH_2·NMe_3$ (**A1**) with $[Cp_2Ti(btmsa)]$ lead to extended B-P-oligomers, which are stabilized in the coordination sphere of Cp_2Ti.[12] Reaction of the phosphanylborane **A1** with Cu(I)I gave two Cu-I-P-clusters.[13]

Herein we present the first investigation about the coordination behavior of the pnictogenylboranes $H_2E–BH_2·NMe_3$ (**A1** E = P; **A2** E = As) towards Cu^+ and Ag^+. Here, **A1** and **A2** represent a special primary phosphine or arsine, respectively. Additionally the coordination behavior of $Ph_2P–BH_2·NMe_3$ (**A3**) which can be viewed as a derivative of the well-known ligand PPh_3 will be presented.

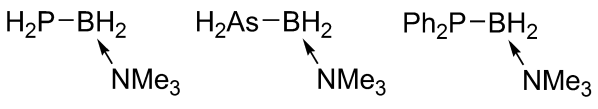

A1 **A2** **A3**

Figure 1: Pnictogenylboranes **A1**, **A2** and **A3**.

10.2 Results and Discussion

Reactions of 4 equivalents of **A1** and **A2** with $[Cu(MeCN)_4][BF_4]$ in MeCN afford the homoleptic, tetracoordinated complexes $[Cu(H_2P–BH_2{\cdot}NMe_3)_4][BF_4]$ (**1**) and $[Cu(H_2As–BH_2{\cdot}NMe_3)_4][BF_4]$ (**2**) in good crystalline yields (68% for **1**, 65% for **2**, Scheme 1). When the sterically demanding phosphanylborane **A3** is reacted with $[Cu(MeCN)_4][BF_4]$ in MeCN the tricoordinated, trigonal planar complex $[Cu(Ph_2P–BH_2{\cdot}NMe_3)_3][BF_4]$ (**3**) is obtained instead in 65% yield. Storing a CH_2Cl_2 solution of **3** for several weeks slowly leads to the formation of $[Cu(Ph_2P–BH_2{\cdot}NMe_3)_2Cl]$ (**4**), which structure could be determined by single-crystal X-ray structure analysis.

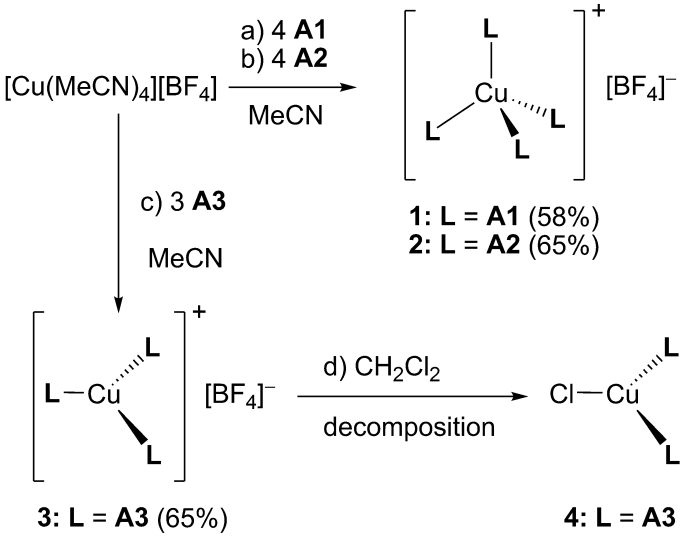

Scheme 1: Coordination of **A1**, **A2** and **A3** towards Cu(I).

The ^{1}H NMR spectra in CD_2Cl_2 shows a doublet of multiplets at δ = 2.2 ppm for the PH_2 group of **1** and a multiplet at δ = 1.2 ppm for the AsH_2 group of **2**. Both are downfield shifted compared to the starting materials (**A1** δ = 1.5 ppm, **A2** δ = 0.8 ppm).[9,10] The ^{31}P NMR spectra reveal a triplet at δ = −183.8 ppm for **1** ($^1J_{H,P}$ = 258 Hz) and a singlet at δ = −38.9 ppm for **3**. While compound **1** shows a significant downfield shift (**A1** δ = −215.5 ppm), the signal for **3** is almost unchanged compared to free **A3** (δ = −39.5 ppm). A broadened signal in the ^{31}P NMR and further unresolved coupling of the EH_2 group in the ^{1}H NMR spectra is indicative for a clear interaction to Cu in solution. ESI mass spectrometry shows signals assignable to the fragments $[Cu(L)_n]$ (**A1**: n = 2,3; **A2**: n = 1,2) with the Cu atom and varying amounts of the corresponding ligands. Single-crystal X-ray diffraction analysis (Figure 2) reveals that **1** and **2** contain a central Cu atom with a nearly ideal tetrahedral coordination environment (E–Cu–E angle 108.81(2) - 110.79(3)° for **1** and 108.32(2) - 111.79(3)° for **2**). The E–Cu bond lengths measure 2.2980(5) Å for

1 (E = P) and 2.3915(6) Å for **2** (E = As) which are slightly longer than the calculated sum of the covalent radii ($\sum r_{cov}$(Cu-P) = 2.23 Å, $\sum r_{cov}$(Cu-As) = 2.33 Å.[14] The P–B bond length of 1.963(3) Å in **1** and the As–B bond length of **2** (2.079(5) Å) are similar to the starting materials (**A1**: 1.976(2) Å, **A2**: 2.071(4) Å). Compound **2** is the first structurally characterized Cu complex containing a primary arsine. Complex **3** exhibits a distorted trigonal planar coordination environment (∑(P–Cu–P) angles = 359.84°), with P–Cu–P angles ranging from 111.45(3) to 124.85(3)°. The P–Cu bond lengths in **3** measure 2.3075(7) - 2.3293(7) Å which are essentially equal to **1**. The P–B bond lengths range from 1.982(3) to 1.990(3) Å for **3** which are slightly longer compared to the starting material (**A3**: 1.975(3) Å). In the solid state each boranyl group adopts another orientation; one lies within the P_3Ag plane while one is above and one below (see figure 2, c).

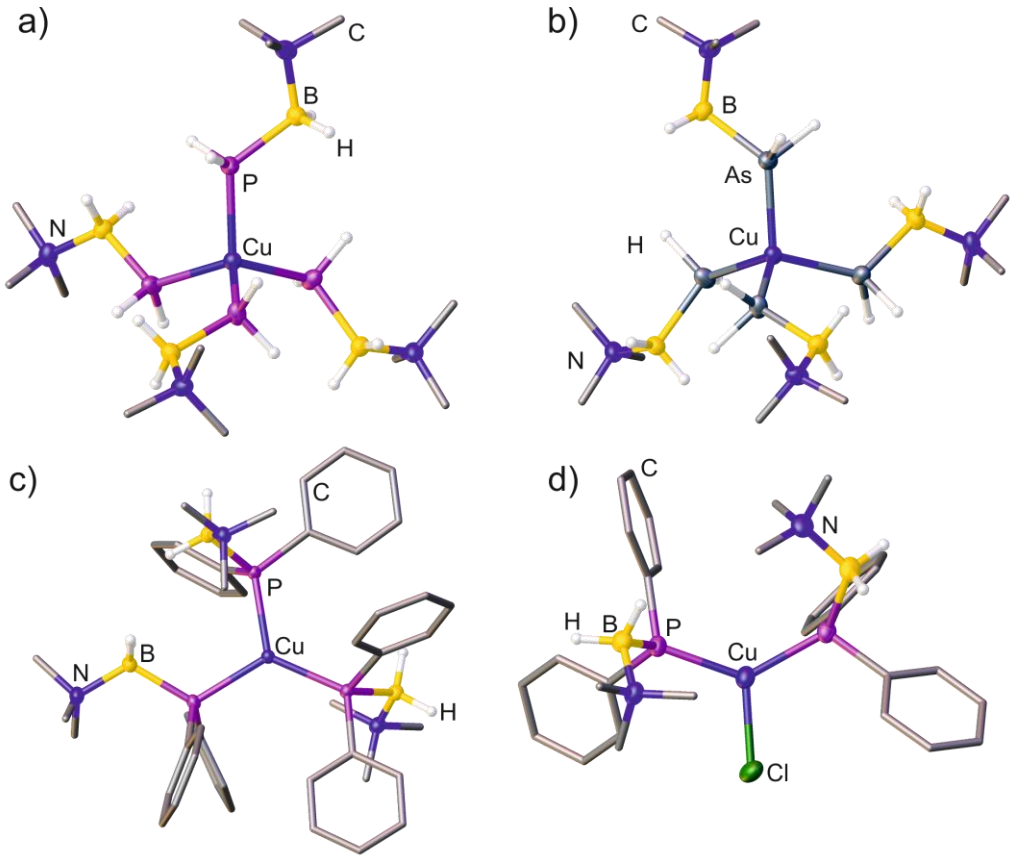

Figure 2: Molecular structure of the Cu complexes **1** (a), **2** (b), **3** (c) and **4** (d). Hydrogen atoms on carbon and counter ions are omitted for clarity. Selected bond lengths [Å] and angles [°]: **1** P–Cu 2.2980(5), P–B 1.963(3), B–P–Cu 123.02(8), P–Cu–P 108.81(2) - 110.79(3); **2** As–Cu 2.3915(6), As–B 2.079(5), B–As–Cu 125.36(17), As–Cu–As 108.32(2) - 111.79(3); **3** P–Cu 2.3075(7) - 2.3293(7), P–B 1.982(3) - 1.990(3), B–P–Cu 118.07(10) - 121.03(9), P–Cu–P 111.45(3) - 124.85(3); **4** P–Cu 2.2571(6) - 2.2649(6), Cu–Cl 2.2861(7), P–B 1.975(3) - 1.984(3), B–P–Cu 119.61(8) - 123.80(8), P–Cu–P 131.49(3), P–Cu–Cl 112.84(2) - 115.67(2).

Reactions of **A1** or **A2** with Ag^+ salts lead to decomposition accompanied by the formation of black precipitate (presumably Ag^0) regardless of the solvent used (CH_2Cl_2 or

MeCN). $[Me_3NH]^+[BF_4]^-$ and $[Me_3N{\cdot}H_2B{\cdot}NCMe]^+[BF_4]^-$) could be identified by single-crystal X-ray structure analysis as two of the decomposition products (Scheme 2). When **A1** was reacted with the Ag^+ salt of the weakly coordinating anion [FAl] = $[FAl\{OC_6F_{10}(C_6F_5)\}_3]$) in one case $[Ag_2(H_2P–BH_2{\cdot}NMe_3)_2][FAl]$ (**5**) was obtained in traces and could be structurally characterized. Compound **5** contains two Ag^+ cations connected by **A1** in an unprecedented coordination mode with simultaneous donation of the P atom and the BH_2 group forming an almost planar six-membered $Ag_2–P_2–B_2$ ring (Figure 3, largest deviation from the plane 0.038 Å for Ag). The Ag^+ cation is coordinated by a P atom of one phosphanylborane (η^1) and the two hydrides of the boranyl group (η^2) of the second phosphanylborane. While some examples are known for the η^2 coordination mode of BH_2 groups for Rh,[15] Ir,[16] Ru and other transition metals,[17] to the best of our knowledge this is unknown for Ag. The coordination sphere of the Ag^+ is further completed by a CH_2Cl_2 molecule in a η^1-coordination mode. The P–B bond length (1.957(5) Å) is slightly shortened compared to free **A1**. The P–Ag bond length measures 2.3884(12) Å and is exactly in the range of the calculated sum of the covalent radii ($\sum r_{cov}$(Ag-P) = 2.39 Å).[14] The B–Ag distance measures 2.505(5) Å and is larger than the calculated sum of the covalent radii of Ag and B ($\sum r_{cov}$(Ag-B) = 2.13 Å),[14] but clearly smaller than the sum of the van der Waals radii ($\sum r_{vdW}$(Ag-B) = 3.64 Å).[18]

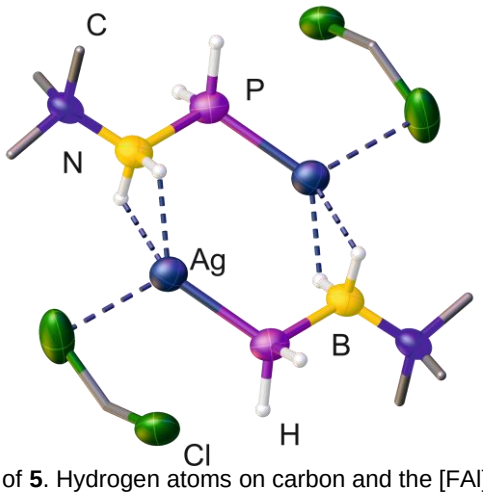

Figure 3: Molecular structure of **5**. Hydrogen atoms on carbon and the $[FAl]^-$ counter ions are omitted for clarity. Coordination of CH_2Cl_2 and BH_2 is illustrated by dashed bonds. Selected bond lengths [Å] and angles [°]: P–Ag 2.3884(12), P–B 1.957(5), Ag–B 2.505(5), Ag–Cl 2.799(4), B–P–Ag 113.66(16), P–Ag–B 137.42(13), P–Ag–B 108.6(2).

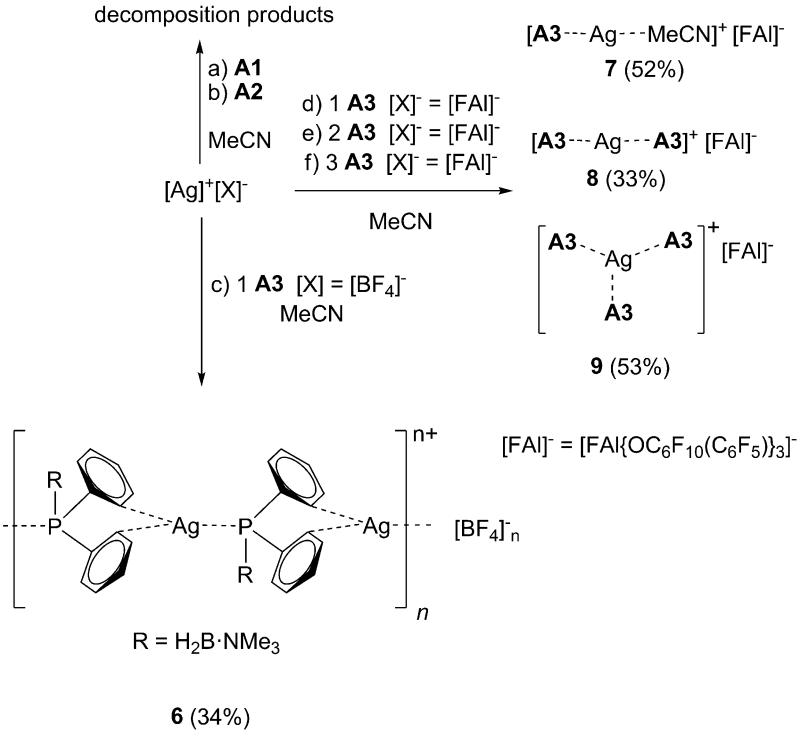

Scheme 2: Reaction of A1, A2 and A3 with Ag(I) salts.

Reactions of $Ph_2P–BH_2·NMe_3$ (**A3**) with Ag^+ salts generally proceed without precipitation of elemental silver. The reaction of **A3** with 1 equivalent of $Ag[BF_4]$ yields the one-dimensional polymer $[Ag(Ph_2P–BH_2·NMe_3)]_n[BF_4]_n$ (**6**). Single-crystal X-ray diffraction analysis of **6** reveals a distorted trigonal planar coordination sphere around Ag (∑(P–Ag–P) angles = 357.22°, Figure 4) by coordination of one P atom and two *ortho* C atoms of the phenyl-groups of the adjacent **A3** molecule. For **6** a P–Ag bond length of 2.4059(14) Å, and a slightly elongated P–B bond compared to free **A3** (1.981(8) Å) is found. The observed Ag–C distances are 2.533(7) and 2.656(6) Å, respectively and are larger than the calculated sum of the covalent radii of Ag and C ($\sum r_{cov}$(Ag-C) = 2.03 Å),[14] but clearly smaller than the sum of the van der Waals radii ($\sum r_{vdW}$(Ag-C) = 3.42 Å).[18] After crystallization from CH_2Cl_2, the polymer is only well soluble in MeCN. In the ^{31}P NMR spectrum a broad doublet is found at δ = –29.7 ppm ($^1J_{P,Ag}$ = 610 Hz), which is shifted downfield compared to **A3** (δ = −39.5 ppm). The ESI mass spectrum shows a peak for $[Ag(Ph_2PBH_2·NMe_3)_2]^+$. Subsequently to the isolation of **6** $Ag[BF_4]$ was also reacted with 2, 3 and 4 equivalents of **A3**. Surprisingly, these reactions did not result in the formation of $[Ag(Ph_2P–BH_2·NMe_3)_n][BF_4]$ and only the polymer **6** could be structurally characterized.

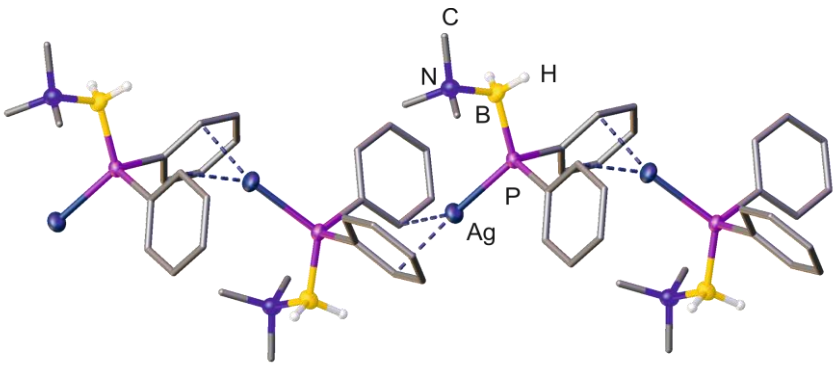

Figure 4: Molecular structure of **6**. Hydrogen atoms on carbon and the $[BF_4]^-$ counter ions are omitted for clarity. Selected bond lengths [Å] and angles[°]: P–Ag 2.4059(14), P–B 1.981(8), Ag–C 2.533(7) and 2.656(6), B–P–Ag 120.5(2), P–Ag–C 129.92(15) a. 142.89(18).

Reactions of different stoichiometric amounts of $Ph_2P–BH_2·NMe_3$ with Ag^+ salts containing the bigger weakly coordinating anion $[FAl]^-$ result in the selective formation of $[Ag(Ph_2P–BH_2·NMe_3)(MeCN)]^+[FAl]^-$ (**7**), $[Ag(Ph_2P–BH_2·NMe_3)_2]^+[FAl]^-$ (**8**) and $[Ag(Ph_2P–BH_2·NMe_3)_3]^+[FAl]^-$ (**9**) (Scheme 2). A fourfold coordination of Ag^+ by **A3** could not be observed. This suggests that due to its boranyl group **A3** has a higher steric demand compared to PPh_3 (for example $[Ag(PPh_3)_4][ClO_4]$ is known).[19] In the solid state **7** and **8** show a distorted linear coordination of the Ag atom (163.85(6)° (**7**), 170.37(3)° (**8**)) with a P–Ag bond length of 2.3633(6) Å (**7**) and 2.3881(8) - 2.3915(8) Å (**8**), respectively. Compound **9** exhibits a distorted trigonal planar coordination environment of Ag (∑(P–Ag–P) angles = 359.82°), with P–Ag–P angles ranging from 112.46(3) to 124.44(3)°. Each boranyl group adopts another orientation, one lies in the AgP_3 plane while the others each point out of the plane on opposite sites (Figure 5). The same structural motif is observed for the Cu complex **3**. The P–Ag bond lengths are between 2.4784(7) to 2.5114(8) Å and longer compared to **7** and **8**. In the ^{31}P NMR spectrum of **7** a broad doublet arises at δ = –25.8 ppm ($^1J_{P,Ag}$ = 628 Hz). Compound **8** shows also a broad doublet at δ = –25.6 ppm ($^1J_{P,Ag}$ = 415 Hz). Both signals are downfield shifted compared to the starting material **A3** (δ = −39.5 ppm). For the trifold-coordinated complex **9** a broad signal is found at δ = –28.8 ppm, but no coupling can be resolved. While **7** and **8** are obtained without formation of any side products, the reaction with 3 equivalents of **A3** shows the formation of new signals in the ^{31}P NMR spectrum (~ 20%) which could not be assigned to **9**. However, crystallization exclusively yields **9**. When 4 equivalents of **A3** are reacted with Ag^+ the obtained NMR spectra of the crude reaction mixture closely resemble the 1:3 complex **9** while the signals for the side products are increasing in intensity along with the occurrence of new signals. In the ESI mass spectra the molecular ion peak is found for $[Ag(Ph_2P–BH_2·NMe_3)MeCN]^+$ (**7**) and $[Ag(Ph_2P–BH_2·NMe_3)_n]$ (**8** n =2, **9** n = 3). The observed reactivity suggests that **A3** is a strong

donor towards Ag^+ forming complexes in a 1:1 (**7**), 1:2 (**8**) and 1:3 (**9**) stoichiometry, respectively. However, probably due to steric repulsion only three ligands **A3** can be coordinated to Ag^+ in solution and in the solid state. In contrast, for PPh_3 complexes with the fourfold coordination ($[Ag(PPh_3)_4]^+$) can be obtained.[20]

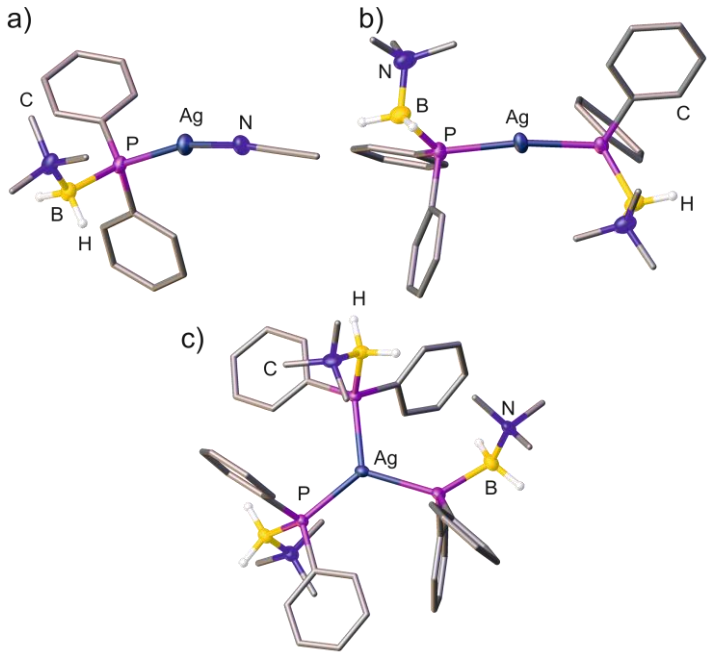

Figure 5: Molecular structure of **7** (a), **8** (b) and **9** (c). Hydrogen atoms on carbon and the $[FAl]^-$ counter ions are omitted for clarity. Selected bond lengths [Å] and angles [°] **7**: P–Ag 2.3633(6), P–B 1.972(3), N–Ag 2.129(2), B–P–Ag 117.72(9), N–Ag–P 163.85(6); **8**: Ag–P 2.3881(8) a. 2.3915(8), P–B 1.965(4) a. 1.984(4), P–Ag–P 170.37(3), B–P–Ag 118.65(13) a. 124.95(13); **9**: Ag–P 2.4784(7) - 2.5114(8), P–B 1.962(4) - 2.004(4), P–Ag–P 112.46(3) - 124.44(3), B–P–Ag 117.13(10) - 129.10(12).

10.3 Conclusion

In summary, it was shown that the pnictogenylboranes $H_2E–BH_2·NMe_3$ (**A1** E = P; **A2** E = As) and $Ph_2P–BH_2·NMe_3$ (**A3**) can be used for the generation of homoleptic complexes of the coinage metals Cu^+ and Ag^+. For Cu^+ the use of the special primary phosphine **A1** and primary arsine **A2** lead to the tetrahedral complexes $[Cu(L)_4]^+$ (L = **A1** (**1**), **A2** (**2**). Among these, complex **2** represents the first Cu complex of a primary arsine. The use of the sterically demanding **A3** leads to a trigonal planar coordination of the Cu^+ ion. For Ag^+ the reaction with **A1** and **A2** leads to decomposition and only side-products were obtained. The organosubstituted phosphanylborane **A3** however, yields a one-dimensional polymer exhibiting Ag-C_{phenyl} interactions for the smaller $[BF_4]^-$ anion. When the bigger $[FAl]^-$ anion is used, complexes containing 1, 2 or 3 ligands **A3** are selectively obtained. The current study conclusively shows the versatility of the easily accessible primary phosphine **A1** or the primary arsine **A2** containin a boranyl group as ligands in coordination chemistry. Despite the academic interest, these ligands may be interesting

for catalytic studies and large variety of different complexes should be accessible. Especially the ligand **A3**, which can be described as a derivative of PPh_3, will be interesting to study, due to the fact that it stabilizes trigonal coordinated metal centers.

10.4 References

[1] a) I. V. Kourkine, S. V. Maslennikov, R. Ditchfield, D. S. Glueck, G. P. A. Yap, L. M. Liable-Sands, A. L. Rheingold, *Inorg.Chem.* **1996**, *35*, 6708–6716; b) P. G. Edwards, B. M. Kariuki, P. D. Newman, H. A. Tallis, C. Williams; *Dalton Trans.* **2014**, *43*, 15532–15545.

[2] P. G. Jones, H. W. Roesky, H. Gruetzmacher, G. M. Sheldrick; *Z. Naturforsch., B: Chem. Sci.* **1985**, *40*, 590–593.

[3] a) O. M. A. Salah, M. I. Bruce, P. J. Lohmeyer, C. L. Raston, B. W. Skelton, A. H. White; *J.Chem.Soc.,Dalton Trans.* **1981**, 962–967; b) G. A. Bowmaker, Effendy, R. D. Hart, J. D. Kildea, E. N. de Silva, B. W. Skelton, A. H. White; *Aust.J.Chem.* **1997**, *50*, 539–552; c) M. F. Davis, M. Jura, W. Levason, G. Reid, M. Webster; *J.Organomet.Chem.* **2007**, *692*, 5589–5597; d) T. Kern, G. Knor, M. Zabel, U. Monkowius; *Acta Crystallogr., Sect. E: Struct. Rep. Online* **2008**, 64, m99; e) J. R. Black, W. Levason, M. D. Spicer, M. Webster; *J. Chem. Soc., Dalton Trans.* **1993**, 3129–3136.

[4] Ph for example: see ref 7b, M. Nardelli, C. Pelizzi, G. Pelizzi, P. Tarasconi; *J. Chem. Soc., Dalton Trans.* **1985**, 321–331; S. W. Ng; *Acta Crystallogr.,Sect. E: Struct. Rep. Online* **2012**, *68*, m1537,

[5] L. Galiano, M. Alcamí, O. Mó, M. Yánez, *J. Phys. Chem. A* **2002,** *106,* 9306–9312.

[6] a) E. Röttinger, H. Vahrenkamp, *J. Organomet. Chem.* **1981**, *213*, 1–9; b) T. Thomas, D. Pugh, I. P. Parkin, C. J. Carmalt, *Dalton Trans.* **2010**, *39*, 5325–5331; c) T. Pugh, A. Kerridge, R. A. Layfield, *Angew. Chem. Int. Ed.* **2015**, *54*, 4255–4258, *Angew. Chem.* **2015**, *127*, 4329–4332.

[7] a) S. Rendler, M. Oestreich, *Angew. Chem. Int. Ed.* **2007**, *46*, 498–504; *Angew. Chem.* **2007**, *119*, 504–510; b) D. H. Appella, Y. Moritani, R. Shintani, E. M. Ferreira, S. L. Buchwald, *J. Am. Chem. Soc.* **1999**, *121*, 9473–9474; c) S. Lal, H. S. Rzepa, S. Díez-González, *ACS Catal.* **2014**, *4*, 2274−2287; d) K. Ramakrishna, M. Murali, C. Sivasankar, *Org. Lett.* **2015**, *17*, 3814−3817.

[8] A. Yanagisawa, T. Arai, *Chem. Commun.* **2008**, 1165–1172.

[9] a) C. Marquardt, T. Jurca, K.-C. Schwan, A. Stauber, A. V. Virovets, G. R. Whittell, I. Manners, M. Scheer, *Angew. Chem. Int. Ed.* **2015**, *54*, DOI: 10.1002/anie.201507084; *Angew. Chem.* **2015**, *127*, DOI: 10.1002/anie.201507084;

b) C. Marquardt, A. Adolf, A. Stauber, M. Bodensteiner, A. V. Virovets, A. Y. Timoshkin, M. Scheer, *Chem. Eur. J.* **2013**, *19*, 11887–11891.

[10] C. Marquardt, C. Thoms, A. Stauber, G. Balazs, M. Bodensteiner, M. Scheer, *Angew. Chem. Int. Ed.* **2014**, *53*, 3727–3730; *Angew. Chem.* **2014**, *126*, 3801–3804; unpublished results, see chapter 5 and 6.

[11] K.-C. Schwan, A. Y. Timoskin, M. Zabel, M. Scheer, *Chem. Eur. J.* **2006**, *12*, 4900–4908; unpublished results, see chapter 7 and 8.

[12] C. Thoms, C. Marquardt, M. Bodensteiner, M. Scheer, *Angew. Chem. Int. Ed.* **2013**, *52*, 5150–5154; *Angew. Chem.* **2013**, *125*, 5254–5259.

[13] K. Schwan, A. Adolf, M. Bodensteiner, M. Zabel, M. Scheer, *Z. Anorg. Allg. Chem.* **2008**, *634*, 1383–1387.

[14] P. Pyykkö, M. Atsumi, *Chem. Eur. J.* **2009**, *15*, 186–197.

[15] M. A. Huertos, A. S. Weller, *Chem. Commun.* **2012**, *48*, 7185–7187.

[16] C. Y. Tang, A. L. Thompson, S. Aldridge, *J. Am. Chem. Soc.* **2010**,*132*, 10578–10591.

[17] G. Alcaraz, S. Sabo-Etienne, *Angew. Chem. Int. Ed.* **2010**, *49*, 7170–7179; *Angew. Chem.* **2010**, *122*, 7326–7335.

[18] a) A. Bondi, *J. Phys. Chem.* **1964**, *68*, 441–451; b) M. Mantina, A. C. Chamberlin, R. Valero, C. J. Cramer, D. G. Truhlar, *J. Phys. Chem. A.* **2009**, *113*, 5806–5812.

[19] L.M. Engelhardt, C. Pakawatchai, A.H. White, P.C. Healy, *J. Chem. Soc., Dalton Trans.* **1985**, 125–133.

[20] R. Meijboom, R. J. Bowen, S. J. Berners-Price, *Coord. Chem. Rev.* **2009**, *253*, 325–342.

10.5 Supporting Information

General Experimental

All manipulations were performed under an atmosphere of dry argon using standard glove-box and Schlenk techniques. All solvents were degassed and purified by standard procedures. The compounds $H_2EBH_2{\cdot}NMe_3$ (E = P, As),[1] $Ph_2PBH_2{\cdot}NMe_3$,[1] Ag[FAl],[2] and Ag[Tef][3] were prepared according to literature procedures. Other chemicals were obtained from Sigma Aldrich ($[Cu(MeCN)_4][BF_4]$, $Ag[BF_4]$). NMR spectra were recorded on a Bruker Avance 400 spectrometer (^{1}H: 400.13 MHz, ^{31}P: 161.976 MHz, ^{11}B: 128.378 MHz, ^{13}C{^{1}H}: 100.623 MHz) with δ [ppm] referenced to external $SiMe_4$ (^{1}H, ^{13}C), H_3PO_4 (^{31}P), $BF_3{\cdot}Et_2O$ (^{11}B). IR spectra were recorded on a DIGILAB (FTS 800) FT-IR

spectrometer. All mass spectra were recorded on a ThermoQuest Finnigan TSQ 7000 (ESI-MS). The C, H, N analyses were measured on an Elementar Vario EL III apparatus.

Synthesis of $[Cu(H_2PBH_2{\cdot}NMe_3)_4)]^+[BF_4]^-$ (1):

A solution of 84 mg (0.8 mmol) $H_2PBH_2{\cdot}NMe_3$ in 1 mL toluene is added to a solution of 63 mg (0.2 mmol) $[Cu(MeCN)_4)]^+[BF_4]^-$ in 10 ml MeCN. After stirring the mixture for 18 h, all volatiles are removed under reduced pressure. After dissolving the solid in CH_2Cl_2 the solution is filtrated and over layered by the 6 fold amount of *n*-hexane. **1** crystallises at r.t. as colourless needles. The crystals are separated and washed with *n*-hexane (3×5 mL). Yield of $[Cu(H_2PBH_2{\cdot}NMe_3)_4)]^+[BF_4]^-$: 66 mg (58%). ^{1}H NMR (CD_2Cl_2, 25 °C): δ = 2.10 (q, 2H, BH_2), 2.20 (dm, $^1J_{H,P}$ = 258 Hz, 4H, PH_2), 2.69 (s, 9H, NMe_3). ^{31}P NMR (CD_2Cl_2, 25 °C): δ = –183.8 (t, br, $^1J_{H,P}$ = 258 Hz). ^{31}P{^{1}H} NMR (CD_2Cl_2,25 °C): δ = –183.8 (s, br). ^{11}B NMR (CD_2Cl_2, 25 °C): δ = –7.8 (m, br, BH_2), –1.4 (s, BF_4). ^{11}B{^{1}H} NMR (CD_2Cl_2, 25 °C): δ = –8.7 (s, br, BH_2), –1.4 (s, BF_4). ^{19}F NMR (CD_2Cl_2, 25 °C): δ = −152.81 (s, $^{11}BF_4$), −152.87 (s, $^{10}BF_4$). ^{13}C{^{1}H} NMR (CD_2Cl_2, 25 °C): δ = 53.2 (d, $^4J_{P,H}$ = 4 Hz). IR (KBr): $\tilde{\nu}$ = 3020 (w, CH), 2948 (w, CH), 2920 (w, CH), 2890 (w, CH) 2835 (w, CH), 2386 (s, br, BH), 2323 (s, PH), 2309 (s, PH), 2250 (w), 2215 (w), 2178 (w), 2143 (w), 2011 (w), 1817 (w), 1735 (w), 1481 (s), 1470 (s), 1408 (m), 1287 (w), 1249 (m), 1151 (s), 1125 (s), 1100 (s), 1061 (vs, BF_4), 978 (m), 849 (vs), 754 (vs), 696 (w), 611 (w), 521 (w), 464 (vw), 434 (vw). ESI-MS (THF): *m/z* = 378 (66%, $[Cu(H_2PBH_2{\cdot}NMe_3)_3)]^+$), 273 (100 %, $[Cu(H_2PBH_2{\cdot}NMe_3)_2)]^+$). Elemental analysis (%) calculated for $C_{12}H_{52}P_4B_5Cu_1F_4N_4$ (**1**): C: 25.25, H: 9.19, N: 9.82; found: C: 25.72, H: 9.09, N: 9.85.

Synthesis of $[Cu(H_2AsBH_2{\cdot}NMe_3)_4)]^+[BF_4]^-$ (2):

A solution of 60 mg (0.4 mmol) $H_2AsBH_2{\cdot}NMe_3$ in 0.8 mL toluene is added to a solution of 31 mg (0.1 mmol) $[Cu(MeCN)_4)]^+[BF_4]^-$ in 10 ml MeCN. After stirring the mixture for 18 h, all volatiles are removed under reduced pressure. After dissolving the solid in CH_2Cl_2 the solution is filtrated and over layered by the 6 fold amount of *n*-hexane. **2** crystallises at r.t. as colourless needles. The crystals are separated and washed with *n*-hexane (3×5 mL). Yield of $[Cu(H_2AsBH_2{\cdot}NMe_3)_4)]^+[BF_4]^-$: 48 mg (65 %). ^{1}H NMR (CD_2Cl_2, 25 °C): δ = 1.21 (m, AsH_2), 2.37 (q, 2H, BH_2), 2.72 (s, 9H, NMe_3). ^{11}B NMR (CD_2Cl_2, 25 °C): δ = –7.8 (t, $^1J_{B,H}$ = 110 Hz, BH_2), –1.4 (s, BF_4). ^{11}B{^{1}H} NMR (CD_2Cl_2, 25 °C): δ = –7.8 (s, br, BH_2), –1.4 (s, BF_4).). ^{19}F{^{1}H} NMR (CD_2Cl_2, 25 °C): δ = −152.25 (s, $^{11}BF_4$), −152.19 (s, $^{10}BF_4$). ^{19}F NMR (CD_2Cl_2, 25 °C): δ = −152.25 (s, $^{11}BF_4$), −152.19 (s, $^{10}BF_4$). ^{13}C{^{1}H} NMR (CD_2Cl_2, 25 °C): δ = 53.7 (s, NMe_3). IR (KBr): $\tilde{\nu}$ = 3017 (w, CH), 3000 (w, CH), 2948 (w, CH), 2920 (w, CH), 2839 (w), 2409 (m, BH), 2382 (m, BH), 2294

(w), 2121 (m, AsH), 2104 (m, AsH), 1484 (m), 1469 (m), 1409 (w), 1249 (w), 1135 (w), 1120 (m), 1099 (m), 1059 (vs, BF_4), 1009 (m), 977 (m), 959 (m), 851 (m), 711 (w), 670 (m), 552 (w), 520 (w). ESI-MS (MeCN): *m/z* = 361 (100 %, $[Cu(H_2AsBH_2{\cdot}NMe_3)_2]^+$), 253 (54 %, $[Cu(H_2AsBH_2{\cdot}NMe_3)MeCN]^+$). Elemental analysis (%) calculated for $C_{12}H_{52}As_4B_5Cu_1F_4N_4$ (**2**): C: 19.32, H: 7.03, N: 7.51; found: C: 19.52, H: 7.06, N: 7.25.

Synthesis of $[Cu(Ph_2PBH_2{\cdot}NMe_3)_3)]^+[BF_4]^-$ (3):

A solution of 154 mg (0.6 mmol) $Ph_2PBH_2{\cdot}NMe_3$ in 10 mL MeCN is added to a solution of 63 mg (0.2 mmol) $[Cu(MeCN)_4)]^+[BF_4]^-$ in 10 ml MeCN. After stirring the mixture for 18 h, all volatiles are removed under reduced pressure. The solid is dissolved in CH_2Cl_2 and the solution is filtrated. The solution is over layered with twice the amount of *n*-hexane. **3** crystallises at -28 °C as colourless blocks. The crystals are separated and washed with *n*-hexane (3×5 mL). Yield of $[Cu(Ph_2PBH_2{\cdot}NMe_3)_3)]^+[BF_4]^-$: 126 mg (65 %). ^{1}H NMR (CD_2Cl_2, 25 °C): δ = 2.37 (s, 9H, NMe_3), 2.49 (br, 2H, BH_2), 7.15 (m, 2H, *m*-Ph), 7.22 (m, 2H, *p*-Ph), 7.36 (m, 4H, *o*-Ph). ^{31}P NMR (CD_2Cl_2, 25 °C): δ = –38.9 (s, br). ^{31}P{^{1}H} NMR (CD_2Cl_2, 25 °C): δ = –38.9 (s, br). ^{11}B NMR (CD_2Cl_2, 25 °C): δ = –5.9 (s, br, BH_2), –1.4 (s, BF_4). ^{11}B{^{1}H} NMR (CD_2Cl_2, 25 °C): δ = –5.9 (s, br, BH_2), –1.4 (s, BF_4). ^{19}F NMR (CD_2Cl_2, 25 °C): δ = −152.91 (s, $^{11}BF_4$), −152.85 (s, $^{10}BF_4$). ^{19}F{^{1}H} NMR (CD_2Cl_2, 25 °C): δ = −152.91 (s, $^{11}BF_4$), −152.85 (s, $^{10}BF_4$). ^{13}C{^{1}H} NMR (CD_2Cl_2, 25 °C): δ = 54.4 (s, NMe_3), 128.4 (s, *p*-Ph), 128.6 (s, *m*-Ph), 134.2 (s, *o*-Ph), 136.3 (s, *i*-Ph). IR (KBr): $\tilde{\nu}$ = 3052 (w, CH), 3005 (w, CH), 2949 (w, CH), 2877 (w, CH), 2842 (w, CH), 2390 (m, br, BH), 1963 (vw), 1892 (vw), 1818 (vw), 1584 (w), 1481 (s), 1463 (s), 1434 (s), 1410 (w), 1426 (w), 1158 (w), 1124 (s), 1063 (vs, BF_4), 970 (m), 856 (m), 739 (s), 698 (s), 512 (m). ESI-MS (pos., MeCN): *m/z* = 577 (100%, $[Cu(Ph_2PBH_2{\cdot}NMe_3)_2]^+$), ESI-MS (neg., MeCN): *m/z* = 87 (100%, $[BF_4]^-$). Elemental analysis (%) calculated for $C_{45}H_{63}B_4Cu_1F_4N_3P_3$ (**3**): C: 58.60, H: 6.89, N: 4.56; found: C: 58.40, H: 6.94, N: 4.14.

Decomposition of $[Cu(Ph_2PBH_2{\cdot}NMe_3)_3)]^+[BF_4]^-$ (3) to $[Cu(Ph_2PBH_2{\cdot}NMe_3)_2Cl)]^+[BF_4]^-$ (4):

Storing a solution of **3** in CH_2Cl_2 leads to traces of **4**. Some crystals were obtained by over layering a solution with *n*-hexane and storing it at r.t..

Typical reaction of the parent compounds $H_2EBH_2{\cdot}NMe_3$ with $[Ag]^+[X]^-$ salts:

0.1 mmol of $[Ag]^+[X]^-$ (X = BF_4, Tef, FAl) were dissolved in MeCN or CH_2Cl_2 and 0.1 mmol $H_2EBH_2{\cdot}NMe_3$ (E = P, As) were added in either toluene or MeCN. In all cases the solution turned immediately dark and a black precipitate formed. Although in one case (E = P, X = BF_4) new signals were observed in ^{11}B (δ = −10.6 ppm) and ^{31}P NMR (δ = −185

ppm), no products could be isolated or characterized. In the reaction of $H_2AsBH_2{\cdot}NMe_3$ and $[Ag]^+[BF_4]^-$ the ionic compound $[Me_3N{\cdot}H_2B{\cdot}NCMe]^+[BF_4]^-$ was isolated and confirmed by single crystal X-Ray structure analysis and ^1H and ^{11}B NMR spectroscopy.

^1H NMR (CD_2Cl_2, 25 °C): δ = 2.33 (q, $^1J_{B,H}$ = 115 Hz BH_2), 2.78 (s, 9H, NMe_3), 2.83 (t, 3H, NCMe). ^{11}B NMR (CD_2Cl_2, 25 °C): δ = –6.7 (t, br, $^1J_{B,H}$ = 115 Hz BH_2), –1.3 (s, BF_4). $^{11}B\{^1H\}$ NMR (CD_2Cl_2, 25 °C): δ = –6.7 (s, br, BH_2), –1.3 (s, BF_4).

Reaction of $H_2PBH_2{\cdot}NMe_3$ and $[Ag]^+[FAl]^-$ gave a mixture of different crystals (<<10 mg). We were able to structurally characterize one compound with the molecular formula "$C_{40}H_{15}AgAlBCl_2F_{46}NO_3P$" (**5**) showing a $[(Ag{\cdot}H_2PBH_2{\cdot}NMe_3)_2]^{2+}$ dimer exhibiting a six-membered ring.

Synthesis of $[Ag(Ph_2PBH_2{\cdot}NMe_3]^+[BF_4]^-$ (6):

A solution of 54 mg (0.21 mmol) $Ph_2PBH_2{\cdot}NMe_3$ in 10 mL MeCN is added to a solution of 39 mg (0.20 mmol) $[Ag]^+[BF_4]^-$ in 10 ml MeCN. Upon addition the solution turns slightly red, the solution is stirred for 1 day. After removal of all volatiles under reduced pressure the remaining solid is dissolved in 5 mL of CH_2Cl_2 and filtrated. The clear solution is over layered by the 6 fold amount of *n*-hexane. **6** crystallises at r.t. as colourless needles. The crystals are separated and washed with *n*-hexane (3×5 mL). Yield of $[Ag(Ph_2PBH_2{\cdot}NMe_3]^+[BF_4]^-$: 32 mg (34 %). ^1H NMR (CD_3CN, 25 °C): δ = 2.58 (q, BH_2), 2.71 (s, 9H, NMe_3), 7.34 – 7.41 (m, 6H, *m*- & *p*-Ph), 7.63 (s, br, 4H, *o*-Ph). ^{31}P NMR (CD_3CN, 25 °C): δ = –29.7 (d, br, $^1J_{P,Ag}$ = 610 Hz). $^{31}P\{^1H\}$ NMR (CD_3CN, 25 °C): δ = –29.7 (d, br, $^1J_{P,Ag}$ = 610 Hz). ^{11}B NMR (CD_3CN, 25 °C): δ = –4.6 (m, BH_2), –0.6 (s, BF_4). $^{11}B\{^1H\}$ NMR (CD_3CN, 25 °C): δ = –4.6 (d, br, $^1J_{B,P}$ = 64 Hz, BH_2), –0.6 (s, BF_4). ^{19}F NMR (CD_3CN, 25 °C): δ = −150.64 (s, $^{11}BF_4$), −150.58 (s, $^{10}BF_4$). $^{19}F\{^1H\}$ NMR (CD_3CN, 25 °C): δ = −150.64 (s, $^{11}BF_4$), −150.58 (s, $^{10}BF_4$). $^{13}C\{^1H\}$ NMR (CD_3CN, 25 °C): δ = 54.5 (s, NMe_3), 129.5 (s, *p*-Ph), 129.9 (s, *m*-Ph), 135.2 (d, $^2J_{C,P}$ = 10 Hz, *o*-Ph), 136.5 (d, $^1J_{B,P}$ = 32 Hz, *i*-Ph). IR (KBr): $\tilde{\nu}$ = 3052 (vw, CH), 3009 (vw, CH), 2950 (vw, CH), 2423 (m, br, BH), 2389 (m, br, BH), 2300 (w), 1568 (vw), 1479 (s), 1466 (m), 1433 (m), 1412 (w), 1312 (vw), 1285 (vw), 1250 (w), 1180 (m), 1115 (s), 1079 (vs), 1073 (vs), 1010 (s), 862 (s), 766 (s), 775 (s), 750 (s), 711 (s), 519 (s), 486 (vw). ESI-MS (CH_2Cl_2): *m/z* = 621 (100%, $[Ag(Ph_2PBH_2{\cdot}NMe_3)_2]^+$), 562 (10%, $[Ag(Ph_2PBH_2{\cdot}NMe_3)(Ph_2PBH_2)]^+$). Elemental analysis (%) calculated for $C_{15}H_{21}AgB_2F_4NP$ (**6**): C: 39.88, H: 4.61, N: 3.10; found: C: 39.75, H: 4.61, N: 3.13.

Synthesis of $[Ag(Ph_2PBH_2{\cdot}NMe_3)(MeCN)]^+[FAl]^-$ (7):

A solution of 12 mg (0.05 mmol) $Ph_2PBH_2{\cdot}NMe_3$ in 5 mL MeCN is added to a solution of 73 mg (0.05 mmol) $[Ag]^+[FAl]^-$ in 5 ml MeCN and the solution is stirred for 1 day. After

removal of all volatiles under reduced pressure the remaining solid is dissolved in 5 mL of CH_2Cl_2 and filtrated. The clear solution is over layered by the 6 fold amount of *n*-hexane. **7** crystallises at r.t. as colourless needles. The crystals are separated and washed with *n*-hexane (3×5 mL). Yield of $[Ag(Ph_2PBH_2{\cdot}NMe_3)(MeCN)]^+[FAl]^-$: 45 mg (52 %). ^{1}H NMR (CD_2Cl_2, 25 °C): δ = 2.36 (s, MeCN), 2.66 (m, 2H, BH_2), 2.69 (s, 9H, NMe_3), 7.35 – 7.46 (m, 6H, *m*- & *p*-Ph), 7.53 – 7.64 (m, 4H, *o*-Ph). ^{31}P NMR (CD_2Cl_2, 25 °C): δ = –25.8 (d, br, $^1J_{P,Ag}$ = 628 Hz). ^{31}P{^{1}H} NMR (CD_2Cl_2, 25 °C): –25.8 (d, br, $^1J_{P,Ag}$ = 628 Hz). ^{11}B NMR (CD_2Cl_2, 25 °C): δ = –5.8 (m, br, BH_2). ^{11}B{^{1}H} NMR (CD_2Cl_2, 25 °C): δ = –5.8 (m, br, BH_2). ^{19}F NMR (CD_2Cl_2, 25 °C): δ = –172.2 ppm (s, AlF), –165.2 (t, $J_{F,F}$ = 18 Hz, 1F), –154.5 (t, $J_{F,F}$ = 22 Hz, 1F), –141.5 (d, $J_{F,F}$ = 277 Hz, 1F), –137.4 (d, $J_{F,F}$ = 277 Hz, 2F), –130.8 (d, $J_{F,F}$ = 277 Hz, 2F), –128.1 (s, 2F), –122.1 (d, $J_{F,F}$ = 277 Hz, 2F), –117.2 (d, $J_{F,F}$ = 277 Hz, 2F), –112.7 (d, $J_{F,F}$ = 283 Hz, 2F). ^{19}F{^{1}H} NMR (CD_2Cl_2, 25 °C): δ = –172.2 ppm (s, AlF), –165.2 (t, $J_{F,F}$ = 18 Hz, 1F), –154.5 (t, $J_{F,F}$ = 22 Hz, 1F), –141.5 (d, $J_{F,F}$ = 277 Hz, 1F), –137.4 (d, $J_{F,F}$ = 277 Hz, 2F), –130.8 (d, $J_{F,F}$ = 277 Hz, 2F), –128.1 (s, 2F), –122.1 (d, $J_{F,F}$ = 277 Hz, 2F), –117.2 (d, $J_{F,F}$ = 277 Hz, 2F), –112.7 (d, $J_{F,F}$ = 283 Hz, 2F). ^{13}C{^{1}H} NMR (CD_2Cl_2, 25 °C): δ = 2.7 (**Me**CN), 54.8 (d, $^3J_{C,P}$ = 7 Hz, NMe_3), 120.1 (s, Me**C**N), 129.5 (d, $^2J_{C,P}$ = 9 Hz, *p*-Ph), 130.4 (s, *m*-Ph), 132.4 (d, $^1J_{B,P}$ = 34 Hz, *i*-Ph), 134.5 (d, $^2J_{C,P}$ = 11 Hz, *o*-Ph). Several signals have been observed from 135-150 ppm for phenyl^F- and from 105 – 115 ppm for cyclohexyl^F-group of FAl-anion, cannot be exactly assigned. IR (KBr): $\tilde{\nu}$ = 3060 (vw, CH), 3019 (vw, CH), 2958 (vw, CH), 2850 (vw, CH), 2440 (w, br, BH), 2387 (w, br, BH), 2361 (w), 2321 (w), 2295 (w), 1653 (m), 1534 (m), 1486 (vs), 1324 (m), 1309 (m), 1268 (s), 1243 (s), 1205 (vs), 1186 (s), 1153 (s), 1104 (s), 1068 (w), 1020 (s), 955 (vs), 911 (m), 858 (w) , 811 (w), 770 (s), 751 (m), 741 (m), 730 (s), 696 (w), 667 (w), 647 (w), 635 (w), 625 (w), 600 (w), 535 (w), 527 (w), 519 (w), 500 (w), 490 (w), 468 (vw). ESI-MS (MeCN, pos): *m/z* = 621 (88%, $[Ag(Ph_2PBH_2{\cdot}NMe_3)_2]^+$), 405 (100%, $[Ag(Ph_2PBH_2{\cdot}NMe_3)(MeCN)]^+$. ESI-MS (MeCN, neg): *m/z* = 1381 (100%, $[FAl]^-$). Elemental analysis (%) calculated for $C_{53}H_{24}AgAlBF_{46}N_2O_3P$ (**7**): C: 35.76, H: 1.35, N: 1.56; found: C: 35.76, H: 1.60, N: 1.44.

Synthesis of $[Ag(Ph_2PBH_2{\cdot}NMe_3)_2]^+[FAl]^-$ (8):

A solution of 24 mg (0.1 mmol) $Ph_2PBH_2{\cdot}NMe_3$ in 5 mL MeCN is added to a solution of 146 mg (0.1 mmol) $[Ag]^+[FAl]^-$ in 5 ml MeCN. Upon addition the solution turns slightly red, the solution is stirred for 1 day. After removal of all volatiles under reduced pressure the remaining solid is dissolved in 5 mL of CH_2Cl_2 and filtrated. The clear solution is over layered by the 6 fold amount of *n*-hexane. Compound **8** crystallises at r.t. as colourless needles. The crystals are separated and washed with *n*-hexane (3×5 mL). Yield of $[Ag(Ph_2PBH_2{\cdot}NMe_3)_2]^+[FAl]^-$: 66 mg (33 %). ^{1}H NMR (CD_2Cl_2, 25 °C): δ = 2.66 (s, 9H,

NMe_3), 2.67 (m, 2H, BH_2), 7.36 – 7.46 (m, 6H, *m*- & *p*-Ph), 7.61 (s, br, 4H, *o*-Ph). ^{31}P NMR (CD_2Cl_2, 25 °C): δ = –25.6 (d, br, $^1J_{P,Ag}$ = 415 Hz). $^{31}P\{^1H\}$ NMR (CD_2Cl_2, 25 °C): –25.6 (d, br, $^1J_{P,Ag}$ = 415 Hz). ^{11}B NMR (CD_2Cl_2, 25 °C): δ = –5.6 (m, br, BH_2). $^{11}B\{^1H\}$ NMR (CD_2Cl_2, 25 °C): δ = –5.6 (m, br, BH_2). ^{19}F NMR (CD_2Cl_2, 25 °C): δ = –172.2 ppm (s, AlF), –165.2 (t, $J_{F,F}$ = 18 Hz, 1F), –154.5 (t, $J_{F,F}$ = 22 Hz, 1F), –141.5 (d, $J_{F,F}$ = 277 Hz, 1F), –137.4 (d, $J_{F,F}$ = 277 Hz, 2F), –130.8 (d, $J_{F,F}$ = 277 Hz, 2F), –128.1 (s, 2F), –122.1 (d, $J_{F,F}$ = 277 Hz, 2F), –117.2 (d, $J_{F,F}$ = 277 Hz, 2F), –112.7 (d, $J_{F,F}$ = 283 Hz, 2F). $^{19}F\{^1H\}$ NMR (CD_2Cl_2, 25 °C): δ = –172.2 ppm (s, AlF), –165.2 (t, $J_{F,F}$ = 18 Hz, 1F), –154.5 (t, $J_{F,F}$ = 22 Hz, 1F), –141.5 (d, $J_{F,F}$ = 277 Hz, 1F), –137.4 (d, $J_{F,F}$ = 277 Hz, 2F), –130.8 (d, $J_{F,F}$ = 277 Hz, 2F), –128.1 (s, 2F), –122.1 (d, $J_{F,F}$ = 277 Hz, 2F), –117.2 (d, $J_{F,F}$ = 277 Hz, 2F), –112.7 (d, $J_{F,F}$ = 283 Hz, 2F). $^{13}C\{^1H\}$ NMR (CD_2Cl_2, 25 °C): δ = 54.7 (s, NMe_3), 129.5 (s, *p*-Ph), 130.3 (s, *m*-Ph), 133.1 (m, *i*-Ph), 134.5 (s, *o*-Ph). Several signals have been observed from 135-150 ppm for phenyl^F- and from 105 – 115 ppm for cyclohexyl^F-group of FAl-anion, cannot be exactly assigned. IR (KBr): $\tilde{\nu}$ = 3080 (w, CH), 3059 (w, CH), 3012 (w, CH), 2955 (w, CH), 2920 (w, CH), 2845 (vw, CH), 2435 (m, br, BH), 2410 (m, br, BH), 1653 (s), 1534 (s), 1484 (vs), 1436 (s), 1407 (w), 1325 (s), 1309 (s), 1268 (s), 1243 (s), 1204 (vs), 1185 (s), 1154 (s), 1134 (s), 1105 (s), 1068 (s), 1030 (s), 1018 (s), 1005 (s), 956 (vs), 910 (s), 857 (s) , 810 (m), 768 (s), 749 (s), 729 (s), 695 (s), 666 (w), 646 (m), 635 (m), 624 (m), 599 (m), 535 (m), 527 (m), 519 (m), 495 (w), 468 (m). ESI-MS (MeCN, pos): *m/z* = 621 (100%, $[Ag(Ph_2PBH_2{\cdot}NMe_3)_2]^+$). ESI-MS (MeCN, neg): *m/z* = 1381 (100%, $[FAl]^-$). Elemental analysis (%) calculated for $C_{66}H_{42}AgAlB_2F_{46}N_2O_3P$ (**8**): C: 39.56, H: 2.11, N: 1.40; found: C: 39.58, H: 2.31, N: 1.35.

Synthesis of $[Ag(Ph_2PBH_2{\cdot}NMe_3)_3]^+[FAl]^-$ (9):

A solution of 78 mg (0.3 mmol) $Ph_2PBH_2{\cdot}NMe_3$ in 5 mL MeCN is added to a solution of 150 mg (0.1 mmol) $[Ag]^+[FAl]^-$ in 5 ml MeCN. Upon addition the solution turns slightly red, the solution is stirred for 1 day. After removal of all volatiles under reduced pressure the remaining solid is dissolved in 5 mL of CH_2Cl_2 and filtrated. The clear solution is over layered by the 6 fold amount of *n*-hexane. **9** crystallises at r.t. as colourless needles. The crystals are separated and washed with *n*-hexane (3×5 mL). Yield of $[Ag(Ph_2PBH_2{\cdot}NMe_3)_3]^+[FAl]^-$: 116 mg (53 %). ^1H NMR (CD_2Cl_2, 25 °C): δ = 2.52 (s, 9H, NMe_3), 2.12 – 2.32 (m, 2H, BH_2), 7.27 – 7.36 (m, 6H, *m*- & *p*-Ph), 7.51 – 7.59 (m, br, 4H, *o*-Ph). ^{31}P NMR (CD_2Cl_2, 25 °C): δ = –28.0 (s, br). $^{31}P\{^1H\}$ NMR (CD_2Cl_2, 25 °C): –28.0 (s, br). ^{11}B NMR (CD_2Cl_2, 25 °C): δ = –5.4 (s, br, BH_2). $^{11}B\{^1H\}$ NMR (CD_2Cl_2, 25 °C): δ = –5.4 (s, br, BH_2). ^{19}F NMR (CD_2Cl_2, 25 °C): δ = –172.2 ppm (s, AlF), –165.2 (t, $J_{F,F}$ = 18 Hz, 1F), –154.5 (t, $J_{F,F}$ = 22 Hz, 1F), –141.5 (d, $J_{F,F}$ = 277 Hz, 1F), –137.4 (d, $J_{F,F}$ = 277 Hz, 2F), –130.8 (d, $J_{F,F}$ = 277 Hz, 2F), –128.1 (s, 2F), –122.1 (d, $J_{F,F}$ = 277 Hz, 2F),

–117.2 (d, $J_{F,F}$ = 277 Hz, 2F), –112.7 (d, $J_{F,F}$ = 283 Hz, 2F). $^{19}F\{^1H\}$ NMR (CD_2Cl_2, 25 °C): δ = –172.2 ppm (s, AlF), –165.2 (t, $J_{F,F}$ = 18 Hz, 1F), –154.5 (t, $J_{F,F}$ = 22 Hz, 1F), –141.5 (d, $J_{F,F}$ = 277 Hz, 1F), –137.4 (d, $J_{F,F}$ = 277 Hz, 2F), –130.8 (d, $J_{F,F}$ = 277 Hz, 2F), –128.1 (s, 2F), –122.1 (d, $J_{F,F}$ = 277 Hz, 2F), –117.2 (d, $J_{F,F}$ = 277 Hz, 2F), –112.7 (d, $J_{F,F}$ = 283 Hz, 2F). $^{13}C\{^1H\}$ NMR (CD_2Cl_2, 25 °C): δ = 54.6 (d, $^3J_{P,C}$ = 6 Hz, NMe_3), 129.2 (d, $^3J_{P,C}$ = 8 Hz, *m*-Ph), 129.6 (s, *p*-Ph), 133.6 (d, $^1J_{P,C}$ = 23 Hz, *i*-Ph), 134.4 (s, $^4J_{P,C}$ = 12 Hz, *o*-Ph). Several signals have been observed from 135-150 ppm for phenyl^F- and from 105 – 115 ppm for cyclohexyl^F-group of FAl-anion, cannot be exactly assigned. IR (KBr): $\tilde{\nu}$ = 3066 (w, CH), 3059 (w, CH), 3005 (w, CH), 2956 (w, CH), 2876 (vw, CH), 2424 (m, br, BH), 2405 (m, br, BH), 1652 (s), 1586 (w), 1533 (s), 1485 (vs), 1436 (s), 1409 (w), 1384 (w), 1332 (s), 1308 (s), 1267 (s), 1224 (s), 1205 (vs), 1186 (s), 1156 (s), 1124 (s), 1104 (s), 1067 (s), 1018 (vs), 955 (vs), 910 (s), 851 (s) , 811 (m), 767 (s), 749 (s), 729 (s), 696 (s), 666 (w), 645 (m), 635 (m), 624 (m), 600 (m), 527 (m), 511 (m), 469 (m). ESI-MS (MeCN, pos): *m/z* = 878 (0.2%, $[Ag(Ph_2PBH_2{\cdot}NMe_3)_3]^+$), 819 (100%, $[Ag(Ph_2PBH_2{\cdot}NMe_3)(Ph_2PBH_2)]^+$), 621 (100%, $[Ag(Ph_2PBH_2{\cdot}NMe_3)_2]^+$). ESI-MS (MeCN, neg): *m/z* = 1381 (100%, $[FAl]^-$). Elemental analysis (%) calculated for $C_{81}H_{63}AgAlB_3F_{46}N_3O_3P_3$ (**9**): C: 43.02, H: 2.81, N: 1.86; found: C: 43.64, H: 3.39, N: 1.69.

X-ray diffraction analysis

The single crystal X-ray diffraction experiments were performed either on a Gemini R Ultra CCD diffractometer (**1**-**4**, **6**, **7**), SuperNova CCD diffractometer (**5**, **8**, $[Me_3N{\cdot}H_2B{\cdot}NCMe]^+[BF_4]^-$) or a SuperNova(Mo) Eos CCD diffractometer (**9**) from Agilent Technologies (formerly Oxford Diffraction) applying Cu-K_α radiation (λ = 1.54178 Å) or Mo-K_α radiation (λ = 0.71073 Å). The measurements were performed at 123 K. Crystallographic data together with the details of the experiments are given below. Absorption corrections were applied semi-empirically from equivalent reflections or analytically (SCALE3/ABSPACK algorithm implemented in CrysAlis PRO software by Agilent Technologies Ltd).[4] All structures were solved using SHELXT,[5] and OLEX 2.[9] Refinements against F^2 in anisotropic approximation were done using SHELXL.[5] The hydrogen positions of the methyl groups were located geometrically and refined riding on the carbon atoms. Hydrogen atoms belonging to BH_2 and PH_2 groups were located from the difference Fourier map and refined without constraints (**1**, **4**, **7**, $[Me_3N{\cdot}H_2B{\cdot}NCMe]^+[BF_4]^-$) or with restrained E–H or B–H distances (**2**, **3**, **5**, **6**, **8**, **9**). The figures were created with OLEX 2.[6] CIF files are deposited on the provided DVD.

Table S1. Crystallographic data for compounds **1** - **2**.

Compound	**1**	**2**
empirical formula	$C_{12}H_{52}B_5CuF_4N_4P_4$	$C_{12}H_{52}As_4B_5CuF_4N_4$
formula weight	570.04	745.85
temperature [K]	123(1)	123(1)
crystal system	tetragonal	tetragonal
space group	*I*-4	*I*-4
a [Å]	15.84420(10)	16.1323(4)
b [Å]	15.84420(10)	16.1323(4)
c [Å]	6.30060(10)	6.3010(4)
α [°]	90	90.00
β [°]	90	90.00
γ [°]	90	90.00
Volume [Å^3]	1581.69(3)	1639.84(12)
Z	2	2
ρ_{calc} [g/cm^3]	1.197	1.511
μ [mm^{-1}]	3.160	5.688
F (000)	604.0	748.0
crystal size [mm^3]	0.23 × 0.15 × 0.08	0.85 × 0.07 × 0.03
radiation	Cu-K_α (λ = 1.54178)	Cu-K_α (λ = 1.54178)
absorption correction	analytical	analytical
T_{min} / T_{max}	0.578 / 0.831	0.220 / 0.866
2Θ range [°]	7.892 to 132.938	7.74 to 132.74
completeness	1.000	1.000
index ranges	−18 ≤ *h* ≤ 18 −13 ≤ *k* ≤ 18 −6 ≤ *l* ≤ 7	−19 ≤ *h* ≤ 15 −18 ≤ *k* ≤ 15 −7 ≤ *l* ≤ 5
reflections collected	6298	2473
independent reflections	1394 [R_{int} = 0.0305, R_{sigma} = 0.0233]	1172 [R_{int} = 0.0443, R_{sigma} = 0.0502]
data/restraints/parameters	1394/0/87	1172/4/83
GOF on F^2	1.058	1.019
R_1/wR_2 [I≥2σ(*I*)]	R_1 = 0.0220 wR_2 = 0.0550	R_1 = 0.0337 wR_2 = 0.0822
R_1/wR_2 [all data]	R_1 = 0.0225 wR_2 = 0.0552	R_1 = 0.0366 wR_2 = 0.0829
max/min $\Delta\rho$ [e·Å^{-3}]	0.29/−0.15	0.84/−0.48
flack parameter	0.005(15)	−0.09(7)

Table S2. Crystallographic data for compounds **3** - **4**.

Compound	**3**	**4**
empirical formula	$C_{47}H_{67}B_4Cl_4CuF_4N_3P_3$	$C_{30}H_{42}B_2ClCuN_2P_2$
formula weight	1091.52	613.20
temperature [K]	123 (1)	123(1)
crystal system	monoclinic	monoclinic
space group	$P2_1/c$	$C2/c$
a [Å]	13.36102(11)	35.8068(5)
b [Å]	15.06251(11)	8.78028(10)
c [Å]	26.9426(2)	20.8866(3)
α [°]	90	90
β [°]	98.0289(7)	106.1251(14)
γ [°]	90	90
Volume [Å^3]	5369.07(7)	6308.26(14)
Z	4	8
ρ_{calc} [g/cm^3]	1.350	1.291
μ [mm^{-1}]	3.652	2.869
F (000)	2272.0	2576.0
crystal size [mm^3]	0.17 × 0.09 × 0.07	0.09 × 0.08 × 0.05
radiation	Cu-K_α (λ = 1.54178)	Cu-K_α (λ = 1.54178)
absorption correction	multi-scan	analytical
T_{min} / T_{max}	0.763 / 1.000	0.803 / 0.877
2Θ range [°]	6.626 to 133.32	8.814 to 133.238
completeness	0.982	0.9763
index ranges	$-15 \le h \le 15$ $-17 \le k \le 17$ $-28 \le l \le 32$	$-42 \le h \le 32$ $-9 \le k \le 10$ $-20 \le l \le 24$
reflections collected	27225	15303
independent reflections	9399 [R_{int} = 0.0342, R_{sigma} = 0.0340]	5504 [R_{int} = 0.0316, R_{sigma} = 0.0316]
data/restraints/parameters	9399/24/656	5504/0/414
GOF on F^2	1.050	1.068
R_1/wR_2 [I≥2σ(I)]	R_1 = 0.0473 wR_2 = 0.1402	R_1 = 0.0354 wR_2 = 0.0894
R_1/wR_2 [all data]	R_1 = 0.0530 wR_2 = 0.1468	R_1 = 0.0418 wR_2 = 0.0936
max/min $\Delta\rho$ [e·Å^{-3}]	0.57/−1.24	0.58/−0.35

Table S3. Crystallographic data for compounds **5** - **6**.

Compound	**5**	**6**
empirical formula	$C_{40}H_{15}AgAlBCl_2F_{46}NO_3P$	$C_{15}NF_4PAgB_2H_{21}$
formula weight	1679.06	451.79
temperature [K]	123(1)	123(1)
crystal system	triclinic	orthorhombic
space group	*P*-1	$P2_12_12_1$
a [Å]	11.2820(3)	11.1197(2)
b [Å]	15.1845(4)	12.5198(2)
c [Å]	17.6051(5)	12.7040(2)
α [°]	72.606(2)	90
β [°]	72.218(2)	90
γ [°]	73.340(2)	90
Volume [Å^3]	2676.42(13)	1768.61(5)
Z	2	4
ρ_{calc} [g/cm^3]	2.083	1.697
μ [mm^{-1}]	6.308	10.334
F (000)	1628.0	904.0
crystal size [mm^3]	0.18 × 0.13 × 0.10	0.23 × 0.04 × 0.04
radiation	Cu-K_α (λ = 1.54178)	Cu-K_α (λ = 1.54178)
absorption correction	analytical	multi-scan
T_{min} / T_{max}	0.490 / 0.649	0.864 / 1.000
2Θ range [°]	6.246 to 148.45	9.918 to 132.904
completeness	0.989	0.984
index ranges	−14 ≤ *h* ≤ 11 −18 ≤ *k* ≤ 17 −21 ≤ *l* ≤ 19	−13 ≤ *h* ≤ 12 −10 ≤ *k* ≤ 14 −14 ≤ *l* ≤ 15
reflections collected	21797	5953
independent reflections	10332 [R_{int} = 0.0269, R_{sigma} = 0.0272]	2926 [R_{int} = 0.0342, R_{sigma} = 0.0351]
data/restraints/parameters	10332/28/916	2926/2/227
GOF on F^2	1.067	1.055
R_1/wR_2 [I≥2σ(*I*)]	R_1 = 0.0495 wR_2 = 0.1434	R_1 = 0.0370 wR_2 = 0.0952
R_1/wR_2 [all data]	R_1 = 0.0515 wR_2 = 0.1458	R_1 = 0.0388 wR_2 = 0.0964
max/min $\Delta\rho$ [e·Å^{-3}]	1.25/−1.54	1.36/−0.75
flack parameter	-	0.424(15)

Table S4. Crystallographic data for compounds **7** – **8.**

Compound	**7**	**8**
empirical formula	$C_{56}H_{30}AgAlB$ $Cl_6F_{46}N_2O_3P$	$C_{66}H_{42}AgAlB_2$ $F_{46}N_2O_3P_2$
formula weight	2042.15	2003.42
temperature [K]	123(1)	123(1)
crystal system	monoclinic	triclinic
space group	$P2_1/n$	P-1
a [Å]	11.39474(4)	11.3066(2)
b [Å]	19.73456(8)	17.6908(3)
c [Å]	31.31366(11)	21.6344(3)
α [°]	90.0	66.0358(15)
β [°]	92.1864(3)	88.8395(14)
γ [°]	90.0	73.5586(17)
Volume [Å^3]	7036.38(4)	3770.45(12)
Z	4	2
ρ_{calc} [g/cm^3]	1.928	1.765
μ [mm^{-1}]	6.310	4.158
F (000)	4000.0	1980.0
crystal size [mm^3]	0.41 × 0.29 × 0.27	0.21 × 0.12 × 0.10
radiation	Cu-K_α (λ = 1.54178)	Cu-K_α (λ = 1.54178)
absorption correction	analytical	analytical
T_{min} / T_{max}	0.202 / 0.362	0.529 / 0.733
2Θ range [°]	5.648 to 133.22	8.202 to 145.924
completeness	0.986	0.993
index ranges	$-13 \le h \le 13$ $-22 \le k \le 23$ $-37 \le l \le 36$	$-13 \le h \le 13$ $-21 \le k \le 21$ $-26 \le l \le 17$
reflections collected	63686	27960
independent reflections	12390 [R_{int} = 0.0276, R_{sigma} = 0.0183]	14497 [R_{int} = 0.0212, R_{sigma} = 0.0327]
data/restraints/parameters	12390/0/1066	14497/4/1130
GOF on F^2	1.038	1.022
R_1/wR_2 [I≥2σ(I)]	R_1 = 0.0334 wR_2 = 0.0909	R_1 = 0.0455 wR_2 = 0.1135
R_1/wR_2 [all data]	R_1 = 0.0360 wR_2 = 0.0924	R_1 = 0.0487 wR_2 = 0.1168
max/min $\Delta\rho$ [e·Å^{-3}]	1.03/−1.03	3.51/−2.14

Table S5. Crystallographic data for compounds **9** and $[Me_3N{\cdot}H_2B{\cdot}NCMe]^+[BF_4]^-$.

Compound	**9**	$[Me_3N{\cdot}H_2B{\cdot}NCMe]^+[BF_4]^-$
empirical formula	$C_{81.45}H_{63.9}AgAlB_3Cl_{0.9}F_{46}N_3O_3P_3$	$C_5H_{14}B_2F_4N_2$
formula weight	2298.75	199.80
temperature [K]	123(1)	123(1)
crystal system	monoclinic	orthorhombic
space group	$P2_1/c$	*Pnma*
a [Å]	11.41518(14)	11.0727(7)
b [Å]	19.8618(3)	7.4319(5)
c [Å]	42.3218(5)	11.8956(8)
α [°]	90	90
β [°]	90.4893(11)	90
γ [°]	90	90
Volume [Å^3]	9595.1(2)	978.90(11)
Z	4	4
ρ_{calc} [g/cm^3]	1.591	1.356
μ [mm^{-1}]	0.432	1.177
F (000)	4587.6	416.0
crystal size [mm^3]	0.58 × 0.12 × 0.07	0.36 × 0.31 × 0.21
radiation	Mo-K_α (λ = 0.71073)	Cu-K_α (λ = 1.54178)
absorption correction	gaussian	multi-scan
T_{min} / T_{max}	0.854 / 0.978	0.610 / 1.000
2Θ range [°]	5.616 to 54.308	10.916 to 148.814
completeness	0.999	0.994
index ranges	$-14 \le h \le 14$ $-25 \le k \le 25$ $-54 \le l \le 54$	$-13 \le h \le 13$ $-6 \le k \le 8$ $-14 \le l \le 14$
reflections collected	146208	2487
independent reflections	21221 [R_{int} = 0.0638, R_{sigma} = 0.0464]	1038 [R_{int} = 0.0210, R_{sigma} = 0.0180]
data/restraints/parameters	21221/12/1342	1038/0/79
GOF on F^2	1.058	1.099
R_1/wR_2 [I≥2σ(*I*)]	R_1 = 0.0410 wR_2 = 0.1310	R_1 = 0.0375 wR_2 = 0.1095
R_1/wR_2 [all data]	R_1 = 0.0567 wR_2 = 0.1354	R_1 = 0.0424 wR_2 = 0.1122
max/min $\Delta\rho$ [e·Å^{-3}]	0.92/−0.76	0.30/−0.28

References

[1] a) C. Marquardt, T. Jurca, K.-C. Schwan, A. Stauber, A. V. Virovets, G. R. Whittell, I. Manners, M. Scheer, *Angew. Chem. Int. Ed.* **2015**, *54*, 13782–13786; *Angew. Chem.* **2015**, *127*, 13986–13991; b) C. Marquardt, A. Adolf, A. Stauber, M. Bodensteiner, A. V. Virovets, A. Y. Timoshkin, M. Scheer, *Chem. Eur. J.* **2013**, *19*, 11887–11891.

[2] T. Köchner, N. Trapp, T. A. Engesser, A. J. Lehner, C. Röhr, S. Riedel, C. Knapp, H. Scherer, I. Krossing, *Angew. Chem. Int. Ed.* **2011**, *50*, 11253–11256; *Angew. Chem.* **2011**, *123*, 11449–11452.

[3] I. Krossing, *Chem. Eur. J.* **2001**, *7*, 490–502.

[4] Agilent Technologies **2006-2011**, CrysAlisPro Software system, different versions, Agilent Technologies UK Ltd, Oxford, UK.

[5] G. M. Sheldrick, *Acta Cryst.* **2008**, *A64*, 112–122.

[6] O.V. Dolomanov, L.J. Bourhis, R.J. Gildea, J.A.K. Howard, H.Puschmann, OLEX2: A complete structure solution, refinement and analysis program, *J. Appl. Cryst*. **2009**, 42, 339–341.

10.6 Author Contributions

The syntheses and characterization of compounds **1**-**7** and $[Me_3N{\cdot}H_2B{\cdot}NCMe]^+[BF_4]^-$ were performed by Christian Marquardt.

The syntheses and characterization of compounds **8** and **9** were performed by Oliver Hegen.

Ag[FAl] and Ag[Tef] was synthesized and provided by Martin Fleischmann and Luis Dütsch.

X-ray structural analyses of all compounds were performed by Christian Marquardt. Refinement was comprehensively supported by Martin Fleischmann.

The manuscript (including supporting information, figures, schemes and graphical abstract) was written by Christian Marquardt with the support of Martin Fleischmann.

11. Thesis Treasury

The following chapter includes preliminary results and by-products, which will be included in future publications or provide a basis for future research targets. Some of the obtained compound could not be fully characterized so far, but all data and knowledge acquired about the described reactions will be presented.

11.1 Alternative synthesis of the pnictogenylboranes $H_2EBH_2{\cdot}NMe_3$ (E = P, As)

For the pnictogenylboranes $H_2EBH_2{\cdot}NMe_3$ (E = P, As) different synthesis have been established over the last decade.[1,2] The most convenient route involves a salt metathesis between $(Me_3Si)_2ELi{\cdot}thf$ (E = P, As) and $ClBH_2{\cdot}NMe_3$, yielding $(Me_3Si)EBH_2{\cdot}NMe_3$ (E = P, As), which can be subsequently transformed into the LB stabilized parent compounds. To avoid the very time consuming and expensive synthesis of $E(SiMe_3)_3$ (E = P, As), which is a starting material for the synthesis of $(Me_3Si)_2ELi{\cdot}thf$, another route to the pnictogenylboranes $H_2EBH_2{\cdot}NMe_3$ (E = P, As) was investigated. The reaction of $IBH_2{\cdot}NMe_3$ with the EH_2 (E = P, As) sources $NaPH_2$ and $LiAsH_2{\cdot}tmeda$ gives the corresponding products in good yields (Scheme 1). All starting materials can be synthesized within a few days and more cost-efficient. It is expected that the reaction of $IBH_2{\cdot}NMe_3$ with AsH_2^- on larger scales should also give higher yields.

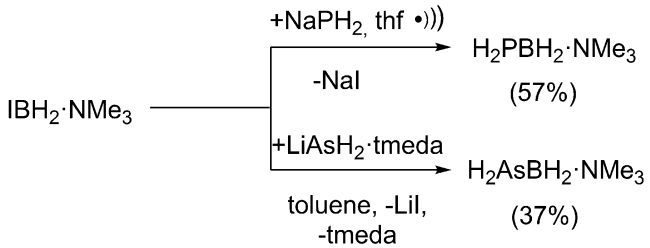

Scheme 1. Synthesis of $H_2EBH_2{\cdot}NMe_3$ (E = P, As). Yields are given in parentheses.

Synthesis of $H_2PBH_2{\cdot}NMe_3$:

A solution of 9.950 g $IBH_2{\cdot}NMe_3$ (50.00 mmol) in 20 mL THF is added to a suspension of 2.800 g (50.00 mmol) $NaPH_2$ in 20 mL THF at −80°C. The suspension is sonicated for 2 hours, the resulting mixture is filtrated over diatomaceous earth and all volatiles are removed under reduced pressure. By using a condensation bridge $H_2PBH_2{\cdot}NMe_3$ is condensed at 65–70 °C under reduced pressure. $H_2PBH_2{\cdot}NMe_3$ forms an emulsion with *n*-hexane. At –28°C crystals are obtained from *n*-hexane. The product can be isolated by

decanting the supernatant at 0°C. Further purification can be achieved by repeated recrystallization from *n*-hexane. Yield of $H_2PBH_2{\cdot}NMe_3$: 3.01 g (57 %); Analytical data are in agreement with the previously published values.[1]

Synthesis of $H_2AsBH_2{\cdot}NMe_3$:

A solution of 120 mg $IBH_2{\cdot}NMe_3$ (0.60 mmol) in 5 mL toluene is added to a suspension of 120 mg (0.60 mmol) $LiAsH_2{\cdot}$tmeda in 5 mL toluene at r.t.. The solution is stirred for 18 hours, than all volatiles are removed under reduced pressure. By using a condensation bridge $H_2AsBH_2{\cdot}NMe_3$ is condensed at 45–50 °C under reduced pressure ($1{\cdot}10^{-3}$ mbar). ^1H and ^{11}B NMR spectrum revealed that the obtained $H_2AsBH_2{\cdot}NMe_3$ was pure. Further purification could be achieved by repeated recrystallization from *n*-hexane. Yield of $H_2AsBH_2{\cdot}NMe_3$: 33 mg (37 %); Analytical data are in agreement with the previously published values.[2]

11.2 Phosphonium salts of Phosphanylboranes and related species

In chapter 4, the reaction of $H_2PBH_2{\cdot}NMe_3$, $AlCl_3$ and $ClBH_2{\cdot}NMe_3$ in CH_2Cl_2 was presented for the synthesis of cationic chains of the phosphanylboranes. Efforts were carried out to structurally characterize the intermediate $Cl_3Al{\cdot}H_2PBH_2{\cdot}NMe_3$. However no single-crystals suitable for X-ray structure determination could be obtained. Instead of the formation of the adduct, the generation of $[H_3PBH_2{\cdot}NMe_3]^+[AlCl_4]^-$ was observed. Most likely it originates from the reaction of $H_2PBH_2{\cdot}NMe_3$, $AlCl_3$ and the solvent CH_2Cl_2 (Scheme 2). Only a small amount of crystals were obtained, thus the by-product $[H_3PBH_2{\cdot}NMe_3]^+[AlCl_4]^-$ was only characterized by X-ray structure analysis (Figure 1). The same reaction is also known for BCl_3.[3]

$$H_2PBH_2{\cdot}NMe_3 + AlCl_3 \xrightarrow{CH_2Cl_2} [H_3PBH_2{\cdot}NMe_3]^+[AlCl_4]^-$$

Scheme 2. Formation of $[H_3PBH_2{\cdot}NMe_3]^+[AlCl_4]^-$.

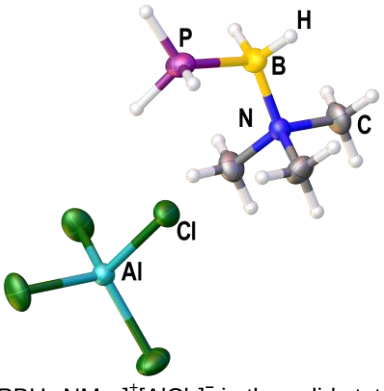

Figure 1. Molecular structure of $[H_3PBH_2{\cdot}NMe_3]^+[AlCl_4]^-$ in the solid state. Thermal ellipsoids are drawn with 50% probability. Selected bond lengths [Å] and angles [°]: P–B 1.987(9), N–B–P 113.2(5).

Table 1. Crystallographic data of $[H_3PBH_2{\cdot}NMe_3]^+[AlCl_4]^-$.

empirical formula	$C_3H_{14}AlBCl_4NP$
formula weight	274.71
temperature [K]	123(1)
crystal system	orthorhombic
space group	$Pna2_1$
a [Å]	12.64740(10)
b [Å]	10.24600(10)
c [Å]	10.09640(10)
α [°]	90
β [°]	90
γ [°]	90
Volume [$Å^3$]	1308.34(2)
Z	4
$\rho_{calc}g/cm^3$	1.395
μ/mm^{-1}	9.647
F(000)	560.0
crystal size [mm^3]	0.1537 × 0.1176 × 0.0975
radiation	Cu*Kα* (*λ* = 1.54178)
absorption correction	analytical
T_{min}/T_{max}	0.383 /0.496
2*Θ* range [°]	6.988 to 133.186
completeness	0.997
index ranges	-14 ≤ *h* ≤ 15 -11 ≤ *k* ≤ 12 -10 ≤ *l* ≤ 12
reflections collected	6699
independent reflections	2187 [R_{int} = 0.0276, R_{sigma} = 0.0265]
data/restraints/parameters	2187/5/124
GOF on F^2	1.043
final R indexes [I>=2σ (I)]	R_1 = 0.0445, wR_2 = 0.1203
final R indexes [all data]	R_1 = 0.0458, wR_2 = 0.1223
max/min Δ*ρ* [$e{\cdot}Å^{-3}$]	1.57/-0.39
flack parameter	0.01(2)

In chapter 5, the synthesis of cationic chains of the diaryl-substituted $Ph_2PBH_2{\cdot}NMe_3$ was presented via the reaction with $IBH_2{\cdot}NMe_3$. It was also investigated if the cationic chains are accessible by the use of $ClBH_2{\cdot}NMe_3$ and the halide abstractor $AlCl_3$ (Scheme 3). However according to ^{31}P NMR and ^{11}B NMR this reaction does not procced as

expected and a variety of signals can be observed. Unfortunately it was only possible to characterize different crystals from the reaction mixture by single-crystal structure analysis. On the one hand the compound $[HPh_2PBH_2{\cdot}NMe_3]^+[AlCl_4]^-$ was obtained (Figure 2), which most probably originate from a side reaction with the solvent CH_2Cl_2 (Scheme 3). The same reaction has also been observed for the parent compound $H_2PBH_2{\cdot}NMe_3$. X-Ray structure analysis of other crystals revealed the compound $Cl_3Al{\cdot}Ph_2PBH_2{\cdot}NMe_3$ (Figure 2). Isolation of the compound from the direct reaction of $Ph_2PBH_2{\cdot}NMe_3$ and $AlCl_3$ failed up to date. Since only small amount of crystals were obtained in a mixture, both compounds were exclusively studied by single-crystal X-ray structure analysis.

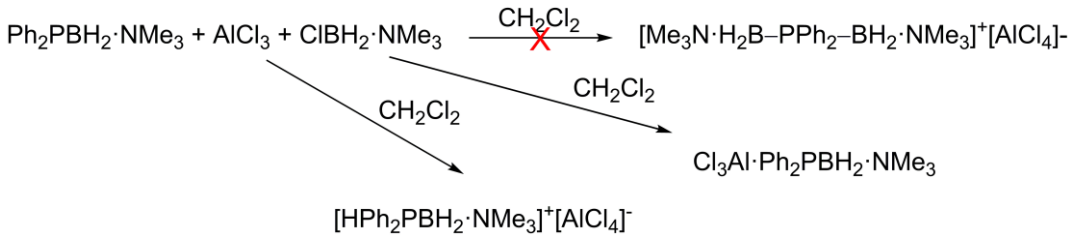

Scheme 3. Reactions of $Ph_2PBH_2{\cdot}NMe_3$ with $AlCl_3$.

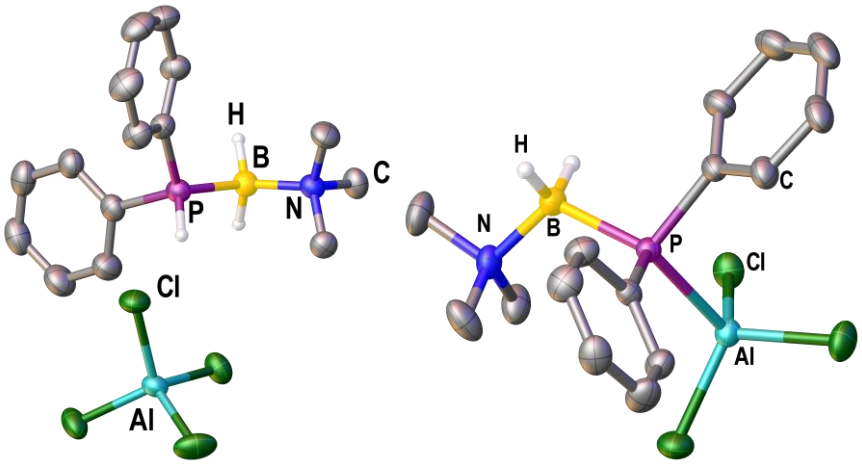

Figure 2. Molecular structure of $[HPh_2PBH_2{\cdot}NMe_3]^+[AlCl_4]^-$ (left) and $Cl_3Al{\cdot}Ph_2PBH_2{\cdot}NMe_3$ (right) in the solid state. Thermal ellipsoids are drawn with 50% probability. Hydrogen atoms bond to carbon are omitted for clarity. Selected bond lengths [Å] and angles [°]:$[HPh_2PBH_2{\cdot}NMe_3]^+[AlCl_4]^-$ P–B 1.955(2), N–B–P 116.47(12), $Cl_3Al{\cdot}Ph_2PBH_2{\cdot}NMe_3$: P–B 1.977(2), P–Al 2.3919(6), N–B–P 115.12(13), B–P–Al 119.99(6).

Table 2. Crystallographic data of $[HPh_2PBH_2{\cdot}NMe_3]^+[AlCl_4]^-$ and $Cl_3Al{\cdot}Ph_2PBH_2{\cdot}NMe_3$.

empirical formula	$C_{15}H_{22}AlBCl_4NP$	$H_{21}C_{15}NAlPCl_3B$
formula weight	426.89	390.44
temperature [K]	123(1)	123(1)
crystal system	orthorhombic	monoclinic
space group	*Pbca*	$P2_1/n$
a [Å]	14.80550(10)	9.4528(2)
b [Å]	11.21530(10)	19.4483(4)
c [Å]	25.8552(3)	10.8006(3)
α [°]	90	90
β [°]	90	91.335(2)
γ [°]	90	90
Volume [$Å^3$]	4293.21(7)	1985.06(7)
Z	8	4
$\rho_{calc}g/cm^3$	1.321	1.306
μ/mm^{-1}	6.082	5.319
F(000)	1760.0	808.0
crystal size [mm^3]	0.27 × 0.08 × 0.08	0.87 × 0.41 × 0.36
radiation	Cu*Kα* (*λ* = 1.54178)	Cu*Kα* (*λ* = 1.54184)
absorption correction	analytical	analytical
T_{min}/T_{max}	0.474 / 0.721	0.051 / 0.321
2*Θ* range [°]	6.838 to 133.36	9.094 to 148.06
completeness	0.992	0.985
index ranges	-17 ≤ *h* ≤ 17 -13 ≤ *k* ≤ 11 -30 ≤ *l* ≤ 29	-10 ≤ *h* ≤ 11 -13 ≤ *k* ≤ 23 -9 ≤ *l* ≤ 12
reflections collected	20560	6416
independent reflections	3775 [R_{int} = 0.0318, R_{sigma} = 0.0213]	3828 [R_{int} = 0.0319, R_{sigma} = 0.0455]
data/restraints/parameters	3775/0/223	3828/0/210
GOF on F^2	1.055	1.045
final R indexes [*I*>=2*σ* (I)]	R_1 = 0.0286, wR_2 = 0.0751	R_1 = 0.0362, wR_2 = 0.0963
final R indexes [all data]	R_1 = 0.0348, wR_2 = 0.0772	R_1 = 0.0389, wR_2 = 0.0987
max/min Δ*ρ* [$e{\cdot}Å^{-3}$]	0.51/-0.4	0.30/-0.50

11.3 Cleavage of $[^tBuHPBH_2]_n$ with N-heterocyclic carbenes and synthesis of the monoaryl-substituted Phosphanylborane $HPhPBH_2 \cdot NMe_3$

In chapter 3 the importance of polymers based on group 13/15 elements was already described. The work focused primarily on the synthesis of poly(phosphinoborane)s. However it has to be emphasized, that the regeneration of monomers by cleavage of the polymers is also very important. Recently it was reported, that aminoborane-oligomers and polymers can be cleaved into the corresponding monomeric species with N-heterocyclic carbenes.[4] With the aid of dmap and NHC^{Me} *Adolf* from our group was able to cleave poly(monophenyphosphinoborane) $[PhHPBH_2]_n$ into the monomers $PhHPBH_2 \cdot LB$ (LB = dmap, NHC^{Me}).[5] Reaction of $[^tBuHPBH_2]_n$ with an equimolar amount of NHC^{Me} yields the monomeric phosphanylborane $^tBuHPBH_2 \cdot NHC^{Me}$ in about 80% yield determined by NMR spectroscopy (Scheme 4). Further addition of NHC^{Me} does not lead to higher yields. $^tBuHPBH_2 \cdot NHC^{Me}$ was extracted with *n*-hexane, however unassigned side products and $[^tBuHPBH_2]_n$ are also soluble, and thus several recrystallization steps are needed to get pure $^tBuHPBH_2 \cdot NHC^{Me}$. This is the reason for the relatively low crystalline yield. In the ^1H NMR spectrum (Figure 5) the resonance signals of the methyl groups of NHC^{Me} arise at δ = 1.14 (C-Me) and 3.15 ppm (N-Me). The CH_3 groups of the ^{t}Bu moiety is found as a doublet at δ = 1.70 ppm ($^3J_{H,P}$ = 10 Hz). A multiplett arises at δ = 2.37 ppm for the BH_2 moiety and a doublet at δ = 2.55 ppm for the PH group ($^1J_{H,P}$ = 173 Hz). In the $^{31}P\{^1H\}$ NMR spectrum a quartet is observed at δ = –63.7 ppm ($^1J_{B,P}$ = 28 Hz) which splits into a doublet in the ^{31}P NMR spectrum ($^1J_{H,P}$ = 173 Hz, Figure 4). The $^{11}B\{^1H\}$ NMR spectrum reveals a doublet at δ = –32.5 ppm ($^1J_{B,P}$ = 28 Hz) which shows further splitting into a triplet of doublets in the ^{11}B NMR spectrum ($^1J_{B,H}$ = 95 Hz, Figure 4). Single crystals are obtained by storing a solution of $^tBuHPBH_2 \cdot NHC^{Me}$ in *n*-hexane at –28°C. The phosphorus atom bears four different substituents leading to a chiral compound, which crystallises as a racemic mixture (Figure 3). In the solid state the P–B bond length is 1.988(2) Å and corresponds to a P–B single bond.

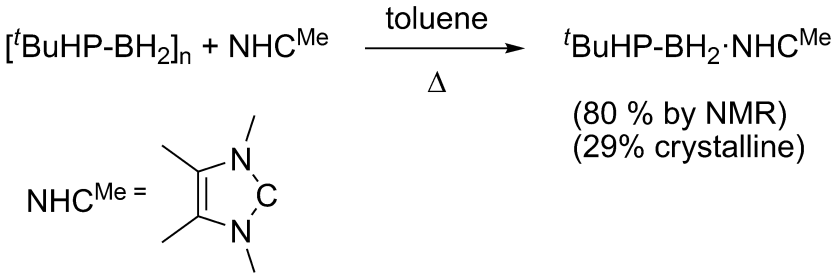

Scheme 4. Synthesis of ^{t}BuHPBH$_2$·NHC^{Me}.

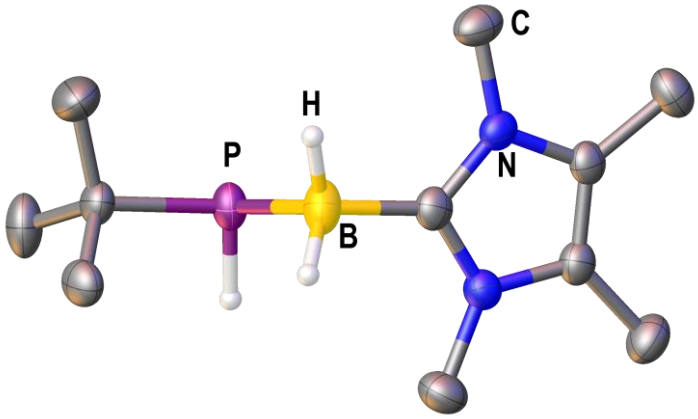

Figure 3. Molecular structure of ^{t}BuHPBH$_2$·NHC^{Me} in the solid state. Thermal ellipsoids are drawn with 50% probability. Hydrogen atoms bond to carbon are omitted for clarity. Selected bond lengths [Å] and angles [°]: P–B 1.988(2), B–C 1.599(3) C–B–P 106.31(9).

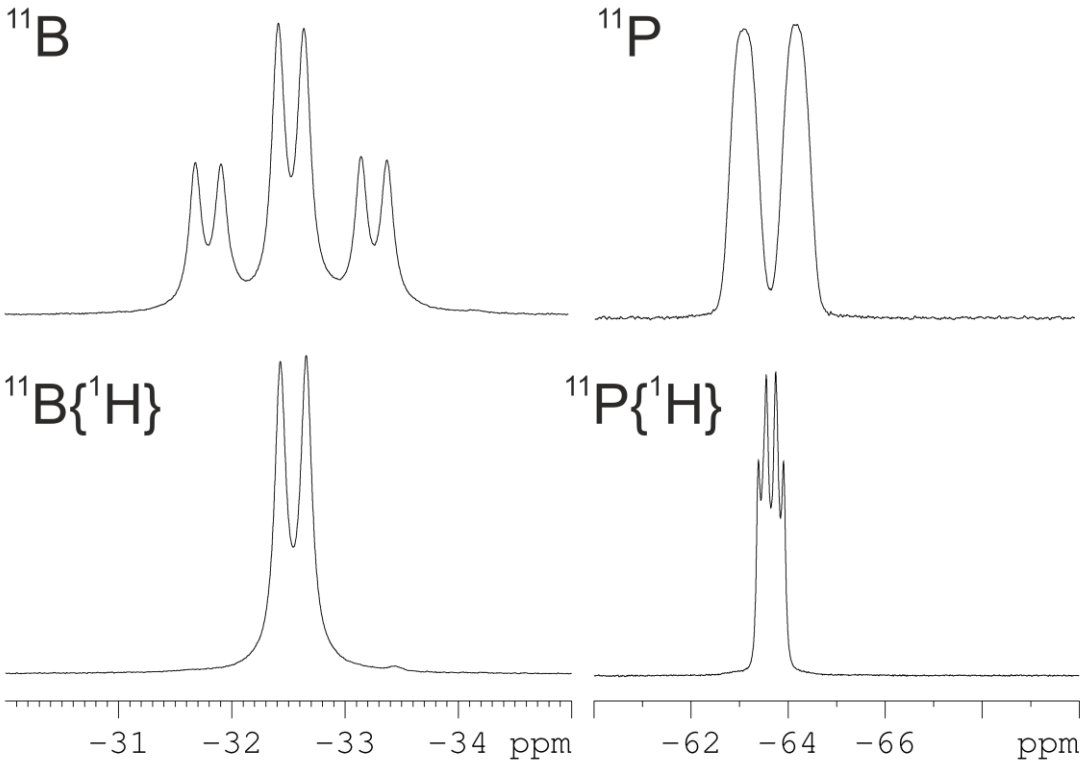

Figure 4. NMR spectra of ^{t}BuHPBH$_2$·NHC^{Me} in C_6D_6.

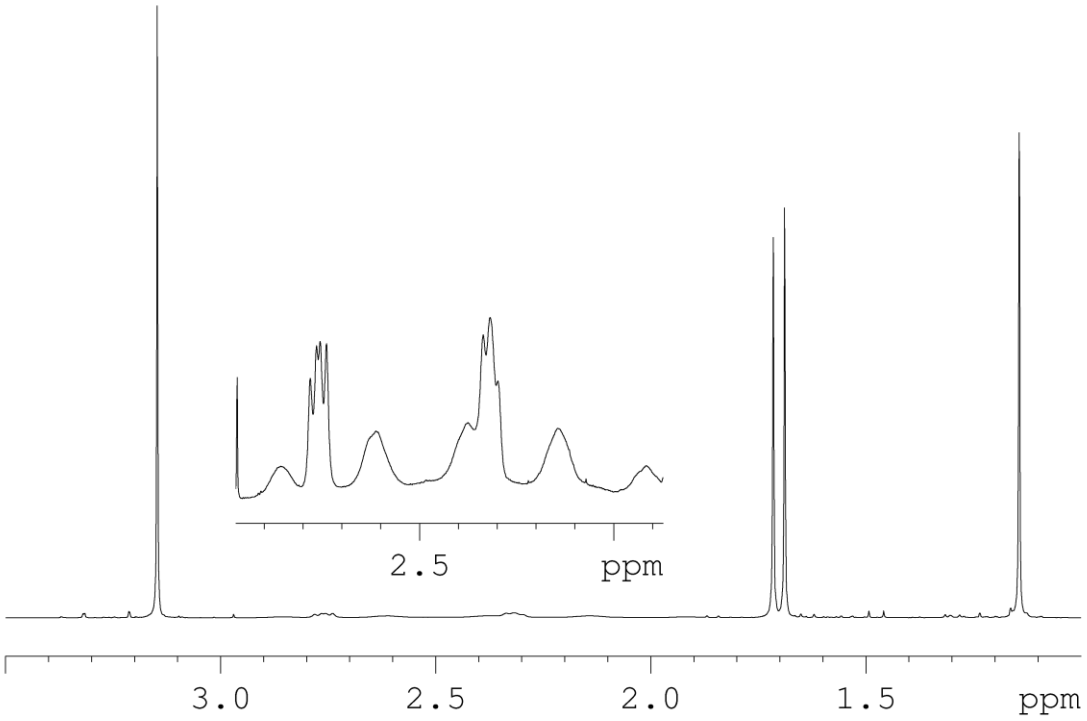

Figure 5. ^{1}H NMR spectrum of ^{t}BuHPBH$_2$·NHC^{Me} in C_6D_6.

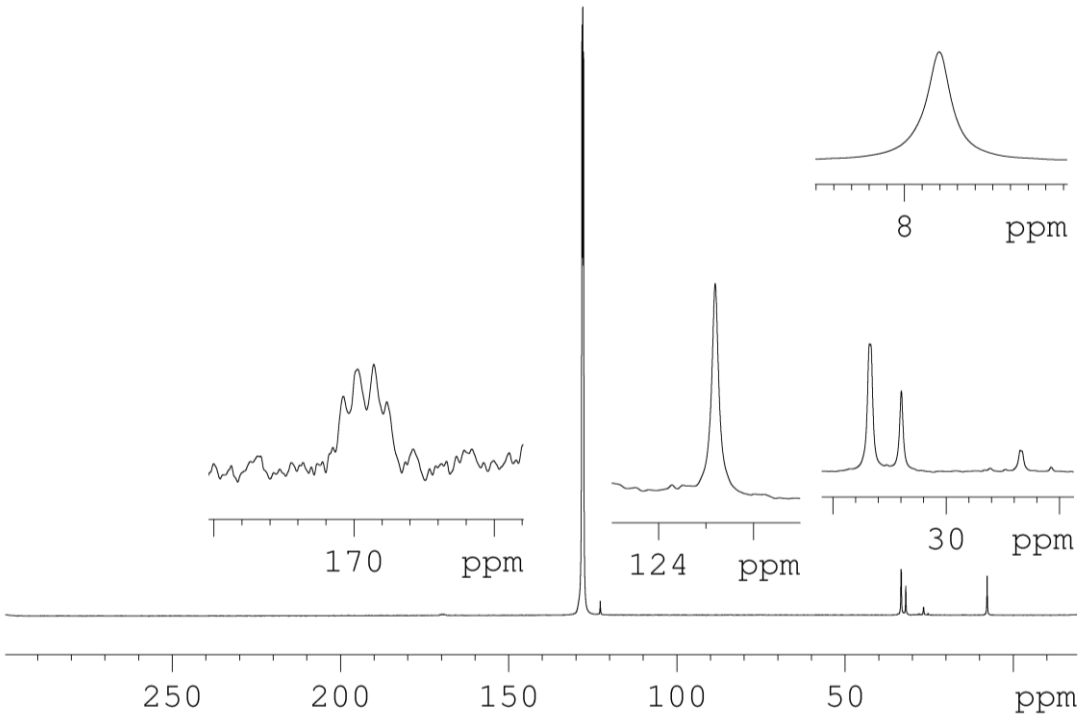

Figure 6. ^{13}C{^{1}H} NMR spectrum of ^{t}BuHPBH$_2$·NHC^{Me} in C_6D_6.

To investigate if $HPhPBH_2{\cdot}NMe_3$ would also be a suitable monomer for the synthesis of poly(phosphinoborane)s, a selective synthesis was developed. In order to synthesize the monophenyl substituted phosphanylborane $HPhPBH_2{\cdot}NMe_3$ many attempts were made. However during the synthesis and upon isolation the stabilizing Lewis base trimethylamine, seems to be too loosely attached to the boron atom leading to elimination and the polymerization to $[HPhP–H_2B]_n$ cannot be avoided (Scheme 5). However in one case a small amount of crystals could be isolated and the proposed structure was confirmed by single crystal X-ray structure analysis and ^{1}H, ^{11}B and ^{31}P NMR spectroscopy. For the synthesis of $HPhPBH_2{\cdot}NMe_3$ the best building blocks are $[LiPPh(SiMe_3)tmeda]_2$ (synthesized on alternative route than reported in the literature) and $IBH_2{\cdot}NMe_3$ (Scheme 5).[6] The best results were obtained with toluene as solvent and when the salt metathesis and methanolysis were carried out at –40°C and the reaction mixture was allowed to reach r.t. (Scheme 5). In the ^{1}H NMR spectrum (Figure 9) of the crystals the signals of the amine NMe_3 arise at δ = 1.80 ppm. The resonance signals of the H atoms of the phenyl group can be found as multipletts at δ = 7.02 (*p*-Ph), 7.15 (*m*-Ph) and 7.73 ppm (*o*-Ph). A multiplet arises at δ = 2.61 ppm for the BH_2-moiety and a doublet at δ = 3.66 ppm for the PH-group ($^{1}J_{H,P}$ = 210 Hz). In the $^{31}P\{^{1}H\}$ NMR spectrum a multiplet is observed at δ = –98.5 ($^{1}J_{B,P}$ = 28 Hz) which splits into doublet in the ^{31}P NMR spectrum ($^{1}J_{H,P}$ = 210 Hz, Figure 8). The $^{11}B\{^{1}H\}$ NMR spectrum reveals a doublet at δ = –4.0 ($^{1}J_{B,P}$ = 35 Hz) which shows further splitting into a triplet of doublets in the ^{11}B NMR ($^{1}J_{B,H}$ = 107 Hz, Figure 8) spectrum. Single crystals are obtained by storing a solution of $PhHPBH_2{\cdot}NMe_3$ in *n*-hexane at –28°C. In the solid state the P–B distance is 1.955(2) Å, corresponding to a P–B single bond (Figure 7).

Heating of a solution of $HPhPBH_2{\cdot}NMe_3$ at 100°C afforded similar overlapping signals in the ^{31}P NMR spectrum (Figure 10), which have been described for the thermolysis (uncatalyzed dehydrocoupling) of $H_2PhP{\cdot}BH_3$.[7] Generation of the free phosphine H_2PhP is also observed.

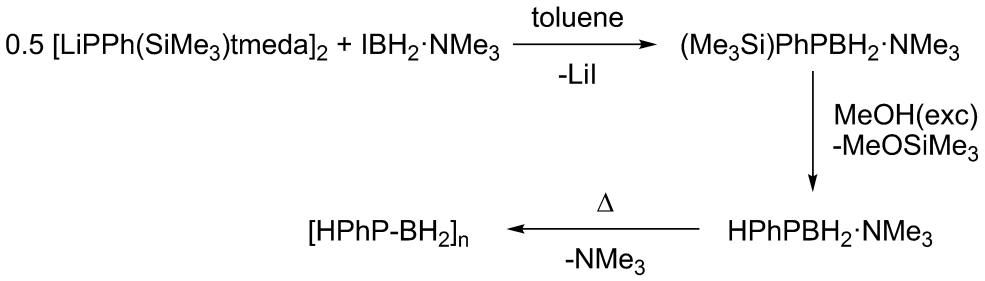

Scheme 5. Synthesis of $HPhPBH_2{\cdot}NMe_3$ and subsequent polymerisation.

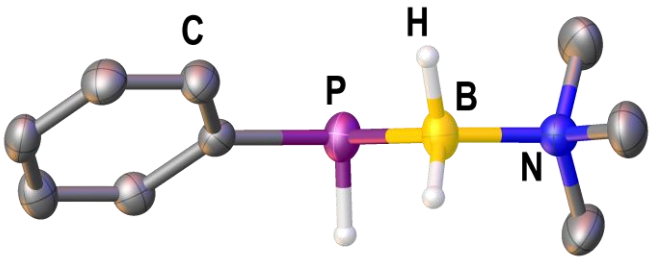

Figure 7. Molecular structure of $HPhPBH_2 \cdot NMe_3$ in the solid state. Thermal ellipsoids are drawn with 50% probability. Hydrogen atoms bond to carbon are omitted for clarity. Selected bond lengths [Å] and angles [°]: P–B 1.955(2), N–B–P 116.47(12).

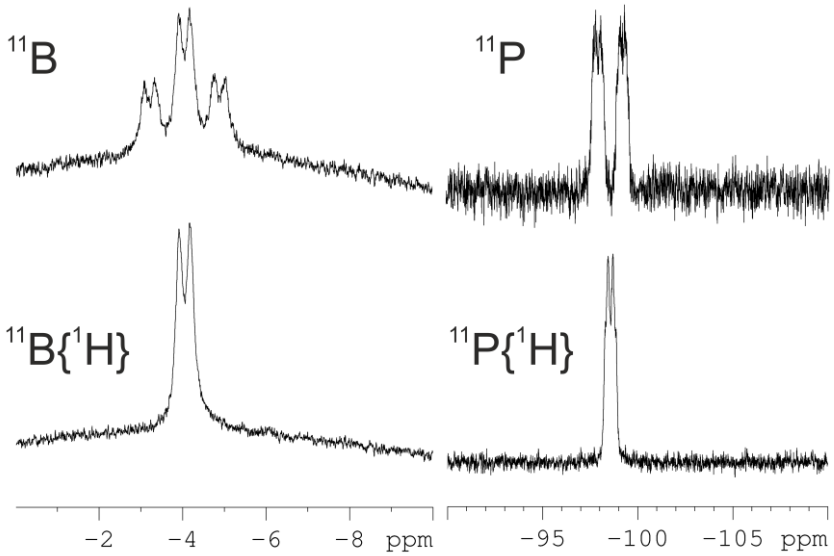

Figure 8. NMR spectra of $HPhPBH_2 \cdot NMe_3$ in C_6D_6.

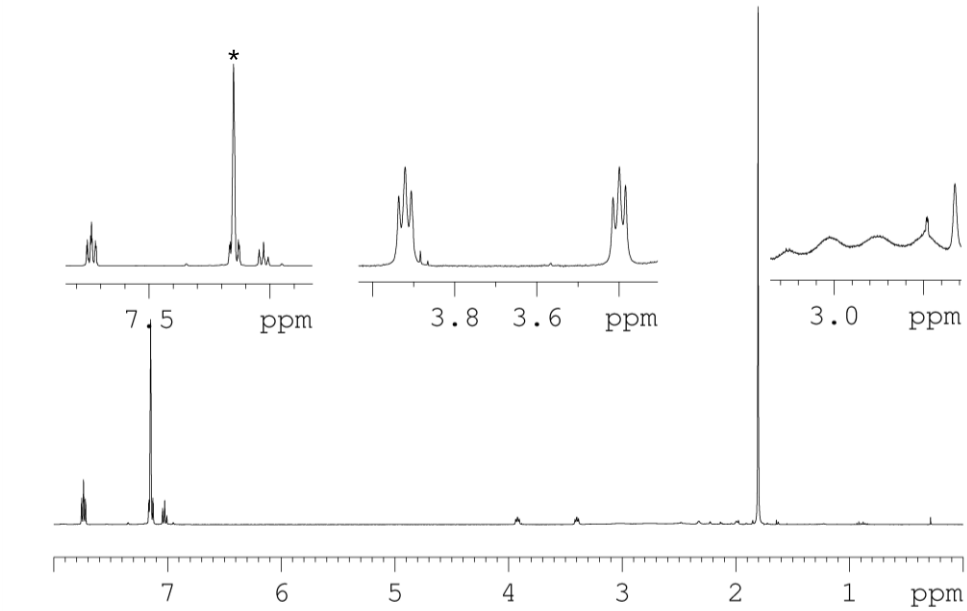

Figure 9. ^1H NMR spectrum of $HPhPBH_2 \cdot NMe_3$ in C_6D_6. * = solvent C_6D_6.

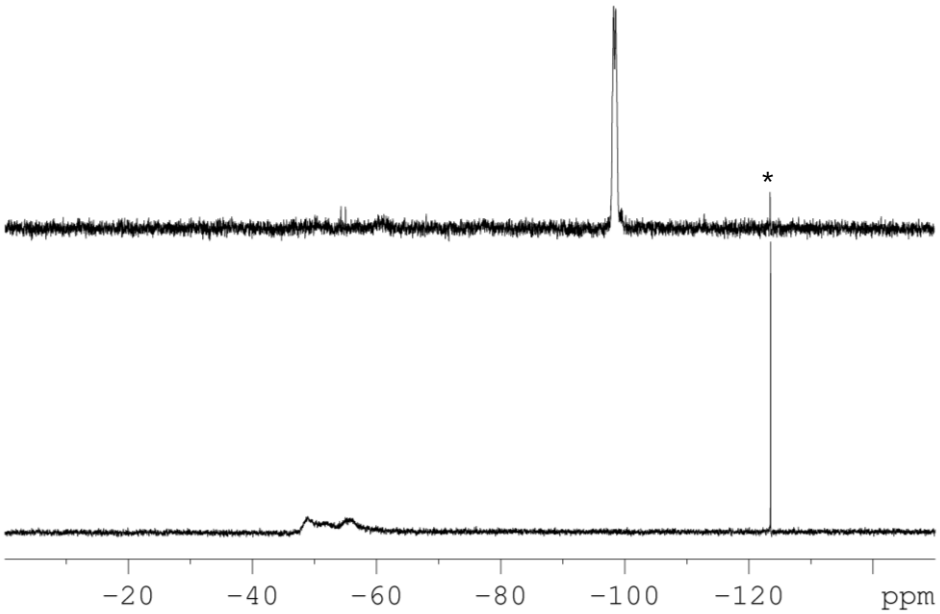

Figure 10. $^{31}P\{^{1}H\}$ NMR spectrum of $HPhPBH_2{\cdot}NMe_3$ (top) and $[HPhPBH_2]_n$ (bottom) in C_6D_6. * = $PhPH_2$

Synthesis of ^{t}BuHPBH$_2$·NHC^{Me}:

A solution of 161 mg (1.00 mmol) $^{t}BuHPBH_2{\cdot}NMe_3$ in 5 mL toluene is stirred at 45°C for 3 days. The completeness of the reaction was confirmed by ^{31}P NMR. The resulting solution of $[^{t}BuHPBH_2]_n$ is added to 124 mg (1.00 mmol) freshly sublimed solid NHC^{Me}. After refluxing the mixture for 2 days, all volatiles are removed under reduced pressure. $^{t}BuHPBH_2{\cdot}NHC^{Me}$ is dissolved in 10 mL of *n*-hexane and filtrated. The solution is concentrated under reduced pressure. $^{t}BuHPBH_2{\cdot}NHC^{Me}$ crystallises at -28 °C as colourless needles. After decanting of the supernatant the crystals are dissolved in a minimum of *n*-hexane and recrystallized for 2 more times. The crystals are separated and washed with cold *n*-hexane (-80°C, 3×5 mL). Yield of of $^{t}BuHPBH_2{\cdot}NHC^{Me}$: 65 mg (29 %). ^{1}H NMR (C_6D_6, 25 °C): δ = 1.14 (s, 6H, C-Me), 1.70 (d, $^{3}J_{H,P}$ = 10 Hz, 9H, ^{t}Bu), 2.37 (m, BH_2), 2.55 (dm, $^{1}J_{H,P}$ = 173 Hz, 1H, PH), 3.15 (s, 6H, N-Me). ^{31}P NMR (C_6D_6, 25 °C): δ = –63.7 (d, $^{1}J_{H,P}$ = 173 Hz, br). $^{31}P\{^{1}H\}$ NMR (C_6D_6, 25 °C): δ = –63.7 (q, $^{1}J_{B,P}$ = 28 Hz). ^{11}B NMR (C_6D_6, 25 °C): δ = –32.5 (td, $^{1}J_{B,H}$ = 95 Hz, $^{1}J_{B,P}$ = 28 Hz). $^{11}B\{^{1}H\}$ NMR (C_6D_6, 25 °C): δ = –32.5 (d, $^{1}J_{B,P}$ = 28 Hz). $^{13}C\{^{1}H\}$ NMR (C_6D_6, 25 °C): δ = 7.8 (s, C**Me**), 26.6 (d, $^{1}J_{C,P}$ = 11 Hz, **C**Me_3), 32.0 (N**Me**), 33.4 (d, $^{1}J_{C,P}$ = 6 Hz, C**Me**$_3$), 122.8 (s, C=C), 169.6 (q, $^{1}J_{C,B}$ = 52 Hz, **C**B). IR (KBr): $\tilde{\nu}$ = 2946 (vs, CH), 2929 (vs, CH), 2887 (s, CH), 2850 (s, CH), 2358 (vs, br, BH), 2300 (s, BH), 2245 (s, PH), 2233 (s, PH), 1656 (m), 1471 (s), 1455 (s), 1431 (s), 1441 (s), 1396 (s), 1355 (m), 1231 (w), 1167 (m), 1111 (w), 1016 (m), 997 (m), 953 (m), 873 (m), 820 (m), 780 (w), 715 (w), 604 (w). EI-MS (toluene): *m/z* = 226 (15 %, $[M]^+$), 137 (100%, $[M-^{t}BuHP]^+$), 57 (9%, $[^{t}Bu]^+$). Elemental

analysis (%) calculated for $C_{11}H_{24}BN_2P$: C: 58.36, H: 10.69, N: 12.38; found: C: 58.29, H: 10.65, N: 12.25.

Alternative synthesis of [LiPPh(SiMe$_3$)tmeda]$_2$:

13.7 g (53.94 mmol) $PhP(SiMe_3)_2$[8] and 11 mL tmeda are dissolved in 60 mL of THF. Under vigorous stirring 34.25 mL of a 1.6 M (54.80 mmol) solution of ^{n}BuLi in *n*-hexane are added drop by drop and the solution is stirred for 12h. After removal of all volatiles under reduced pressure the resulting [LiPPh(SiMe$_3$)tmeda]$_2$ is washed 2 times with 10 mL of toluene and 2 times with 10 mL of *n*-hexane. The solid is dried under reduced pressure. Yield of [LiPPh(SiMe$_3$)tmeda]$_2$: 14.6 g (89%). All analytical data are in accordance with the previously published values.[6]

Synthesis of (Me$_3$Si)PhPBH$_2$·NMe$_3$:

A solution of 199 mg (1.0 mmol) $IBH_2 \cdot NMe_3$ in 10 mL of toluene is added to a solution of 304 mg (0.50 mmol) [LiPPh(SiMe$_3$)tmeda]$_2$ in 10 ml toluene at –40°C. The reaction mixture is stirred for 18 h upon slow warming to r.t.. The solution is filtrated over diatomaceous earth and all volatiles are removed under reduced pressure. The resulting white wax is characterized by NMR spectroscopy, as isolation as a pure product failed so far. ^{31}P NMR (C_6D_6, 25 °C): δ = –129.5 (m, br). ^{31}P{^{1}H} NMR (C_6D_6, 25 °C): δ = –129.5 (m, br). ^{11}B NMR (C_6D_6, 25 °C): δ = –3.5 (m). ^{11}B{^{1}H} NMR (C_6D_6, 25 °C): δ = –3.5 (m).

Synthesis of HPhPBH$_2$·NMe$_3$:

A solution of 199 mg (1.0 mmol) $IBH_2 \cdot NMe_3$ in 10 mL of toluene is added to a suspension of 304 mg (0.50 mmol) [LiPPh(SiMe$_3$)tmeda]$_2$ in 10 ml toluene at –40°C. After stirring the reaction mixture for 18 h at r.t. the solution is filtered over diatomaceous earth and is cooled to –40°C. 0.5 mL of methanol are added and the mixture is stirred for further 18 h. All volatiles are removed under reduced pressure and the remaining solid is extracted with *n*-hexane (3 x 50 mL) and filtered over diatomaceous earth. The solution is concentrated under reduced pressure. Storing the solution at 3°C affords a small amount of crystals as colourless needles. ^{1}H NMR (C_6D_6, 25 °C): δ = 1.80 (s, NMe_3), 2.61 (m, BH_2), 3.66 (dt, $^1J_{H,P}$ = 210 Hz, $^3J_{H,H}$ = 6 Hz, PH), 7.02 (m, 1H, *p*-Ph), 7.15 (m, 2H, *m*-Ph), 7.73 (m, 2H, *o*-Ph). ^{31}P NMR (C_6D_6, 25 °C): δ = –98.5 (dm, br, $^1J_{H,P}$ = 210 Hz). ^{31}P{^{1}H} NMR (C_6D_6, 25 °C): δ = –98.5 (m). ^{11}B NMR (C_6D_6, 25 °C): δ = –4.0 (dt, $^1J_{B,P}$ = 35 Hz, $^1J_{B,H}$ = 107 Hz). ^{11}B{^{1}H} NMR (C_6D_6, 25 °C): δ = –4.0 (d, $^1J_{B,P}$ = 35 Hz). IR (KBr): $\tilde{\nu}$ = 3065 (w, CH), 3059 (w, CH), 2994 (w, CH), 2942 (w, CH), 2916 (w, CH), 2383 (s, B-H), 2296 (sh), 2264 (m, P-H), 1951 (w), 1584 (m), 1480 (vs), 1463 (s), 1447 (m), 1431 (m), 1404 (m), 1385 (w), 1251 (s), 1158 (m), 1123 (s), 1074 (s),

1062 (s), 1030 (m), 1011 (m), 980 (m), 952 (w), 907 (w), 887 (m), 851 (s), 745 (s), 738 (s), 696 (s), 575 (w), 551 (w), 480 (w), 462 (w).

Table 3 Crystallographic data of ^{t}BuHPBH$_2$·NHC^{Me} and HPhPBH$_2$·NMe$_3$.

empirical formula	$C_{11}H_{24}BN_2P$	$C_9H_{17}BNP$
formula weight	226.10	181.01
temperature [K]	123(1)	123(1)
crystal system	monoclinic	monoclinic
space group	$P2_1/c$	Pn
a [Å]	20.4072(4)	6.26140(16)
b [Å]	12.16809(19)	8.4380(2)
c [Å]	11.9600(2)	10.2943(3)
α [°]	90	90
β [°]	106.177(2)	94.756(3)
γ [°]	90	90
Volume [Å^3]	2852.27(9)	542.01(3)
Z	8	2
ρ_{calc}g/cm^3	1.053	1.109
μ/mm^{-1}	1.479	1.814
F(000)	992.0	196.0
crystal size [mm^3]	0.28 × 0.12 × 0.08	0.37 × 0.08 × 0.06
radiation	Cu$K\alpha$ (λ = 1.54184)	CuKα (λ = 1.54184)
absorption correction	multi-scan	analytical
T_{min}/T_{max}	0.608 / 1.000	0.746 / 0.918
2Θ range [°]	8.554 to 147.73	10.484 to 133.096
completeness	0.996	0.993
index ranges	-25 ≤ h ≤ 25 -15 ≤ k ≤ 14 -10 ≤ l ≤ 14	-7 ≤ h ≤ 7 -10 ≤ k ≤ 9 -12 ≤ l ≤ 8
reflections collected	15424	3759
independent reflections	5573 [R_{int} = 0.0420, R_{sigma} = 0.0360]	1425 [R_{int} = 0.0355, R_{sigma} = 0.0384]
data/restraints/parameters	5573/4/321	1425/3/124
GOF on F^2	1.023	1.025
final R indexes [I>=2σ (I)]	R_1 = 0.0506, wR_2 = 0.1338	R_1 = 0.0412, wR_2 = 0.1051
final R indexes [all data]	R_1 = 0.0551, wR_2 = 0.1394	R_1 = 0.0418, wR_2 = 0.1062
max/min $\Delta\rho$ [e·Å^{-3}]	0.43/-0.31	0.24/-0.17
flack parameter	-	-0.04(4)

11.4 Synthesis of $IAlH_2 \cdot NMe_3$

In the chapters 4, 5 and 9 it was shown, that monoiodoboranes of the type $IH_2B \cdot LB$ (LB = SMe_2, NMe_3, NHC^{Me}) are on the one hand valuable building blocks for the synthesis of cationic oligomeric units and on the other hand can easily be used for the synthesis of a variety of pnictogenylboranes. Consequently it was worthwhile to investigate whether alanes can also be transferred into the monoiodoalane adducts and consequently be used for the synthesis of cationic chains and pnictogenylalanes. It was found, that $H_3Al \cdot NMe_3$ can easily be transferred into the corresponding monoiodoalanes. Reaction of $H_3Al \cdot NMe_3$ with 0.5 equivalents of elemental iodine leads almost selectively to $IH_2Al \cdot NMe_3$ (Scheme 6). Whilst the ^1H NMR spectrum shows a clean conversion (Figure 12), a definitive statement for the signal in the ^{27}Al NMR spectrum cannot be given (Figure 13). The ^1H NMR shows a sharp singlet for the amine at δ = 1.84 ppm and a very broad signal at δ = 4.48 ppm for the AlH_2 group (Figure 12). The broadness of the resonance signal of the AlH_2 group is due to the quadrupole moment of the ^{27}Al nucleus. The ^{27}Al NMR spectrum allows no definitive statement, as different broad signals are obtained and no coupling to the H atoms can be determined (Figure 13). In the solid state $IH_2Al \cdot NMe_3$ reveals a N–Al bond length of 1.985(4) Å and an Al–I bond length of 2.5635(12) Å (Figure 11). Further conversion into cationic chains or pnictogenylalanes was not successful to date, presumably to the high reactivity of the Al–H bond, which readily eliminates H_2 in combination with compounds containing E–H bonds (E = P, As, Sb; e.g. $H_2PBH_2 \cdot NMe_3$).

$$AlH_3 \cdot NMe_3 + 0.5\ I_2 \xrightarrow{\text{benzene}} IAlH_2 \cdot NMe_3 + 0.5\ H_2 \quad (93\ \%)$$

Scheme 6. Synthesis of $IAlH_2 \cdot NMe_3$.

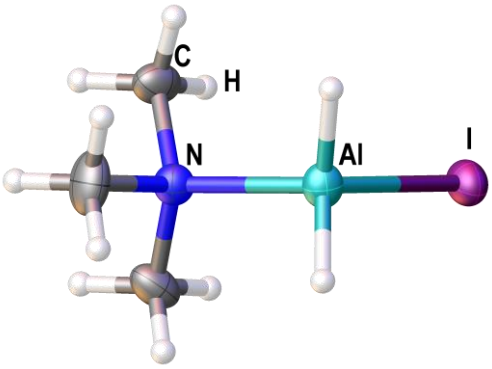

Figure 11. Molecular structure of $IH_2Al \cdot NMe_3$ in the solid state. Thermal ellipsoids are drawn with 50% probability. Selected bond lengths [Å] and angles [°]: N–Al 1.985(4), Al–I 2.5635(12), N–Al–I 105.22(11).

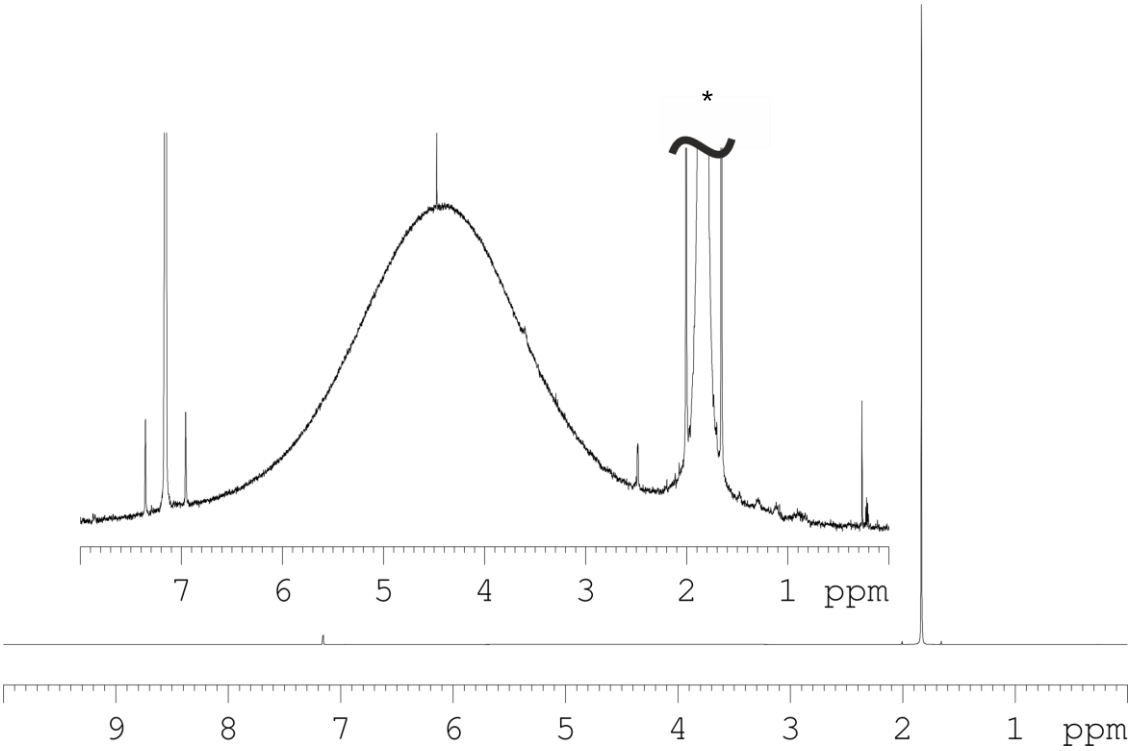

Figure 12. ^{1}H NMR spectrum of $IH_2Al{\cdot}NMe_3$ in C_6D_6. * = NMe_3.

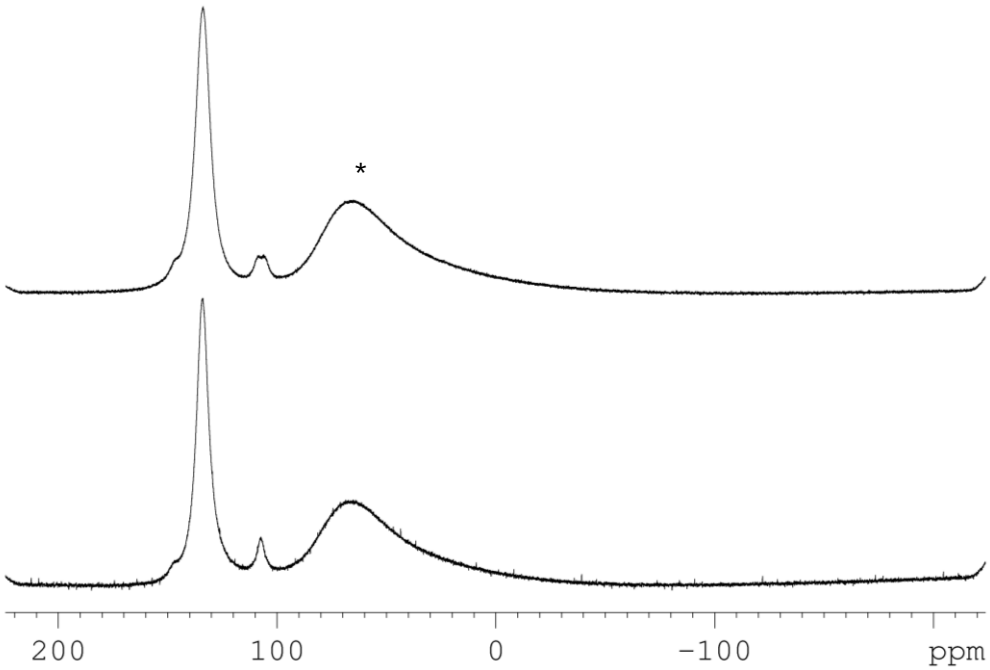

Figure 13. $^{27}Al\{^{1}H\}$ (bottom) and ^{27}Al (top) NMR spectrum of $IH_2Al{\cdot}NMe_3$ in C_6D_6. * = aluminium content of NMR tube.

Synthesis of $IH_2Al{\cdot}NMe_3$:

89 mL (1.0 mmol) $H_3Al{\cdot}NMe_3$ is dissolved in 15 mL of benzene and 254 mg of I_2 (1.0 mmol) is added in portions. Upon addition I_2 is immediately consumed. A clear colourless solution is obtained. All volatiles are removed under reduced pressure.

Crystals of $IH_2Al{\cdot}NMe_3$ (dull, colourless blocks) are obtained by dissolving a small quantity of $IH_2Al{\cdot}NMe_3$ in *n*-hexane or diethylether and storring the solution at –28°C. Yield of $IH_2Al{\cdot}NMe_3$: 200 mg (93%). ^{1}H NMR (C_6D_6, 25 °C): δ = 1.84 (s, 9H, NMe_3), 4.48 (s, br, 2H AlH_2).

Table 4 Crystallographic data of $IAlH_2{\cdot}NMe_3$.

empirical formula	$C_3H_{11}AlIN$
formula weight	215.01
temperature [K]	123(1)
crystal system	orthorhombic
space group	*Pbca*
a [Å]	6.80086(11)
b [Å]	11.97608(14)
c [Å]	19.9797(3)
α [°]	90
β [°]	90
γ [°]	90
Volume [Å^3]	1627.30(4)
Z	8
ρ_{calc}g/cm^3	1.755
μ/mm^{-1}	31.153
F(000)	816.0
crystal size [mm^3]	0.4951 × 0.3619 × 0.244
radiation	Cu*Kα* (*λ* = 1.54184)
absorption correction	multi-scan
T_{min}/T_{max}	0.040 / 1.000
2*Θ* range [°]	8.852 to 132.986
completeness	0.999
index ranges	-8 ≤ *h* ≤ 6 -10 ≤ *k* ≤ 14 -23 ≤ *l* ≤ 23
reflections collected	12340
independent reflections	1432 [R_{int} = 0.0865, R_{sigma} = 0.0380]
data/restraints/parameters	1432/2/66
GOF on F^2	1.105
final R indexes [I>=2σ (I)]	R_1 = 0.0403, wR_2 = 0.1067
final R indexes [all data]	R_1 = 0.0420, wR_2 = 0.1092
max/min Δ*ρ* [e·Å^{-3}]	2.79/-1.02

11.5 Synthesis of Lewis Base stabilized monoiodoboranes IBH_2·LB (LB = dmap, NH_3)

Besides H_3B·NMe_3 and H_3B·SMe_2, other boranes were also transformed into their monoiodoborane derivatives. The borane complexes BH_3·LB (LB = dmap, NH_3) were chosen, as dmap is a very strong LB and promises similar properties like NHC^{Me} which is known, to stabilize reactive compounds (chapter 9). IBH_2·NH_3 on the other hand would allow the synthesis of 13/15 compounds which bear only hydrogen substituents on every group 15 atom. The reactions of BH_3·LB (LB = dmap, NH_3) with 0.5 equivalents of I_2 lead to IBH_2·LB (LB = dmap, NH_3) in good yields (Scheme 7). The boranes were characterized by ^1H and ^{11}B NMR spectroscopy. In the $^{11}B\{^1H\}$ NMR spectrum IBH_2·NH_3 reveals a singlet at δ = –20.6 ppm which splits into a triplet ($^1J_{B,H}$ = 130 Hz) in the ^{11}B NMR spectrum (Figure 14). The ^1H NMR spectrum of IBH_2·NH_3 allows no definitive statement due to the broadness of the signals. IBH_2·dmap shows in the $^{11}B\{^1H\}$ NMR spectrum also a singlet at δ = –11.9 ppm which splits into a triplet ($^1J_{B,H}$ = 130 Hz) in the ^{11}B NMR spectrum (Figure 15). The ^1H NMR spectrum of IBH_2·dmap reveals a quartet for the BH_2 group at δ = 4.51 ppm and for dmap the methyl group is observed at δ = 1.78 ppm (s, 6H, Me), and the aromatic protons at δ = 5.37 (*meta*) and 7.88 ppm (*ortho*, figure 16).

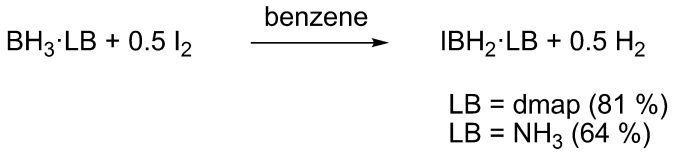

Scheme 7. Synthesis of monoiodoboranes IBH_2·LB (LB = dmap, NH_3). Yields are given in parentheses.

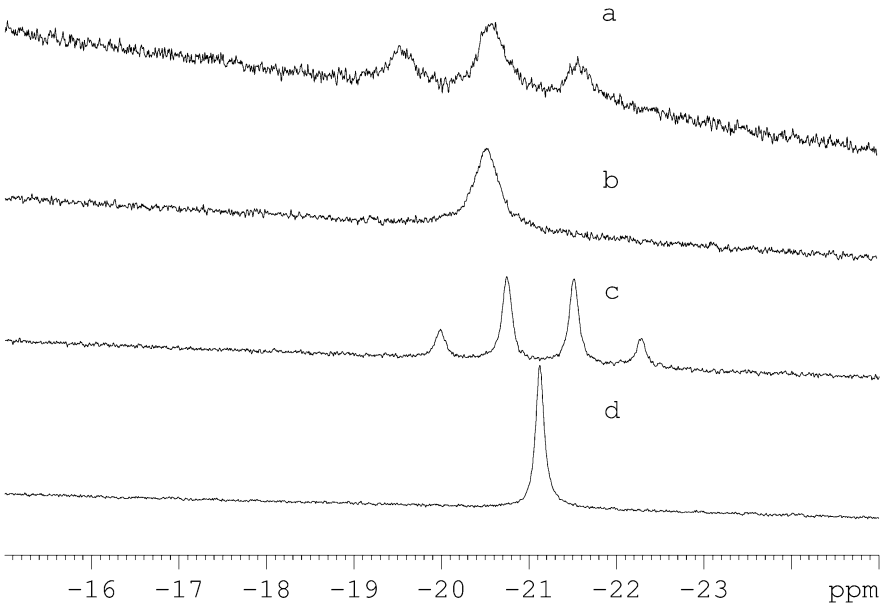

Figure 14. $^{11}B\{^1H\}$ NMR spectrum of IBH_2·NH_3 (b) and BH_3· NH_3 (d) and ^{11}B NMR spectrum of IBH_2· NH_3 (a) and BH_3· NH_3 (c) in C_6D_6.

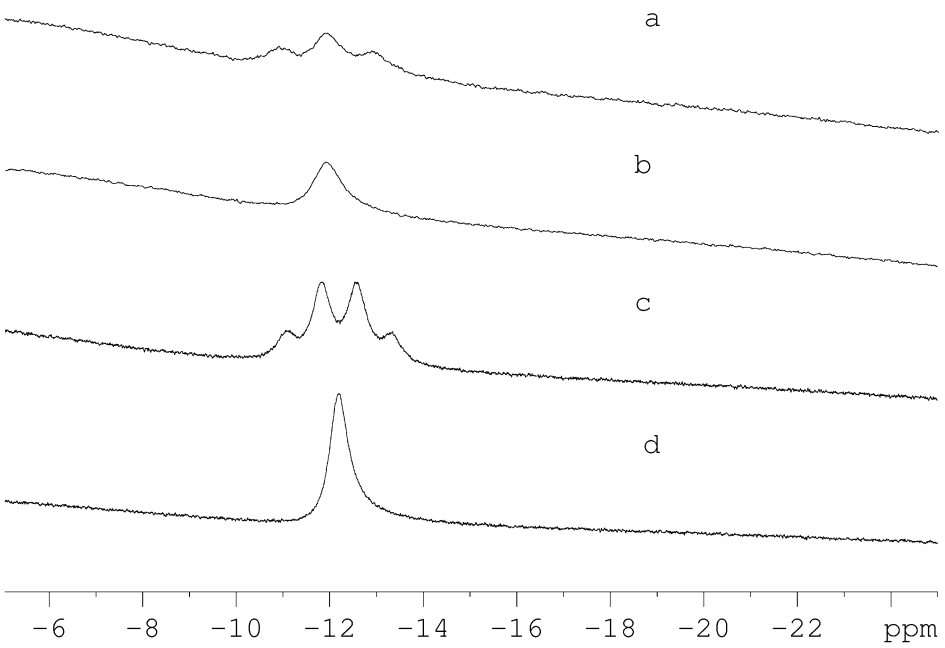

Figure 15. $^{11}B\{^{1}H\}$ NMR spectrum of IBH_2·dmap (b) and BH_3·dmap (d) and ^{11}B NMR spectrum of IBH_2·dmap (a) and BH_3·dmap (c) in C_6D_6.

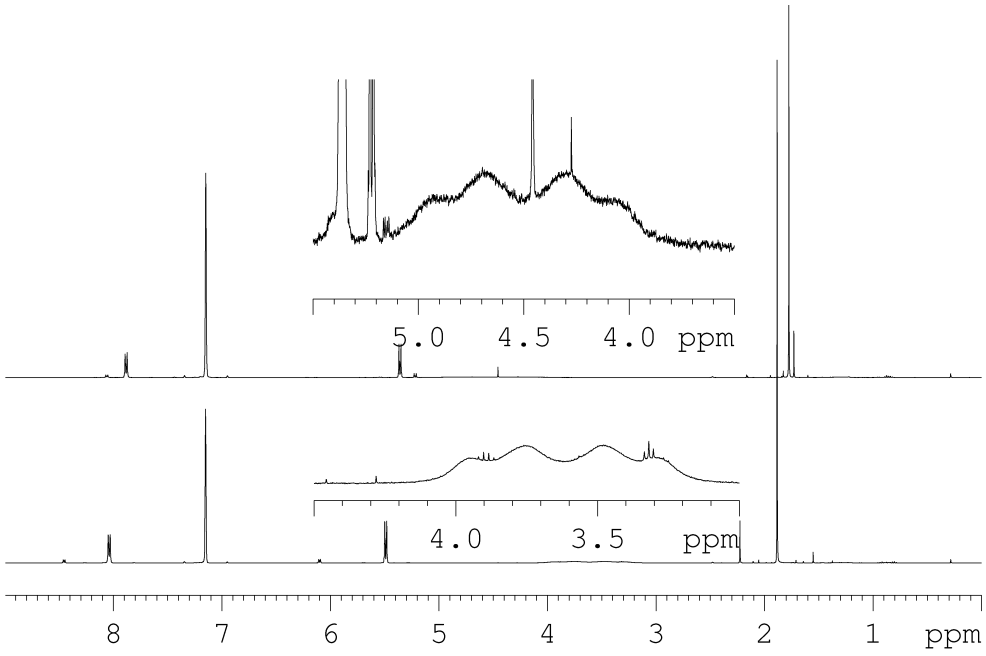

Figure 16. ^{1}H NMR spectrum of IBH_2·dmap (top) and BH_3·dmap (bottom) in C_6D_6.

Synthesis of IBH_2·NH_3:

To a solution of 31 mg (1.00 mmol) H_3B·NH_3 in 15 mL of Et_2O 127 mg (0.5 mmol) I_2 are added at r.t.. A white powder precipitates. After stirring for 18h, the supernatant is decanted off and all volatiles are removed under reduced pressure. The white solid is washed with *n*-hexane (2×5 mL) and dried under reduced pressure. Yield of IBH_2·NH_3:

100 mg (64 %). ^{1}H NMR (C_6D_6, 25 °C): signals cannot be assigned. ^{11}B NMR (C_6D_6, 25 °C): δ = –20.6 (t, $^{1}J_{B,H}$ = 130 Hz, BH_2). $^{11}B\{^{1}H\}$ NMR (C_6D_6, 25 °C): δ = –20.6 (s, BH_2).

Synthesis of BH_3·dmap:

610 mg (5.0 mmol) of dmap are dissolved in 40 mL of toluene. After addition of 5 mL of a 1.0 M H_3B·thf solution a white solid precipitates. All volatiles are removed and the solid is dried under reduced pressure. The solid is washed 2 times with 10 mL of *n*-hexane and dried under reduced pressure. Yield of BH_3·dmap: 355 mg (52 %). ^{1}H NMR (C_6D_6, 25 °C): δ = 1.89 (s, 6H, Me), 3.63 (q, 3H, BH_3), 5.49 (m, 2H, *meta*-H), 8.04 (m, 2H, *ortho*-H). ^{11}B NMR (C_6D_6, 25 °C): δ = –12.2 (t, BH_2). $^{11}B\{^{1}H\}$ NMR (C_6D_6, 25 °C): δ = –12.2 (s, BH_2).

Synthesis of IBH_2·dmap:

272 mg (2.0 mmol) of BH_3·dmap are dissolved in 45 mL of benzene. 250 mg (0.98 mmol) of I_2 are slowly added at r.t.. Gas evolution is observed and the solution gets slightly turbid. After stirring for 2 h, all volatiles are removed under reduced pressure and the solid is washed with 15 mL of *n*-hexane. IBH_2·dmap is obtained as a white solid. Yield of IBH_2·dmap: 425 mg (81 %). ^{1}H NMR (C_6D_6, 25 °C): δ = 1.78 (s, 6H, Me), 4.51 (q, 2H, BH_2), 5.37 (m, 2H, *meta*-H), 7.88 (m, 2H, *ortho*-H). ^{11}B NMR (C_6D_6, 25 °C): δ = –11.9 (t, $^{1}J_{B,H}$ = 130 Hz, BH_2). $^{11}B\{^{1}H\}$ NMR (C_6D_6, 25 °C): δ = –11.9 (s, BH_2).

11.6 H_2PBH_2–H_2PBH_2·NMe_3, H_2PBH_2–H^tBuPBH_2·NMe_3 and the longer cationic chain $[Me_3N{\cdot}H_2B–P^tBuH–H_2B–PH_2–BH_2–H_2P–BH_2–H^tBuP–BH_2{\cdot}NMe_3]^+I^-$

The anionic compound $[Na]^+[H_2P–BH_2–PH_2]^-$ introduced in chapter 6, is a very unique species. With accessible lone pairs at each phosphorus atoms, it is an interesting starting material for further conversions. In a first approach we targeted on the synthesis of $H_3B{\cdot}H_2PBH_2$–$H_2PBH_2{\cdot}NMe_3$ via the reaction of $[Na]^+[H_2P–BH_2–PH_2]^-$, $IBH_2{\cdot}NMe_3$ and H_3B·thf in THF. However, the desired product could not be obtained. Instead some crystals of H_2PBH_2–$H_2PBH_2{\cdot}NMe_3$ could be isolated. The structure was confirmed by single-crystal X-ray structure analysis. However this compound seems to be extremely unstable. ^{31}P NMR spectroscopic investigations at room temperature reveal that most probably it decomposes to $H_2PBH_2{\cdot}NMe_3$ and $[H_2PBH_2]_n$ polymer (Scheme 7). The signals could not be clearly assigned. Stoichiometric reaction of $[Na]^+[H_2P–BH_2–PH_2]^-$ with $IBH_2{\cdot}NMe_3$ does not lead to better results (Scheme 7). The same behaviour is observed, when $H_3B{\cdot}H_2PBH_2{\cdot}NMe_3$ is transformed to $IH_2B{\cdot}H_2PBH_2{\cdot}NMe_3$ and reacted

with $NaPH_2$. Whilst the first reaction step yields quantitatively $IH_2B{\cdot}H_2PBH_2{\cdot}NMe_3$ (Figure 18, 19) the transformation into $H_2PBH_2{-}H_2PBH_2{\cdot}NMe_3$ leads to decomposition/ polymerization. $IH_2B{\cdot}H_2PBH_2{\cdot}NMe_3$ was characterized by NMR spectroscopy in solution and could not be isolated for further characterization. In the solid state $H_2PBH_2{-}H_2PBH_2{\cdot}NMe_3$ reveals P–B which measure 1.947(2), 1.954(2) and 1.967(3) Å and correspond to P–B single bonds (Figure 17).

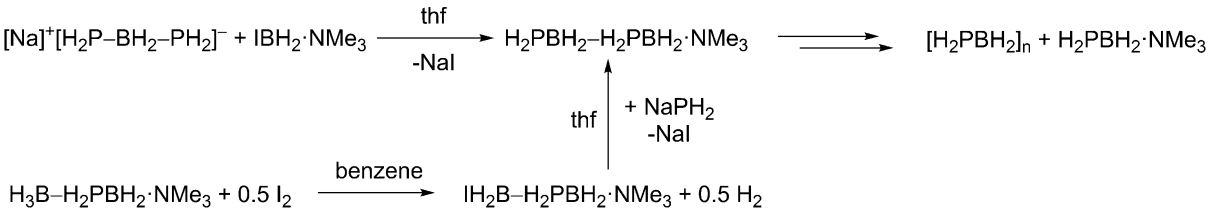

Scheme 7. Synthesis and decomposition of $H_2PBH_2{\cdot}H_2PBH_2{\cdot}NMe_3$.

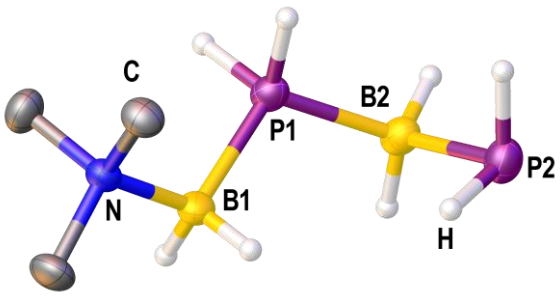

Figure 17. Molecular structure of $H_2PBH_2{\cdot}H_2PBH_2{\cdot}NMe_3$ in the solid state. Hydrogen atoms bonded to carbon are omitted for clarity. Thermal ellipsoids are drawn with 50% probability. Selected bond lengths [Å] and angles [°]: P1–B1 1.954(2), P1–B2 1.947(2), P2–B2 1.967(3), N1–B1 1.601(3), B2–P1–B1 112.84(10), N1–B1–P1 115.39(13), P1–B2–P2 109.85(12).

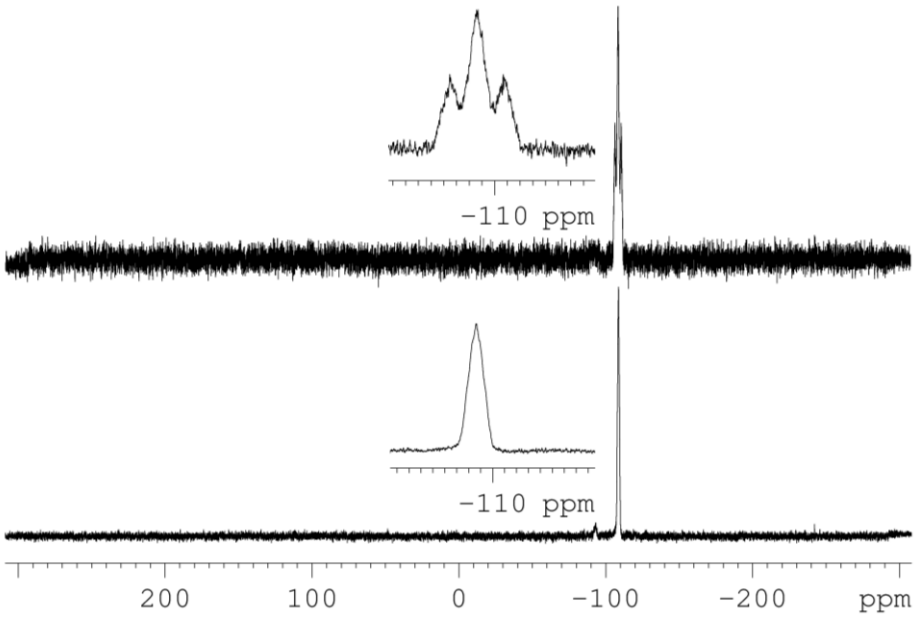

Figure 18. $^{31}P\{^{1}H\}$ (bottom) and ^{31}P (top) NMR spectrum of $IH_2B{\cdot}\ H_2PBH_2{\cdot}NMe_3$ in C_6D_6.

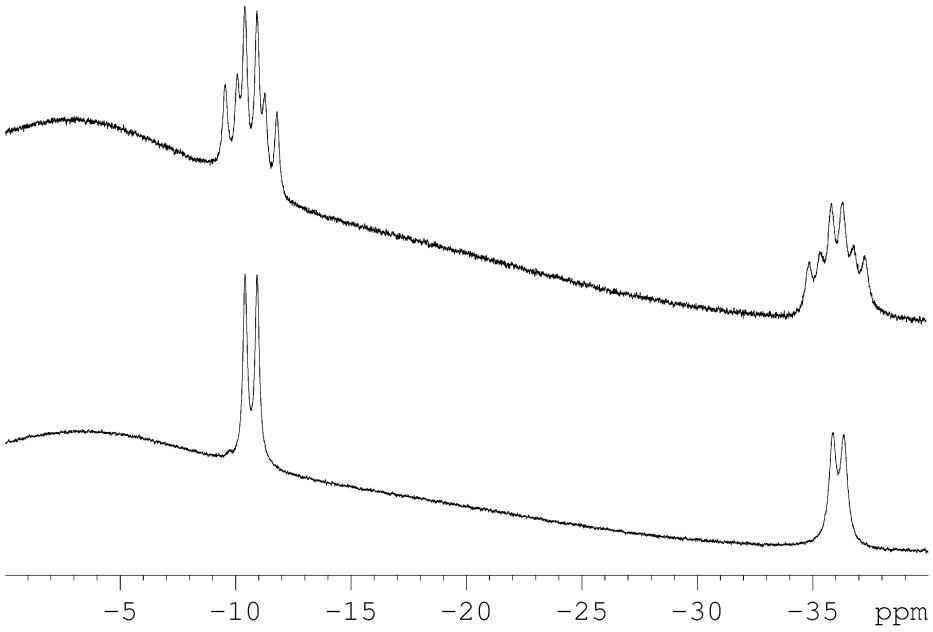

Figure 19. $^{11}B\{^{1}H\}$ (bottom) and ^{11}B (top) NMR spectrum of $IH_2B\cdot H_2PBH_2\cdot NMe_3$ in C_6D_6.

With H_2PBH_2–$H_2PBH_2\cdot NMe_3$ being very prone toward polymerization the synthesis of H_2PBH_2–$H^tBuPBH_2\cdot NMe_3$ was developed, as it was expected to be more stable. Due to the higher donation properties of the ^{t}Bu substituted P atom which should lead to a more stable of the P–B bond. Reaction of the anionic species $[Na]^+[H_2P–BH_2–P^tBuH]^-$ with $IBH_2\cdot NMe_3$ leads selectively to H_2PBH_2–$H^tBuPBH_2\cdot NMe_3$ (Scheme 8). Since H_2PBH_2–$H^tBuPBH_2\cdot NMe_3$ shows good solubility in *n*-hexane it can be easily be isolated by extraction with *n*-hexane and filtration over diatomaceous earth. However all attempts to isolate it as a pure product or crystallize it failed to date. Characterization was only achieved by ^{31}P and ^{11}B NMR spectroscopy. Subsequent reaction with $IBH_2\cdot SMe_2$ leads to a long cationic chain which backbone contains 5 boron and 4 phosphorus atoms (Scheme 8). Crystallization and isolation of a pure product of this cationic species was not successful to date, however the existence of the chain was undoubtedly confirmed by mass spectrometry and ^{31}P and ^{11}B NMR spectroscopy (Figure 20).

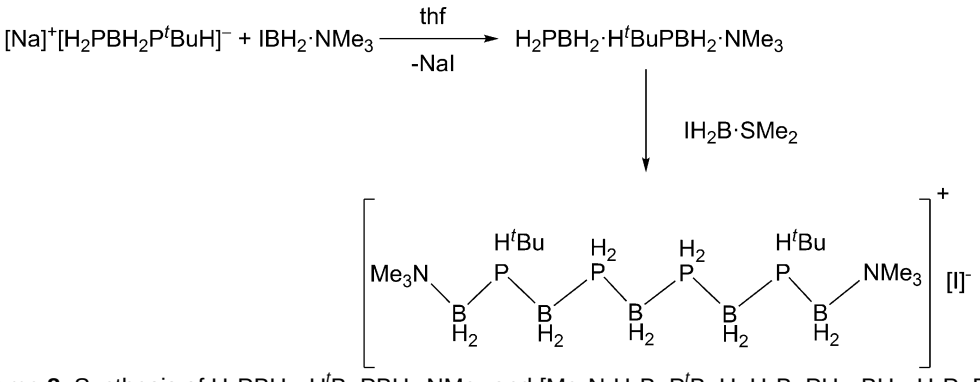

Scheme 8. Synthesis of H_2PBH_2–$H^tBuPBH_2\cdot NMe_3$ and $[Me_3N\cdot H_2B–P^tBuH–H_2B–PH_2–BH_2–H_2P–BH_2–H^tBuP–BH_2\cdot NMe_3]^+I^-$.

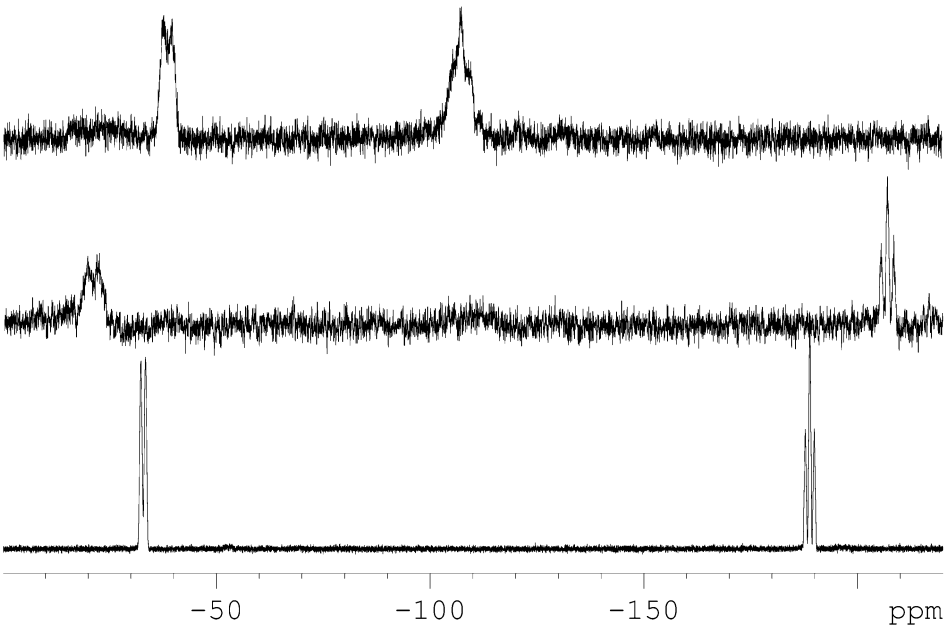

Figure 20. ^{31}P NMR spectrum of $[Na]^+[H_2P–BH_2–P^tBuH]^-$ (bottom), $H_2PBH_2–H^tBuPBH_2·NMe_3$ (middle) and $[Me_3N·H_2BP^tBuH–H_2BPH_2–BH_2–H_2PBH_2–H^tBuPBH_2·NMe_3]^+I^-$ (top).

Synthesis of $H_2PBH_2–H_2PBH_2·NMe_3$:

A solution of 102 mg (0.25 mmol) $[Na]^+[H_2PBH_2PH_2]^-$ in 10 mL THF is added at −80°C to a solution of 22 mg (0.25 mmol) $H_3B·thf$ and 50 mg (0.25 mmol) $IH_2B·NMe_3$ in THF and is stirred for 18 h. After removal of all volatiles under reduced pressure, the solid was extracted 3 times with 10 mL of *n*-hexane and filtrated over diatomaceous earth. The solution was concentrated under reduced pressure and stored at −80°C. A very small amount (~2 mg) of crystals of $H_2PBH_2·H_2PBH_2·NMe_3$ was isolated.

Stoichiometric reaction:

To a solution of 112 mg (2mmol) $NaPH_2$ in 20 mL of thf 212 mg (2 mmol) $H_2PBH_2·NMe_3$ were added and the mixture was sonicated for 3h. The resulting $[Na]^+[H_2PBH_2PH_2]^-$ was added at −80°C to a solution of 400 mg (2.00 mmol) $IH_2B·NMe_3$ in THF and is stirred for 18 h. The ^{31}P NMR spectrum of the reaction mixture showed only the decomposition products mentioned before.

Synthesis of $IBH_2·H_2PBH_2·NMe_3$:

To a solution of 53 mg (0.50 mmol) $H_2PBH_2·NMe_3$ in 10 mL THF 0.5 mmol of $H_3B·thf$ were added at r.t. and the mixture was stirred for 2 h. After removal of all volatiles under reduced pressure, the solid was dissolved in benzene and 63 mg (0.25mmol) of I_2 were added. After stirring for 2 days all volatiles were removed under reduced pressure and the orange oil was dissolved in toluene. Isolation of $IBH_2·H_2PBH_2·NMe_3$ failed up to date, however ^{31}P and ^{11}B NMR spectroscopy show a quantitative conversion to $IBH_2·H_2PBH_2·NMe_3$.

Conversion to H_2PBH_2–H_2PBH_2·NMe_3

Subsequent reaction with 28 mg (0.5 mmol) $NaPH_2$ in THF leads to the same signal pattern in ^{31}P NMR spectrum, as observed for the other pathway.^{31}P NMR (C_6D_6, 25 °C): δ = –108.7 (d, br, $^1J_{H,P}$ = 340 Hz). $^{31}P\{^1H\}$ NMR (C_6D_6, 25 °C): δ = –108.7 (s, br). ^{11}B NMR (C_6D_6, 25 °C): δ = –36.11 (dt, $^1J_{B,P}$ = 63 Hz, $^1J_{B,H}$ = 125 Hz, BH_2I), –10.7 (dt, $^1J_{B,P}$ = 70 Hz, $^1J_{B,H}$ = 110 Hz). $^{11}B\{^1H\}$ NMR (C_6D_6, 25 °C): δ = –36.11 (d, $^1J_{B,P}$ = 63 Hz, BH_2I), –10.7 (d, $^1J_{B,P}$ = 70 Hz, Me_3NBH_2).

Synthesis of H_2PBH_2–H^tBuPBH_2·NMe_3 and subsequent reaction to $[Me_3N{\cdot}H_2B$–P^tBuH–H_2B–PH_2–BH_2–H_2P–BH_2–H^tBuP–$BH_2{\cdot}NMe_3]^+I^-$

To a solution of 112 mg (1.00 mmol) Na^{t}BuPH in THF, 105 mg (1.00 mmol) of H_2PBH_2·NMe_3 were added and the mixture was sonicated for 2 hours. The mixture was added to a solution of 199 mg (1.00 mmol) IBH_2·NMe_3 in THF at −80°C and was stirred overnight. All volatiles were removed under reduced pressure and the residue was extracted with *n*-hexane (3 x 10 mL). Even in concentrated solutions at low temperatures no crystals could be obtained. The solution was added to (0.50 mmol) IBH_2·SMe_2 in CH_2Cl_2 and the solution was stirred overnight. Though many attempts were made, $[Me_3N{\cdot}H_2B$–P^tBuH–H_2B–PH_2–BH_2–H_2P–BH_2–H^tBuP–$BH_2{\cdot}NMe_3]^+I^-$ could not be crystallized.

H_2PBH_2–H^tBuPBH_2·NMe_3

^{31}P NMR (C_6D_6, 25 °C): δ = –207.0 (t, br, $^1J_{H,P}$ = 183 Hz, PH_2), –21.0 (d, br, $^1J_{H,P}$ = 317 Hz, P^{t}BuH). $^{31}P\{^1H\}$ NMR (C_6D_6, 25 °C): δ = –207.0 (m, br, PH_2), –21.0 (s, br, P^{t}BuH).

$[Me_3N{\cdot}H_2B$–P^tBuH–H_2B–PH_2–BH_2–H_2P–BH_2–H^tBuP–$BH_2{\cdot}NMe_3]^+I^-$

^{31}P NMR (C_6D_6-cap, 25 °C): δ = –107.3 (t, br, PH_2), –38.3 (d, br, P^{t}BuH). $^{31}P\{^1H\}$ NMR (C_6D_6, 25 °C): = δ –107.3 (s, br, PH_2), –38.3 (s, br, P^{t}BuH). ^{11}B NMR (C_6D_6, 25 °C): δ = –38.7 (m, br, P–BH_2–P), –10.3 (m, br, P–BH_2–NMe_3). $^{11}B\{^1H\}$ NMR (C_6D_6, 25 °C): δ = –38.7 (d, br, P–BH_2–P), –10.3 (t, br, P–BH_2–NMe_3).). ESI-MS (MeCN): *m/z* = 426 (100%, $[Me_3N{\cdot}H_2B$–P^tBuH–H_2B–PH_2–BH_2–H_2P–BH_2–H^tBuP–$BH_2{\cdot}NMe_3]^+$).

Table 5. Crystallographic data of H_2PBH_2–$H_2PBH_2{\cdot}NMe_3$.

empirical formula	$C_3H_{17}B_2NP_2$
formula weight	150.73
temperature [K]	123(1)
crystal system	monoclinic
space group	$P2_1/n$
a [Å]	10.2429(4)
b [Å]	9.2237(3)
c [Å]	11.0740(5)
α [°]	90
β [°]	113.455(5)
γ [°]	90
Volume [Å^3]	959.79(7)
Z	4
ρ_{calc}g/cm^3	1.043
μ/mm^{-1}	3.458
F(000)	328.0
crystal size [mm^3]	0.16 × 0.07 × 0.05
radiation	CuK_α (λ = 1.54178)
absorption correction	analytical
T_{min}/T_{max}	0.712 / 0.849
2Θ range [°]	9.958 to 146.818
completeness	0.988
index ranges	-11 ≤ h ≤ 12 -10 ≤ k ≤ 11 -13 ≤ l ≤ 5
reflections collected	3230
independent reflections	1851 [R_{int} = 0.0314, R_{sigma} = 0.0396]
data/restraints/parameters	1851/0/108
GOF on F^2	1.068
final R indexes [I>=2σ (I)]	R_1 = 0.0453, wR_2 = 0.1234
final R indexes [all data]	R_1 = 0.0509, wR_2 = 0.1327
max/min $\Delta\rho$ [e·Å^{-3}]	0.53/-0.35

11.7 Synthesis of $(Me_3Si)_2Bi–BH_2·dmap$

Whereas phosphanyl- and arsanylboranes are known for decades, the heavier analogues of the pnictogenylboranes remain unknown. Compounds with a direct E–B (E = Sb, Bi) are very scarce in the literature. In chapter 9, a strategy was developed to access the stibanylboranes via a salt metathesis reaction. This is the first report on the isolation and characterization of the parent compound of the stibanylboranes and some of its derivatives. It was worthwhile to investigate, if the heavier analogue - the bismuthanylborane - is also experimentally accessible. The reaction of $LiBi(SiMe_3)_2·DME$ with $IBH_2·dmap$ gives the corresponding silylated bismuthanylboranes (Scheme 9). ^{11}B NMR spectroscopic studies show, that the salt metathesis proceeds selectively to give the silylated species. For dmap as Lewis base some crystals could be isolated and were characterized by single-crystal X-ray structure analysis. This compound is one of the first examples for a compound containing a covalent 2c-2e-σ Bi–B bond with 2.424(5) Å. In the solid state the substituents along the Bi–B bond show a synclinal arrangement (Figure 21). In the $^{11}B\{^1H\}$ NMR spectrum a singlet is observed at δ = –15.4 ppm which shows further splitting into a triplet ($^1J_{B,H}$ ~ 120 Hz, BH_2) in the ^{11}B NMR spectrum. The ^1H NMR spectrum reveals a singlet for the $SiMe_3$-group at δ = 0.99 ppm. For the methyl group of dmap a singlet is found at δ = 1.83 ppm, and the aromatic protons can be found at δ = 5.40 (*meta*) and 8.05 ppm (*ortho*). The boranyl moiety is found at δ = 4.86 ppm. With $IBH_2·NMe_3$ no reaction was observed for the salt metathesis. Until now, cleavage of the $SiMe_3$ groups was not successful, rendering the parent compound $H_2Bi–BH_2$ not accessible. Attempts for the cleavage of the $SiMe_3$ groups were performed by the addition of MeOH, mixtures of MeOH/MeONa or KF·HF (see experimental part for further information).

$$LiBi(SiMe_3)_2·3dme + IBH_2·dmap \xrightarrow[-LiI\ -dme]{-80°C\text{ - r.t.}\ \text{toluene}} (Me_3Si)_2BiBH_2·dmap$$

Scheme 9. Synthesis of $(Me_3Si)_2Bi–BH_2·dmap$.

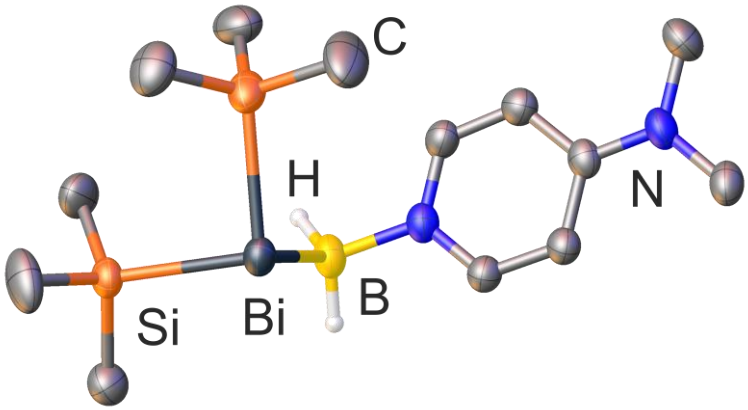

Figure 21. Molecular structure of $(Me_3Si)_2Bi–BH_2$·dmap in the solid state. Hydrogen atoms bonded to carbon are omitted for clarity. Thermal ellipsoids are drawn with 50% probability. Selected bond lengths [Å] and angles [°]: Bi–B 2.424(5), N–B 1.578(5), N–B–Bi 106.9(2).

Synthesis of $(Me_3Si)_2Bi–BH_2$·dmap:

To a solution of 1.28 g (1.89 mmol) $LiBi(SiMe_3)_2$·3dme in toluene 440 mg (1.6 mmol) IBH_2·dmap at –80°C. The solution is stirred for 2 h and then it is stored for 18h at –28°C. The mixture is allowed to reach –10°C and is reaction control was perfomed by ^{11}B NMR spectroscopy, which shows full conversion. The mixture was allowed to reach r.t., whereby NMR showed no change. The solution is filtrated and stored at –28°C. Some crystals of $(Me_3Si)_2Bi–BH_2$·dmap were formed and could be characterized by X-ray structure analysis.^1H NMR (C_6D_6, 25 °C): δ = 0.99 (s, 18H, $SiMe_3$), 1.83 (s, 6H, Me), 4.86 (q, 2H, BH_2), 5.40 (m, 2H, *meta*-H), 8.05 (m, 2H, *ortho*-H). ^{11}B NMR (C_6D_6, 25 °C): δ = –15.4 (t, $^1J_{B,H}$ ~ 120 Hz, BH_2). $^{11}B\{^1H\}$ NMR (C_6D_6, 25 °C): δ = –15.4 (s, br, BH_2).

Attempted cleavage of $SiMe_3$-groups:

I) To a solution of 0.8 mmol $(Me_3Si)_2Bi–BH_2$·dmap in toluene, an excess of MeOH (1 mL) was added at -80°C, the reaction was stirred 4h at -80°C and transferred into a NMR tube. The solution was allowed to reach r.t.. In the ^{11}B and ^1H NMR spectra only signals of the starting materials are present.

II) A solution of 0.8 mmol $(Me_3Si)_2Bi–BH_2$·dmap in toluene, was added to 1 mL of MeOH containing ~10 mg NaOMe at -80°C, the reaction was stirred 4h at -80°C and transferred into a NMR tube. The solution was allowed to reach r.t.. In the ^1H NMR spectrum only signals of the starting materials are present.

III) A solution of 0.8 mmol $(Me_3Si)_2Bi–BH_2$·dmap in THF was stirred over KF·HF (80 mg, 1mmol) at -80°C and was allowed to reach r.t.. In the ^1H NMR spectrum only signals of the starting materials are present.

Table 6. Crystallographic data of $(SiMe_3)_2Bi–BH_2$·dmap.

empirical formula	$C_{13}H_{30}BBiN_2Si_2$
formula weight	490.36
temperature [K]	123(1)
crystal system	triclinic
space group	*P*-1
a [Å]	7.3161(2)
b [Å]	9.8444(2)
c [Å]	15.3209(3)
α [°]	90.6300(10)
β [°]	103.624(2)
γ [°]	103.085(2)
Volume [$Å^3$]	1042.14(4)
Z	2
$\rho_{calc}g/cm^3$	1.563
μ/mm^{-1}	17.621
F(000)	476.0
crystal size [mm^3]	0.2232 × 0.1182 × 0.0982
radiation	Cu*Kα* (*λ* = 1.54178)
absorption correction	analytical
T_{min}/T_{max}	0.112 / 0.337
2*Θ* range [°]	9.244 to 133.164
completeness	0.985
index ranges	$-7 \le h \le 8$ $-11 \le k \le 11$ $-18 \le l \le 16$
reflections collected	10095
independent reflections	3613 [R_{int} = 0.0278, R_{sigma} = 0.0248]
data/restraints/parameters	3613/0/188
GOF on F^2	1.090
final R indexes [I>=2σ (I)]	R_1 = 0.0202, wR_2 = 0.0526
final R indexes [all data]	R_1 = 0.0221, wR_2 = 0.0532
max/min Δ*ρ* [$e·Å^{-3}$]	0.72/-0.54

11.8 Synthesis of the Tl complexes $[Tl(H_2E–BH_2·NMe_3)_3]^+[Tef]^–$ (E = P, As) and $[Tl]^+[Tef]^–$ mediated P-P coupling

In chapter 10 it was shown, that coordination of different pnictogenylboranes gives access to a variety of unprecedented Cu and Ag complexes, respectively. For the first time a copper-arsine-complex, bearing primary arsines was reported. Likewise, there are no reports on homoleptic Tl complexes with primary arsines or phosphines. The reaction of 3 equivalents $H_2E–BH_2·NMe_3$ (E = P, As) with $[Tl]^+[Tef]^–$ (Tef = $[Al\{OC(CF_3)_3\}_4]$) leads to $[Tl(H_2E–BH_2·NMe_3)_3]^+[Tef]^–$ (E = P, As, scheme 10). While for the phosphorus derivative $[Tl(H_2P–BH_2·NMe_3)_3]^+[Tef]^–$ only twinned crystals are obtained, single-crystal structure determination was performed for $[Tl(H_2As–BH_2·NMe_3)_3]^+[Tef]^–$. In the solid state $[Tl(H_2As–BH_2·NMe_3)_3]^+[Tef]^–$ reveals a trigonal-pyramidal coordination at the Tl atom (sum coordination angles 244.53(12)°, Figure 22). From every BH_2 moiety one hydride is pointed towards the next Tl atom (H···Tl distance 3.093 Å), leading to columns in the solid state and a pseudo-octahedral coordination. The found bond length for As–Tl is with 3.1154(14) Å above the sum of covalent radii for Tl and As ($\sum r_{cov}$(Tl-As) = 2.67 Å)[9] but far below the sum of the van der Waals radii ($\sum r_{vdW}$(Tl-As = 3.81 Å)[10]. The As–B bond length measures 2.081(14) Å and the N–B bond length 1.586(17)Å and are in the expected range of a single bond. The phosphorus derivative showed very similar unit cell parameters (see table 8), however due to crystal twinning only the parameters were determined and a poor model was obtained.

The ^{1}H NMR spectrum of $[Tl(H_2As–BH_2·NMe_3)_3]^+[Tef]^–$ reveals for the AsH_2 group a multiplet at δ = 1.30 ppm (Figure 23). The boranyl moiety is found at δ = 2.43 ppm and the amine arises as a singlet at δ = 2.72 ppm. The $^{11}B\{^1H\}$ NMR spectrum reveals a singlet at δ = –6.5 which splits into a triplet in the ^{11}B NMR spectrum ($^1J_{B,H}$ = 111 Hz, Figure 24).

$[Tl(H_2P–BH_2·NMe_3)_3]^+[Tef]^–$ shows in the ^{1}H NMR spectrum a doublet at δ = 2.11 ppm ($^1J_{H,P}$ = 220 Hz) for the PH_2 group (Figure 25). At δ = 2.20 ppm the BH_2 group is found and NMe_3 arises as a singlet at δ = 2.68 ppm. In the $^{31}P\{^1H\}$ NMR spectrum a broad singlet is found at δ = –161.4 ppm which splits into a further triplet in the ^{31}P NMR spectrum ($^1J_{H,P}$ = 220 Hz, Figure 26). The $^{11}B\{^1H\}$ NMR spectrum reveals a singlet at δ = –8.1 ppm which shows further splitting into a triplet in the ^{11}B NMR spectrum ($^1J_{B,H}$ = 103 Hz, Figure 26).

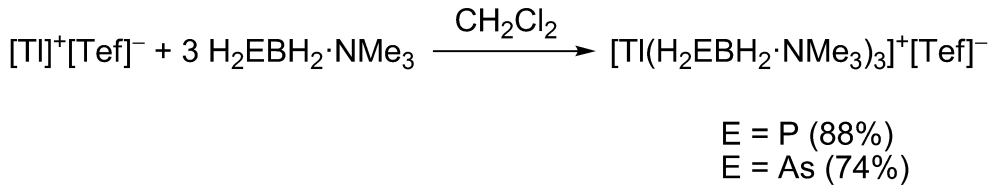

Scheme 10. Synthesis of $[Tl(H_2E–BH_2·NMe_3)_3]^+[Tef]^-$ (E = P, As). Yields are given in parentheses.

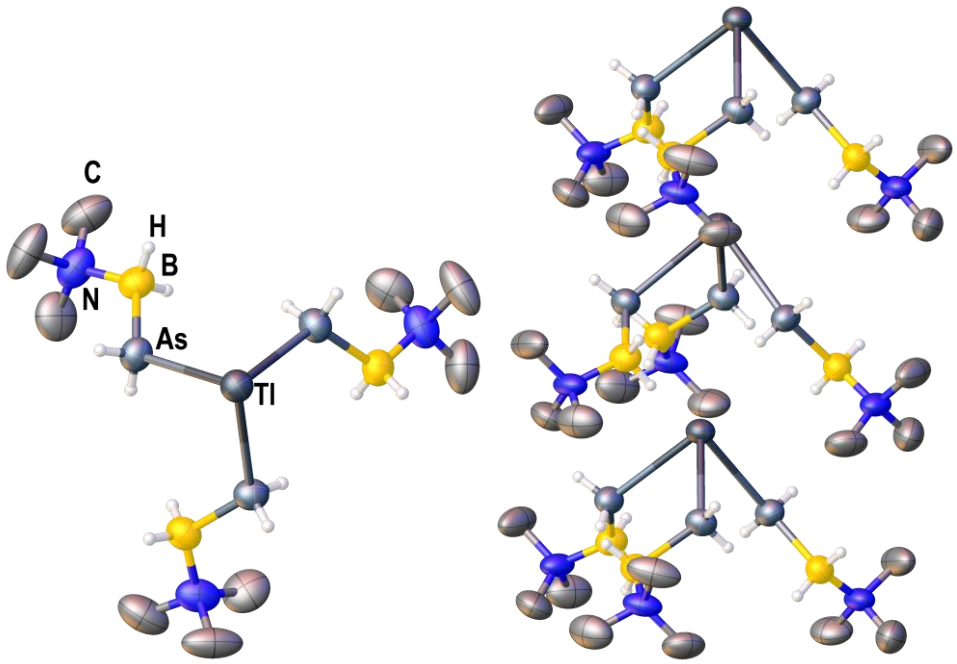

Figure 22. Molecular structure of $[Tl(H_2As–BH_2·NMe_3)_3]^+[Tef]^-$ in the solid state. Hydrogen atoms bonded to carbon and the counter ion are omitted for clarity. Thermal ellipsoids are drawn with 50% probability. Selected bond lengths [Å] and angles [°]: As–Tl 3.1154(14), As–B 2.081(14), N–B 1.586(17), B–As–Tl 126.1(4), As–Tl–As 81.51(4), N–B–As 117.5(9).

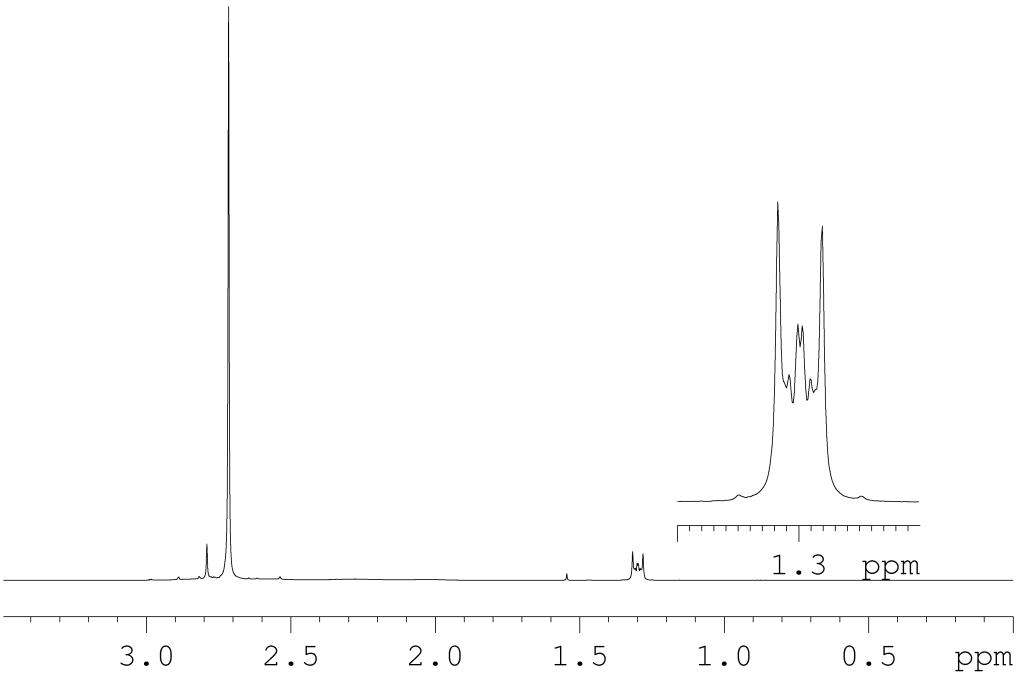

Figure 23. ^1H NMR spectrum of $[Tl(H_2As–BH_2·NMe_3)_3]^+[Tef]^-$ in CD_2Cl_2.

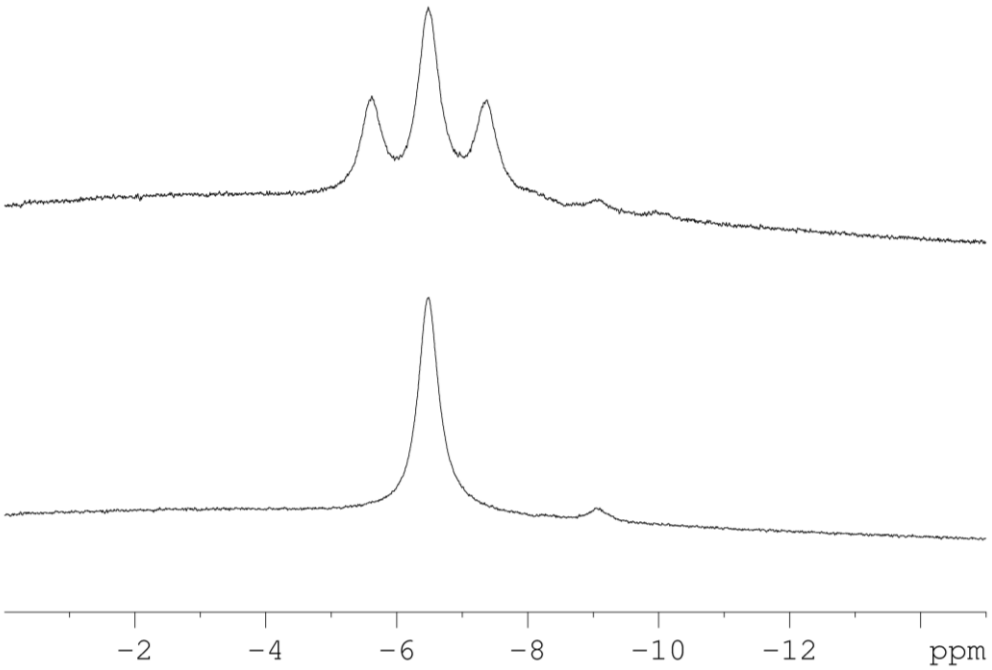

Figure 24. NMR spectra of $[Tl(H_2As–BH_2{\cdot}NMe_3)_3]^+[Tef]^-$ $^{11}B\{^1H\}$ bottom ^{11}B top in CD_2Cl_2.

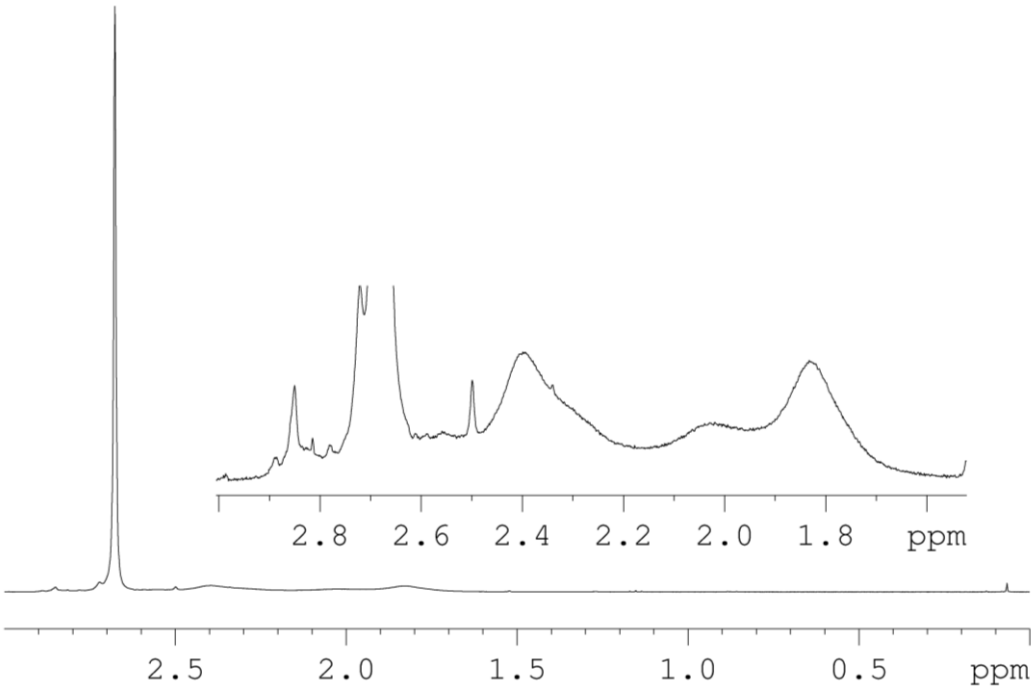

Figure 25. ^1H NMR spectrum of $[Tl(H_2P–BH_2{\cdot}NMe_3)_3]^+[Tef]^-$ in CD_2Cl_2.

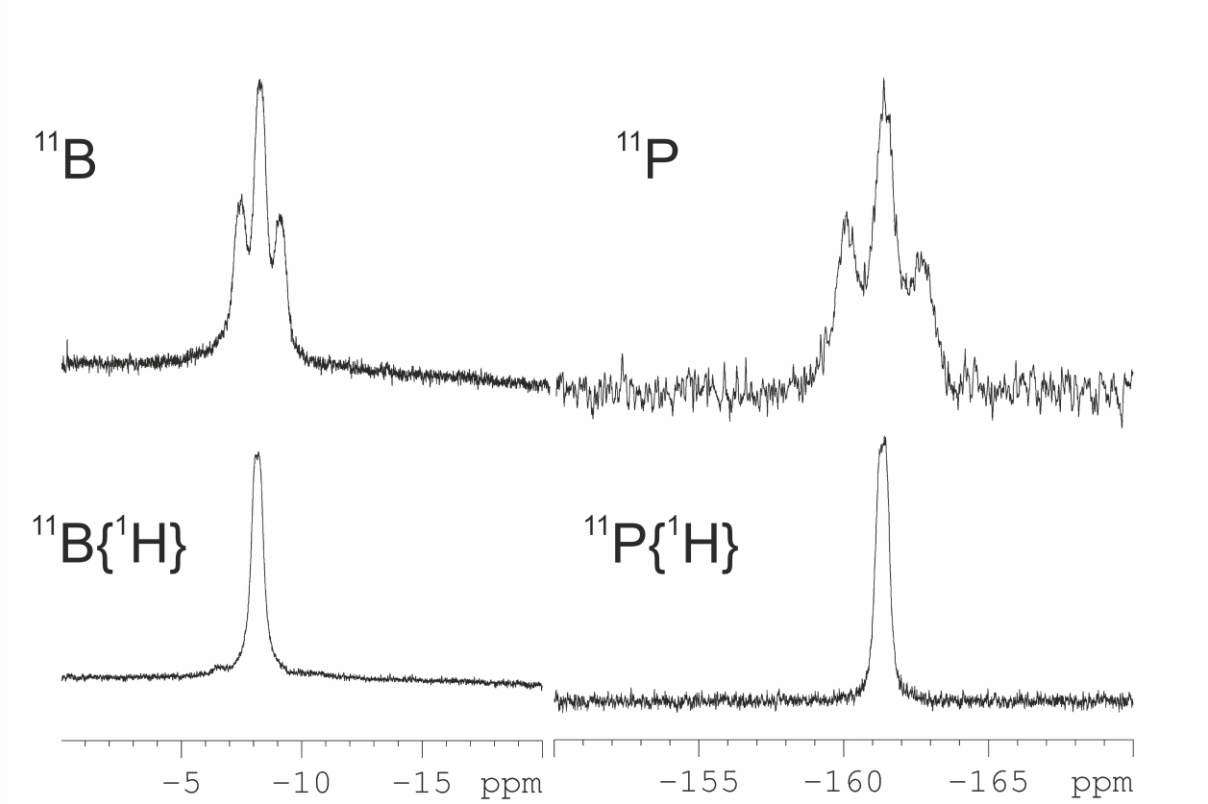

Figure 26. NMR spectra of $[Tl(H_2P–BH_2·NMe_3)_3]^+[Tef]^-$ in CD_2Cl_2.

While $[Tl(H_2As–BH_2·NMe_3)_3]^+[Tef]^-$ is stable in CH_2Cl_2 solution, the compound $[Tl(H_2P–BH_2·NMe_3)_3]^+[Tef]^-$ showed a subsequent reaction under involvement of the solvent CH_2Cl_2. Thorough investigation of this reaction with different stoichiometry of Tl and $H_2P–BH_2·NMe_3$ revealed a clean conversion for the 1:2 stoichiometry in CH_2Cl_2 determined by ^{31}P NMR spectroscopic studies. Excess of $H_2P–BH_2·NMe_3$ leads to another unassignable product which shows a very broad peak in the ^{31}P NMR spectra.

Stirring a mixture of 2 equivalents of $H_2P–BH_2·NMe_3$ with $[Tl]^+[Tef]^-$ in CH_2Cl_2 leads to a Tl mediated P-P coupling (Scheme 11). We assume, that the Tl^+ ion abstracts a chlorine from CH_2Cl_2 leading to $[CH_2Cl]^+$ and the precipitation of TlCl. X-ray powder diffraction pattern of the precipitated powder revealed pure TlCl (Figure 31). $[CH_2Cl]^+$ reacts further with $H_2P–BH_2·NMe_3$ giving $[HP–BH_2·NMe_3]^+$ and CH_3Cl, which formation was confirmed by ^1H NMR spectroscopy (Figure 30).[11] The $[HP–BH_2·NMe_3]^+$ instantly reacts with the second equivalent of $H_2P–BH_2·NMe_3$ to $[Me_3N·H_2B–H_2P–HP–BH_2·NMe_3]^+$ (Scheme 11). The presence of $[Me_3N·H_2B–H_2P–HP–BH_2·NMe_3]^+[Tef]^-$ was confirmed by ^{31}P NMR spectroscopy (Figure 28, new signals at δ = –91.3, –199.6 ppm) and mass spectrometry. ^{31}P ^{31}P COSY experiments revealed cross peaks indicative of a direct coupling between the two phosphorus atoms ($^1J_{P,P}$ = 255 Hz, figure 27). However a crystal structure could not be determined as up to date no suitable counter ion was

found, allowing a directed packing of the cation. X-ray structure analysis of the crystals reveal only the anionic part, and NMR shows the same signals as found for the reaction mixture. However weakly coordinating anions play a crucial role in this reaction. Test reactions with other Tl^+ salts failed (e.g. $TlPF_6$), and the only successful reactions were observed with $[Tef]^-$, FAl ($[FAl\{OC_6F_{10}(C_6F_5)\}_3]$) and $[BAr^{Cl}]^-$ ($[B(C_6H_3Cl_2)_4]$).

To our knowledge this is the first example for a Tl-mediated P-P coupling reactions. Further investigations have to be made to verify this reaction by single-crystal X-ray structure determination and to evaluate the scope of substrates.

$$[Tl]^+[Tef]^- + 2\ H_2PBH_2{\cdot}NMe_3 + CH_2Cl_2 \xrightarrow{CH_2Cl_2} [Me_3N{\cdot}H_2BHP{-}PH_2BH_2{\cdot}NMe_3]^+[Tef]^- + TlCl\downarrow + CH_3Cl$$

Scheme 11. Synthesis of $[Me_3N{\cdot}H_2B{-}H_2P{-}HP{-}BH_2{\cdot}NMe_3]^+[Tef]^-$.

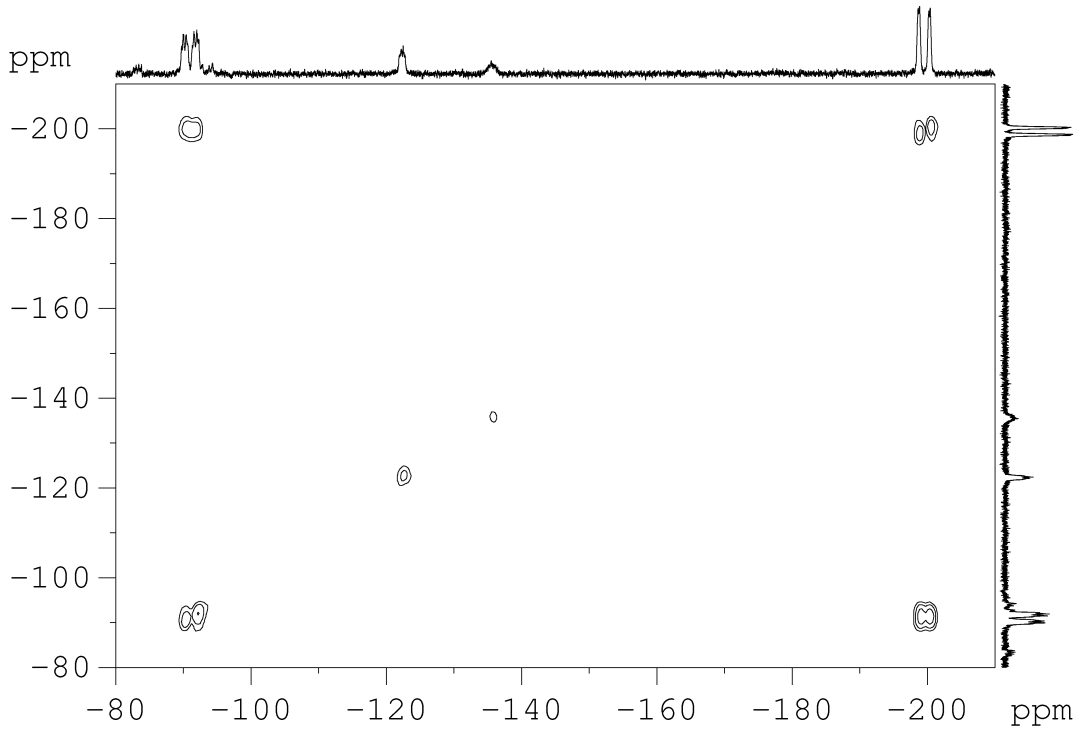

Figure 27. $^{31}P\ ^{31}P$ COSY of $[Me_3N{\cdot}H_2B{-}H_2P{-}HP{-}BH_2{\cdot}NMe_3]^+[Tef]^-$ in CD_2Cl_2 showing coupling of the two P signals.

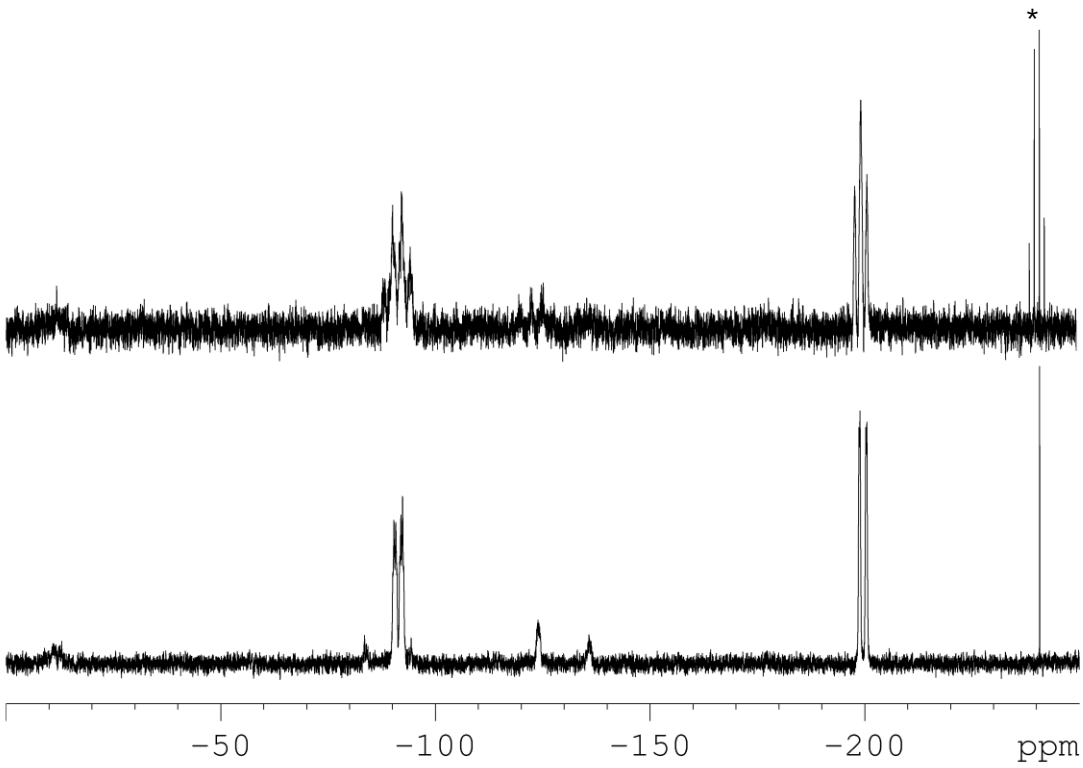

Figure 28. ^{31}P (top) and $^{31}P\{^{1}H\}$ NMR of a reaction mixture of $[Me_3N{\cdot}H_2B{-}H_2P{-}HP{-}BH_2{\cdot}NMe_3]^+[Tef]^-$ in CD_2Cl_2. * =PH_3.

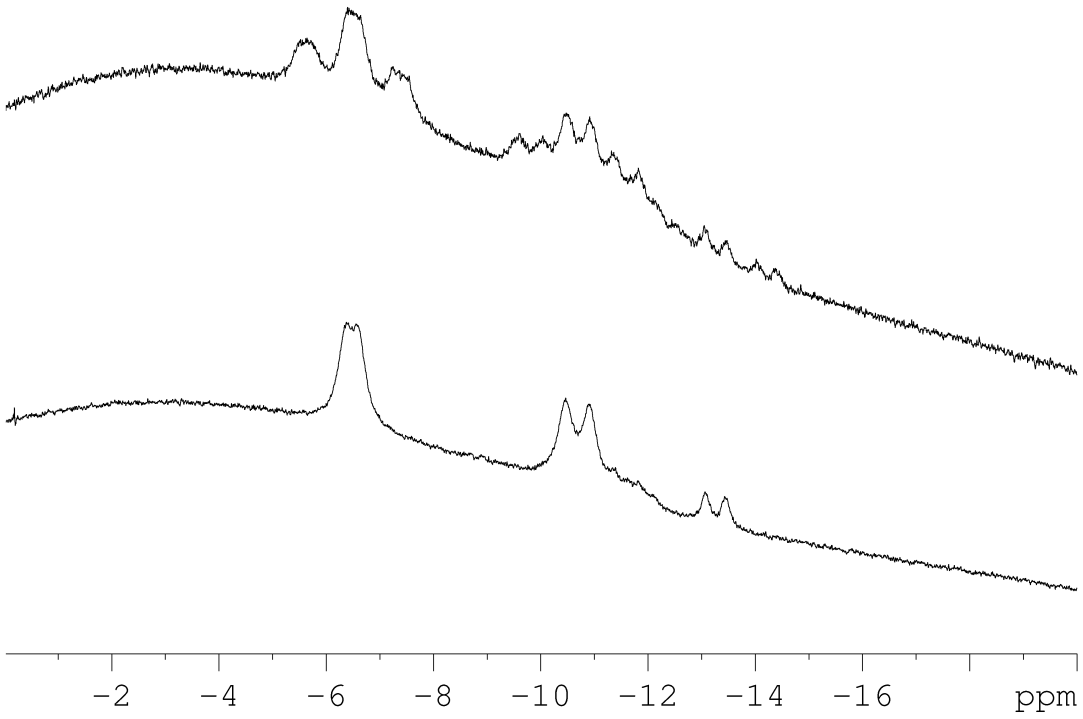

Figure 29. ^{11}B (top) and $^{11}B\{^{1}H\}$ NMR of a reaction mixture of $[Me_3N{\cdot}H_2B{-}H_2P{-}HP{-}BH_2{\cdot}NMe_3]^+[Tef]^-$ in CD_2Cl_2.

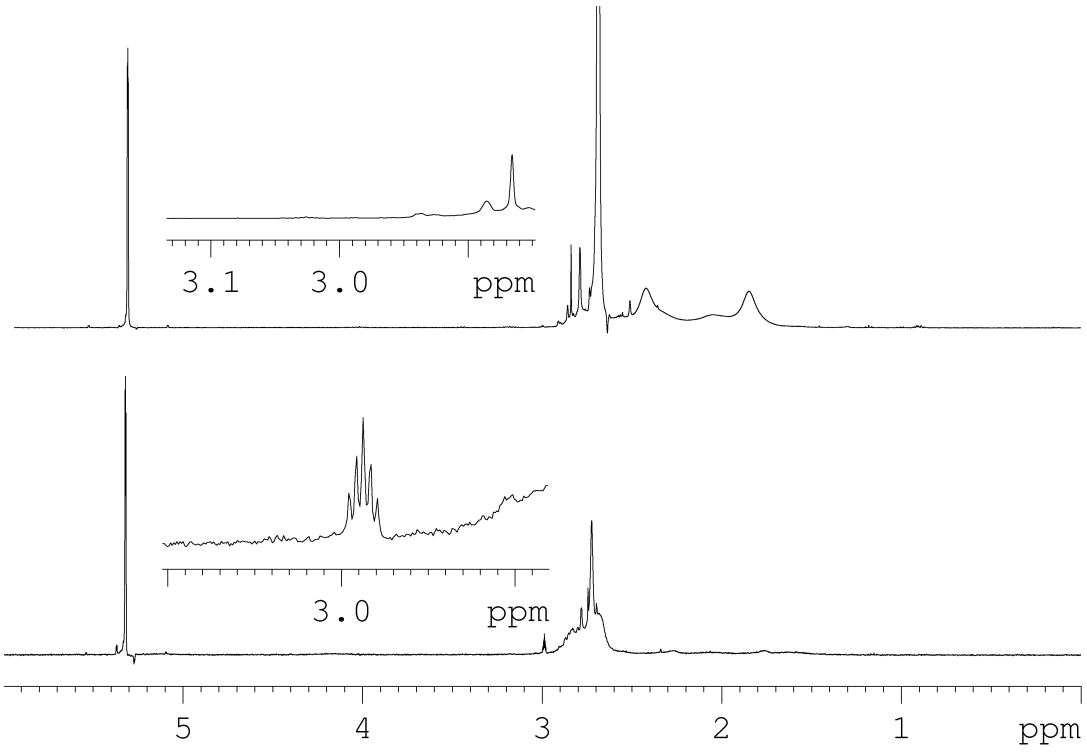

Figure 30. ^{1}H NMR spectrum of $[Tl(H_2P–BH_2{\cdot}NMe_3)_3]^+[Tef]^-$ (top) and ^{1}H NMR spectrum of a solution of $[Tl(H_2P–BH_2{\cdot}NMe_3)_3]^+[Tef]^-$ after decomposition to $[Me_3N{\cdot}H_2B–H_2P–HP–BH_2{\cdot}NMe_3]^+[Tef]^-$ in CD_2Cl_2. Evolution of CD_2HCl can be clearly observed at δ = 3.00 ppm.

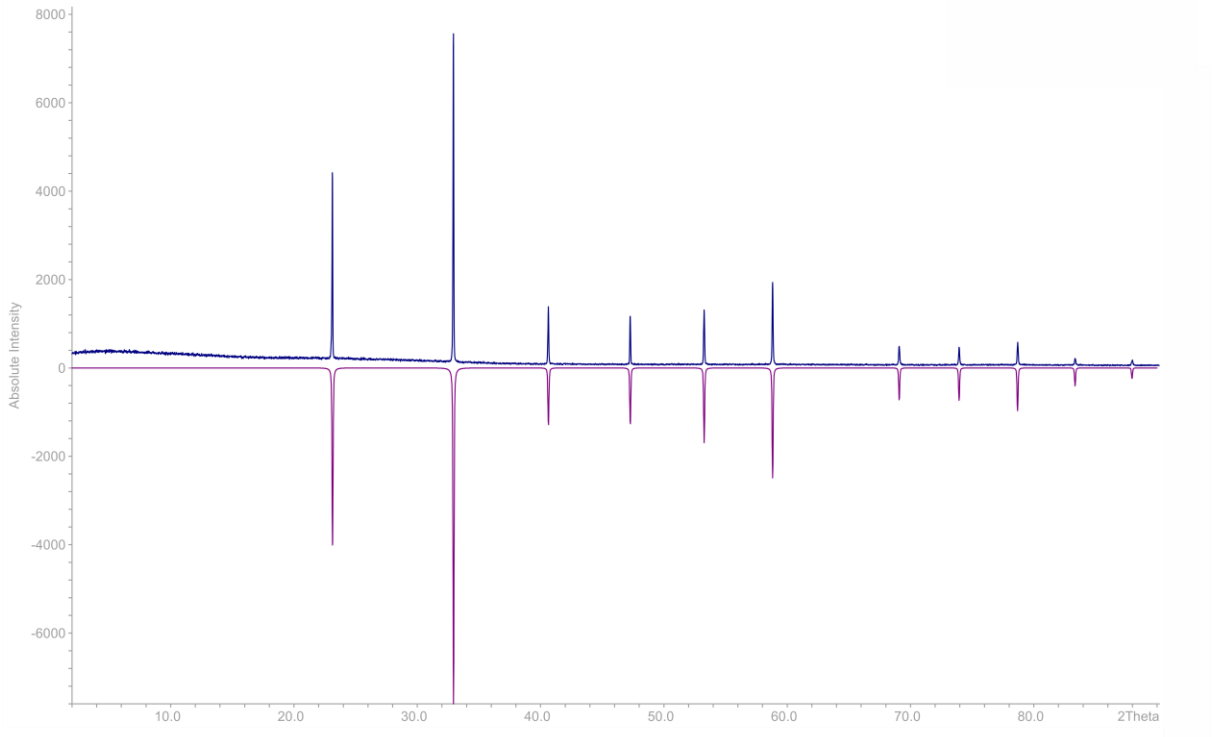

Figure 31. X-ray powder diffraction pattern of the precipitated powder (top) vs theoretical pattern of TlCl (bottom). The measurements were carried out with a STOE Stadi P diffractometer with monochromatic Cu-$K_{\alpha1}$-radiation (λ = 1.540598 Å, Ge-monochromator) and a Mythen 1 K detector at 293 K.

Synthesis of $[Tl(H_2P–BH_2·NMe_3)_3]^+[Tef]^–$:

To a solution of 117 mg (0.1 mmol) $[Tl]^+[Tef]^–$ in 5 mL of CH_2Cl_2 32 mg (0.3 mmol) $H_2P–BH_2·NMe_3$ are added at r.t.. The mixture is stirred for 30 min and filtrated. The solution is over layered by the 6 fold amount of *n*-hexane. $[Tl(H_2P–BH_2·NMe_3)_3]^+[Tef]^–$ crystallizes at −28°C as colorless needles. The crystals are separated and washed with *n*-hexane (3×5 mL). Yield of $[Tl(H_2P–BH_2·NMe_3)_3]^+[Tef]^–$: 127 mg (88 %). ^{1}H NMR (CD_2Cl_2, 25 °C): δ = 2.11 (d, $^1J_{H,P}$ = 220 Hz, PH), 2.20 (m, BH_2), 2.68 (s, NMe_3). ^{31}P NMR (CD_2Cl_2, 25 °C): δ = –161.4 (t, $^1J_{H,P}$ = 220 Hz, br). ^{31}P{^{1}H} NMR (CD_2Cl_2, 25 °C): δ = –161.4 (s, br). ^{11}B NMR (CD_2Cl_2, 25 °C): δ = –8.1 (t, $^1J_{B,H}$ = 103 Hz). ^{11}B{^{1}H} NMR (CD_2Cl_2, 25 °C): δ = –8.1 (s). ^{19}F NMR (CD_2Cl_2, 25 °C): δ = –75.6 (s). ^{19}F{^{1}H} NMR (CD_2Cl_2, 25 °C): δ = –75.6 (s). ^{13}C{^{1}H} NMR (CD_2Cl_2, 25 °C): δ = 53.2 (d, $^4J_{P,H}$ = 3Hz). IR (KBr): $\tilde{\nu}$ = 3017 (w, CH), 2956 (w, CH), 2403 (m, br, BH), 2393 (m, br, BH), 2373 (m, BH), 2316 (m, PH), 1486 (w), 1469 (w), 1452 (w), 1409 (w), 1352 (m), 1305 (s), 1277 (s), 1242 (s), 1218 (s), 1167 (m), 1123 (m), 1091 (m), 1051 (m), 1013 (w), 973 (s), 848 (m), 833 (w), 727 (s), 694 (w), 561 (w), 537 (w), 446 (w). ESI-MS (MeCN): *m/z* = 415 (10%, $[Tl(H_2P–BH_2·NMe_3)_2]^+$), 310 (100%, $[Tl(H_2P–BH_2·NMe_3)]^+$), 205 (15%, $[Tl]^+$). Elemental analysis (%) calculated for $C_{25}H_{39}AlB_3F_{36}N_3O_4P_3Tl$: C: 20.18, H: 2.64, N: 2.82; found: C: 20.37, H: 2.70, N: 2.76.

Synthesis of $[Tl(H_2As–BH_2·NMe_3)_3]^+[Tef]^–$:

To a solution of 117 mg (0.1 mmol) $[Tl]^+[Tef]^–$ in 5 mL of CH_2Cl_2 45 mg (0.3 mmol) $H_2As–BH_2·NMe_3$ are added at r.t.. The mixture is stirred for 30 min and filtrated. The solution is over layered by the 6 fold amount of *n*-hexane. $[Tl(H_2As–BH_2·NMe_3)_3]^+[Tef]^–$ crystallizes at −28°C as yellow needles. The crystals are separated and washed with *n*-hexane (3×5 mL). Yield of $[Tl(H_2As–BH_2·NMe_3)_3]^+[Tef]^–$: 120 mg (74 %). ^{1}H NMR (CD_2Cl_2, 25 °C): δ = 1.30 (m, 2H, AsH_2), 2.43 (q, $^1J_{B,H}$ = 111 Hz, BH_2), 2.72 (s, NMe_3). ^{19}F NMR (CD_2Cl_2, 25 °C): δ = –75.6 (s). ^{19}F{^{1}H} NMR (CD_2Cl_2, 25 °C): δ = –75.6 (s). ^{11}B NMR (CD_2Cl_2, 25 °C): δ = –6.5 (t, $^1J_{B,H}$ = 111 Hz). ^{11}B{^{1}H} NMR (CD_2Cl_2, 25 °C): δ = –6.5 (s). ^{13}C{^{1}H} NMR (CD_2Cl_2, 25 °C): δ = 53.7 (s, NMe), 123.7 (q, $^1J_{C,F}$ = 293 Hz, CF_3). IR (KBr): $\tilde{\nu}$ = 3018 (w, CH), 2957 (w, CH), 2924 (w, CH), 2417 (w, br, BH), 2374 (w, BH), 2110 (w, AsH), 1627 (w), 1486 (w), 1468 (w), 1353 (m), 1305 (s), 1278 (s), 1243 (s), 1219 (s), 1167 (m), 1119 (m), 1071 (m), 1048 (m), 1013 (w), 973 (s), 850 (m), 833 (w), 728 (s), 648 (w), 561 (w), 537 (w), 445 (w). ESI-MS (MeCN): *m/z* = 354 (100%, $[Tl(H_2As–BH_2·NMe_3)]^+$), 205 (75%, $[Tl]^+$). Elemental analysis (%) calculated for $C_{25}H_{39}AlAs_3B_3F_{36}N_3O_4Tl$: C: 18.56, H: 2.43, N: 2.60; found: C: 18.77, H: 2.39, N: 2.44.

Synthesis of $[Me_3N{\cdot}H_2B–H_2P–HP–BH_2{\cdot}NMe_3]^+[Tef]^–$:

To a solution of 117 mg (0.1 mmol) $[Tl]^+[Tef]^–$ in 5 mL of CH_2Cl_2 21 mg (0.2 mmol) $H_2P–BH_2{\cdot}NMe_3$ are added at r.t.. The mixture is stirred for 1 day upon which TlCl precipitates. After filtration the solution is over layered by the 6 fold amount of *n*-hexane. $[Me_3N{\cdot}H_2B–H_2P–HP–BH_2{\cdot}NMe_3]^+[Tef]^–$crystallizes at −28°C as colorless needles. The crystals are separated and washed with *n*-hexane (3×5 mL). ^{31}P NMR (CD_2Cl_2, 25 °C): δ = –91.3 (m, PH_2), –199.6 (t, br, PH). $^{31}P\{^1H\}$ NMR (CD_2Cl_2, 25 °C): δ = –91.3 (d, $^1J_{P,P}$ = 255 Hz, br, PH_2), –199.6 (d, $^1J_{P,P}$ = 255 Hz, br, PH_2). ^{11}B NMR (CD_2Cl_2, 25 °C): δ = –10.7 (t, $^1J_{B,H}$ = 119 Hz, $^1J_{B,P}$ = 55 Hz, BH_2), –6.5 (td, $^1J_{B,H}$ = 113 Hz, BH_2). $^{11}B\{^1H\}$ NMR (CD_2Cl_2, 25 °C): δ = –10.7 (d, $^1J_{B,P}$ = 55 Hz, BH_2), –6.5 (s, $^1J_{B,P}$ = 25 Hz, BH_2). ^{19}F NMR (CD_2Cl_2, 25 °C): δ = –75.6 (s). $^{19}F\{^1H\}$ NMR (CD_2Cl_2, 25 °C): δ = –75.6 (s). ESI-MS (CH_2Cl_2, pos. mod.): *m/z* = 209 (100%, $[Me_3N{\cdot}H_2B–H_2P–HP–BH_2{\cdot}NMe_3]^+$), 149 (30%, $[Me_3N{\cdot}H_2B–H_2P–HP–BH_2]^+$), 135 (15%, $[Me_3N{\cdot}H_2B–HP–HP]^+$), 104 (7%, $[Me_3N{\cdot}H_2B–HP]^+$). ESI-MS (CH_2Cl_2, neg. mod.): *m/z* = 967 (100%, $[Tef]^–$).

Table 7. Determined unit cell of $[Tl(H_2P–BH_2{\cdot}NMe_3)_3]^+[Tef]^–$.

crystal system	trigonal
a [Å]	16.7796(18)
b [Å]	16.7796(18)
c [Å]	10.5406(18)
α [°]	90.00
β [°]	90.00
γ [°]	120.00
Volume [Å^3]	2570.2(6)

Table 8. Crystallographic data of $[Tl(H_2As–BH_2·NMe_3)_3]^+[Tef]^-$.

empirical formula	$H_{39}C_{25}N_3O_4F_{36}AlAs_3TlB_3$
formula weight	1618.13
temperature [K]	123(1)
crystal system	trigonal
space group	*P*31*c*
a [Å]	16.92690(10)
b [Å]	16.92690(10)
c [Å]	10.50350(10)
α [°]	90
β [°]	90
γ [°]	120
Volume [$Å^3$]	2606.27(4)
Z	2
$\rho_{calc}g/cm^3$	2.062
μ/mm^{-1}	9.788
F(000)	1548.0
crystal size [mm^3]	0.3956 × 0.2046 × 0.1444
radiation	Cu*Kα* (*λ* = 1.54178)
absorption correction	analytical
T_{min}/T_{max}	0.101 / 0.399
2*Θ* range [°]	6.028 to 133.026
completeness	0.999
index ranges	-20 ≤ *h* ≤ 20 -20 ≤ *k* ≤ 20 -12 ≤ *l* ≤ 12
reflections collected	46858
independent reflections	3069 [R_{int} = 0.0495, R_{sigma} = 0.0151]
data/restraints/parameters	3069/7/237
GOF on F^2	1.039
final R indexes [I>=2σ (I)]	R_1 = 0.0374, wR_2 = 0.0976
final R indexes [all data]	R_1 = 0.0377, wR_2 = 0.0979
max/min Δ*ρ* [$e·Å^{-3}$]	0.58/-0.95
flack parameter	-0.058(5)

General Experimental

All manipulations were performed under an atmosphere of dry argon using standard glove-box and Schlenk techniques. All solvents are degassed and purified by standard procedures. The compounds $H_2EBH_2{\cdot}NMe_3$ (E = P, As),[2] $ClBH_2{\cdot}NMe_3$,[12] $IBH_2{\cdot}NMe_3$,[13] $IBH_2{\cdot}SMe_2$,[13] $LiAsH_2{\cdot}tmeda$,[14] $NaPH_2$,[15] $LiBi(SiMe_3)_2{\cdot}DME$[14], $Ph_2PBH_2{\cdot}NMe_3$,[16] ^{t}BuHPBH$_2{\cdot}$NMe$_3$,[16] $Na[H_2P–BH_2–PH_2]^-$,[17] $Na[^t$BuHP–BH$_2$–PH$_2]^-$,[17] $AlH_3{\cdot}NMe_3$,[18] NHC^{Me},[19] $PhP(SiMe_3)_2$,[20] and Tl[Tef][21] were prepared according to literature procedures. Other chemicals were obtained from Sigma-Aldrich ($AlCl_3$, I_2, dmap, $BH_3{\cdot}NH_3$, KF·HF) or STREM Chemicals, INC. ($BH_3{\cdot}SMe_2$, $BH_3{\cdot}NMe_3$, $BH_3{\cdot}$thf). The NMR spectra were recorded on a Bruker Avance 400 spectrometer (^{1}H: 400.13 MHz, ^{31}P: 161.976 MHz, ^{11}B: 128.378 MHz, ^{13}C{^{1}H}: 100.623 MHz, ^{27}Al: 104.261 MHz) with δ [ppm] referenced to external $SiMe_4$ (^{1}H, ^{13}C), H_3PO_4 (^{31}P), $BF_3{\cdot}Et_2O$ (^{11}B), $CFCl_3$ (^{19}F) or $Al(NO_3)_3{\cdot}9\ H_2O$ (^{27}Al). IR spectra were measured on a DIGILAB (FTS 800) FT-IR spectrometer. All mass spectra were recorded on a ThermoQuest Finnigan TSQ 7000 (ESI-MS) or a Finnigan MAT 95 (FD-MS and EI-MS). The C, H, N analyses were measured on an Elementar Vario EL III apparatus.

X-ray diffraction analysis

The single crystal X-ray diffraction experiments were performed either on a Gemini R Ultra CCD diffractometer or a GV1000 diffractometer from Agilent Technologies (formerly Oxford Diffraction) applying Cu-K_α radiation (λ = 1.54178 Å) at 123 K. Preliminary CIF files and SHELX instruction files (*.ins) containing refinement details are deposited on the provided DVD. The figures were created with OLEX 2.[22]

References

[1] K.-C. Schwan, A. Y. Timoskin, M. Zabel, M. Scheer, *Chem. Eur. J.* **2006**, *12*, 4900–4908.

[2] C. Marquardt, A. Adolf, A. Stauber, M. Bodensteiner, A. V. Virovets, A. Y. Timoshkin, M. Scheer, *Chem. Eur. J.* **2013**, *19*, 11887–11891.

[3] K.-Ch. Schwan, PhD thesis, University of Regensburg (Germany), **2006**.

[4] N. E. Stubbs, T. Jurca, E. M. Leitao, C. H. Woodall, I. Manners, *Chem. Commun.* **2013**, *49*, 9098–9100.

[5] A. Adolf, PhD thesis, University of Regensburg (Germany), **2007**.

[6] a) E. Hey, C. L. Raston, B. W. Skelton, A. H. White, *J. Organomet. Chem.* **1989**, *362*, 1–10; b) C. Marquardt, C. Thoms, A. Stauber, G. Balazs, M.

Bodensteiner, M. Scheer, *Angew. Chem. Int. Ed.* **2014**, *53*, 3727–3730; *Angew. Chem.* **2014**, *126*, 3801–3804.

[7] a) H. Dorn, R. A. Singh, J. A. Massey, J. M. Nelson, C. A. Jaska, A. J.Lough, I. Manners, *J. Am. Chem. Soc.* **2000**, *122*, 6669–6678; b) H. Dorn, R. A. Singh, J. A. Massey, A. J. Lough, I. Manners, *Angew. Chem.* **1999**, *111*, 3540–3543; *Angew. Chem. Int. Ed.* **1999**, *38*, 3321–3323.

[8] W. Uhlig, A. Tzschach, *Z. anorg. allg. Chem.* **1989**, *576*, 281–283.

[9] P. Pyykkö, M. Atsumi, *Chem. Eur. J.* **2009**, *15*, 186–197.

[10] A. Bondi, *J. Phys. Chem.* **1964**, *68*, 441–451.

[11] AIST: Integrated Spectral Database System of Organic Compounds. (Data were obtained from the National Institute of Advanced Industrial Science and Technology (Japan))

[12] G. E. Ryschkewitsch, J. W. Wiggins, *Inorg. Synth.,* **1970**, *12*, 116.

[13] C. Marquardt, C. Thoms, A. Stauber, G. Balazs, M. Bodensteiner, M. Scheer, *Angew. Chem. Int. Ed.* **2014**, *53*, 3727–3730; *Angew. Chem.* **2014**, *126*, 3801–3804;

[14] W. A. Herrmann, G. Brauer, *Synthetic Methods of Organometallic and Inorganic Chemistry*, *Vol.* 3 *,* **1996** *,* Thieme Publishers*,* Stuttgart.

[15] H. Jacobs, K. M. Hassiepen, *Z. Anorg. Allg. Chem.***1985**, *531*, 108–118.

[16] C. Marquardt, T. Jurca, K.-C. Schwan, A. Stauber, A. V. Virovets, G. R. Whittell, I. Manners, M. Scheer, *Angew. Chem. Int. Ed.* **2015**, *54*, DOI: 10.1002/anie.201507084; *Angew. Chem.* **2015**, *127*, DOI: 10.1002/anie.201507084.

[17] Unpublished results C. Marquardt, see chapter 6.

[18] K. Ruff, *Inorg. Synth.* **1967**, *9*,30–97.

[19] N. Kuhn, T. Kratz, *Synthesis* **1993**, 561–562.

[20] W. Uhlig, A. Tzschach, *Z. Anorg. Allg. Chem.* **1989**, *576*, 281–283.

[21] M. Gonsior, I. Krossing, N. Mitzel, *Z. Anorg. Allg. Chem.* **2002**, *628*, 1821-1830.

[22] O.V. Dolomanov, L.J. Bourhis, R.J. Gildea, J.A.K. Howard, H.Puschmann, OLEX2: A complete structure solution, refinement and analysis program, *J. Appl. Cryst*. **2009**, 42, 339–341.

12. Conclusion

12.1 Poly(phosphinoborane)s

The polymerization of the parent compound of the phosphanylboranes $H_2P–BH_2·NMe_3$ (**C1**) by simple thermal treatment, was reinvestigated. Due to the low solubility of the resulting polymer $[H_2P–BH_2]_n$ (**C4**), the characterization of this polymer was limited. To circumvent the problems with the solubility, a straightforward synthesis of organosubstituted monomeric phosphanylboranes, stabilized only by a Lewis base has been developed, to obtain the aryl-substituted compound $Ph_2P–BH_2·NMe_3$ (**C2**) and the alkyl-substituted derivative ^{t}BuHP–BH_2•NMe_3 (**C3**, Scheme 1)**.** Simple thermal treatment of the monomeric Lewis base stabilized parent and organosubstituted phosphanylboranes leads to the formation of new oligomeric and polymeric compounds. Those compounds were characterized in close collaboration with the *Manners* group from Bristol. Polymerization of $Ph_2P–BH_2·NMe_3$ leads to short chain oligomers $[Ph_2P–BH_2]_n$ (**C5**) which could be characterized by multinuclear NMR spectroscopy, and mass spectrometry. However, polymerization of ^{t}BuPH–$BH_2·NMe_3$ affords the polymer $[^t$BuPHP–$BH_2]_n$ (**C6**) with high molar mass (M_n = 27.800 – 35.000 g mol^{-1}) and reasonably low polydispersity index (PDI = 1.6-1.9) characteristic of a mainly linear material. The high molecular weight poly(phosphinoborane) $[^t$BuPHP–$BH_2]_n$ (**C6**) is not accessible via transition metal-catalyzed catalytic dehydrocoupling routes, presumably due to the deactivated P-H bond in alkylphosphinoborane monomers RH_2P•BH_3.

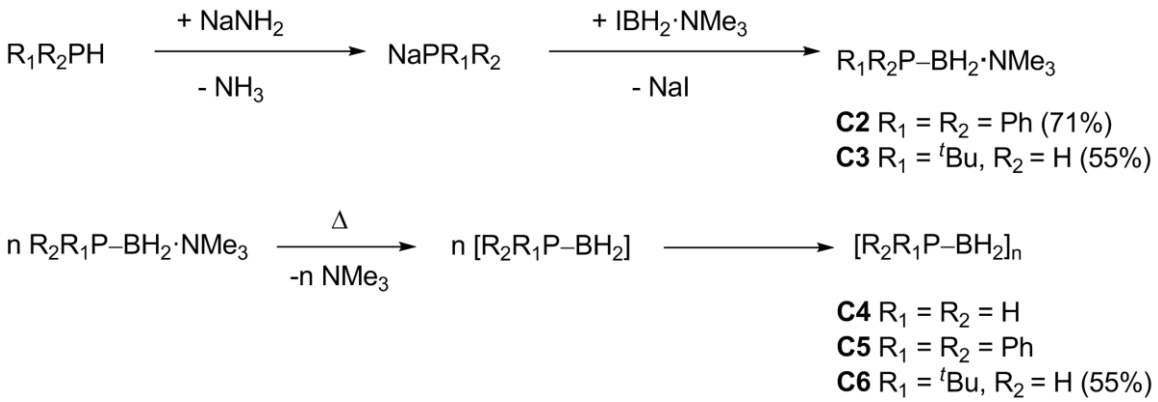

Scheme 1. Top: Synthesis of **C2** and **C3**. Yields are given in parentheses. Bottom: Polymerization of the phosphanylboranes **C1**, **C2** and **C3**.

It could be shown, that the polymerization process is also reversible. Treatment of $[^t\text{BuPHP–BH}_2]_n$ with an equivalent amount of NHC^{Me} in boiling toluene leads to $^t\text{BuPH–BH}_2\cdot\text{NHC}^{\text{Me}}$ (**C7**, Scheme 2).

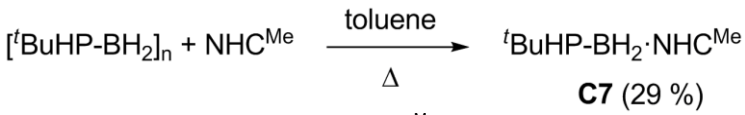

Scheme 2. Cleavage of the polymer **C6** by NHC^{Me}. Isolated yield is given in parentheses.

With a salt metathesis reaction between $[\text{LiPPh(SiMe}_3\text{)tmeda}]_2$ and $\text{IBH}_2\cdot\text{NMe}_3$ the mono-aryl substituted phosphanylborane $\text{HPhP–BH}_2\cdot\text{NMe}_3$ (**C8**, Scheme 3) can also be generated. However this monomer is not stable and already at low temperatures a polymerization process takes place, rendering **C8** to a disadvantageous monomer for the intended studies.

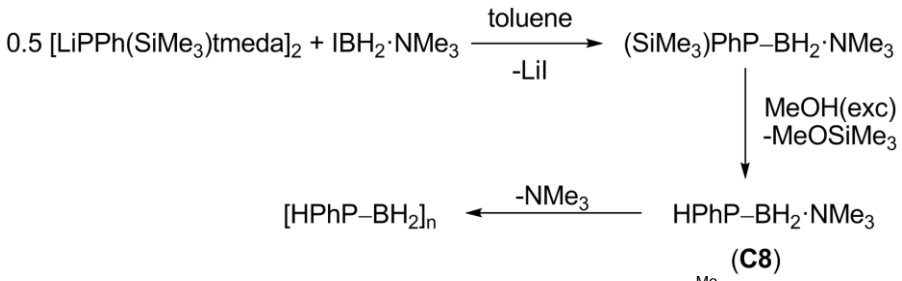

Scheme 3. Cleavage of the polymer **C8** by NHC^{Me}.

Based on these results, the new metal-free polymerization method described offers considerable promise for the preparation of a range of new poly(phosphinoborane)s with alkyl substituents on phosphorus that are of interest as elastomers, flame retardant materials, and as ceramic precursors.

12.2 Comparative studies of the substituted Phosphanylboranes

In addition to the polymerization experiments of the substituted phosphanylboranes $\text{R}_1\text{R}_2\text{P–BH}_2\cdot\text{NMe}_3$ (**C2**: $R_1 = R_2 = \text{Ph}$; **C3**: $R_1 = \text{tBu}$, $R_2 = \text{H}$) reactions including the oxidation with elemental chalcogens and coordination towards boron centered Lewis acids were performed. The elemental chalcogens sulfur, selenium and tellurium and the oxygen source bis(trimethylsilyl)peroxide are applied for the oxidation of the tertiary and secondary phosphanylboranes $\text{Ph}_2\text{P–BH}_2\cdot\text{NMe}_3$ (**C2**) and $^t\text{BuHP–BH}_2\cdot\text{NMe}_3$ (**C3**). The corresponding mono-oxidation products are obtained in good yields and have been characterized thoroughly (**C9**, **C10**, Scheme 4). While the first oxidation step proceeds

selectively for all chalcogens, further oxidation was observed for the ^{t}Bu derivative **C3** with O_2, S_8 and Se which only proceed selectively for oxygen and sulfur (**C11**, Scheme 4).

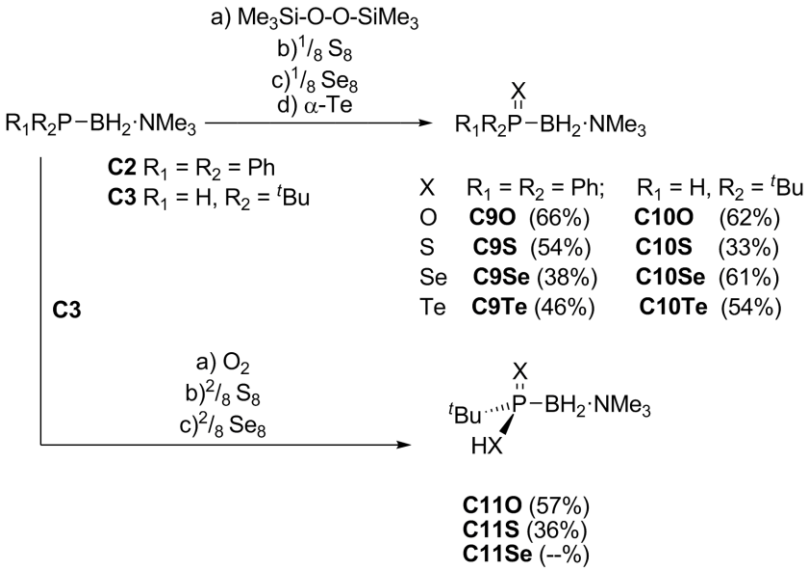

Scheme 4. Oxidation of the phosphanylboranes **C2** and **C3** with chalcogens. Yields are given in parentheses.

Whilst the parent compound **C1** can also be easily oxidized with elemental chalcogens, its reaction does not proceed as selective as found for the organosubstituted derivatives **C2** and **C3** (see below). For S and Se the mono-oxidized species $H_2P(X)–BH_2·NMe_3$ (X = S, Se) were obtained. The oxidation with elemental O_2 however leads to a phosphonic acid derivative; whereas a selective oxidation with $ONMe_3$ was not possible. In contrast to the parent compound, the oxidation reactions proceed selectively and we were able to isolate and fully characterize the mono oxidation product, for $Ph_2P(X)–BH_2·NMe_3$ (**C9X**, X = O, S, Se, Te) and ^{t}BuHP(X)–$BH_2·NMe_3$ (**C10X**, X = O, S, Se, Te). Furthermore, $Ph_2P(Te)–BH_2·NMe_3$ (**C9Te**) and ^{t}BuHP(Te)–$BH_2·NMe_3$ (**C10Te**) represent the first examples for neutral compounds with a B–P–Te unit.

The special primary phosphine $H_2PBH_2·NMe_3$ is a good σ-donor and was used for instance for the coordination to main group Lewis acids like BH_3 and BCl_3. Reaction of $Ph_2P–BH_2·NMe_3$ (**C2**) and ^{t}BuHP–$BH_2·NMe_3$ (**C3**) with $H_3B·LB$ (LB = thf, SMe_2) and BBr_3 (Scheme 5) yields the adducts $H_3B·Ph_2P–BH_2·NMe_3$ (**C2**·BH_3), $H_3B·^{t}$BuHP–$BH_2·NMe_3$ (**C3**·BH_3), $Br_3B·Ph_2P–BH_2·NMe_3$ (**C2**·BBr_3) and $Br_3B·^{t}$BuHP–$BH_2·NMe_3$ (**C3**·BBr_3), respectively.

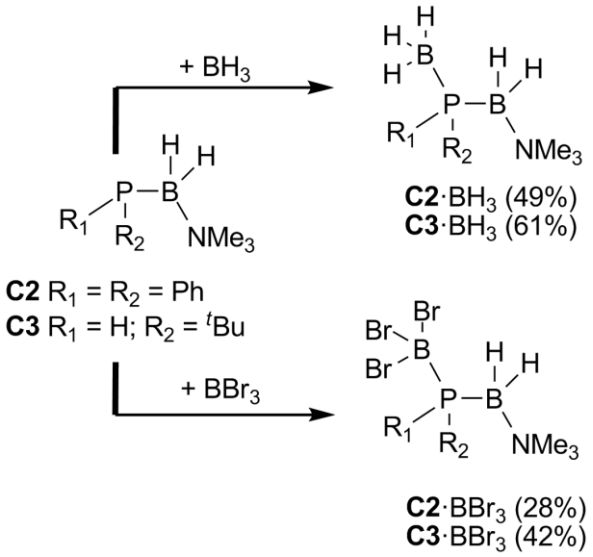

Scheme 5. Coordination of **C2** and **C3** towards BH_3 and BBr_3. Yields are given in parentheses.

Like for the parent compound $H_2PBH_2{\cdot}NMe_3$ the phosphanylborane derivatives **C2** and **C3** are good σ-donors. The formation of adducts with boron centered LAs like BH_3 and BBr_3 can be easily achieved (Scheme 5), and the resulting compounds were thoroughly characterized.

12.3 Cationic oligomers of Arsanyl- and Phosphanylboranes

To investigate if besides the polymeric chains linear oligomeric units can also be obtained, we developed a new method to transform the parent compounds of the phosphanyl- and arsanylboranes and the substituted derivatives into cationic oligomeric chains.

The reaction of the phosphanyl- or the arsanylborane $H_2EBH_2{\cdot}NMe_3$ (**C1**: E = P, **C12**: E = As) with one equivalent of $AlCl_3$ and $ClBH_2{\cdot}NMe_3$ leads to the formation of the cationic chains $[Me_3N{\cdot}BH_2{-}EH_2{-}BH_2{\cdot}NMe_3]^+[AlCl_4]^-$ (**C13**: E = P, **C14**: E = As, Scheme 6) in good crystalline yields. When $IBH_2{\cdot}NMe_3$, is treated with **C1** or **C12** no halogen abstracting agent is necessary to form $[Me_3N{\cdot}BH_2{-}EH_2{-}BH_2{\cdot}NMe_3]^+[I]^-$ (**C13**: E = P, **C14**: E = As, Scheme 6), due to the much better leaving group iodine. Reaction with a monoiodoborane stabilized by a more labile Lewis base leads to more extended frameworks (Scheme 6). The reaction of $IBH_2{\cdot}SMe_2$ with **C1** or **C12** leads to the formation of $[Me_3N{\cdot}BH_2{-}EH_2{-}BH_2{-}EH_2{-}BH_2{\cdot}NMe_3]^+[I]^-$ (**C15**: E = P, **C16**: E = As). Whereas the P derivative is stable, the As compound is prone towards decomposition in solution and in the solid state and reacts in the presence of MeCN to the 6-membered heterocycle (**C17**, Scheme 5). The Natural Population Analysis (NPA) shows a relatively strong charge separation within the cationic chains with the positive charges being accumulated on the pnictogen atoms, whereas the B atoms are negatively charged.

Based on the charge distribution the cationic chains can formally be described as a phosphonium or arsonium cations.

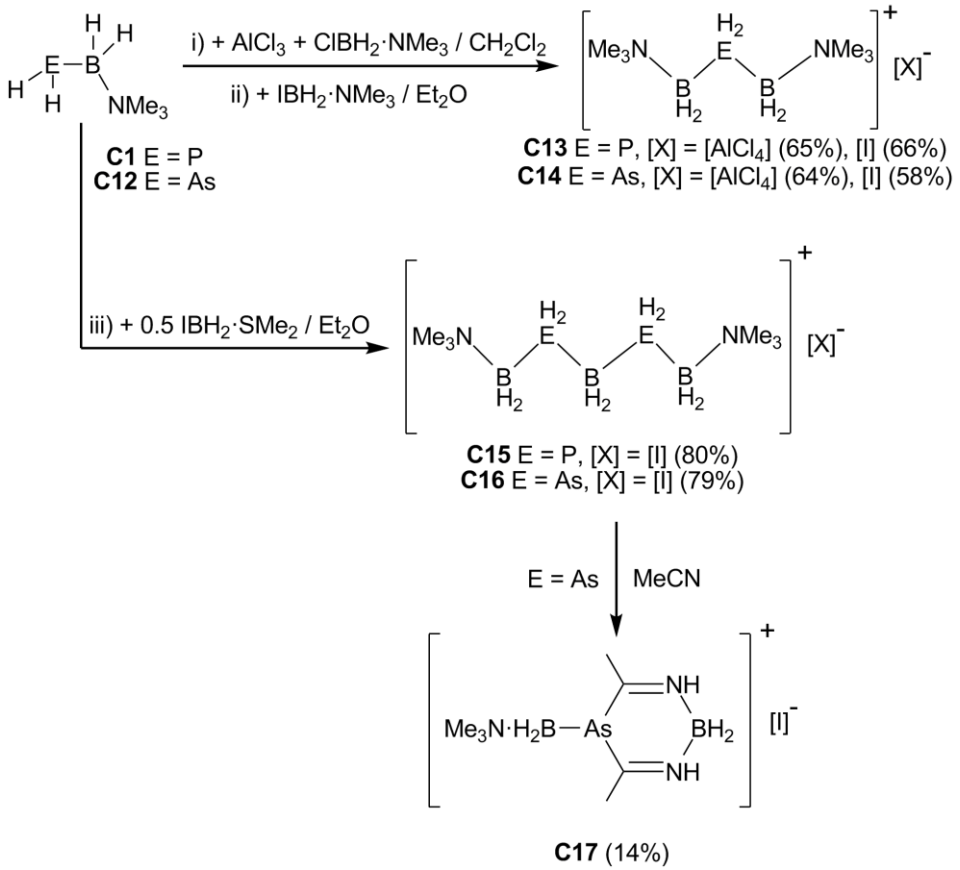

Scheme 6. Reaction of **C1** and **C12** with $H_2BI{\cdot}NMe_3$ and $H_2BI{\cdot}SMe_2$. Isolated yields are given in parentheses.

The generality of this reaction type for phosphanylboranes was demonstrated by the reaction of $Ph_2P–BH_2{\cdot}NMe_3$ (**C2**) and $^tBuPH–BH_2{\cdot}NMe_3$ (**C3**) with $IBH_2{\cdot}NMe_3$ and $IBH_2{\cdot}SMe_2$, respectively (Scheme 7). The resulting products $[Me_3N{\cdot}H_2B–PR_1R_2–BH_2{\cdot}NMe_3]^+I^-$ (**C18**: $R_1 = R_2 = Ph$; **C19**: $R_1 = H$, $R_2 = {}^tBu$)and $[Me_3N{\cdot}H_2B–PR_1R_2–BH_2–PR_1R_2–BH_2{\cdot}NMe_3]^+I^-$ (**C20**: $R_1 = R_2 = Ph$; **C21**: $R_1 = H$, $R_2 = {}^tBu$) are obtained in good yields and were fully characterized. Those compounds were also observed in electron impact mass spectrometry studies of the polymers **C5** and **C6.**

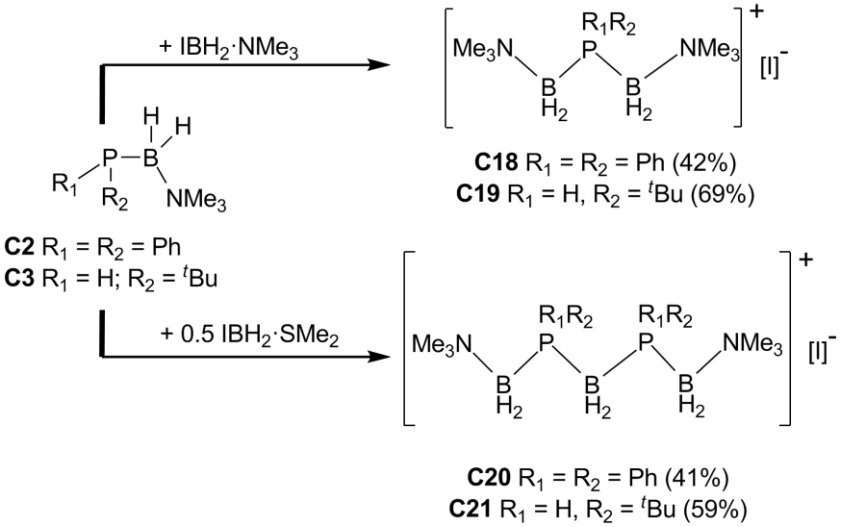

Scheme 7. Reaction of **C2** and **C3** with $H_2BI{\cdot}NMe_3$ and $H_2BI{\cdot}SMe_2$. Isolated yields are given in parentheses.

The results show the advantages of the used monomeric pnictogenylboranes as remarkable building blocks for unprecedented cationic chain compounds, which can be build-up in a stepwise manner, and in high yields. They are structurally and electronically related to *n*-alkanes. These first phosphanylborane chains are unique representatives of the cationic class of group 13/15 catena compounds, and they are the longest X-ray structurally characterized group 13/15 chain-compounds. The first examples for mixed arsenic-boron chains have also been isolated (**C14**, **C16**, Scheme 6). The chains show excellent thermodynamic stability, and the presented concepts will allow the formation of more extended chain molecules and also of more complex hydrocarbon-related structures. The presented reaction is a versatile way for the generation of cationic oligomers based on phosphorus- and arsenic-donors. These results contribute to our knowledge about the C/PB relationship.

12.4 Anionic oligomers of Phosphanylboranes

As the cationic chains of the phosphanyl- and arsanylboranes were easily accessible and showed a surprising thermodynamic stability, we also investigated if the phosphanylborane **C1** can be used as a starting material for the generation of anionic species. The reactions of the phosphanylborane **C1** with sodium salts of PH_2^-, $^tBuPH^-$ and Ph_2P^-, leads to the formation of $[Na]^+[H_2P–BH_2–PH_2]^-$ (**C22**), $[Na]^+[H_2P–BH_2–P^tBuH]^-$ (**C23**) and $[Na]^+[H_2P–BH_2–PPh_2]^-$ (**C24**), respectively, containing anionic phosphorus-boron chain like units (Scheme 8). By using a different stoichiometry and reaction conditions the species $[Na]^+[H_2P–BH_2–PPh_2–BH_2–PH_2]^-$ (**C25**), containing a longer B–P unit, can be obtained (Scheme 8).

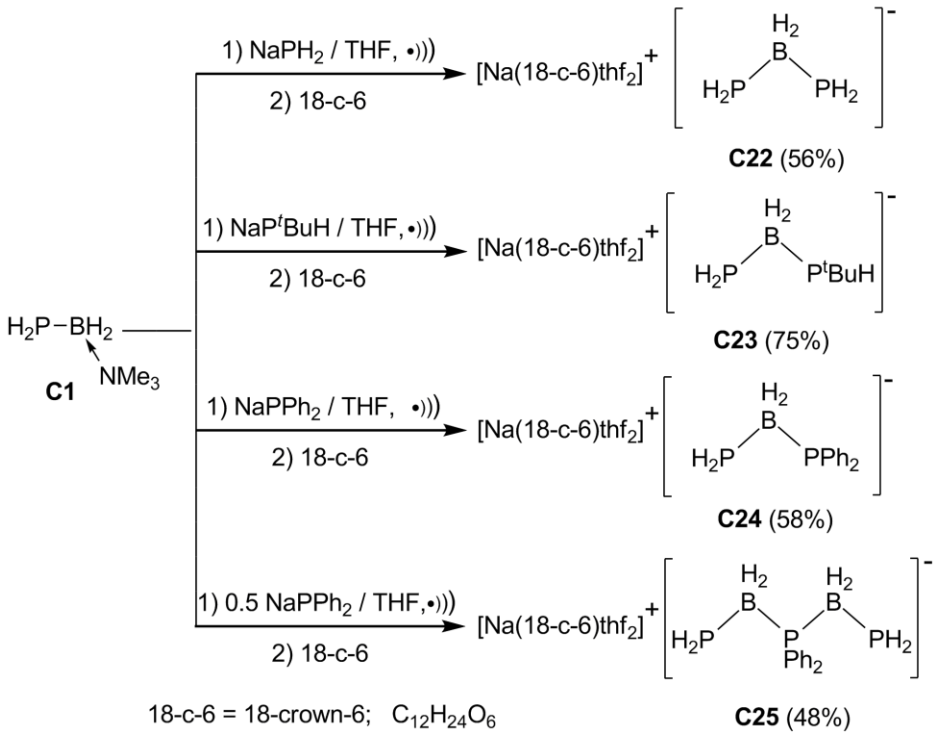

Scheme 8. Transformation of **C1** into the anionic species **C22** – **C25**. Yields are given in parentheses.

The results show that the parent phosphanylborane $H_2PBH_2{\cdot}NMe_3$ is a valuable precursor for the generation of anionic mixed group 13/15 chains. For the first time the structural characterization of the unprecedented, anionic chains was possible. These unique 13/15 compounds represent the anionic counterparts to the above mentioned cationic species. The compounds are stable under inert conditions, and preliminary investigations have shown, that they are excellent starting materials for the preparation of longer linear phosphanylboranes, extended ionic group 13/15 chains, cycles and polymers.

12.5 Heavier analogs of the Pnictogenylboranes

Since the synthesis of the arsanylborane **C12** was reported very recently, it was worthwhile to examine if pnictogenylboranes of the heavier congeners Sb and Bi are also accessible. However, compounds with a well-defined 2-center-2-electron bond between Sb and B or Bi and B, respectively, are quite scarce. In the present work a new strategy via salt metathesis was developed, which can be used for the synthesis of such unprecedented bonds. By a salt metathesis route the silyl substituted compounds $(Me_3Si)_2Sb–BH_2{\cdot}LB$ (**C26**: LB = NMe_3, **C27**: LB = NHC^{Me}) have been synthesized (Scheme 9). They represent unique derivatives with a Sb-B σ-bond. Under very mild conditions they could be transformed to the target compounds $H_2Sb–BH_2{\cdot}NMe_3$ (**C28**), which is unstable and decomposes to $Me_3N{\cdot}H_2B–HSb–BH_2{\cdot}NMe_3$ (**C30**) and $H_2Sb–$

$BH_2{\cdot}NHC^{Me}$ (**C29**) respectively (Scheme 9). Usage of the strong Lewis base dmap allowed the stabilization of $(Me_3Si)_2Bi–BH_2{\cdot}$dmap (**C31**), which is one of the first bimuthanylboranes known so far. Unfortunately, the cleavage of the Bi-Si bonds and an evidence for the presence of the parent compounds of the bismuthanylboranes $H_2Bi–BH_2{\cdot}$dmap - representing the first example for a primary bismuthane - failed so far.

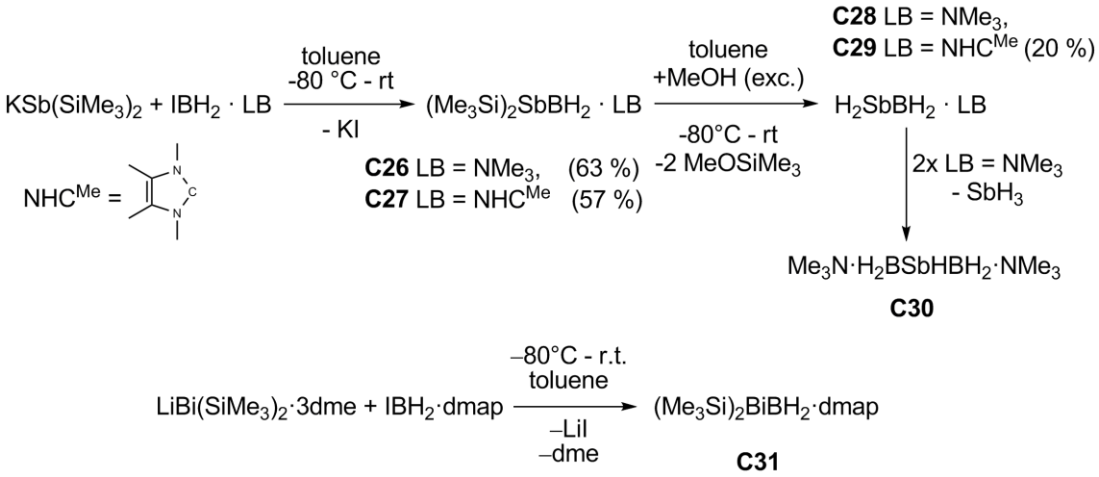

Scheme 9. Synthesis of stibanyl- and bismuthanylboranes. Yields are given in parentheses.

By using the monoiodo-borane adducts $IBH_2{\cdot}LB$ (LB = NMe_3, NHC^{Me}, dmap) a direct synthesis and isolation of a series of stable stibanylboranes is achieved. The silylsubstituted compounds $(Me_3Si)_2Sb–BH_2{\cdot}LB$ (**C26**: LB = NMe_3, **C27**: LB = NHC^{Me}) are unique representatives with a well-defined 2-center-2-electron-σ-bond between antimony and boron. The silyl-substituted compound $(Me_3Si)_2Bi–BH_2{\cdot}$dmap is one of the first representatives with a well-defined 2-center-2-electron-σ-bond between bismuth and boron. Furthermore, it was possible for the first time to synthesize, isolate and characterize comprehensively the Lewis base stabilized monomeric parent compound of the stibanylboranes "H_2SbBH_2". This compound represents a unique primary stibine without a bulky substituent as usually needed for the stabilization of the reactive SbH_2 unit. The diboranylstibine **C30** was obtained as a decomposition product of the primary stibine, revealing a first longer neutral B-Sb-B chain. Additionally it was shown that this route - the application of $IBH_2{\cdot}NMe_3$ - also enables an easier approach for the synthesis of phosphanyl- and arsanylboranes. Alkalimetal salts of PH_2^- and AsH_2^- can be used for the synthesis of the parent compounds which bypasses the highly time-, material- and energy-consuming synthesis of tris(trimethylsilyl)phosphine and –arsine.

12.6 Coordination towards Cu^+, Ag^+ and Tl^+

As a last aspect of this work the coordination behavior of $H_2EBH_2{\cdot}NMe_3$ (**C1** E = P, **C12** E = As) and $Ph_2PBH_2{\cdot}NMe_3$ (**C2**) towards the monovalent metal cations Cu, Ag and Tl with weakly coordinating anions was investigated. Reaction with $[Cu(MeCN)_4(BF_4)]$ affords the homoleptic, tetracoordinated complexes $[Cu(H_2P–BH_2{\cdot}NMe_3)_4(BF_4)]$ (**C32**) and $[Cu(H_2As–BH_2{\cdot}NMe_3)_4(BF_4)]$ (**C33**) in good crystalline yields (Scheme 10). If the sterically higher demanding phosphanylborane **C2** is used only the tricoordinated trigonal planar complex $[Cu(Ph_2P–BH_2{\cdot}NMe_3)_3(BF_4)]$ (**C34**) is obtained. All compounds have been comprehensively characterized by spectroscopic methods and their structures were determined by single-crystal X-ray diffraction. Complex **C34** slowly decomposes to $[Cu(Ph_2P–BH_2{\cdot}NMe_3)_2Cl]$ in CH_2Cl_2 solution (Scheme 10), determined by X-ray structure analysis of the product.

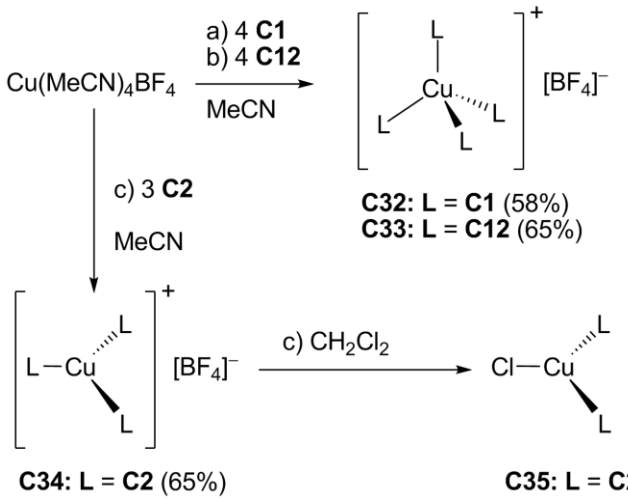

Scheme 10. Coordination of **C1**, **C2** and **C12** towards Cu. Yields are given in parentheses.

In contrast to the reactions mentioned before, reactions of **C1** and **C12** with Ag^+ however do not proceed smoothly. The parent compounds **C1** and **C12** decompose upon reaction with Ag^+, and in MeCN only decomposition products were obtained (Scheme 11). Only once a compound containing a six membered ring was obtained from the reaction of $H_2P–BH_2{\cdot}NMe_3$ with $[Ag]^+[Fal]^-$. It exhibits the dimeric unit $[(Ag{\cdot}H_2P–BH_2{\cdot}NMe_3)_2]^{2+}2[FAl]^-$ with a central six membered $Ag_2–P_2–B_2$ ring. Reaction of $Ph_2P–BH_2{\cdot}NMe_3$ (**C2**) with $[Ag]^+$ salts proceeds without decomposition. The stoichiometric reaction of **C2** with 1 equivalent $[Ag]^+[BF_4]^-$ yields the one dimensional coordination polymer **C36** (Scheme 11), exhibiting Ag-C_{phenyl} interactions. Subsequently $Ag[BF_4]$ was also reacted with 2, 3 and 4 equivalents of **C2**. Surprisingly, these reactions did not result in the formation of $[Ag(Ph_2P–BH_2{\cdot}NMe_3)_n][BF_4]$ and only polymeric **C36** could be

structurally characterized. Reactions of different stoichiometric amounts of $Ph_2P–BH_2·NMe_3$ with Ag^+ salts containing the bigger weakly coordinating anion $[FAl]^-$ result in the selective formation of $[Ag(Ph_2P–BH_2·NMe_3)(MeCN)]^+[FAl]^-$ (**C37**), $[Ag(Ph_2P–BH_2·NMe_3)_2]^+[FAl]^-$ (**C38**) and $[Ag(Ph_2P–BH_2·NMe_3)_3]^+[FAl]^-$ (**C39**) (Scheme 11). While complexes **C37** and **C38** show linear coordination of the Ag atom, compound **C39** shows a trigonal planar coordination environment for Ag. A fourfold coordination of Ag^+ by **C2** could not be observed.

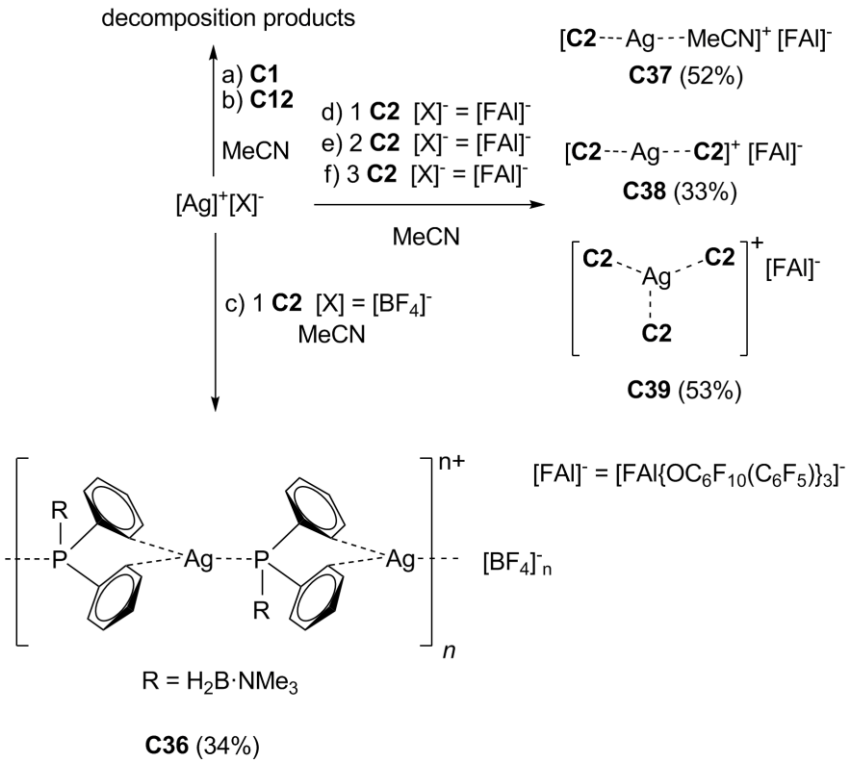

Scheme 11. Coordination of **C2** towards Ag. Yields are given in parentheses.

The obtained complex **C32** is a very rare example of a homoleptic complex with a primary phosphine. A homoleptic complex with a primary arsine at a Cu-center (**C33**) is also described for the first time. The reaction of the phosphanylboranes with Ag^+ salts affords new homoleptic coordination compounds. For the first time a one dimensional polymer of a group 13/15 compound with Ag was observed (**C36**). This study conclusively shows the versatility of the easily accessible primary phosphine **C1** or the primary arsine **C12** containing a boranyl group as ligands in coordination chemistry. Despite the pure academic interest, these ligands may be interesting for catalytic studies and large variety of suitable complexes should be accessible. Especially the ligand **C2**, which can be described as a derivative of PPh_3, will be interesting due to the fact that it stabilizes trigonal coordinated metal centers.

For Tl also no homoleptic complexes are known with primary arsines or phosphines. Reaction of 3 equivalents of $H_2E–BH_2·NMe_3$ (**C1** E = P, **C2** E = As) with $[Tl]^+[Tef]^-$ leads to $[Tl(H_2E–BH_2·NMe_3)_3]^+[Tef]^-$ (**C40** E = P, **C41** E = As, Scheme 12). In the solid state compounds **C40** and **C41** reveal one-dimensional columns in which three pnictogen atoms coordinate a Tl atom, and a hydride from each boranyl group is interacting with the next Tl atom. In the case of the P derivative the complex is not stable. Stirring a mixture of 2 equivalents of $H_2P–BH_2·NMe_3$ with $[Tl]^+[Tef]^-$ leads to a Tl mediated P-P coupling. The Tl^+ ion abstracts a chlorine atom from CH_2Cl_2 leading to $[CH_2Cl]^+$ which reacts with $H_2P–BH_2·NMe_3$ to give $[HP–BH_2·NMe_3]^+$. $[HP–BH_2·NMe_3]^+$ reacts instantly with the second equivalent of $H_2P–BH_2·NMe_3$ to form $[Me_3N·H_2B–H_2P–HP–BH_2·NMe_3]^+$ (**C42**, Scheme 12). The presence of $[Me_3N·H_2B–H_2P–HP–BH_2·NMe_3]^+[Tef]^-$ (**C42)** was confirmed by ^{31}P NMR spectroscopy and mass spectrometry.

$$[Tl]^+[Tef]^- + 3\ H_2EBH_2·NMe_3 \xrightarrow{CH_2Cl_2} [Tl(H_2EBH_2·NMe_3)_3]^+[Tef]^-$$

C40 E = P (88%)
C41 E = As (74%)

$$[Tl]^+[Tef]^- + 2\ H_2PBH_2·NMe_3 + CH_2Cl_2 \xrightarrow{CH_2Cl_2} [Me_3N·H_2BHP–PH_2BH_2·NMe_3]^+[Tef]^- + TlCl\downarrow + CH_3Cl$$

C42

Scheme 12. Coordination of **C1** and **C12** towards Tl. Yields are given in parentheses.

The products **C40** and **C41** are the first examples of Tl complexes with primary phosphines and arsines. In the case of the P derivative a very interesting and yet unknown Tl-mediated P-P coupling reaction is observed, which might be a powerful tool for P-P bond formation reactions in the future.

13. Appendices

13.1 Alphabetic List of Abbreviations

18-c-6	18-crown-6, $C_{12}H_{24}O_6$
Å	Angstroem, 1 Å = $1 \cdot 10^{-10}$ m
°C	degree Celsius
br(NMR)	broad
btmsa	bis(trimethylsilyl)acetylene
COSY	correlation spectroscopy
cod	cycloocta-1,5-diene
cov	covalent
Cp	cyclopentadienyl, C_5H_5
d(NMR)	doublet
DLS	Dynamic light scattering
$E°_0$	reaction energy
$H°_{298}$	standard reaction enthalpy
$S°_{298}$	standard reaction entropy
$G°_{298}$	standard gibbs reaction energy
δ	chemical shift
Da	Dalton
DFT	density functional theory
Dipp	2,6-diisopropylphenyl
dmap	4-Dimethylaminopyridine
dme	1,2-dimethoxyethane
E	element of the 15th group, E = N, P, As, Sb, Bi
E’	element of the 13th group, E’ = B, Al, Ga, In, Tl
e^-	electron
EI MS	electron impact mass spectrometry
ESI MS	electron spray ionization mass spectrometry
FAl	[FAl{$OC_6F_{10}(C_6F_5)$}$_3$])
Fc	Ferrocene
FD MS	field desorption ionization mass spectrometry
FLP	frustrated Lewis pair
GPC	Gel permeation chromatography

HOMO	highest occupied molecular orbital
Hz	Hertz
^{i}Bu	*iso*-butyl, C_4H_9
^{i}Pr	*iso*-propyl, C_3H_7
IR	infrared spectroscopy
J(NMR)	coupling constant
L	ligand (specified in text)
LA	Lewis acid
LB	Lewis base
LUMO	lowest unoccupied molecular orbital
M	molecular ion peak
M_n	number-average molar mass
m/*z*	mass to charge ratio
Me	methyl, CH_3
Mes	mesityl, 2,4,6-trimethylphenyl
MHz	Megahertz, 10^6 Hz
MOCVD	metalorganic chemical vapor deposition
nacnac	*β*-diketiminate
^{n}Bu	*n*-butyl, C_4H_9
NHC	N-heterocyclic carbene
NMR	nuclear magnetic resonance
NPA	Natural Population analysis
PDI	polydispersity index
$\tilde{\nu}$	frequency/wavenumber
$\omega_{1/2}$	half width
OTf^-	triflate, $CF_3SO_3^-$
Ph	phenyl, C_6H_5
PPA	poly(aminoborane)
PPB	poly(phosphinoborane)
ppm	parts per million
q(NMR)	quartett
R	organic substituent
R_h	hydrodynamic radius
r	radius
r.t.	room temperature
s(IR)	strong
s(NMR)	singlet

sept(NMR)	septet
sh(IR)	shoulder
sMes	2,4,6-tri-tertbutylphenyl
Tef	$[Al\{OC(CF_3)_3\}_4]$
^{t}Bu	*tert*-butyl, C_4H_9
t(NMR)	triplet
THF	tetrahydrofurane, C_4H_8O
tmp	2,2,6,6-Tetramethylpiperidine
TMS	tetramethylsilane, $Si(CH_3)_4$
vdW	van der Waals
VE	valence electron
VT	Various Temperature
w(IR)	weak

13.2 Acknowledgments

Finally special thanks got to:

- Prof. Dr. Manfred Scheer for giving me the opportunity to work on this very interesting project, providing excellent working conditions and the freedom to pursue my own ideas in the lab.
- Dr. Gábor Balázs for spending so much time on discussing, giving helpful advice, accurate proof-reading and tons of DFT calculations. Without his knowledge and input, major parts of this work would not have been possible.
- Prof. Dr. Alexey Timoshkin for a lot of discussions and putting so much effort into DFT calculations, helping to understand the presented chemistry.
- Prof. Dr. Ian Manners and co-workers for a very pleasant research stay at the School of Chemistry in Bristol, UK, which was a very rewarding experience. And in particular Dr. Titel Jurca for putting a lot of effort into this collaboration.
- Dr. Alexander V. Virovets and Dr. Eugenia Peresypkina for comprehensive help with X-ray structure analyses, and fighting a lot of problems.
- All staff and co-workers of the Central Analytical Services of the University of Regensburg: X-ray (Dr. Michael Bodensteiner, Sabine Stempfhuber, Katharina Beier), mass spectrometry department (Josef Kiermaier, Wolfgang Söllner), elementary analysis department (Helmut Schüller, Barbara Baumann, Wilhelmina Krutina) and in particular the NMR Department (Dr. Ilya Shenderovich, Anette Schramm, Georgine Stühler, Fritz Kastner) for recording countless spectra and satisfying all special requests.
- The staff of the glass blowing, electronics and mechanics facilities of the University of Regensburg.
- My former lab colleagues (Andreas, Bianca, Jens, Olli, Tobi) for the unforgettable time and funny and high-class discussions.
- The whisky-connection (Christian, Basti, Wast, Moartl) for the very entertaining tastings.
- All present and former members of the Scheer group for a pleasant working atmosphere and an unforgettable time: Andi, Andrea, Barbara K., Barbara T., Bianca, Boudi, Claudi, Conny, Dani, David, Eric, Eva, Fabian D., Fabian S., Felix, Gábor, Hannes, Helena, Jens, Julian, Karin, Kathl, Küken, Liese, Luigi, Luis, Matthias H., Matthias L., Mehdi, Mia, Michi, Miriam, Moartl, Moni, Mo, Musch, Muschine, Oime, Olli, Patrick, Petra, Reini, Robert, Rudi, Sabine, Schotti, Sµ, Stubi, Susanne, Thomsi, Tobi, Valentin, Walter, Wast, Welschi, Wurzl.
- And especially to my family and all my friends for their enduring support.